γ

GEND-INF- 013
May 1984

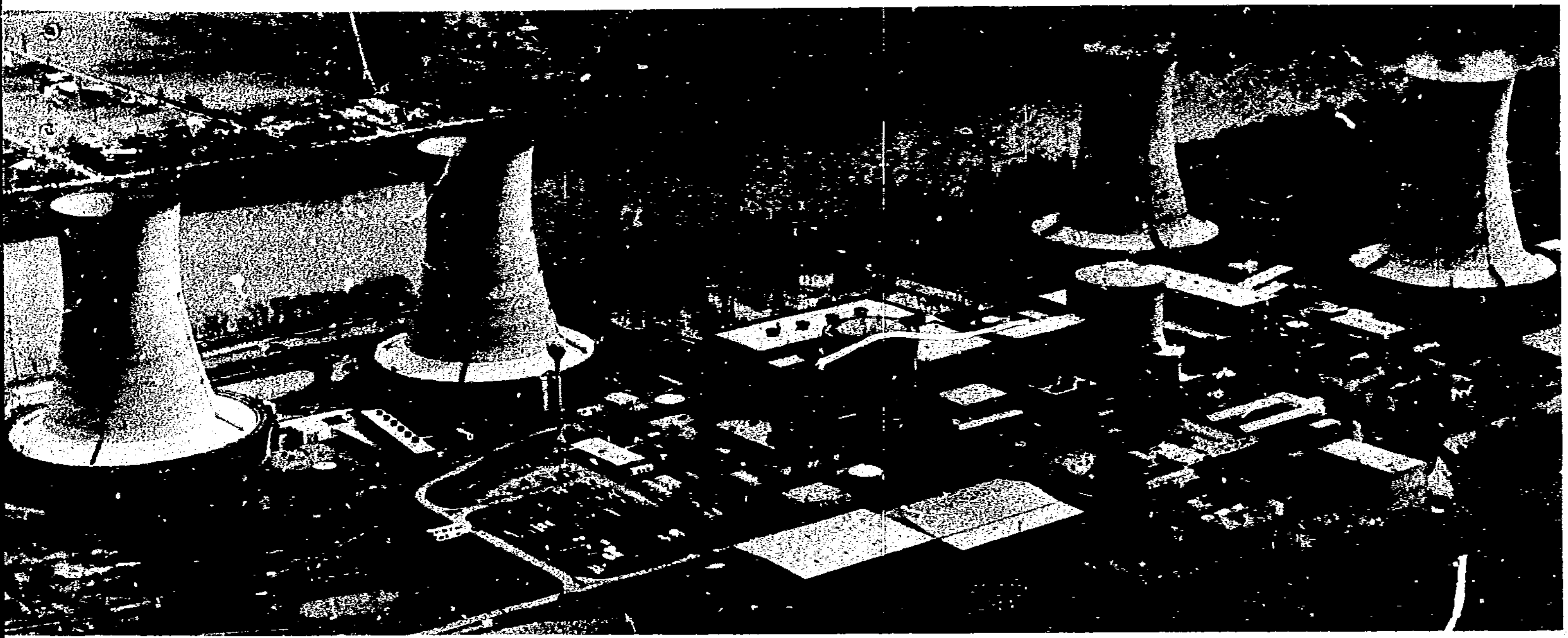

This is an informal report intended for use as a preliminary or working document

GEND

General Public Utilities • Electric Power Research Institute • U.S. Nuclear Regulatory Commission • U.S. Department of Energy

TMI-2 Purification Demineralizer Resin Study

Joseph D. Thompson
Thomas R. Osterhoudt

Prepared for the
U.S. Department of Energy
Three Mile Island Operations Office
Under DOE Contract No. DE-AC07-76ID01570

DISTRIBUTION OF THIS DOCUMENT IS UNLIMITED

GEND-INF--013

DE84 014736

TMI-2 PURIFICATION DEMINERALIZER RESIN STUDY

Joseph D. Thompson
EG&G Idaho, Inc.
Idaho Falls, Idaho 83415

Thomas R. Osterhoudt
GPU Nuclear Corporation
Middletown, PA 17057

Published May 1984

Prepared for the
U.S. Department of Energy
Three Mile Island Operations Office
Under DOE Contract No. DE-AC07-76ID01570

ABSTRACT

Study of the Makeup and Purification System demineralizers at TMI-2 has established that fuel quantities in the vessels are low, precluding criticality, that the high radioactive cesium concentration on the demineralizer resins can be chemically removed, and that the demineralizer resins can probably be removed from the vessels by sluicing through existing plant piping. Radiation measurements from outside the demineralizers established that there is between 1.5 and 5.1 (probably 3.3) lb of fuel in the A vessel and less than that amount in the B vessel. Dose rates up to 2780 R per hour were measured on contact with the A demineralizer. Remote visual observation of the A demineralizer showed a crystalline crust overlaying amber-colored resins. The cesium activity in solid resin samples ranged from 220 to 16,900 µCi/g. Based on this information, researchers concluded that the resins cannot be removed through the normal pathway in their present condition. Studies do show that the resins will withstand chemical processing designed to rinse and elute cesium from the resins. The process developed should work on the TMI-2 resins.

CONTENTS

NOTE: The appendixes are presented on microfiche contained in an envelope on the inside back cover of the report.

TMI-2 PURIFICATION DEMINERALIZER RESIN STUDY

INTRODUCTION

The TMI-2 Makeup and Purification System demineralizers were in use for at least 18 h, 35 min during the March 28, 1979 TMI-2 accident. These demineralizers, the dimensions of which are shown in Figure 1, are located in shielded cubicles in the TMI-2 Auxiliary Building. They process primary coolant system water and return it to various locations within the primary coolant system and storage tanks. General Public Utilities Nuclear Corporation (GPU Nuclear) has estimated that 46,000 gal of highly contaminated reactor coolant passed through the demineralizer vessels during the accident.

In normal plant operation, the demineralizer system is used to remove soluble contaminants from primary system water. Periodically, expended demineralizer resins are removed by sluicing them through installed piping to spent resin storage tanks. The demineralizer vessels' process connections are shown in Figure 2.

During the accident, the resins absorbed significant quantities of fission products. Most notable are ^{137}Cs, which has a 30-year half life and for the most part is still present, and isotopes of iodine, which are essentially gone. The iodine, however, presented a relatively high heat source when the vessels were isolated, causing overheating of the resin bead media. In addition, some fuel particles were transported through the letdown piping into the demineralizer vessels. This combination presented three separate and distinct problems which had to be understood prior to treating the contents of the demineralizers. First, knowledge regarding the amount of fuel present was necessary to address the criticality potential during processing and handling. Second, the cesium represents a high potential handling dose rate for which the impacts must be minimized. Third, knowing the physical state of the resins as a result of overheating was important in order to establish which physical removal processes would be feasible. If the material congealed, then this problem would be exacerbated.

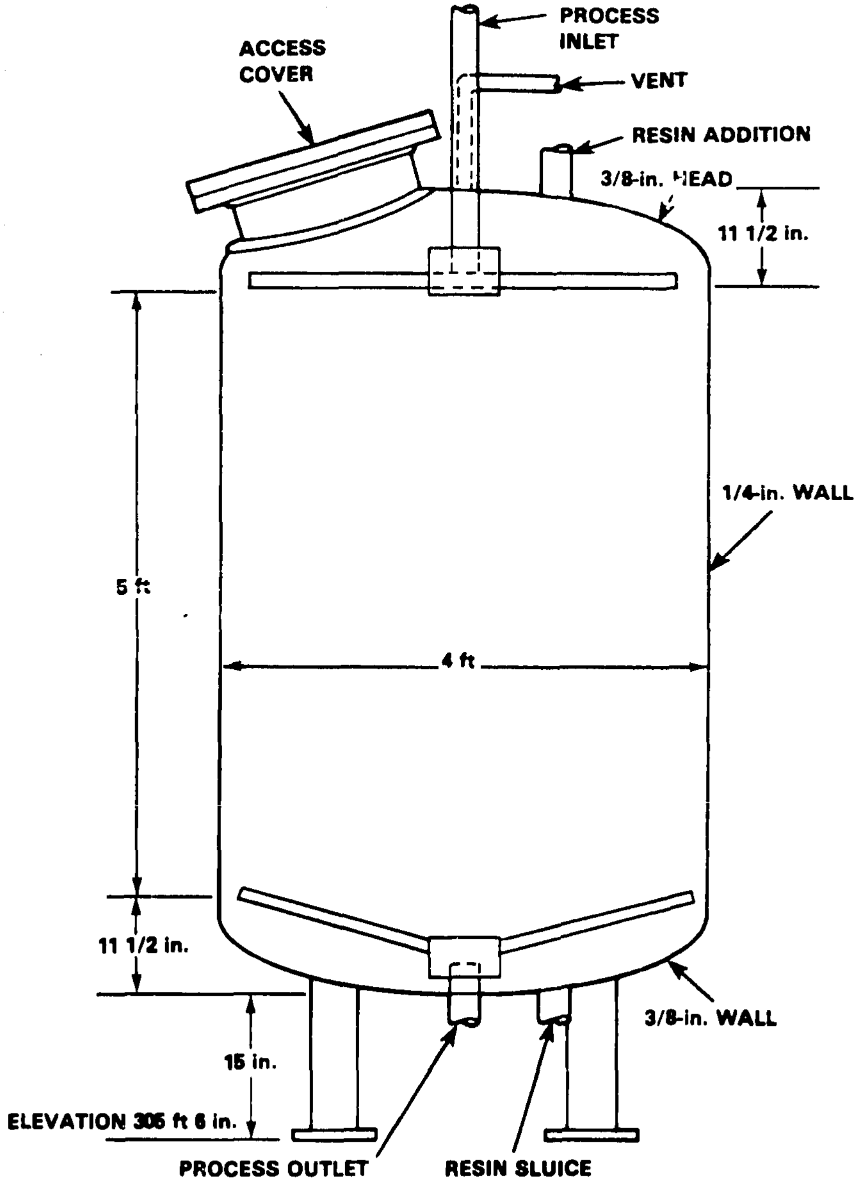

MU-K-1A, B
MAKE-UP AND PURIFICATION
DEMINERALIZERS

TOP CONNECTIONS
- PROCESS INLET
- VENT
- RESIN ADDITION
- ACCESS COVER

BOTTOM CONNECTIONS
- PROCESS OUTLET
- RESIN SLUICE

TOP LATERALS
- 12 TOTAL
- 18-in. LONG
- 3/4-in. Φ, 304SS
- 21 HOLES, 3/16-in. PER LATERAL

BOTTOM LATERALS
- 12 TOTAL
- 20-in. LONG
- 3/4-in. Φ, 304 SS
- 21 HOLES, 3/16-in. PER LATERAL
- 100 MESH WIRE SCREEN

TANK VOLUME
- 560 GALLONS

Figure 1. Dimensions of demineralizer vessel.

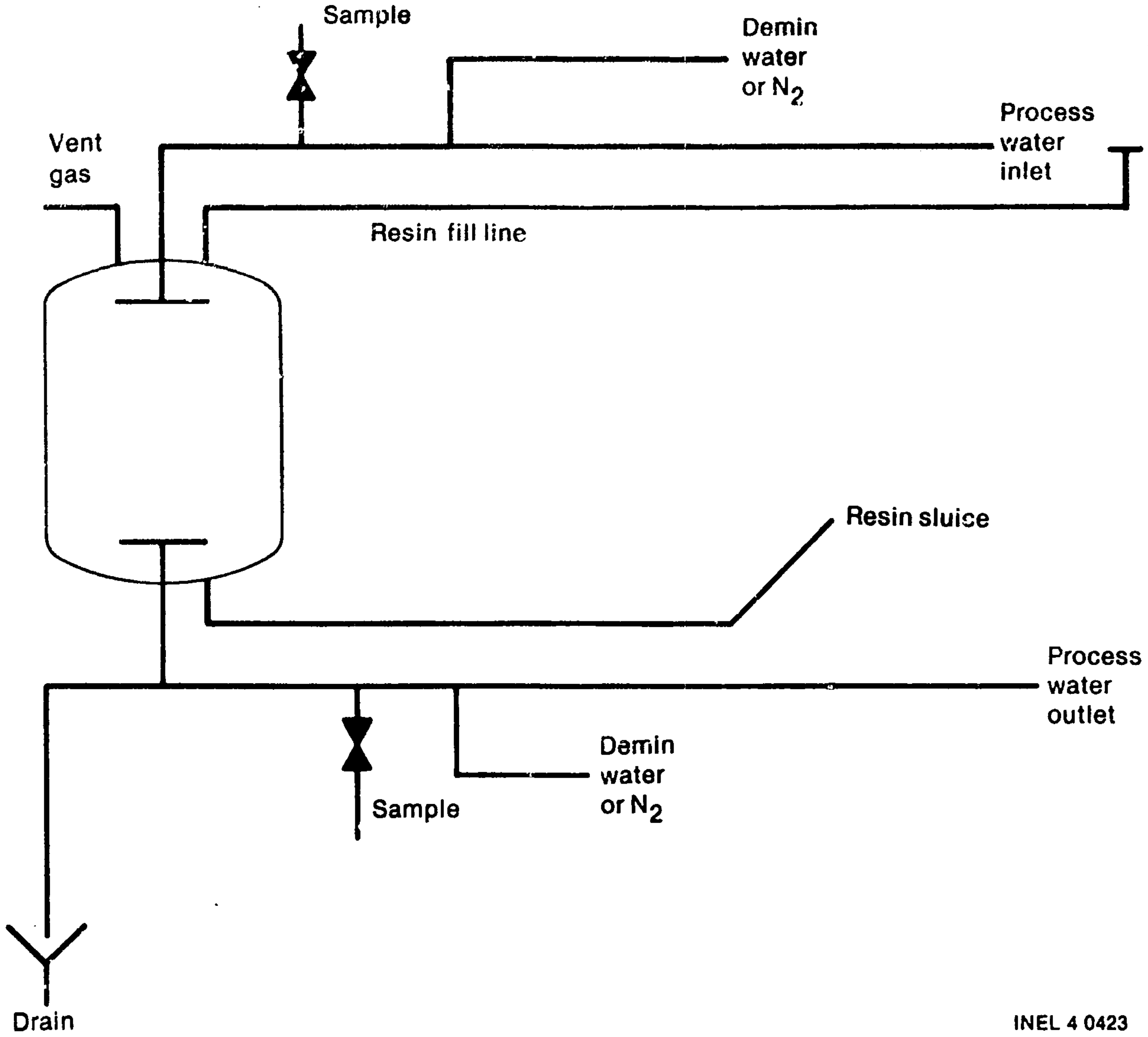

Figure 2. Demineralizer vessel connections.

This report presents a summary of the results of several studies undertaken to plan for removal and subsequent disposal of demineralizer resins from the system. The technical reports documenting these activities are contained in Appendixes A through J of this report. Three separate assessments of the fuel content of the demineralizers were made, the dose rates in the demineralizer cubicles were measured by several methods, and samples of the demineralizer resin and liquid were obtained and analyzed.

Based on the results obtained from sample analyses and cesium elution studies, processing methods and equipment alternatives have been evaluated, and processing equipment choices have been made. A resin radioactivity reduction process and a resin removal method have been selected. Still under evaluation are packaging, disposal, and waste form options for the spent resin and fuel debris. Present plans call for the Department of Energy (DOE) to dispose of the resins in suitable packaging and to be reimbursed for the cost involved.

CUBICLE SURVEYS AND LABORATORY SIMULATION OF RESIN CONDITION

To assess the condition of the demineralizers, a program of remote visual inspection of the cubicles and vessel dose rate monitoring was instituted by GPU Nuclear. Westinghouse Hanford Company (WHC) supplied a small robot equipped with television surveillance cameras and a programmable arm, which was adapted for contamination surveys inside each cubicle. The layout of the cubicles is shown in Figure 3.

The robot entered both cubicles A and B. GPU Nuclear engineers and technicians measured dose rates by attaching a radiation detector probe to the programmable arm of the robot. Measurements in the A cubicle were augmented by radiation detectors and solid state track recorders (SSTRs) lowered into the cubicle from penetration 891. The gamma dose rates obtained are shown in Figures 4 and 5 and are explained in detail in Appendix E. The robot obtained the measurements near the floor.

The radiation detector obtained two vertical radiation dose rate profiles in cubicle A. Locations of the devices were determined with a television camera attached to the robot arm. One dose rate profile was taken approximately 2 ft from the demineralizer. Another dose rate profile was obtained at the surface of the vessel. Figure 6 shows the two dose rate profiles and extrapolated dose rates at different distances from the vessel. Surface contamination readings were taken on the floor, walls, and equipment surfaces. Values were generally low except for the area immediately inside the cubicle doorway, where it appears that settling of airborne activity produced a location of higher smearable activity.

Visual surveillance using the television camera on the robot's arm showed piping and equipment to be unaffected by the accident. White crystals were observed on the floor of cubicle A near a floor drain and the discharge of the pressure relief line of the A demineralizer. Subsequently, the robot obtained samples of these crystals. Radiation measurements of the crystals were made on site by GPU Nuclear, and it was concluded that the deposits were residue from preaccident drain operations.

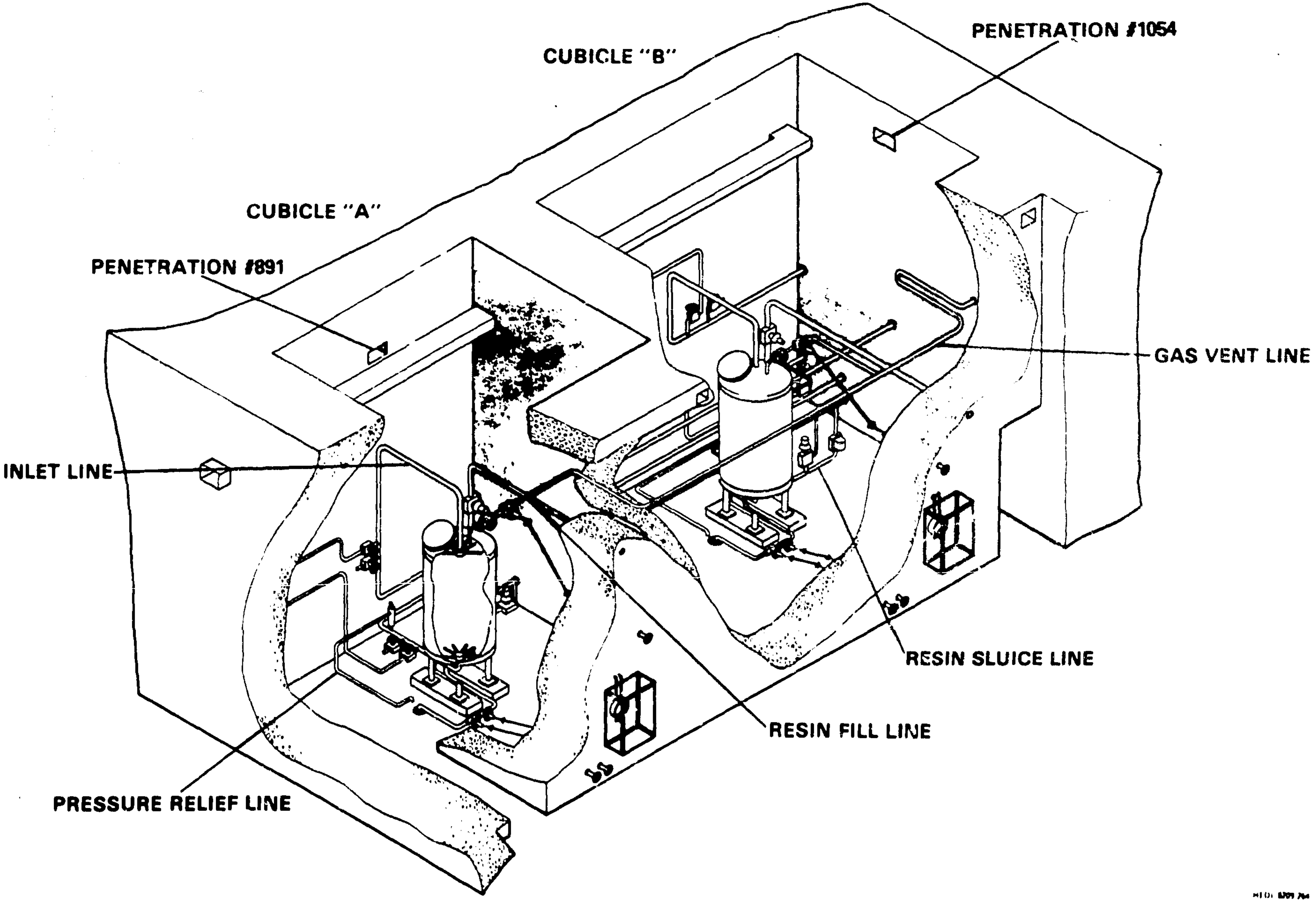

Figure 3. TMI-2 makeup and purification demineralizer cubicles.

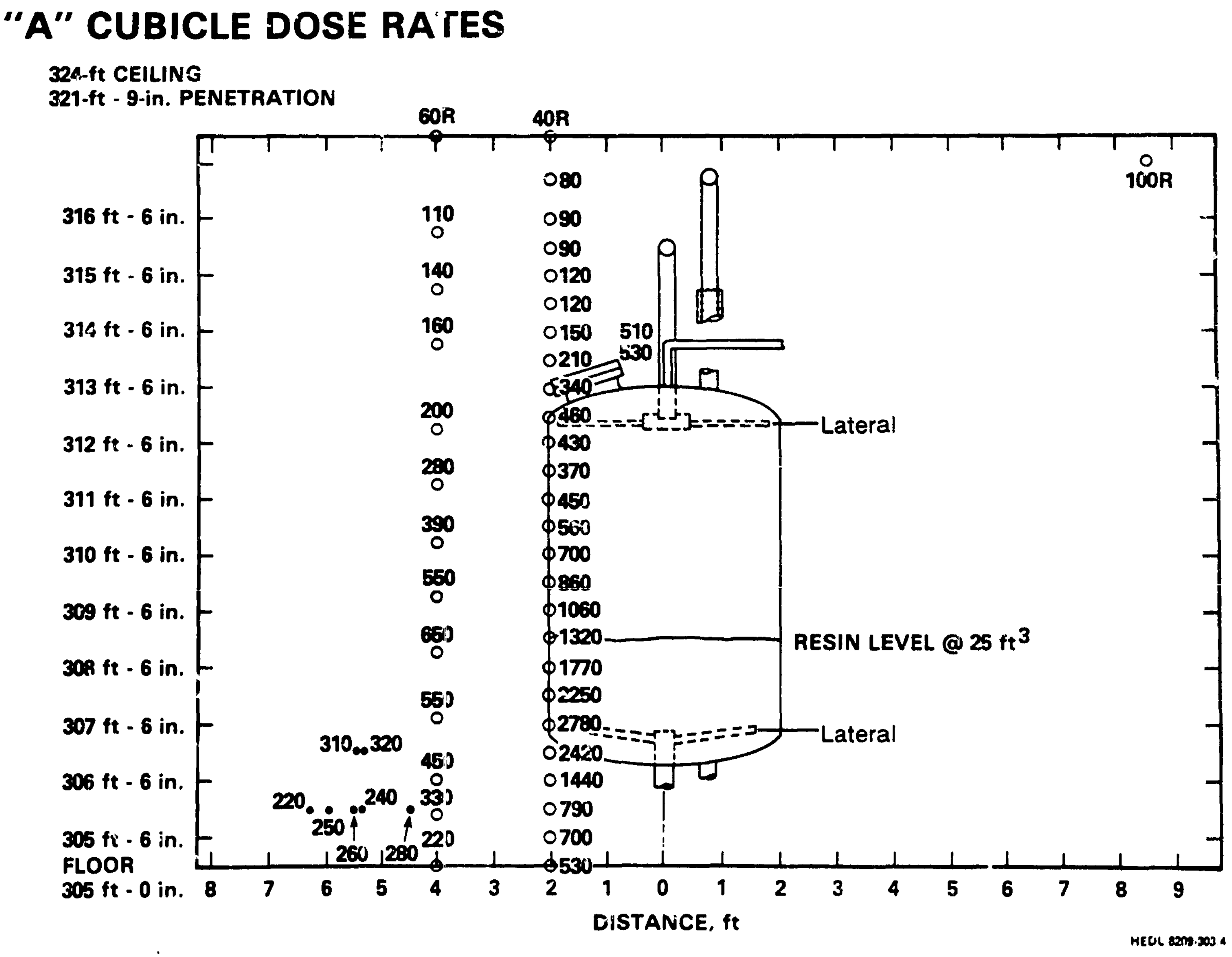

Figure 4. Gamma dose rates in cubicle A.

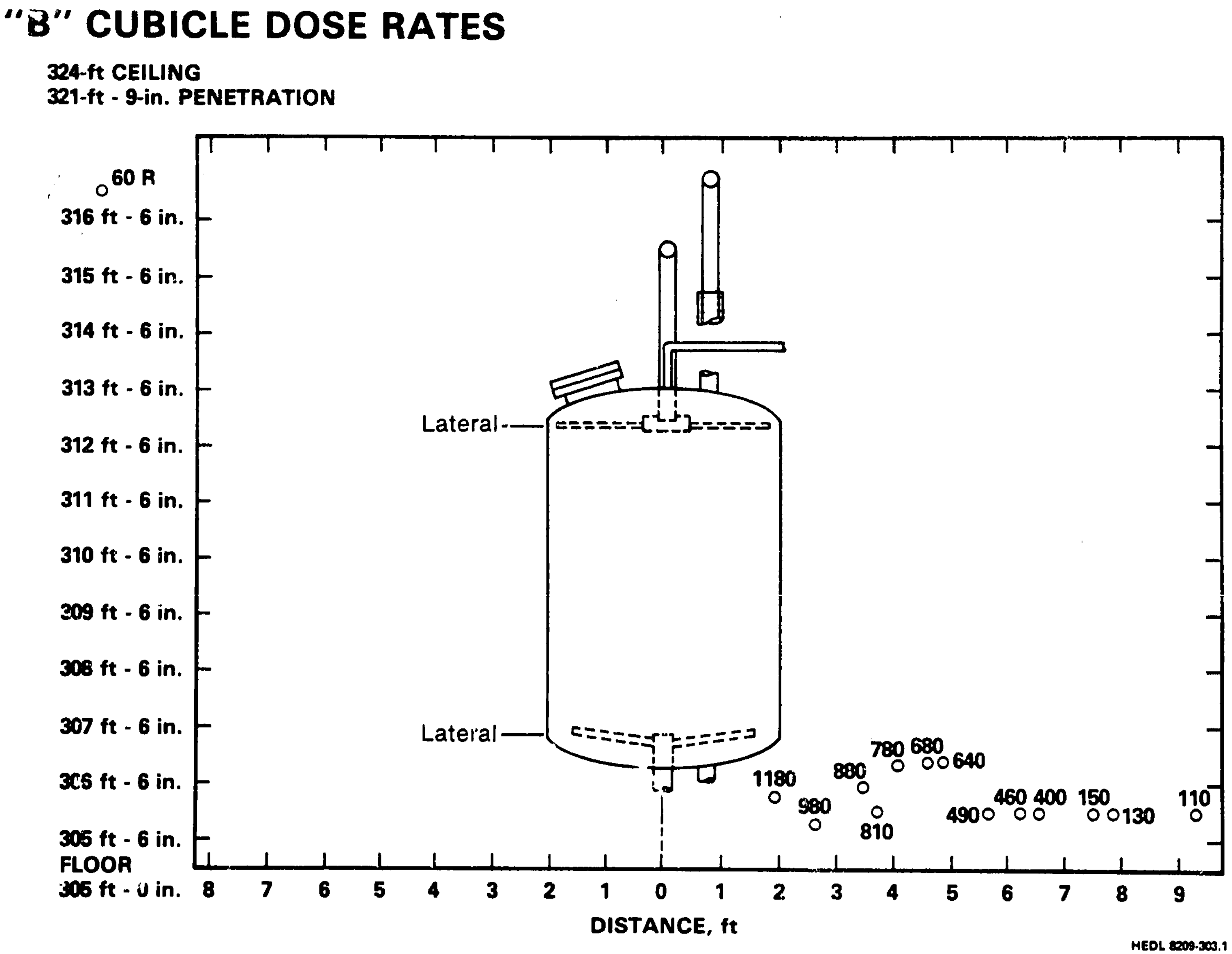

Figure 5. Gamma dose rates in cubicle B.

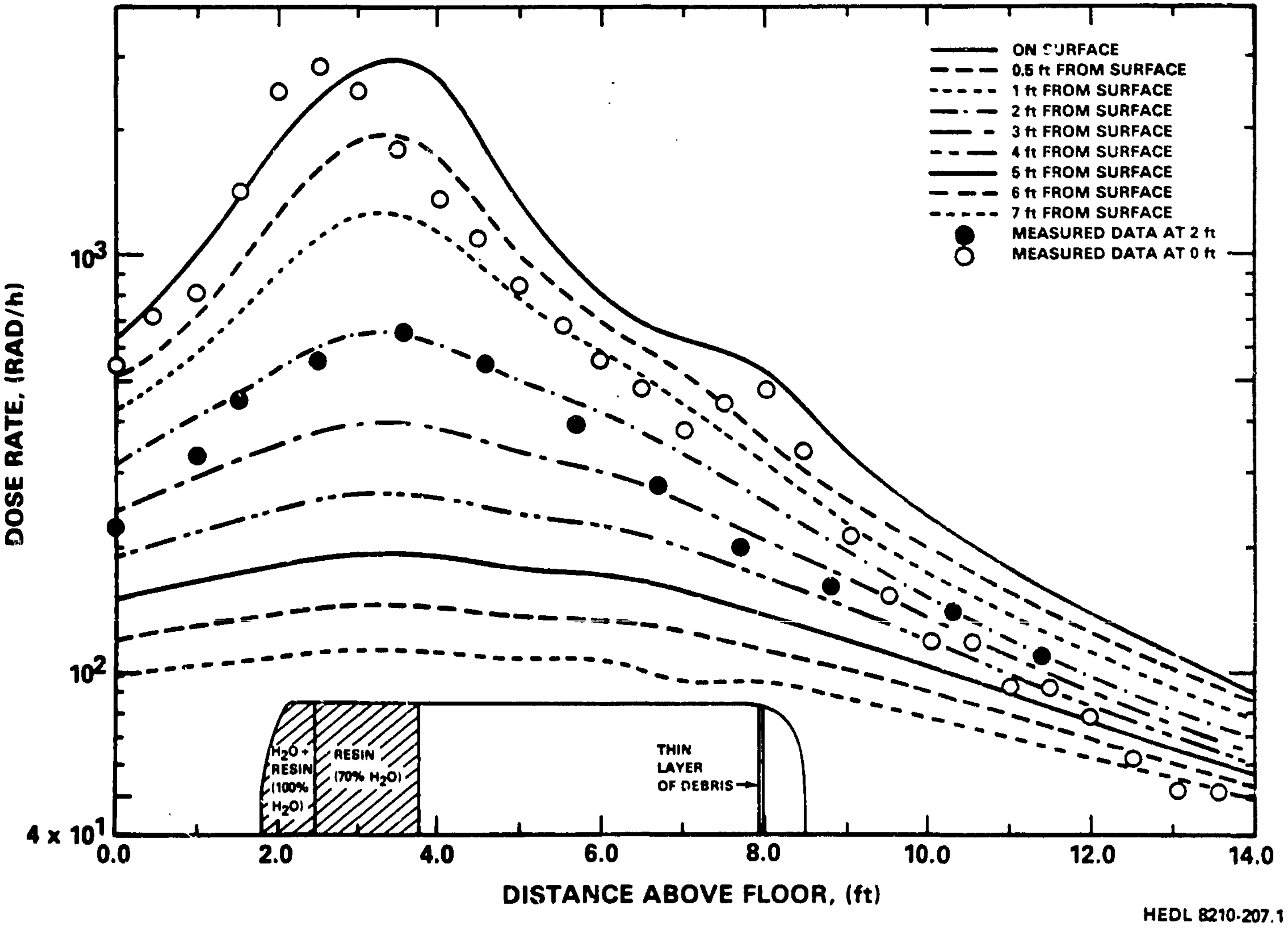

Figure 5. Cubicle A dose rates normalized to maximum measured data.

The radiation dose rate profiles were used to estimate the source distribution in the vessel. Figure 6 shows the best estimate obtained. The resin was assumed to be 2 ft deep in the vessel, and the vessel was assumed to be dry above the resin. A uniformly distributed cylindrical source was assumed.

Similar radiation profiles were not obtained for the B cubicle since penetration 1054 is not accessible because of local contamination outside the cubicle. Therefore, no estimate of source distribution could be made. A comparison of robot data approximately 2 ft off the floor indicated higher gamma activity in the B cubicle. In general, cubicle B dose rates were higher.

Laboratory Simulation of Resin Condition

In order to further assess the condition of the demineralizer resins, technicians at Battelle Pacific Northwest Laboratory performed a laboratory simulation of the thermal and radiation history of ion exchange resin similar to that in the demineralizer system. In these tests, samples of ion exchange resin from the same manufacturer were prepared by the same method used at TMI. They were subjected to 2×10^9 R in both wet and dry conditions and heated to 360, 500, 700, and 1000°F. The results of this testing are summarized below and are found in detail in Appendix E.

- At dose levels of 2×10^9 R, both dry and wet IRN-150 Li-form resins remain in a particulate form.

- Sluicing tests indicate that exposed resins sluice more readily than as-received resin.

- The gas analyses taken during ^{60}Co irradiation show that large amounts of H_2 (20-90 mole%) are formed without an equivalent amount of oxygen. The products of irradiation are probably H_2 and H_2O_2. No oxygen is released in an organic medium probably because the H_2O_2 depletes itself in an oxidative process.

- Resin irradiated to 1.7×10^9 R in water shows a weight and volume loss of about 50%.

- Resin heated to 500°F lost 63 wt% but retained its original structure. At 1000°F in an N_2 atmosphere, the resin structure was completely destroyed, was a solid mass, and was changed into coke.

FUEL QUANTITY ASSESSMENT

During the TMI-2 accident, previously undetermined amounts of fuel material were deposited in the purification demineralizers. If large quantities of fuel were present, extra precautions in cleanup would be necessary to ensure that there would be no inadvertent criticality.

Each demineralizer is located in a separate shielded room as shown in Figure 3. Radiation levels in both rooms precluded direct personnel access; therefore, detailed fuel measurements were performed using remote positioning devices. One device was pushed in the doorway using a long-handled tool. A rigid metal boom carried a second measuring device into cubicle A through penetration 891. The third measuring device was lowered in and left beside the vessels for a month.

Fuel quantities in the A demineralizer were estimated in three ways. One test measured the quantity of ^{144}Ce/Pr present using a beryllium (Be [γ, n]) detector. A second method measured the same ^{144}Ce/Pr quantity using a collimated lithium-drifted silicon (Si[Li]) detector. A third test measured the spontaneous neutrons from the fuel in the demineralizer using solid state fission track recorders. Access for these last two measurements was through penetration 891. Since contamination outside the B cubicle penetration prevented access there, fuel measurement was restricted to use of a remote positioning device on the floor of that cubicle. An approximate fuel inventory was established based on this measurement.

Before either the Be (γ, n) or Si(Li) readings could be used to estimate the fuel quantity present, researchers first had to establish the amount of ^{144}Ce/Pr present in the fuel before the accident. This task was accomplished by using information on the original ^{235}U enrichment of the fuel and the power history of the core as input to computer programs. The ^{144}Ce in the fuel was calculated using both the Origen II and Cinder computer codes. The amount of ^{144}Ce/Pr was assumed to be proportional to the amount of fuel present. That is, the study assumed that the fission product cerium did not migrate out of the uranium fuel.

Beryllium Detector

During October 1982, Los Alamos National Laboratory used a Be (γ, n) detector, sensitive to gamma rays with energies above 1.667 MeV, to estimate the quantity of ^{144}Ce/Pr present in the A and B demineralizers. In the interpretation of data from this measurement, it was necessary to model the source distribution of the cerium in the vessel. Monte Carlo modeling of the source distribution and material density was carried out to make data interpretation possible.

The Be (γ, n) detector collected data indicating the strength of the gamma ray flux above 1.667 MeV. Since ^{144}Ce/Pr, which emits a 2.16 MeV gamma, is the principal fission product emitting gamma rays above this energy level, accurate determination of the fuel was possible by measuring the gamma field in this energy range. Having determined the source strength of gamma rays with energies above 1.667 MeV, the physical geometry of the material in the vessel was modeled. The gross gamma flux was measured and was used to determine the amount of fuel present when various source distributions were assumed to be in the vessel. Using the assumption that the gamma ray source is evenly distributed in the resin, the amount of fuel present for various source distributions was calculated. Finally, the shape of the gamma ray flux for various assumed distributions was calculated to determine what best approximated the flux measurement. A source height of 24 in. provided the most accurate fit with the shape of the observed flux distribution for scans taken adjacent to the vessel and 12 in. from the vessel surface. This source height agrees with the height estimated from other radiation profiles, as discussed earlier in the section Cubicle Surveys.

In interpreting the data from this measurement, a variety of material densities and geometries for the fuel in the lower 24 in. of the vessel were assumed. Using combinations of these assumptions, fuel amounts varying between 1.5 and 14.8 lb were calculated.

By remotely positioning the Be (γ, n) detector through the doorway to the B cubicle, the ^{144}Ce/Pr present in the B demineralizer was measured, and 1.5 lb of fuel was determined to be present in the B vessel. Appendix A of this document presents a detailed discussion of the method used and the technical data obtained in the Be (γ, n) detector work in both cubicles.

Lithium-drifted Silicon Compton Recoil Gamma-ray Spectrometry

During October 1982, engineers from GPU Nuclear and WHC used a collimated Si(Li) Compton recoil gamma-ray spectrometer to measure gamma spectra at various locations in the A demineralizer cubicle. The addition of 77 lb of shielding to the spectrometer permitted operation in gamma fields up to 2000 R/h. The spectral data obtained with this device were used to determine the intensity of the 2.18 MeV gamma ray from the ^{144}Ce/Pr fission product as a function of the position of the detector with respect to the A demineralizer vessel.

Before the results obtained could be meaningfully interpreted, technicians had to determine the source distribution, including the amount of water, resin, and other attenuating media inside the vessel. The calculation of the amount of fuel in the vessel is strongly dependent on the resin level assumed in those calculations. A vessel resin level of approximately 2 ft was established by determining the response of the Si(Li) detector to the cesium 0.662 MeV gamma in a laboratory with a water attenuator. A ^{137}Cs source was used with varying amounts of water attenuator between the source and the detector. The response of the detector showed an increasing continuum below 0.662 MeV due to collisions of the gamma rays within the attenuator. The data generated in the laboratory were within 2% of TMI-2 data when the attenuating media and the resin were assumed to be evenly distributed in the bottom 2 ft of the vessel. This assumption permitted relatively accurate determination of the amount of fuel present. Assuming that the ^{144}Ce/Pr did not migrate out of the fuel, the fuel present was calculated from the ^{144}Pr measured.

This measurement determined that 2.9 ± 1.3 lb of fuel is in the A demineralizer. In addition, spectral data were used to predict the ^{137}Cs content, which was found to be 3400 ± 2500 Ci. A detailed report of this experiment is presented in Appendix B of this document.

Uranium-235 Foil Neutron Dosimeter

In this measurement, WHC determined the amount of fuel in the A demineralizer by using neutron dosimetry. Dosimeters were prepared by placing 93% enriched ^{235}U foil on both sides of an aluminum support plate and placing mica strips over the uranium foil, as shown in Figure 7. This assembly was then sandwiched between two lucite sheets, which provided rigidity to the dosimeter and enhanced fission in the ^{235}U by thermalizing the incoming neutrons. Dosimeters of this type are called solid state track recorders (SSTRs). Neutrons striking the ^{235}U foil cause fission in the dosimeter, and fission fragments cause damage to the mica. This damage is called a fission track. These tracks are chemically developed in the laboratory after exposure, and the number of tracks per unit area in the mica is counted under a microscope. Using appropriate calibration data, the fission tracks can be used to estimate neutron fluence in the SSTRs. Finally, the neutron fluence and duration of exposure of the SSTRs can be used to ascertain the amount of fuel present.

SSTRs were assembled at TMI-2 and placed in the A demineralizer cubicle on September 14, 1982 by GPU Nuclear technicians. Both horizontal and vertical strings of SSTRs were placed in the cubicle, and their position was verified using a robot-transported camera. The dosimeters were left in place for 29 days and removed on October 13, 1982. Figure 8 shows the location of the SSTRs in the cubicle. The background neutron dose rate was determined by preparing identical SSTRs and exposing them in a cubicle where no fuel was present. The measurement determined that 3.75 ± 1.39 lb of fuel is present in the A demineralizer. A detailed technical report of this measurement is contained in Appendix C.

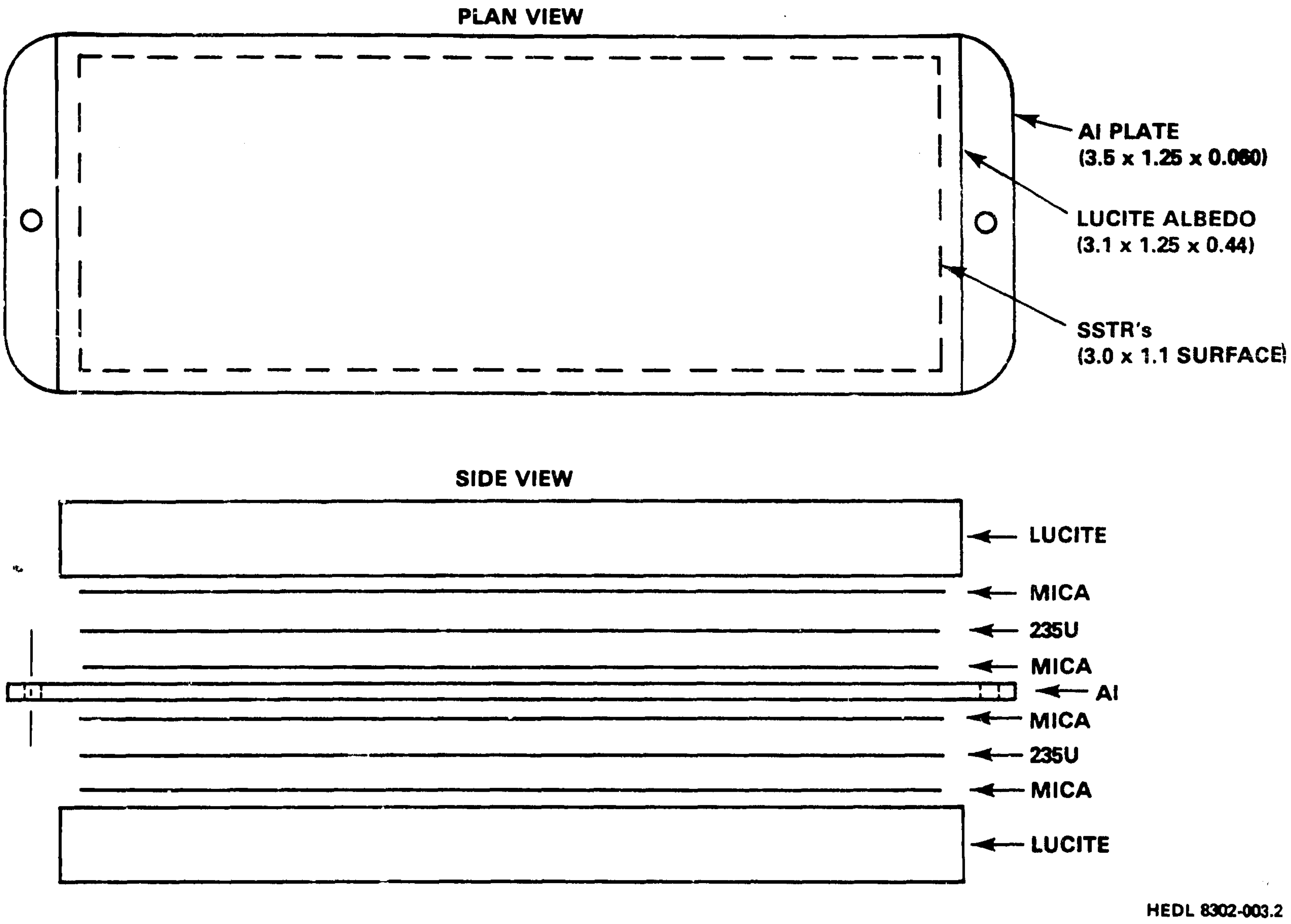

Figure 7. SSTR neutron dosimeter holder for demineralizer A measurements.

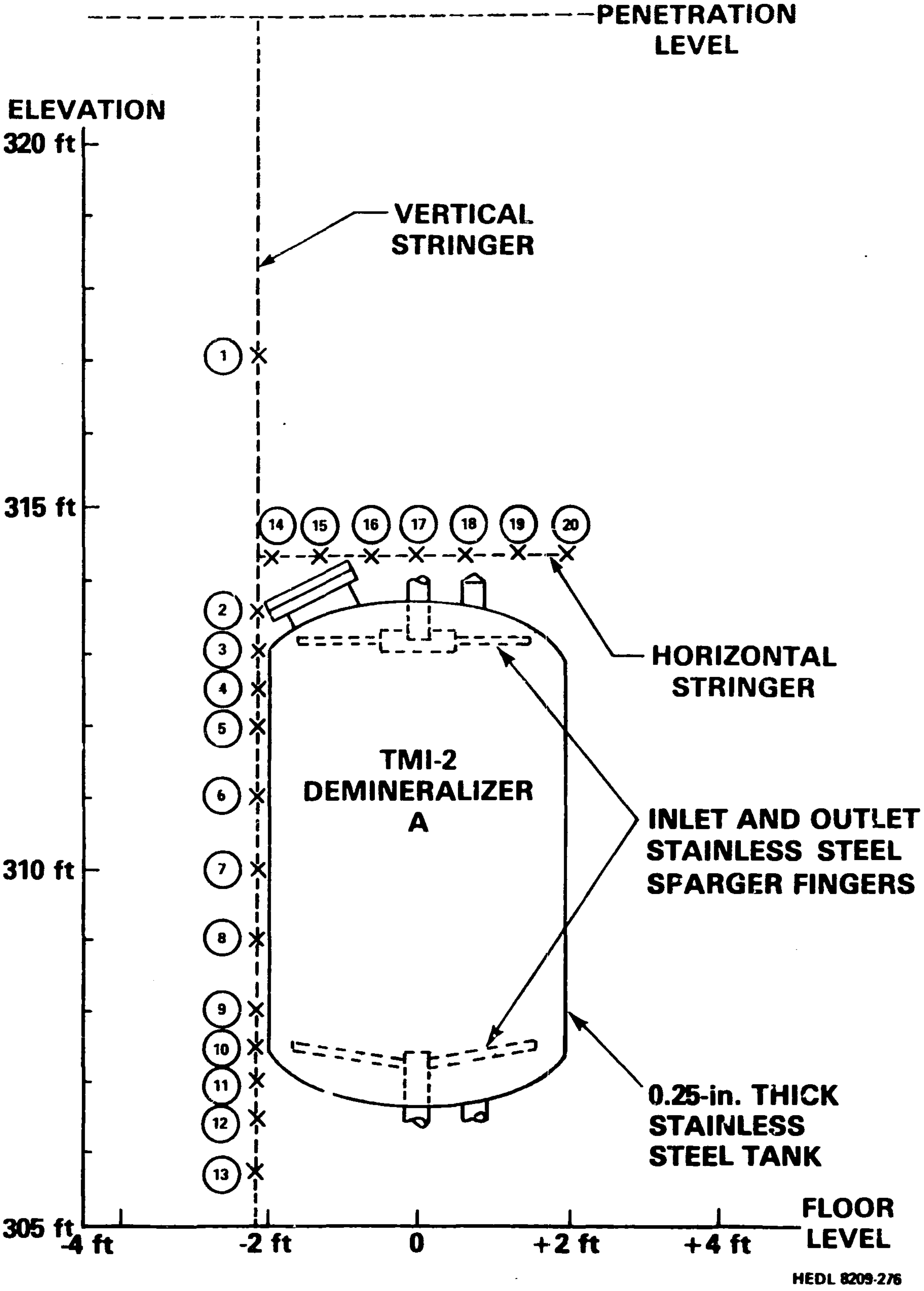

Figure 8. Location of SSTR neutron dosimeters during exposure.

ACQUISITION AND ANALYSIS OF RESIN SAMPLES

The first samples to be obtained from both the A and B vessels were gas samples taken by GPU Nuclear from the void space above the resin beds. The results of the gas sample analyses showed that there were high hydrogen and low oxygen gas concentrations and a substantial quantity of nondiatomic gases. These results had been predicted by resin irradiation experiments performed in laboratory scoping studies in 1982 to determine the effects of temperatures and irradiation on organic resins. These studies are reported in Appendix E. From a comparison of the actual gas samples to the scoping study results, it was concluded that conditions in the demineralizer after the accident were such that the resins in both vessels were wet when irradiated.

After the vessels were gas sampled, they were purged with nitrogen gas to remove hydrogen gas. The next step was to purge the resin fill line with nitrogen gas in preparation for obtaining resin and liquid samples from the vessels. The resin fill lines are 3-in.-diameter pipes through which new resin is sluiced from above into the vessels. GPU Nuclear engineers and technicians cut these fill lines just outside the demineralizer cubicles and placed sampling equipment in the vessel through the fill line and the fill line's diaphragm valve.

First attempts to obtain resin and liquid samples were made with a vacuum sampler. A Teflon tube was used to obtain a 100-mL sample of liquid from the B vessel. A sample could not be obtained from the A vessel since the resin was dry. The difficulty in trying to obtain an A vessel sample led to the use of a radiation tolerant, fiberoptic scope to see what was in the vessel. The scope, inside a polyethylene guide tube, was pushed into the vessel through the resin fill line and passed easily through the resin fill line diaphragm valve. Observations during the fiberscope inspection concluded that the A vessel contained a boron crystal coating on top of the bed of resin. The center of the bed has a large cavity that appears to be above the resin sluicing outlet line. The resin in the bed is agglomerated and amber-colored below the crystalline crust.

Using mechanical probes and the vacuum sampling system, a 10-g solid sample of the A vessel resin was obtained. This sample had radiation readings of 3 rad/h beta and 150 mR/h gamma. The mechanical probe inserted into the B vessel found the resin bed approximately 12 in. below the top of the water and 18 in. thick. Samples from various depths in the B resin bed resulted in a 75-mL slurry with approximately 50 mL of solids. Radiation readings taken without shielding at the top of the B sample shipping container were 40 rad/h beta and 800 mR/h gamma.

The liquid and resin samples obtained from the B vessel in March and April 1983 and the solid sample obtained from the A vessel in April 1983 were analyzed at Oak Ridge National Laboratory (ORNL). Selected preliminary results are listed in Table 1. All samples confirm that the fuel content of the demineralizer resins is very low. But the samples also indicate cesium activity levels that far exceed known values for any other accident-generated waste (other than the fuel itself) in the plant. The ^{137}Cs activity ranged from 220 µCi/g in the A vessel solid sample to 16,900 µCi/g in the B vessel solid sample obtained in April 1983. Appendix D presents the available information from this resin sample analysis.

Physical manipulation of the B resin sample by ORNL technicians has shown that the resin can be sluiced from the demineralizer tank. Chemical testing has shown that 90% of the cesium sorbed on this resin can be removed by elution, and that virtually 100% of the cesium removed by elution can be recaptured by zeolite ion exchange material in the Submerged Demineralizer System.

TABLE 1. SAMPLE ANALYSIS OF RESINS IN THE A AND B DEMINERALIZER VESSELS

	March 1983 Sample		April 1983 Sample		
Element	B Solution (ppm)	B Solid (ppm)	B Solution (ppm)	B Solid (ppm)	A Solid (ppm)
Cs	30	--[a]	30	100	100
Sr	1	--[a]	<1	1	4
U	0.064	1,620	0.109	283	1,250
Pu	0.72 E-3	3.550	0.64 E-3	0.787	3.520
Isotope	(μCi/g)	(μCi/g)	(μCi/g)	(μCi/g)	(μCi/g)
^{134}Cs	181	778	101	1,130	15
^{137}Cs	2,640	11,200	1,430	16,900	220
^{90}Sr	14	490	9,460	880	200

---

[a] No analysis conducted.

Because insufficient data had been obtained in the initial sampling of the A demineralizer, GPU Nuclear engineers developed a plan to resample the A demineralizer in a wet condition. After analyzing components making up the A demineralizer and pressurizing the system to determine leak integrity, 200 gal of water were added to the vessel. This water was allowed to soak and was sparged with nitrogen in an attempt to redissolve the crust which had been observed during previous sample attempts. Additionally, it was thought that the sparging would aid in breaking the bed up to allow a sample to be taken. During February 1984, resampling was attempted using the mechanical sampling tool which had successfully sampled the B demineralizer. The sampling resulted in the acquisition of approximately a 90-mL sample consisting of 40 mL of solids and 50 mL of liquid. This sample was also given to ORNL for analysis.

Although the sample analysis was incomplete at this writing, preliminary results indicate that the A demineralizer resins will also be sluiceable and the resin may be eluted using techniques similar to those planned for the B demineralizer. Microscopic examination of the beads in the ORNL hot cells indicated significantly more charring in the A resins than observed in the B resins. GPU Nuclear designed testing methods to determine filtering characteristics; SDS compatibility tests are also planned. A detailed report on the ORNL analyses, cesium elution studies, and flowsheet proof-of-principle tests will be available at the completion of the ORNL work.

In both the A and B resin studies undertaken at ORNL, the physical size and method of acquisition of the sample material required that caution be used in interpreting the results. In both cases, only a tiny portion of the resin bed could be sampled. Because of the physical difficulty of sampling, no attempt was made to replicate the samples for greater accuracy. Engineering for treatment and handling was based on a smaller-than-ideal sampling program.

PROCESSING PLANS

In normal plant operations, demineralizer resins are removed by sluicing them through installed piping to the spent resin storage tanks. Tests performed on samples of the B demineralizer contents confirm that these resins are sluiceable, and preliminary studies of the A resins suggest they too can be sluiced. However, the high activity in these resins would make normal sluicing a high-radiation exposure task for plant workers. The DOE Waste Immobilization Program participants, EG&G Idaho, Inc., ORNL, and WHC together with GPU Nuclear have developed a three-phase plan to first remove the cesium from the resins and then sluice the resins from the vessels for packaging.

During Phase 1, ^{137}Cs will be removed from the resins and processed through the plant's Submerged Demineralizer water processing system. To remove the cesium from the resins, GPU Nuclear engineers have developed a chemical addition process, which will first add water to the vessels to rinse the contents. The resins will be rinsed with borated water and "fluffed" with nitrogen gas, and then the water will be decanted. This process will dilute the activity contained in the water in the B demineralizer. Essentially the same operation will take place during elution; however, chemicals such as sodium borate will be added to the flush water to remove additional radioactive cesium from the resin. During both the rinse and elution steps, the flow rate of water through the vessels will be restricted to less than 5 gpm, a rate slow enough to ensure that very little solid material will be carried out with the rinse water. To guard against particle carryover to other parts of the plant, a filter may be installed in the effluent flow path.

Current estimates indicate that about 2000 gal of water will have to flow through each demineralizer vessel before the cesium activity is reduced sufficiently to allow sluicing of the solids. The water will be added to the vessels in 200-gal batches. Each vessel will be rinsed several times and then eluted. The number of times rinsing and elution must be repeated to satisfactorily complete each step will be determined by

GPU Nuclear engineers during processing. Because the cesium concentrations are so high, the discharge stream from each vessel will have to be diluted with additional process water immediately after the rinse water leaves the demineralizer cubicle. The entire procedure can be repeated if it appears that still more cesium could be removed from the resins. Cesium removal will reduce the dose rates in the demineralizer cubicles and along the sluice path to the spent resin storage tanks. Removal of the cesium will also minimize the handling problems associated with packaging the sluiced resins for shipment. Once the resins have undergone rinsing and elution, Phase 2 of the removal plan may begin. This phase includes sluicing the resin to the spent resin storage tank. Phase 3 encompasses packaging and disposal of the resin.

A description of the conceptual design of the rinse and elution process is included in Appendix E of this document. Necessary plant modifications to support resin transfer and packaging, and proposed resin transfer and packaging activities are described in Appendix F of this document.

Many alternatives for resin processing have been considered throughout the Purification Demineralizer resin removal project. Before the original sample-taking and analysis, no information was available on the condition of the resins and what would have to be done to remove the resins. The possibility that the resins were agglomerated and fused was considered. Alternatives for processing considered over the course of the demineralizer study are explored in Appendixes E, F, and G.

Many possible choices of equipment, pipe runs, tank usage, and the location of equipment in the plant were also considered during the design stages of the project. Details of these considerations are presented in Appendixes H, I, and J.

APPENDIXES

A. J. R. Phillips, J. K. Halbig, P. M. Rinard, G. E. Bosler, NDA Measurement of the Demineralizers at TMI-2, LA-9795-MS, August 1983.

B. J. P. McNeece, B. J. Kaiser, R. Gold, W. W. Jenkins, Fuel Assessment of the Three Mile Island Unit 2 Makeup Demineralizers by Compton Recoil Continuous Gamma-Ray Spectrometry, HEDL-7285, October 1983.

C. F. H. Ruddy, J. H. Roberts, R. Gold, C. C. Preston, J. A. Ulseth, Solid State Track Recorder Neutron Dosimetry Measurements for Fuel Debris Assessment of TMI-2 Makeup and Purification Demineralizer, HEDL-TC-2492, October 1983.

D. G. J. Quinn ltr to Distribution, "Demineralizer Resin Sample Study Results From Experiments at Oak Ridge National Laboratory," GJQ-46-83, October 6, 1983.

E. M. K. Mahaffey, E. J. Renkey, W. W. Jenkins, L. M. Northey, R. D. Hensyel, Resin and Debris Removal System Conceptual Design, Three Mile Island Nuclear Station Unit 2 Makeup and Purification Demineralizers, HEDL-7335, May 1983.

F. C. A. Negin, C. G. Hitz, Technical Plan Makeup and Purification Demineralizers Resin Removal, TPO/TMI-072, August 1983.

G. E. J. Renkey, W. W. Jenkins, Planning Study Resin and Debris Removal System, Three Mile Island Nuclear Station Unit 2 Makeup and Purification Demineralizers, HEDL-7377, June 1983.

H. W. W. Jenkins, Concepts for Mechanical Removal of Resin and Debris and Loading Shipping Containers, June 1983.

I. W. W. Jenkins, TMI-2 Resin Removal Concepts for Use of Spent Resin Storage Tanks.

J. W. W. Jenkins, TMI-2 Alternate Skid Locations.

LA-9795-MS

Los Alamos National Laboratory is operated by the University of California for the United States Department of Energy under contract W-7405-ENG-36.

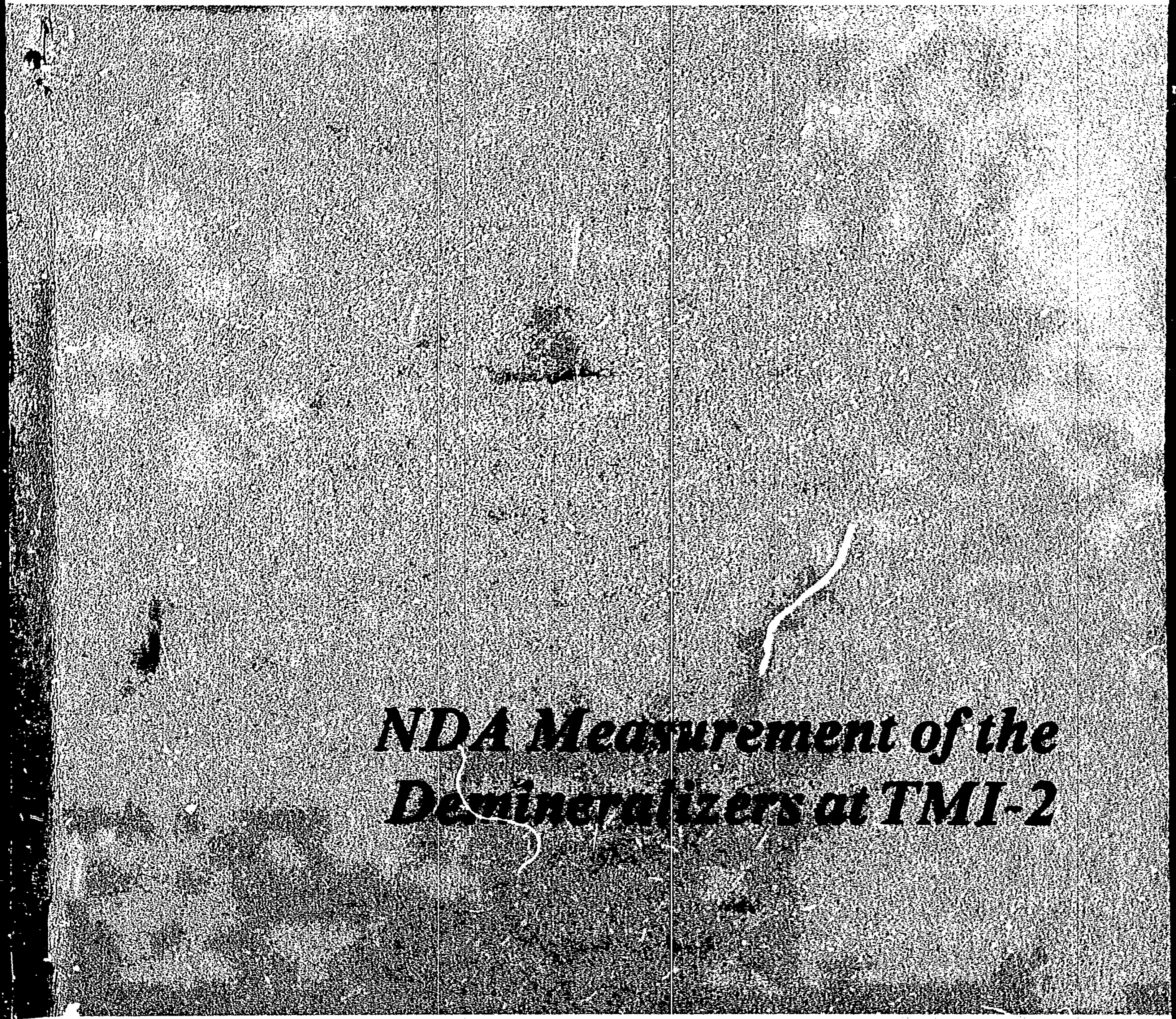

NDA Measurement of the Demineralizers at TMI-2

Los Alamos Los Alamos National Laboratory
Los Alamos, New Mexico 87545

This work was supported by the US Depatment of Energy, TMI-2 Program.

Edited by Serene Rein
Prepared by Edith K. Williams, Group Q-4

LA-9795-MS

UC-15
Issued: August 1983

NDA Measurement of the Demineralizers at TMI-2

J. R. Phillips
J. K. Halbig
P. M. Rinard
G. E. Bosler

Los Alamos
Los Alamos National Laboratory
Los Alamos, New Mexico 87545

EXECUTIVE SUMMARY

During the TMI-2 accident in March 1979 undetermined amounts of fuel material were deposited in the water purification demineralizers. The Los Alamos National Laboratory and the Hanford Engineering and Development Laboratory were asked to assist the facility operator in determining the quantity of material present in each of the two demineralizers. If a large quantity of fuel were present, extra precautions in cleanup would be needed to ensure that there would be no criticality problem.

Each of the demineralizers is located in a separate, shielded room. Radiation levels in both rooms precluded direct personnel access; therefore, all measurements were performed using remote positioning devices. We used a gross gamma-ray measuring device to determine the horizontal and vertical activity distribution of fission products in Demineralizer A. Access to Demineralizer A was obtained through a small (6 by 9 in.) penetration near the top of the room. There was no similar penetration in the room containing Demineralizer B; we were unable therefore to measure its distributions of fission products.

A Be(γ,n) detector was used to measure the quantity of ^{144}Ce - ^{144}Pr present in each of the demineralizers. This detector is only sensitive to gamma rays having energies above 1.667 MeV. The principal gamma ray in a fission product spectrum with an energy above this threshold is the 2.186-MeV gamma ray from ^{144}Ce - ^{144}Pr. We had routinely used this type of detector in the measurements of a variety of spent-fuel material; consequently, a specially designed, high-efficiency detector was fabricated to perform these measurements.

Six source distributions for Demineralizer A and one source distribution for Demineralizer B were modeled using the Los Alamos Monte Carlo transport code to calculate the fraction of gamma rays that would strike the calibrated detector with energies above the 1.667-MeV threshold. The following table summarizes the results of our measurements and calculations.

Demineralizer Tank	Source Distribution	Material Density (g/cm^3)	Estimated Amount of Uranium (kg)
A	Uniform, 61 cm high	2.07	4.6
A	Uniform, 61 cm high	1.00	2.8
A	Crust, 10 cm atop 51-cm attenuating material	2.07	6.7
A	Crust, 10 cm atop 51-cm attenuating material	1.00	3.6
A	Cylindrical ring, 30 cm thick, inside surface of tank	1.00	2.7
A	Point	0.0	2.5
B	Uniform, 160 cm high	1.0	0.7

The estimated amount of uranium metal depends on the assumed source distribution and material density as well as on the specific orientation of the detector. We estimate an upper limit to be in the range of 7 kg and a lower limit to be 2 kg for Demineralizer A. Demineralizer B is estimated to contain approximately 0.7 kg of uranium.

CONTENTS

NDA MEASUREMENT OF THE DEMINERALIZERS AT TMI-2

by

J. R. Phillips, J. K. Halbig, P. M. Rinard,
and G. E. Bosler

ABSTRACT

Nondestructive measurements were performed to estimate the amount of fuel material deposited in the two demineralizers during the accident at TMI-2. Gross gamma-ray measurements were used to characterize the horizontal and vertical activity profiles of gamma-emitting fission products in Demineralizer A. A Be(γ,n) detector, sensitive to gamma rays with energies above 1.667 MeV, was used to estimate the quantity of ^{144}Ce - ^{144}Pr present, which was assumed to be directly proportional to the amount of fuel present. A variety of source distributions was modeled using the Los Alamos Monte Carlo transport code to calculate the fraction of gamma rays that would strike the detector with energies above the 1.667-MeV threshold. The estimated amount of uranium depends on the assumed source distribution and material density as well as on the specific orientation of the detector. We estimate an upper limit to be in the range of 7 kg and a lower limit to be 2 kg for Demineralizer A. Demineralizer B is estimated to contain approximately 0.7 kg of uranium.

I. INTRODUCTION

During the TMI-2 accident in March 1979 undetermined amounts of fuel material were deposited in the water purification demineralizers. The Los Alamos National Laboratory and the Hanford Engineering and Development Laboratory were asked to assist the facility operator (General Public Utilities) in determining the quantity of material present in each of the two purification demineralizers. If a large quantity of fuel were present, extra cleanup precautions would ensure that there would be no possibility of criticality problems.

During the past few years, the Safeguards Groups at Los Alamos have been actively involved in the development and implementation of nondestructive measurement techniques for the assay of spent-fuel materials. Both gamma-ray and neutron measurement techniques have been evaluated. Based on this experience we identified three measurement techniques that would complement the Compton recoil spectrometry and solid-state track recorder (SSTR) techniques previously proposed by the Hanford Engineering and Development Laboratory (HEDL):

(1) high-resolution gamma spectrometry,
(2) Be(γ,n) detector for ^{144}Ce-^{144}Pr, and
(3) gross gamma-ray and neutron detectors.

Each of these techniques can provide specific information about the transuranic or fission-product inventory and distribution in the demineralizer tanks.

Each of the demineralizers is located in a separate shielded room. Radiation levels in both rooms precluded direct personnel access, therefore all measurements used remote positioning devices. The high-resolution gamma spectrometry (HRGS) system would have required a large amount of shielding, approximately 800 pounds of lead, to reduce the background radiation to a level in which the germanium detector could operate. Because of this requirement, as well as other considerations, we were advised to concentrate on the latter two techniques.

Access to Demineralizer A was possible through a small (6 x 9 in.) penetration near the top of one of the walls and through the personnel entry doorway. Demineralizer B was accessible only through the personnel entry doorway. We used a gross gamma-ray measuring device to determine the horizontal and vertical activity distributions of fission products in Demineralizer A by passing the detectors through the penetration using a positioning apparatus provided by HEDL.

A Be(γ,n) detector was used to measure the quantity of ^{144}Ce - ^{144}Pr present in each of the demineralizers. This detector is only sensitive to gamma rays having energies above 1.667 MeV. The principal gamma ray in a fission product spectrum with an energy above this threshold is the 2.186-MeV gamma ray from ^{144}Ce - ^{144}Pr. We have routinely used this type of detector in the measurements of a variety of spent-fuel material. A specially designed, high-efficiency detector was fabricated to perform these measurements.

We assembled the Be(γ,n) and gross gamma-ray detectors and electronics unit (ION-1) and performed the measurements from October 25 to 28, 1982. Prior to the measurements at TMI-2, we calibrated the ion chambers used in the gamma-ray measurements. Following the measurement we calibrated the Be(γ,n) detector and calculationally simulated various source geometries using Monte Carlo gamma-ray transport techniques[1] to obtain our estimated values of 6.7 to 2.7 kg of fuel in Demineralizer A and about 0.7 kg of fuel in Demineralizer B. These values are sensitive to the source distributions and densities that we assume exist in the tanks but which are not well known at the present time.

This report includes six sections: Introduction; Instrumentation; Calibration; Data Collection, Analysis, and Results; Conclusions; and Appendices. We have attempted to include all the pertinent information to allow an independent evaluation of the data by the reader.

II. INSTRUMENTATION

A. Be(γ,n) Detector

The Be(γ,n) detector was developed to measure the high-energy gamma rays emitted from irradiated fuel material. The detector is based on the threshold photoneutron reaction in beryllium that produces a neutron for incident gamma rays with energies above 1.667 MeV (or 1667 keV). The neutron is thermalized in polyethylene and then detected using a thermal neutron detector (^{235}U fission chamber). In irradiated fuel materials the principal source of gamma rays with energies above this threshold is ^{144}Pr, which has a 17.3-min half-life and is in secular equilibrium with its parent ^{144}Ce ($t_{1/2}$ = 284.5 days). Figure 1 shows a typical spectrum of spent-fuel material with the

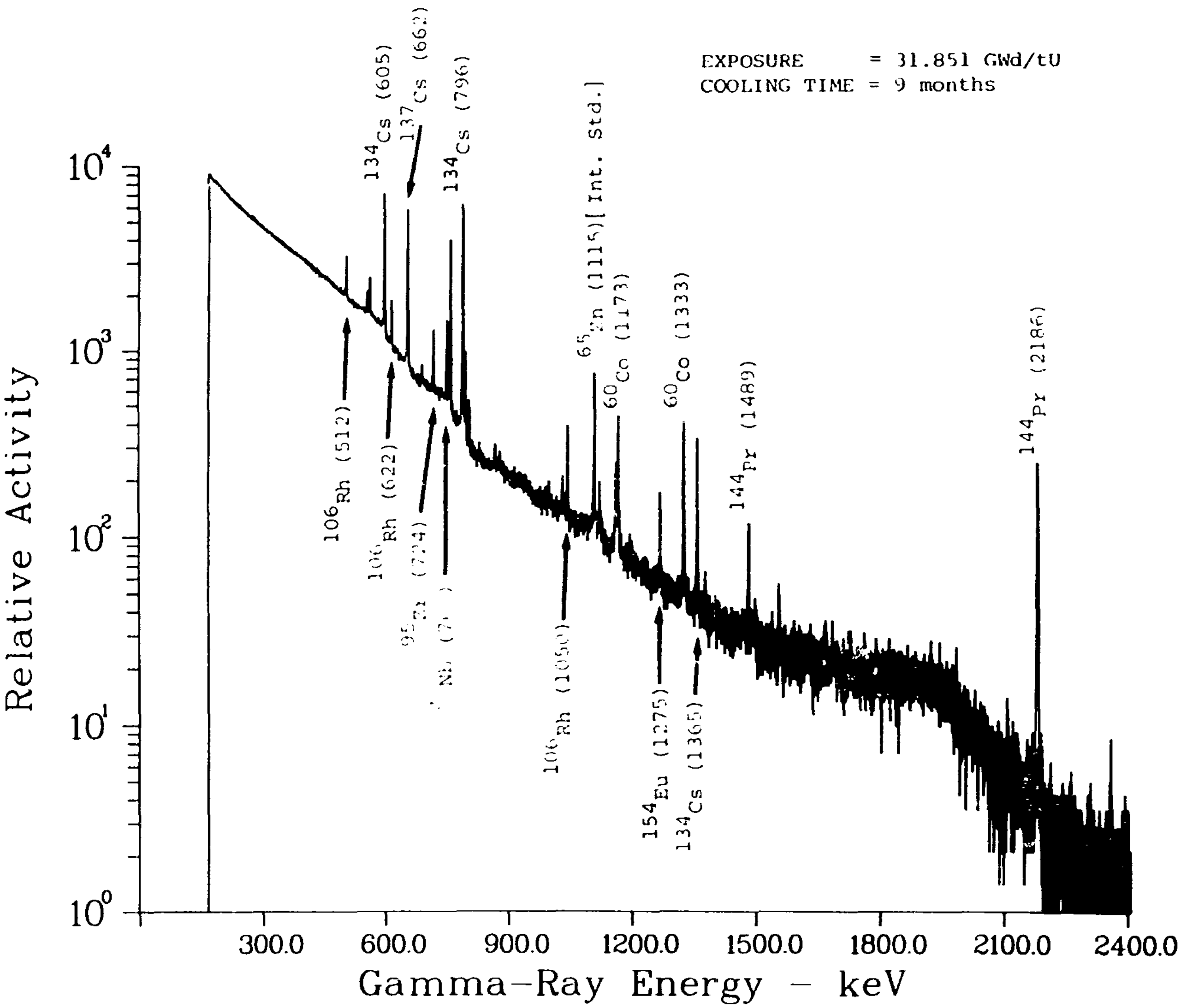

Fig. 1. Gamma-ray spectra of a PWR fuel assembly with the dominant 2186-keV peak of ^{144}Ce-^{144}Pr above the Be(γ,n) threshold of 1667 keV.

more prominent lines identified. Above the 1667-keV threshold of the beryllium gamma-n reaction, the prominent peak is the 2186-keV peak from the ^{144}Ce-^{144}Pr decay. The chemistry of the ^{144}Ce would be expected to be similar to that of the uranium and plutonium under these conditions, therefore, a measurement of the amount of cerium should be directly proportional to the amount of fuel material present.

There is the possibility of ^{106}Ru-^{106}Rh interfering with these measurements because of the relatively low-intensity gamma rays with energies above the 1667-keV threshold of beryllium. The individual gamma rays from ^{106}Rh have such a low intensity that they are not distinguishable from the continuum under the 2186-keV peak of ^{144}Ce-^{144}Pr. If we assume that the ^{106}Ru-^{106}Rh concentration were the $3.76 \bullet 10^6$ nCi/g listed in Table I, the isotope could contribute approximately 5 to 8% to the ^{144}Ce-^{144}Pr signal.

TABLE I

MEASURABLE FISSION AND ACTIVATION PRODUCTS

Isotope	Half-Life (yr)	Gamma-Ray Energy (keV)	Activity[a] (nCi/g)
^{134}Cs	2.062	604.6, 795.8, 1167.9, 1365.1	$5.73 \bullet 10^5$
^{137}Cs	30.17	661.6	$9.58 \bullet 10^6$
^{106}Ru-^{106}Rh	1.011	622.2, 1050.5, 1562.2[b]	$3.76 \bullet 10^6$
^{144}Ce-^{144}Pr	0.78	1489, 2186	$1.48 \bullet 10^7$
^{125}Sb	2.73	427, 601, 636	$2.80 \bullet 10^5$

---

[a] Based on entire core inventory for fission and activation products present on July 28, 1982, using the EPRI-CINDER code.[2,3]

[b] Rhodium-106 has approximately 30 very low-intensity gamma rays with energies above 1667 keV.

Because of its high volatility, bp ~100°C, ruthenium may have escaped from the fuel material as the tetroxide during the accident. If it had concentrated in the tank (which is unlikely because the resin probably would not have trapped the ruthenium) it may have escaped because of the heat generated by the decaying fission products. For all of our measurements we have assumed that the source was entirely ^{144}Ce-^{144}Pr, therefore we slightly overestimated the amount of fuel present (equivalent to the contribution from the ^{106}Ru-^{106}Rh present).

Figure 2 shows a schematic of the Be(γ,n) detector used in these measurements. A photograph of the detector is shown in Fig. 3. The detector was mounted on four wheels and was positioned in the demineralizer rooms using a push rod that could be assembled in 6-ft sections to a maximum length of 24 ft. We designed the detector to maximize the counting efficiency.

B. Gamma-Ray and Neutron Detector

A detector probe (Figs. 4 and 5) containing an ion chamber and a neutron detector was fabricated to measure horizontal and vertical gamma and neutron activity profiles for Demineralizer A. A variety of neutron detectors could be used in the detector probe depending upon the intensity of the gamma-ray field: ^{235}U fission chambers, ^{10}B-lined detectors, and ^{3}He neutron detectors.

The number of neutrons being emitted by spent fuel with a burnup of only 3.3 GWd/tU is expected to be very low. Based on calculated actinide inventories on July 28, 1982, we estimated the neutron-source strength for the principal neutron-producing isotopes, and the results are presented in Table II. For these neutron-source strength estimates, actinide inventories were obtained from Ref. 2 and the neutron-yield data were obtained from Ref. 4. The results are normalized assuming an initial total uranium mass of 82 tonnes.

For a 10-kg mass of uranium, ~2200 n/s would be emitted. If this source were concentrated in the middle of a spherical, 4-ft-diam tank, the flux on the surface of the sphere, not considering multiplication or absorption effects, would be ~0.05 n/s-cm^2. Even if the actual flux on the surface were an order of magnitude higher than this, the flux would still be very low and thereby difficult to measure.

The detector probe was designed to be compatible with the positioning boom installed by HEDL for its Compton recoil-spectrometer measurements.

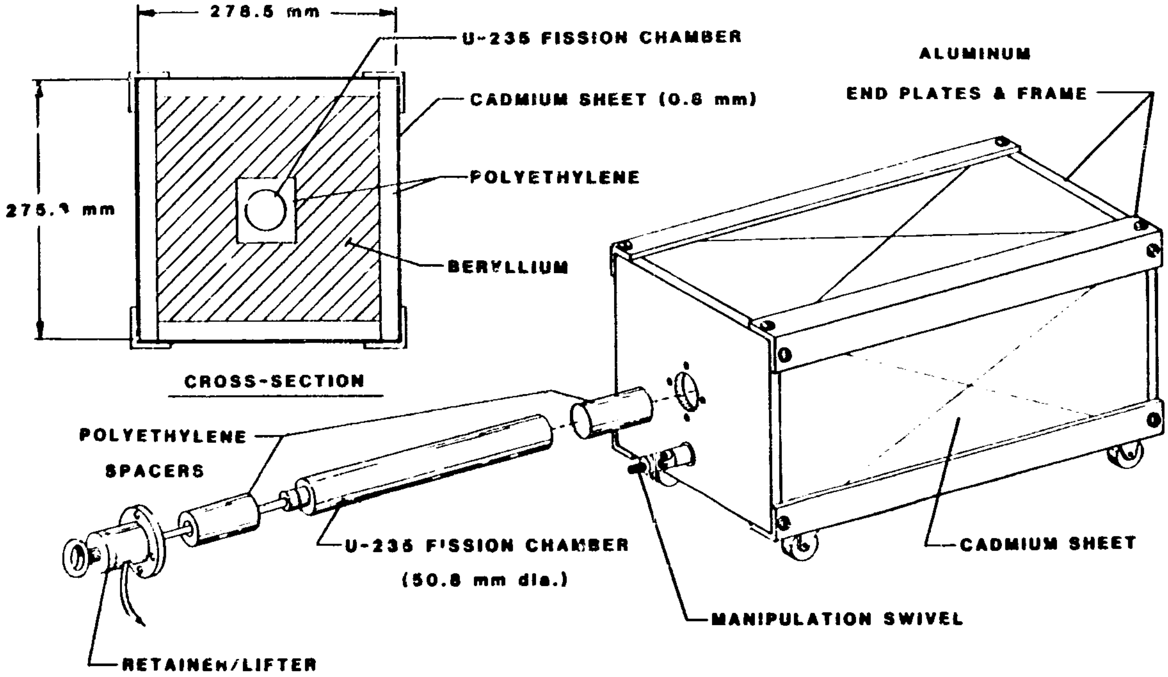

Fig. 2. Beryllium gamma-n detector used for the measurement of demineralizers.

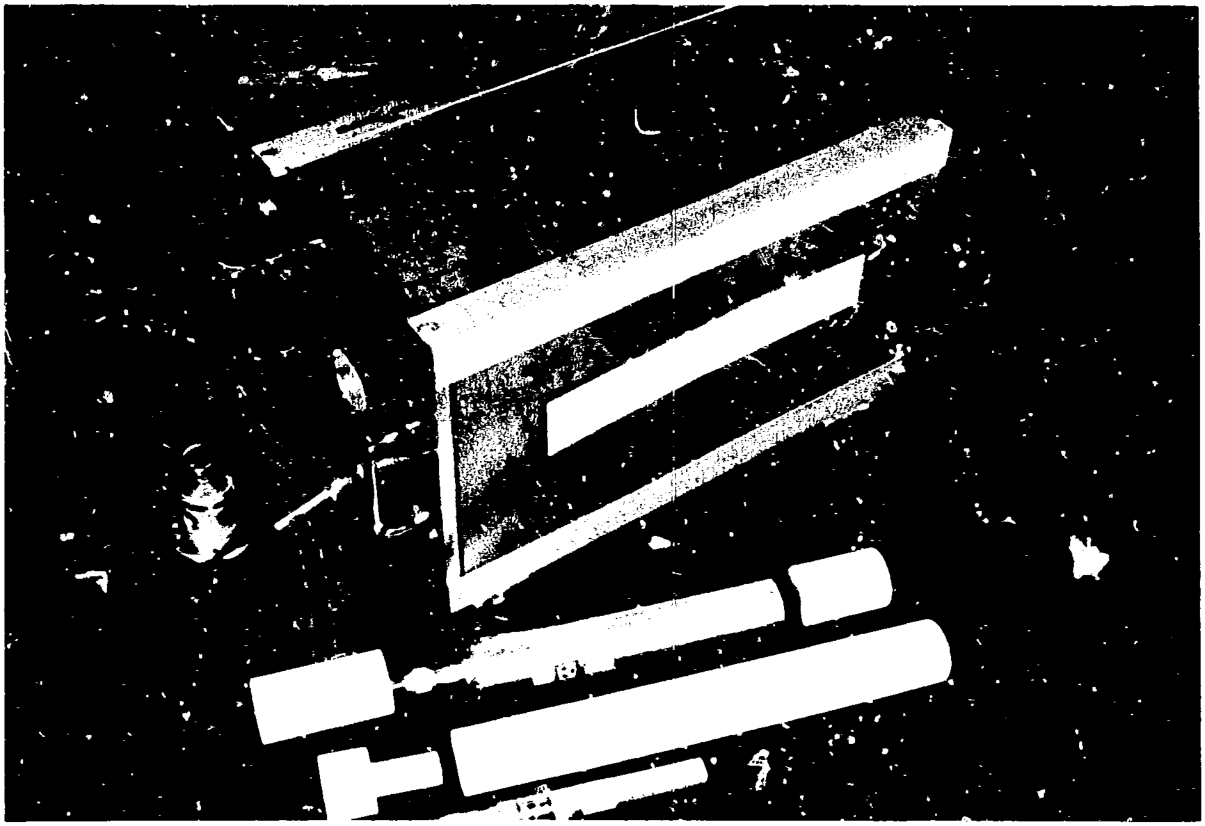

Fig. 3. The assembled Be(γ,n) detector.

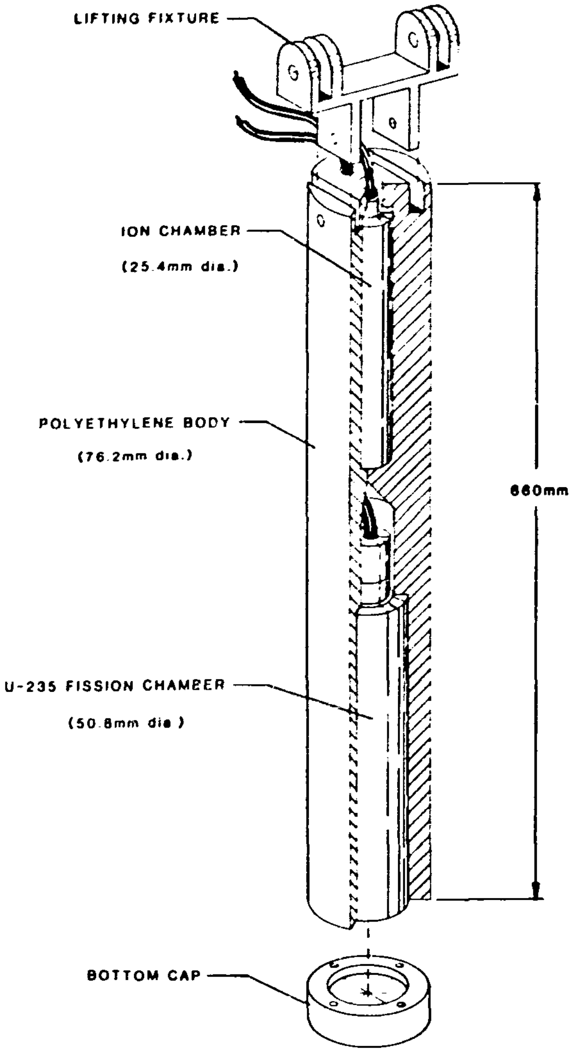

Fig. 4. Gross gamma-ray and neutron measurement probe showing relative position of the detectors.

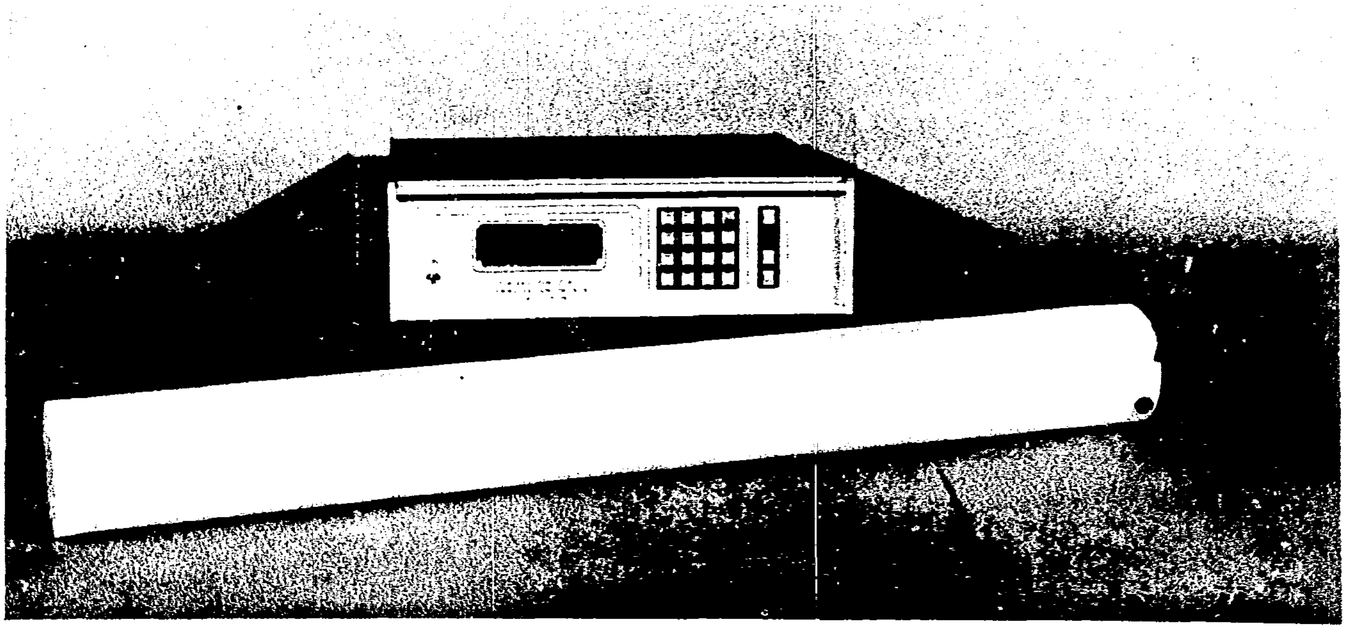

Fig. 5. Detector probe used to map the horizontal and vertical gross gamma-ray fields around Demineralizer A.

TABLE II

NEUTRON SOURCES IN LOW-EXPOSURE(3.36 GWd/tU) FUEL MATERIAL

Isotope	Half-Life (yr)	Total Mass in Core (kg)	Neutron Production[a] (n/g/s)	Production per Unit UO_2 mass[b] ($n/gUO_2/s$)
^{235}U	$7.04 \bullet 10^{8}$	1806.1	$1.01 \bullet 10^{-3}$	$1.96 \bullet 10^{-5}$
^{238}U	$4.47 \bullet 10^{9}$	78877.0	$1.37 \bullet 10^{-2}$	$1.16 \bullet 10^{-2}$
^{238}Pu	$8.78 \bullet 10^{1}$	0.0457	$1.60 \bullet 10^{4}$	$7.87 \bullet 10^{-3}$
^{239}Pu	$2.41 \bullet 10^{4}$	132.9	$3.82 \bullet 10^{1}$	$5.45 \bullet 10^{-2}$
^{240}Pu	$6.55 \bullet 10^{3}$	9.885	$1.05 \bullet 10^{3}$	$1.11 \bullet 10^{-1}$
^{241}Pu	$1.47 \bullet 10^{1}$	1.403	$1.27 \bullet 10^{1}$	$1.91 \bullet 10^{-4}$
^{242}Pu	$3.76 \bullet 10^{5}$	0.0542	$1.71 \bullet 10^{3}$	$9.95 \bullet 10^{-4}$
^{241}Am	$4.32 \bullet 10^{2}$	0.2422	$2.69 \bullet 10^{3}$	$7.00 \bullet 10^{-3}$
^{242}Cm	$4.46 \bullet 10^{-1}$	$1.664 \bullet 10^{-6}$	$2.48 \bullet 10^{7}$	$4.43 \bullet 10^{-4}$
^{244}Cm	$1.81 \bullet 10^{1}$	$1.482 \bullet 10^{-5}$	$1.09 \bullet 10^{7}$	$1.73 \bullet 10^{-4}$
		Total for 10 kg UO_2		$1.95 \bullet 10^{-1}$
		Total for 10 kg U		$2.2 \bullet 10^{-1}$

---

[a] Grams are of isotopic mass.
[b] Multiply the UO_2 mass by 0.88 to obtain the uranium mass.

C. Electronics Unit (ION-1)

Both the probe and Be(γ,n) detectors used the same electronics unit to collect data and provide the necessary power to the detectors. The ION-1 shown in Fig. 5 is an intelligent, portable spent-fuel gamma-ray and neutron detector. This electronics package provides digital readout of the current-mode response produced by gamma rays in an ion chamber and provides amplification and scaling of pulses received from a neutron detector. This instrument[5] was developed for use by the International Atomic Energy Agency (IAEA) inspectors, and therefore was designed to assist the user by:

- prompting the user through programmed operating and experimental procedures,
- prompting for external information required,

- calculating and providing results and error estimates, and
- performing internal diagnostics.

These features allow the user to concentrate on performing the measurement correctly without being adversely distracted by operations in the plant. Because the measurements can be fully automated, there is excellent control of the measurement procedure.

III. CALIBRATION

A. Be(γ,n) Detector

A small sample of irradiated fuel material was dissolved by the Analytical Chemistry Group at Los Alamos to obtain a 30-mℓ solution containing 8.38 Ci of ^{144}Ce and 1.83 Ci of ^{106}Ru. Although the fraction of curies from ^{106}Ru is nearly 18%, most of the ^{106}Ru gamma rays lie below the 1667-keV threshold of the Be(γ,n) reaction. Approximately 5 to 8% of the ^{106}Ru gamma rays lie above this threshold. Therefore, this standard is similar in composition to the fuel material measured in the demineralizers. The assay procedure and calculation are presented in Appendix A. The response of the detector to this point source was measured at various distances and elevations of the source relative to the detector. Table III lists the measured efficiencies obtained in these calibrations with the source placed on the center line of the detector's square front.

The counting efficiency of the Be(γ,n) detector was calculated by determining the solid angle subtended by the detector for a source located 64 in. from the detector's face and 24 in. above the floor using the following equation.

$$\text{Efficiency} = \frac{\text{Measured counts per second}}{\text{Number of gamma rays striking the surface/s}} \quad . \tag{1}$$

This equation becomes

$$= \frac{\text{Measured counts per second}}{\begin{array}{l}\text{Curies in source} \bullet \text{disintegration per second} \\ \text{per curie} \bullet \text{number of gammas per disintegration} \\ \bullet \text{ fraction of sphere subtended by the detector}\end{array}} \tag{2}$$

$$= \frac{1.02 \pm 0.04}{8.38\ \text{Ci} \bullet 3.70 \bullet 10^{10}\text{dps/Ci} \bullet 0.007\ \text{gammas/dis} \bullet 1.8417 \bullet 10^{-3}} \tag{3}$$

$$= 2.55 \pm 0.10 \bullet 10^{-7}\ \text{counts/gamma.}$$

TABLE III

ABSOLUTE COUNTING EFFICIENCY OF THE Be(γ,n) DETECTOR

Horizontal Distance from Front Surface (in.)	Vertical Distance above the Floor (in.)	Absolute Efficiency[a] (counts/s
36	0	0.163 ± 0.003[b]
64	24	1.02 ± 0.04
88	24	0.60 ± 0.01

---

[a] Assuming only ^{144}Ce contributes to the counting rate.
[b] When the source was placed facing the long side of the detector, we obtained 0.234 ± 0.004.

B. Gamma-Ray and Neutron Detector

The ion chambers were calibrated at the Radiation Instrument Calibration Facility.[6] Field strengths of up to 836 R/h were used. The gamma field was produced by three ^{60}Co sources. We used these data (Fig. 6) to obtain the calibration for dose rate in roentgen per hour (Table IV).

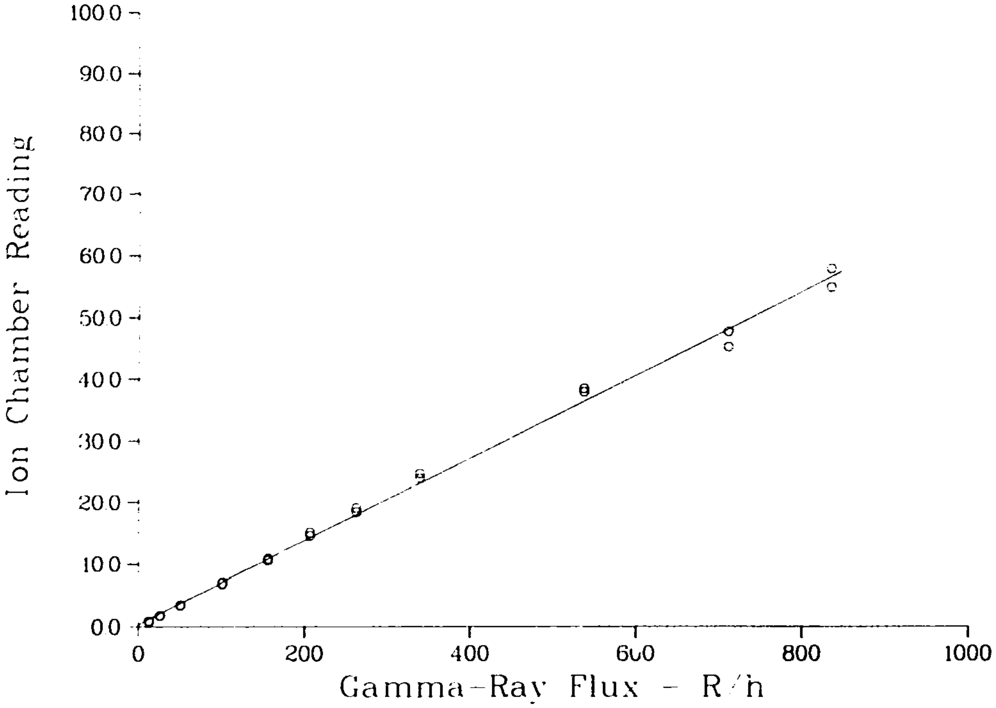

Fig. 6. Calibration curve for the ion chamber used at TMI-2.

Three types of neutron detectors were tested in various gamma radiation fields: ^{235}U fission chamber, ^{10}B-lined detector, and ^{3}He detector. We have operated ^{235}U fission chambers in gamma fields up to 50 000 R/h. The ^{10}B-lined detector (1-in. diam with 1-cm lead shielding) appeared to operate well in fields up to ~1000 R/h. The ^{3}He detector (1-in. diam with 1-cm lead shielding) operated in fields below 100 R/h.

IV. DATA COLLECTION, ANALYSIS, AND RESULTS

A. Gross Gamma-Ray and Neutron Measurements

Using the probe of Fig. 4 with detectors for gross gamma rays and neutrons and the positioning boom designed by HEDL, horizontal and vertical scans were made of tank A. With these uncollimated detectors, it was not possible to obtain the same spatial resolution that the HEDL personnel could obtain using their collimated detector, but with the probe very close to the tank an accurate profile of the activity from the tank could be measured (this is especially true for the vertical profile).

TABLE IV

GAMMA-RAY CALIBRATION DATA

Declared Dose Rate[a] (R/h)	Measured Ion-Chamber Calibration Values[b]			
	Run 1	Run 2	Run 3	Run 4
12.8	0.86	0.84		
25.8	1.74	1.71		
50.6	3.47	3.37		
101.0	7.01	6.88	6.911	
156.0	10.84	10.52	10.52	
207.0	15.02	14.50	14.46	
263	19.05	18.41	18.37	
340	24.72	23.93	23.81	23.85
538	38.44	37.89	37.89	37.73
712	47.63	45.16	45.32	45.16
836	57.61	54.68	54.68	54.68
15.1	1.02			
31.8	2.16			
63.8	4.54			
235	16.1			
347	22.98			
478	30.31			
591	40.94			

---

[a] Dose Rate = $\frac{\text{Ion chamber} - 0.3490}{0.06697}$

[b] Ion-Chamber Value = a + b • dose rate

$a = 0.3490$

$b = 0.06697$

$R^2 = 0.9964$

The gross neutron count rates were not significantly greater than the background rates. As was discussed in the instrumentation section, the neutron yields were expected to be low. Without greatly extended counting times, it was not possible to obtain any useful gross neutron data with this probe.

The gross gamma-ray measurements from the ionization chamber provide important information for interpreting the data from the Be(γ,n) detector. The ionization-chamber results indicate the distribution of the gross gamma-ray source in the tank. The ionization chamber responds to gamma rays of all energies. For these measurements we assumed that the ionization chamber results represent the distribution of the cerium isotope in the tank. With this distribution, Monte Carlo models can estimate the fraction of gamma rays that reach the Be(γ,n) detector. This fraction is a component of the total detection efficiency during the measurements on the demineralizer tanks.

The results of a horizontal scan over the top of tank A, shown in Fig. 7 and Table V, suggest that the material's distribution is nearly uniform in the radial direction, with variations of ~5%. It was assumed in most of the calculations that the density of the cerium was the same at all points in a horizontal section of the tank. A recent physical inspection of the interior revealed a hollow core in the contents of tank A. This may account for the slight dip in the curve in Fig. 7.

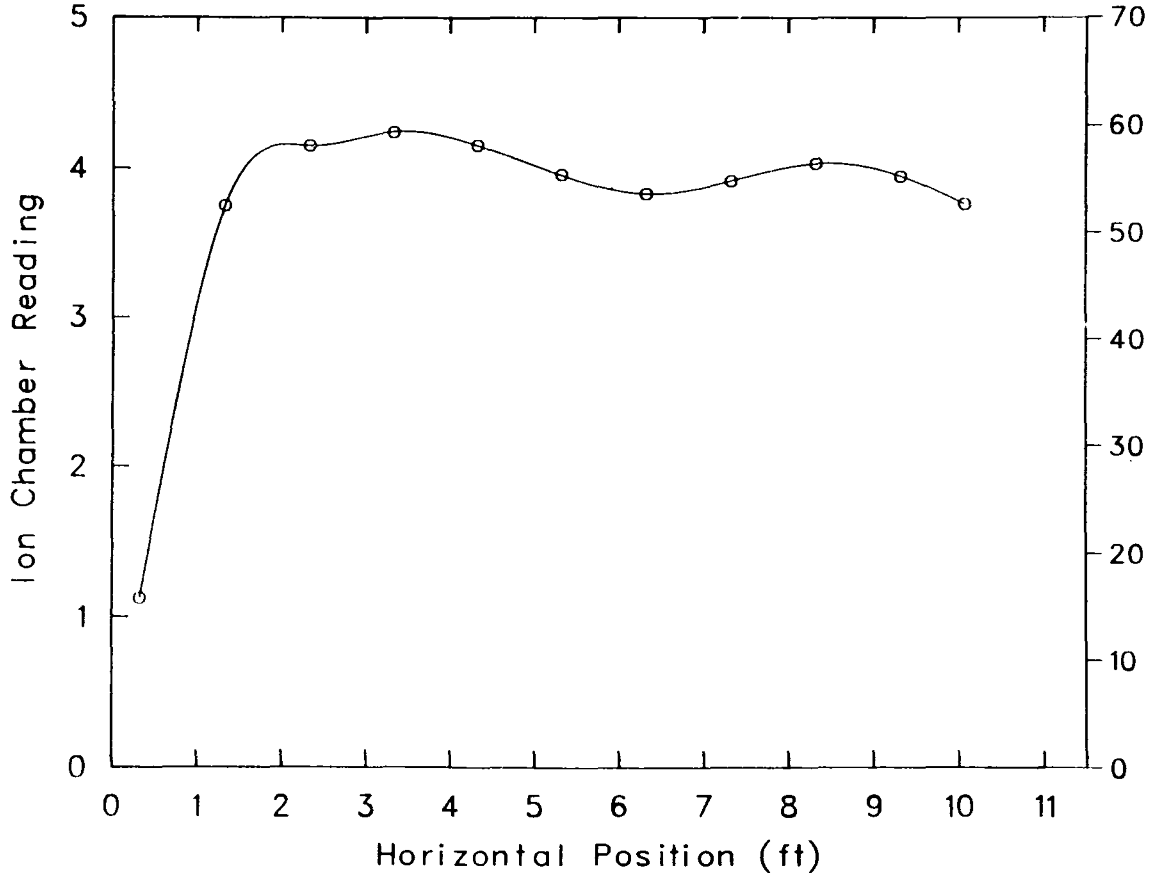

Fig. 7. Gross gamma-ray scan over the top of Demineralizer A.

TABLE V

HORIZONTAL SCAN AT 321-ft 9-in. ELEVATION FOR DEMINERALIZER A

Distance from Wall Penetration[a] (ft.)	(in.)	Ion-Chamber Reading[b]	Dose Rate (R/h)
	4	1.127	11.6
1	4	3.753	50.8
2	4	4.154	56.8
3	4	4.242	58.1
4	4	4.154	56.8
5	4	3.958	53.9
6	4	3.831	52.0
7	4	3.919	53.3
8	4	4.036	55.1
9	4	3.948	53.7
10	1	3.762	51.0

---

[a] Position of centerline of ion chamber.
[b] Uncertainty values of ±0.004 to ±0.005 should be associated with individual measurements.

The vertical scans along the sides of tank A give the data in Fig. 8 and Table VI. The vertical scan on the north side has a maximum activity about 20% higher than the scan has on the south side. The distribution for both the north and south side scans were similar. These scans show the source of gamma rays to be most dense at the bottom of the tank and to become much less dense at the top.

The decrease in the response at the bottom of the tank was attributed to its rounded shape in which less material could be held than in the same thickness of a cylindrical portion.

B. Monte Carlo Calculations

The Los Alamos National Laboratory's Monte Carlo transport code, MCNP,[1] was used to model the gamma-ray source in the demineralizer tank and to calculate the fraction of gamma rays with energies above the 1.667-MeV threshold that would strike the front surface of the Be(γ,n) detector. We investigated various models for the source distribution to obtain one that approximated the measured gross gamma-ray distribution (Fig. 8). Using

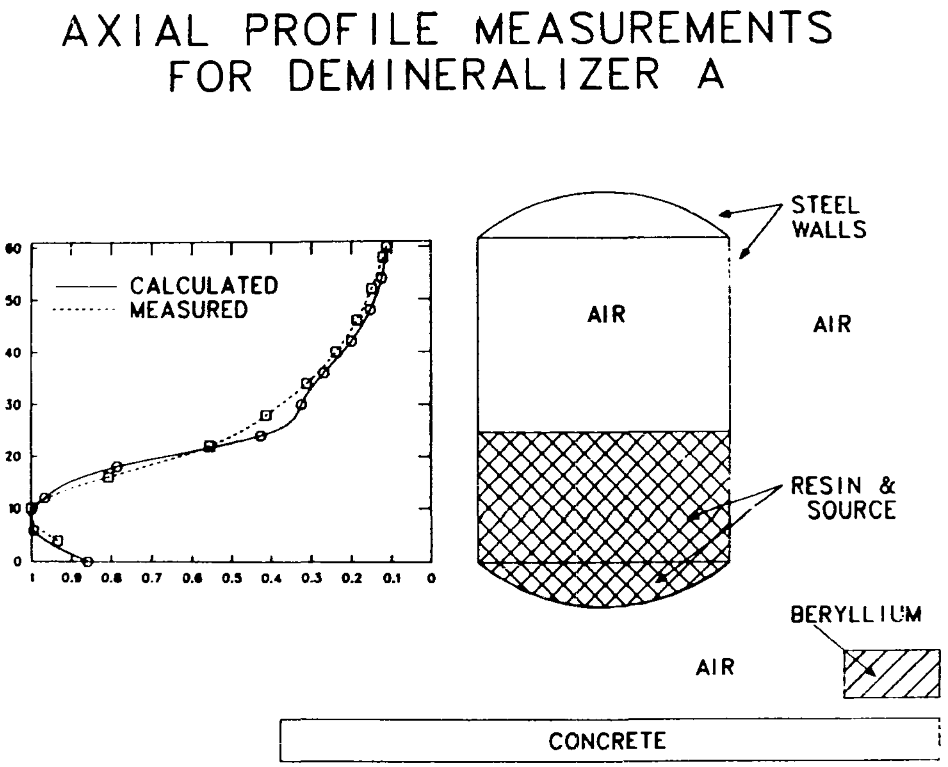

Fig. 8. Vertical gross gamma-ray scans along the sides of Demineralizer A.

the source distribution that best models the observed data, we then calculated the fraction (of the 2.186-MeV gamma rays escaping from the tank with a minimum energy of 1.667 MeV) that would pass through a unit area where the Be(γ,n) detector was located. A summary of the calculations is given immediately below, with a more detailed description in Appendix B.

1. Determination of Gamma-Ray Source Distribution. With only the profile measurements as a guide, we assumed that the gamma-ray source was uniformly distributed in a cylinder that contained a mixture of elements found in the demineralizer resin. The densities of the material were assumed to be 1.0 and 2.07 g/cm^3.

Various heights were selected for the cylindrical source and then the axial gamma-ray flux distributions were calculated to determine what height best approximated the measured distributions in Fig. 8.

TABLE VI

AXIAL SCAN RESULTS FOR DEMINERALIZER A

Elevation		North Side		South Side	
(ft)	(in.)	Ion-Chamber Reading	Dose Rate (R/h)	Ion-Chamber Reading	Dose Rate (R/h)
319	6	3.22 ± 0.0049	42.9	3.69	49.9
319		3.6	48.5	4.08	55.7
318	6	3.99 ± 0.0049	54.4	4.538 ± 0.0049	62.6
318		4.47	61.5	5.08	70.6
317	6	5.007 ± 0.0049	69.6	5.712 ± 0.0049	80.1
317		5.46	76.3	6.46	91.3
316	6	6.005 ± 0.0049	84.5	7.198 ± 0.0049	102.3
316		6.68	94.5	8.2	117.3
315	6	7.599 ± 0.0049	108.3	9.48 ± 0.0049	136.4
315		8.8	126.2	10.8	156.1
314	6	14.47 ± 0.020	210.9	12.90 ± 0.035	187.4
314		18.3	268.1	15.76	230.1
313	6	22.01 ± 0.0196	323.5	18.38 ± 0.0845	269.3
313		22.7	333.8	20.4	299.4
312	6	25.61 ± 0.0196	377.2	24.44 ± 0.020	359.7
312		31.7	468.2	30.0	442.8
311	6	39.47 ± 0.078	584.2	36.29 ± 0.067	536.7
311		50.5	748.9	46.0	681.7
310	6	65.99 ± 0.078	986.2	60.53 ± 0.078	898.7
310		87.5	1301.4	77.5	1152.1
309	6	117.5 ± 0.078	1749.4	103.8 ± 0.078	1544.8
309		171	2548.3	140.0	2085.4
308	6	211.9 ± 0.31	3159.1	175.6 ± 0.427	2617.0
308		198.1 ± 0.31	2956.0	165.0 ± 0.3125	2458.7

A source height of 61 cm appears to fit the measured data best. Varying the density from 1 to 2 g/cm^3 did not significantly affect the shape of the calculated profile. This source distribution fitted the data taken from the two scans adjacent to the demineralizer tank as well as another scan taken 1 ft away from the tank. We also calculated the effect that a layer of water above the source would have on the results. For both scanning positions, the measured results would have shown a much steeper gradient. After a physical inspection of tank A revealed a hollow central region, a cylindrical ring model was also used. It had the height of 61 cm and the radius of the hollow core was 30 cm, leaving a 30-cm-thick ring of material on the inner surface of the tank.

2. Fraction of Gamma-Rays Reaching the Be(γ,n) Detector.

We used five different source distributions to model the fraction of gamma rays reaching the Be(γ,n) detector for the measurements on the A demineralizer. For the measurements of tank A we assumed the Be(γ,n) detector was 5 ft from the center line of the tank; for tank B we used a distance of 7 ft as shown in Fig. 9. We originally assumed that the source was uniformly distributed on the entire 61-cm-high cylindrical source. Calculations were performed assuming average densities of 1.0 g/cm^3 and 2.07 g/cm^3. The first density value was based on the assumption that one-half of the resin had escaped from the tank. For the second density value, 2.07 g/cm^3, we assumed all the resin remained in the demineralizer and was compressed to lie within the 61-cm depth.

A second set of calculations was run for these two densities with the assumption that the fuel material was deposited in a

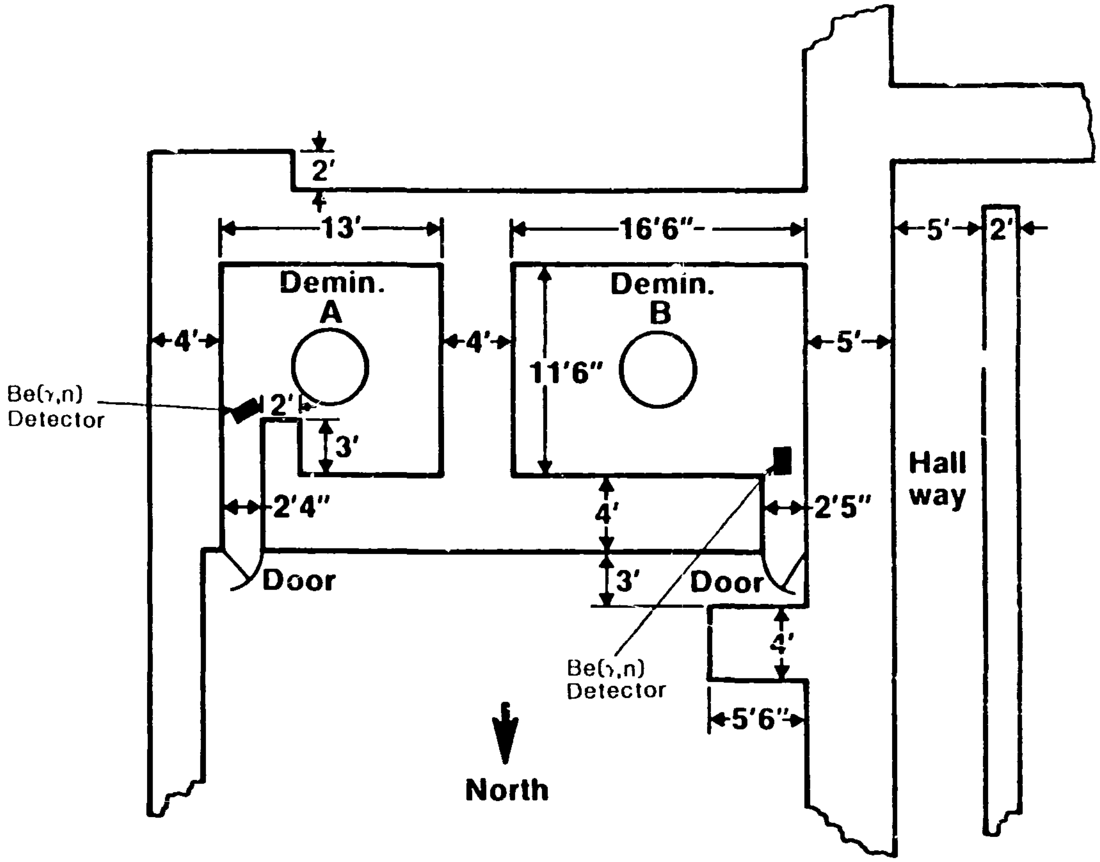

Fig. 9. Estimated locations of Be(γ,n) measurements in an overhead view of the two demineralizer cubes.

10-cm layer at the top of the 61-cm depth of resin. The model would have been applicable if the demineralizer were acting as a mechanical filter instead of as an ion-exchange resin.

The fifth model assumes that a large fraction of the resin material was no longer present in the demineralizer. The resin in the demineralizer was assumed to be deposited in a ring 30 cm thick (12 in. thick) around the inner surface of the tank. Results for the five models investigated are given in Table VII. The result for a point source located in the bottom of the demineralizer tank is also included for comparison. Only one source distribution was modeled for the B demineralizer.

C. Grams of Uranium per Curie of ^{144}Ce

Based on calculated results from the EPRI-CINDER[2,3] single point depletion code, we obtained the following for the core average values.

Grams of initial uranium = $82.069 \bullet 10^6$
Curies of ^{144}Ce (October 27, 1982) = $9.74 \bullet 10^5$
One curie ^{144}Ce = 84.3 grams uranium

D. Be(γ,n) Measurements and Results

Figure 9 shows the approximate locations of the Be(γ,n) detector during the measurements of Demineralizers A and B. We were able to obtain gamma-ray-profile measurements for Demineralizer A but were unable to obtain corresponding data for Demineralizer B because we did not have sufficiently long signal cables for the ion chambers. Table VIII gives the results for the Be(γ,n) measurements.

1. Curies of ^{144}Ce in the Demineralizer. Rearranging Eq. (3) we obtain the following.

$$\text{Curies of } {}^{144}\text{Ce} = \frac{\text{Measured counts/s}}{3.70 \bullet 10^{10}\,\text{dps/Ci} \bullet \text{branching ratio} \bullet f(\Omega,\mu,\rho,x,y,z) \bullet \text{detector efficiency}}$$

where

branching ratio = 0.007 gamma/disintegration.

$f(\Omega,\mu,\rho,x,y,z)$ = Fraction of gamma rays escaping from the demineralizer and striking the surface of the Be(γ,n) detector. These values were calculated using the Monte Carlo code.

detector efficiency = The probability of a gamma ray striking the surface of the detector producing a count.

= 2.55×10^{-7} counts/gamma.

TABLE VII

FRACTION OF INITIAL GAMMA RAY STRIKING THE FRONT SURFACE OF THE Be(γ,n) DETECTOR

Tank	Material Density (g/cm^3)	Source Distribution	Probability
A	2.07	Uniform, 61 cm high	0.000995
A	1.00	Uniform, 61 cm high	0.00168
A	2.07	Crust, 10-cm source on top of 51-cm attenuating material	0.000686
A	1.00	Crust, 10-cm source on top of 51-cm attenuating material	0.00127
A	1.00	30-cm-thick ring	0.0020
A	--	Point source	0.00184
B	1.00	Uniform, 160 cm deep	0.000976

TABLE VIII

MEASUREMENTS OF DEMINERALIZERS

Demineralizer	Count Time (s)	Net neutron from Be(γ,n)	Net Gamma of Ion Chamber
A	300	919 ± 30	15.76 ± 0.02
	300	951 ± 30	15.76 ± 0.02
	300	963 ± 31	15.72 ± 0.06
	300	948 ± 31	15.84 ± 0.02
	300	924 ± 30	15.84 ± 0.02
	300	952 ± 31	15.76 ± 0.02
	300	1003 ± 32	15.64 ± 0.02
	300	964 ± 31	15.72 ± 0.06
	300	1000 ± 31	15.64 ± 0.04
	300	941 ± 31	15.88 ± 0.02
	300	967 ± 31	15.80 ± 0.02
	300	943 ± 31	[a]
	300	971 ± 31	[a]
	300	907 ± 30	[a]
	300	932 ± 30	[a]
	300	975 ± 31	[a]
	300	875 ± 31	[a]
	300	899 ± 30	[a]
	300	921 ± 30	15.50 ± 0.09
	300	902 ± 30	15.48 ± 0.02
Average		946.4 ± 30.3 3.15 Counts/s	15.72 ± 0.13 or 229 R/h
B	300	153 ± 12.4	
	300	163 ± 12.8	
	300	147 ± 12.1	
	300	147 ± 23.1	
	300	160 ± 12.7	
	300	149 ± 12.2	
	300	140 ± 11.8	
	300	134 ± 11.6	
	300	169 ± 13.0	
Average		151.3 ± 11.2 0.504 Counts/s	

---

[a] Values were not recorded because they were relatively constant.

Substituting the values from Table VII and incorporating the conversion factor for curies of ^{144}Ce to grams of uranium metal, we obtain the results given in Table IX.

TABLE IX

CURIES ^{144}Ce AND AMOUNT OF URANIUM METAL

Tank	Material Density (g/cm^3)	Source Distribution	^{144}Ce (Ci)	U Metal (kg)
A	2.07	Uniform, 61 cm high	55.1	4.6
A	1.07	Uniform, 61 cm high	32.7	2.8
A	2.07	Crust, 10-cm source on top of 51-cm attenuating material	80.0	6.7
A	1.00	Crust, 10-cm source on top of 51-cm attenuating material	43.2	3.6
A	1.00	30-cm-thick ring	27.4	2.7
A	--	Point source	29.8	2.5
B	1.00	Uniform, 160 cm deep	7.8	0.7

2. Measurement Variables. There are several variables that could affect the calculated results significantly.

(a) Detector position with respect to the tanks.

(b) Orientation of detector.

(c) Distribution and density of material in the tank.

(d) Fraction of high-energy gamma rays above 1.667 MeV from ^{106}Ru.

We can only estimate the real positions and orientations of the detectors during this measurement. The position of the detector with respect to a tank could influence the results from 10 to 30% depending on whether the detector were 5 ft or 6 ft from the tank's center line. We expect this effect to be at the lower end of this range because of our assumption that the tank was an extended source. Therefore, the effect would not necessarily vary as the square of the distance. The detector has directional sensitivity and is ~50% more efficient if it is oriented with its long side facing the source. The measurement geometry of the detector in the B cubicle may have been such that a significant number of gamma rays could have struck the side of the detector; hence our efficiency factor could have been higher, reducing our estimated inventory of fuel proportionally. For our calculations, we assumed that the front surface of the detector was normal to the center line of the tank. In the actual measurements, the extended source distribution and the possibility of the detector not being perfectly aligned would affect the geometry efficiency factor, $f(\Omega,\mu,\rho,x,y,z)$, in the calculations. If this factor were increased, our estimates of the uranium inventories would be reduced proportionally.

Another unknown factor was the real density of the matrix material in the tanks. We have assumed uniform densities of 1.0 and 2.07 g/cm^3; if the true effective density were greater than that, as might be the case if all the original resin had been in the lower region of the tank, our estimates would be low. Similarly, if the effective density were less than 1.0, our fuel estimates would be high. If we assumed the density to be that of air, and the source to be a point source as was the case in our hot-cell calibration, we would estimate a fuel inventory of approximately 2.5 kg.

The fraction of gamma rays above 1.667 MeV not arising from ^{144}Ce-^{144}Pr was assumed to be not more than 5%. If ^{106}Ru (the only plausible interference) had concentrated in the demineralizers, our values would be biased too high. From the preliminary results obtained from HEDL, this does not appear to be a significant problem.

V. CONCLUSIONS

Each of the factors discussed in the previous sections can influence the calculation of the fuel inventories in the two demineralizers. The specific value is strongly dependent on the assumed distribution of the source and the density of the material in the tank. The detectors' positions and orientations are important but were known only approximately. We assumed also that no ^{106}Ru remained in the resin. For these reasons, only a fairly wide range of results for tank A is given. Also, we have included all of our data to allow others the opportunity to review our results. Keeping in mind all of the previous considerations, we estimate the inventories from data shown in Table VII to be

2 to 7 kg of fuel in Demineralizer A,
0.7 kg of fuel in Demineralizer B.

ACKNOWLEDGMENTS

The authors appreciate the assistance of the DOE and EG&G personnel at TMI-2 in performing these experiments. H. Sanchez and G. Quinn were instrumental in the successful completion of the project. We are also indebted to N. Stalnaker for preparing the calibration standard and to W. Wood and T. Romero for calibrating the detector.

REFERENCES

1. W. L. Thompson, "MCNP - A General Monte Carlo Code for Neutron and Photon Transport," Los Alamos Scientific Laboratory report LA-7396-M (1978).

2. T. R. England, W. B. Wilson, "TMI-2 Decay Power: LASL Fission-Product and Actinide Decay Power Calculations for the Presidents Commission on the Accident at Three Mile Island," Los Alamos Scientific Laboratory report LA-8041-MS (revised) (March 1980).

3. W. B. Wilson, R. J. LaBauve, and T. R. England, "Calculations of Spent Thermal Reactor Fuel Nuclide Inventories and Comparison with Measurements," Proceedings of Seminar/Workshop on Thermal Reactor, Benchmark, Calculations, Techniques, Results, and Applications, May 17-18, 1982 (to be published by EPRI).

4. G. E. Bosler, J. R. Phillips, W. B. Wilson, R. J. LaBauve, and T. R. England, "Production of Actinide Isotopes in Simulated PWR Fuel and Their Influence on Inherent Neutron Emission," Los Alamos National Laboratory report LA-9343 (July 1982).

5. S. F. Klosterbuer, and J. K. Halbig, "Portable Spent-Fuel Gamma-Ray and Neutron Detector Electronics User Manual," Los Alamos National Laboratory report LA-8707-M (to be published).

6. R. W. Davis and E. R. Graves, "The Radiation Instrument Calibration Facility at the Los Alamos Scientific Laboratory" Los Alamos Scientific Laboratory report LA-4090 (June 1969).

APPENDIX A

PREPARATION OF STANDARD ^{144}Ce SOLUTION FOR CALIBRATION OF THE Be(γ,n) DETECTOR

A 1.25-cm section of an experimental (uranium, plutonium) carbide fuel pin from the fast reactor fuel development program was used to prepare a standard ^{144}Ce solution for calibration of the Be(γ,n) detector. The fuel pin had an average burnup of 8.7% and was removed from the reactor on March 26, 1982. Because it was a mixed carbide fuel sample, the amount of ^{106}Ru present was significantly higher than what would be found in a LWR fuel sample because of the much higher fission yield of ^{106}Ru from ^{239}Pu compared to ^{235}U. Chemical separation of the ruthenium was accomplished by dissolution of the fuel section in nitric acid followed by a sodium hydroxide precipitation and oxidation of the ruthenium to the base-soluble perruthenate. The perruthenate-containing solution was decanted off the precipitate, which was washed with sodium hydroxide and then dissolved in nitric acid. Thirty milliliters of this acid solution was used as the gamma-ray calibration standard for the Be(γ,n) detector.

The radiochemical assay of the solution gave $3.08 \cdot 10^{11}$ dps/30 mℓ or 8.38 Ci of ^{144}Ce. Assay for ^{106}Ru gave $6.78 \cdot 10^{10}$ dps/30 mℓ or 1.83 Ci after the separation. For our calibration standard, the ratio of ^{144}Ce/^{106}Ru was 4.6, which was similar to the expected ratio of 3.9 for the TMI-2 fuel. Assay procedure and calculations are summarized below.

A. Dilution Sequence

(1) 1.007 mℓ of source solution diluted to 189.76 mℓ with 1 N HNO_3.

(2) Two 0.010 mℓ aliquots of 189.76 mℓ each diluted to 10 mℓ in volumetric flask with 1 N HNO_3.

(3) One mℓ of first 10-mℓ dilution was counted.

(4) Two mℓ of second 10-mℓ dilution was counted.

B. Cerium-144 assay

Energy peak used for assay = 133 keV

Abundance = 0.108 gamma/disintegration

Detector efficiency = $4.06 \bullet 10^{-2}$ counts/gamma

Count time = 1000 s (live time)

Sample 1

Gross Peak Area = 287 497 counts

Background = 49 065 counts

Sample 2

Gross Peak Area = 604 987 counts

Background = 126 997 counts

Average dps/mℓ of source = $1.026 \pm 0.002 \bullet 10^{10}$

Source dps = $(1.026 \bullet 10^{10})$ (30) = $3.078 \bullet 10^{11}$

C. Ruthenium-106 assay

Energy peak used for assay = 512 keV

Abundance = 0.205 gamma/disintegration

Detector efficiency = $1.03 \bullet 10^{-2}$ counts/gamma

Count time = 1000 s (live time)

Sample 1

Gross Peak Area = 37 387 counts

Background = 12 458 counts

Sample 2

Gross Peak Area = 69 543 counts

Background = 18 220 counts

Average dps/mℓ of source = $2.26 \pm 0.05 \bullet 10^{9}$

Source dps = $(2.26 \bullet 10^{9})$ (30) = $6.78 \bullet 10^{10}$

APPENDIX B

PROBABILITY OF A SOURCE GAMMA RAY STRIKING THE Be(γ,n) DETECTOR

The calibration of the Be(γ,n) detector provides the probability of a count being recorded for a gamma ray entering the detector. This was found experimentally using a point-like source of gamma rays of known activity where the probability of a gamma ray passing through the detector could be calculated using simple geometry considerations.

With the more complicated source distributed within a demineralizer tank, the probability of a gamma ray passing through the detector is not easily obtained. A model of the tank and detector was examined using the Los Alamos Monte Carlo computer code, MCNP. The model detector was positioned at the distance from the tank estimated by the General Public Utility (GPU) personnel who positioned the detector in the demineralizer room. We assumed that the detector was aligned with its long axis pointed toward the center line of the tank. The vast majority of the gamma rays that enter the detector in this orientation do so through the top and front surfaces; the small additional number that enter through the sides were not included in these calculations. A layer of concrete simulated the floor to allow for scatter of gamma rays into the detector, but this was found to have a very minor effect.

The gamma-ray profile scan was approximated by our assuming a uniform source distribution that filled the bottom spherical cap of the tank and then continued upward for about 61 cm. This is in general agreement with the estimated location of the material given by a physical probe placed into the tank. In these calculations we assumed that the source and resin have uniform densities.

If all the resin is still in the tank, its density would be about 2.07 g/cm^3; if about half has escaped, the density might be about 1.00 g/cm^3. These two densities were used to examine the effects of density on the calculations.

The Monte Carlo code gives the flux of gamma rays entering a square centimeter normal to the direction of motion, divided by the number of source gamma rays. The models used here always had the bottom spherical cap filled with resin; for Tank A, 61 cm of resin was in the lower cylindrical portion; for Tank B, 160 cm of resin was in the cylindrical portion. For Tank A, an extra case was used in which the source is confined to the uppermost 10 cm of the 61 cm of resin. This model does not match the measured gamma-ray profile but is used simply to help establish bounds on the calculated values. After an inspection revealed a hollow core in the resin of tank A, a cylindrical ring of resin was used in the Monte Carlo model. The ring was 61 cm high and had a central hollow region 30 cm in diameter. Table B-I gives the results for these cases.

TABLE B-I

RESULTS OF MONTE CARLO CALCULATIONS

Tank	Density	Source Distribution	Flux[a]		Projected Area		Probability
			Top	Front	Top	Front	
A	2.07	Uniform	0.8609	1.359	450	447	0.000995
A	1.00	Uniform	1.650	2.215	391	467	0.00168
A	2.07	10-cm crust	0.6837	0.6455	625	400	0.000686
A	1.00	10-cm crust	1.225	1.390	550	432	0.00127
A	1.00	Ring	1.950	2.554	420	460	0.0020
B	1.00	Uniform	0.9081	1.245	522	403	0.000976
Point Source Calibration			2.165	2.870	154	511	0.00180

---

[a] The flux units are $10^{-6}/cm^2$, with estimated accuracies of about 10%.

The fluxes must be multiplied by the projections of the areas of the top and front surfaces of the detector. These projections are normal to the direction of gamma rays from the tank. With the extended sources within the tanks, these projected areas can only be averages.

From a point within the tank, lines were drawn to the centers of the top and front surfaces. The projections of the areas were normal to these lines. We imagined a line that was four mean-free-path lengths inside the tank and in the plane containing the center line of the tank and the detector. The end points of this line coincided with the top and bottom of the gamma-ray source region. For these two points, projected areas of a surface of the detector were calculated; the average of these areas is shown in Table B-I and was used to multiply a corresponding flux. A probability in Table B-I is thus the flux for the top surface times its projected area, plus the flux for the front surface times its projected area.

Printed in the United States of America
Available from
National Technical Information Service
US Department of Commerce
5285 Port Royal Road
Springfield, VA 22161

Microfiche (A01)

Page Range	NTIS Price Code	Page Range	NTIS Price Code	Page Range	NTIS Price Code	Page Range	NTIS Price Code
001-025	A02	151-175	A08	301-325	A14	451-475	A20
026-050	A03	176-200	A09	326-350	A15	476-500	A21
051-075	A04	201-225	A10	351-375	A16	501-525	A22
076-100	A05	226-250	A11	376-400	A17	526-550	A23
101-125	A06	251-275	A12	401-425	A18	551-575	A24
126-150	A07	276-300	A13	426-450	A19	576-600	A25
						601 up*	A99

*Contact NTIS for a price quote.

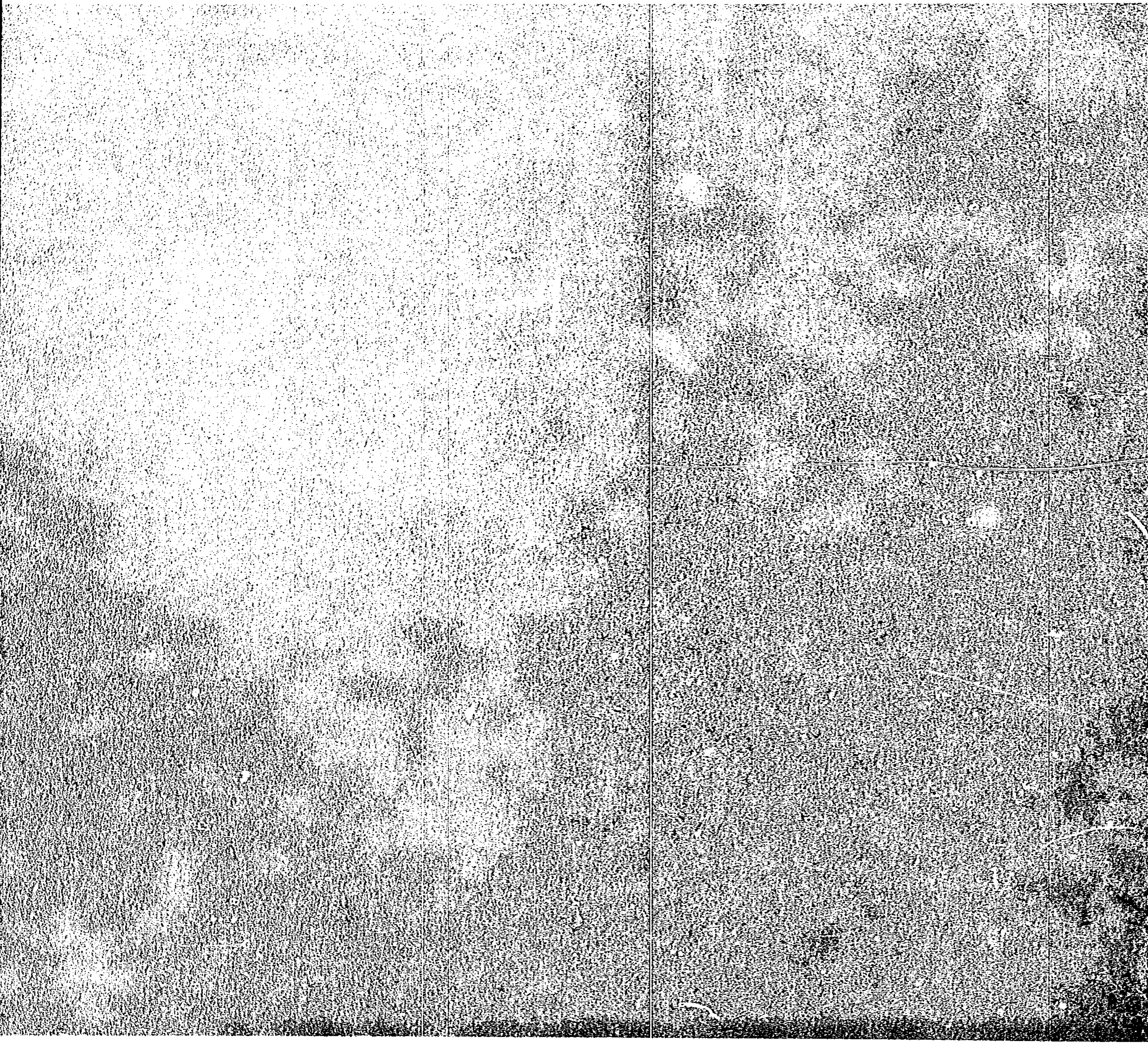

Los Alamos

RRB (6)

Westinghouse Hanford Company

HEDL-7285

FUEL ASSESSMENT OF THE THREE MILE ISLAND UNIT 2 MAKEUP DEMINERALIZERS BY COMPTON RECOIL CONTINUOUS GAMMA-RAY SPECTROMETRY

U.S. Department of Energy

HANFORD ENGINEERING DEVELOPMENT LABORATORY Operated by Westinghouse Hanford Company P.O. Box 1970
Richland, WA 99352 A Subsidiary of Westinghouse Electric Corporation Prepared for the U.S. Department of Energy
Assistant Secretary for Nuclear Energy Office of Terminal Waste Disposal and Remedial Action under Contract
No. DE-AC06-76FF02170 B&R No. AG-30-05

Westinghouse Hanford Company

HEDL-7285

FUEL ASSESSMENT OF THE THREE MILE ISLAND UNIT 2 MAKEUP DEMINERALIZERS BY COMPTON RECOIL CONTINUOUS GAMMA-RAY SPECTROMETRY

J.P. McNeece
B.J. Kaiser
R. Gold
W.W. Jenkins
October 1983

U.S. Department of Energy

HANFORD ENGINEERING DEVELOPMENT LABORATORY Operated by Westinghouse Hanford Company P.O. Box 1970 Richland, WA 99352 A Subsidiary of Westinghouse Electric Corporation Prepared for the U.S. Department of Energy Assistant Secretary for Nuclear Energy Office of Terminal Waste Disposal and Remedial Action under Contract No. DE-AC06-76FF02170 B&R No. AG-30-05

FUEL ASSESSMENT OF THE THREE MILE ISLAND UNIT 2 MAKEUP DEMINERALIZERS BY COMPTON RECOIL CONTINUOUS GAMMA-RAY SPECTROMETRY

James P. McNeece, Bruce J. Kaiser,
Raymond Gold, and William W. Jenkins

ABSTRACT

During October, 1982, gamma spectrometry measurements were carried out to assess the fuel debris content of the TMI-2 makeup demineralizers. A shielded Si(Li) Compton recoil gamma ray spectrometer was used to measure the gamma spectra at various locations within the cell. The shield weighed 78 pounds and permitted operation in gamma fields up to 2000 R/hr. The spectral data were used to determine the intensity of the 2.18 MeV gamma ray from the fission product ^{144}*Ce.* Assuming this fission product does not migrate out of the fuel, the quantity of* ^{144}*Ce is directly related to the quantity of fuel present. These spectral measurements also provided data for determining the* ^{137}*Cs loading on the demineralizer resin.*

A small diameter collimator opening in the side of the detector's lead shield allowed accurate mapping of the source configuration within the demineralizer tank. Collimated horizontal traverses across the top of the tank and vertical traverses down the sides were made. The observed horizontal source distributions show gross nonuniformity for both the ^{144}*Ce and* ^{137}*Cs. The observed vertical distributions show the source to be volume distributed over the two-foot region from elevation 307' to 309'. Analysis of the* ^{137}*Cs electron spectral shapes indicate there is no significant attenuating material above the 309' elevation. The observed gross nonuniformities in the source distribution leads one to conclude there has been, in turn, gross nonuniformity in the radiation damage to the resin bed.*

Based on the observed source geometry and the measured flux of the ^{144}*Ce 2.18 MeV gamma-rays, the fuel content of the A demineralizer is calculated to be 1.3 ± 0.6 Kg. In addition, as based on these measurements, the* ^{137}*Cs content is calculated to be 3400 ± 2500 Curies. Both estimates are as of mid-October, 1982.*

**This gamma-ray is actually emitted by* ^{144}*Pr, which is the daughter of* ^{144}*Ce.*

CONTENTS

FIGURES

FIGURES (Cont'd)

TABLES

1.0 Introduction

Assessment of the fuel content of the Three Mile Island Unit-2 (TMI-2) makeup demineralizers is necessary prior to removal of the highly radioactive ion exchange resin from the demineralizer tanks. Since both the A and B demineralizers were on-line during the accident, significant amounts of fuel may have been trapped in the resin beds. Estimates of the fuel debris present can be made by measuring the intensity of specific gamma rays associated with fission products and by measuring the neutron flux from spontaneous fission and (α,n) reactions in the fuel. Continuous gamma-ray spectrometry provides the means for carrying out the gamma ray measurements. Solid state nuclear track recorders are applicable for the neutron measurements,(1) and results are provided in a companion report.(2)

This report provides data and results obtained from continuous gamma-ray spectrometry measurements in the A and B demineralizer cells. In Section 2 the continuous gamma-ray spectrometry method is described with emphasis on adaptations introduced to carry out measurements in the intense radiation environment of the TMI-2 demineralizer cells. The actual measurement campaign is described in Section 3. Analysis of the data to locate and quantify the fuel debris is given in Section 4. Additional characterization in terms of the total ^{137}Cs activity loading of the A demineralizer is provided in Section 5.

2.0 Measurement Technique

Gamma spectra measurements were made using a unique Si(Li) Compton recoil spectrometer. The ability of this Si(Li) spectrometer to determine absolute gamma ray continua has been well established.(3-5) In addition, the spectrometer has the ability to accurately determine the absolute intensity of widely spaced line spectra. From preliminary measurements of a TMI sludge sample, it was shown that the gamma ray lines were widely spaced, thereby making this an ideal application for the Compton recoil spectrometer.

A photograph of the physical packaging of the spectrometer/preamplifier assembly is shown in Figure 1. To reduce the intense background radiation from ^{137}Cs, the detector was surrounded by a 5.5" diameter lead shield 8" in length. Two shields were used to provide different levels of background attenuation. Both

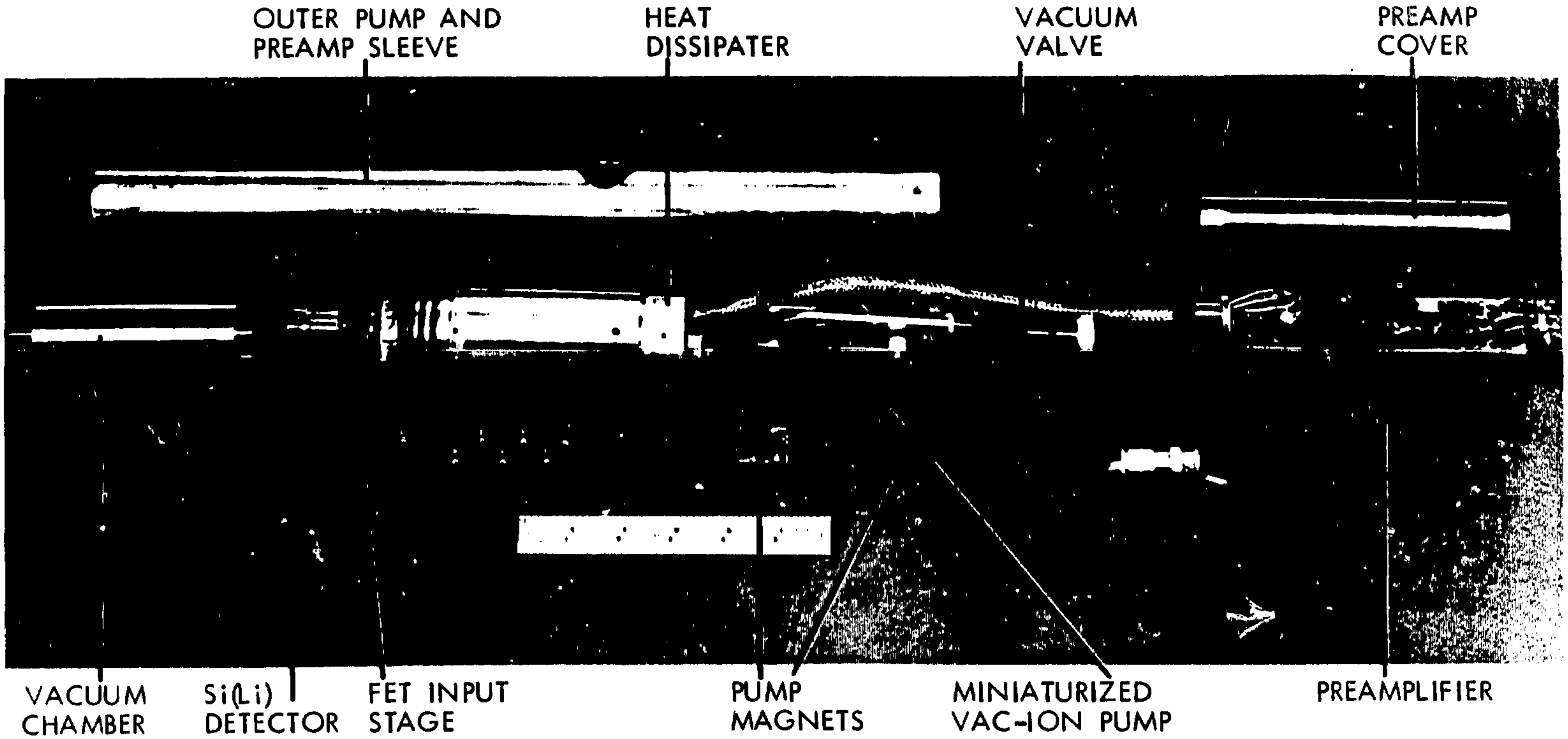

FIGURE 1. Photograph of the Si(Li) compton recoil spectrometer.

are shown in Figures 2 and 3. Small diameter collimator holes in the shields' sides permitted accurate mapping of the geometrical source distribution within the demineralizer tank.

Access to the A-Cell was limited to a 6" x 9" opening at the 321'9" elevation (penetration #891 shown in Figure 4, which is approximately 8 feet above the demineralizer tank). A special boom and winch assembly was fabricated to remotely position the spectrometer/shield package inside the cell. The boom provided for horizontal movement of the detector over the complete width of the cell. A swing arm and winch provided for lowering the detector down both the north and south sides of the tank. Tape measures attached to the boom allowed for accurate positioning of the detector.

A small, remotely operated transporter was used to position a video camera inside the cell. It proved to be an invaluable aid in positioning of the spectrometer.

3.0 Demineralizer A Measurements

An overall isometric view of the makeup demineralizer cells is shown in Figure 4. Elevation and plan views of the demineralizer A cell are shown in Figures 5 and 6, respectively. Horizontal traverses were made across the top of the tank at the 321'9" elevation and vertical traverses were made down both the north and south sides of the tank. Both detector shields were used for the horizontal traverses. Only the symmetrical shield was used for the vertical traverses.

Two sets of data were taken--one set with the collimator opening plugged (background) and the other set with the collimator opening toward the tank (foreground). The source geometrical distributions are obtained by subtracting the background data from the foreground data. This difference is the response due only to the uncollided gamma rays that enter through the collimator opening. The collimator limits the field of view of the detector to small diameter regions, thereby allowing the relative source intensity distribution to be accurately mapped. On the other hand, flux distributions are obtained from the background data only. The flux at any location is obviously a function of the total source within the cell, not just the emission from a small region.

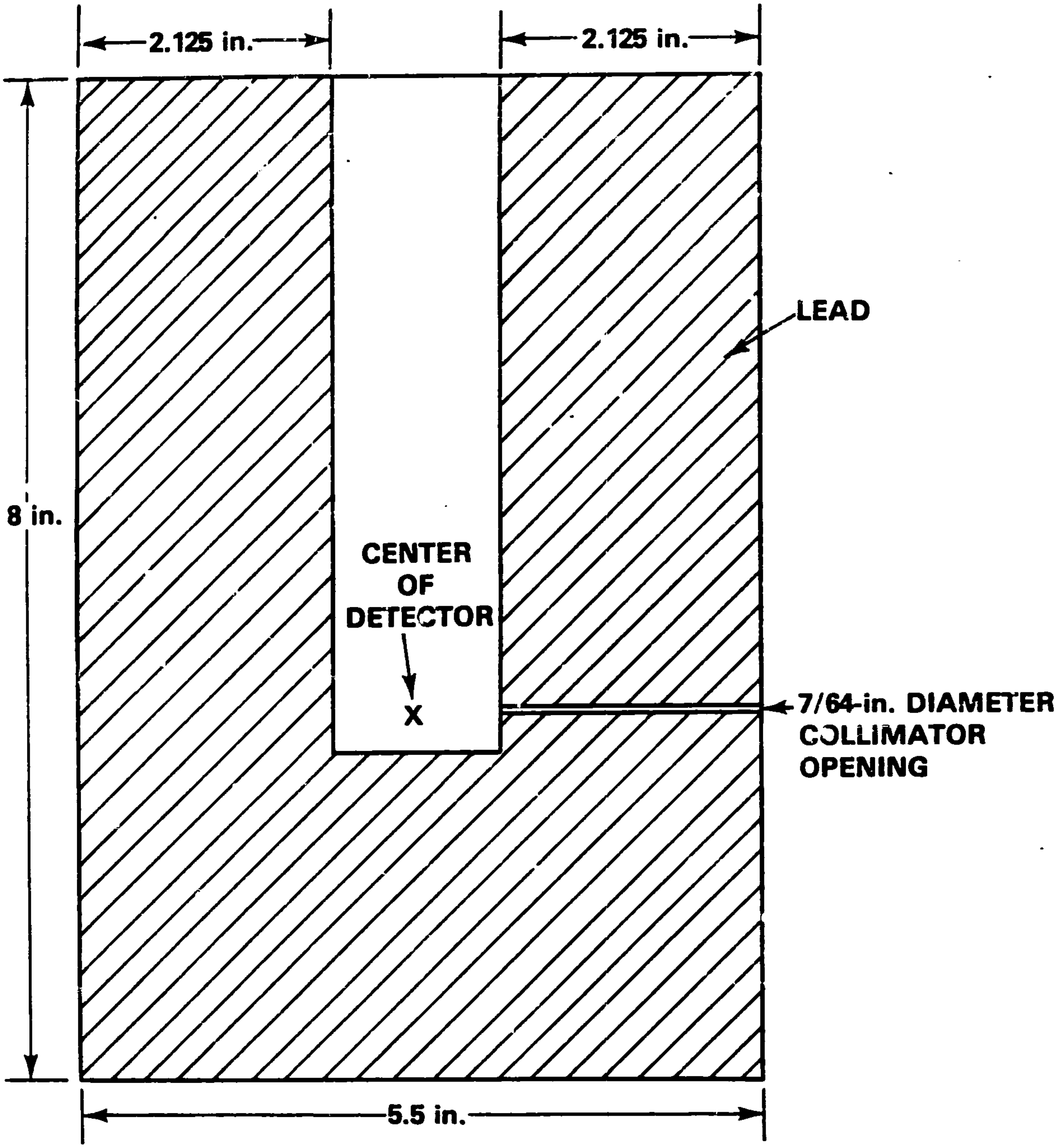

HEDL 8212-080.3

FIGURE 2. Cutaway drawing of the symmetrical shield.

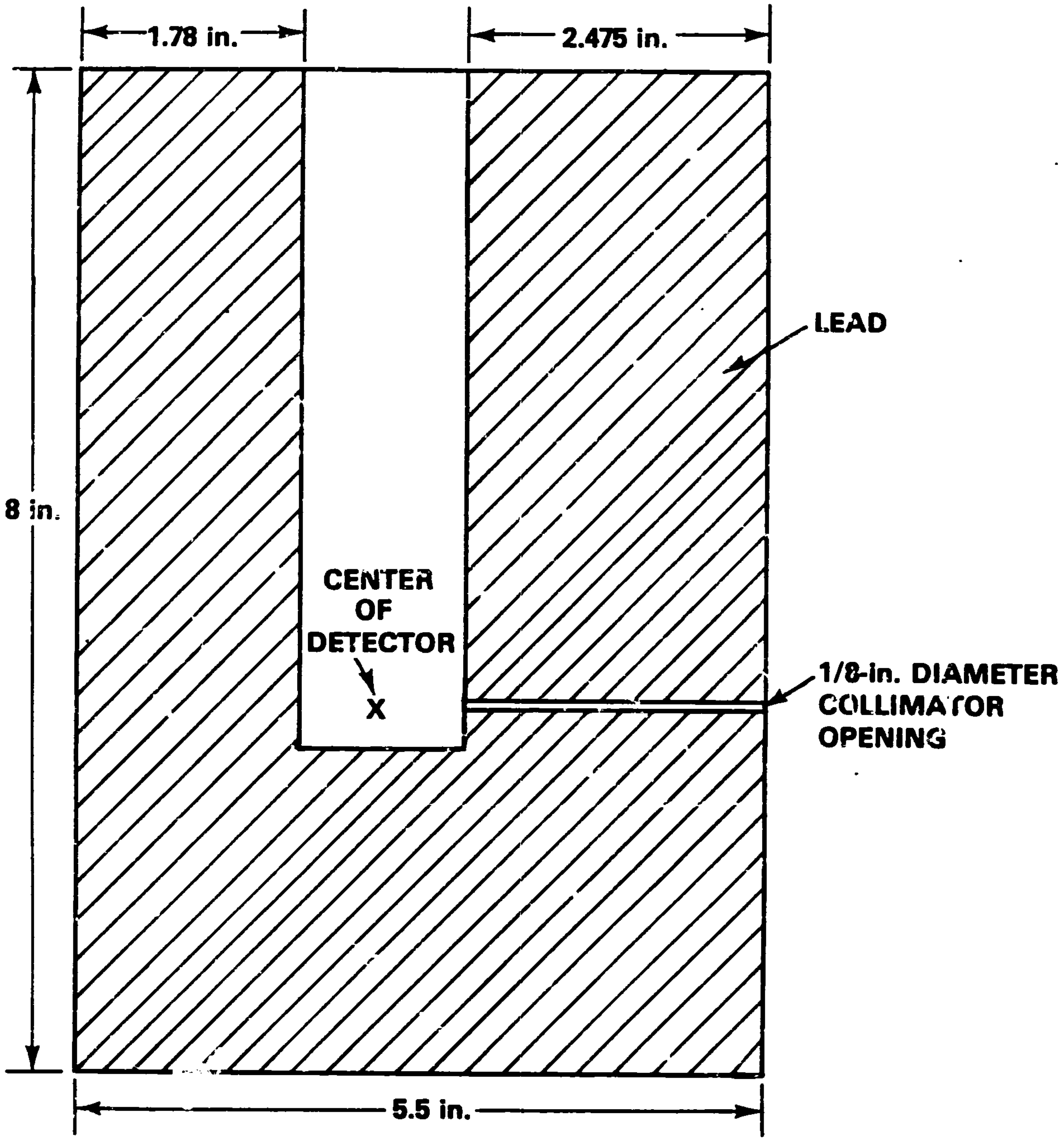

HEDL 8212-080.4

FIGURE 3. Cutaway drawing of the asymmetrical shield.

TMI-2 MAKE-UP & PURIFICATION DEMINERALIZERS

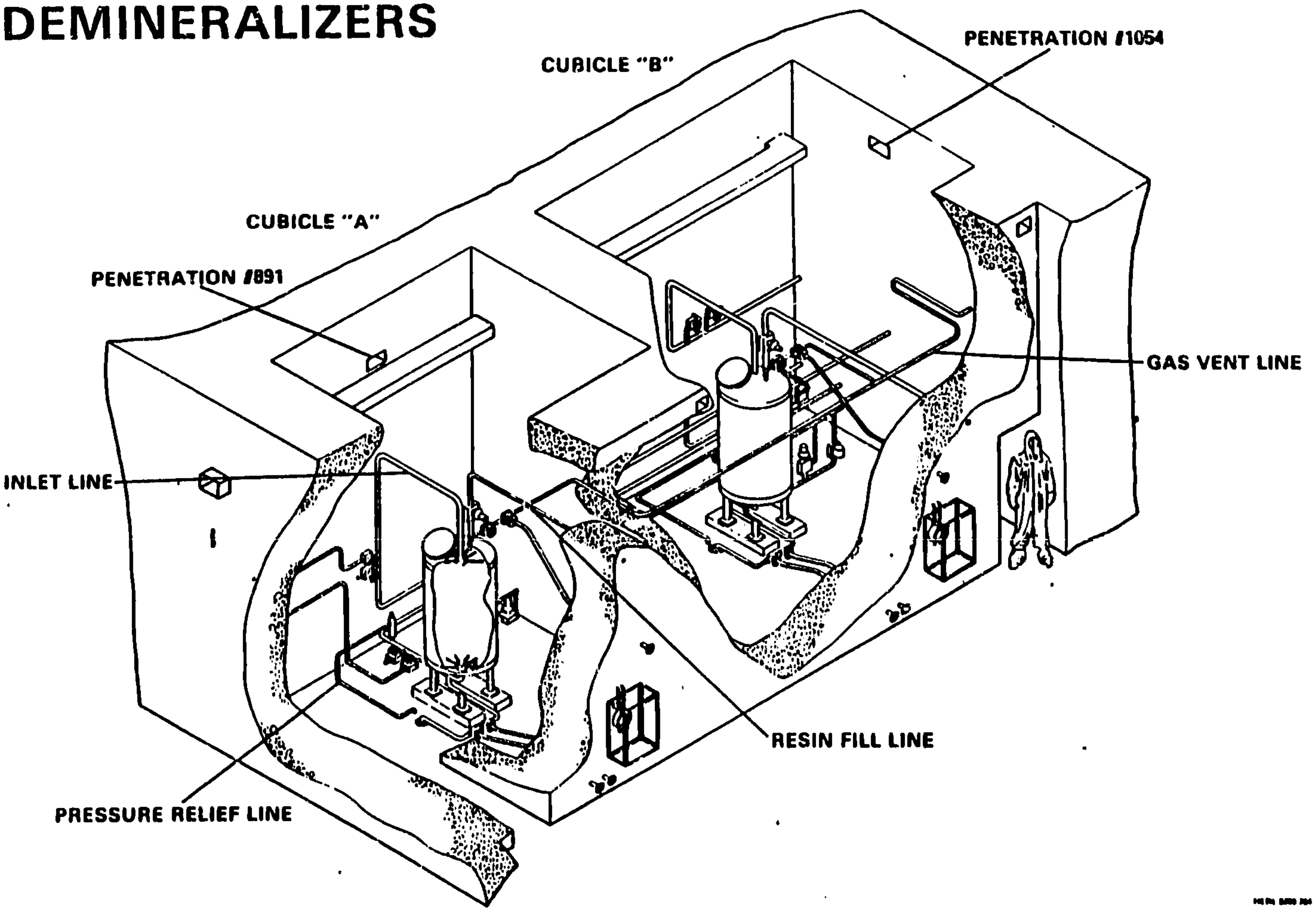

FIGURE 4. Isometric view of the makeup demineralizer cells.

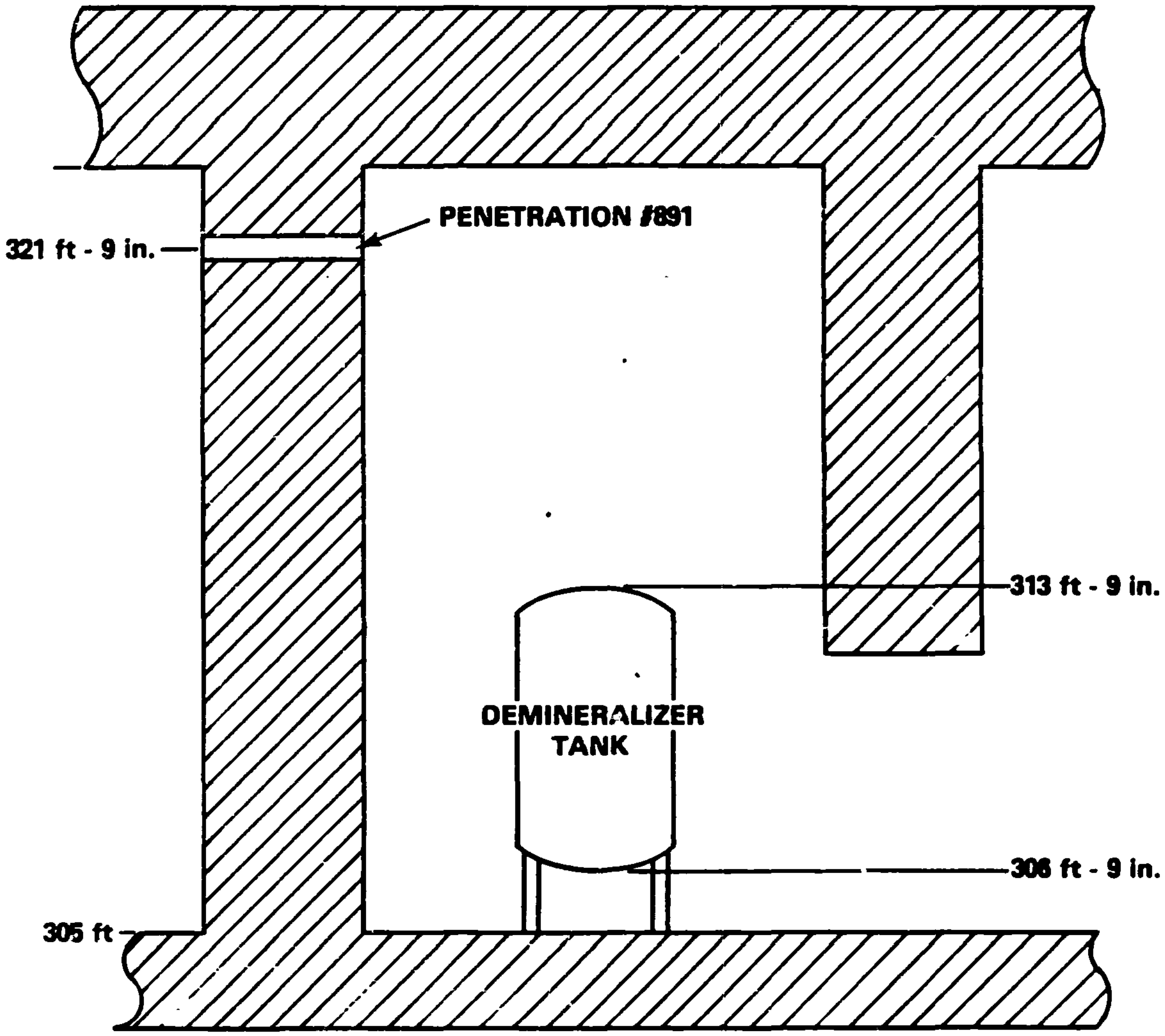

FIGURE 5. Elevation view of the "A" demineralizer cell.

HEDL 8212-080.1

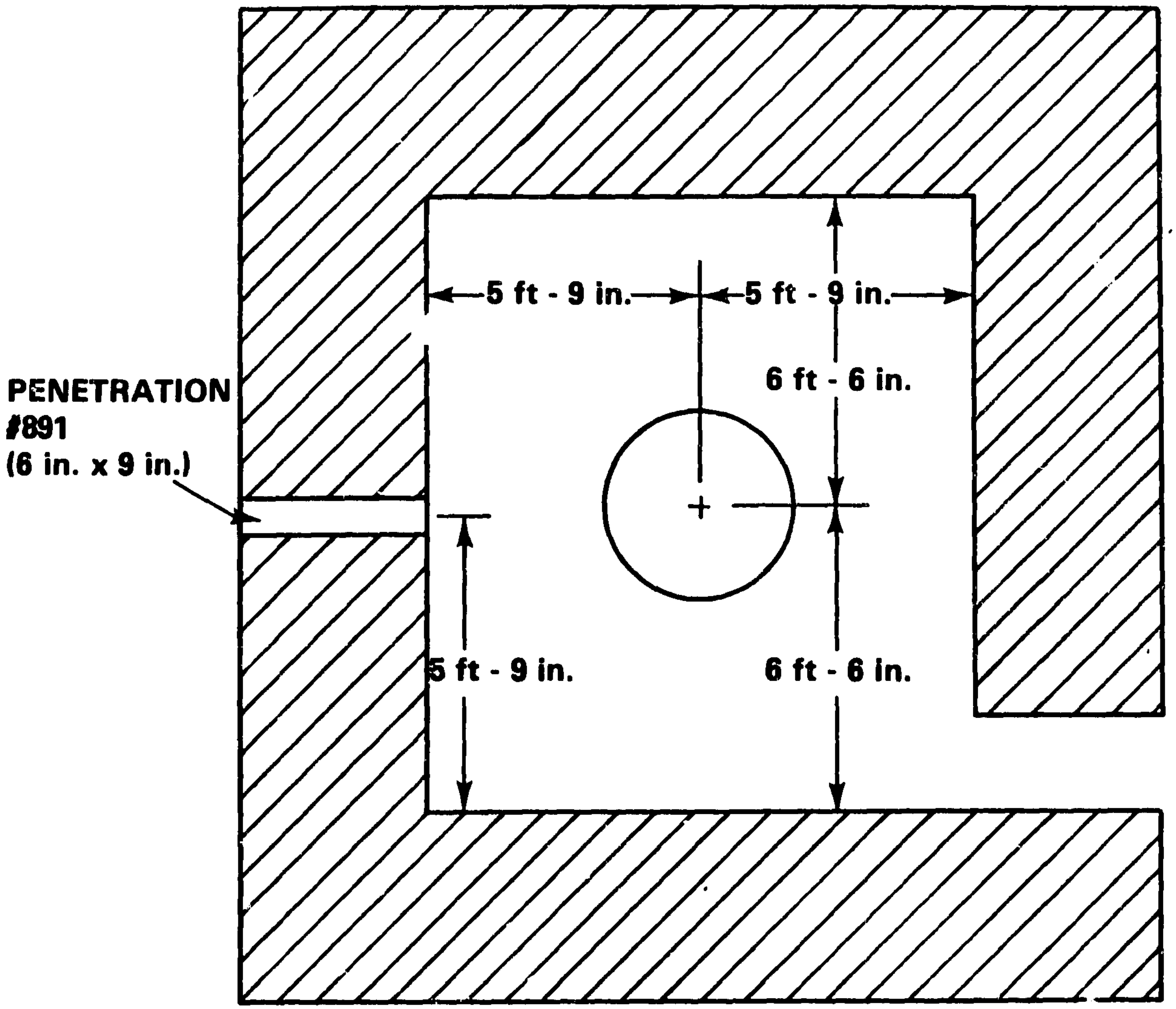

HEDL 8212-080.2

FIGURE 6. Plan view of the "A" demineralizer cell.

Results of the horizontal traverses over the region one foot south of the tank to one foot north of the tank are shown in Figures 7-10. Figures 7 and 8 show the relative source distributions for the ^{137}Cs and ^{144}Ce, respectively. Both the ^{137}Cs and ^{144}Ce show dramatically skewed horizontal source distributions. The horizontal flux distribution for ^{137}Cs 0.662 MeV gamma ray is shown in Figure 9. Figure 10 displays the ^{144}Ce 2.18 MeV gamma ray flux. As expected, the flux distributions follow the source distributions but are not as severely skewed.

Only the vertical traverses on the south side of the tank were successful. The high source intensity observed on the north side prohibited measurements on that side. The traverses on the south side were made at 1'10" from the tank wall. Figures 11 and 12 show the relative vertical source distributions for the ^{137}Cs and ^{144}Ce. The observed distributions show both the ^{137}Cs and ^{144}Ce to be limited to a region below the 309' elevation. Above 309' there is virtually no ^{144}Ce source. Some ^{137}Cs source is present above the 309' elevation. The ^{137}Cs source above 309' may be due to residual contamination left on the tank wall as the resin bed subsided due to radiation damage and thermal degradation. The vertical flux distributions for the ^{137}Cs and ^{144}Ce are shown in Figures 13 and 14.

A typical Compton recoil electron spectrum obtained in the background mode is shown in Figure 15. The Compton edges corresponding to the most significant gamma rays are labeled. Figure 16 is the foreground electron spectrum at the same location (321'9" elevation, one foot north of the tank center line). Note that Figure 16 is plotted on a 7-decade log scale whereas Figure 15 is a 6-decade log scale. The gamma ray spectrum is obtained from the observed electron spectrum by an iterative unfolding technique.(6,7) The unfolding method requires the use of a response matrix whose column elements are the responses of the detector for a given gamma ray energy. The response matrix is derived from the observed responses from a set of monoenergetic gamma ray calibration sources. Figure 17 displays the unfolded gamma ray spectrum from the electron spectrum in Figure 15.

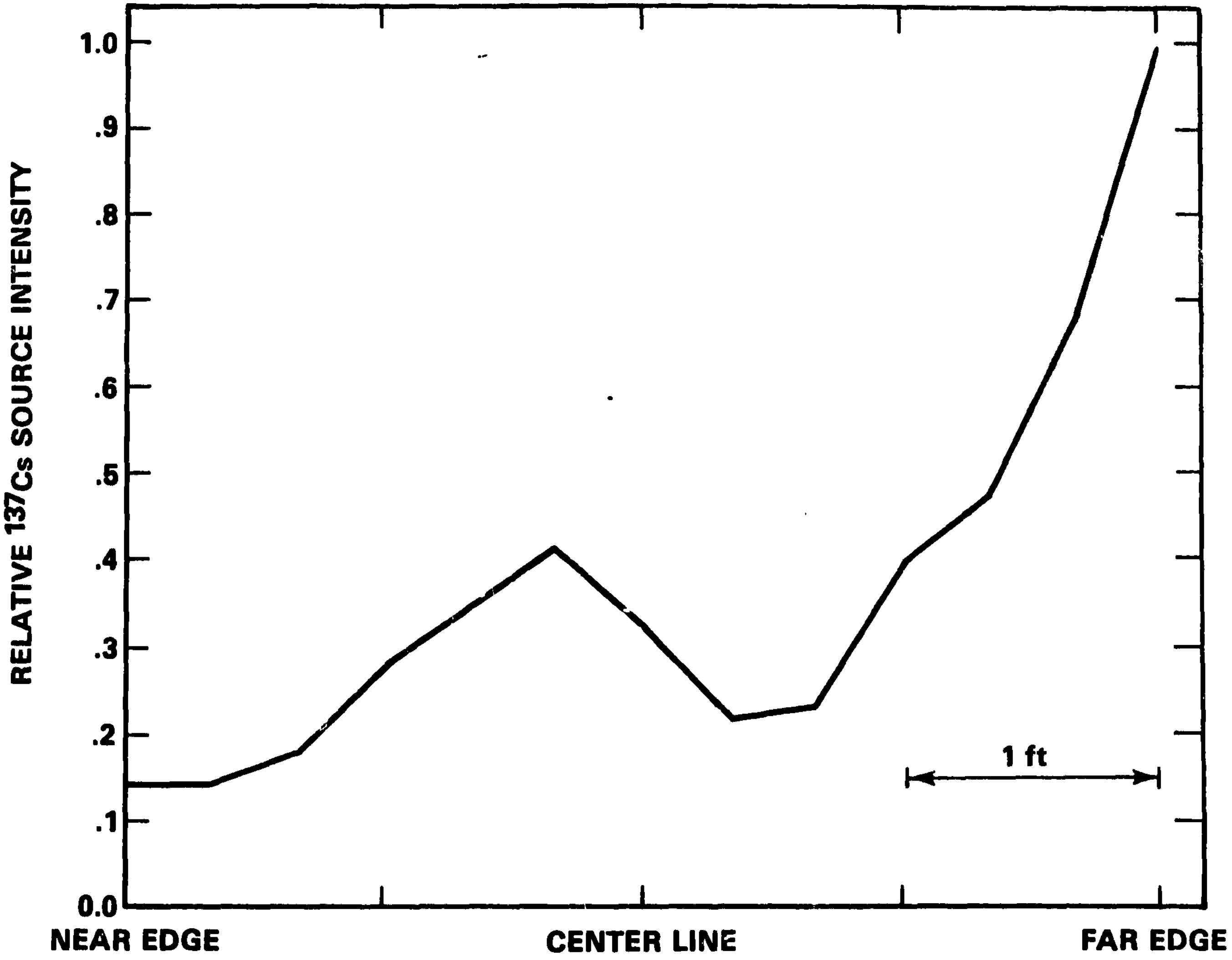

HEDL 8212-080.11

FIGURE 7. Horizontal distribution of the ^{137}Cs source intensity.

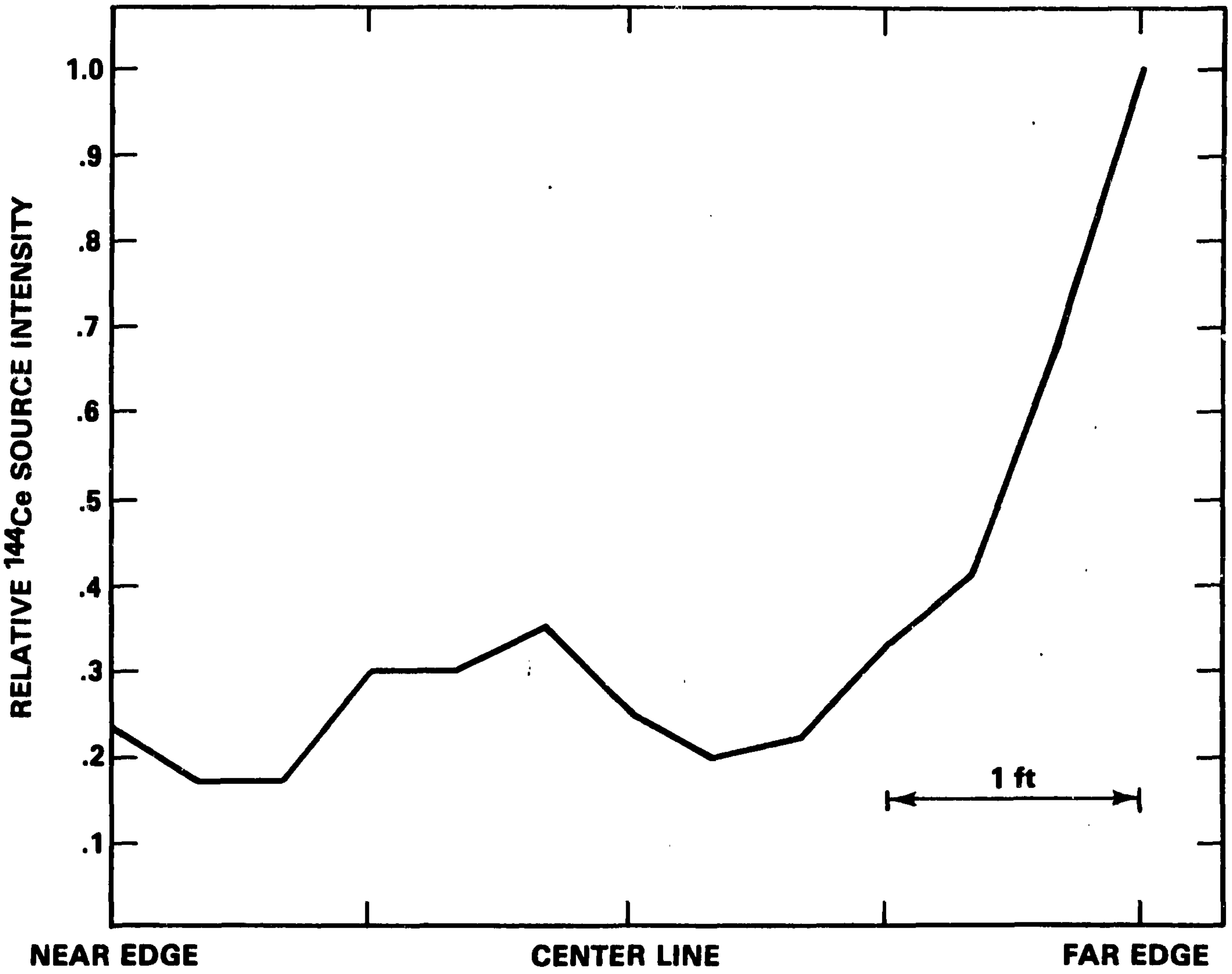

HEDL 8212-080.10

FIGURE 8. Horizontal distribution of the ^{144}Ce source intensity.

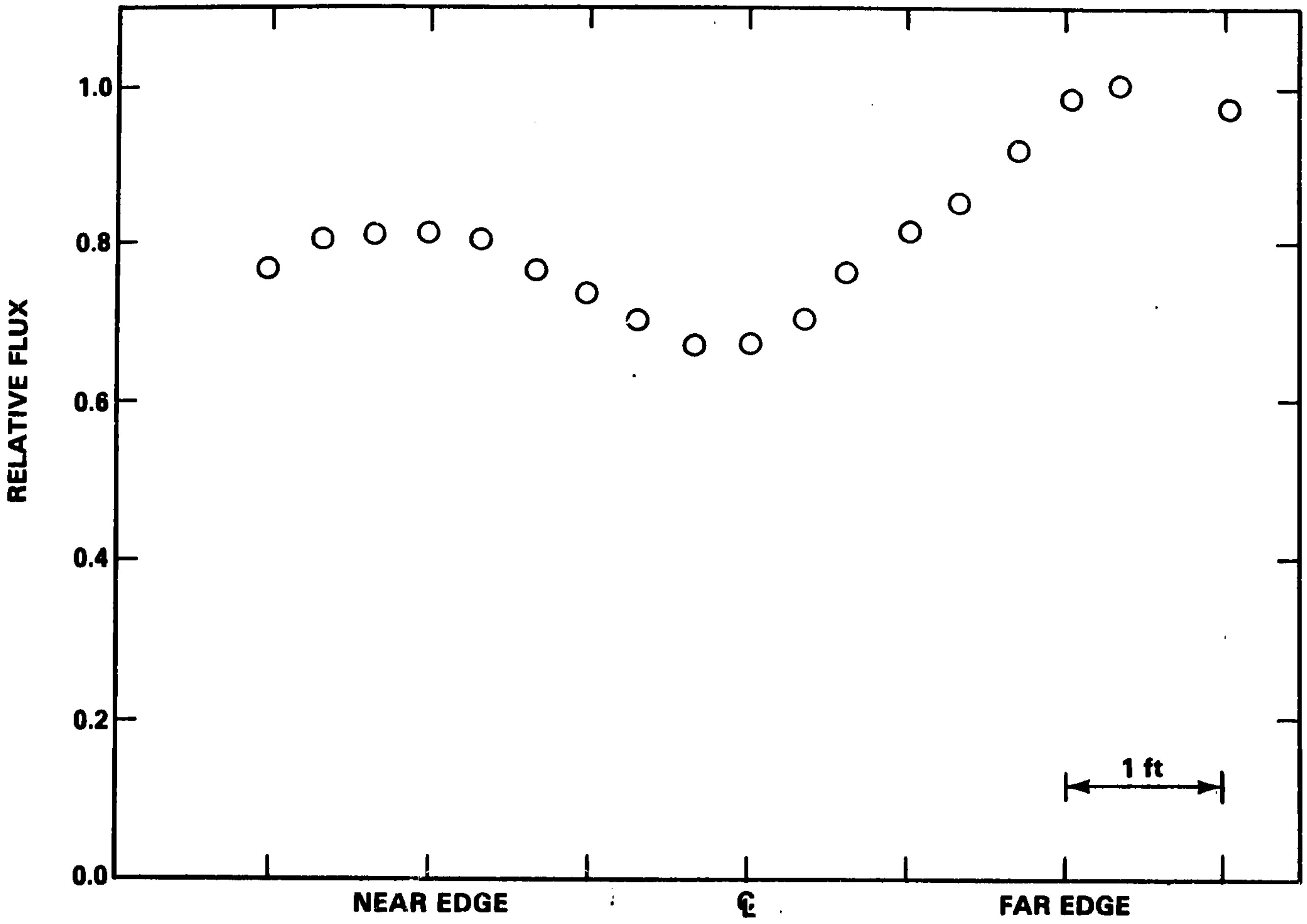

HEDL 8212-080.8

FIGURE 9. Horizontal flux distribution at 321′ 9″ for the 0.662 MeV ^{137}Cs gamma ray.

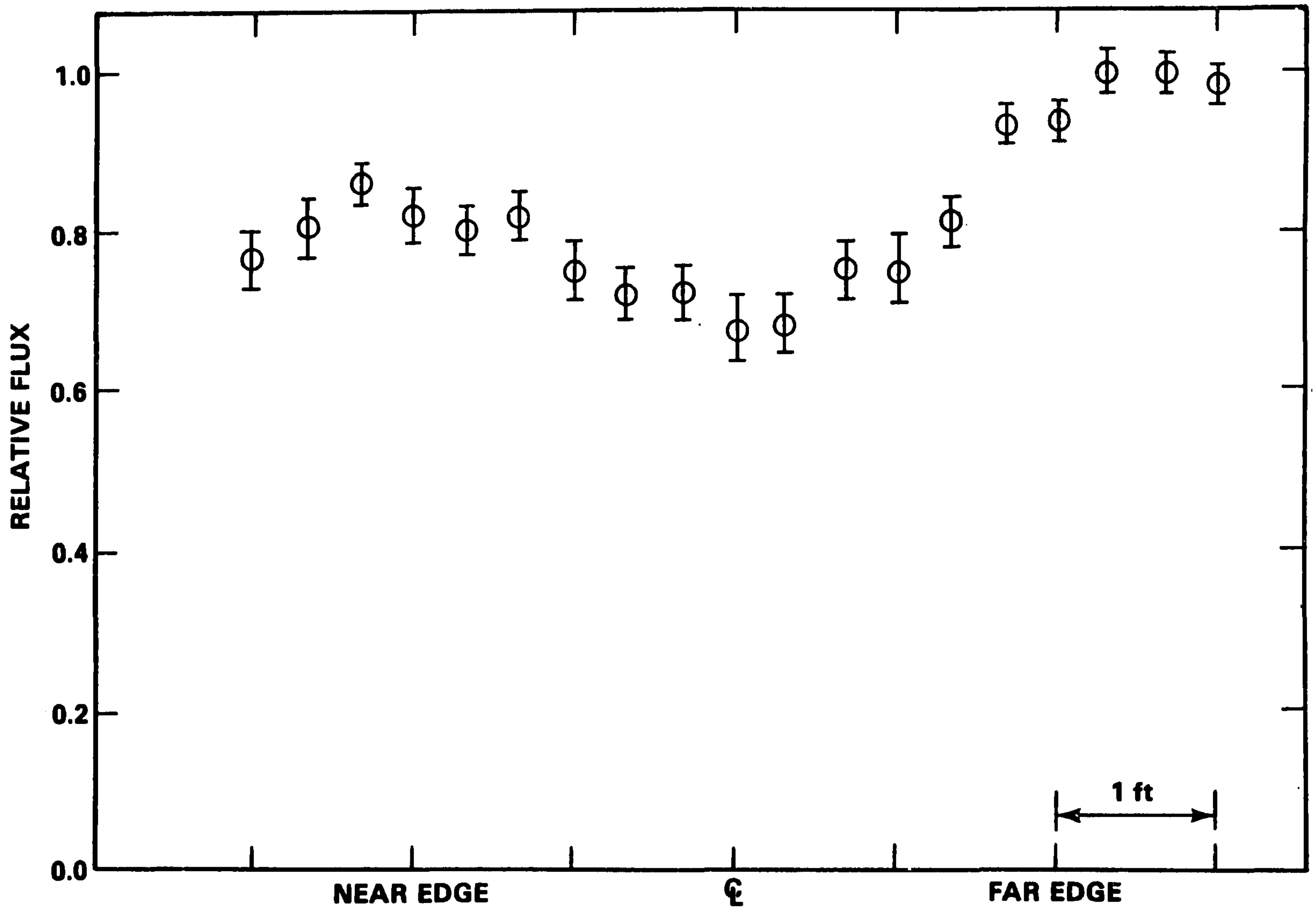

HEDL 8212-080.9

FIGURE 10. Horizontal flux distribution at 321′ 9″ for the 2.18 MeV ^{144}Ce gamma ray.

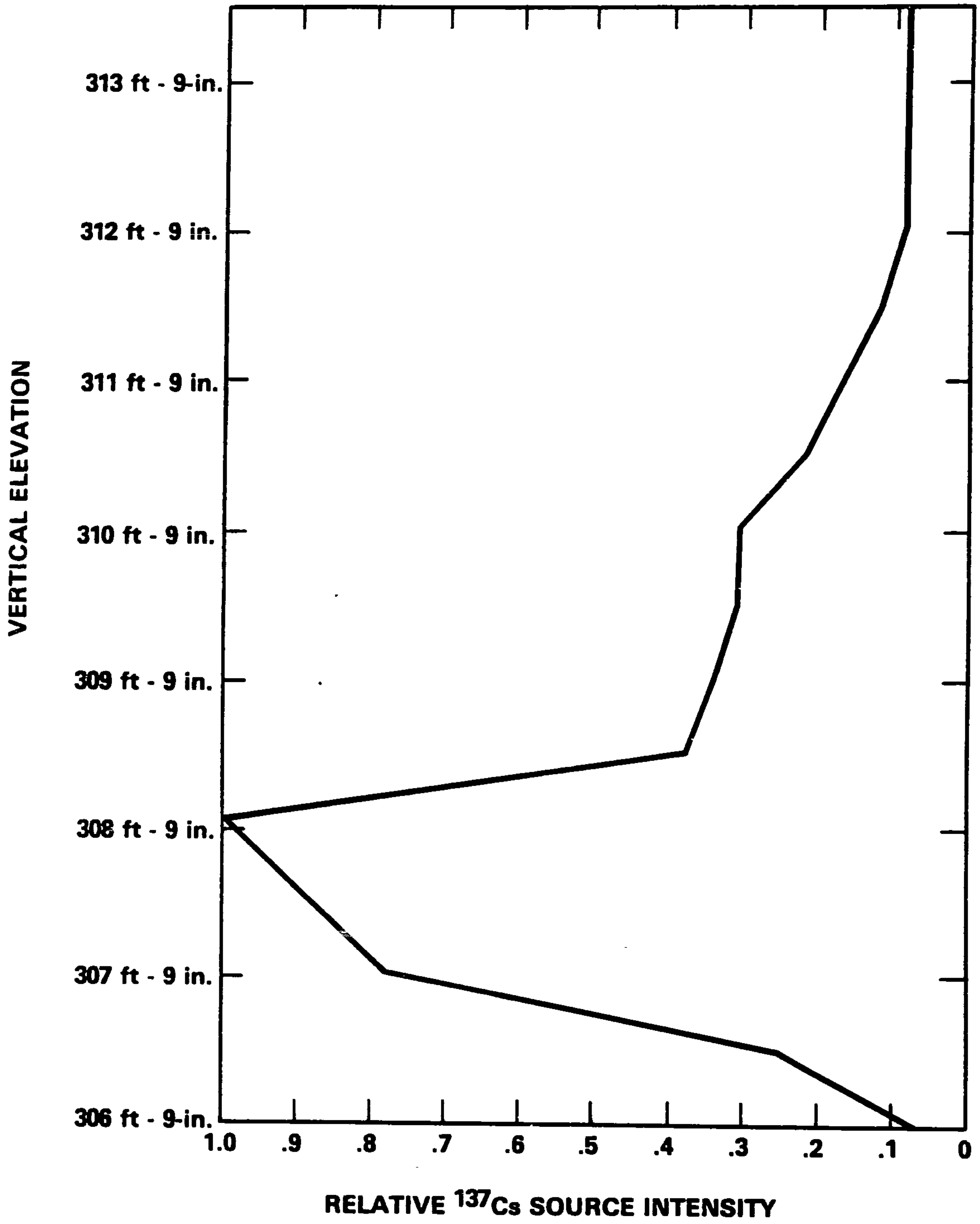

HEDL 8212-080.6

FIGURE 11. Vertical distribution of the ^{137}Cs source intensity.

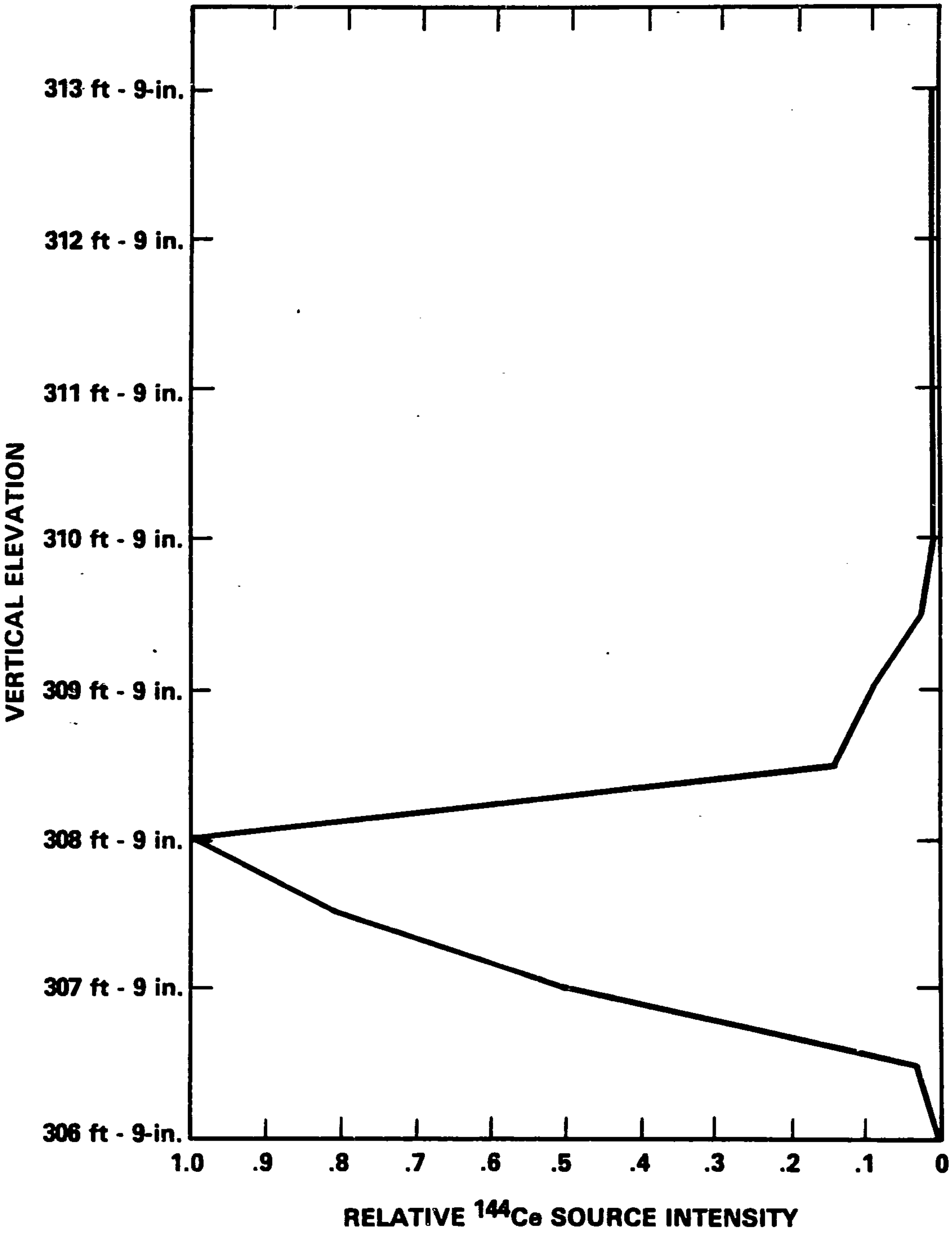

HEDL 8212-080.7

FIGURE 12. Vertical distribution of the ^{144}Ce source intensity.

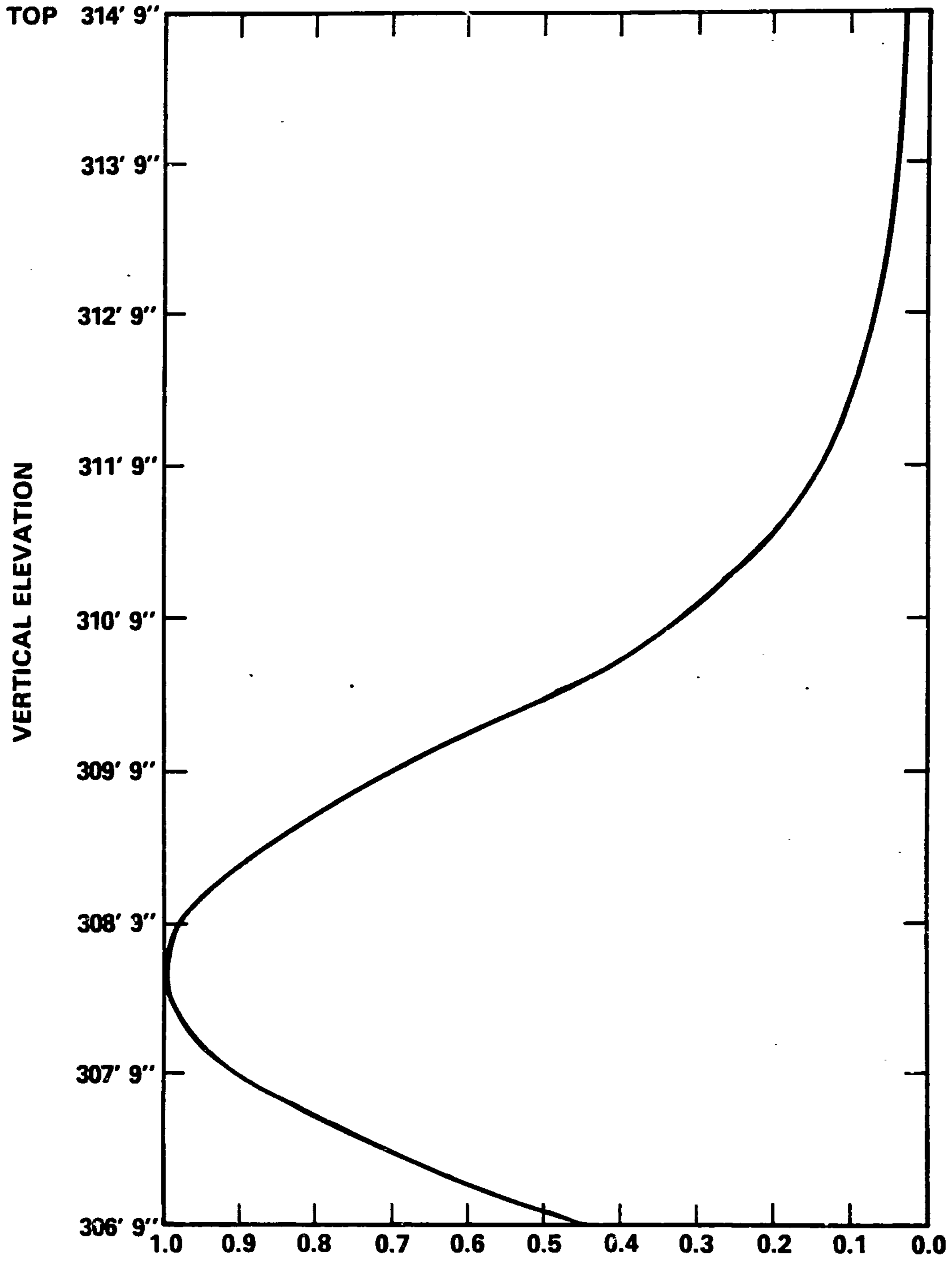

HEDL 8212-080.24

FIGURE 13. Vertical flux distribution for the 0.662 MeV ^{137}Cs gamma ray.

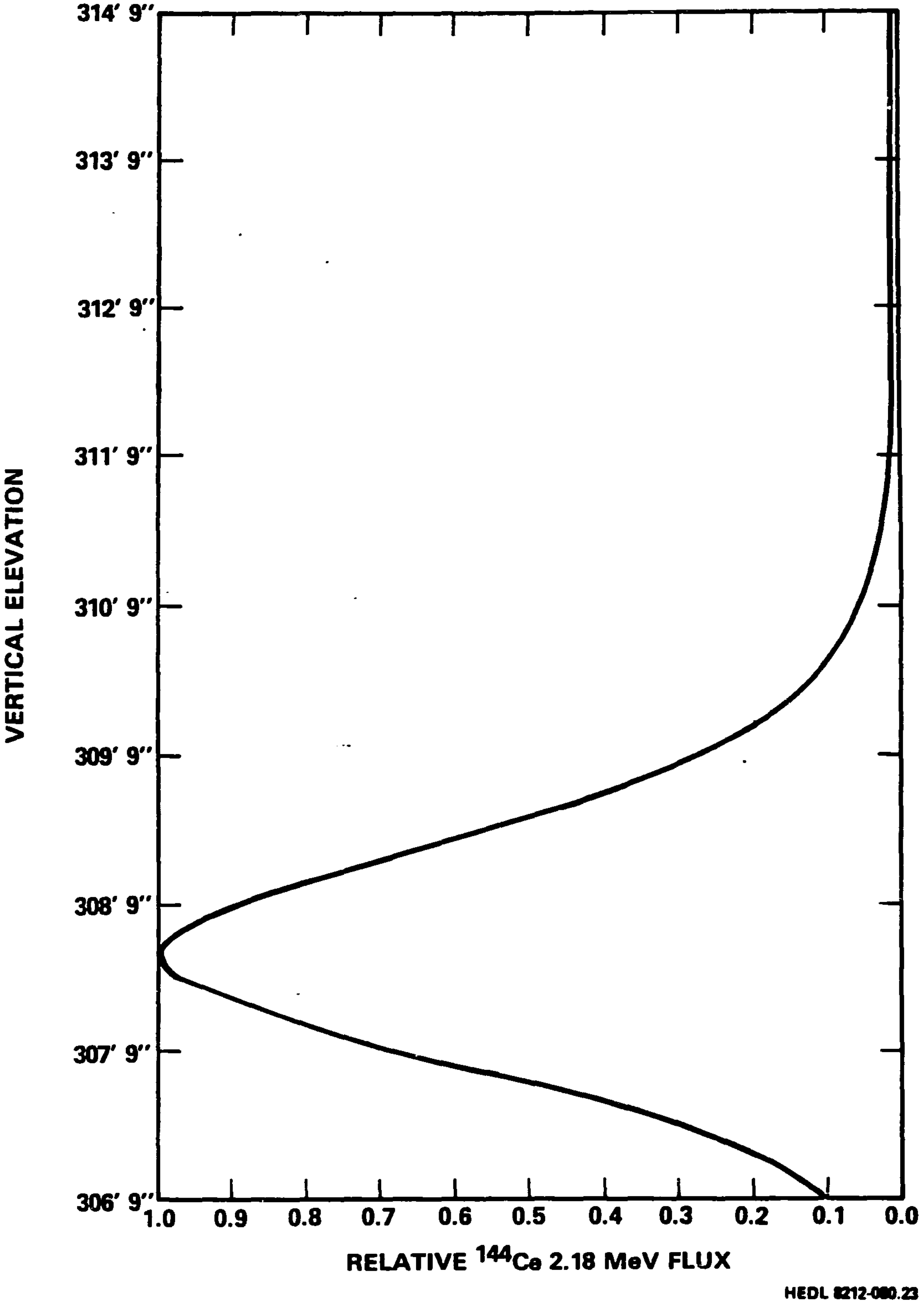

FIGURE 14. Vertical flux distribution for the 2.18 MeV ^{144}Ce gamma ray.

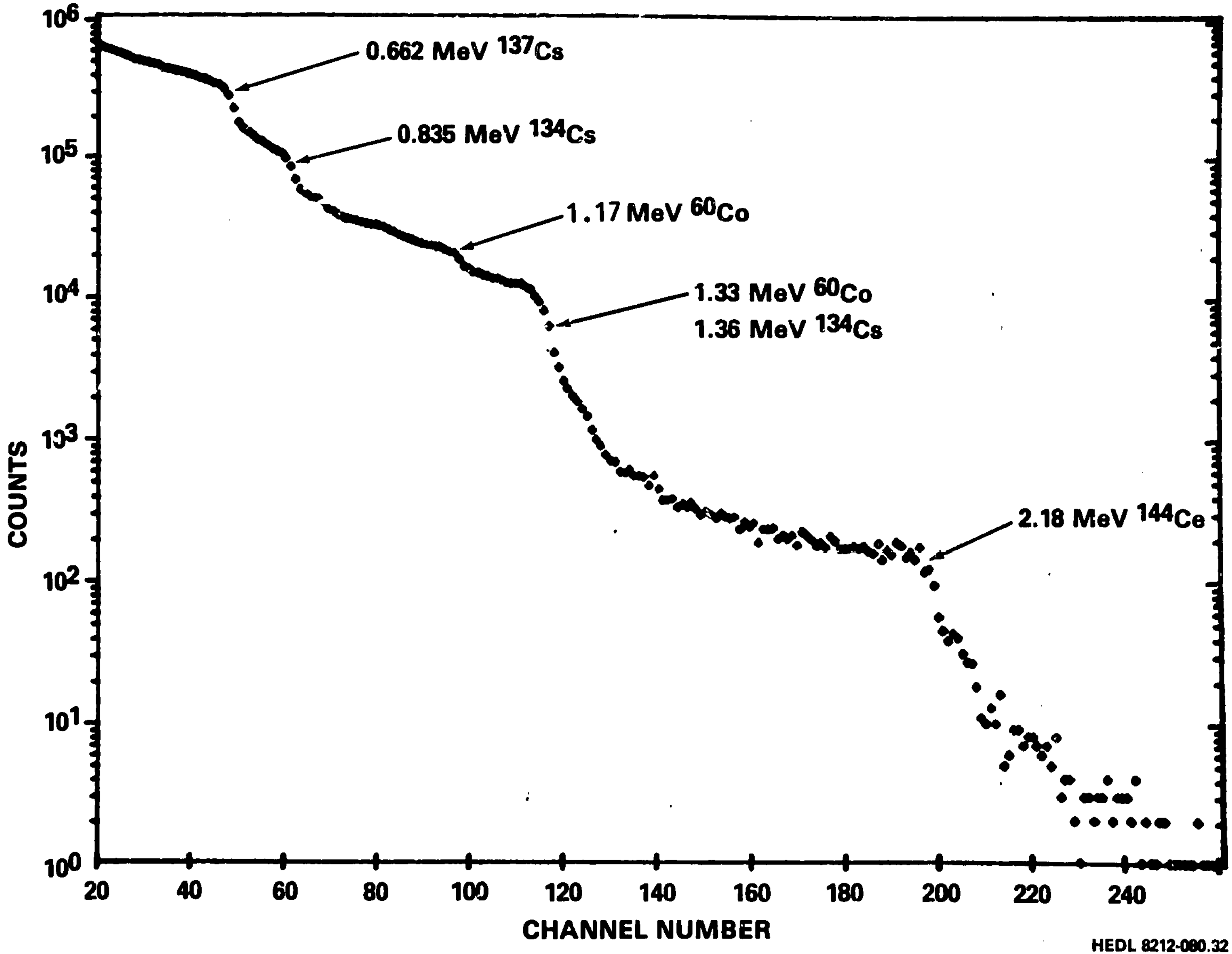

HEDL 8212-080.32

FIGURE 15. Background Compton recoil spectrum at 321′ 9″.

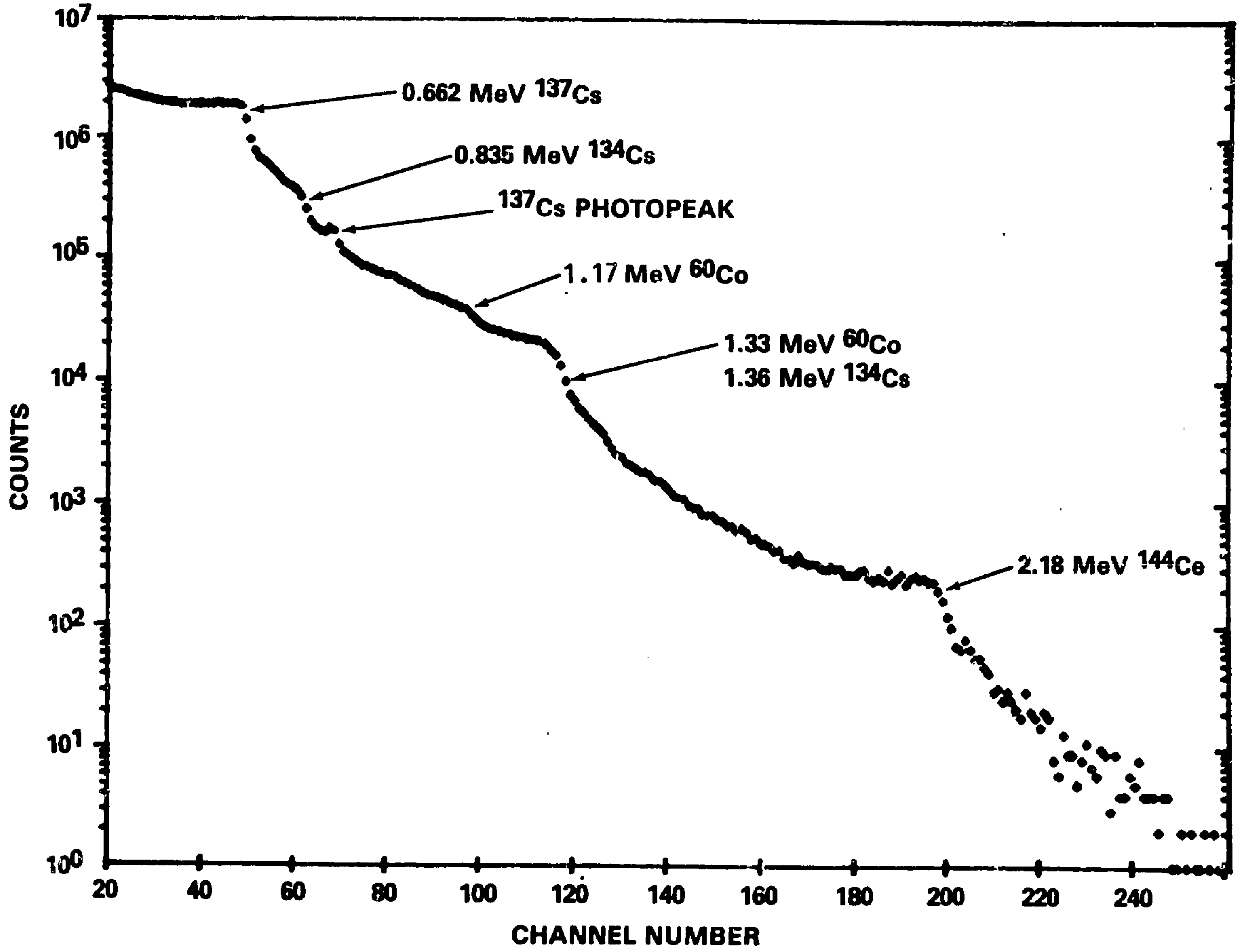

HEDL 8212-080.31

FIGURE 16. Foreground Compton recoil electron spectrum at 321′ 9″.

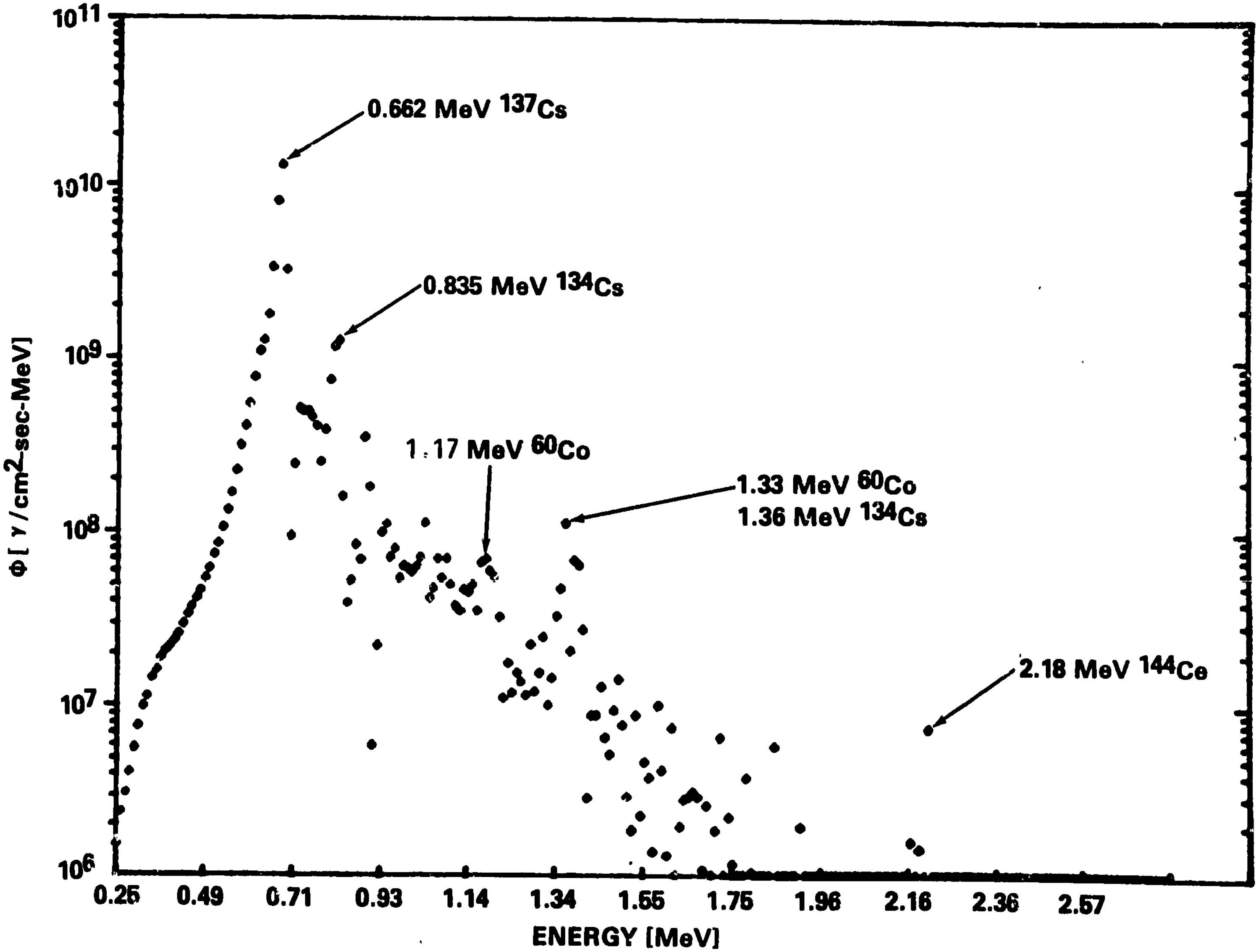

HEDL 8212-080.21

FIGURE 17. Unfolded gamma ray spectrum at the 321′ 9″ elevation.

4.0 Data Analysis

Before the ^{144}Ce flux data can be used to determine the amount of fuel in the demineralizer tank, it is necessary to establish the amount of attenuating medium inside the tank. The difference between a tank full of water and a dry tank results in a significant difference in the calculation of the fuel content. This fact is dramatically illustrated in Figure 18. Here the quantity of fuel is plotted as a function of the amount of water between the source and the spectrometer.

The Compton recoil electron spectrum from the 0.662 MeV ^{137}Cs gamma was used to determine the water equivalent attenuator in the tank. A foreground minus background spectrum at the 321'9" elevation was used. The spectrum is shown in Figure 19. A ^{137}Cs spectrum taken in the laboratory with no attenuation is shown in Figure 20.

Placing an attenuator (water) between the ^{137}Cs source and the collimated spectrometer causes the gamma flux spectrum at the detector to change. There are fewer uncollided 0.662 MeV gamma-rays and an increasing gamma continuum below 0.662 MeV due to collisions within the attenuator. The resulting Compton recoil spectrum reflects this change. Quantifying this change was accomplished with laboratory calibration experiments in which foreground and background spectra were measured for various thicknesses of water attenuator. A diagram of the experimental setup is shown in Figure 21. The resulting foreground minus background spectra for 2, 4, 8, 12 and 18 inches of water are shown in Figures 22 through 26. The two most dramatic effects of adding attenuator are broadening of the peak near the Compton edge and a decrease in the peak-to-valley ratio. It is clear from a comparison between the TMI ^{137}Cs spectrum (Figure 19) and the experimental spectra that some attenuating material is present in the tank.

It is known from the vertical traverse (see Figure 11) that the ^{137}Cs source is volume distributed within a region below the 309' elevation. The thickness is approximately two feet. The composition of the material in the tank is radiation damaged and thermally degraded ion exchange beads possibly intermixed with water. If the medium is assumed to be water equivalent in its attenuation of the ^{137}Cs,

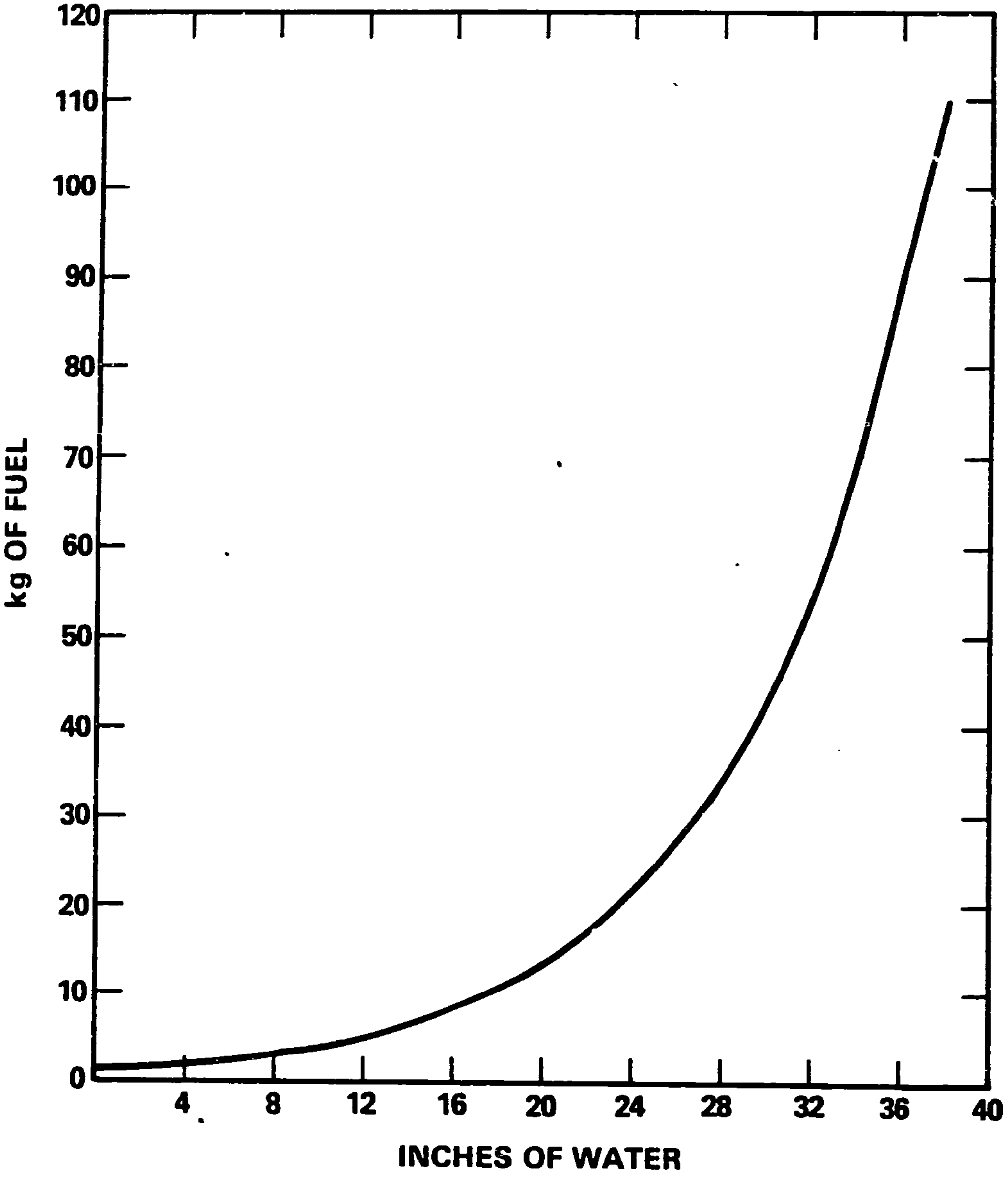

HEDL 8212-080.22

FIGURE 18. Effect of water on the calculation of the amount of fuel present in the demineralizer tank.

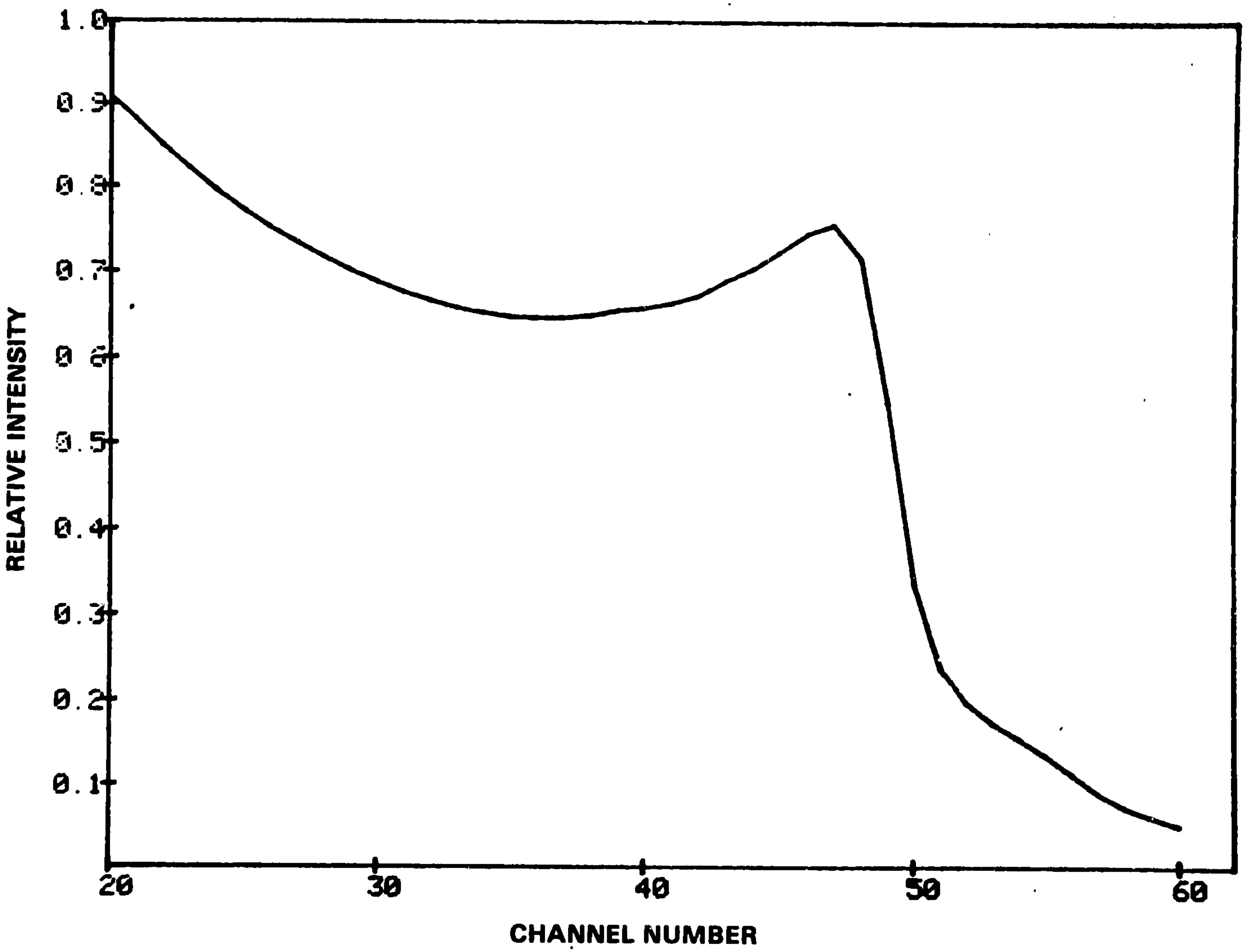

HEDL 8212-080.17

FIGURE 19. TMI foreground - background ^{137}Cs electron spectrum at 321′ 9″.

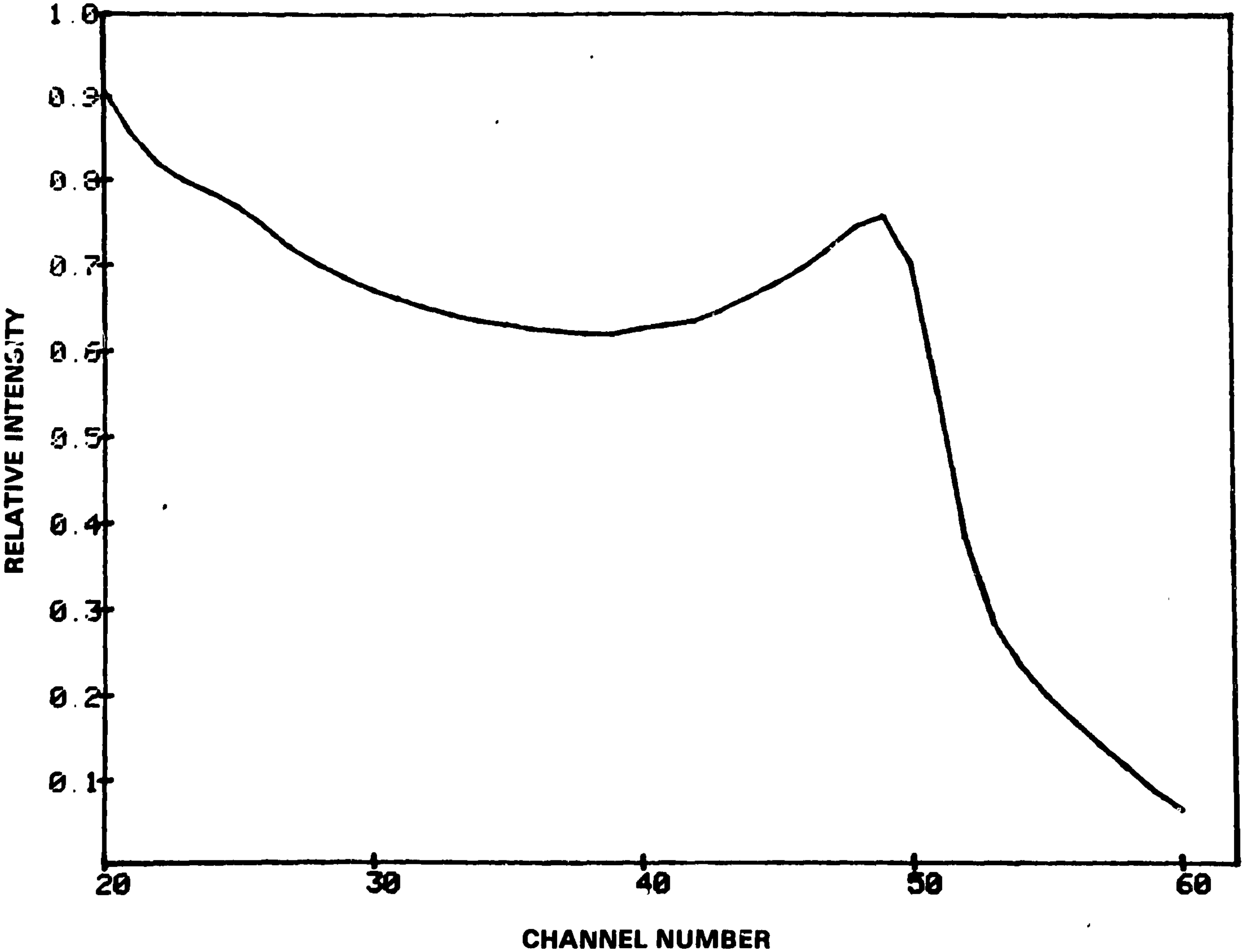

HEDL 8212-080.19

FIGURE 20. ^{137}Cs electron spectrum with no water attenuation.

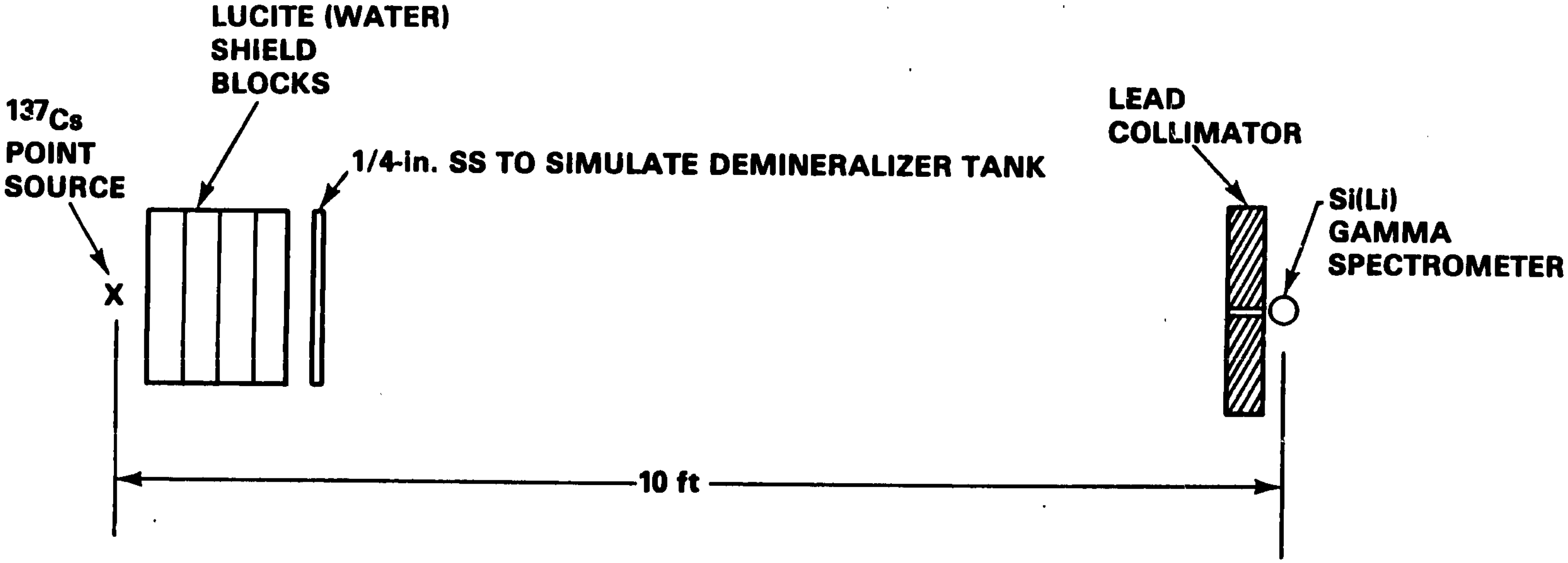

HEDL 8212-080.5

FIGURE 21. Experimental setup for measuring the effect of water attenuation on the ^{137}Cs compton recoil spectrum.

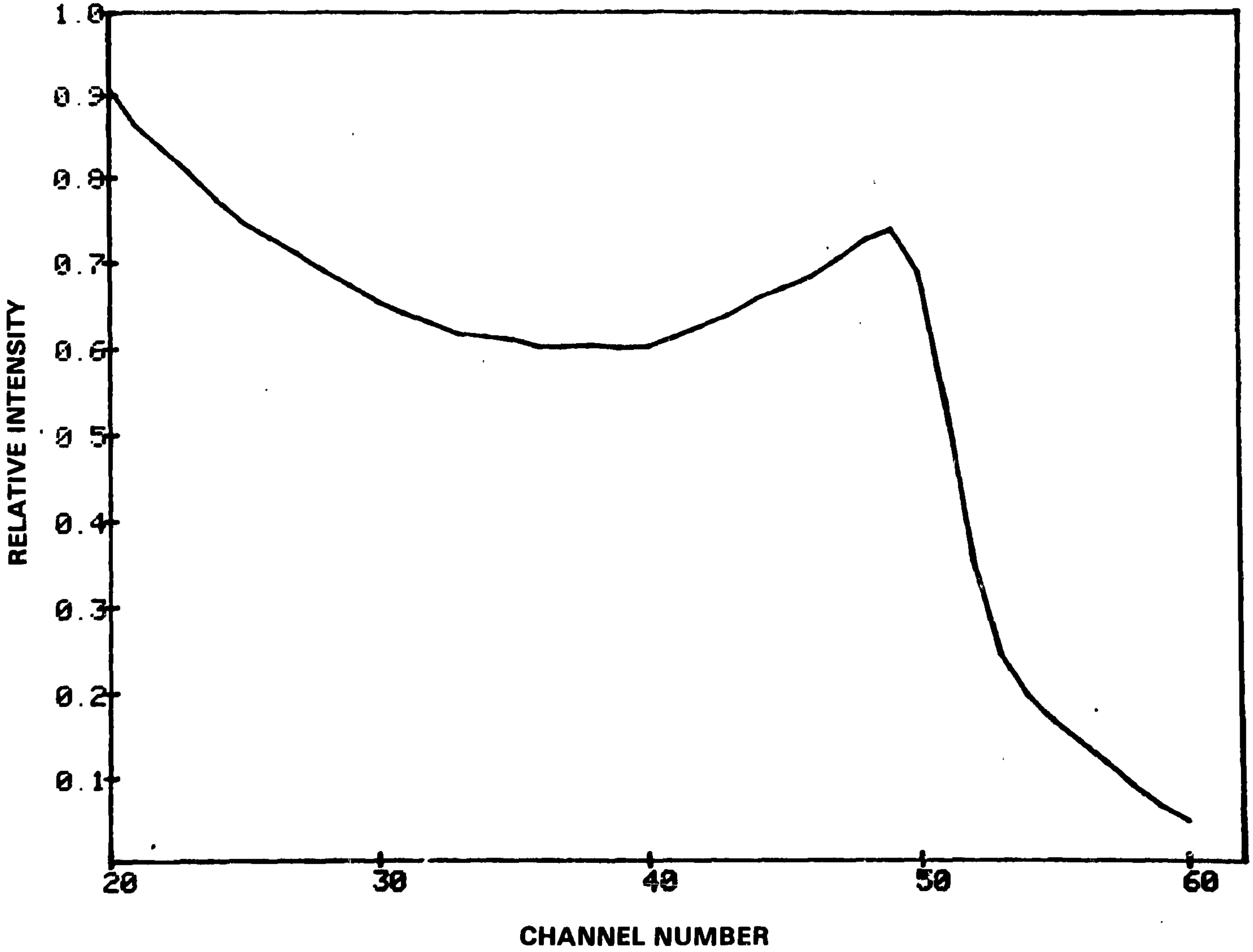

HEDL 8212-080.16

FIGURE 22. ^{137}Cs electron spectrum for 2 inches of water attenuation.

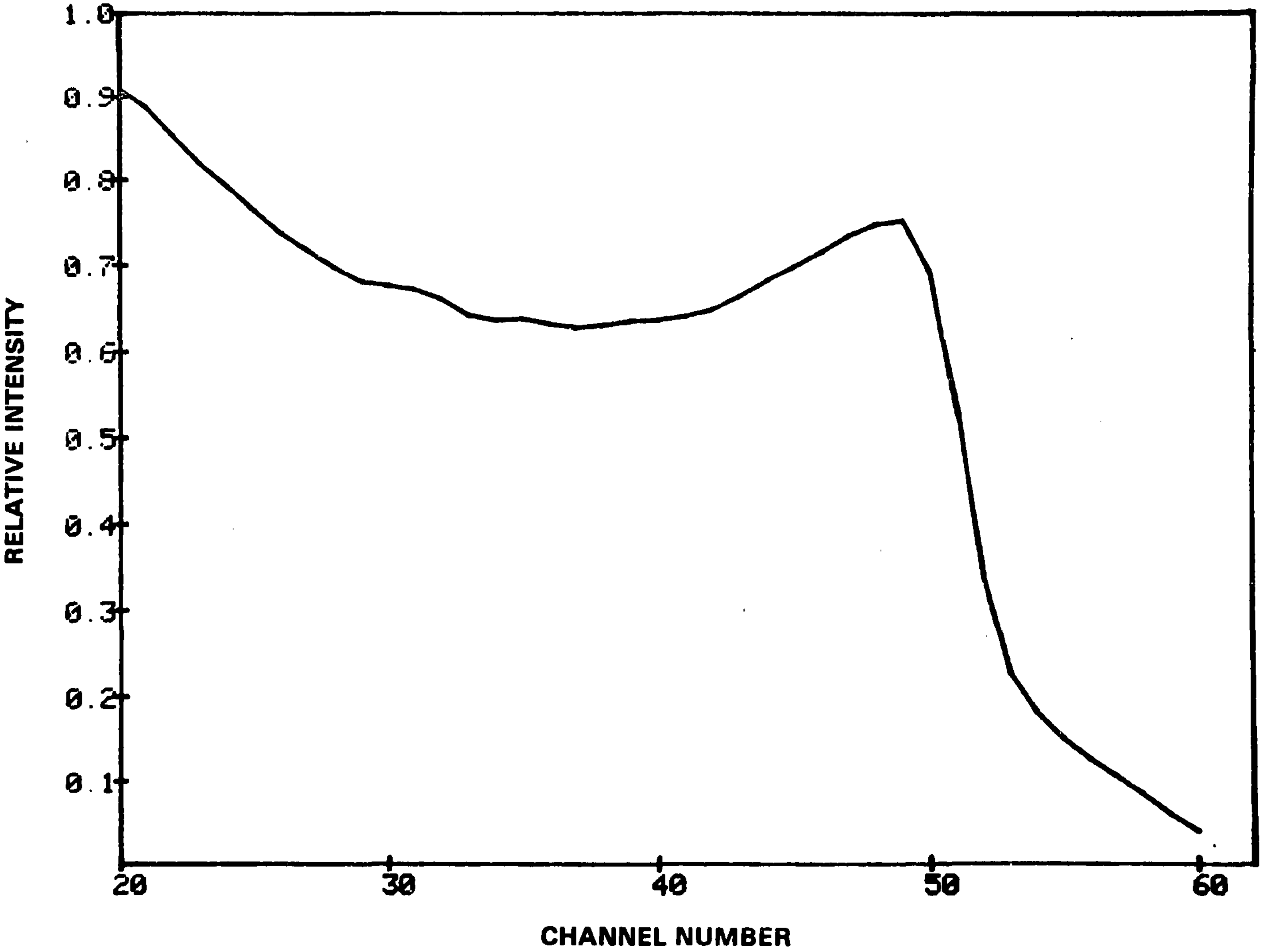

HEDL 8212-090.15

FIGURE 23. ^{137}Cs electron spectrum for 4 inches of water attenuation.

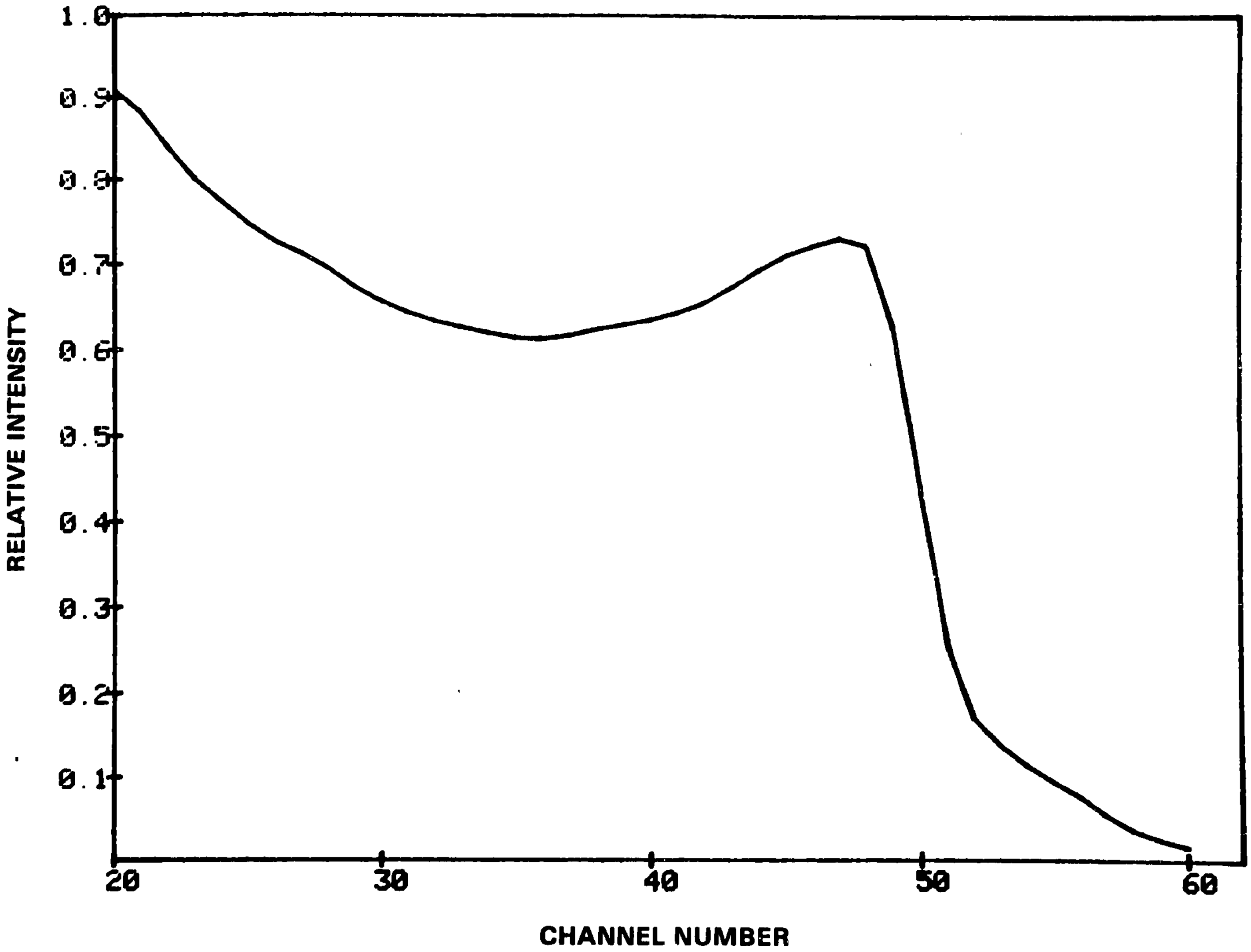

HEDL 8212-080.14

FIGURE 24. ^{137}Cs electron spectrum for 8 inches of water attenuation.

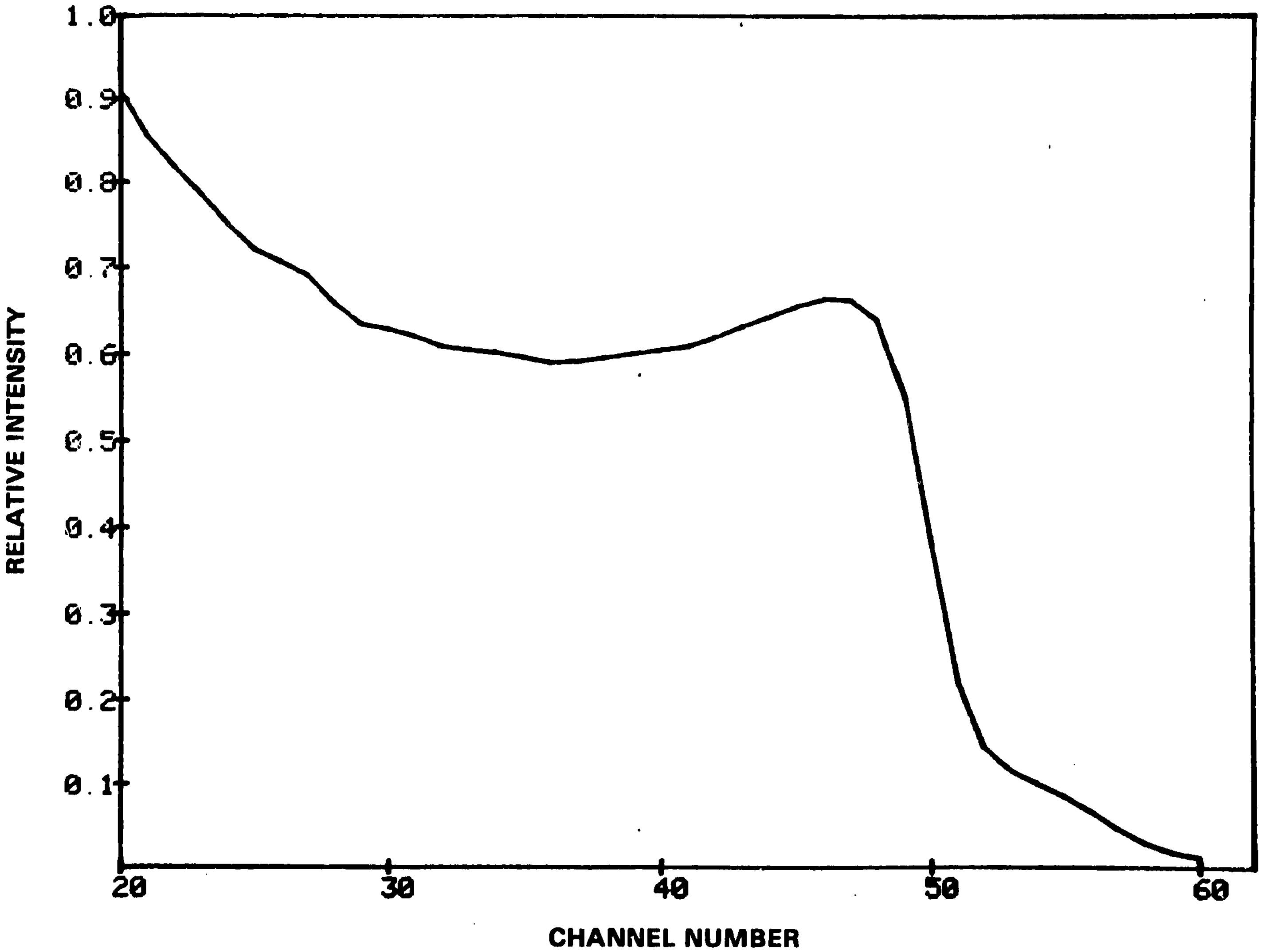

HEDL 8212-080.13

FIGURE 25. ^{137}Cs electron spectrum for 12 inches of water attenuation.

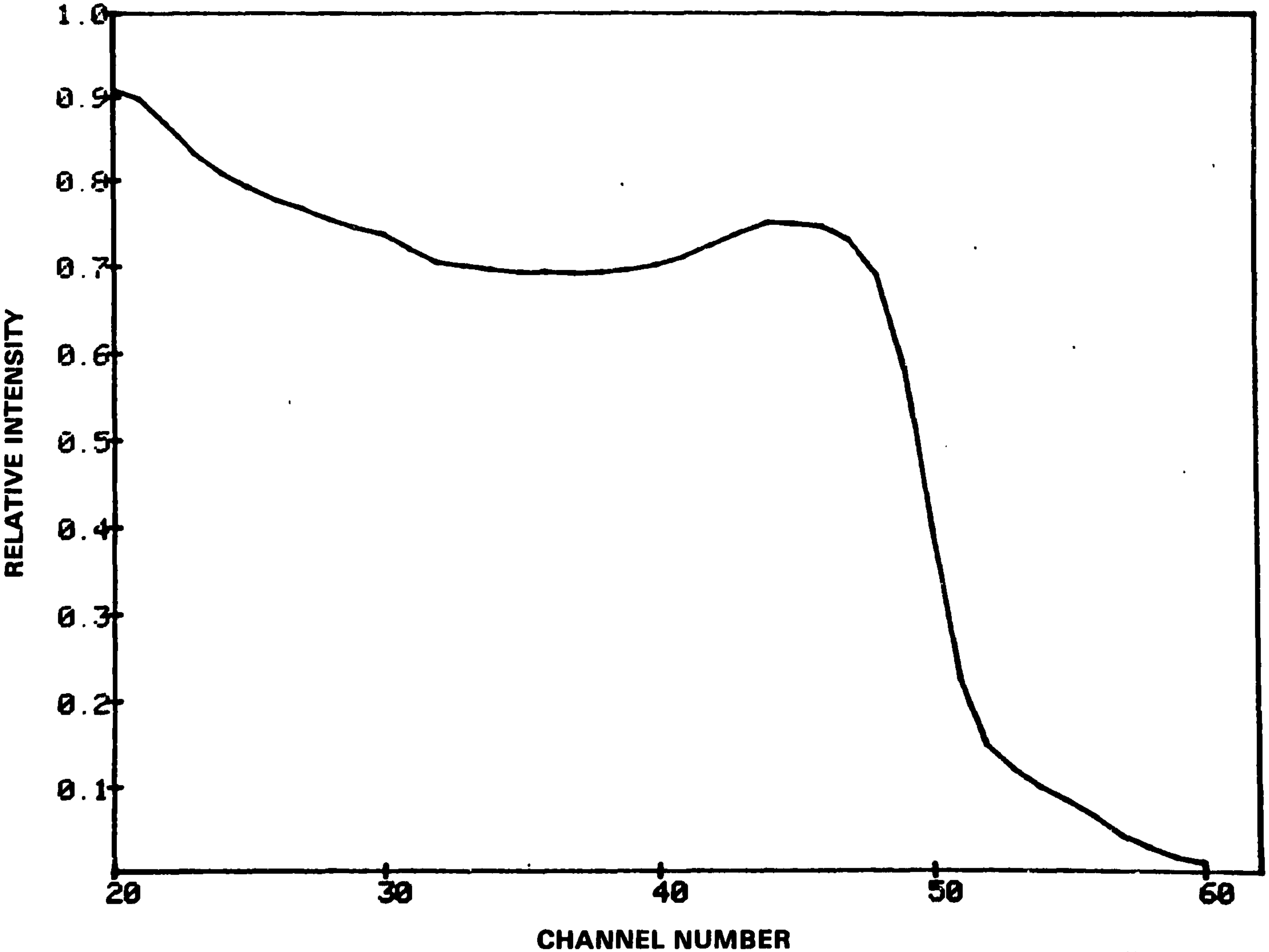

HEDL 8212-080.12

FIGURE 26. ^{137}Cs electron spectrum for 18 inches ofwater attenuation.

the source distribution from the vertical traverse can be combined with the electron spectral distributions from the experimental water attenuation calibration data to obtain the expected Compton recoil spectrum. That is, if

$P(x)$ = source intensity as a function of depth into the source

$C(x,E)$ = shape distribution of the Compton recoil spectrum as a function of water equivalent attenuator (x) and electron energy, E.

Then the observed electron spectrum, $C_{obs}(E)$ is simply:

$$C_{obs}(E) = \int P(x)C(x,E)dx \qquad [1]$$

or, as an approximation,

$$C_{obs}(E) = \sum_i P(x_i)C(x_i,E) \qquad [2]$$

The $C(x_i,E)$ were measured for x_i = 2, 4, 8, 12 and 18 inches of water equivalent absorber. The relative source intensity is obtained from the vertical traverse data fitted to a polynomial of the form

$$P(x_i) = P(o)\ (A_1+A_2x_i+A_3x_i^2) \qquad [3]$$

For the ^{137}Cs data, the polynomial is

$$P(x_i) = P(o)\ (1.0 + .13x_i - .38x_i^2) \qquad [4]$$

Using equation [4] to form the sum in equation [2] produces the Compton recoil electron spectrum shown in Figure 27. The ratio of $C_{obs}(E)$ to the TMI-2 spectrum (Figure 19) is given in Table 1. It can be seen that $C_{obs}(E)$ matches the TMI-2 spectrum within 2%.

This excellent agreement implies that the source can be defined as a simple volume distributed source in a water equivalent medium. There is no additional attenuating medium above the 309' elevation. The neutron flux measurements made with the

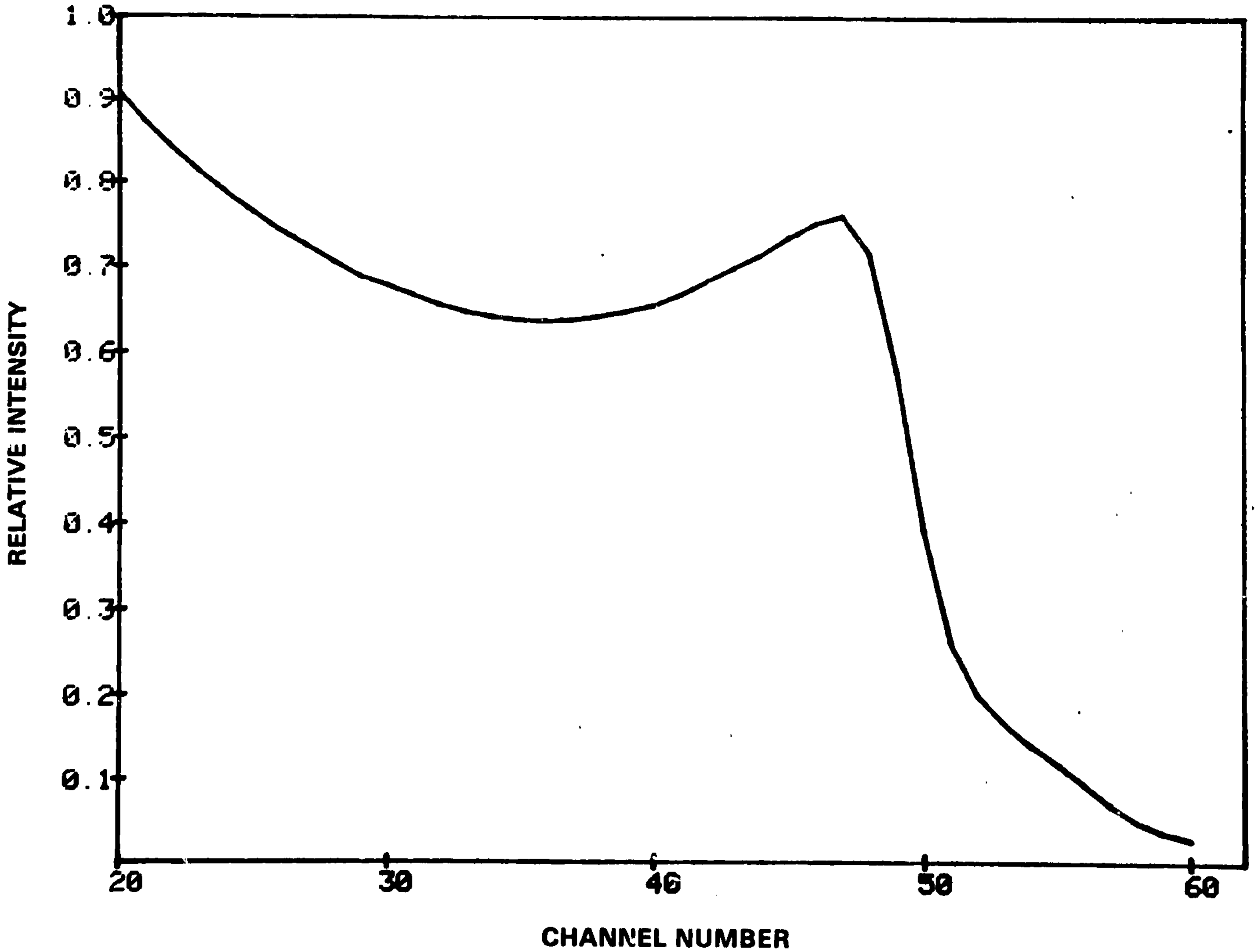

FIGURE 27. ^{137}Cs electron spectrum calculated from equation [2].

Table I. Ratio of the TMI ^{137}Cs Spectrum to the ^{137}Cs Spectrum Obtained from Equation [2].

Channel No.	Ratio of TMI ^{137}Cs/Experimental ^{137}Cs
20	1.000
21	1.008
22	1.009
23	1.010
24	1.008
25	1.009
26	1.011
27	1.014
28	1.016
29	1.019
30	1.015
31	1.015
32	1.018
33	1.018
34	1.018
35	1.018
36	1.019
37	1.017
38	1.013
39	1.012
40	1.005
41	0.996
42	0.986
43	0.988
44	0.984
45	0.987
46	0.991
47	0.995

solid state track recorder corroborate the conclusion that no water is present above the 309' elevation.(2) With the source geometry so defined the absolute source intensities for the ^{144}Ce and ^{137}Cs can be calculated.

Calculation of the total source is based on flux measurements at the 321'9" elevation and a source made up of 4' diameter disks at various depths in a water equivalent medium. The relative source intensity as a function of depth is given by polynomial fits to the vertical ^{144}Ce traverse data (see Figure 11):

$$P(x_i) = P(o)\cdot(1.0 - .237x_i - .27x_i^2) \qquad [5]$$

The equation for the flux from a disk source is

$$\phi = S_A/4 \ln (R^2/L^2 + 1)\, e^{-\mu x} \qquad [6]$$

where

ϕ = flux

S_A = source/unit area

R = radius of source

L = distance from center of source to the detector

μ = attenuation coefficient for water

x = distance below 309'

This is not an exact representation of the flux from a disk source. However, it is accurate to better than 5% for the R/L ratio of the TMI flux measurements.

Therefore, the flux measured at the 321'9" elevation is given by the sum:

$$\phi = S_A/4 \sum_i P(x_i) \ln (R^2/L^2 + 1)\, e^{-\mu x} \quad , \qquad [7]$$

where the $P(x_i)$ are the polynomial fits to the vertical ^{144}Ce traverse data. If the absolute flux, ϕ, is known, then equation [7] can be solved for the source term, S_A. The total ^{144}Ce source strength S_γ is then given by

$$S_\gamma = A \cdot S_A \cdot \sum_i P(x_i) \qquad , \qquad [8]$$

where A is the area of the disk source.

The absolute flux of 2.18 MeV gamma-rays from ^{144}Ce can be obtained from the background measurements made at the six locations of the horizontal scan at the 321'9" elevation. The absolute flux, Φ, is given by

$$\phi = C_\gamma \cdot N \cdot e^{\mu\tau}/T \qquad , \qquad [9]$$

where

C_γ = calibration constant

N = number of counts in the Compton edge

$e^{\mu\tau}$ = attenuation correction for a lead shield of thickness τ

T = live time of the data collection interval

Since the ^{144}Ce 2.18 MeV gamma-ray is the highest energy gamma-ray present in the source (see Figure 15), conversion can be made directly from the observed number of counts in the Compton edge to gamma-ray fluence. The calibration constant for this conversion, C_γ, has been obtained from response function measurements with a relative error of five percent.(8)

Table 2 presents the ^{144}Ce 2.18 MeV gamma fluxes observed at the six positions of the horizontal scan at the 321'9" elevation. Using the average of these values in equations [7] and [8], the ^{144}Ce activity is calculated to be $S_\gamma = 4.1 \times 10^9$ γ/sec.

The fuel content of demineralizer A, S_F, can be determined from the expression

$$S_F = S_\gamma / C_F \qquad [10]$$

Table 2. Observed Gamma Ray Fluxes for ^{144}Ce and ^{137}Cs from Horizontal Traverses at the 321'9" Elevation.

Horizontal Position Relative to Tank Center Line. + is North, - is South of Center Line.	Gamma Ray Flux (γ/cm^2-sec) ^{144}Ce 2.18 MeV	^{137}Cs 0.662 MeV
-3.0	1.16×10^3	2.17×10^7
-2.0	1.12×10^3	2.30×10^7
-1.0	1.24×10^3	2.06×10^7
0.0	1.03×10^3	1.89×10^7
+1.0	1.08×10^3	2.30×10^7
+2.0	1.55×10^3	2.77×10^7
+3.0	-	2.74×10^7
Average Flux	1.20×10^3	2.32×10^7

where C_F is the conversion factor representing the amount of ^{144}Ce 2.18 MeV gamma-ray activity per Kg of TMI-2 fuel. This conversion factor has been derived from the calculated fuel fission product inventory.$^{(9)}$ The value for C_F is 3.16 x 10^9 γ/sec-Kg corrected to mid-October, 1982. Using these results in equation [10] gives the fuel content of demineralizer A as

$$S_F = \frac{4.1 \times 10^9}{3.16 \times 10^9} = 1.30 \text{ Kg.}$$

It must be stressed that this value of fuel content assumes complete retention of the ^{144}Ce fission product in the TMI-2 fuel. This assumption is supported by the similar chemical behavior of Ce and TMI-2 uranium oxide fuel as well as examination of samples taken at different locations in the TMI-2 primary coolant system.

Experimental error of these measurements can be obtained from equations [7], [8] and [9]. From equation [9] the relative error in the flux, (σ_ϕ/ϕ), can be expressed as

$$\left(\frac{\sigma_\phi}{\phi}\right)^2 = \left(\frac{\sigma_N}{N}\right)^2 + \left(\frac{\sigma_{C_\gamma}}{C_\gamma}\right)^2 + \left(\frac{\sigma_T}{T}\right)^2 + (\mu\tau)^2 \left(\frac{\sigma_\mu}{\mu}\right)^2 \quad . \qquad [11]$$

The relative errors in N, C_γ, and T are 7, 5 and 1 percent, respectively. The relative error in μ, the attenuation coefficient of lead, is approximately 10%. Since $\mu\tau \cong 3.2$, the last term in equation [11] dominates. On the basis of these estimates, equation [11] yields a relative error of 33 percent in the ^{144}Ce 2.18 MeV gamma-ray flux.

The relative error in S_γ, the ^{144}Ce 2.18 MeV gamma-ray activity, can be estimated in a similar manner from equations [7] and [8]. Here additional uncertainties arise from: (1) the analytical representation ($\sim$5%), (2) the attenuation coefficient of 2.18 MeV gamma-rays in water ($\sigma_\mu/\mu \sim$ 10%), and (3) the polynomial fit P(x) of the observed vertical scan ^{144}Ce data ($\sim$15%).

Accounting for these additional uncertainties in appropriate quadrature with the results of equation [11] gives a relative error, $\sigma_{S_\gamma}/S_\gamma \simeq$ 41 percent.

Using equation [10], the relative error in the fuel content of demineralizer A can be written as

$$(\sigma_{S_F}/S_F)^2 = (\sigma_{S_\gamma}/S_\gamma)^2 + (\sigma_{C_F}/C_F)^2 \quad . \qquad [12]$$

Since the uncertainty of the conversion factor C_F, as based on the fission product inventory calculation, is roughly 10%, the estimated overall relative uncertainty in the fuel content is $(\sigma_{S_F}/S_F) \cong 43$ percent. Therefore the fuel content of the A demineralizer tank is 1.3 ± 0.6 Kg.

High radiation field levels outside the demineralizer B cell prevented personnel from operating the boom and winch assembly for gamma spectrometry measurements within the B cell. Gamma spectrometry was conducted only at a single location in the B cell by mounting the shielded spectrometer on a small hand cart that was pushed in through the B cell doorway.

On the basis of the foregoing analysis, it is obviously not possible to obtain a quantitative estimate of the fuel content in demineralizer B using data from this single location. Nevertheless the following qualitative speculations can be advanced using these results; namely that (1) demineralizer B contains significantly less fuel than demineralizer A, and (2) demineralizer B contains significantly more ^{137}Cs than demineralizer A.

5.0 ^{137}Cs Determination

The ^{137}Cs content of the A demineralizer is calculated in a similar manner as the ^{144}Ce source computation. The major difference is the computation of the gamma intensity from the observed electron spectrum. Unlike the ^{144}Ce gamma-ray, the ^{137}Cs 0.662 MeV gamma-ray appears in the low energy part of the spectrum. Unfolding of the spectrum as described in Section 3.0 is necessary to determine absolute gamma-ray intensity.

Table 2 shows the gamma-ray intensities at each of the horizontal locations. Using the average of these values along with the polynomial

$$P(x_i) = P(o)\ (1.0 + .13x_i - .38x_i^2)$$

already given in equation [4], yields a total ^{137}Cs source of 3400 Curies.

The uncertainty in the ^{137}Cs flux can be found from equation [11] and is completely dominated in this case by the term for the attenuation by the lead shield. Since $\mu\tau \simeq 7.4$ and $\sigma_\mu/\mu = .1$, the relative error in the flux is $\sigma_\phi/\phi \simeq .74$. This uncertainty likewise dominates the source calibration, that is $\sigma_{S_\gamma}/S_\gamma \simeq .74$. The ^{137}Cs source is, therefore 3400 ± 2500 Curies.

Knowledge of the absolute ^{137}Cs content of the demineralizer is important for the determination of the physical condition of the ion exchange resin beads. High radiation doses are known to drastically modify the physical properties of the resin. In the case of ^{137}Cs, not only is there a dose to the resin from the 0.662 MeV gamma-ray, but there is also a significant dose contribution from the beta decay particles of ^{137}Cs, whose average energy is approximately 0.25 MeV.(10) Any dose calculations must include the dose from these electrons.

Finally, it should be stressed that the error in both the ^{144}Ce and ^{137}Cs fluxes (i.e., 33 and 74 percent, respectively) can be significantly reduced. By direct experimental calibration, the shield attenuation factor could be determined to an experimental error of better than 10 percent. Unfortunately, as a result of this TMI-2 campaign, this shield (see Figure 2) has become contaminated and therefore has not as yet been available for such experimental determinations.

ACKNOWLEDGMENTS

The support and exchange of ideas with government agencies, industrial participants and advisory groups associated with TMI-2 recovery is acknowledged; notably DOE, EPRI, NRC, GPU and the Technical Assistance and Advisory Group (TAAG) Committee for TMI-2 recovery. Continued WHC management support on the TMI-2 demineralizer resin removal program provided the incentive for demonstrating the advanced gamma detection capabilities using the Si(Li) Compton recoil gamma ray spectrometer.

Numerous individuals were involved in the preparation for the TMI-2 campaign. Gerry Crouch and Dale Selle (WHC) were responsible for fabrication of the spectrometer. Evan Jensen, Fred Holt, Gary Jones (WHC) and Margaret Kress (PNL) assisted in the calibration of the detector. Bill McElroy, Frank Ruddy, Parvin Lippincott and Jim Roberts (WHC) provided encouragement and suggestions throughout the campaign.

The assistance of Herb Sanchez (EG&G) and Ken Lionarons (GPU) during the measurements is acknowledged.

References

1. R. Gold, F. H. Ruddy, J. H. Roberts, C. C. Preston, J. A. Ulseth, W. N. McElroy, F. J. Leitz, B. R. Hayward, and F. A. Schmittroth, "Calibration of SSTR Neutron Dosimetry for TMI-2 Applications," Proceedings of the Fifth Pacific Northwest Working Group on Nuclear Track Registration, July 28-29, 1982, Richland, Washington.

2. F. H. Ruddy, J. H. Roberts, R. Gold, C. C. Preston, and J. A. Ulseth, "Solid State Track Recorder Neutron Dosimetry Measurements for Fuel Debris Assessment of TMI-2 Makeup and Purification Demineralizer-A" Hanford Engineering Development Laboratory, HEDL-TC-2492, 1983.

3. R. Gold, B. J. Kaiser, F. S. Moore, Jr., W. L. Bunch, W. N. McElroy, and E. M. Sheen, "Continuous Gamma Ray Spectrometry in the Fast Flux Test Facility," ANS Topical Meeting on 1980 Advances in Reactor Physics and Shielding, Sun Valley, Idaho, September 14-17, 1980. ISDN #0-89448-107-X, p. 803 (1980).

4. B. J. Kaiser, R. Gold, and J. P. McNeece, Si(Li) Gamma-Ray Dosimetry, W. N. McElroy Ed., LWR Pressure Vessel Dosimetry Improvement Program: PCA Experiments and Blind Test, NUREG/CR-1861, p. 5.3-1 (1981).

5. R. Gold, B. J. Kaiser, and J. P. McNeece, "Gamma-Ray Spectrometry in Light Water Reactor Environments," Fourth ASTM-EURATOM International Symposium on Reactor Dosimetry, NBS, Washington, D. C., March 1982 (invited paper).

6. R. Gold and I. K. Olson, Analysis of Componton Continuum Measurements, ANL-7611 Argonne Natinal Laboratory, Argonne, Illinois 1970.

7. R. Gold, An Iterative Unfolding Method for Response Matrices, ANL-6984 Argonne National Laboratory, Argonne, Illinois 1964.

8. R. Gold and B. J. Kaiser, Gamma Ray Spectrometry, W. N. McElroy, Ed., LWR Pressure Vessel Dosimetry Improvement Program: PCA Experiments and Blind Tests, NUREG/CR-1861 p. 5.2-1 (1981).

9. Krishna Vinjamuri, et al Nondestructive Techniques for Assaying Fuel Deliris in Piping at Three Mile Island Unit 2, GEND-018, EG&G Idaho Inc., Idaho Falls, Idaho 1981.

10. T. R. England, W. B. Wilson, and R. E. Schenter, ENDF/B-V Mod "0" Summary Data for Fission Products and Actinides, LA-UR 81-1418 Los Alamos Scientific Laboratory, Los Alamos, New Mexico 1981.

DISTRIBUTION FOR HEDL-7285

D. G. Doran	W/A-57	J. P. McNeece	W/A-56
E. A. Evans	W/C-23	W. J. McShane	W/B-12
R. Gold	W/C-39	E. J. Renkey	W/B-17
B. R. Hayward	W/C-44	J. H. Roberts	W/C-39
W. W. Jenkins	W/B-84	F. H. Ruddy	W/C-39
R. L. Knecht	W/A-40	F. A. Schmittroth	W/A-4
F. J. Leitz	W/C-27	W. F. Sheely	W/C-44
E. P. Lippincott	W/C-39	D. L. Swannack	W/B-84
M. K. Mahaffey	W/B-12	H. H. Yoshikawa	W/C-44
W. N. McElroy	W/C-39	Central Files	W/C-123

External

DOE/RL

J. J. Schreiber, Director
Waste Management Division

K. R. Absher

R. J. Myjak, AMAR Operations (w/o enclosure)

P. F. X. Dunigan, Jr. (3)

F. R. Standerfer

EG&G/TIO

G. J. Quinn (7)

PNL

D. E. Knowlton

RHO

R. E. Smith

ORNL

W. D. Bond

LANL

J. Halbig

HEDL-TC-2492

SOLID STATE TRACK RECORDER NEUTRON DOSIMETRY MEASUREMENTS FOR FUEL DEBRIS ASSESSMENT OF TMI-2 MAKEUP AND PURIFICATION DEMINERALIZER

PATENT STATUS

This document copy, since it is transmitted in advanced of patent clearance, is made available in confidence solely for use in performance of work under contracts with the U.S. Department of Energy. This document is not to be published nor its contents otherwise disseminated or used for purposes other than specified above before patent approval for such release or use has been secured, upon request, from the RL Patent Attorney, Richland Operations Office, U.S. DOE, Richland, Washington 99352.

Hanford Engineering Development Laboratory

HANFORD ENGINEERING DEVELOPMENT LABORATORY
Operated by Westinghouse Hanford Company
P.O. Box 1970 Richland, WA 99352
A Subsidiary of Westinghouse Electric Corporation
Prepared for the U.S. Department of Energy
Assistant Secretary for Nuclear Energy
Office of Terminal Waste Disposal and Remedial Action
under Contract No. DE-AC06-76FF02170
B&R NO. AG-30-05

Operated by
Westinghouse
Hanford Company
for the U.S. DOE

Contract No.
DE-AC06-76FF02170

A Subsidiary of
Westinghouse Electric
Corporation

P.O. Box 1970
Richland, WA 99352

Hanford Engineering Development Laboratory

INFORMATION CONCERNING USE OF THIS DOCUMENT

PURPOSE OF DOCUMENT

This is a working document required to perform, direct or integrate work under U.S. Department of Energy contracts.

NOTICE

PRELIMINARY DOCUMENT

This document contains information of a preliminary nature prepared in the course of work under U.S. DOE Contract DE-AC06-76FF02170. This information is subject to corrections or modification upon the collection and evaluation of additional data.

HEDL-TC-2492

SOLID STATE TRACK RECORDER NEUTRON DOSIMETRY MEASUREMENTS FOR FUEL DEBRIS ASSESSMENT OF TMI-2 MAKEUP AND PURIFICATION DEMINERALIZER

PATENT STATUS

This document copy, since it is transmitted in advanced of patent clearance, is made available in confidence solely for use in performance of work under contracts with the U.S. Department of Energy. This document is not to be published nor its contents otherwise disseminated or used for purposes other than specified above before patent approval for such release or use has been secured, upon request, from the RL Patent Attorney, Richland Operations Office, U.S. DOE, Richland, Washington 99352.

Hanford Engineering Development Laboratory

F.H. Ruddy
J.H. Roberts
R. Gold
C.C. Preston
J.A. Ulseth
October 1983

HANFORD ENGINEERING DEVELOPMENT LABORATORY
Operated by Westinghouse Hanford Company
P.O. Box 1970 Richland, WA 99352
A Subsidiary of Westinghouse Electric Corporation
Prepared for the U.S. Department of Energy
Assistant Secretary for Nuclear Energy
Office of Terminal Waste Disposal and Remedial Action
under Contract No. DE-AC06-76FF02170
B&R NO. AG-30-05

HEDL-TC-2492

SOLID STATE TRACK RECORDER NEUTRON DOSIMETRY MEASUREMENTS FOR FUEL DEBRIS ASSESSMENT OF TMI-2 MAKEUP AND PURIFICATION DEMINERALIZER-A

Frank H. Ruddy, James H. Roberts,
Raymond Gold, Christopher C. Preston,
and James A. Ulseth

December, 1982

Revised September, 1983

Hanford Engineering Development Laboratory
Richland, Washington

TABLE OF CONTENTS

Appendices

FIGURES

TABLES

SOLID STATE TRACK RECORDER NEUTRON DOSIMETRY MEASUREMENTS FOR FUEL DEBRIS ASSESSMENT OF TMI-2 DEMINERALIZER-A

Frank H. Ruddy, James H. Roberts, Raymond Gold, Christopher C. Preston, and James H. Ulseth

ABSTRACT

Solid State Track Recorder (SSTR) neutron dosimetry measurements have been made in TMI-2 makeup Demineralizer A Cubicle in order to assess the amount of fuel debris present by means of the specific neutron activity of TMI-2 fuel. Based on recent calibration data and the results of the TMI-2 SSTR neutron dosimetry, the amount of fuel present is estimated to be 1.7 ± 0.6 kg. This value is in excellent agreement with a value determined independently by Compton recoil gamma-ray spectrometry. Sources of uncertainty in and proposed refinements of the present SSTR measurements are discussed.

SOLID STATE TRACK RECORDER NEUTRON DOSIMETRY MEASUREMENTS FOR FUEL DEBRIS ASSESSMENT OF TMI-2 DEMINERALIZER-A

Frank H. Ruddy, James H. Roberts, Raymond Gold, Christopher C. Preston, and
James H. Ulseth

1.0 Introduction

As a result of the Three Mile Island Unit 2 (TMI-2) accident on March 28, 1979, fuel debris was dispersed into the primary coolant system of the reactor. Two makeup and purification demineralizers, A and B, which maintain coolant water purity, were in operation at the time of the accident. Due to the high gamma ray intensities in the location of these demineralizers, fuel was presumed to be located in the demineralizers. As part of the TMI-2 recovery task and WHC TMI-2 Demineralizer Resin Removal Program, the amount of fuel debris in these demineralizers required quantification before other phases of the ion exchange resin removal program could proceed.

The presence of fuel may be traced by using the radiation emitted by the fuel or fuel products. TMI-2 fuel emits two easily detectable forms of radiation which are (1) gamma rays from fission products, and (2) neutrons from actinide buildup in the fuel.

A companion paper(1) describes the use of Compton recoil electron gamma ray spectrometry to detect ^{144}Ce (which is correlated with the fuel), ^{137}Cs, and ^{134}Cs absolute gamma ray fluxes . This report describes neutron detection using solid state track recorders (SSTRs). TMI-2 fuel has an estimated average neutron specific activity of about 300 n/sec/kg,(2,3) which results mainly from Pu buildup. Assuming that Pu is a good chemical tracer for uranium, SSTR neutron dosimetry can be used to assess the location and quantity of fuel present.

The use of SSTRs for fuel detection applications has been described previously.(3) Briefly, enriched ^{235}U foils are placed in firm contact with mica SSTRs, and the neutron induced fission fragments from ^{235}U register as regions of damage (tracks) in the mica. These tracks are chemically developed to a size that is visible with a microscope. The number of tracks per unit area in the mica is proportional to the number of fissions per unit area in the adjacent uranium foil. Using appropriate calibration data, this fission rate can be used to deduce the neutron fluence. The neutron fluence and duration of exposure of the SSTRs can then be used to ascertain the amount of fuel present.

This report describes the SSTR neutron dosimetry measurements that were made in the TMI-2 Demineralizer A Cubicle and the relevant calibration measurements that were made at Hanford Engineering Development Laboratory (HEDL). On the basis of these measurements and calibrations, the amount of fuel present in TMI-2 Demineralizer A is estimated.

2.0 TMI-2 Measurements

SSTR neutron dosimeters were constructed as shown in Figures 1 and 2. Two 3" x 1" sheets of 0.004" thick 93% enriched ^{235}U were sandwiched between two pieces of mica and pressed in firm contact against an aluminum support plate between two 0.25" thick pieces of lucite. The lucite was used to enhance the neutron signal via the albedo effect which has been reported previously.(3) The total SSTR area of this neutron dosimeter is approximately 85 cm². These dosimeters were assembled at TMI-2 immediately prior to the exposure (Figures 3 and 4) to

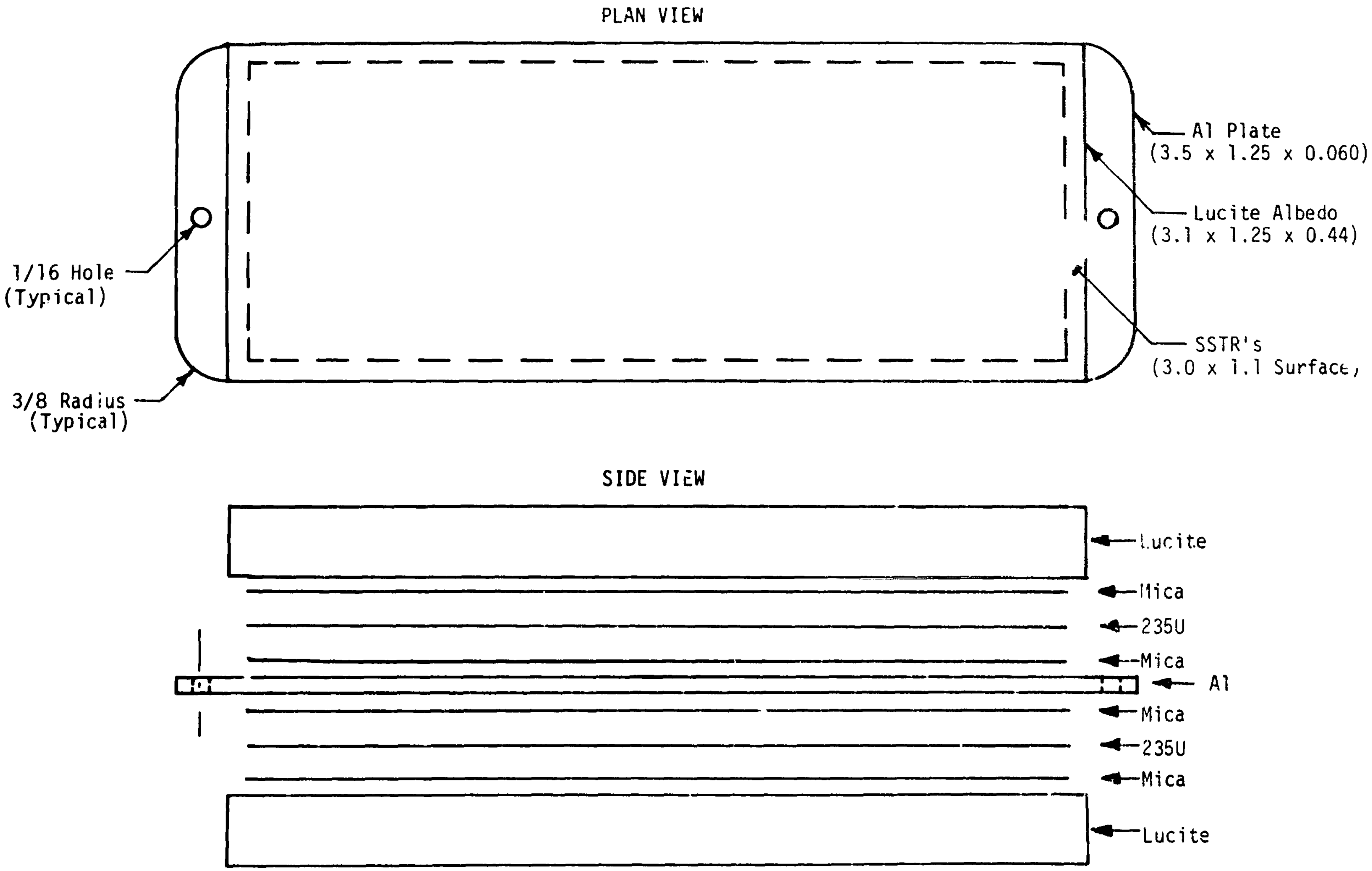

FIGURE 1. SSTR Neutron Dosimetry Holder for TMI-2 Demineralizer A Measurements. (All dimensions in inches.)

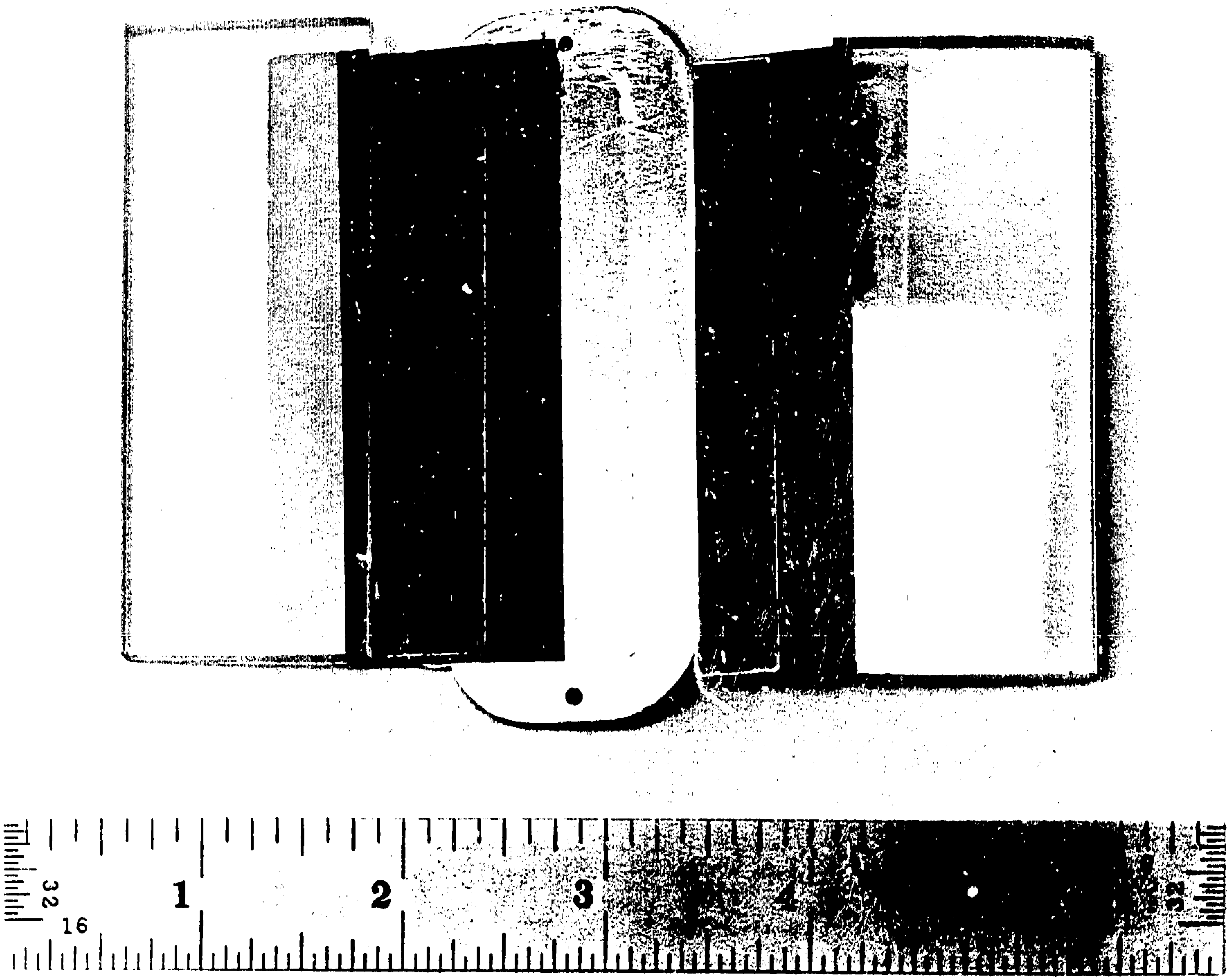

FIGURE 2. Photograph of Disassembled SSTR Neutron Dosimetry Holder. Parts are Assembled as Shown in Figure 1.

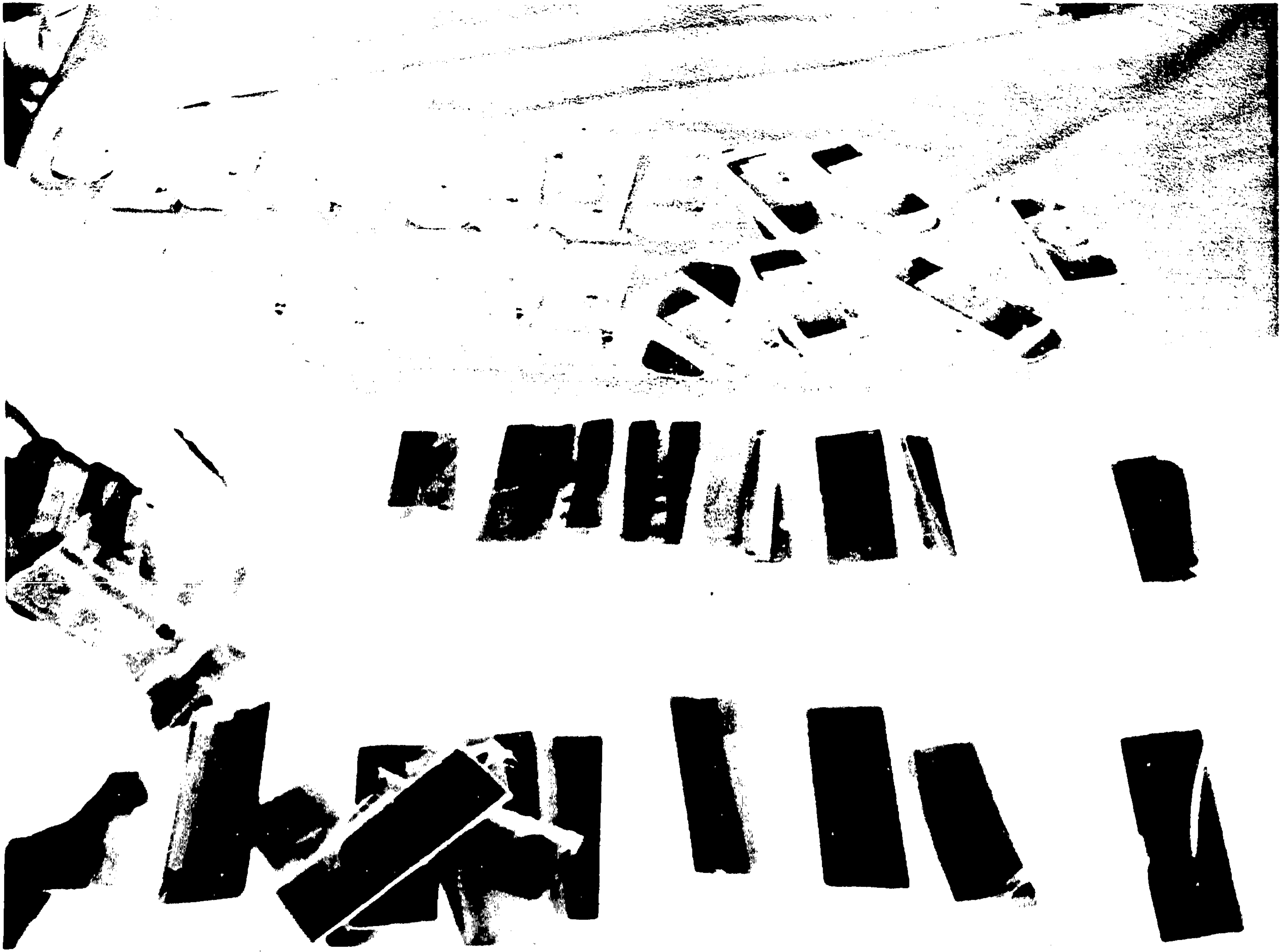

FIGURE 3. SSTR Neutron Dosimeters During Assembly. Mica and ^{235}U foils are wrapped in polyethylene bags in foreground.

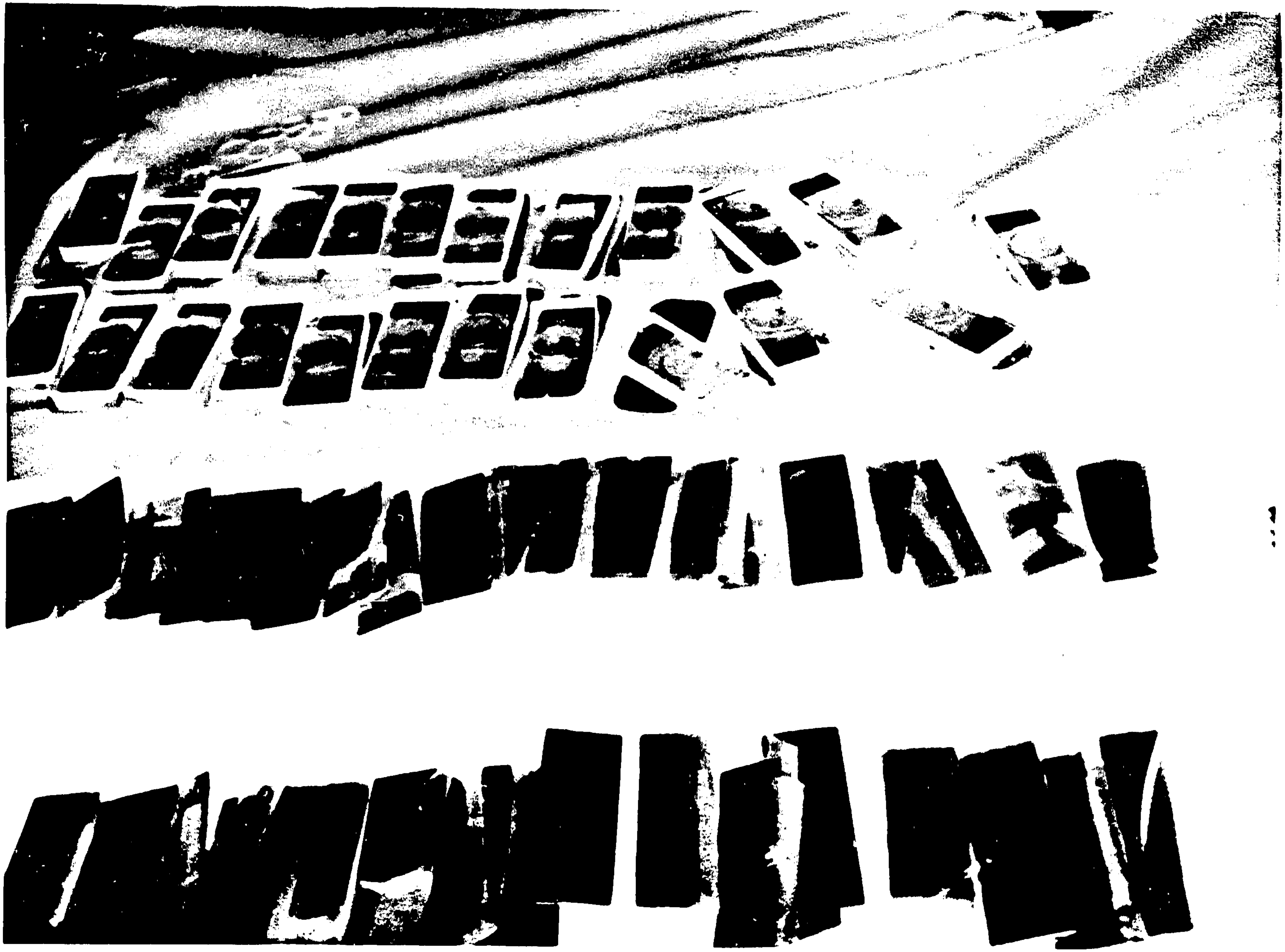

FIGURE 4. SSTR Neutron Dosimeters During Assembly. Fully assembled dosimeters are in background.

reduce background due to cosmic ray neutron induced fission and from spontaneous fission of the ^{238}U in the uranium. Also circular (1" diameter) CR-39 SSTRs were attached to the outer surface of each dosimeter (see Figure 4) to measure the high energy (E > ~0.5 MeV) neutron flux.

An overview of TMI-2 Demineralizer A and B Cubicles is shown in Figure 5. Due to the intense gamma ray fields present near the demineralizers, neutron dosimeters had to be placed remotely from outside the cubicle. The demineralizer A cubicle was accessible through penetration #891 shown in Figure 5.

A vertical stringer was prepared by fastening together SSTR dosimeters at measured intervals using fishing line. This stringer was enclosed in plastic tubing to protect the dosimeters from contamination inside the demineralizer cubicle. A horizontal set of dosimeters was prepared by attaching the dosimeters to a pipe which was then enclosed in plastic tubing. Both the horizontal and vertical stringers were inserted into the cubicle through penetration #891 as shown in Figures 6, 7 and 8. The dosimeters were inserted at 11:55 p.m. on September 14, 1982, and occupied the positions shown in Figure 9. The location of the vertical stringer was confirmed during a robot entry of the cubicle. The dosimeters were left in place for twenty-nine days and removed on October 13, 1982, at 6:20 p.m. Some difficulties were encountered during removal, resulting in a maximum uncertainty of 3% in the vertical stringer exposure time. In order to measure the detector background, control dosimeters were assembled at the same time and exposed in a demineralizer cubicle (D) where fuel was not present. Assembly and disassembly of all of the dosimeters required a few hours so that background cosmic ray neutron exposure is approximately the same for all detectors. A summary of the detector positions and labels is given in Tables 1 and 2. After exposure, the SSTRs were

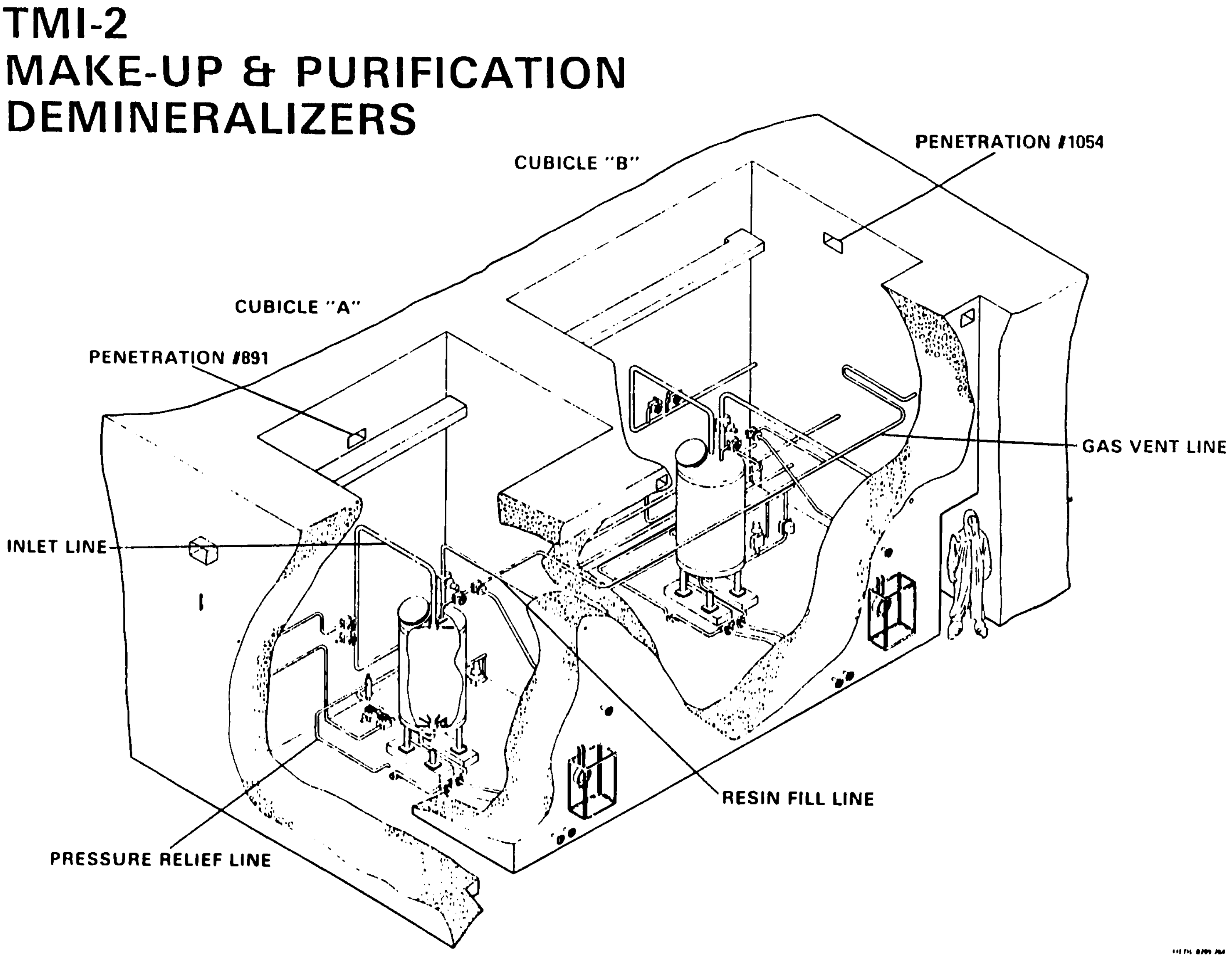

FIGURE 5. Isometric View of Makeup Demineralizer Cells A and B.

FIGURE 6. Emplacement of SSTR Neutron Dosimeters--Attaching Vertical Stringer to Support Pole.

FIGURE 7. Emplacement of SSTR Neutron Dosimeters--Measurement of Reference Point for Stringer Location.

FIGURE 8. Emplacement of SSTR Neutron Dosimeters--Final Insertion Through Penetration #891.

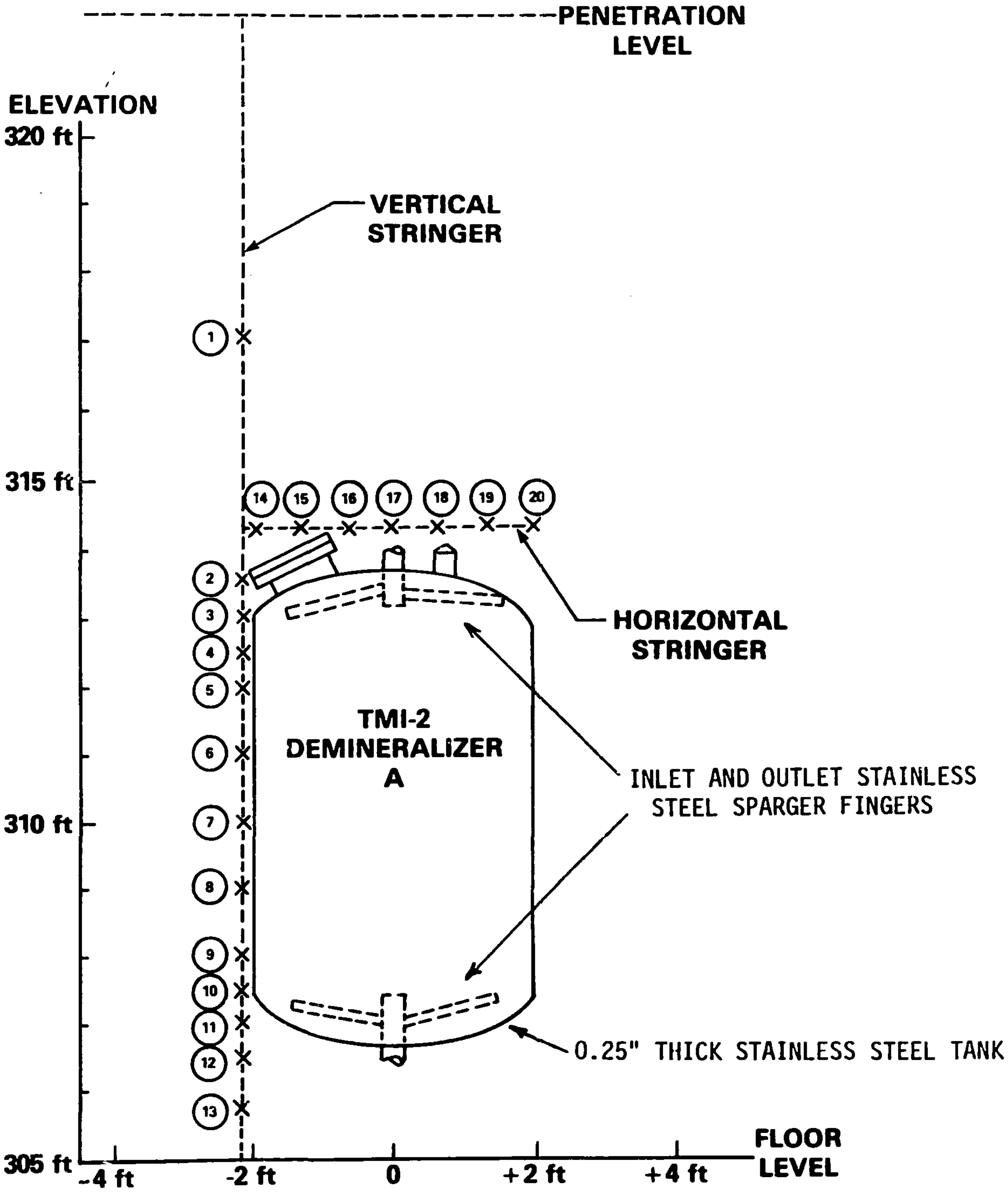

HEDL 8209-276

FIGURE 9. Locations of SSTR Neutron Dosimeters During Exposure.

TABLE 1. SUMMARY OF DETECTOR LABELS AND LOCATIONS FOR THE VERTICAL STRINGER

Holder Number	SSTR Labels	Demineralizer Location	Elevation
1	TMI-253-253'* -254,254'	A	317'0"
2	TMI-255,255' -256,256'	A	313'6"
3	TMI-257,257' -258,258'	A	313'0"
4	TMI-259,259' -260,260'	A	312'6"
5	TMI-261,261' -262,262'	A	312'0"
6	TMI-263,263' -264,264'	A	311'0"
7	TMI-265,265' -266,266'	A	310'0"
8	TMI-267,267' -268,268'	A	309'0"
9	TMI-269,269' -270,270'	A	308'0"
10	TMI-271,271' -272,272'	A	307'6"
11	TMI-273,273' -274,274'	A	307'0"
12	TMI-275,275' -276,276'	A	306'0"
13	TMI-277,277' -278,278'	A	305'9"
21	TMI-293,293' -294,294'	D	307'6"
23	TMI-297,297'	D	311'6"

---

* Mica SSTRs were numbered in sequence. Unprimed numbers correspond to SSTRs nearest to lucite. Primed numbers correspond to SSTRs nearest to aluminum.

TABLE 2. SUMMARY OF DETECTOR LABELS AND LOCATIONS FOR THE HORIZONTAL STRINGER

Holder Number	SSTR Labels	Demineralizer A Location
14	TMI-279,279' -280,280'	-2',0"
15	TMI-281,281' -282,282'	-1',4"
16	TMI-283,283' -284,284'	-0',8"
17	TMI-285,285' -286,286'	0
18	TMI-287,287' -288,288'	+0',8"
19	TMI-289,289' -290,290'	+1',4"
20	TMI-291,291' -292,292'	+2',0"

transported to HEDL where they were processed by etching with 49% HF at room temperature for 90 minutes. The developed tracks from selected dosimeters were manually counted with the aid of several observers and microscopes. The measured ^{235}U fission fragment track densities for this exposure are given in Table 3.

3.0 Analysis and Results

The SSTR ^{235}U track densities from Table 3 are plotted in Figure 10. Shown for comparison is a curve resulting from gamma scanning(1) of the ^{144}Ce activity present in the demineralizer tank. Within experimental limitations, the positions of the two peaks are the same, indicating the presence of fuel at the 309' elevation. The assumptions are made here that ^{144}Ce and Pu both are closely associated with the fuel, resulting in fuel traceable gamma rays and neutrons, respectively.

The SSTR intensity distribution in Figure 10 is asymmetric, decreasing less rapidly above the 309' elevation than below. A probable explanation (later substantiated by direct observations) is that the tank is dry above the 309' elevation and contains degraded resin and possibly boronated water below this level. The resin attenuates fuel neutrons below 309', whereas the slower falloff in intensity above 309' results from the increasing distance between the SSTR neutron dosimeters and the neutron source.

Although the background measurements give a track density of about 5 tracks/cm^2 due to cosmic radiation, the baseline for the measurements in the demineralizer cubicle is about 10 tracks/cm^2. The 5 tracks/cm^2 difference is due to room return resulting from thermalization of source neutrons in the walls of the cubicle. This effect, which is discussed in detail in Appendix B, can be used to derive

TABLE 3

MEASURED SSTR TRACK DENSITIES AT SELECTED LOCATIONS IN THE TMI-2 DEMINERALIZER A CUBICLE

			Measured Tracks/cm^2			
Dosimeter Number	SSTR Label	Elevation	Obs. 1	Obs. 2	Avg.	Avg-Bkgd
1	TMI-253	317'	11.1		11.1	6.1 ± 2.0
5	TMI-261	312'	26.1		26.1	21.1 ± 2.8
6	TMI-263	311'	25.2	27.0	26.1	21.1 ± 2.7
7	TMI-265	310'	30.1	30.6	30.4	25.4 ± 3.2
8	TMI-267	309'	36.8	36.1	36.4	31.4 ± 4.2
9	TMI-269	308'	13.3	12.4	12.8	7.8 ± 1.7
11	TMI-273	307'	10.2		10.2	5.2 ± 1.9
13	TMI-277	305'9"		8.3	8.3	3.3 ± 2.0
17	TMI-285	*	9.3		9.3	4.3 ± 2.0
20	TMI-291	*		11.5	11.5	6.5 ± 2.0
—	TMI-293	**	4.8	5.3	5.0 ± 1.1	—

*Horizontal Stringer (Elevation 314'6")

**Located in Cubicle D - Background Measurement

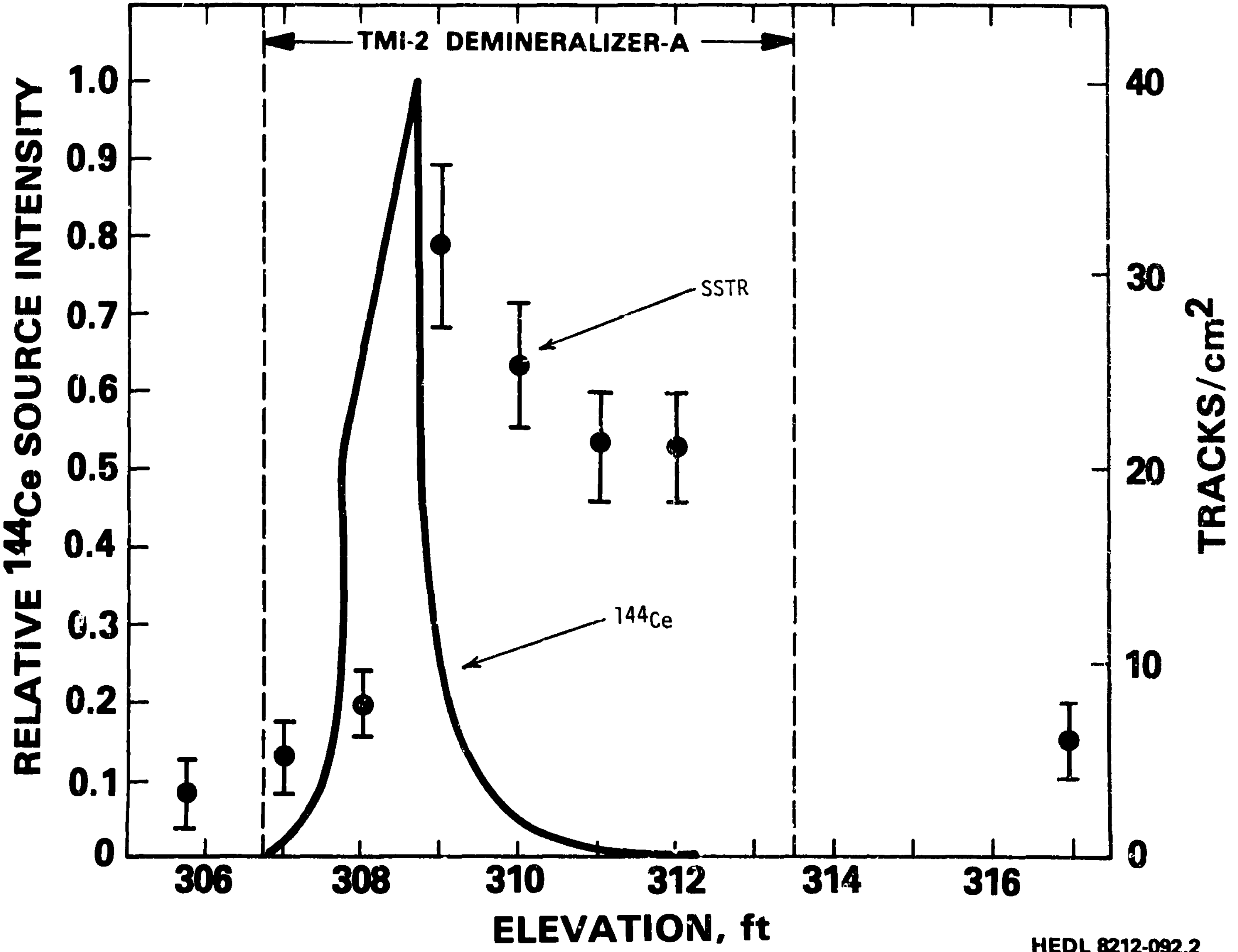

FIGURE 10. Track Density as a Function of Axial Location for SSTR Neutron Dosimeters Exposed in TMI-2 Demineralizer A Cubicle.

the most reliable estimate of the total amount of fuel present in the demineralizer cubicle, since the room return response integrates over the complex source geometry of the neutron emitting fuel yielding a total response that is proportional to the total amount of fuel present in the demineralizer cubicle.

By averaging the detector responses at the positions most distant from the fuel and correcting for background, a room return response of 5.1 ± 1.9 tracks/cm^2 was obtained in the demineralizer vault. The exposure time of 29 days yields 1.24×10^{-4} tracks/cm^2/min. An identical albedo-type dosimeter exposed to a $(3.08 \pm 0.42) \times 10^8$ n/sec ^{252}Cf source in a closed cubicle gave a room return response of 74.8 ± 7.5 tracks/cm^2/min (see Appendix B). If the room return response in the ^{252}Cf calibrations is assumed to have the same proportionality as the room return response in the demineralizer cubicle (as is shown to be likely by calibration data in Appendix B), the total neutron emission rate in the demineralizer cubicle is found to be

$$\left(\frac{1.24 \times 10^{-4}\ \text{tracks/cm}^2\text{/min}}{74.8\ \text{tracks/cm}^2\text{/min}}\right)\left(3.08 \times 10^8\ \text{n/sec}\right) = 511\ \text{n/sec}$$

If an average neutron specific activity of 300 n/sec/kg is assumed for TMI-2 fuel, an SSTR neutron source intensity derived value of fuel debris of 1.70 ± 0.63 kg is obtained.

This estimate is subject to error from a number of sources, the most important being the unknown amounts of moderators (mainly hydrogenous materials such as water and ion exchange resins) and absorbers such as boron. After the SSTR measurements were performed, the demineralizer tank was found to be dry (as was predicted by the results of the SSTR measurements) and the resin is thought to be substantially degraded (dehydrogenated), so that the presence of moderators is probably not a serious source of error. The amount of boron in the demineralizer is unknown. The indeterminant error resulting from these sources probably does not exceed a factor of two.

An independent estimate of the amount of fuel present has been made using the shape of the response curve and simple geometric arguments (see Appendix C). This less reliable estimate, 0.9 ± 0.5 kg, is consistent with the room return estimate, lending confidence that the indeterminant errors in the room return estimate are small. Also, the room return estimate is in excellent agreement with the estimate based on the gamma spectrometry measurements, 1.3 ± 0.6 kg.(1)

Analysis of the direct geometrical SSTR dosimeter response (Appendix C) indicates that the neutron source is concentrated near the back wall of the demineralizer tank, consistent with the results of the collimated gamma ray spectrometer measurements.

The response of the SSTR dosimeter closest to the fuel and with the maximum response indicates a neutron flux of (1.5 ± 0.2) x 10^{-3} n/cm^2/sec (see Appendix C). The present SSTR neutron dosimetry is the only known method capable of detecting such a low neutron flux.

During unloading of the dosimeters, the lucite albedo blocks were observed to have been discolored by radiation damage. The intensity of the discoloration appears to be proportional to the intensity of the gamma ray dose at the location of each dosimeter, as can be seen in Figure 11. Quantitative light absorption or transmission measurements should be made on these lucite blocks to determine if usable gamma ray dose information can be derived.

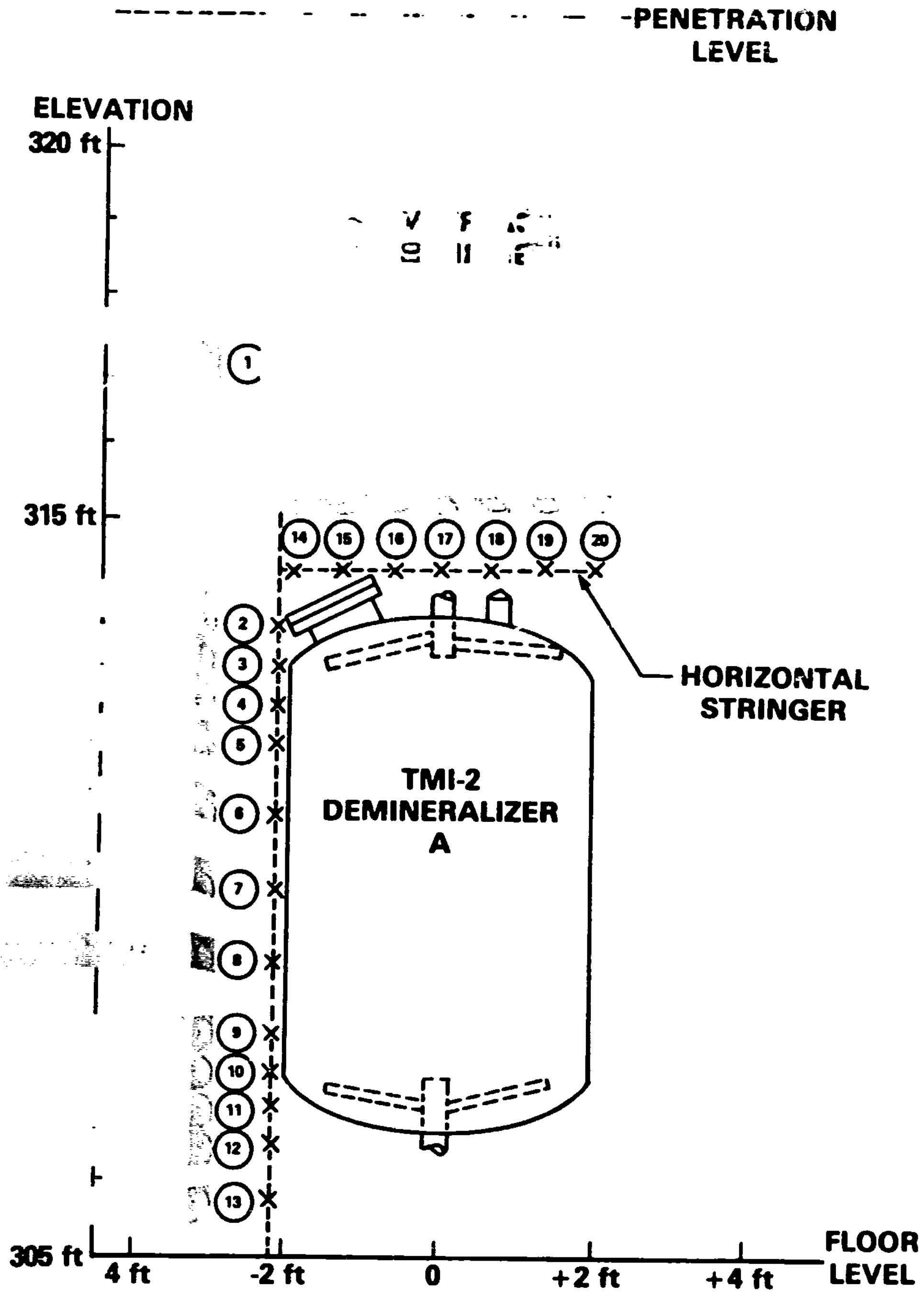

HEDL 8209-276

FIGURE 11. Lucite Blocks from SSTR Neutron Dosimeters that were Exposed in Demineralizer Cubicle A. Discoloration is the Result of Accumulated Radiation Damage from Gamma Ray Exposure. The Maximum Discoloration Corresponds to the Location of Highest Gamma Ray Dose.

4.0 Summary

Based on the room return response of the SSTR neutron dosimeters, the amount of fuel present in TMI-2 Demineralizer A is estimated to be 1.7 ± 0.6 kg whereas the analysis of the SSTR data with a point source model yields 0.9 ± 0.5 kg. These estimates assume that the demineralizer is dry above the 309' level, an assumption that was predicted by the shape of the axial response data and later verified by direct observations. The presence of unknown amounts of degraded resin and boron below the 309' level could increase the room return estimate by a maximum of a factor of two. On the other hand, the uncertainty of the point source estimate is dominated by the lack of proper calibration data as well as uncertainty associated with the spatial distribution of the source. For reasons discussed in the previous section, the room return estimate is considered to be more reliable.

These SSTR estimates are consistent with the value 1.3 ± 0.6 kg obtained in independent Compton recoil gamma ray spectrometry measurements.(1) Source distribution data from these gamma ray measurements were used to guide the direction and planning of the SSTR calibration measurements. In turn, the SSTR prediction that the demineralizer tank is dry above the 309' level provided guidance for reduction of the Compton recoil spectrometer data. Thus, the two methods provide independent but complementary data.

The present SSTR estimates of the fuel quantity could be refined by the following:

(1) Improved knowledge of the neutron specific activity of TMI-2 fuel. The 300 n/sec/kg estimate is based on calculations. Previous experience(4,5) has shown that such estimates are lower than what is found experimentally. Also, the neutron specific activity will vary with the reactor core location of the

irradiated fuel. Since an estimated average value has been used for this analysis, measurements of the neutron specific activity of representative samples of TMI-2 fuel should be made.

(2) Further calibrations using experimental mockups containing moderators and absorbers that are more characteristic of the contents of the demineralizer tank.

(3) Further scanning of the mica SSTR dosimeters to obtain more tracks and the concomitant higher statistical accuracy. Also, the CR-39 SSTRs could be processed, scanned, and analyzed to obtain data on the high energy ($E > 0.5$ MeV) neutron flux (the accuracy of the higher energy neutron data may be limited by a low signal to background ratio).

The present fuel estimates resulted from neutron dosimetry measurements in a field where the neutron flux was less than 2×10^{-3} neutrons/cm^2/sec. Thus, the high sensitivity and cost effectiveness of the SSTR method makes it an excellent candidate for further TMI-2 applications involving fuel debris tracing by neutron dosimetry.

ACKNOWLEDGMENTS

These measurements were undertaken as a result of the interaction and exchange of ideas with a number of organizations; among these are DOE, EPRI, GPU, NRC, EG&G, HEDL, and the Technical Assistance Advisory Group (TAAG) Committee for TMI-2 Recovery. Support and further encouragement for this work was received through the WHC TMI-2 Demineralizer Resin Removal Program, under the direction of Mike Mahaffey of WHC.

During the calibration measurements, assistance was received from G. Jones, R. Tomlinson, and W. Mallory of WHC, and L. Nichols of PNL.

The assistance of Ken Lionarons and Ted Rekart of GPU, Herb Sanchez of EG&G, and Bruce Kaiser, Jim McNeece, and Bill Jenkins of WHC, during the placement and removal of the dosimeters at TMI-2 is gratefully acknowledged.

Leslie Dunn, Jess Smart, Cesar Icayan, and Tom Cross of WHC provided track recorder scanning assistance.

The additional support, encouragement, and/or technical assistance provided by Fred Leitz, Ben Hayward, Wally Sheely, Bill McElroy, Parvin Lippincott, Frank Schmittroth, Don Doran, Herb Yoshikawa, and Ersel Evans of WHC, and Geoff Quinn of EG&G, are gratefully acknowledged.

REFERENCES

1. J. P. McNeece, B. J. Kaiser, R. Gold, and W. W. Jenkins, "Fuel Assessment of the Three Mile Island Unit 2 Makeup Demineralizers by Continuous Gamma-Ray Spectrometry", HEDL-7285, 1983.

2. K. Vinjamuri, C. V. McIsaac, L. S. Beller, L. Isaacson, J. W. Mandler, and R. R. Hobbins, Jr., "Nondestructive Techniques for Assaying Fuel Debris in Piping at Three Mile Island Unit 2", General Public Utilities, Electric Power Research Institute, U.S. Nuclear Regulatory Commission, and U.S. Department of Energy Report GEND-018, 1981.

3. R. Gold, F. H. Ruddy, J. H. Roberts, C. C. Preston, J. A. Ulseth, W. N. McElroy, F. J. Leitz, B. R. Hayward, and F. A. Schmittroth, "Application of Solid State Recorder Neutron Dosimetry for Three Mile Island Unit 2 Reactor Recovery", Nuclear Track Detection 7, pp. 13-30 (1983).

4. R. Gold, F. H. Ruddy, E. P. Lippincott, W. N. McElroy, and J. H. Roberts, "Neutron Emissions Observed from Spent Thermal Reactor Fuel Assemblies", Third ASTM-EURATOM Symposium on Reactor Dosimetry, EUR6873, Vol. II, p. 858 (1980).

5. R. Gold, F. H. Ruddy, E. P. Lippincott, W. N. McElroy, and J. H. Roberts, "Neutron Dosimetry Characterization of Spent Thermal Reactor Fuel Assemblies," Trans. Am. Nucl. Soc., 32, p. 634 (1979).

6. P. H. White, "The Room Scattered Background Produced by a Neutron Source in a Laboratory With Concrete Walls", Nuclear Instruments and Methods 39, p. 256 (1966).

APPENDIX A

SSTR NEUTRON DOSIMETER RESPONSE

In order to convert observed fission track density into neutron fluence, calibration data on the response of the SSTR neutron dosimeter is required. This response will depend on the energy spectrum as well as the intensity of the incident neutrons. Neutrons from the source (fuel in the demineralizer) will be moderated, absorbed, and reflected by the surroundings, and the resultant neutron spectrum will be sensitive to the presence of moderators such as water or materials with high neutron absorption cross sections. Calibration data has been obtained(3) using a ^{252}Cf source in an experimental configuration designed to "mock-up" the demineralizer and its surroundings. At the time these calibrations were carried out it was believed that the demineralizer was filled with 1100 ppm borated water.

On the basis of the present work and subsequent direct observations, the demineralizer can be assumed to be dry above the 309' elevation. Below this elevation, degraded resin is present containing unknown amounts of hydrogen and boron. Nevertheless, the previous dosimeter calibrations(3) provide insight into the response of the ^{235}U fission rate as a function of moderation and absorption of source neutrons. Figure A-1 shows the response of SSTR dosimeters to a ^{252}Cf source immersed in borated water at various depths. Note that the SSTR response peaks directly above the source but drops off rapidly for other positions as a result of the attenuation (absorption) of source neutrons by the borated water. This effect is also shown in Figure A-2 where the peak intensity is plotted as a function of water depth. This response is the basis of the argument presented in Section 3.0 that the tank is dry above the 309' level. If water were present, the response curve

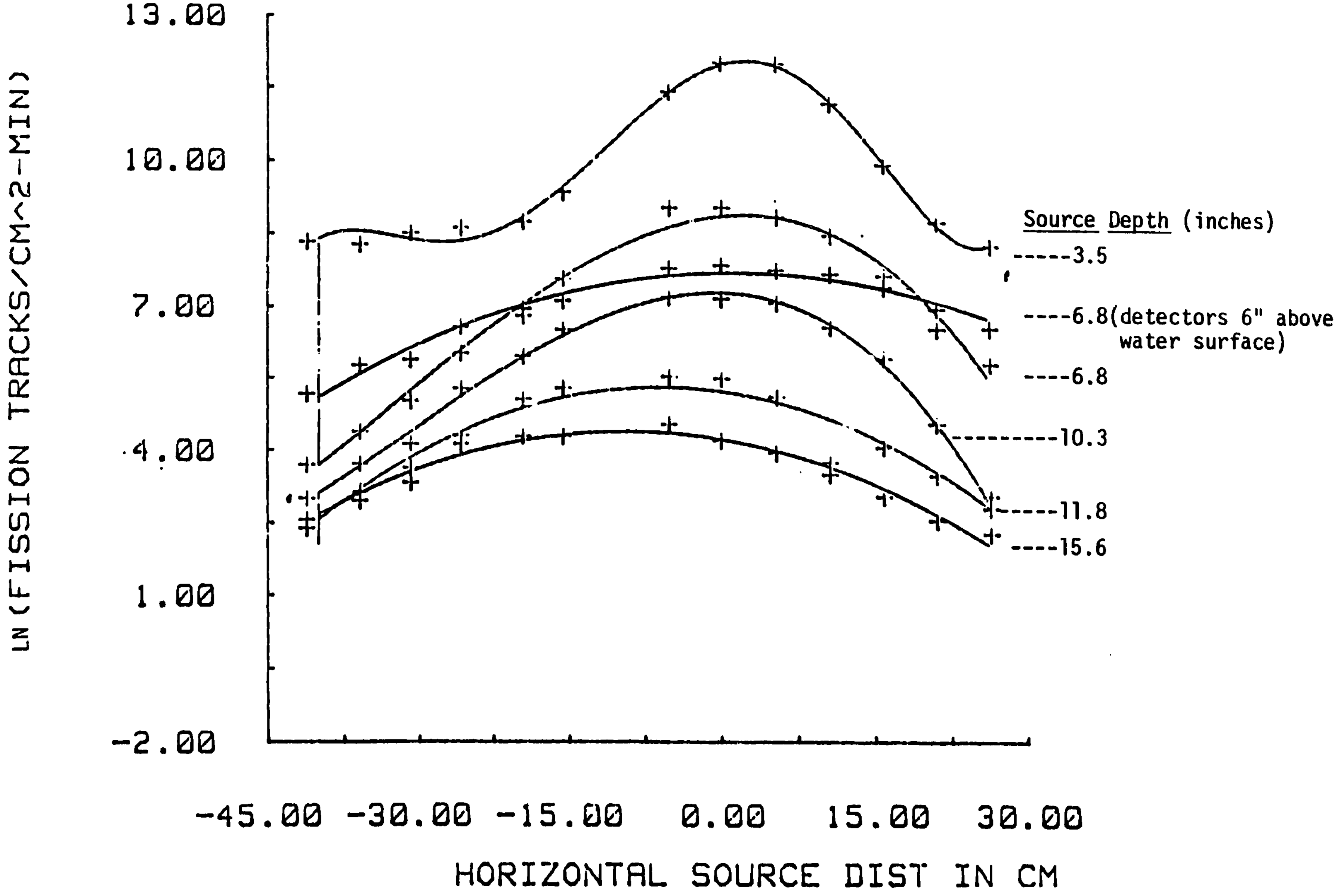

FIGURE A-1. SSTR Neutron Dosimeter Response Along the Surface of a Tank of 1100 ppm Borated Water Containing a ^{252}Cf Source Located at Various Depths.

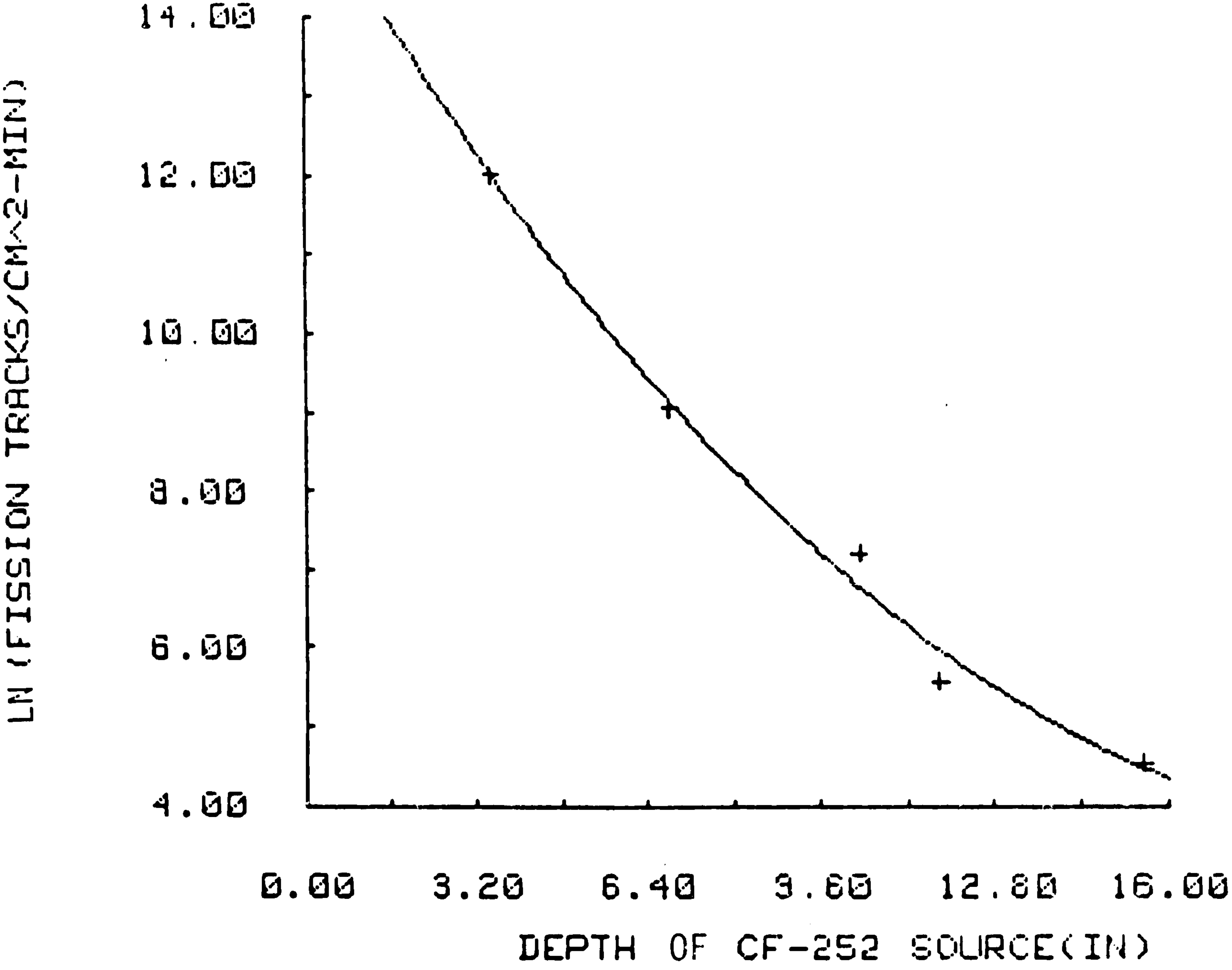

FIGURE A-2. SSTR Neutron Dosimeter Response as a Function of Depth of a ^{252}Cf Source in 1100 ppm Borated Water.

plotted in Figure 10 would decrease much more rapidly above the 309' level (see also, Appendix C).

The dosimeter design shown in Figure 1 differs from the design used for previous calibrations(3) in that two layers of 0.004" uranium are used to increase the detector surface area and lucite albedo blocks are used to increase the neutron response of the ^{235}U by contributing further moderation of the neutron spectrum. In order to calculate the relative response of the two SSTR neutron dosimeters, additional ^{252}Cf exposures were carried out. These ^{252}Cf calibrations were carried out in a concrete walled cubicle in order to approximate the room return effects observed in the enclosed demineralizer vault. Since these results were dominated by room return effects, they are summarized in the following appendix.

The ^{252}Cf source used for most of these measurements was calibrated directly using SSTR techniques. The fission rate of ^{238}U was measured by placing a ^{238}U-SSTR dosimeter in known geometry (at a distance of 2') from the ^{252}Cf source. Since ^{238}U has an energy threshold for neutron induced fission of about 1 MeV, the effects of neutron down scattering are not dominant, and the $^{238}U(n,f)$ fission neutron energy spectrum averaged cross section may be used to convert measured fission rate into fast neutron flux. This fast neutron flux may then be converted to total source output using point source geometry, since neutron scattering by the surroundings will not be an important consideration for the high energy portion of the neutron spectrum which induces fission in ^{238}U. The intensity of the ^{252}Cf source was found to be $(3.08 \pm 0.42) \times 10^8$ n/sec.

APPENDIX B

SSTR ROOM RETURN RESPONSE

Whenever neutron dosimetry is conducted in a laboratory bounded by walls containing moderator materials (hydrogeneous concrete in the present case), the source neutrons will be transported, scattered, and absorbed throughout the environment and particularly in the walls if the dimensions of the laboratory are small. Room return neutrons are the last vestiges of neutrons originally emitted by the source, and, indeed, these neutrons has been scattered so often that they have attained thermal equilibrium with their environment. The intensity of these room return neutrons is independent of position within the laboratory. They retain no knowledge of their origin with the exception of their intensity, which is proportional to the total emission rate of the source.

The effects of room return can be seen in data taken in the vicinity of a spent fuel subassembly housed in a hot cell.(3) Fission rates were measured for ^{235}U, ^{238}U, ^{237}Np, and ^{232}Th. The axial and radial distributions for these fission rates are shown in Figures B-1 and B-2, respectively. The isotopes with threshold neutron response (^{238}U, ^{237}Np, and ^{232}Th) respond to fast neutrons from the source and show the expected spatial distributions, that is they decrease geometrically with distance from the source (the intensity is inversely proportional to the radial distance from the planar source). The ^{235}U-bare fission rates result mainly from thermal neutrons and are roughly constant at all positions indicating that the thermal neutron intensity is independent of position relative to the source within the hot cell. The calmium covered ^{235}U fission rates are indicative of

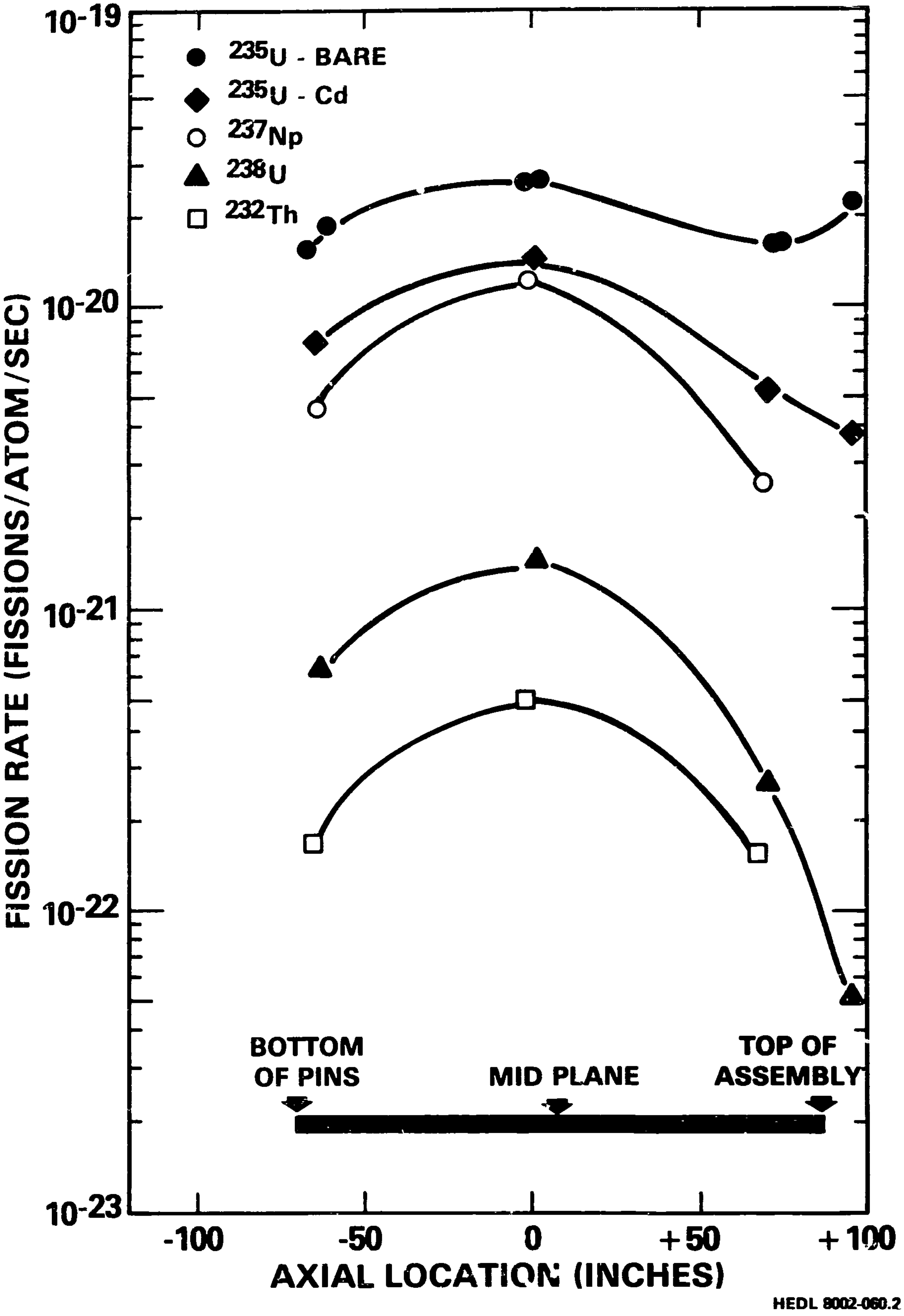

FIGURE B-1. Axial Fission Rate Distributions Measured Along the Face of a Reactor (PWR) Spent Fuel Assembly.

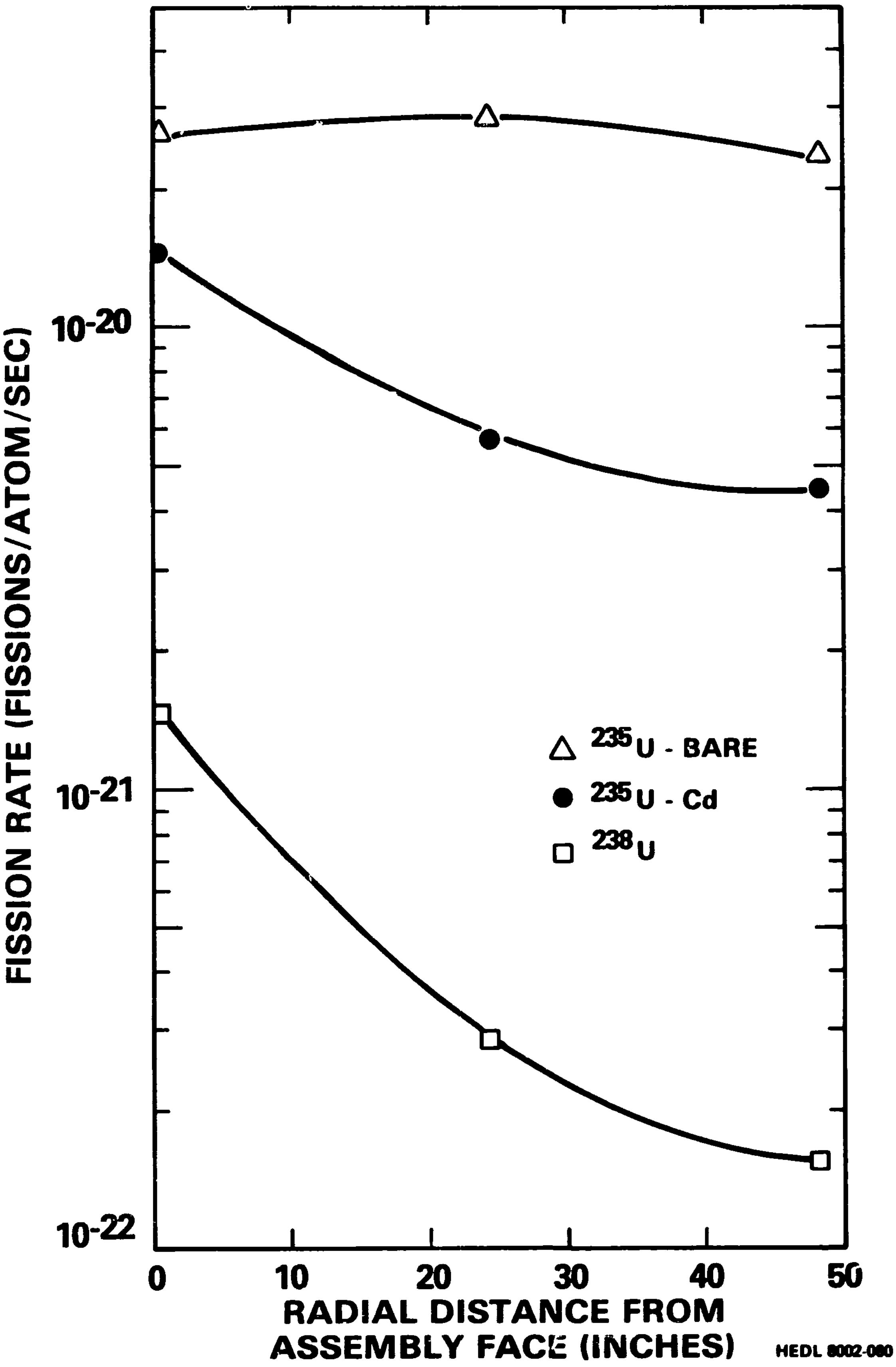

FIGURE B-2. Fission Rates as a Function of Radial Distance from a Reactor (PWR) Spent Fuel Assembly.

epithermal neutron fluxes, and behave in a manner intermediate between the thermal and threshold cases.

The ^{235}U-bare fission rates depend mainly upon the room return thermal neutron intensity which is proportional to the total amount of fuel present in the hot cell.

The SSTR ^{235}U fission rate data from demineralizer A shown in Figure 10 and summarized in Table 3 show a constant response at positions distant from the source, and this room return response should also be proportional to the total amount of fuel present in the demineralizer cubicle.

A detailed analysis of the room return phenomenon has been given by White$^{(6)}$ who used diffusion theory to describe experimental data obtained in a laboratory bounded by concrete walls. According to this analysis, the thermal neutron flux can be expressed as

$$\phi = C \cdot S_n / R^2 \quad , \qquad [1]$$

where S_n is the neutron emission of the source in neutrons/sec, C is a constant and R is the effective radius of the laboratory given by

$$R^{-2} = 1/6 \sum_{i=1}^{6} D_i^{-2} \quad , \qquad [2]$$

where D_i, i = 1, . . . 6 are the six distances from the source to each wall of the laboratory. A value of R that is pertinent to the TMI-2 Demineralizer A Cubicle can be derived from the known dimensions of the cubicle and the approximate location of the fuel as derived from the Compton gamma ray spectrometer data.(1) These gamma-ray results show that the source can be approximately represented by a point source which lies two feet from the bottom of the demineralizer tank and very close to the north side of the tank. On this basis, one finds a value of approximately 5.1' for R.

In order to experimentally determine the room return response of the SSTR dosimeters, calibrations were carried out in a cubicle where similar values of R would be obtained. A ^{252}Cf source was suspended at two different heights (2' and 3.5') in a cubicle with overall dimensions 11.5' x 8' and a height of 8' and dosimeters were placed at the locations shown in Figure B-3. With the ^{252}Cf source at 2' and 3.5', the corresponding values of R are 3.6' and 4.3', respectively. The bulk of the measurements were made with ^{235}U-bare dosimeters of the type used for the calibration measurements described in Appendix A and Reference 3. These dosimeters were then cross-calibrated with dosimeters of the design shown in Figure 1 which were used in the demineralizer measurement.

The ^{235}U-bare radial response results for source heights of 2' and 3.5' are shown in Figures B-4 and B-5. Here, ^{235}U dosimeters with no albedo devices were used, and no water was present in the tank. The response is seen to be roughly constant for both cases with the exception of the 2' radial measurement with the source at 2' which corresponds to the smallest source to dosimeter distance and the highest response. Axial response distributions at a radial distance of 4' are shown for the 2' and 3.5' source heights in Figure B-6. In both cases, the response is flat and constant for both source heights. Apparently, equation [1] is not valid for the small room dimensions addressed here. Because of the closeness of

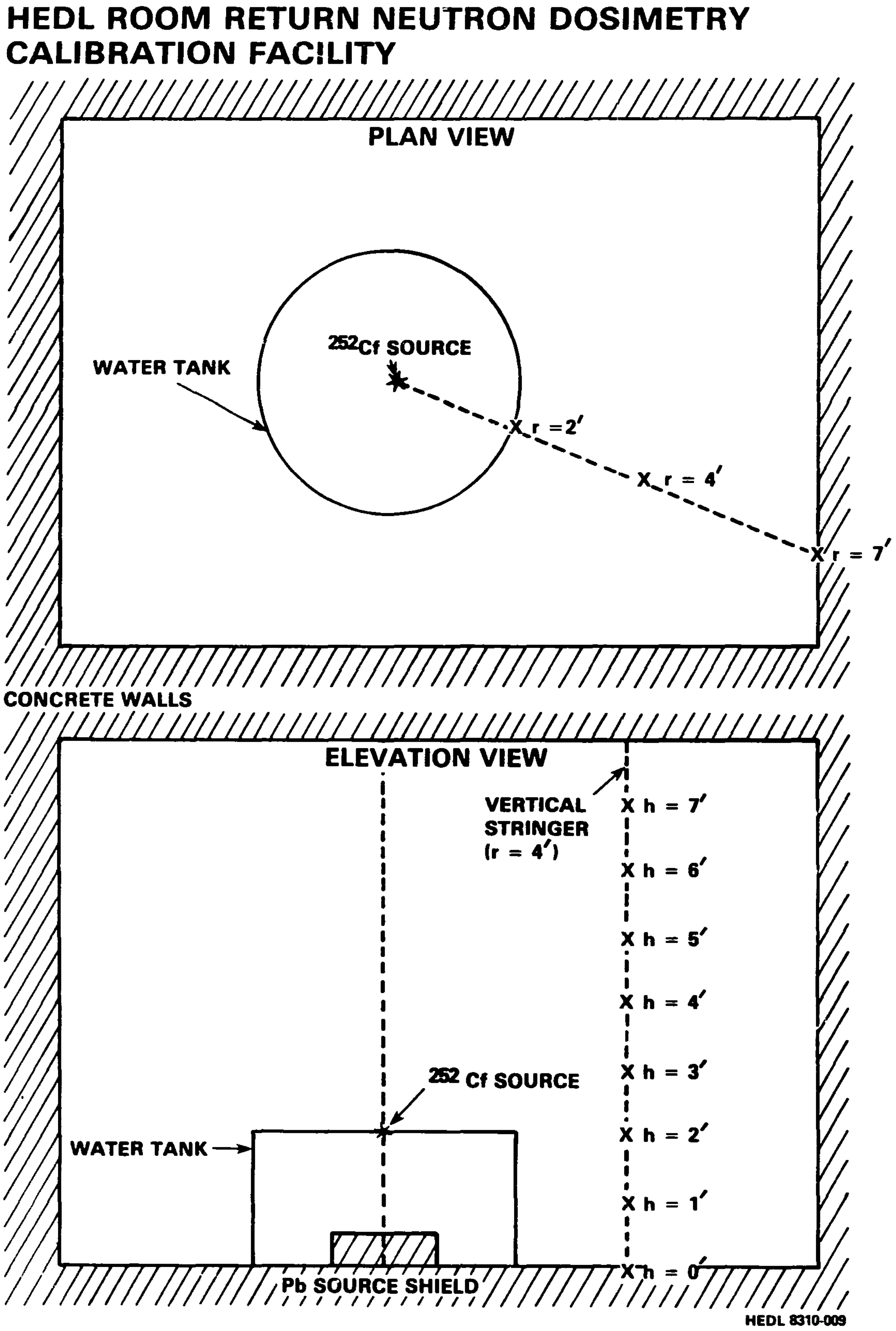

FIGURE B-3. Schematic of source and detector positions for ^{252}Cf SSTR calibrations carried out in a closed cubicle.

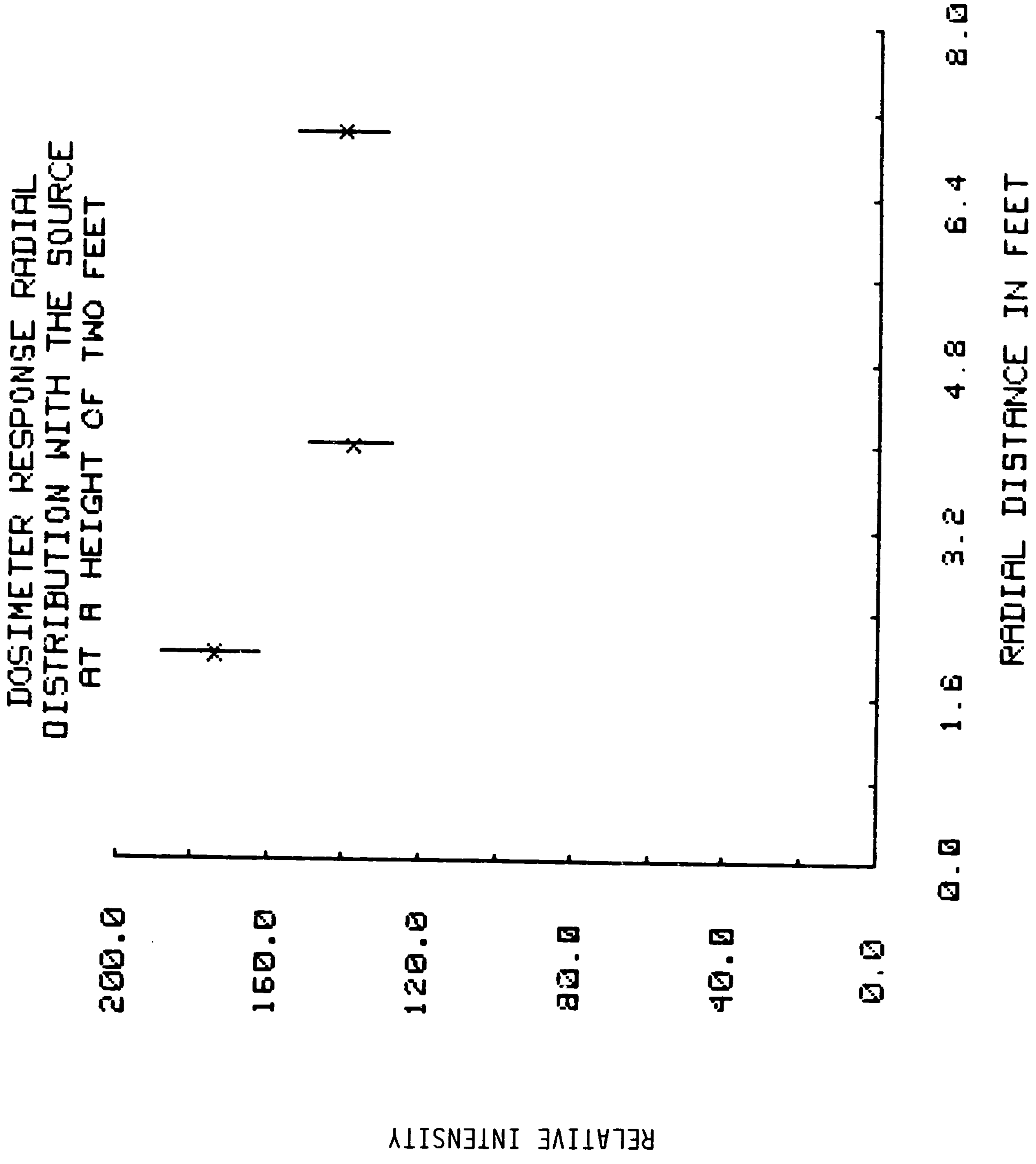

FIGURE B-4. Response as a Function of Radial Location for SSTR Neutron Dosimeters Exposed to a ^{252}Cf Source Suspended at 2' from the Floor in the Center of a Concrete Cubicle with Overall Dimensions 11.5' x 8' and a Height of 8'.

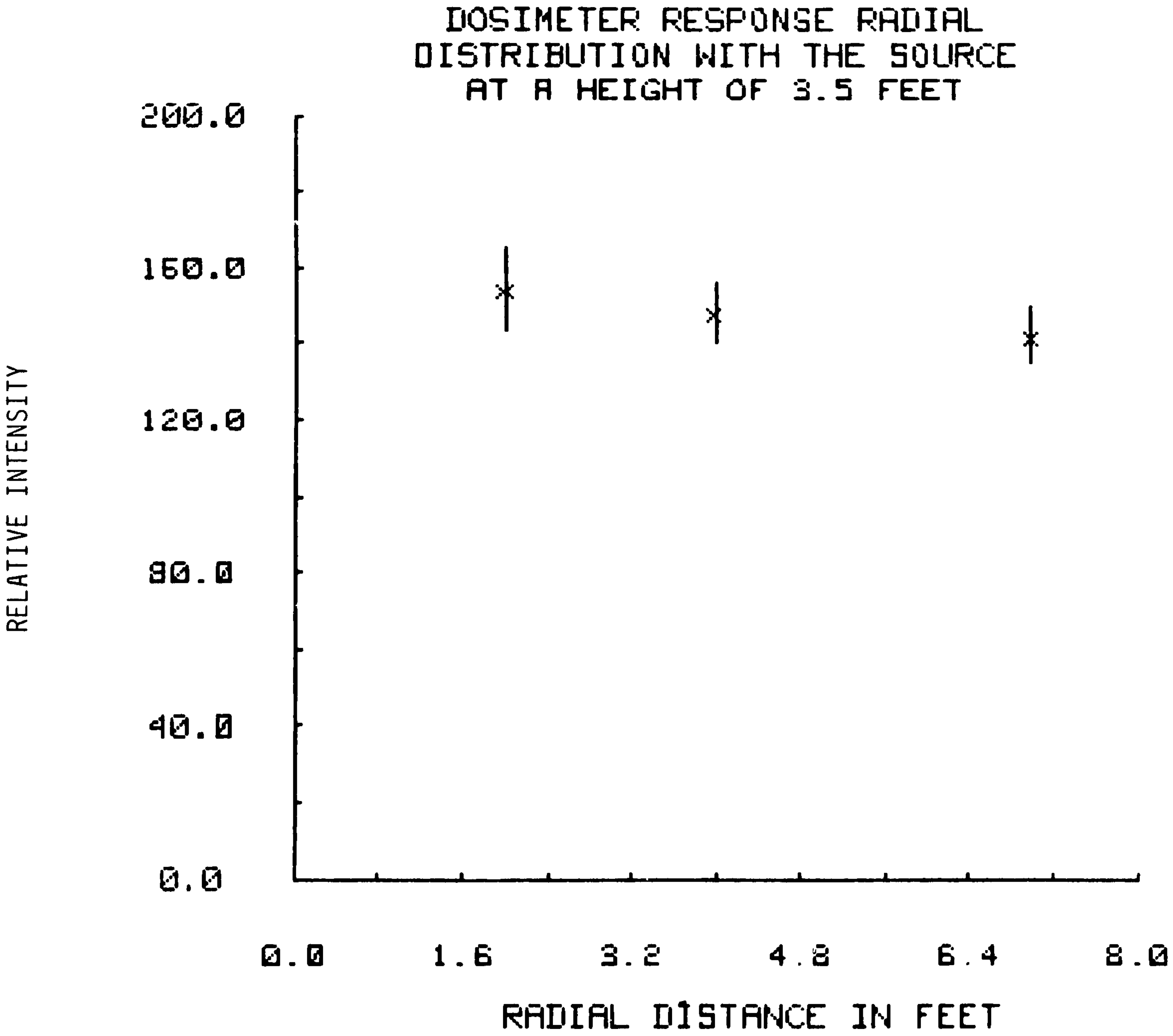

FIGURE B-5. As in Figure B-4, with a Source Height of 3.5'.

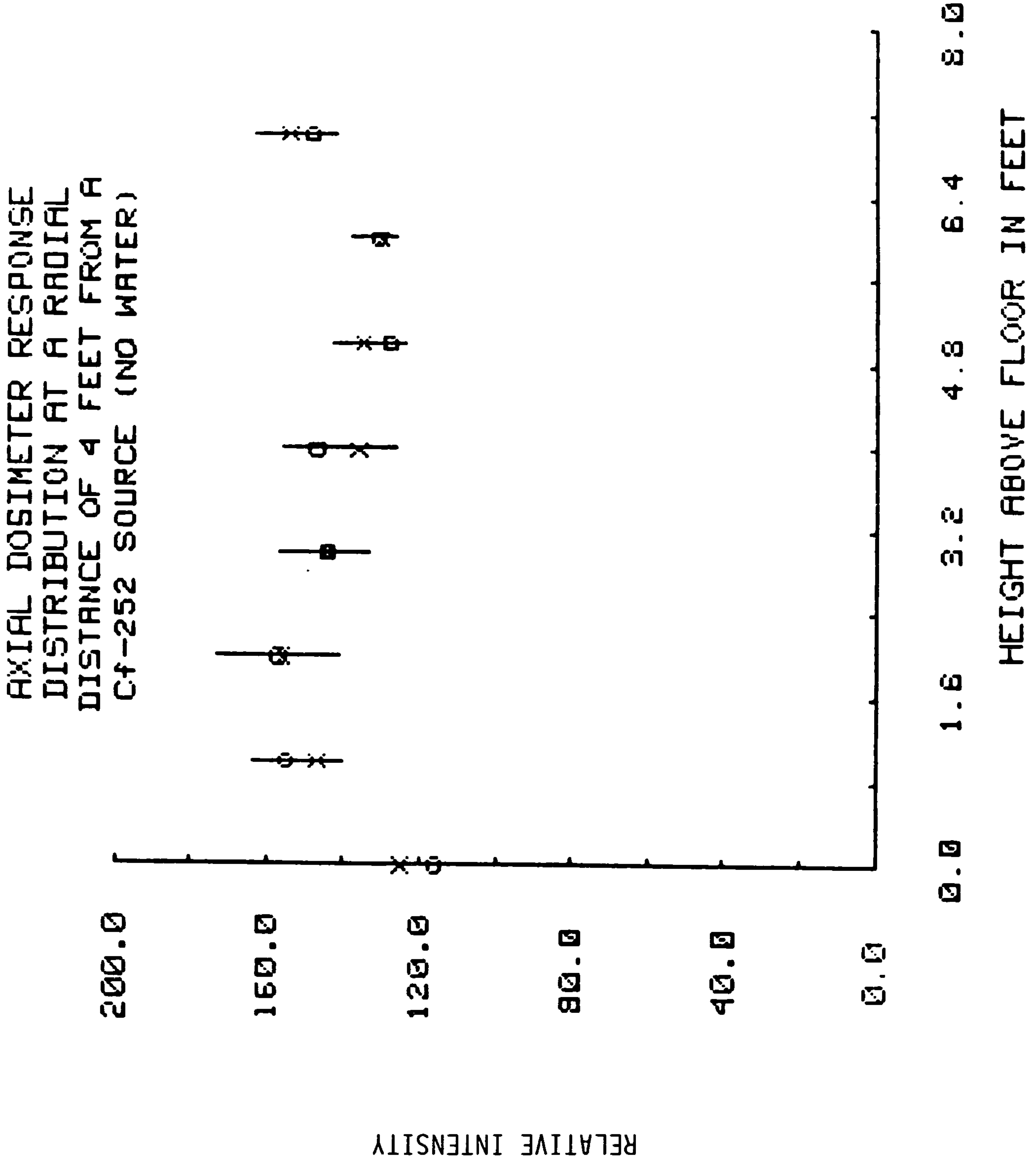

FIGURE B-6. SSTR Neutron Dosimeter Axial Responses at a Radial Distance of 4' from a ^{252}Cf Source.

X Source Height 2'
O Source Height 3.5'

the effective radius in the demineralizer vault to the two calibration cases which show constant response, this constant room return response has been taken to be valid for the demineralizer measurements.

The constant response of the bare ^{235}U-SSTR dosimeters was cross calibrated to the also constant response of albedo-type dosimeters of the type shown in Figure 1. The albedo dosimeter response was found to be 74.8 ± 7.5 tracks/cm^2/min. The response per unit area of this type of dosimeter is less than that for a bare ^{235}U dosimeter because of the flux depression caused by the stacked 0.004" ^{235}U foils. The increased overall SSTR area (85 cm^2) leads to a higher overall response, and the albedo devices allow source position information to be obtained in the presence of a dominant room return thermal neutron spectrum since the albedo device converts the source geometry dependent fast neutrons into more detectable thermal neutrons at the detector positions.

The SSTR response may be effected by a number of factors. The most important factors that must be taken into account are the absorption and moderation of neutrons in the laboratory. These effects are particularly significant when hydrogenous media may exist in the laboratory as in the case for the Demineralizer A cubicle. Neutron absorption decreases the number of neutrons which attain thermal equilibrium in the cubicle. On the other hand, moderation by a hydrogenous medium produces a softer neutron spectrum incident upon the laboratory walls, thereby increasing neutron reflection and the thermal neutron room return flux. Consequently, these two effects work in opposite directions and tend to cancel each other. Obviously, the specific laboratory environment and geometry will play a dominant role in the relative weighting of these effects.

In order to explore the effect of having hydrogenous media present, SSTR calibration measurements were done with the ^{252}Cf source suspended at a height of 2' at the surface of the water in a 2' high by 4' diameter tank. The radial dosimeter response data for bare ^{235}U dosimeters are shown in Figure B-7. The response is less by a factor of about two from that shown in Figures B-4 and B-5, but it is still flat. The decrease in intensity is due to thermalization and absorption of source neutrons in the water which subtends about 50% of the geometry of the source. The axial response distribution at a distance of 4' is shown in Figure B-8. As in the corresponding axial distributions of Figure B-6, no albedo devices were used. Below the level of the water, the response is quite low due to neutron absorption in the water. From 2' to 5' the response is reasonably flat and above 5' increases slightly as the 8' ceiling of the cubicle is approached. This measurement was repeated using albedo dosimeters identical to those used in the measurements in the Demineralizer A cubicle, yielding the data plotted in Figure B-9. The shape of this albedo response is qualitatively similar to the axial distribution of Figure 10 obtained for Demineralizer A.

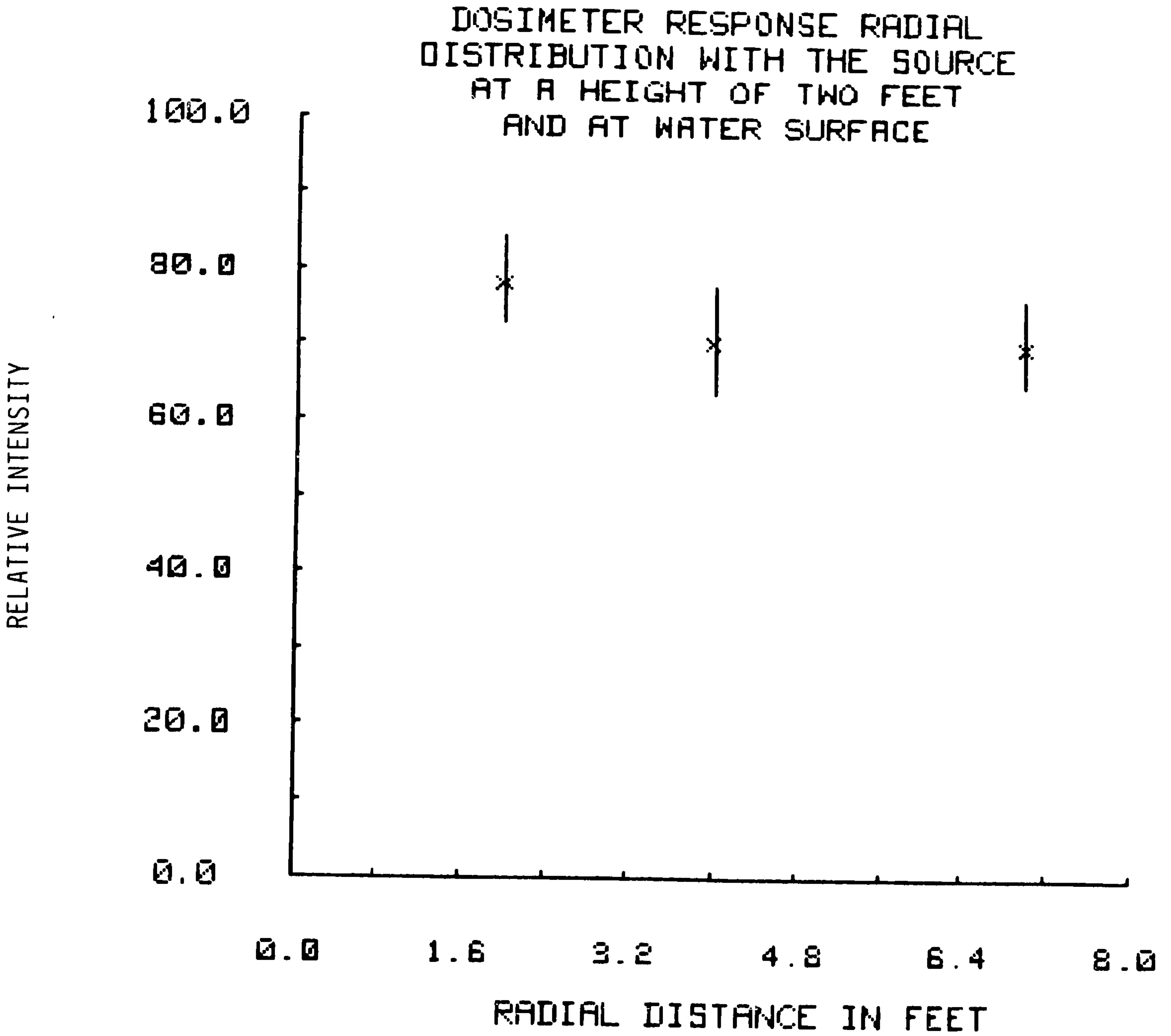

FIGURE B-7. Response as a Function of Radial Location for SSTR Neutron Dosimeters Exposed to a ^{252}Cf Source Suspended at the Center of the Surface of a 2' High by 4' Diameter Tank of Water

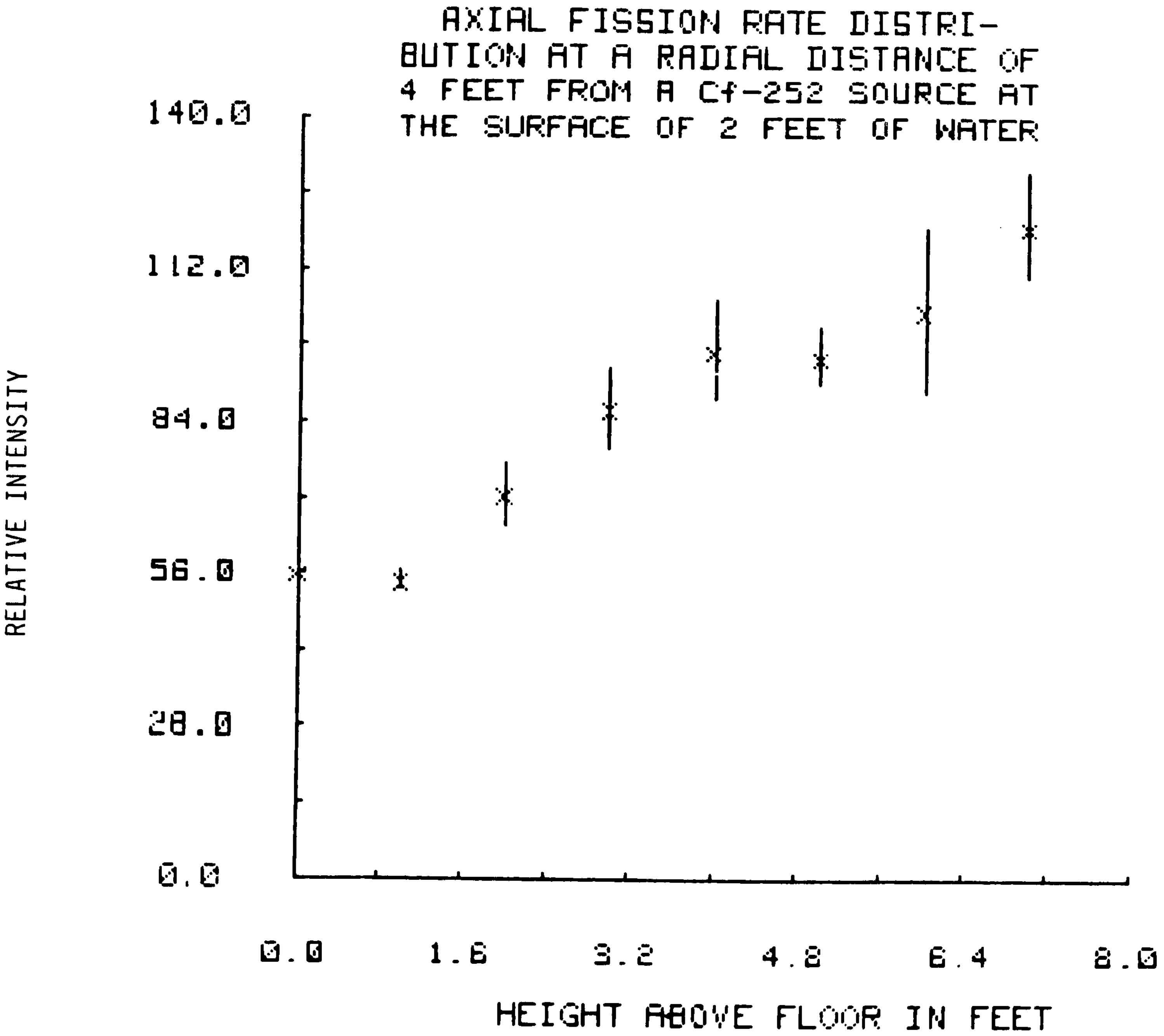

FIGURE B-8. SSTR Neutron Dosimeter Axial Response at a Radial Distance of 4' to a ^{252}Cf Source Suspended at the Center of the Surface of a 2' High by 4' Diameter Tank of Water.

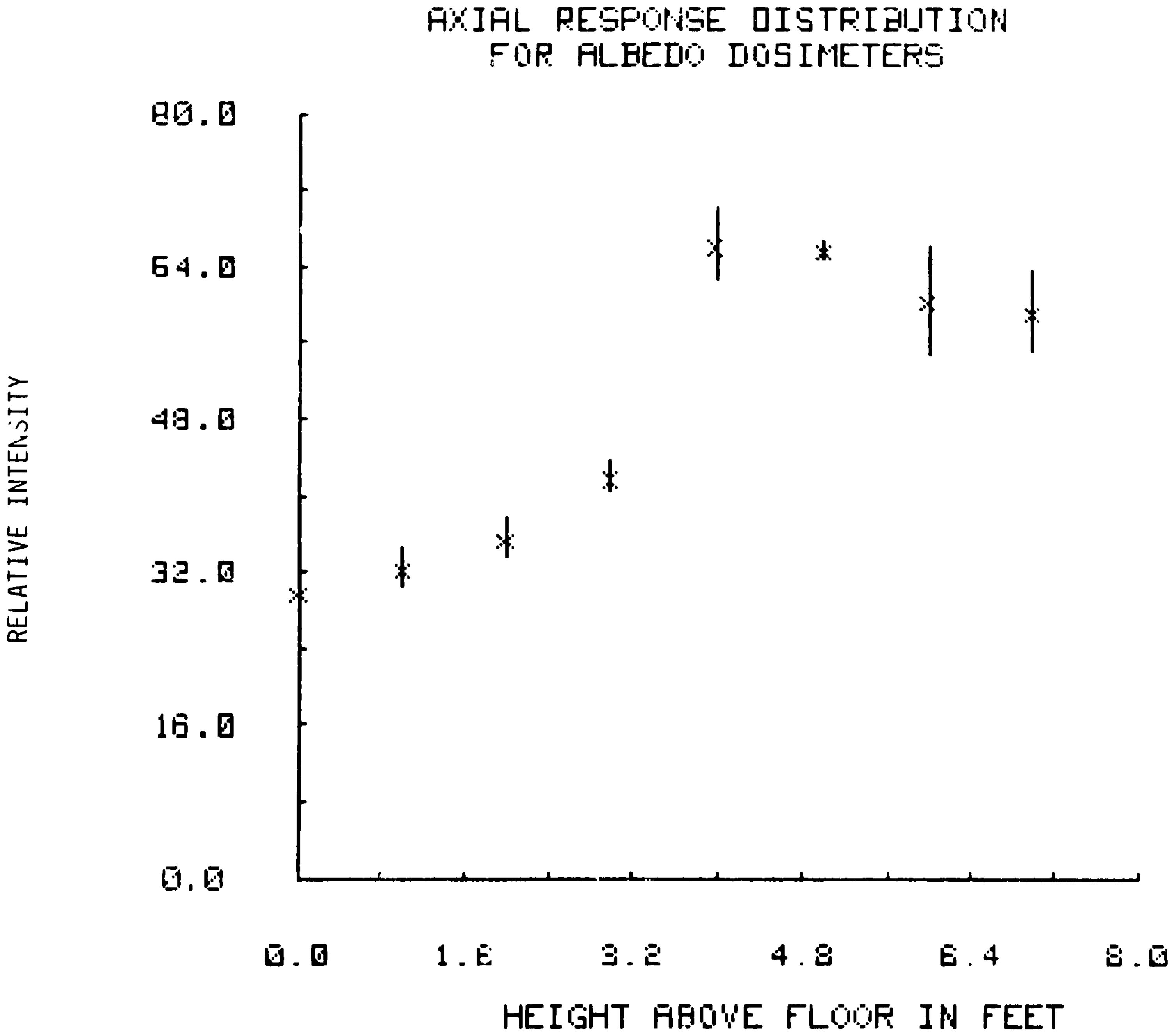

FIGURE B-9. As in Figure B-8 but with Albedo Dosimeters of the Design Shown in Figure 1.

APPENDIX C

POINT SOURCE RESPONSE OF SSTR NEUTRON DOSIMETRY

An estimate of the amount of fuel in the demineralizer has been made from the distribution of the fission tracks/cm^2 observed in SSTR along the vertical stringer above the peak observed in the gamma ray distribution. Let us assume that the bulk of the fuel, near the far side of the demineralizer according to the gamma ray measurements, occupies a space small relative to the distance from the SSTR's so that it can be treated as a "point" source. If there is then no or little moderator between the fuel and these SSTR, one would expect that the intensity of neutrons over and above cosmic ray and room return neutrons would approximate a $1/R^2$ behavior, where R is the distance between the fuel and the SSTR. Let X be the horizontal distance between the fuel and the vertical row of SSTR's, and let Z be the distance each SSTR is above the horizontal plane containing the source. Then $R^2 = X^2 + Z^2$. If we let F be the fission tracks/cm^2, then

$$F = \frac{C}{R^2} = \frac{C}{X^2 + Z^2} \quad , \qquad [3]$$

where C is a constant.

It is useful to work with $1/F = \frac{X^2 + Z^2}{C}$, since if we let $\nu = Z^2$, we have the linear relationship

$$1/F = a + b\nu, \qquad [4]$$

where $a = \frac{X^2}{C}$ and $b = 1/C$.

Table C-1 gives the measured values of F and the estimated values of Z for the nearest four SSTR above the horizontal source plane.

TABLE C-1

VARIATION OF SSTR FISSION TRACK DENSITY WITH VERTICAL DISTANCE (Z)

SSTR Label	Z(ft.)	F(fission tracks/cm^2)
TMI-267	0.29	26.5 ± 6.0
TMI-265	1.29	20.3 ± 5.1
TMI-263	2.29	15.2 ± 5.0
TMI-261	3.29	16.1 ± 5.1

Figure C-1 shows a linear least squares fit, including statistics, to $1/F = a + b\nu$, giving $a = (4.03 \pm 0.75) \times 10^{-2}$, and $b = (2.60 \pm 1.91) \times 10^{-3}$. Calculating C and X from these, we obtain

$$C = 385 \pm 283 \qquad [5a]$$

and

$$X = 3.94 \begin{smallmatrix} + 1.29 \\ - 2.01 \end{smallmatrix} \text{ ft.} \qquad [5b]$$

Note that the value of X is consistent with the fuel being near the far side of the tank. Figure C-2 shows a plot of $F = C/R^2$ and the data points, indicating that the results are also at least consistent with a $1/R^2$ distribution. The fitted value of F for the SSTR at Z = 0.29 ft. is 24.7 ± 6.0. (The actual value of σ would be a little less, but this uncertainty does not dominate in the measurements, as the following analysis will show.)

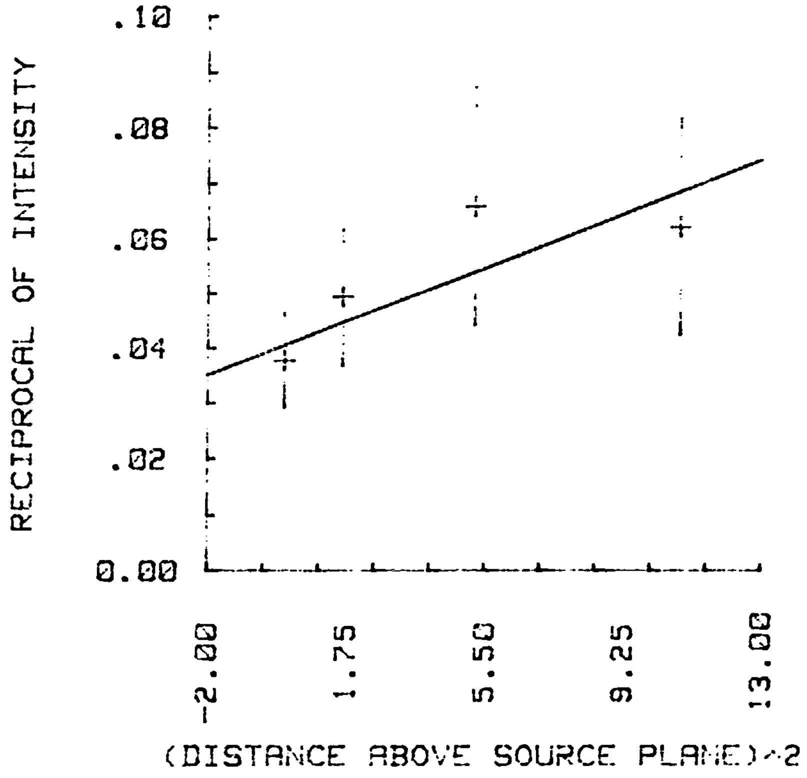

FIGURE C-1. TMI Demineralizer SSTR Data Test of $1/R^2$ Fit.

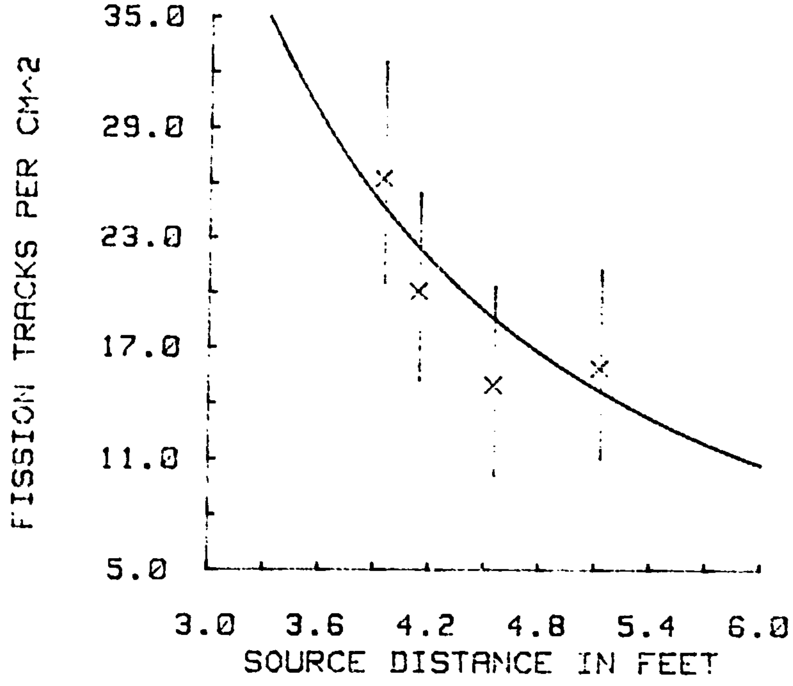

FIGURE C-2. 1/R^2 Fit of the SSTR Demineralizer Data.

In Figure B-4 is shown the fission tracks per cm^2/min. for the ^{252}Cf source suspended 2 ft. above the floor, and the bare SSTR-^{235}U assemblies at the same height but at different horizontal distances from the source. The result for the SSTR 2 ft. from the source is 175 fission tracks/cm^2/min. and for the other positions 140 fission tracks/cm^2/min.. If we assume the latter as the room return level, 35 tracks/cm^2/min. would be due to the proximity of the source. If we assume a $1/R^2$ fall off of these, this signal at 3.95 ft. would be 9.0 tracks/cm^2/min., and the fraction above room return 0.064. In the case of the SSTR giving the highest response at the demineralizer, the corresponding ratio is 24.7/5.0 = 4.94 or a factor of 4.94/.064 = 77.2 higher.

Two factors would be expected to contribute to the difference in these ratios: (1) in the calibration experiment the SSTR is bare (no lucite) so that its response to fast neutrons coming from the source is reduced; (2) in the demineralizer with resin near the fuel, many neutrons will be moderated sufficiently to increase the response of the albedo detector, but will still have a "memory" of their source. Considering the assumptions, however, we assign an uncertainty of 50% to this ratio.

With the ^{252}Cf source, having an emission rate of 3.08×10^8 neutrons/sec., and the SSTR having a response like the albedo detector placed 0.29 ft. above the source plane in the demineralizer environment we would expect the response to the neutrons coming from source region to give 9.0 x 77.2 = 695 tracks/cm^2/min.. The neutron flux producing these tracks would be

$$\frac{3.08 \times 10^8 \times 60}{4\Pi(3.95 \times 12 \times 2.54)^2} = 1.015 \times 10^5 \text{ neutrons/cm}^2\text{/min.} \qquad [6]$$

If n is the number of kg of fuel having an emission rate of 300 neutrons/sec/kg, the flux would be

$$\frac{300\ n \times 60}{4\Pi(3.95 \times 12 \times 2.54)^2} = (9.882 \times 10^{-2})n \text{ neutrons/cm}^2\text{/min.} \qquad [7]$$

The SSTR response is given by 24.7/(29 x 24 x 60) = 5.91×10^{-4} tracks/cm^2/min..
We thus have the relationship of proportions,

$$\frac{n(9.88 \pm 1) \times 10^{-2}}{(1.02 \pm 0.1) \times 10^5} = \frac{(5.91 \pm 0.6) \times 10^{-7}}{(695 \pm 350)}$$

$$\therefore n = \frac{(1.02 \pm 0.1) \times 10^5 \times (5.91 \pm 0.6) \times 10^{-4}}{(9.88 \pm 0.9) \times 10^{-2} \times (695 \pm 350)} \qquad [8]$$

$$n = (0.9 \pm 0.5) \text{ kg.}$$

This result is consistent with that obtained from room return and from the gamma ray measurements, but is less reliable because of inadequate calibration data. In fact, it is the best that can be done short of conducting further more detailed calibration experiments and obtaining more detailed information on the source spatial distribution.

DISTRIBUTION LIST FOR HEDL-TC-2492

Internal

D. G. Doran - W/A-57
E. A. Evans - W/C-23
R. Gold - W/C-39
B. R. Hayward - W/C-44
W. W. Jenkins - W/B-84
R. L. Knecht - W/A-40
F. J. Leitz - W/C-27
E. P. Lippincott - W/C-39
M. K. Mahaffey - W/B-12
W. N. McElroy - W/C-39
J. P. McNeece - W/A-56
W. J. McShane - W/B-112
L. M. Northey - W/B-84
E. J. Renkey - W/B-17
J. H. Roberts - W/C-39
F. H. Ruddy - W/C-39
F. A. Schmittroth - W/A-4
W. F. Sheely - W/C-44
D. L. Swannack - W/B-84
H. H. Yoshikawa - W/C-44
Central Files (3) - W/C-110
Publication Services (2) - W/C-115
Documentation Services - W/C-123
Microfilming - W/C-123

External

DOE/RL

J. J. Schreiber, Director
Waste Management Division

K. R. Absher

R. J. Myjak, AMAR Operations (w/o enclosure)

P. F. X. Dunigan, Jr. (3)

F. R. Standerfer

EG&G/TIO

G. J. Quinn (7)

PNL

D. E. Knowlton

RHO

R. E. Smith

ORNL

W. D. Bond

LANL

J. Halbig

EG&G Idaho, Inc.
PO Box 88, Middletown, PA 17057

From Quinn 10-10-83 -10

DCC: H. M. Burton
F. C. Fogarty
K. C. Sumpter

October 6, 1983

DISTRIBUTION

DEMINERALIZER RESIN SAMPLE STUDY RESULTS FROM EXPERIMENTS AT OAK RIDGE NATIONAL LABORATORY - GJQ-46-83

Ref: G. J. Quinn ltr to Distribution, GJQ-42-83, Demmineralizer Resin Sample Studies at Oak Ridge National Laboratory, September 20, 1983

Attached is a copy of the meeting minutes from a meeting held September 27, 1983 at TMI to discuss results from experimental studies with demineralizer resin samples performed at Oak Ridge National Laboratory.

Very truly yours,

G J Quinn

[redacted]aste Immobilization Program Manager

cmr

Attachment:
As Stated

Distribution:

GPUNC
J. J. Bevelacqua
E. D. Showalter
J. Galanto
T. Osterhoudt
W. J. Marshall
S. J. Eichfeld
C. G. Hitz

Geocenters
L. Isaacson

WHC
E. J. Renkey

DOE
J. K. Reilly

NRC
D. Hennart
J. A. Thomas
T. Moslak

ORNL
W. D. Bond

cc: B. K. Kanga, GPUNC

Attachment 1
October 6, 1983
GJQ-46-83
Page 1 of 2

Experimental Studies with Demineralizer Resin Samples From TMI Meeting, September 27, 1983

Meeting Minutes

A GPUNC developed preliminary flowsheet for the stripping of Cs from the makeup and purification demineralizers was tested at Oak Ridge National Laboratory (ORNL) using a B demineralizer vessel resin sample. A copy of the slides used in the presentation is attached.

The first slide shows that ORNL has completed the tests and summarizes the results. As indicated, the GPUNC flowsheet test was successful (see slide 2), organics removal by charcoal was not very effective (see Appendix A, Table A-4), the effects of organics on zeolites were minor (see slide 7) and a 0.5 micron filter will remove finely divided solids.

Slide 2 is a graph of instantaneous and cumulative Cs137 removal using the GPUNC developed process flowsheet. Table A-2 in Appendix A provides for each stage of this process: the elution agent, the Cs137 effluent concentration, the instantaneous and cumulative percentages of Cs137 removal, the distribution coefficient (Kd) values, the organics concentration in the effluent and the cumulative mass of organics leached from the resin. While the first twelve stages were per the GPUNC flowsheet, by this stage instantaneous removal had reached less than 3% removal and ORNL used NaOH to see the relative increase in removal rate and total removal achievable.

Slide 3 shows the graph of instantaneous and cumulative Cs137 removal for a test for which results had first been presented at TMI on July 14, 1983 (see Ref. 1). The graph was included here to clarify that total removal had reached 93% as shown in Table A-1 which provides detailed results for this test. ORNL indicated that after the July 14 meeting another analysis of the resin loading showed the starting value for the stripping process to be 21.8 mCi of Cs137 per gram which affected the results originally presented.

Slide 4 shows a graph of ppm of organics leached per batch for the various solutions in the GPUNC flowsheet. Values are provided in Table A-2.

Slide 5 shows the sodium ion concentration dependence of the distribution coefficient values. The Kd values for sodium ion concentrations between 0.26M and 0.032M would be on this straight line.

Slide 6 shows a graph for organics concentration in the effluent for three tests. The curve marked Zeolite-1 is the removal of the organics from raw feed by zeolite only. Curve (SK-4)-1 is the removal by charcoal of the organics remaining after the zeolite. Curve (SK-4)-2 is the removal of the organics from raw feed by SK-4 charcoal only. The charcoal did not retain any significant amount of Cs in this test.

007010628

Slide 7 shows the Cs removal by zeolite for both raw (1st SDS run curve) and charcoal treated feed (2nd SDS run curve) (See Table A-5). Initial concerns were the effect of organics on the SDS zeolites and these have been shown to be minor.

Slide 8 is a list of isotopes found by a gamma scan from solids removed by a 0.5 micron filter. From approximately 5 ml of 0.5 mCi/ml solution generated from the first 6 stages of the GPUN flowsheet tests, a maximum of 1 mg of material was left on the filter. Some sulfur, titanium, stainless steel and zirconium have been identified in the solids.

Appendix A provides the data for the tests performed by ORNL.

As a result of these tests GPUNC will reevaluate the proposed use of a charcoal filter to remove organics from the demineralizer Cs removal process streams before these solutions are introduced in to plant piping via the MUF5B filter housing.

EXPERIMENTAL STUDIES WITH DEMINERALIZER RESIN SAMPLES FROM TMI

W. D. BOND, ORNL
J. B. KNAUER, ORNL

Presentation at Three Mile Island
September 27, 1983

STATUS OF WORK

- COMPLETED SECOND MULTISTAGE BATCH ELUTION TEST ON B-2 RESIN
- SK-4 CHARCOAL NOT VERY EFFECTIVE FOR REMOVAL OF CARBONACEOUS COMPOUNDS
- EFFECTS OF CARBONACEOUS COMPOUNDS IN SDS COLUMN TESTS WERE MINOR
- FINELY DIVIDED SOLIDS IN EARLY ELUATES OF BATCH ELUTION ARE REMOVED BY 0.5 µ MILLIPORE FILTER

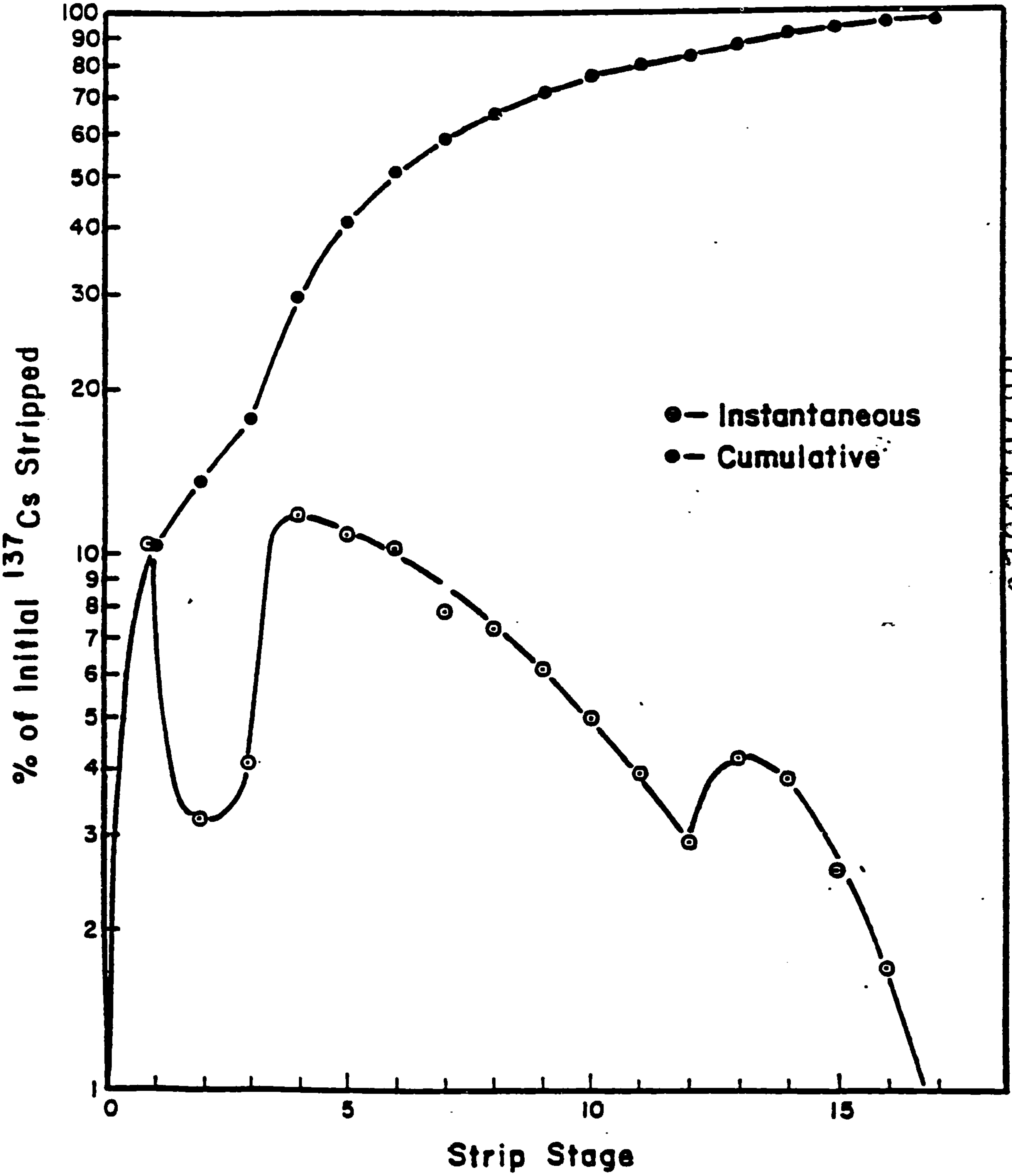

BATCH ELUTION TEST 2 OF B-2 SOLIDS

SLIDE 2

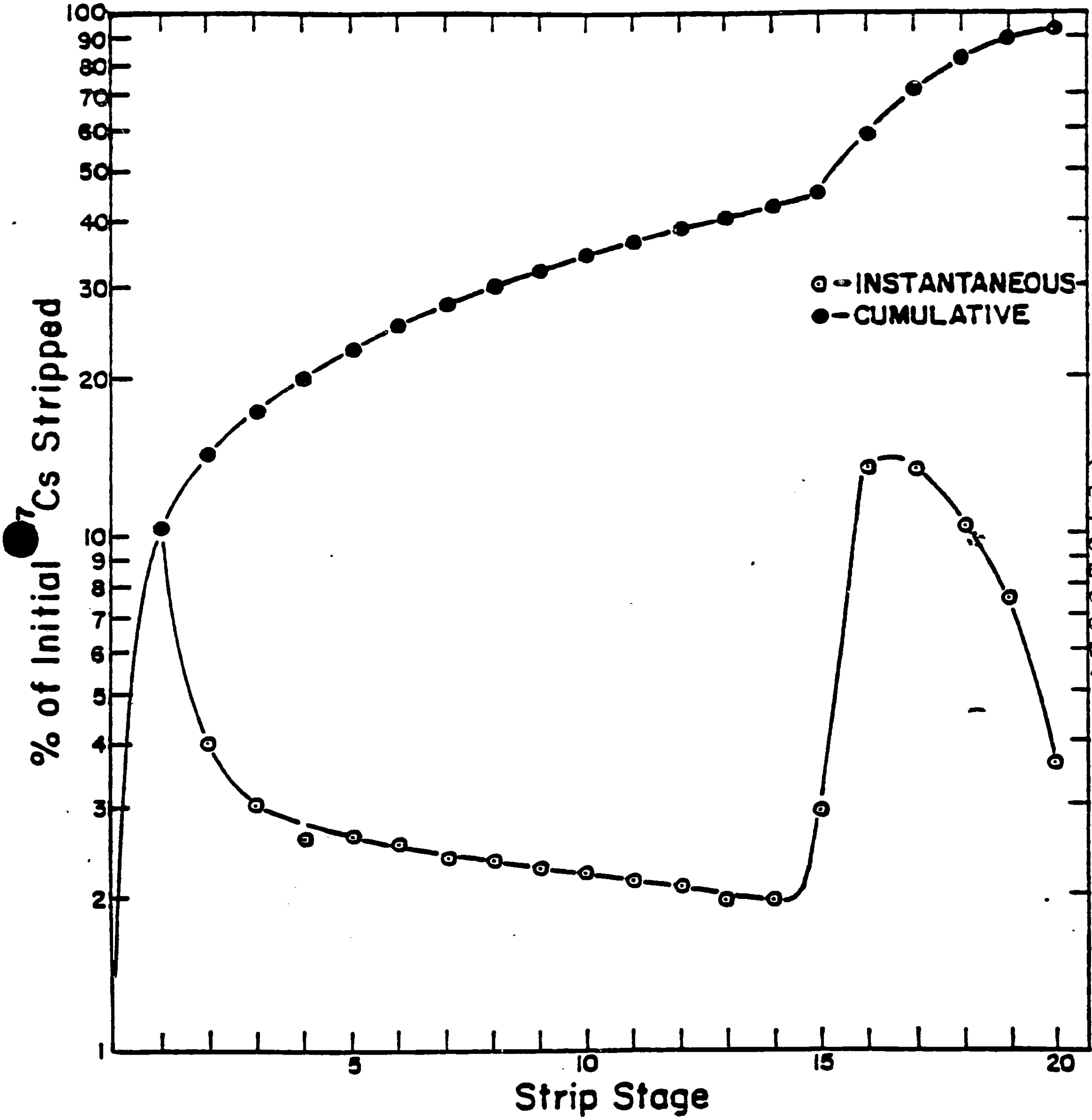

BATCH ELUTION TEST-1 OF B-2 SOLIDS

SLIDE 3

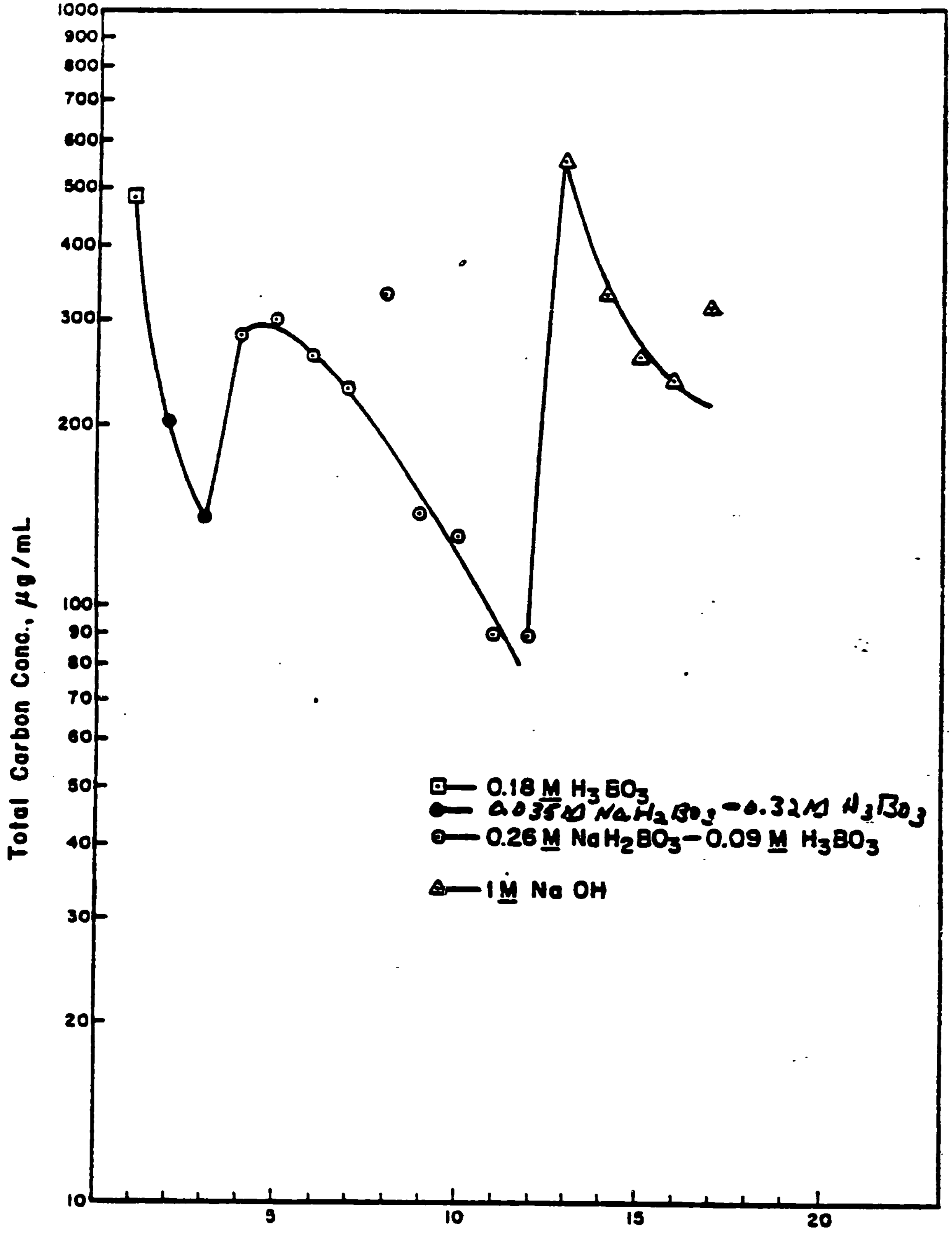

LEACHING OF CARBONACEOUS COMPOUND IN BATCH ELUTION – TEST 2

SLIDE 4

SODIUM CONCENTRATION DEPENDENCE IN B-2 RESIN ELUTION TESTS

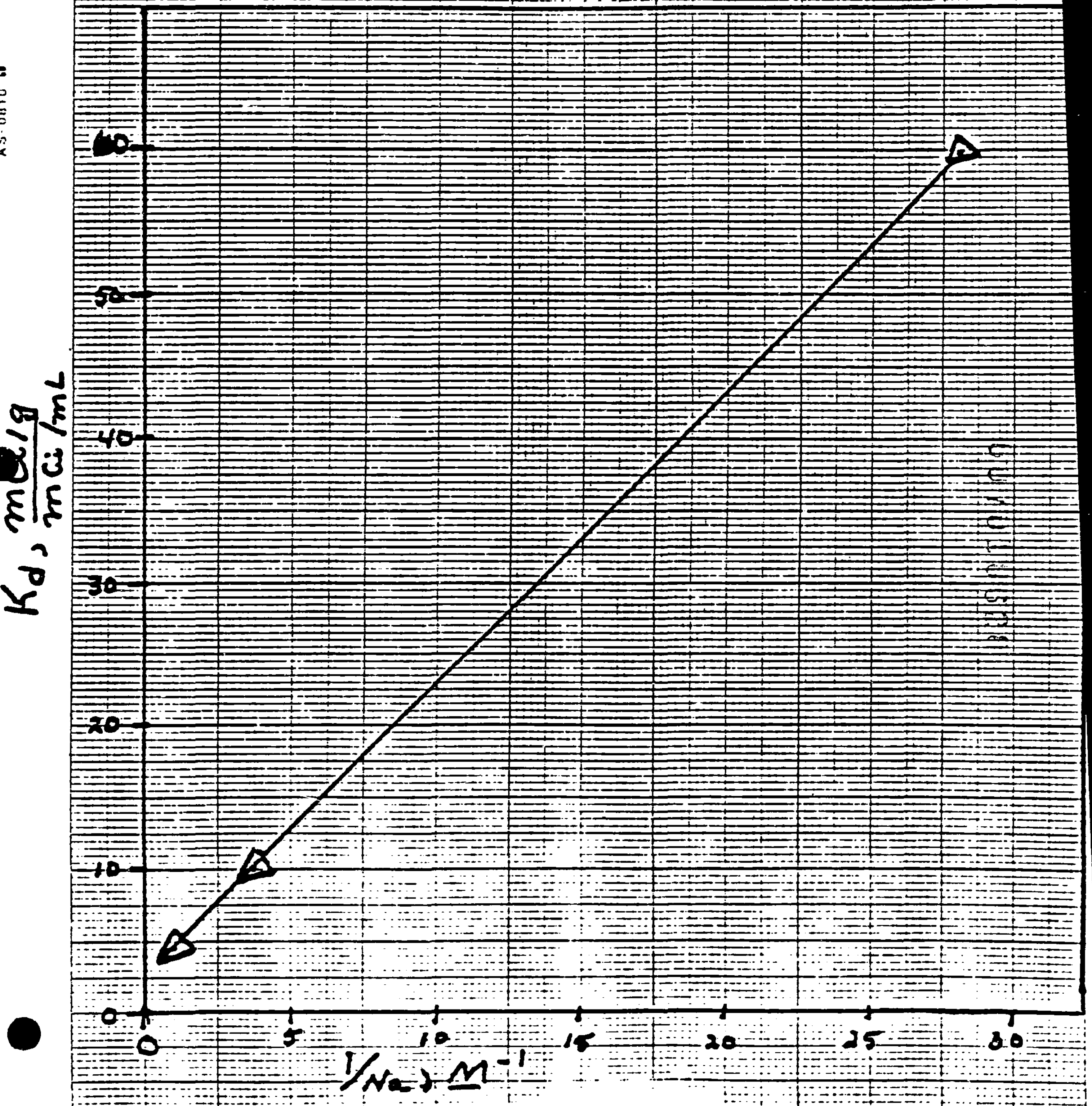

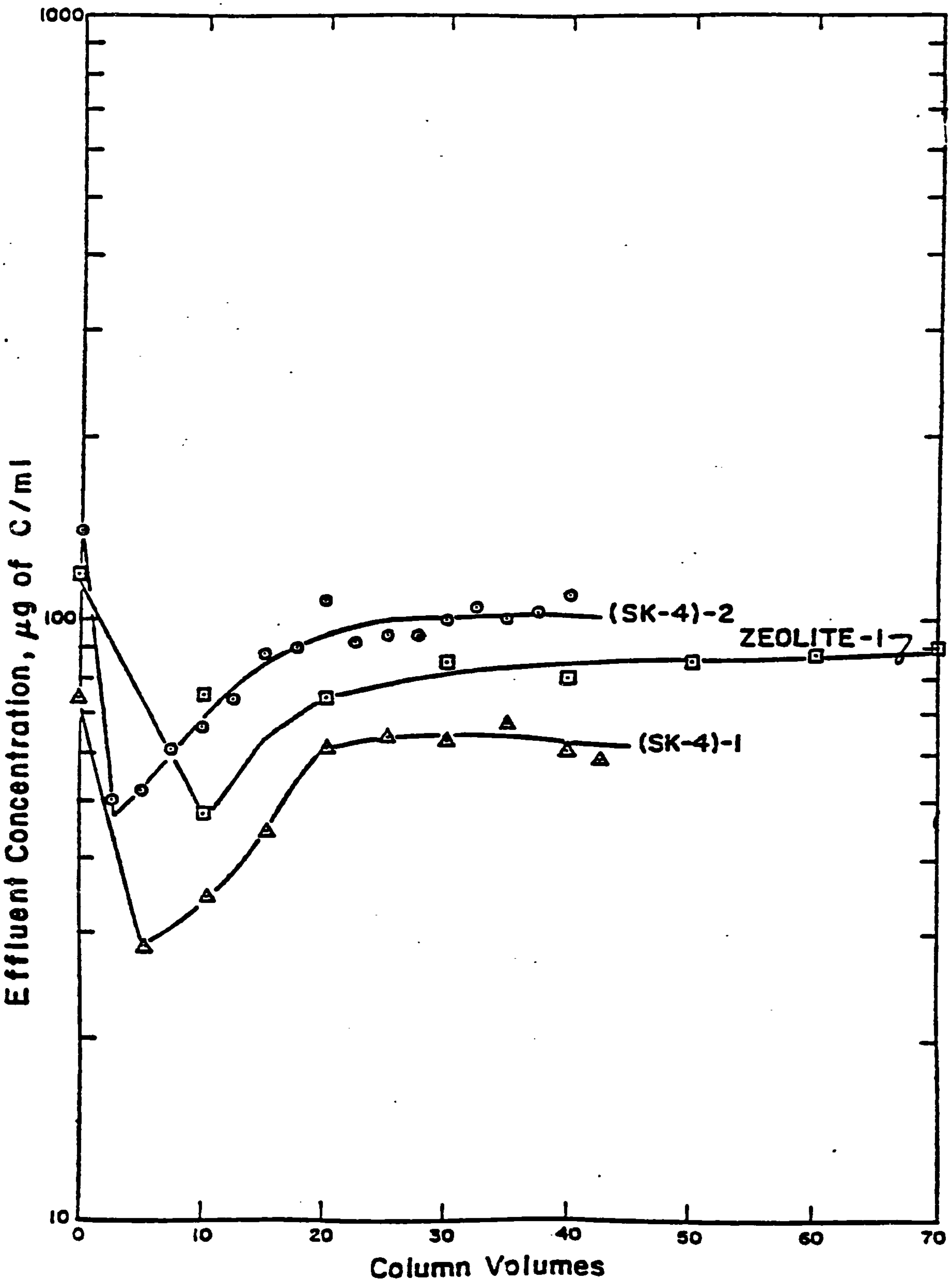

SORPTION OF SOLUBLE CARBONACEOUS SPECIES ON ZEOLITE AND ON SK-4 CHARCOAL BEDS

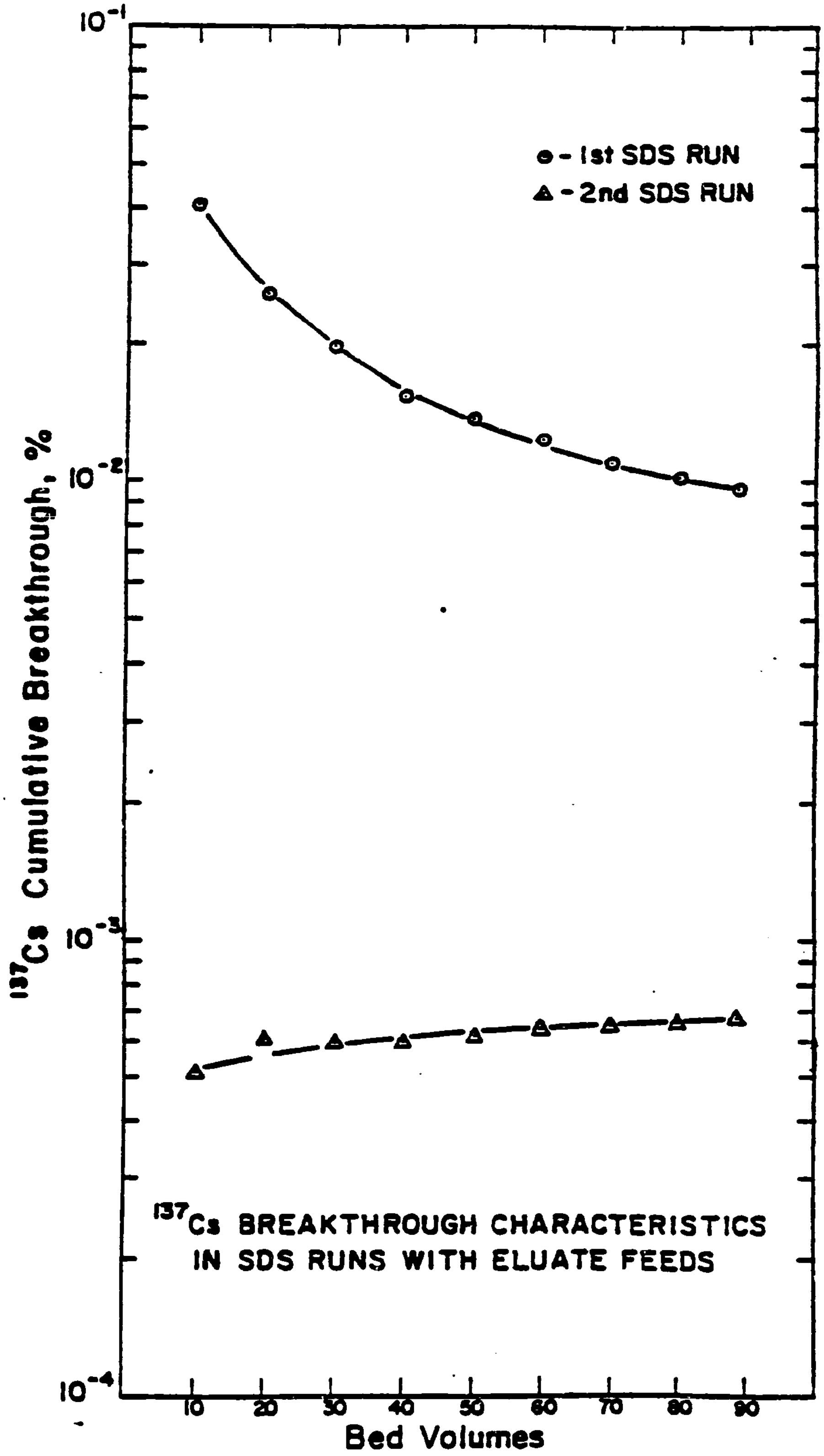

^{137}Cs BREAKTHROUGH CHARACTERISTICS IN SDS RUNS WITH ELUATE FEEDS

SLIDE 7

GAMMA SCAN OF FILTER SOLIDS

Isotope	Activity, dis/s
$^{60}\mathrm{Co}$	27
$^{125}\mathrm{Sb}$	310
$^{134}\mathrm{Cs}$	1.66×10^{3}
$^{137}\mathrm{Cs}$	2.69×10^{4}
$^{144}\mathrm{Ce}$	52

APPENDIX A

DETAILED COMPILATION OF DATA AND RUN CONDITIONS FOR THE BATCH RESIN ELUTION, SDS ZEOLITE COLUMN, AND CHARCOAL BED TESTS

BATCH ELUTION OF B-2 RESIN: TEST 1

Conditions: 7.48 g of resin (~10 mL); 21.8 mCi of ^{137}Cs/g; contacted with 15 mL of elution agent for 30 min.

Stage Number	Elution Agent	^{137}Cs in effluent (mCi/mL)	% of Initial ^{137}Cs Eluted		K_d $\frac{(mCi/g)}{(mCi/mL)}$	Total Carbon	
			Instan.	Cumul.		Eluate Conc. (µg/mL)	Cumulative Mass Leached (mg/g of resin)
1	0.035 M NaH_2BO_3-0.32 M H_3BO_3	1.119	10.3	10.3	17.5	370	0.7
2		0.432	4.0	14.3	43.3	140	1.0
3		0.330	3.0	17.3	54.6	200	1.4
4		0.281	2.6	19.9	62.1	75	1.6
5		0.284	2.6	22.5	59.5	73	1.7
6		0.273	2.5	25.0	59.9	74	1.9
7		0.255	2.4	27.4	62.1	72	2.0
8		0.252	2.3	29.7	60.8	54	2.1
9		0.245	2.2	31.9	60.6	60	2.3
10		0.240	2.2	34.1	59.8	62	2.4
11		0.231	2.1	36.2	60.1	130	2.7
12		0.225	2.1	38.3	59.8	70	2.8
13		0.214	2.0	40.3	60.8	60	2.9
14		0.212	2.0	42.3	59.4	50	3.0
15		0.316	2.9	45.2	37.8	100	3.2
16	1 M NaOH	1.443	13.3	58.5	6.3	870	5.0
17		1.424	13.1	71.6	4.4	430	5.8
18		1.111	10.2	81.8	3.6	430	6.7
19		0.822	7.6	89.4	2.8	250	7.2
20		0.492	3.6	93.0	3.1	250	7.7

BATCH ELUTION OF B-2 RESIN: TEST 2

Conditions: 7.22 g of resin (~10 mL); 21.8 mCi of ^{137}Cs/g; contacted with 15 mL of elution agent for 30 min.

Stage Number	Elution Agent	^{137}Cs in effluent (mCi/mL)	% of Initial ^{137}Cs Eluted		K_d (mCi/g)/(mCi/mL)	Total Carbon	
			Instan.	Cumul.		Eluate Conc. (μg/mL)	Cumulative Mass Leached (mg/g of resin)
1	0.18 M H_3BO_3	1.09	10.4	10.4	17.9	480	1.0
2	0.035 M NaH_2BO_3-0.32 H_3BO_3	0.340	3.2	13.6	55.4	200	1.4
3		0.420	4.0	17.6	42.8	140	1.7
4	0.26 M NaH_2BO_3-0.09 M H_3BO_3	1.23	11.7	29.3	12.5	290	2.3
5		1.14	10.9	40.2	11.4	300	3.0
6		1.05	10.0	50.2	10.3	260	3.5
7		0.870	7.7	57.9	10.5	230	3.9
8		0.757	7.2	65.1	10.0	330	4.6
9		0.632	6.0	71.1	9.9	140	4.8
10		0.516	4.9	76.0	10.1	130	5.1
11		0.405	3.9	79.9	10.8	88	5.3
12		0.343	2.8	82.7	10.9	88	5.5
13	1 M NaOH	0.432	4.1	86.8	6.6	560	6.7
14		0.395	3.8	90.6	5.1	340	7.4
15		0.264	2.5	93.1	5.6	260	7.9
16		0.175	1.7	94.8	6.4	240	8.4
17		0.097	0.8	95.6	9.7	320	8.5

SORPTION OF CARBONACEOUS COMPOUNDS ON SDS ZEOLITE BED

Conditions: 2 mL of zeolite, superficial bed residence time of 8.4 min.

Column Volumes	% Breakthrough[a] Raw Feed	% Breakthrough[a] Charcoal Treated Feed	Bed Loading, mg of C/mL of zeolite Raw Feed	Bed Loading, mg of C/mL of zeolite Charcoal Treated Feed
10	40	42	0.7	0.5
20	62	71	1.2	0.7
30	71	76	1.5	0.9
40	67	71	1.9	1.1
50	71	74	2.3	1.3
60	73	79	2.6	1.5
70	75	80	2.9	1.6
80	84	85	3.1	1.8
87.5	78	92	3.3	1.8

[a] Concentrations of total carbon in the raw and charcoal treated feeds were 120 and 80 μg of C/mL, respectively.

SORPTION OF CARBONACEOUS COMPOUNDS ON SK-4 CHARCOAL BED

Conditions: Superficial bed residence time of 10.4 min., 80-100 mesh SK-4 charcoal (Alltech. Assoc./Applied Sciences Division)

Column Volumes	% Breakthrough[a]		Bed Loading, mg of C/g of charcoal[b]	
	Zeolite Treated Feed	Raw Feed	Zeolite Treated Feed	Raw Feed
2.5		34		0.5
5.0	38	36	0.5	1.0
7.5		42		1.5
10.0	46	46	1.0	1.9
12.5		51		2.3
15.0	59	61	1.3	2.6
17.5		62		2.9
20.0	83	75	1.4	3.1
22.5		63		3.4
25.0	85	66	1.6	3.7
27.5		66		4.0
30.0	84	69	1.7	4.2
32.5		72		4.5
35.0	91	69	1.8	4.7
37.5		71		4.9
40.0	80	76	1.9	5.1
42.5	79		2.0	

[a] Feed concentrations of the zeolite treated feed and the raw feed were 75 and 140 μg of C/mL, respectively.

[b] A 2-mL (0.91 g) bed was employed in the run with zeolite-treated feed and a 6-mL (2.71 g) bed was used in the run with raw feed.

CUMULATIVE ^{137}Cs DECONTAMINATION FACTORS (DFs) AND EFFLUENT CONCENTRATIONS ACHIEVED WITH SDS ZEOLITE COLUMNS USING RAW AND CHARCOAL-TREATED FEEDS

Conditions: 2 mL bed of zeolite (60 vol % Ionsiv-96 and 40 vol % A-51); superficial residence time of 8.4 min.

Bed Volumes	^{137}Cs Concentration in Effluent[a] (mCi/mL)		Cumulative DF	
	Run Z-1	Run Z-2	Run Z-1	Run Z-2
10	1.43×10^{-1}	1.76×10^{-3}	2.44×10^{3}	1.97×10^{5}
20	3.95×10^{-2}	2.41×10^{-3}	3.84×10^{3}	1.65×10^{5}
30	2.53×10^{-2}	2.04×10^{-3}	5.02×10^{3}	1.68×10^{5}
40	6.89×10^{-3}	2.07×10^{-3}	6.50×10^{3}	1.68×10^{5}
50	2.38×10^{-2}	2.37×10^{-3}	7.32×10^{3}	1.62×10^{5}
60	2.06×10^{-2}	2.60×10^{-3}	8.09×10^{3}	1.57×10^{5}
70	1.05×10^{-2}	2.59×10^{-3}	9.07×10^{3}	1.53×10^{5}
80	1.40×10^{-2}	2.40×10^{-3}	9.84×10^{3}	1.52×10^{5}
87.5	1.48×10^{-2}	2.70×10^{-3}	1.04×10^{4}	1.50×10^{5}

---

[a] Concentrations of ^{137}Cs in the feed for Runs Z-1 and Z-2 were 3.49×10^{2} and 3.46×10^{2} mCi/mL, respectively. Raw feed was used in Run Z-1, whereas charcoal-treated feed was used in Run Z-2.

HEDL-7335

RESIN AND DEBRIS REMOVAL SYSTEM CONCEPTUAL DESIGN

THREE MILE ISLAND NUCLEAR STATION UNIT 2 MAKE-UP AND PURIFICATION DEMINERALIZERS

Hanford Engineering Development Laboratory

HANFORD ENGINEERING DEVELOPMENT LABORATORY
Operated by Westinghouse Hanford Company
P.O. Box 1970 Richland, WA 99352
A Subsidiary of Westinghouse Electric Corporation
Prepared for the U.S. Department of Energy
Assistant Secretary for Nuclear Energy
Office of Terminal Waste Disposal
and Remedial Action
under Contract No. DE-AC06-76FF02170
B&R No. AG 30-0[illegible]

Printed in the United States of America

HEDL-7335

RESIN AND DEBRIS REMOVAL SYSTEM CONCEPTUAL DESIGN

THREE MILE ISLAND NUCLEAR STATION UNIT 2 MAKE-UP AND PURIFICATION DEMINERALIZERS

Hanford Engineering Development Laboratory

M.K. Mahaffey
E.J. Renkey
W.W. Jenkins
L.M. Northey
R.D. Hensyel
May 1983

HANFORD ENGINEERING DEVELOPMENT LABORATORY
Operated by Westinghouse Hanford Company
P.O. Box 1970 Richland, WA 99352
A Subsidiary of Westinghouse Electric Corporation
Prepared for the U.S. Department of Energy
Assistant Secretary for Nuclear Energy
Office of Terminal Waste Disposal
and Remedial Action
under Contract No. DE-AC06-76FF02170

RESIN AND DEBRIS REMOVAL SYSTEM
CONCEPTUAL DESIGN
THREE MILE ISLAND NUCLEAR STATION
UNIT 2 MAKEUP AND PURIFICATION DEMINERALIZERS

M. K. Mahaffey
E. J. Renkey
W. W. Jenkins
L. M. Northey
R. D. Hensyel

ABSTRACT

Quantities of fuel, core debris and fission products were released from the Three Mile Island Nuclear Station Unit 2 reactor vessel and significant quantities of these materials are believed to be deposited in the pressurized water makeup and purification demineralizers. The various methods of characterizing these highly radioactive contents are described, as well as a summary of the results. A five-step process is presented for remotely removing the resin and debris. The process includes elution of ^{137}Cs *and transferring the demineralizer contents to shipping containers by utilization of two slurrying steps. The selection criteria for shipping containers and casks is discussed and possible research programs for the resin and debris are proposed.*

CONTENTS

CONTENTS (Cont'd)

CONTENTS (Cont'd)

FIGURES

FIGURES (Cont'd)

TABLES

RESIN AND DEBRIS REMOVAL SYSTEM
CONCEPTUAL DESIGN
THREE MILE ISLAND NUCLEAR STATION
UNIT 2 MAKEUP AND PURIFICATION DEMINERALIZERS

1.0 INTRODUCTION

The pressurized water letdown flow and makeup systems of the Three Mile Island Nuclear Station Unit 2 (TMI-2) were on-line during a portion of the time of the March 28, 1979 accident. Quantities of fuel, core debris and fission products were released from the reactor vessel and circulated through various components making up the auxiliary systems. Significant quantities of these accident by-products are believed to be deposited in the pressurized water makeup and purification demineralizers.

These demineralizers are located in shielded cubicles of the auxiliary building of the TMI-2 nuclear plant. High radioactivity precludes normal access to the demineralizer cubicles as well as normal disposal of the resin using existing plant systems.

Westinghouse Hanford Company was selected as lead contractor to coordinate the Department of Energy Richland Operations efforts in a program of demineralizer chararacterization as well as the evaluation of alternatives for removal of the demineralizer contents. This report describes the results of the characterization efforts and provides a conceptual design for removal of the demineralizer contents. Possible research uses of the resin are also discussed.

1.1 REMOVAL SYSTEM FUNCTIONS

The resin and debris removal system shall provide the following specific functions:

A. Removal of essentially all radioactive solids and liquids from the Make-up and Purification Demineralizers, MU-K-1A and 1B.

B. Treatment of all liquid effluents to assure compatibility with onsite water processing systems (Submerged Demineralizer System and EPICOR II)

C. Onsite handling of radioactive demineralizer contents consistent with normal TMI-2 practices.

D. Containerization of the radioactive demineralizer contents in a form suitable for use in a DOE research and development program.

E. Transportation of radioactive demineralizer contents to a DOE site using licensed or licensable containers and casks.

F. Flushing of lines after resin removal is complete.

1.2 REMOVAL SYSTEM PROCESS REQUIREMENTS

A. Existing TMI-2 systems and equipment shall be used to the maximum extent practical.

B. Selection of existing piping and routing of new piping shall minimize personnel exposure consistant with ALARA considerations in place at TMI-2. Maximum use should be made of existing architectural features.

C. Operational process selection shall result in minimizing personnel exposure consistent with ALARA considerations in place at TMI-2.

D. The resin and debris removal system shall perform its required functions only during normal plant operating and clean-up conditions.

E. The resin and debris removal system is a temporary system and shall be removed when its required functions have been performed. Any modifications to the existing TMI-2 systems shall include provisions for returning those systems to their original configuration. Radiation levels in the permanent piping shall be left in a condition acceptable for the original design usage.

F. Materials used in the removal system shall be compatible with the conveyed and contained internal fluids and with the surrounding environment including the anticipated radiological dosage.

G. Operation of the resin and debris removal process shall be independent of the handling, storage and transportation of the waste packages.

H. TMI-2 plant demineralized water, processed water, reactor coolant grade water and nitrogen sources may be utilized provided that precautions exist to preclude backflow into these systems.

1.3 CODES AND STANDARDS

A. USNRC Regulatory Guide 1.143, Design Guidance for Radioactive Waste Management Systems, Structures, and Components Installed in Light-Water-Cooled Nuclear Power Plants.

B. ASME Boiler and Pressure Vessel Code, Section VIII Division 1.

C. ANSI B31.1 Power Piping Systems.

D. Title 49, Code of Federal Regulations, Part 173, Department of Transportation Hazardous Material Regulations.

E. NEC - National Electric Code.

F. NEMA - National Electrical Manufacturers' Association.

G. ASME/ANSI NQA-1, Quality Assurance Requirements for Nuclear Power Plants.

2.0 SYSTEM DESCRIPTION AND CURRENT STATUS

The two makeup and purification demineralizers, MU-K-1A and MU-K-1B, are a part of the pressurized water makeup and purification system which is designed to provide chemistry control to the reactor primary coolant system. The demineralizers contain a 3:2 ratio mixed bed of anion and cation organic resins to control the concentrations of potentially corrosive minerals and to reduce the buildup of radioactive deposits in the circulating system.

2.1 MAKEUP AND PURIFICATION SYSTEM

The schematic of the makeup and purification system is shown in Figure 1. Letdown flow is taken off of the primary system upstream of the primary pump. Flow is routed through the letdown coolers, through a block orifice to reduce pressure, to the makeup filters MU-F-5A and MU-F-5B and then to the two demineralizers MU-K-1A and MU-K-1B. At flow rates below 70 gpm one filter and one demineralizer are on line; above 70 gpm both filters and demineralizers are in service.

The accident was initiated March 28, 1979 at approximately 0400 by a turbine trip on low feedwater flow rate. During the accident, letdown flow varied from 40 to 150 gpm. Significant core damage is believed to have occurred from 100 to 200 minutes into the accident. In the several hours following the accident, flow was lost to the letdown coolers and temperatures in the letdown system are known to have reached $160^{o}F$. Late on March 28, 1979 letdown flow was lost due to plugging either in the filters, block orifice, or letdown coolers. In the early morning hours of March 29, 1979, letdown flow was reestablished. Makeup filters MU-F-5A, 5B and the demineralizers were bypassed with flow going directly from the block orifice to makeup filters MU-F-2A and 2B. On March 31, 1979 a routine operator entry in the plant log shows that the demineralizers were isolated, and manual isolation valves closed.

Surveys have been made of the makeup and purification system by gamma spectrometry; filter cartridges have been removed; and samples of filter sludge

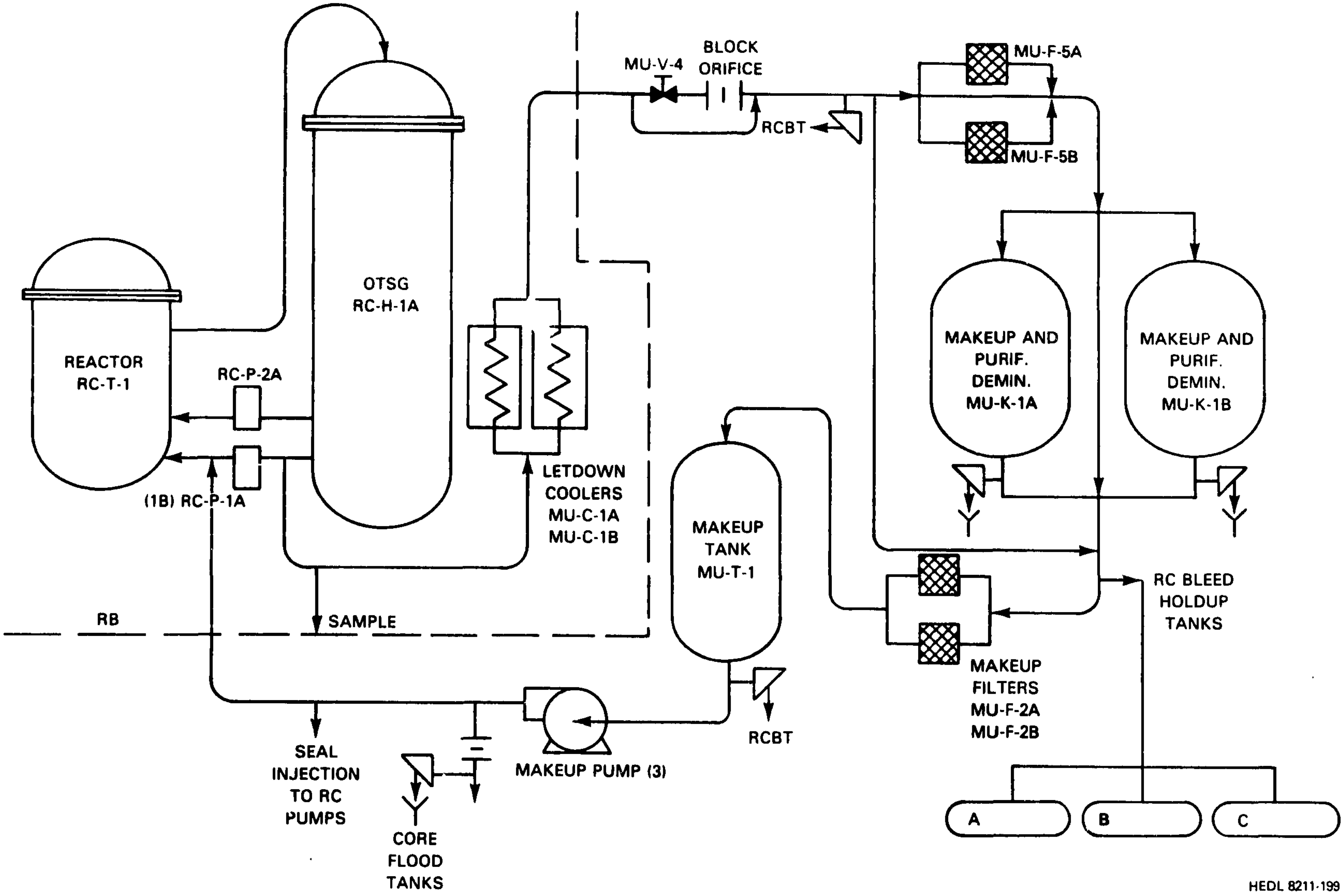

HEDL 8211-199

FIGURE 1. Makeup and Purification System - TMI-2

obtained and analyzed. Sludge samples have also been obtained from the reactor coolant bleed holdup tanks. Quantities of fuel and core structural debris have been identified in various locations. Preliminary radiation surveys of the demineralizer cubicles indicated high concentrations of fission products, primarily ^{137}Cs.

General Public Utilities (GPU) made an evaluation of fission product levels in the demineralizers based on fission product concentrations found in a coolant sample taken March 28, 1979, 2 hours and 45 minutes after the accident. A fuel estimate was also made based on another coolant sample taken one day after the accident. GPU estimated the total flow to the demineralizers at 46,000 gallons at an average flowrate of 46.5 gpm. GPU assumed the demineralizers were isolated 18 hours and 35 minutes after the start of the accident. Table I shows the results of the GPU analysis for fission products. Since the split of flow between demineralizers A and B was not known, no attempt was made to apportion the fission products between the two demineralizers.

Table I

GPU Calculated Fission Product Activity in Makeup and Purification Demineralizers

March 28, 1979 2235 pm

Isotope	Activity (Ci)	Isotope	Activity (Ci)
^{85}Kr	8,950	^{134}I	57,000
^{89}Sr	445	^{135}I	7,550
^{90}Sr	30	^{134}Cs	2,650
^{95}Zr	9,500	^{131}Cs	12,000
^{95}Nb	4,750	^{137}Cs	12,200
^{98}Nb	845	^{138}Cs	10,100
^{131}I	1.25×10^6	^{140}Ba	14,800
^{132}I	3.45×10^5	^{133}Xe	8,220
^{133}I	1.93×10^6	^{135}Xe	3,200

The fuel concentration from the coolant sample was found to be 68 milligrams per liter with a size distribution shown in Table II. Based on 46,000 gallons, the maximum fuel entering the demineralizers would be 11.8 kilograms.

Table II

Fuel Particle Size Distribution
Coolant Sample - March 29, 1979

Particle Size, microns	mg/l
5	33.33
1.2 - 5	14.28
0.45 - 1.2	20.63
	68.24

It was originally thought that a significant portion of the fuel and core debris would be retained in the filter housings of MU-F-5A and 5B. When the filters were opened, and the cartridges removed, it was found that the paper backing in the cartridges had partially disintegrated, thus destroying their filtering capability. Examination of the filter housings and gamma spectrometry indicated approximately 70 grams of uranium in MU-F-5B. MU-F-5A was not surveyed prior to cartridge removal but has been estimated to have contained approximately 200 grams of uranium based on ratioing overall radiation measurements. Chemical analysis of filter debris from MU-F-5B indicates 4 to 6% UO_2 by weight.

2.2 DEMINERALIZER AND CONTENTS - PRE-ACCIDENT

The mechanical characteristics of the demineralizers are depicted in Figure 2. The demineralizer tanks are stainless steel and are designed for 150 psig. Various connections to the demineralizers are shown schematically in Figure 3.

The tanks were charged with a mixed bed resin as shown in Table III. The total amount initially charged was 50 ft^3 per vessel. Fresh batches of resin

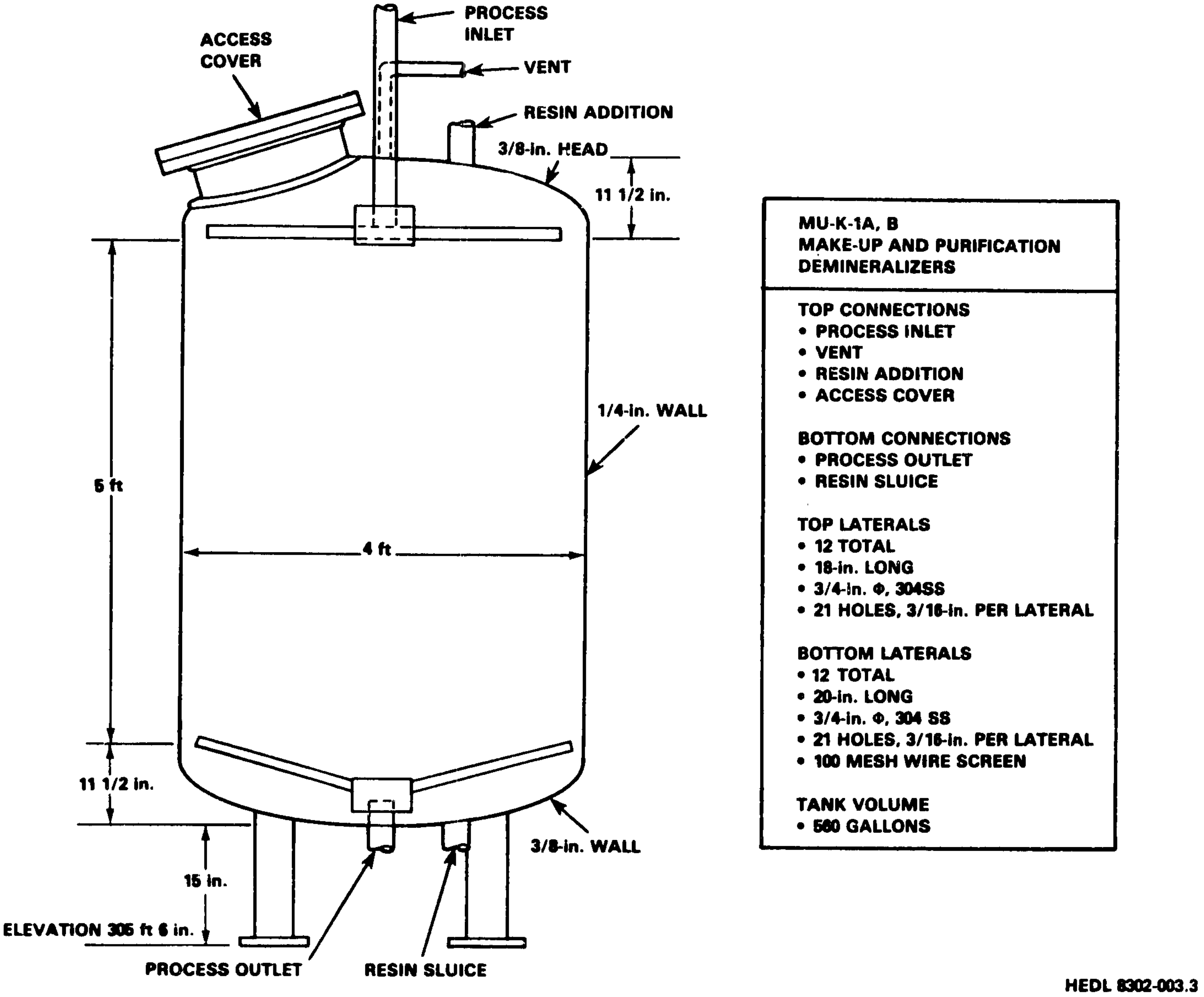

MU-K-1A, B
MAKE-UP AND PURIFICATION DEMINERALIZERS

TOP CONNECTIONS
- PROCESS INLET
- VENT
- RESIN ADDITION
- ACCESS COVER

BOTTOM CONNECTIONS
- PROCESS OUTLET
- RESIN SLUICE

TOP LATERALS
- 12 TOTAL
- 18-in. LONG
- 3/4-in. Φ, 304SS
- 21 HOLES, 3/16-in. PER LATERAL

BOTTOM LATERALS
- 12 TOTAL
- 20-in. LONG
- 3/4-in. Φ, 304 SS
- 21 HOLES, 3/16-in. PER LATERAL
- 100 MESH WIRE SCREEN

TANK VOLUME
- 560 GALLONS

Figure 2. Demineralizer Tank.

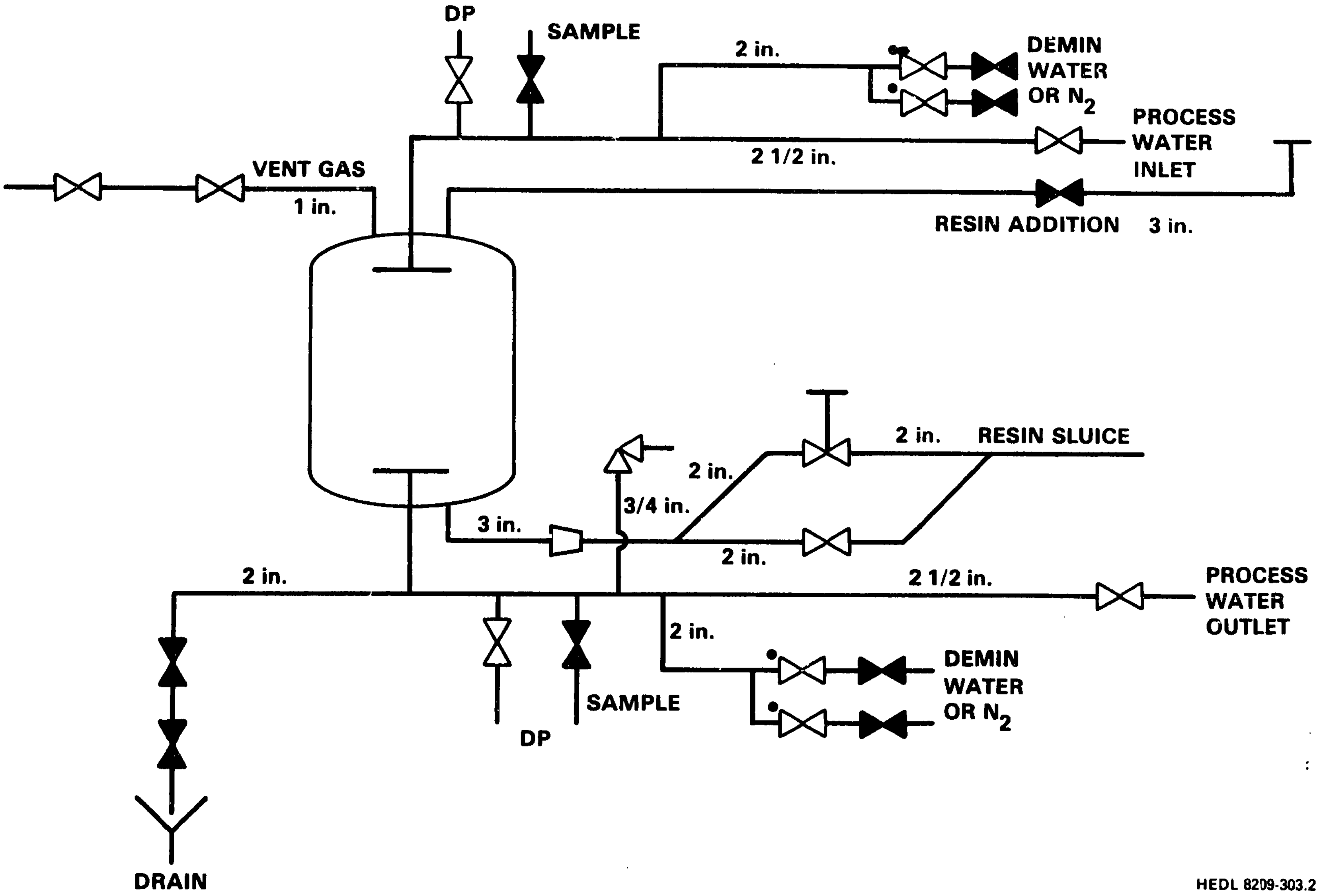

Figure 3. Demineralizer Tank Connections.

Table III

Ion Exchange Resin

TMI-2 Demineralizer, IRN-217

	IRN-218	IRN-78
	Cation Exchange	Anion Exchange
Volume, %	40	60
Moisture, %	55	60
Volume Capacity, Meq/ml	1.76*	1.2*
Screen Analysis, on 16 mesh	5% max	5% max
thru 50 mesh	0.5%	0.5%
Ionic Form	Li^{+7}	OH^-
% Regenerated, As Supplied		
Li form	99 min	
OH form		90 min
Effective Size, mm	0.5 to 0.60	0.38 to 0.45
Density, lb/ft^3	42.8	

---

*0.7 Meq/ml of IRN-217

were added a few months before the accident.The resin is a 3:2 mixture of anion and cation resin to chemically balance the positive and negative ion exchange sites available.

The demineralizers are located in cubicles in the auxiliary building on the 305' elevation, as shown in Figure 4. The cubicles are shown isometrically in Figure 5. Included in the cell is a pressure relief valve dumping to a floor drain. The valve setting is 150 psig.

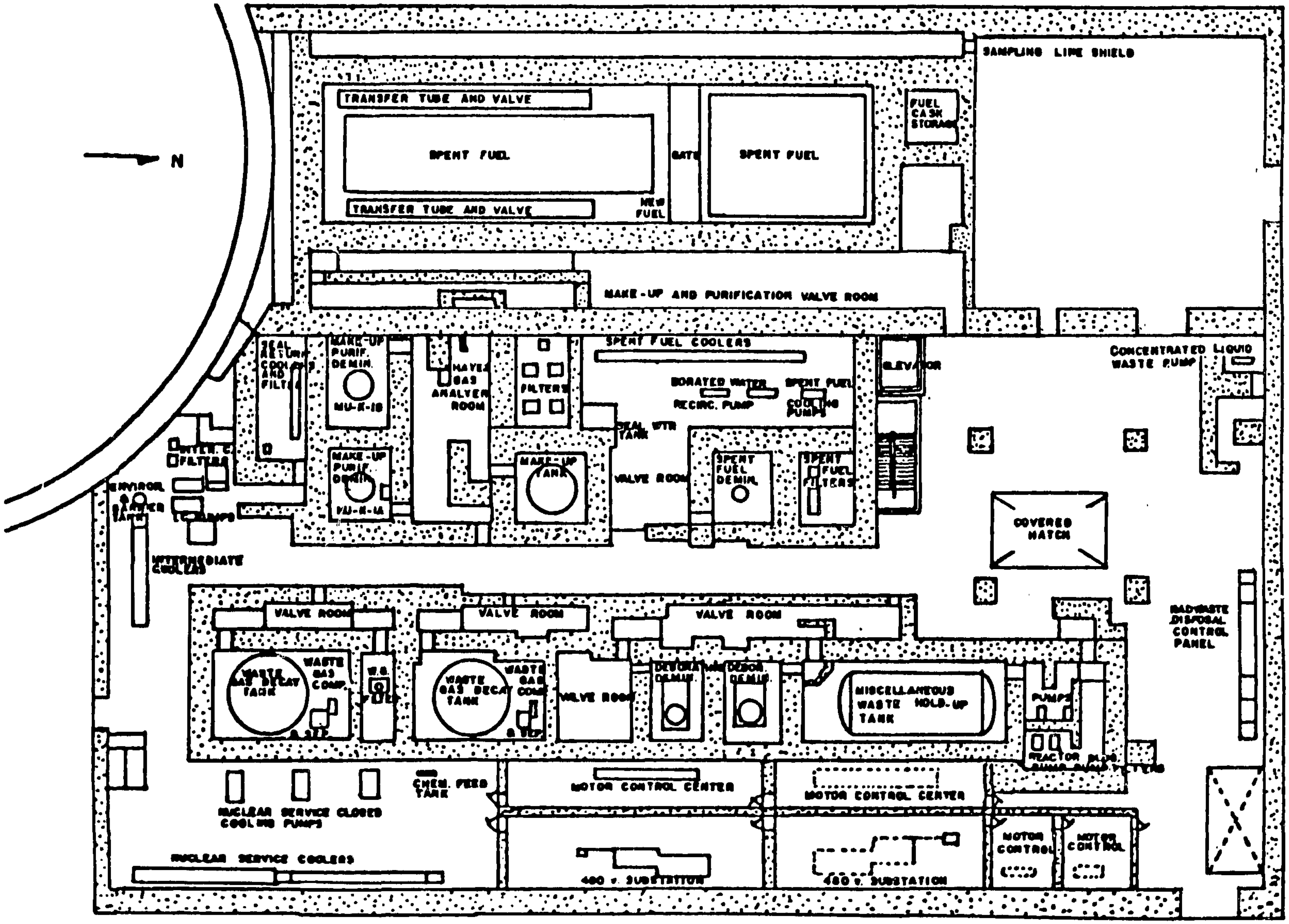

FIGURE 4. El. 305' Unit 2 Auxiliary and Fuel Handling Buildings.

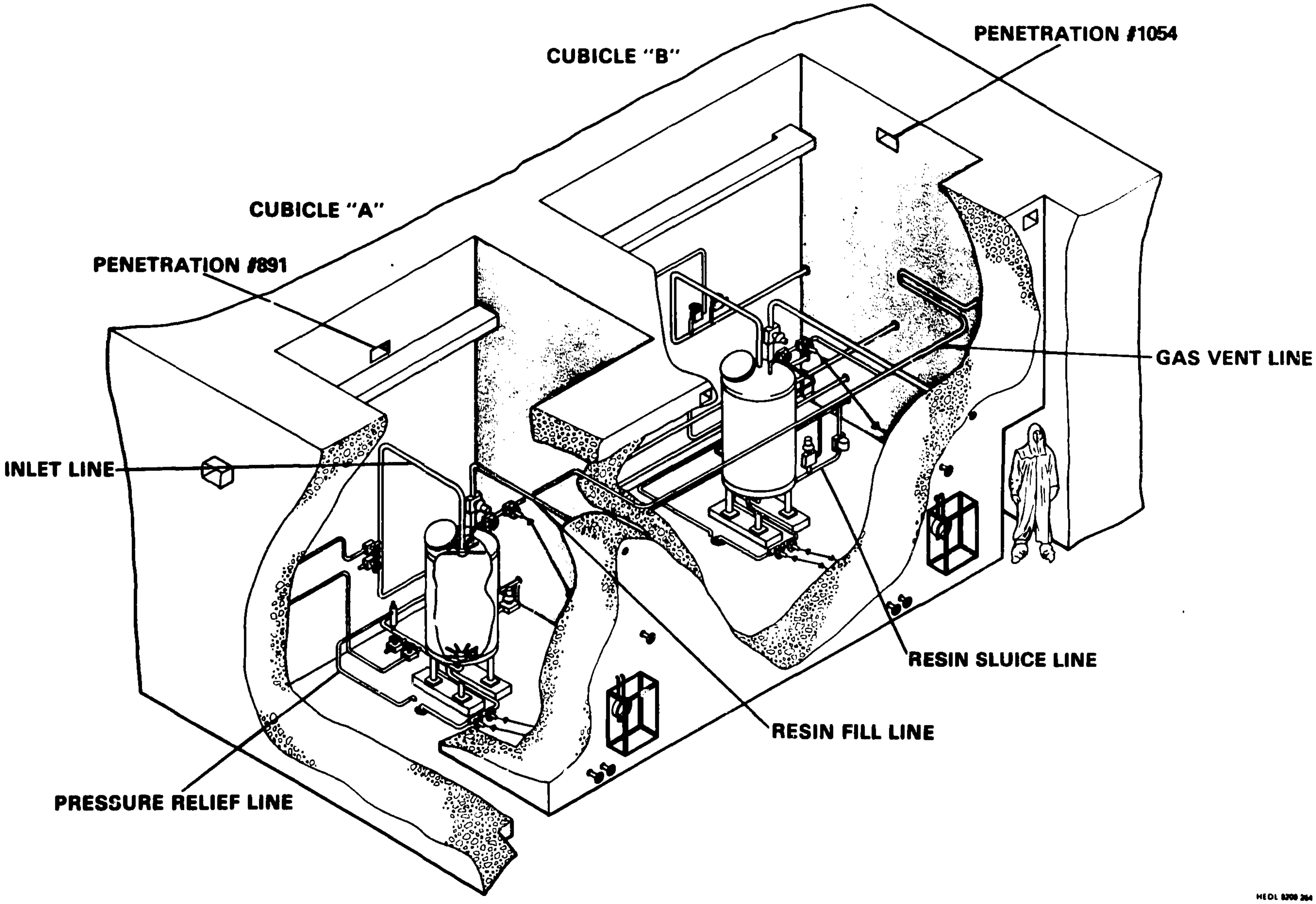

Figure 5. TMI-2 Makeup and Purification Demineralizers.

3.0 CHARACTERIZATION OF DEMINERALIZER CONTENTS

The introduction of substantial quantities of radioactivity and debris into the demineralizer is expected to produce physical changes in the resin. A series of scoping tests were run at Pacific Northwest Laboratories (PNL) to explore the effect of radiation and temperature on resin form and chemical capacity. In parallel, onsite activities were initiated to obtain cell dose rate and contamination surveys as well as fuel quantity assessments.

3.1 RESIN DEGRADATION EXPERIMENTS

The introduction of radioactivity into the demineralizers resulted in a high radiation dose to the resin as well as possible overheating after flow to the demineralizers was shut off. A program was set up to independently evaluate the effects of radiation and temperature on resin physical form and chemical exchange capacity. Tests were performed with IRN-150 resin which when treated with Lithium Hydroxide becomes chemically identical to IRN-217, which was in use at TMI-2. The resins are physically identical. Detailed Test Reports are included in Appendix A.

3.1.1 Effects of Irradiation on Resin

Bounding analysis by GPU, using the radioisotopes shown in Table I, indicated a cumulative resin dosage range of 1 to 5 x 10^9 rads depending on the distribution of activity between demineralizers.

Irradiation was found to substantially affect the physical form and chemical capacity of the resin. Two resin samples were irradiated. One sample designated "A" was irradiated in water at 150^{O}F simulating the case with some flow through the demineralizer. A second sample "B" was preheated to 360^{O}F in nitrogen and then irradiated dry simulating the case where steam or hydrogen generation had produced sufficient pressure to drive water from the demineralizer. The 360^{O}F value was selected since this is the boiling point of water at 150 psig which is the pressure relief setting for the system. During irradiation the resin temperature was maintained at 220^{O}F.

Both samples were irradiated to 1.7×10^9 R at a rate of 8×10^6 R/hr. The rate was a function of the ^{60}Co gamma facility used at the Hanford Engineering Development Laboratory.

Results of test "A" included a significant loss of resin volume and a smaller increase in resin density. Heating significantly affected the resin in test "B". Detail results are shown in Table IV.

Table IV

Resin Changes Due to Irradiation

	Original	1.7×10^9 R	Percent Change
Test A Wet			
Volume cm^3	410	177.5	-56.7
Weight, g	281.1	134.7	-52.1
Density lb/ft^3	42.8	47.4	+10.8

	Original	After 360°F Heating	Percent Change
Test B Dry			
Volume, cm^3	400	124	-69
Weight, g	281	104.7(a)	-62.7
Density, lb/ft^3	42.8	52.7	+23.1

	After Heating	After Irradiation	Percent Change
Test B Dry			
Volume, cm^3	124	124	0
Weight, g	95.3(a)	94.7	-0.6
Density, lb/ft^3	52.7	52.7	0

(a) 9.4 grams removed for analysis

Appreciable quantities of gases were generated in test "A" (41 cm^3/hr) which were composed of 80 - 90% hydrogen. Early samples showed significant concentrations of trimethylamine. The liquid in the sample became discolored due to the dissolution of organic residues from resin disintegration. The appearance of the resin was not significantly changed. Test B showed significantly different gas composition with higher concentrations of carbon compounds and lower hydrogen levels. The "B" test gas generation rate was 2 - 3 cm^3/hr.

Subsequent testing was performed to assess resin exchange capacity for anions and cations and sluicability. Sluicibility of irradiated resin exceeded that for pre-test resin. This effect was evaluated by measuring the expansion of a resin column with varying flow rates introduced at the bottom. Anion and cation capacity was evaluated by measuring lithium retained and by treatments with NaOH and HCl. The resins were then eluted with HNO_3 and the resulting solutions analyzed for Na^+ and Cl^-. Results are shown tabulated below.

Table V

Cation and Anion Exchange Capacity

	Irradiation Effects	
	Cation Sites Lost	Anion Sites Lost
Test A Irradiated Wet	40-70%	90%
Test B Preheated to 360°F Irradiated Dry	0%	90%
	Heating Effects	
225°F	0%	76%
500°F	0%	99%

3.1.2 Effects of Temperature on Resin

In extreme cases, with the demineralizer isolated and heat rejection modes limited, the resin can be subjected to higher temperatures. GPU performed bounding calculations for the activity burden early in the accident assuming conductive heat transfer only. Centerline resin temperatures were calculated to approach 1000°F. Tests of a scoping nature were therefore conducted to assess the effects of temperatures up to 1000°F. Samples of resin were heated in nitrogen and in moist steam environments. At 1000°F the resin tends to agglomerate, become a solid mass, and is changed into carbon. Resin in this form would need to be mechanically separated or treated chemically.

When heated to 750°F the resin beads retained their spherical shape but also were transformed into carbon. The particles are free flowing and exhibit no tendency to adhere to each other. Sluicing should be easily achievable. Below 750°F the resin retained its bead shape and colorations. Water is evaporated or driven off. The anion resin is highly susceptible to temperature degradation as shown in Table V, but mixtures are readily sluicable.

3.1.3 Conclusions from Resin Scoping Tests

The scoping tests provide valuable insights into possible resin conditions. However, the exact conditions to which the resin has been exposed are not known with an acceptable degree of certainty. In situ irradiation combined with heating may produce different effects than the conditions produce separately. Other studies (Ref. 1) have shown that in situ radiation causes more damage to organic resins than does external radiation. It does appear that settling or compaction of the resin bed is to be expected. Based on sluicing tests it appears that the resin will be sluicable.

Resin sampling of the demineralizer contents should be attempted prior to the implementation of any process for resin removal. The sampling should confirm expected resin location and consistency as well as fuel content and fission product activity.

3.2 CELL SURVEYS

To assess the condition of the demineralizers a program of cell access and dose rate monitoring was instituted by GPU. Westinghouse Hanford supplied a small robot equipped with TV surveillance cameras and a programmable arm which was adapted for contamination surveys inside the cubicles.

Robot access was obtained into cubicles "A" and "B". Dose rates were measured by attaching a radiation detector probe to the programmable arm of the robot. The gamma dose rates are shown in Figures 6 and 7. Measurements in the "A" cubicle were augumented by thermo-luminescent dosimeters (TLD) on a stringer and by insertion of the radiation detector through penetration #891 shown in Figure 5. Two vertical radiation dose profiles were obtained. The first was taken approximately 2' from the demineralizer. Locations were determined by a visual survey made with a TV camera attached to the robot arm. The second profile was obtained immediately adjacent to the tank but precise locations are not certain since visual access was not possible on the day of the measurements. Both profiles are plotted in Figure 6.

TLD measurements generally supported radiation detector readings but were less precise due to the exposure during handling operations. Surface contamination readings were taken on the floor, walls and equipment surfaces. Values were generally low except for the area immediately adjacent to the Hayes gas analyzer room, where it appeared that prior decontamination efforts had produced a location of higher activity. Visual surveillance showed piping and equipment to be in satisfactory condition. White crystals were observed on the floor of cubicle "A" near a floor drain and the discharge of the pressure relief line of demineralizer "A". Subsequently, the robot was used to obtain samples of the crystals. Radiation measurements of the crystals were made on site by GPU and it was concluded that the deposits were residues from preaccident drain operations.

Attempts were made to fit the radiation profiles in demineralizer "A" with various source distributions. Figure 8 shows the best estimate obtained. The resin was assumed to be below the 309' elevation and the tank was assumed to be dry above the resin. A uniformly distributed cylindrical source was assumed. The strength of the source was estimated to be about 50% of the GPU estimate for both demineralizers or about 5,500 curies of ^{137}Cs.

Similar radiation profiles were not obtained for the "B" cubicle since penetration 1054 is not accessible because of local contamination. Therefore, no

"A" CUBICLE DOSE RATES

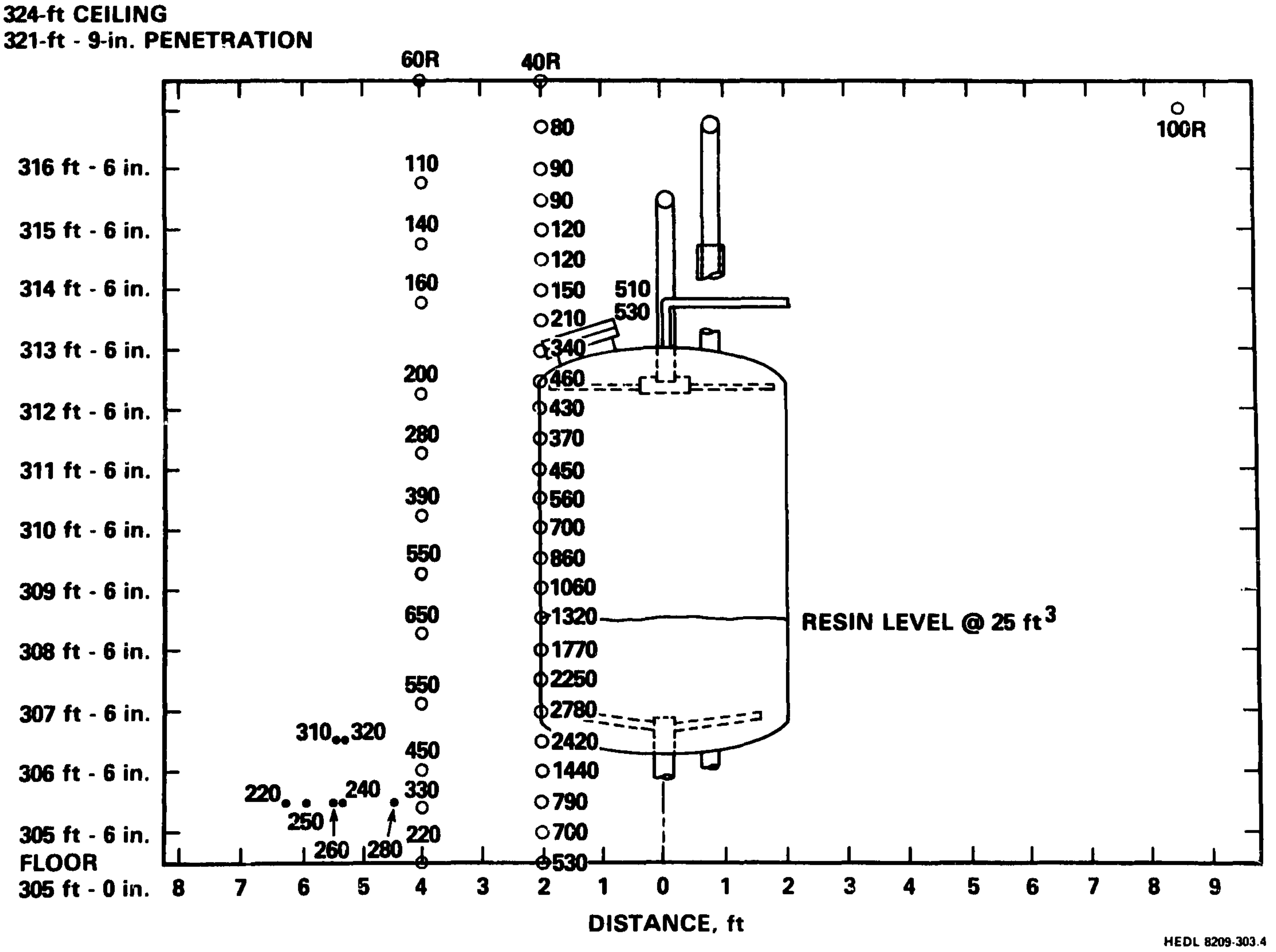

FIGURE 6.

"B" CUBICLE DOSE RATES

324-ft CEILING
321-ft - 9-in. PENETRATION

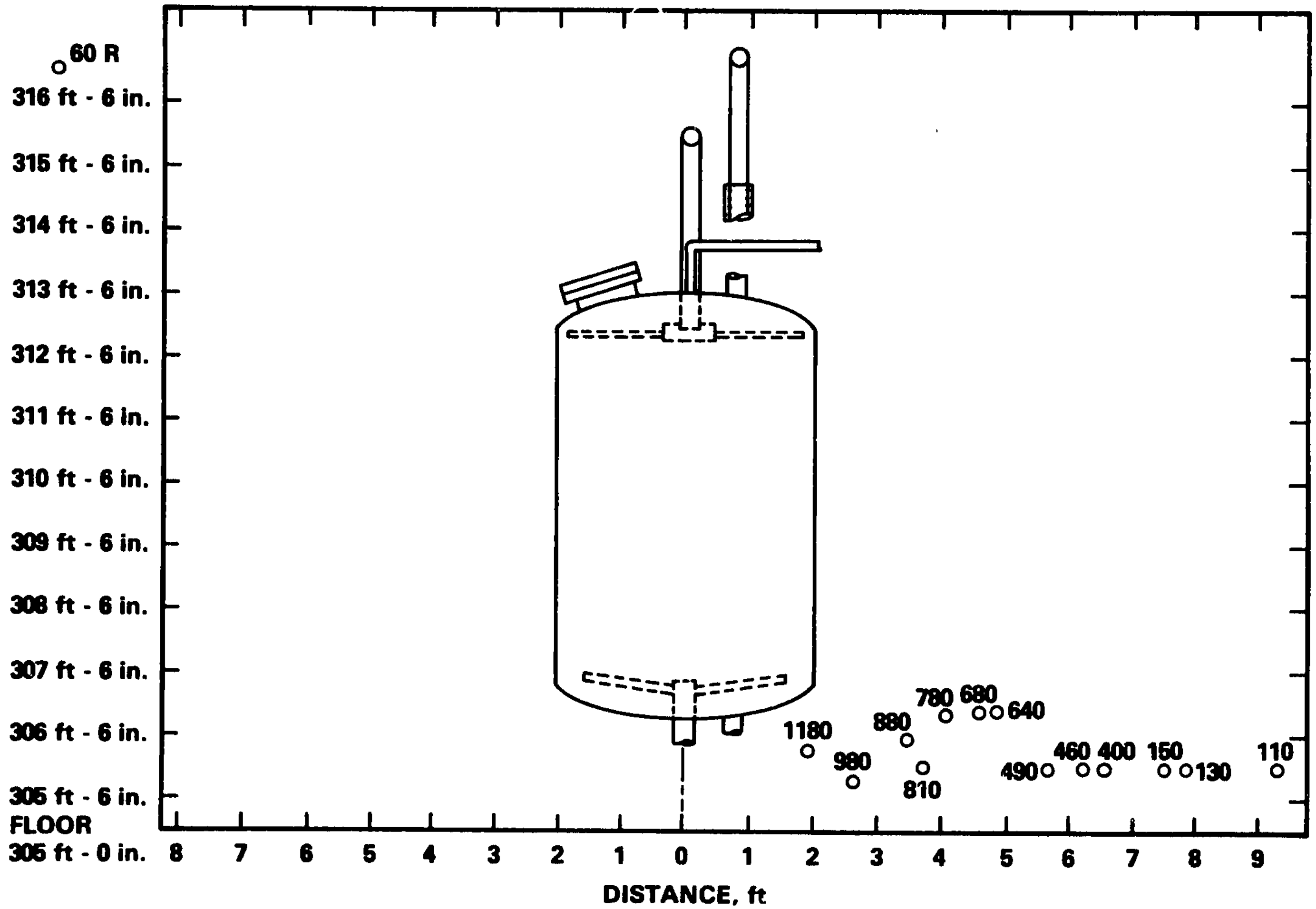

HEDL 8208-303.1

FIGURE 7.

CUBICLE A DOSE RATE TRAVERSES

PARALLEL TO TMI-2 DEMIN SIDE
SOURCES -- TOP DISK + LOW 1/2
NORMED TO MAX. MEASURED DATA

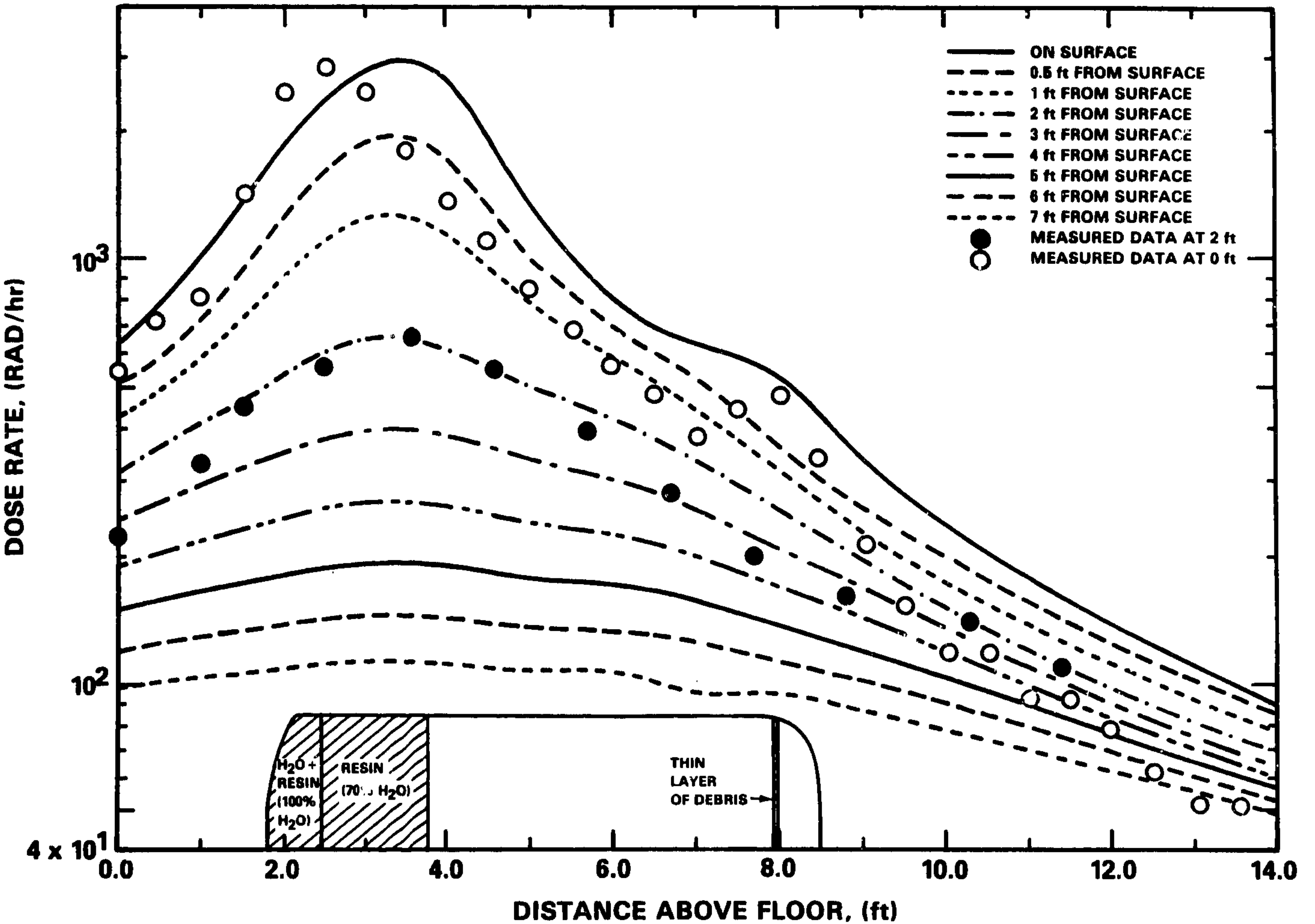

FIGURE 8.

HEDL 8210-207.1

estimate of source distribution could be made. A comparison of robot data approximately two feet off the floor indicated higher gamma activity in the "B" cubicle. Cell dose rates were in general higher.

3.3 FUEL QUANTITY ASSESSMENT

Concern had been expressed about the uncertainty of the fuel assessment made by GPU. Fuel concentrations in the coolant could have varied considerably during the accident. The poor condition of makeup filters MU-F-5A and 5B indicated a potential for the accumulation of appreciable fuel and core debris in the demineralizers.

A program was instituted to assess fuel quantity by several techniques. Two of these techniques were performed by WHC. The first was a passive technique employing mica strips attached to ^{235}U foils (Figure 9). Neutrons emitted by spontaneous fissions in the fuel or alpha-neutron reactions will cause fissions in the ^{235}U. Fission products from the ^{235}U leave charged particle tracks in the mica which can be developed and examined microscopically to determine the number of fissions which have occurred. From these data a neutron flux due to the fuel can be calculated. This flux can then be used to calculate the amount of fuel present. The technique, deployment of the detectors, and results are discussed in detail in Reference 2. Only demineralizer "A" was instrumented. The detectors were positioned remotely on stringers inserted through penetration #891 (Figure 10). The solid state track recorders confirmed that the tank was dry above the 309' level and estimated 1.7 ± 0.6 kg of uranium was present in the "A" demineralizer.

The second technique employed was gamma spectroscopy to detect the 2.18 MeV gamma ray associated with the ^{144}Pr daughter of the fission product ^{144}Ce. Cerium is known to have similar chemical properties with uranium and has been shown generally to stay within the fuel matrix. Reactor burnup codes are used to calculate the amount of ^{144}Ce present in TMI-2 fuel and the ^{144}Ce measured is then used to calculate the amount of fuel present. Details of the experiment are described fully in Reference 3. A delivery device for positioning a

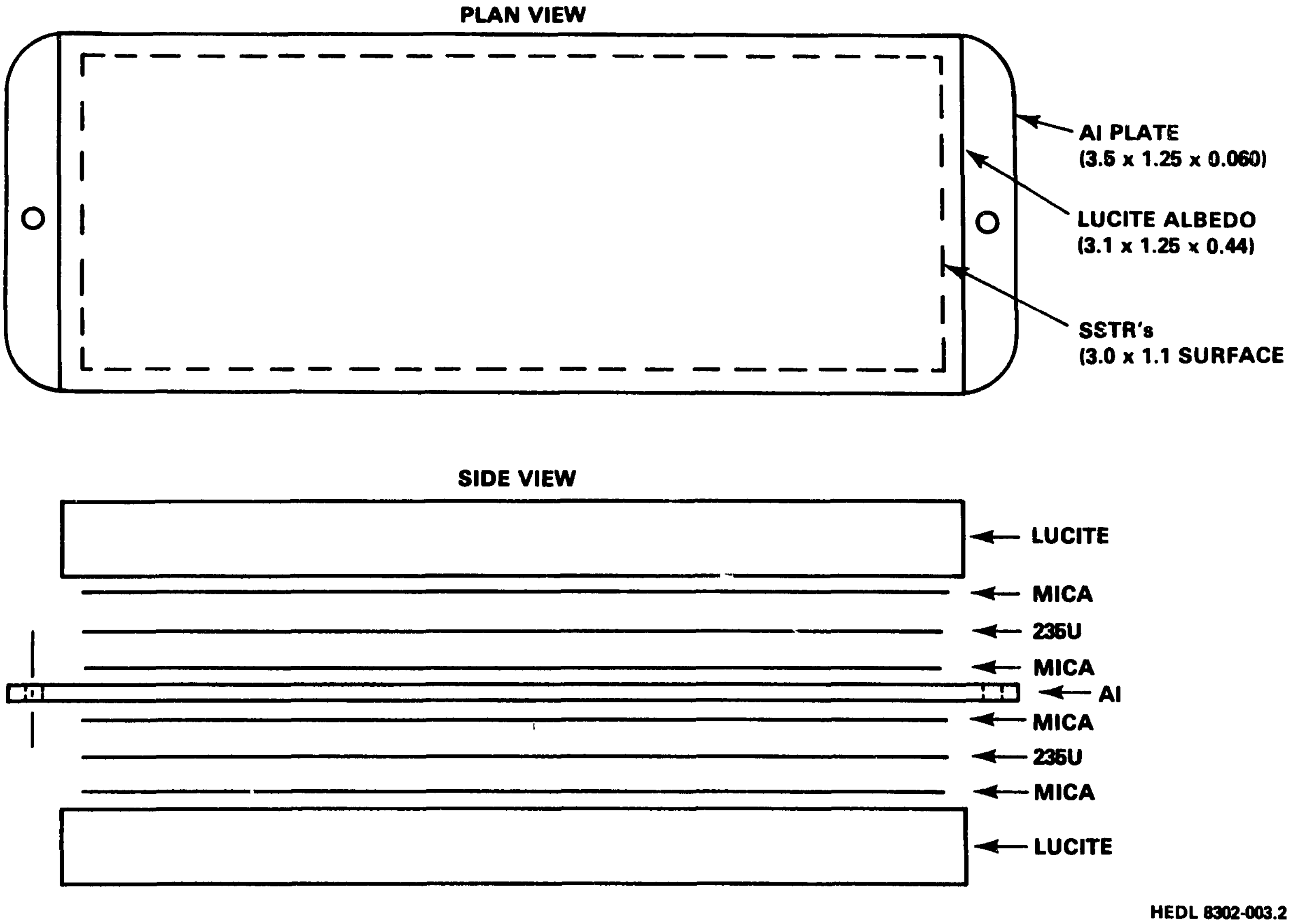

FIGURE 9. SSTR Neutron Dosimetry Holder for TMI-2 Demineralizer "A" Measurements.

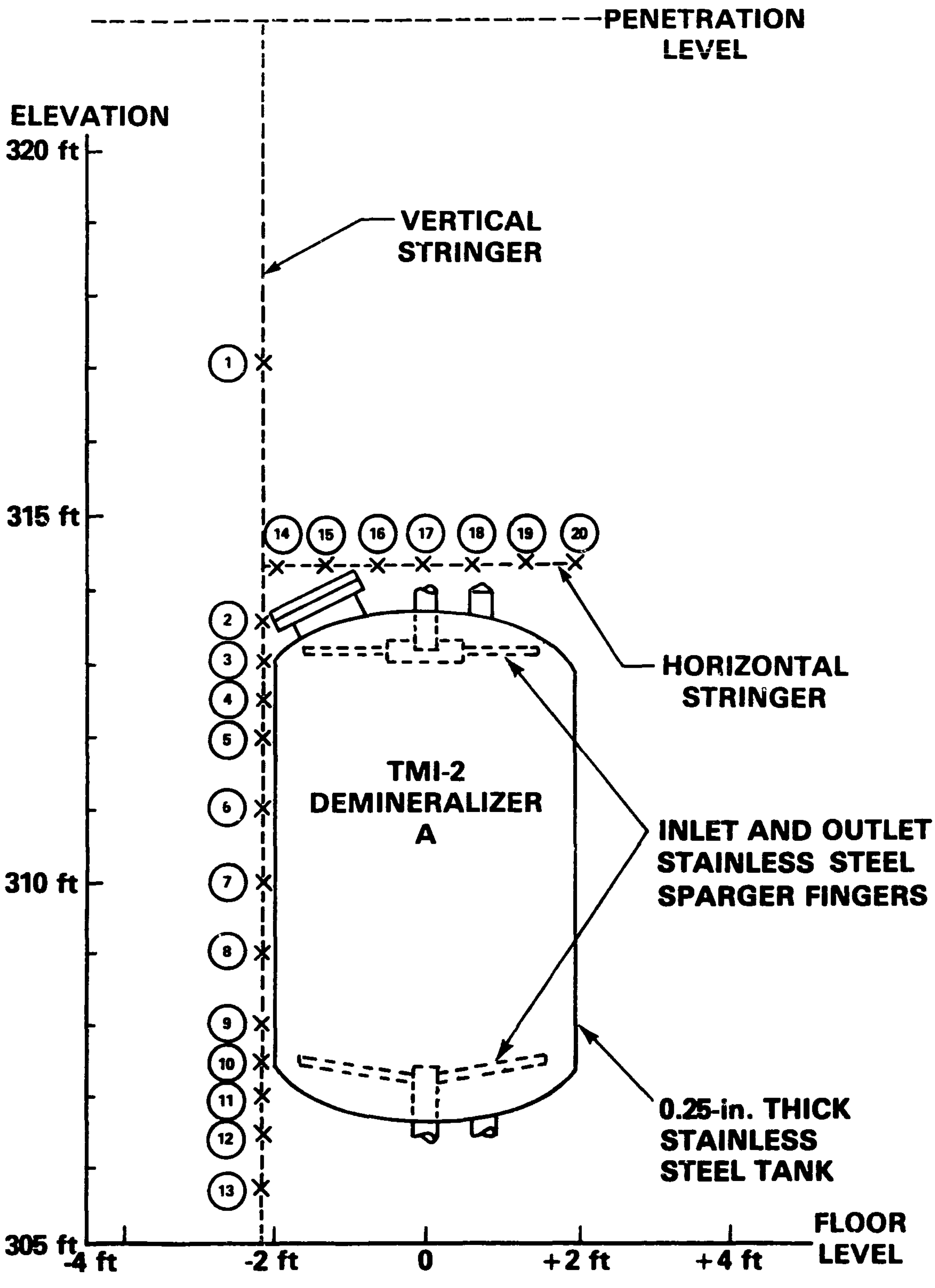

FIGURE 10. Locations of SSTR Neutron Dosimeters During Exposure.

Compton recoil spectrometer was designed for insertion into the demineralizer "A" cubicle through penetration #891. A cart was used to obtain readings in the "B" demineralizer cubicle. The spectrometer was developed by Westinghouse Hanford and employs a silicon crystal which is lithium drifted. The spectrometer can operate in higher gamma fields than a more conventional Ge-(Li) system. The spectrometer was operated with a lead collimator weighing 78 pounds, for use in gamma fields up to 2000 R/hr.

The Si-(Li) system predicted 1.3 ± 0.6 kg U in the "A" demineralizer. In addition spectral data was also used to predict the ^{137}Cs content which was found to be 3400 ± 2500 curies as of mid October 1982. Vertical source distributions indicated that most of the fuel was located between the 307' and 309' elevation, consistent with earlier estimates. Horizontal traverses across the top of the demineralizer showed significant nonuniformity in the radial source distribution. This could produce gross differences in the radiation damage in various areas of the resin bed.

Data from the "B" cubicle was limited by the exposure of personnel maneuvering the cart through the doorway and into the cubicle. In the time available, statistical information which would allow a quantitative estimate of fuel content was not obtained. Qualitatively, less fuel is expected in the "B" demineralizer but higher ^{137}Cs activity. A forthcoming GEND report will describe the other techniques.

3.4 TRU ASSESSMENT

Once the amount of fuel is known, an estimate can be made of the transuranic (TRU) content. The ORIGEN code was used to calculate the quantities of transuranics produced in TMI-fuel prior to the accident. The activity was then decayed three and one-half years to mid October 1982. The major transuranic contributor of radiation was found to be ^{241}Pu which decays to ^{241}Am. The value calculated was 2 x 10^5 nano curies TRU per gram of TMI-2 fuel expressed as Uranium.

3.5 SUMMARY OF CHARACTERIZATION EFFORTS

The various activities directed at assessing the contents of the demineralizer have resulted in the estimates shown in Table VI.

Table VI

Estimated Demineralizer Loadings
Based Upon Mid-October 1982 Characterizations

	Initial	A Vessel	B Vessel
1. Resin			
Volume, ft^3	50	22	22
Weight, lb	2,139	1,025	1,025
^{137}Cs, Ci	0	3,500	7,000
^{134}Cs, Ci	0	270	540
2. Liquid			
Volume, ft^3	44	3	3
Weight, lb	2,746	193	193
3. Debris			
U, lb		5	1
Core Debris, lb		95	19
^{137}Cs, Ci		177	35
^{134}Cs, Ci		16	3
^{106}Ru, Ci		21	4
^{144}Ce, Ci		28	5
^{125}Sb, Ci		116	23
TRU, Ci		0.5(a)	0.1(a)
4. Gas			
Volume, ft^3		54	54
Temp, °F		80	80
Pressure, psig		11	10.5

(a) α activity only

Apparently shrinkage of the resin bed has occurred. The shrinkage observed is identical to that produced in laboratory experiments at 1.7×10^9 rads, i.e. -56%. The higher dose rate observed in the "B" cubicle may indicate higher radiation exposure and a lower resin level. This will be confirmed by resin sampling operations planned for both demineralizers later this year. The

^{137}Cs is probably tied up by the resin. Calculations of exchange capacity for cations in the degraded resin indicate that only 0.1% of resin capacity would be required to accommodate the 3400 curies of Cesium. The fuel and core debris are probably in the form of fine particles since the laterals have 3/16" holes. Portions of the laterals may, however, be plugged with filter debris. The debris which entered the demineralizer is expected to be in the top portion of the resin.

Examination of radiation profiles indicate the probable existance of water particularly in the lower portion of the resin. The water will probably contain organic degradation products of the resin and low Cesium concentrations. The lower laterals may also be plugged at the 100 mesh screen which is wrapped around them.

The level of the resin bed may not be even due to the nonuniformity of the radiation dose. Wide temperature variations may also have occurred.

The bed is predicted to have been blown dry by the gases generated in the resin bed and steam generation. This is expected to have occurred prior to system isolation. The gas composition can vary depending on the amount of water present. Dry resin produces less gas than wet resin when irradiated. Gas sampling of the demineralizer is to be performed by GPU. Analysis of the gas composition should provide additional information on the status of the resin and provide information on the status of the inlet line.

The presently estimated TRU activity indicates a possible problem with resin disposal. Assuming a uniform mixture, the demineralizer "A" contents will have a TRU concentration of 900 nCi/gm which exceeds commercial burial limitations of 100 nCi/gm.

4.0 SYSTEM ASSESSMENT

A study by Westinghouse Hanford evaluated integrated doses at certain equipment within the demineralizer cubicles. Results of this evaluation are shown in Table VII. Of particular concern for resin removal were the valves associated with the resin fill and sluice lines. The table shows that dose rates have not reached the range where operation would be affected.

The integrated dose values are calculated based on the GPU activity estimates in Table I. Dose rates were estimated from radiation surveys and extrapolated back to the accident to establish integrated doses. If the "B" cubicle contains twice the activity in approximately the same location integrated doses will approach twice the value shown for the "A" cubicle.

The status of the lines leading to each demineralizer is somewhat questionable. Letdown flow has been circulated subsequent to the accident through the bypass line. Flushing operations were performed in October 1980. However, the makeup and purification filters and demineralizers have been isolated. The filters have been subsequently removed and housings flushed and vacuumed. Reactor coolant processing has reduced dose rates in some areas such as the letdown orifice which communicate with the primary system.

The characterization scoping tests, dose rate calculations, and general data collection performed to date have provided the basis for making the following assumptions upon which all of the resin and debris removal conceptual design is based. They are:

A. The contents of the demineralizers can be agitated into a slurry and then sluiced.

B. All required valves are operable or can be made to be operable.

COMPONENT STATUS - "A" CUBICLE

EQUIPMENT #	USE	"A" CUBICLE CURRENT DOSE RATE, R/HR	INTEGRATED DOSE, 10^7 RADS	PROGNOSIS
MU-111A, GRINNELL	RESIN FILL VALVE	510	8.3	NORDELL DIAPHRAGM PROBABLY USABLE
MU-R5A, CROSBY	PRESSURE RELIEF	400	6.6	METAL OR BUNA-N SEAT - ACCEPTABLE
MU-V1116A, VELAN	GAS VENT	530	8.7	PROBABLY ACCEPTABLE
MU-217A, VELAN	GAS VENT	510	8.3	PROBABLY ACCEPTABLE
MU-V192A, VELAN	LIQUID SAMPLE TAP	500	8.1	PROBABLY ACCEPTABLE
MU-V194B, VELAN	ΔP LINE	650	10.5	PROBABLY ACCEPTABLE
MU-V194A, VELAN	ΔP LINE	250	4.2	PROBABLY ACCEPTABLE
MU-V193A, VELAN	LIQUID SAMPLE TAP	300	5.1	PROBABLY ACCEPTABLE
MU-V108A, GRINNELL	RESIN SLUICE	650	10.5	PROBABLY ACCEPTABLE
MU-V238A, GRINNELL	RESIN SLUICE	600	9.9	PROBABLY ACCEPTABLE
MU-V240A, VELAN	DRAIN LINE	300	5.1	PROBABLY ACCEPTABLE
MU-V109A, VELAN	DRAIN LINE	300	5.1	PROBABLY ACCEPTABLE
B&W MU-8 PI-1	DIFFERENTIAL PRESSURE SWITCH	200	3.	PROBABLY ACCEPTABLE

HEDL 8211-069.1

Table VII

5.0 RESIN AND DEBRIS REMOVAL METHODS

Initially, three basic approaches were considered for resin removal. Removal of the demineralizer tanks in shielded containers was evaluated but was eliminated early in the design process. The high radiation dose rates in the demineralizer cubicle would make access possible only by remote means. Pipes would have to be severed and capped, walls penetrated, shielding and transportation devices designed, fabricated and tested. It was concluded that personnel exposures would be high and building operations severely restricted because of the high potential for contamination.

In-situ methods of resin treatment were also considered to break down the resin into soluble products. Results of these evaluations are described in Appendix B. Laboratory scale experiments indicated that iron catalized Hydrogen Peroxide would react with the resin. Concern was expressed over controlling the chemical activity of Hydrogen Peroxide. Offgassing systems would be required. If the resin has carbonized, sodium hypochlorite processing will perform better. The technique was considered viable but less attractive than the third approach which involved transferring of the resin from the tanks.

Normal resin removal is accomplished by sluicing the resin in slurry form through the resin sluice line to spent resin storage tanks. The slurry is produced by circulating demineralized water through the demineralizer tanks. In light of sluicability tests performed on irradiated resin as part of the scoping studies described in Appendix A, sluicing appeared feasible. The main concern in sluicing through the normal system was the high activity contained in the resin. Methods were evaluated to elute the activity from the resin prior to sluicing.

5.1 RESIN AND DEBRIS REMOVAL SYSTEM DESIGN DESCRIPTION

5.1.1 Piping and Instrumentation

The piping system for the demineralizers is shown in Figure 11. In normal operation, reactor coolant water flows through makeup and purification filter

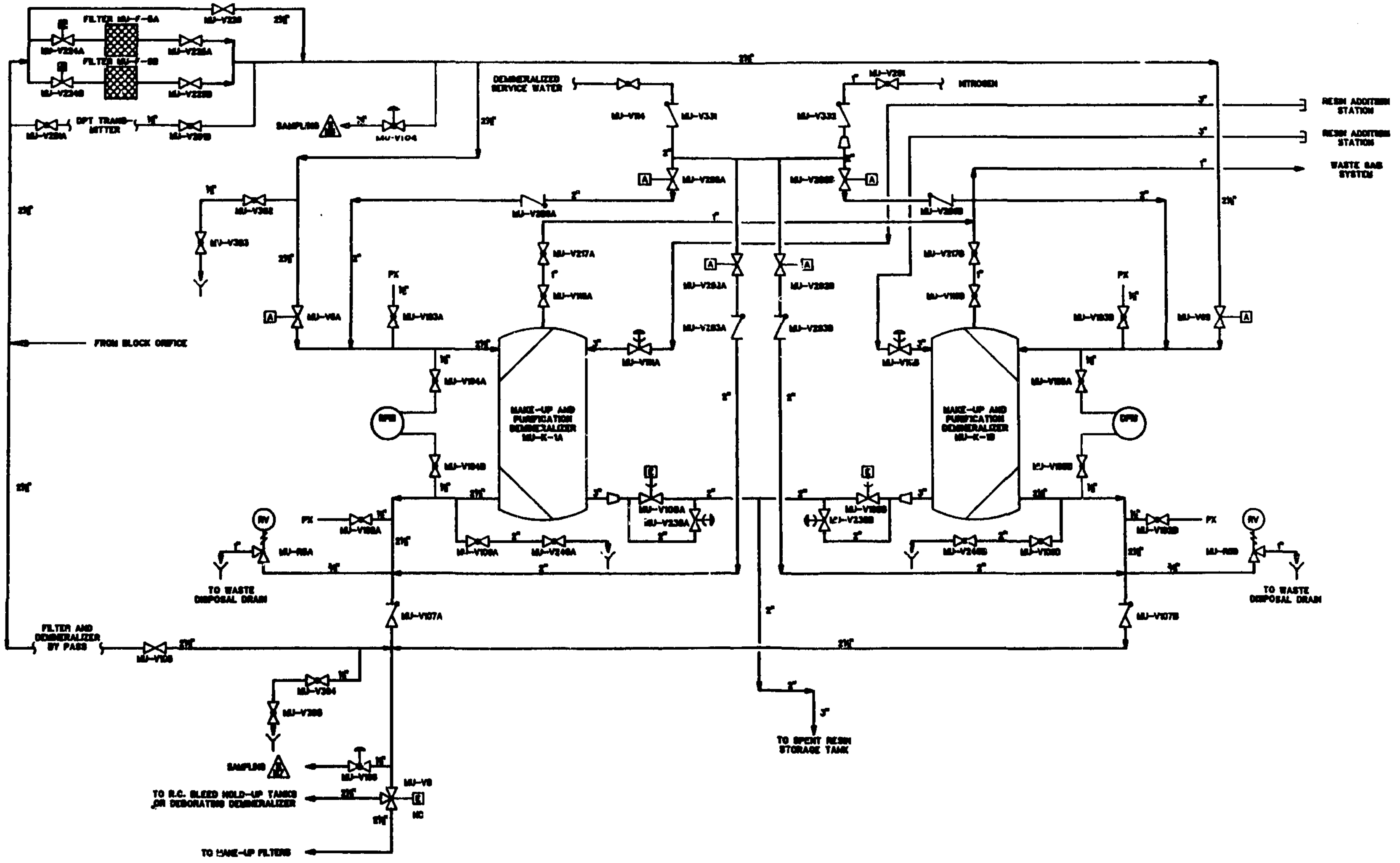

FIGURE 11. Makeup and Purification Piping System.

MU-F-5A or 5B and enters the demineralizer tank. The processed water then flows through the 2-1/2" outlet at the bottom of the tank, through stop check valve MU-V107 to MU-V8 where it can be directed to holdup tanks or more generally to the makeup filters. Old resin is sluiced from the bottom of the tank through MU-V108 or MU-V238 to the spent resin storage tank. Demineralized water is added through MU-V-292 to the bottom of the tank to agitate the resin bed in preparation for sluicing. Fresh resin is added through MU-V111. Nitrogen can also be added through the bottom inlet to the demineralizer to assist in agitating the bed prior to sluicing. A gas vent is provided on the top of each demineralizer tank. Operations are monitored in the control room and at local stations in the auxiliary building. All piping is stainless steel.

The demineralized water system and nitrogen system are believed to be operable. Furthermore, the resin removal process described below assumes that the valves in the demineralizer system are, or can be made, operable.

5.1.2 Resin Removal Process

The normal process for removing resin is to sluice it to a spent resin storage tank located on the 280'-6" elevation below the demineralizer. From the laboratory tests performed by PNL on wet and dry irradiated resin (Appendix A), and assuming that the debris consists of particles that will not clog the resin sluice line that exits from the bottom of the demineralizer, the resin and debris should be sluicable. However, there are reasons why the normal sluicing process should not be attempted. These are:

1. Transferring the resin from the demineralizer to the spent resin storage tanks does not accomplish the overall objective of removing the abnormally contaminated resins from TMI. In fact, it would result in additional components becoming contaminated to high levels.

2. The irradiated resin can provide information that may benefit the industry at a future date. Therefore, a certain quantity should be retained for this purpose.

3. The irradiated resin, in solution, will possibly release complex compounds which cannot be retained in the SDS and EPICOR II cleaning systems. If the sluice water enters these systems, it will contaminate the processed water at TMI-2.

Based on the above, a multi-step process is proposed for resin and debris removal. The major steps in this process are:

1. Slow upflow recirculation to remove complex organic compounds.
2. Slow upflow recirculation to remove cesium.
3. Fast upflow recirculation to transfer the contents.
4. Fast downflow recirculation to transfer the contents.
5. Resin and debris transfer to shipping containers.

Resin and debris are removed from one demineralizer at a time. The removal system process piping and equipment locations are shown in Figures 12 and 13. Temporary process piping is connected to the existing system at four major locations which are described briefly below and in detail in Section 5.2. The locations are:

1. In the resin sluice line upstream of the spent resin storage tanks. This connection is in the valve room (280'-6" elevation). The tie-in point is near the ceiling of the valve room. This tie-in point is illustrated in Figure 12.

2. In each of the resin fill lines, upstream of MU-V111A and MU-V111B. These connections are in the Hayes gas analyzer room. The connections will be made at the point where these lines were opened to obtain resin samples to minimize additional penetrations into the demineralizer system piping.

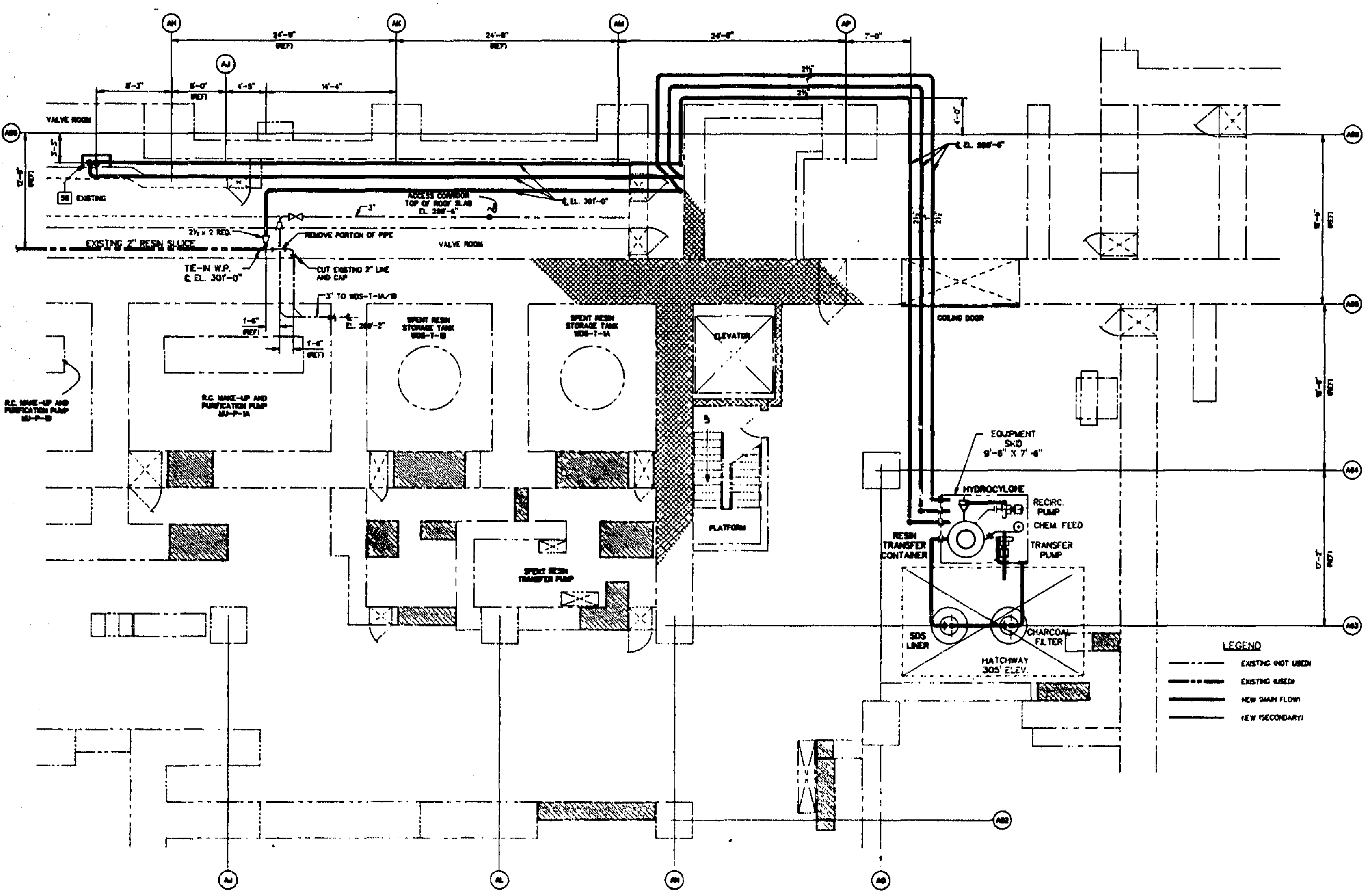

FIGURE 12. Piping Arrangement - 280'-6" Elevation.

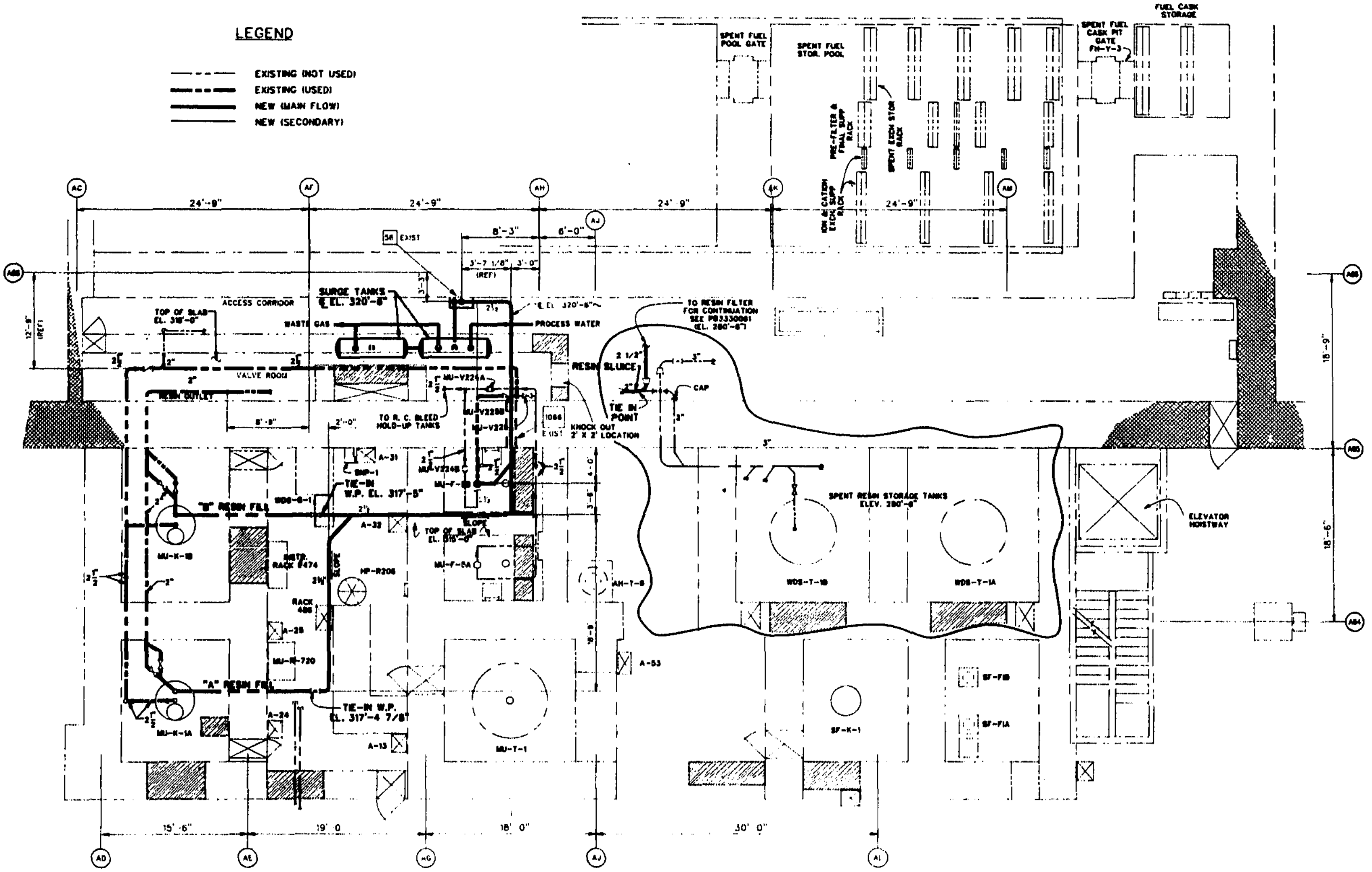

FIGURE 13. Piping Arrangement - 305' Elevation.

3. In the filter housing of filter MU-F-5A or MU-F-5B. The filter cubicles are adjacent to the Hayes gas analyzer room on the 305'-0" elevation. This tie-in point is not required for resin and debris removal. However, it will provide for removing debris from the 2-1/2-inch normal inlet piping including the upper laterals. This section of piping is located downstream of filter housings MU-F-5A and 5B.

With the exception of the tie-in point described in 1) above (resin sluice line) all are readily accessible. The radiation levels near the sluice line are not extremely high, however, this area should be cleaned prior to making the tie-in at this location. Auxiliary tie-ins will be provided by GPU.

Step 1 - Slow Upflow Recirculation to Remove Complex Organic Compounds

Research performed by PNL on irradiated resins (Appendix A) revealed the formation of soluble complex organic compounds. The effect of these compounds on the Submerged Demineralizer System and EPICOR II is not known. However, it is possible that these compounds could damage the cleanup capability of these systems or the compounds could pass through these systems and contaminate the processed water. This step is designed to capture any organic compounds prior to release of the effluent to the normal TMI-2 cleanup systems.

The flow path for this step is shown in Figure 14. Water enters the bottom of the demineralizer through the resin sluice line and exits the top of the demineralizer through the resin fill line. The slow upward flow rate of approximately 5 to 10 gpm is sufficient to clear the resin from the short section of resin sluice line between valves MU-V-108 and MU-V-238 and the bottom of the demineralizer but is not sufficient to cause resin carryover into the resin fill line. The normal water inlet line at the top of the demineralizer is not used (MU-V6 remains shut) until all resin and debris are removed in Step 4 of the resin removal process.

STEP 1
SLOW UPFLOW
REMOVE COMPLEX COMPOUNDS

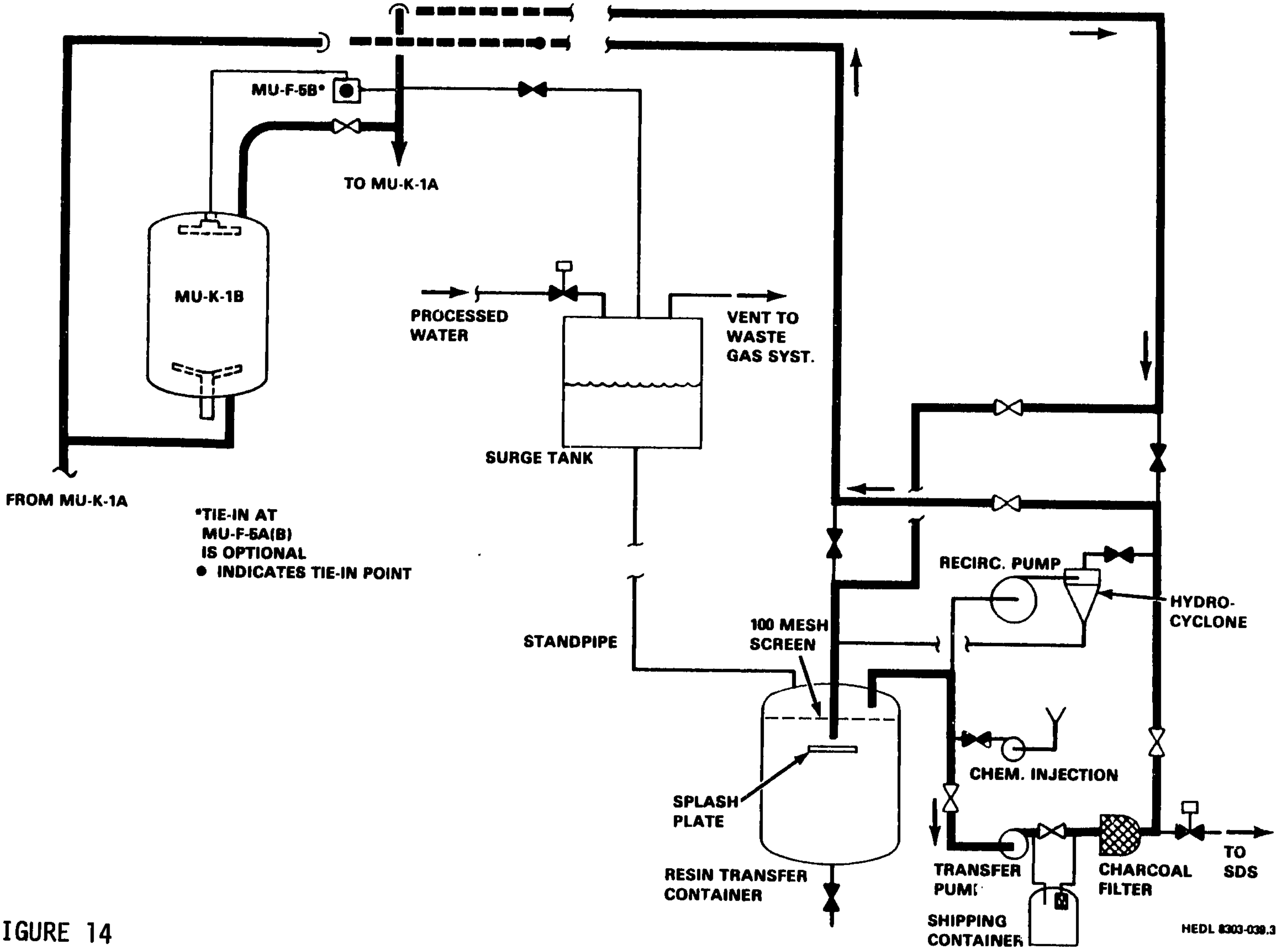

FIGURE 14

All effluent from the demineralizer flows out the resin fill line and into the resin transfer container which will be located on the 280'-6" elevation of the Fuel Handling and Auxiliary Building. The effluent passes upward in the resin transfer container through a 100 mesh screen (0.0059 inch openings), enters the transfer pump which provides for recirculation and continues on through a charcoal filter which removes the complex compounds that may be in solution. All effluent is passed through the charcoal filter during Steps 1 and 2 of the processs.

From the charcoal filter, the effluent is returned to the bottom of the demineralizer through the resin sluice line. Recirculation continues until sampling indicates that the charcoal filter has removed sufficient complex compounds to enable release of the effluent to the SDS.

Step 2 - Slow Upflow Recirculation to Remove Cesium

ALARA considerations make it desirable to remove the ^{137}CS from the demineralizers, resin, and debris prior to removal of the resin and debris from the demineralizers. The elution of the ^{137}Cs will permit disposal of this isotope within the SDS zeolites. Subsequent sluicing and transfer operations can then be performed at lower activity levels and at a lower exposure risk to personnel operating the removal system. If the total estimated ^{137}Cs content of 10,000 Ci is eluted to the SDS, 10% of one SDS liner's loading capacity will be expended.

Numerous possibilities exist for elution of the resin to remove the ^{137}Cs. Some preliminary evaluations are discussed in Appendix A. Oak Ridge National Laboratory (ORNL) will perform additional analyses in this area. It may be possible to use reactor coolant grade water as an eluent. Its chemical composition is shown in Table VIII.

Table VIII

Reactor Coolant Grade Water Chemical Composition

3500 ppm Boron as Boric Acid
1000 ppm Na^+ as NaOH
<5 ppm Cl^-
<6 ppm SO_4^{--}
pH = 7.8

Recirculation provides the capability for sampling and adjustment of the demineralizer effluent. The removal process equipment will be designed such that the liquids which are generated during cleanup of the demineralizers will be suitable for processing by the on-site systems.

The low upward velocity through the demineralizer is continued during Step 2 (see Figure 15) to minimize resin carryover into the system piping. If required, additional sodium ions can be injected at the transfer pump inlet to alter the equilibrium concentration and thus improve the probability of displacing cesium from the cation resin in the demineralizer. The sodium ion solution can continue to be injected and circulated while bleeding the system to SDS through the charcoal filter. The charcoal filter, in addition to removing complex compounds, removes all particles larger than 1 micron prior to release of the effluent to SDS. Makeup water is added to the surge tank where the water level is controlled automatically. This elution and feed/bleed process is continued until temporary radiation monitors installed in the demineralizer cubicle indicate no further reduction in radiation is being attained.

Step 3 - Fast Upflow Recirculation to Transfer Resin

When elution has been satisfactorily accomplished, the recirculation rate is increased to effect carryover of the resin into the resin fill line. To

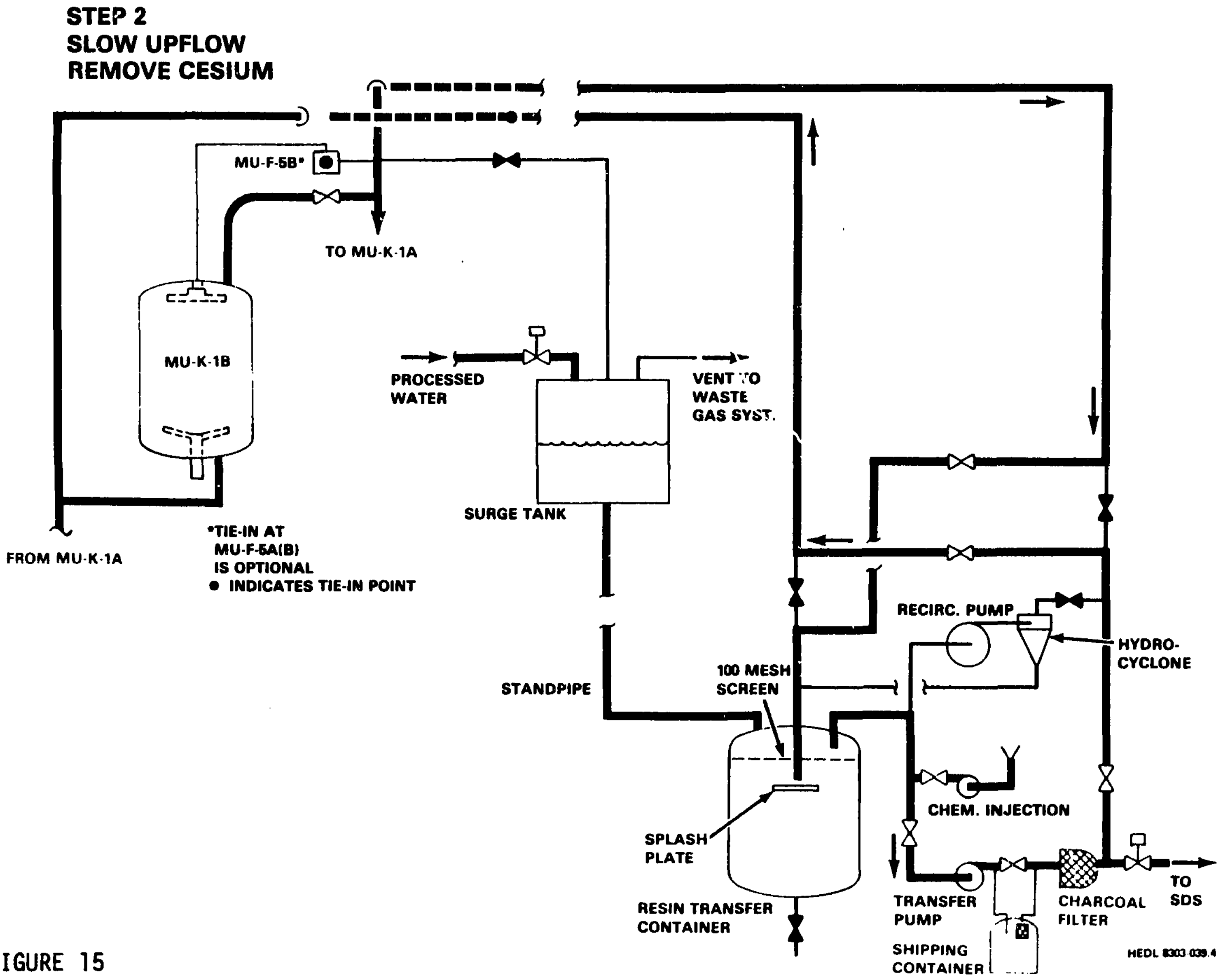
STEP 2
SLOW UPFLOW
REMOVE CESIUM
MU-F-5B*
TO MU-K-1A
MU-K-1B
FROM MU-K-1A
*TIE-IN AT
MU-F-5A(B)
IS OPTIONAL
● INDICATES TIE-IN POINT
PROCESSED
WATER
VENT TO
WASTE
GAS SYST.
SURGE TANK
STANDPIPE
100 MESH
SCREEN
SPLASH
PLATE
RESIN TRANSFER
CONTAINER
RECIRC. PUMP
HYDRO-
CYCLONE
CHEM. INJECTION
TRANSFER
PUMP
SHIPPING
CONTAINER
CHARCOAL
FILTER
TO
SDS
HEDL 8303-038.4

FIGURE 15

accomplish the higher recirculation rate, the transfer pump is secured and the recirculation pump is started (see Figure 16). The recirculation pump will provide an upward flow of approximately 120 gallons per minute which will result in an upflow velocity of approximately 1-1/4 feet per minute (23 meters per hour) in the demineralizer. Tests performed on irradiated resin by PNL (See Figure 3, Appendix A) indicate that the vertical expansion of the resin bed will be in excess of 700%. Therefore, if the initial depth of the bed is 2 feet, the column height of the expanded resin will be in excess of 14 feet. Since the height of the demineralizer is approximately 7 feet, some resin will carry over into the resin fill line at an upward flow rate of 120 gallons per minute.

The rate of resin removal during upflow can be controlled by adjusting the upflow velocity. This is not the case during fast downflow (Step 4) where maximum flow must be maintained to keep the concentrated resin slurry in suspension in the long horizontal runs of piping. Upflow will not remove the higher density resin beads or the larger fuel fines. However, the quantity of materials that are removed will be significant and will minimize the possibility of plugging the sluice line when the remainder of the resin and debris are transferred by downflow as discussed in Step 4 below.

The effluent is sent to the resin transfer container and is discharged below a horizontal 100 mesh screen. The discharge is directed toward a splash plate in the container which will be designed to minimize agitation of the resin that has settled to the bottom of the container. The resin transfer container is a 4 foot diameter container with outside dimensions similar to an EPICOR II liner. The 100 mesh horizontal screen will prevent carryover of the resin to the recirculation pump. Some small fuel fines are expected to be carried out the top of the demineralizer since their terminal velocity in water is less than the 1-1/4 feet per minute upward velocity. The size of these fuel fines is less than 40 microns (specific gravity 10.2 g/cm^3). Some of these fines will settle-out into the transfer container while all fines larger than 4 microns will be removed by the hydrocyclone. Therefore, the water that is recirculated to the demineralizer will be essentially free of resin and debris. This will minimize the spread of contaminated particles throughout the system.

STEP 3
FAST UPFLOW
REMOVE RESIN

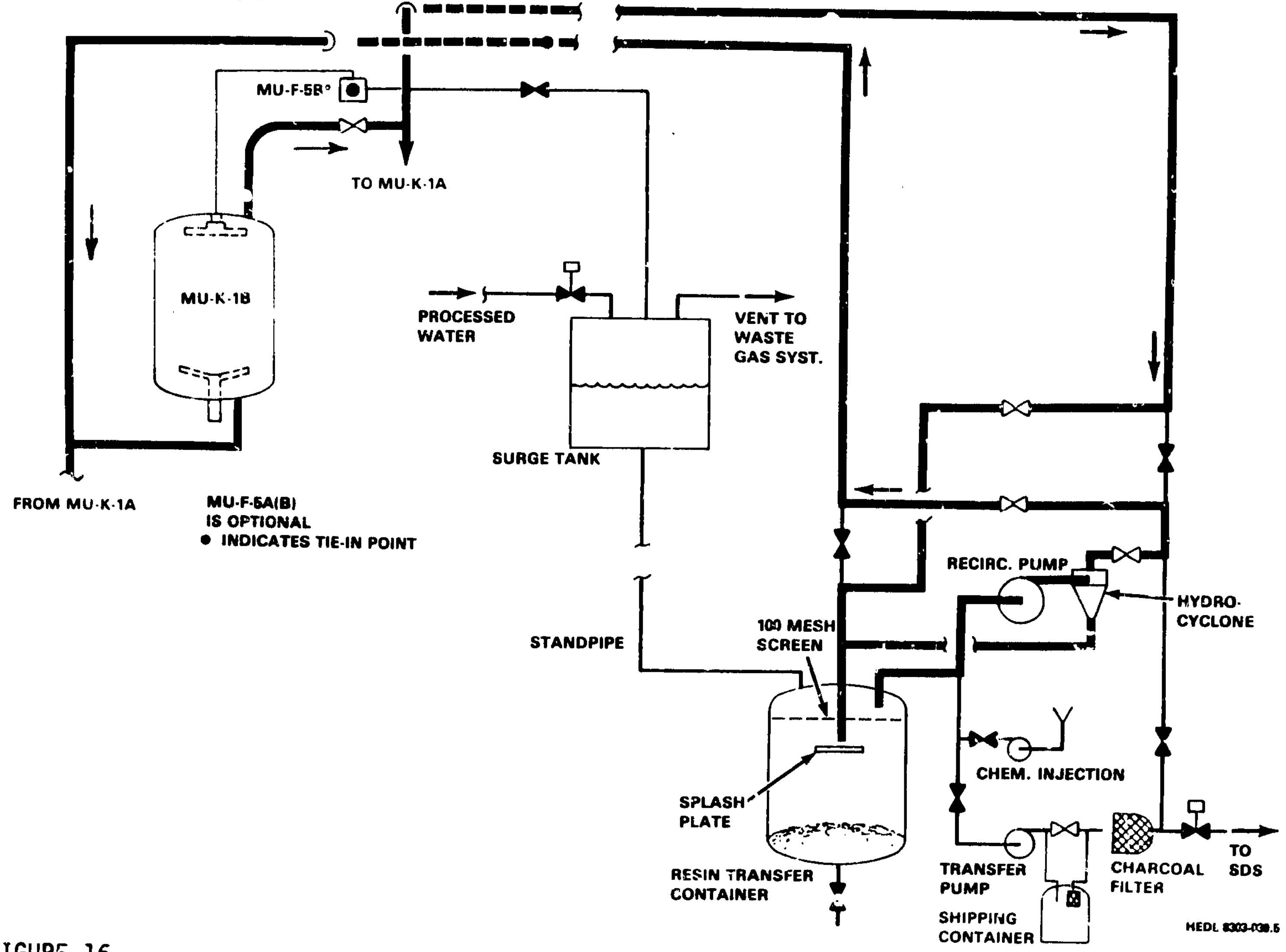

FIGURE 16

Additional agitation of the resin bed can be accomplished (including a higher rate of upflow in the demineralizer) by injecting demineralized water into the bottom of the demineralizer through valve MU-V-292. Since the addition of water through MU-V-292 will increase the water level in the surge tank, provisions will be included in the final design to permit the release of water through the charcoal filter to SDS with the transfer pump secured (this detail is not shown in the Figures).

Step 4 - Fast Downflow Recirculation to Transfer Resin and Debris

Downflow utilizes the same piping systems with the flow reversed (Figure 17). Since sluicing severely degraded resin from demineralizers has not been attempted and since the form of the debris in the demineralizers is presently unknown, suitable precautions must be taken when downflowing to prevent plugging up the resin sluice line. The objective during downflow is to transfer all remaining resin and debris into the resin transfer container.

To initiate downflow, the water level in the surge tank is lowered to provide for addition of demineralized water to the system through the normal demineralizer outlet line (through MU-V 292). Water addition at this location will agitate the resin bed to improve sluicability. While adding demineralized water through the normal outlet line, fast upflow recirculation is initiated as described in Step 3 to clear resin and debris from the section of piping between valves MU-V 238 and MU-V 108 and the demineralizer. When the water level in the surge tank approaches the high level limit, all inflow to the bottom of the demineralizer is secured and the valves on the resin removal process equipment skid (Figure 12) are realigned to reverse the flow direction through the demineralizer. The recirculation pump is then restarted to sluice the remaining resin and debris to the transfer container.

The 100 mesh screen will retain the resin in the container and the majority of the higher density fuel fines will settle to the bottom. Any resin fines or debris that pass through the 100 mesh screen will be processed through the hydrocyclone which will be designed to remove all resin fines greater than 70 microns and all fuel fines greater than 4 microns. Samples of wet

STEP 4
FAST DOWNFLOW
REMOVE RESIN AND DEBRIS

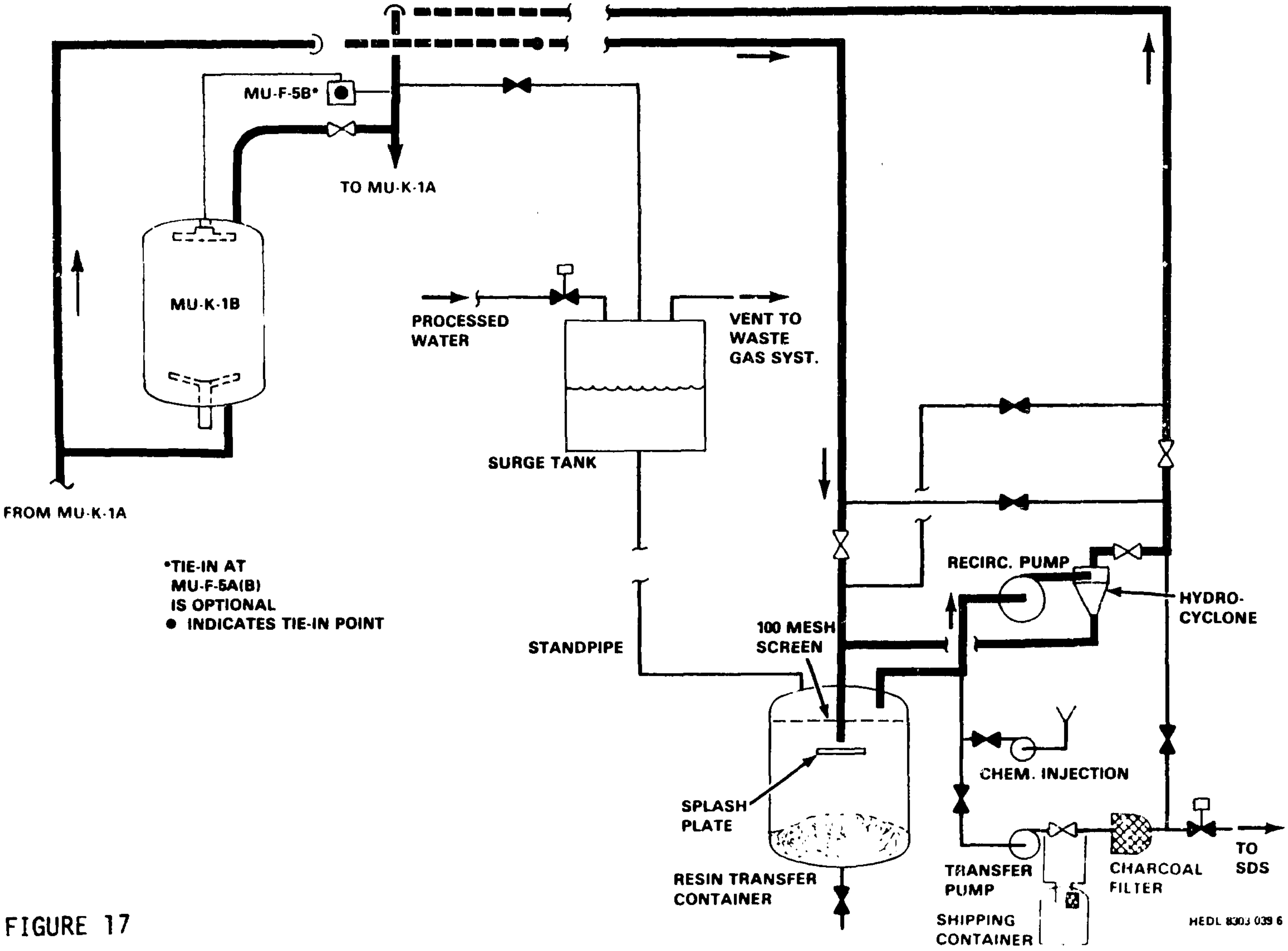

*TIE-IN AT
MU-F-5A(B)
IS OPTIONAL
● INDICATES TIE-IN POINT

FIGURE 17

irradiated resin (1.7 x 10^9 R) and new Li-form IRN-150 resin were wet sieved by PNL to determine size distribution. The results are shown in Table IX.

TABLE IX

Sizing of New and Irradiated Ion Exchange Resin

Mesh	Openings		Percent Retained on Mesh	
	Inches	Microns	Irradiated	New Resin
20	0.0331	841	ND	>13.7
30	0.0234	594	>49.C	71.6
40	0.0165	419	43.0	12.3
60	0.0098	249	7.8	2.4
80	0.0070	178	0.2	0.015

Table IX indicates that the 100 mesh screen and the hydrocyclone will remove essentially all resin from circulation. A hydrocyclone that is designed to remove all fuel fines above 4 microns will also remove some fuel fines less than 4 microns. In practice, a hydrocyclone with a separator size classification of 2 microns (for particles of a given specific gravity) results in a 50% split between the number of 2 micron particles that are released to the overflow (recirculated) and the number of particles retained in the underflow (returned to the resin transfer container). A properly designed hydrocyclone of the size considered here will result in a maximum overflow particle size of approximately twice the value of the classification size. Therefore, the maximum size particle recirculated will be approximately 4 microns.

By incorporating the resin transfer container as a settling tank and with the 100 mesh screen and the hydrocyclone operating in series, the amount of recirculation of contaminated particles will be held to the minimum practical limit. It should be noted that the piping used in this process, both existing and temporary, is (or will be) designed for sluicing resin and is therefore free of deadlegs and crevices that would otherwise collect small particles of resin and debris.

After all resin and debris have been removed from the demineralizer, the normal inlet line between filters MU-F-5A (5B) and the demineralizers can be back flushed by opening MU-V 6 and MU-V 225 and recirculating in the upflow direction as described in Step 3. Any debris that may be in this section of piping could be flushed from the filter housing and into the resin transfer container through a tie-in point at the top of one of the filter housings. The method of tying into the top of the filter housing is illustrated in Figure 18 and is discussed in Section 5.2. This tie-in point is optional since it is not needed to remove resin and debris from the demineralizers. However, a tie-in at this point will provide a method for filtering the effluent prior to sending it to SDS or the reactor coolant bleed holdup tanks through MU-V 8.

Unplugging this section of piping, including the top laterals in the demineralizers, will also make the top laterals available for final rinsing of the internal surfaces of the demineralizer. This would be accomplished after the resin transfer container was drained (following Step 5 below). Demineralized water would enter the top of the demineralizer through existing piping by opening MU-V-285.

Step 5 - Resin and Debris Transfer to Shipping Containers

The shipping containers for resin and debris are modified SDS liners (Section 6). They are installed downstream of the transfer pump as shown in Figure 19. Resin transfer to the shipping containers can be initiated following Step 3 (fast upflow recirculation) to minimize the amount of solids in the bottom of the resin transfer container prior to starting Step 4 (fast downflow recirculation to transfer resin and debris). The resin transfer operation is independent of operations associated with recirculation. This allows system operators to give their full attention to each individual phase or step in the overall resin removal operation. Loading the shipping containers is accomplished by adding water to the bottom of the resin transfer container to agitate the resin. The slurry is then pumped to the shipping container using the transfer pump. A 5-micron backflushable metallic filter is installed in the outlet line of the shipping container to retain resin and debris. Effluent that passes through the 5-micron filter will go to the charcoal filter which contains a 1-micron filter. Effluent from the charcoal filter is sent to the SDS. Adding water to the resin transfer container and transferring the slurry to the shipping container will cause fluctuations in the surge tank level which will be accommodated by the automatic level control system for the surge tank.

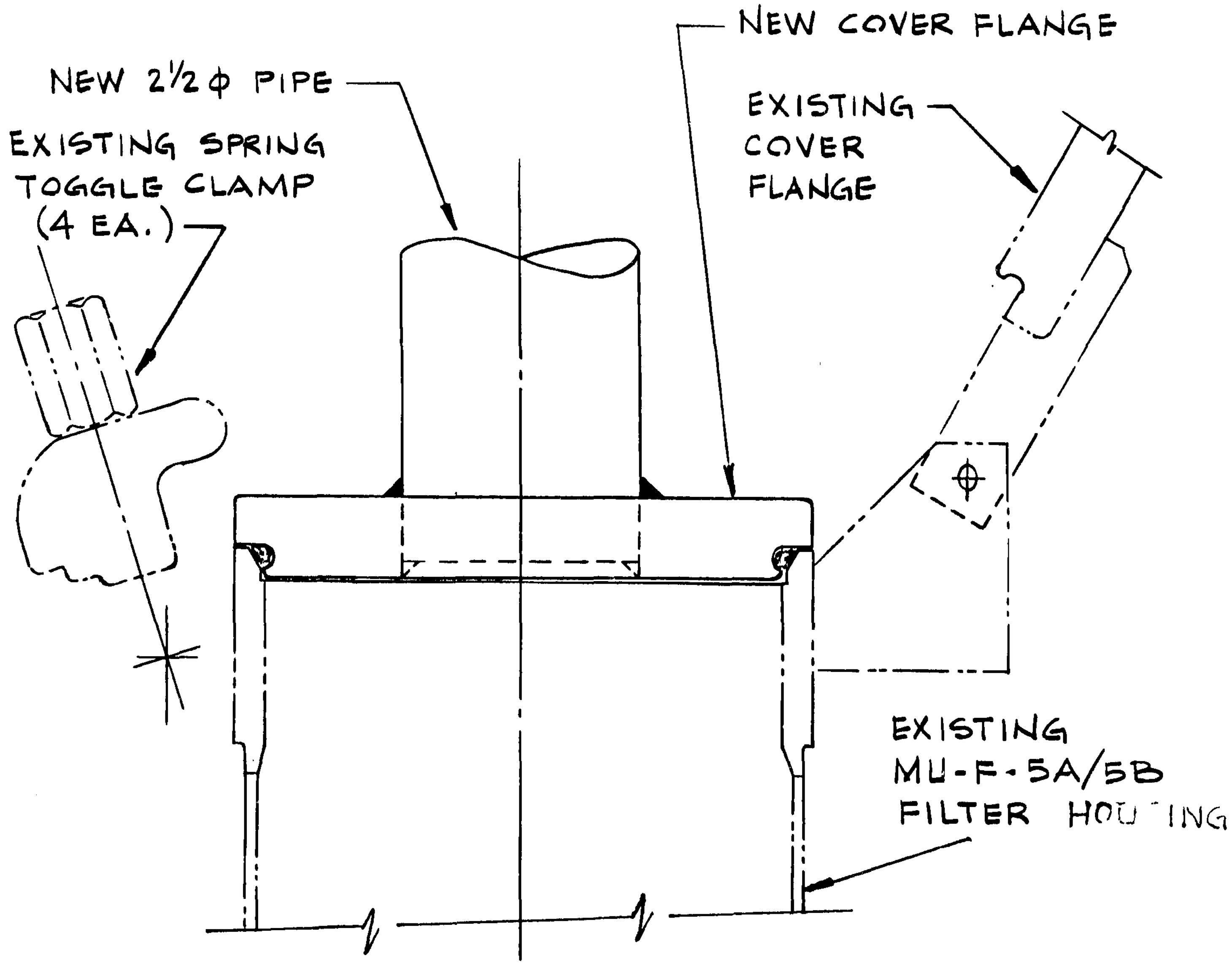

FIGURE 18. Modified Filter Housing Closure.

STEP 5

RESIN AND DEBRIS TRANSFER TO SHIPPING CONTAINER

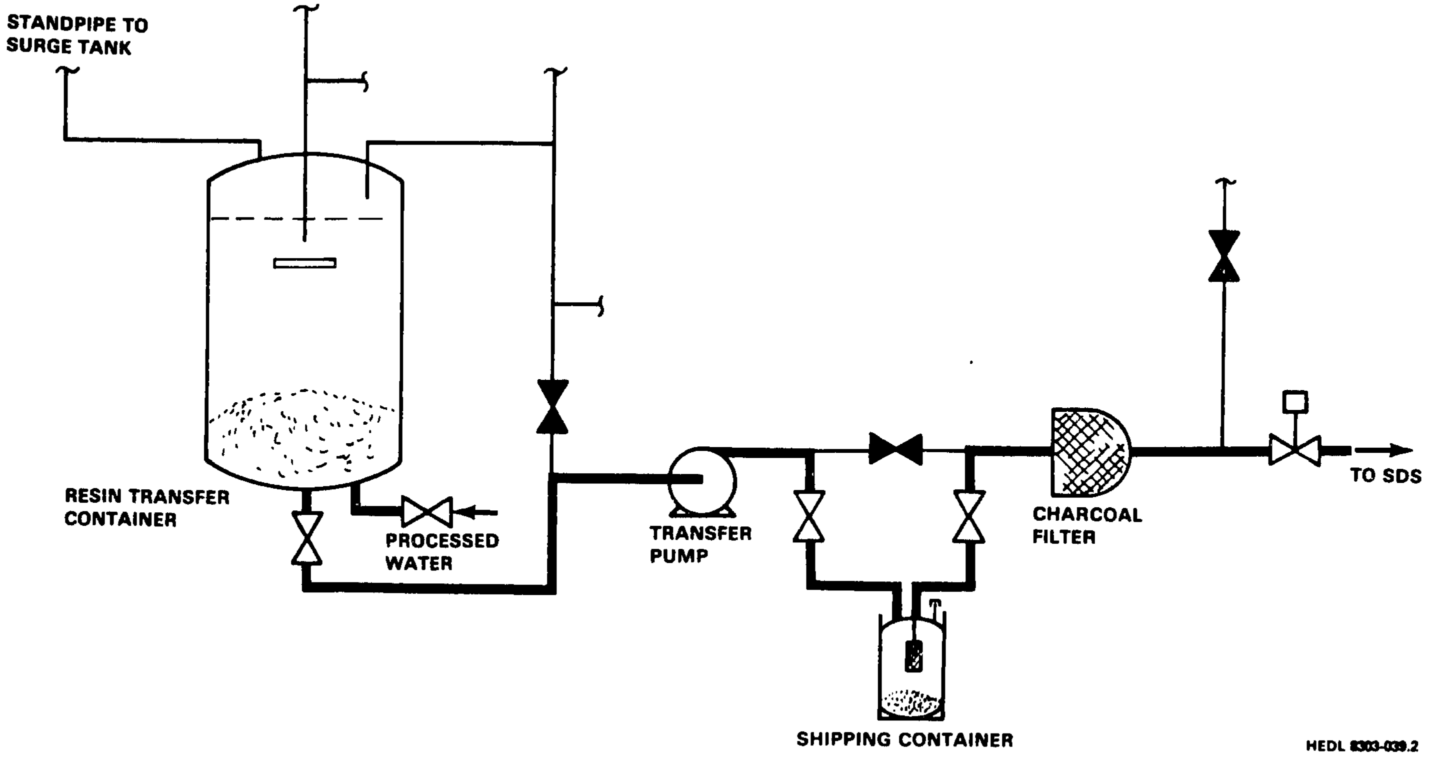

FIGURE 19

Instrumentation will be provided to monitor and control the level of resin and debris in the shipping container prior to sealing for shipment. Instrumentation will also be provided to monitor the pressure drop across the filter elements in the shipping containers and the charcoal filter. These filter elements will be capable of being backflushed with processed water in the event that partial plugging results in excessive pressure drop across the elements.

The shipping containers will include all connections and provisions required to dewater and degas the containers in preparation for safe shipment. Particular attention will be directed toward the design features required to eliminate or minimize hydrogen accumulation during shipment and storage.

5.2 TIE-IN POINTS

Tie-in points are locations where the resin and debris removal process piping is connected to the existing piping system. Four major tie-in points will be required. These are:

1) Resin sluice line
2) Resin fill line - A demineralizer
3) Resin fill line - B demineralizer
4) Filter housing MU-F-5A or MU-F-5B (optional)

The remaining tie-in points for miscellaneous vents, drains, reactor coolant grade water supply and a return line to SDS are located in noncontaminated (or low level contamination) piping that will be selected and provided by GPU during the preliminary equipment design phase. Details of the four major tie-in points are discussed below.

5.2.1 Resin Sluice Line

The resin sluice line is a 2-inch line with a long horizontal run between the demineralizers and the spent resin storage tank. This line is shown in Figures 12 and 13. As seen in Figure 12, there are a number of sluice lines that

STEP 5
RESIN AND DEBRIS
TRANSFER TO SHIPPING CONTAINER

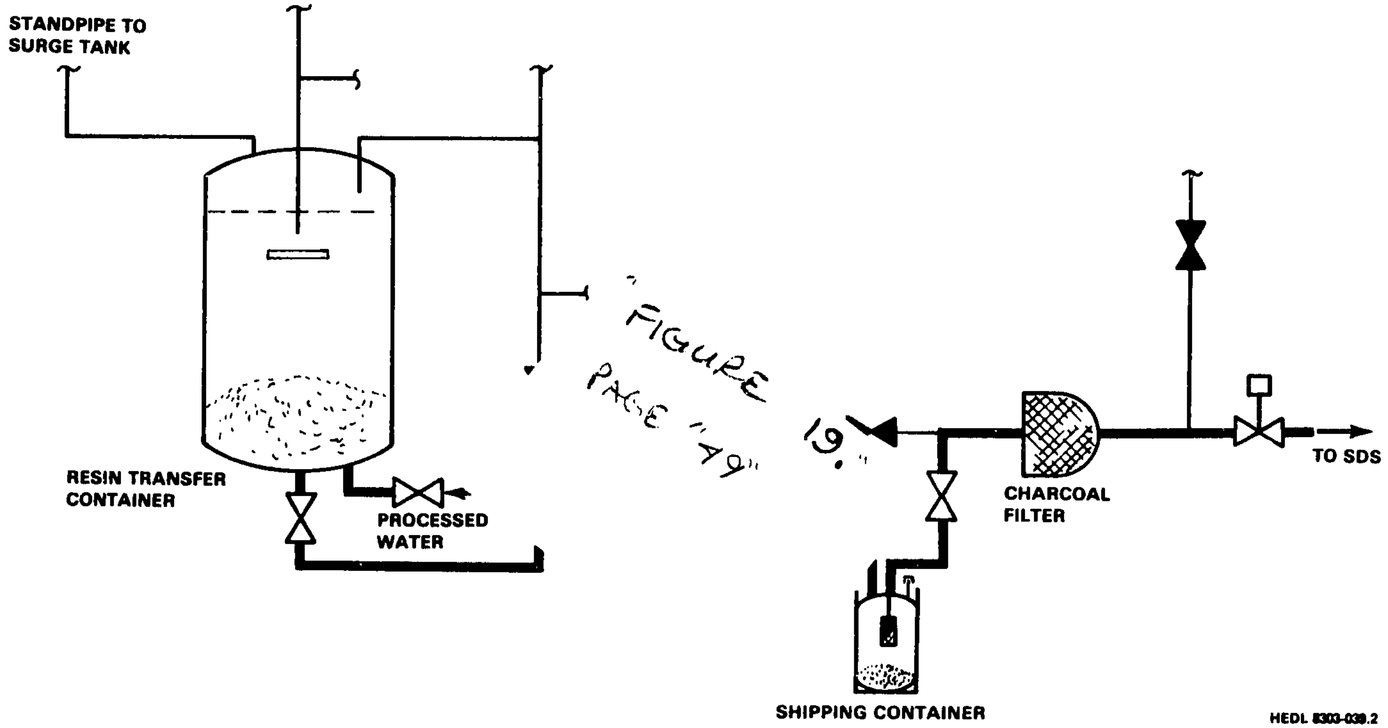

"FIGURE 19."
PAGE "49"

FIGURE 18

Instrumentation will be provided to monitor and control the level of resin and debris in the shipping container prior to sealing for shipment. Instrumentation will also be provided to monitor the pressure drop across the filter elements in the shipping containers and the charcoal filter. These filter elements will be capable of being backflushed with processed water in the event that partial plugging results in excessive pressure drop across the elements.

The shipping containers will include all connections and provisions required to dewater and degas the containers in preparation for safe shipment. Particular attention will be directed toward the design features required to eliminate or minimize hydrogen accumulation during shipment and storage.

5.2 TIE-IN POINTS

Tie-in points are locations where the resin and debris removal process piping is connected to the existing piping system. Four major tie-in points will be required. These are:

1) Resin sluice line
2) Resin fill line - A demineralizer
3) Resin fill line - B demineralizer
4) Filter housing MU-F-5A or MU-F-5B (optional)

The remaining tie-in points for miscellaneous vents, drains, reactor coolant grade water supply and a return line to SDS are located in noncontaminated (or low level contamination) piping that will be selected and provided by GPU during the preliminary equipment design phase. Details of the four major tie-in points are discussed below.

5.2.1 Resin Sluice Line

The resin sluice line is a 2-inch line with a long horizontal run between the demineralizers and the spent resin storage tank. This line is shown in Figures 12 and 13. As seen in Figure 12, there are a number of sluice lines that lead to the spent resin storage tank. Since a major objective of the resin removal operation is to prevent the spread of contaminants to additional components at TMI-2, the tie-in point has been located upstream of the spent resin storage tank and upstream of the remaining sluice lines that feed into the main collection header (3-inch pipe) near the top of the spent resin storage tanks. To complete this tie-in, a section of the 2-inch sluice line will be removed. The open line on the downstream (spent resin storage tank) side will be plugged. A temporary fitting will be welded to the demineralizer side to provide the connection to the resin removal process piping. The preferred location is in the valve room, near the ceiling of the 280'-6" elevation as shown in Figures 12 and 13. General radiation levels in this area are 10-50 mR/hr (beta). An alternate location is in the Make-Up and Purification Pump 1-A cubicle on elevation 280'-6". The reasons for selecting the valve room as the preferred location are: 1) there will be one supply line, one return line, and a stand pipe to the surge tank in this location that can be run side by side to make use of common shielding and; 2) the cubicle housing pump 1-A is expected to require more effort to clean up than the valve room.

5.2.2 Resin Fill Lines

The resin fill lines are 3 inch diameter lines that pass through the Hayes gas analyzer room on elevation 305'-0". The Hayes gas analyzer room has recently been decontaminated to the point where it can be considered an accessible area. Radiation exposure to personnel making the connections in this area will be minimal. The resin fill lines will have been previously cut to obtain resin samples and flanged fittings will be available for connecting the resin removal process piping. Lines in proximity of normal personnel access areas will be shielded.

5.2.3 Filter Housing MU-F-5A and MU-F-5B

The filter housings are located inside an enclosed cubicle adjacent to the Hayes gas analyzer room. The cartridges have been removed from housings MU-F-5A and 5B and the housings have been flushed. Hands-on access to the housings is not required since the closures on these housings have been designed to be removed remotely. To accomplish this, a 12-inch diameter shielded plug is removed from the top of the filter cubicle and extension tools are lowered through the plug opening to manipulate the bolts on the closure.

The filter housing closure is illustrated in Figure 18. With the closure in the open position, a special closure will be installed which consists of a section of 2-1/2 inch piping with a flange welded at one end. The flange sealing surface is designed to be identical to the closure (and will in all probability be a modified closure procured from the filter housing manufacturer). The flange can be installed using the available tooling that is used for installation and removal of the normal closure device.

5.3 REMOVAL EQUIPMENT SELECTION AND LOCATION

Equipment shown in Figures 12 and 13 is discussed in the following sections including the rationale for its selection and location. All special equipment items listed below which include the resin transfer container, hydrocyclone, recirculation pump, transfer pump, chemical injection pump, shipping container, charcoal filter and the majority of the valves and instrumentation required to control the resin removal process equipment are located on the 280'-6" elevation as shown in Figure 12. The primary reason for selecting this location is to enable change-out of the shipping containers (and charcoal filter if necessary) by manipulating the connections to these containers remotely from the open hatch on the 305' elevation. In addition, the open hatch, and the installed 25 ton capacity beam above the hatch, provide the capability of removing the containers in shielded handling casks from the 280'-6" elevation to the 305' elevation and into the model room and truck bay. The containers can then be transferred to the spent fuel storage pool for interim storage in preparation for removal from TMI. Remote handling will be necessary since the radiation levels near the connections will prevent hands-on operations in accordance with ALARA objectives.

In addition to the above, activities on the 280'-6" elevation are minimal compared to those on the higher elevations. Therefore, location of equipment there will cause minimum interruption to on-going operations at TMI-2.

5.3.1 Surge Tank

The surge tank provides a constant pressure at the recirculation and transfer pump inlets which will enable the system operator to control pressure in the demineralizer by throttling the pump outlet. The surge tank also provides for expansion and contraction of the total system volume due to temperature changes or due to water addition and removal operations. The tank will be located above the valve alley with a tank centerline (average water level) elevation of 320'-6". The space above the valve alley is limited since the ceiling is at elevation 324'-0". Therefore, the surge tank will actually consist of two interconnected horizontal cylindrical tanks with a combined volume of approximately 300 gallons.

The high water level elevation in the surge tank will be above the high point in the overall system (see Figure 20). The high point in the system will be in a section of temporary piping between the resin fill lines and the resin transfer container. This section of piping will include a high point vent valve which will be opened only during initial fill of the system. This high point vent will be routed to the gas space in the surge tanks. The cover gas in the surge tanks will be vented to the waste gas system. An automatic water level control system will be included to prevent overflow of liquid to the waste gas system and to assure a constant head of water on the resin transfer container (which is at approximately the same pressure as the recirculation and transfer pump inlets).

5.3.2 Resin Transfer Container

The resin transfer container is a cylindrical vessel 4 feet in diameter and approximately 4 feet high. These dimensions were selected to permit handling and shielding of the container with existing equipment designed for the

HYDRAULIC PROFILE

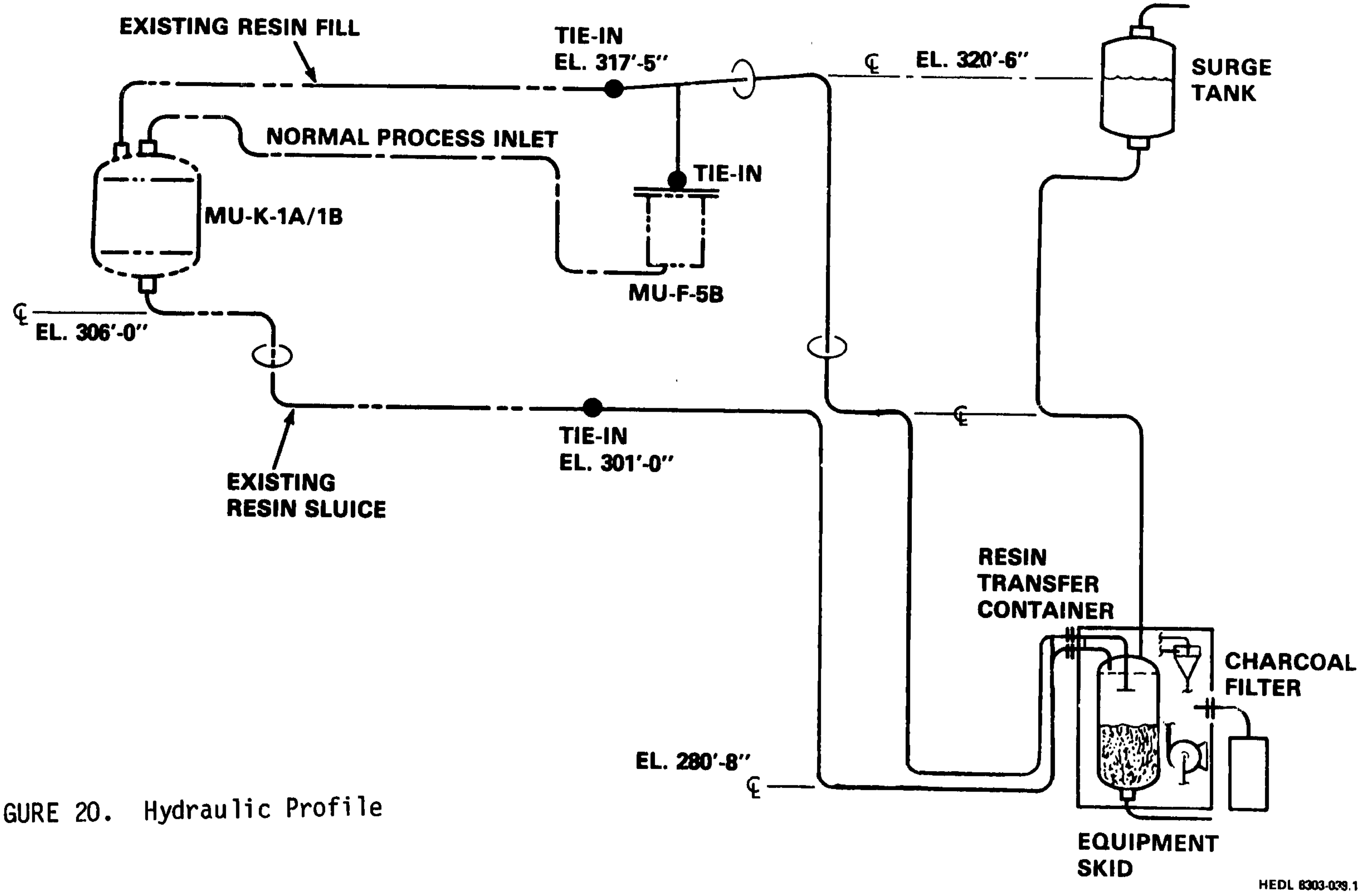

FIGURE 20. Hydraulic Profile

EPICOR II system. The volume is approximately 40 cubic feet (300 gallons). The container will be constructed of carbon steel in accordance with Section VIII of the ASME code. The normal operating pressure of approximately 20 psig is the pressure due to the static head of the system. Design pressure will be 100 psig. The resin transfer container serves as an interim hold point in the overall process of transferring the resin and debris from the demineralizers to the shipping containers.

The container includes a large area horizontal 100 mesh (0.0059 inch opening) screen, or set of screens, which serve to remove the resin from the flow stream during fast upflow and fast downflow operations. The effluent from the demineralizers is discharged below the 100 mesh screen and the majority of the resin and debris will collect on the underside of the screen or will settle to the bottom of the container when recirculating at maximum flow.

Provisions will be included in the design of the resin transfer container for agitation of the resin and debris during transfer operations to the shipping containers. A penetration at the bottom of the resin transfer container, in addition to the drain line, will provide for addition of water for initial system fill and agitation of the contents during transfer operations to the shipping containers. The bottom penetration will also provide for addition of nitrogen prior to initial fill to displace the air and oxygen from the system.

5.3.3 Hydrocyclone

The hydrocyclone will be designed to remove all fuel fines (specific gravity 10.2 g/cm^3) greater than 4 microns and all resin fines (approximate specific gravity 1.025 g/cm^3) greater than 70 microns. The inlet flow rate will be approximately 125 gallons per minute and the underflow (return flow to the resin transfer container) will be approximately 5 gallons per minute. Pressure drop through the cyclone, which will have an inlet diameter of approximately 1.0 inches, will be approximately 77 psig. These parameters are preliminary and will be further evaluated and tested during final design of the system.

5.3.4 Recirculation Pump

The recirculation pump is a single stage horizontal shaft canned centrifugal pump. Maximum output is 125 gpm at a head of 325 ft of water. The pump casing shall be designed for 175 psig minimum to accommodate the pressure rise across the pump with an inlet pressure of 20 psig (resin transfer container operating pressure). Materials shall be stainless steel. Power shall be electric.

5.3.5 Transfer Pump

The transfer pump is a low volume (10 gpm) low head (50 ft) single stage centrifugal pump. It is located between the resin transfer container and the shipping container and provides for recirculating the effluent through the charcoal filter, sending the filtered effluent to SDS, and for transferring the resin and debris from the resin transfer container to the shipping container. The transfer pump may also be used to partially dewater the shipping containers and charcoal filter container prior to removing these containers from the system.

5.3.6 Chemical Injection Pump and Injection Station

The chemical injection pump provides the capability of introducing chemicals for resin elution or system decontamination. The capacity of the pump is variable up to a maximum rate of 1 gallon/min and is a positive displacement design. Standard materials for this type of pump are stainless steel. Chemicals are placed into solution in the feed tank prior to injection into the recirculation pump inlet line.

5.3.7 Shipping Container

The shipping container is essentially an empty SDS liner and is equipped with a 5.0 micron metallic filter to retain the resin and debris that are pumped from the resin transfer container. All existing design features of the SDS liners shall be retained. In addition, filter backflush capability and a resin level indicating system shall be provided. The filter capacity will be sized to permit flows up to 10 gpm. Further details on the shipping container (modified SDS liner) are included in Section 6.1.

5.3.8 Charcoal Filter

The charcoal filter is installed in series with, and downstream of, the shipping container. This filter is essentially an SDS liner containing charcoal in place of the normal zeolite bed. Alternatives to charcoal, i.e., special resins, will be evaluated during the preliminary design phase. The filter shall be designed for cleaning by backflushing and shall permit flows up to 10 gpm. The purpose of the charcoal filter is twofold: 1) to remove complex organic compounds from the demineralizer effluent that would otherwise degrade the SDS and EPICOR II systems; and 2) to retain fuel fines down to 1 micron to assure that they do not accumulate in other TMI-2 systems such as the Reactor Coolant Bleed Holdup Tanks prior to being processed by the SDS.

5.3.9 Piping

All piping will be welded and in accordance with ANSI B31.1. Exceptions to welded connections are at the four tie-in points discussed in Section 5.2 and at the connections to process equipment items such as pumps and containers. All temporary piping runs comprising the main recirculating path will be constructed of 2-1/2 inch schedule 40 stainless steel and will be installed in accordance with Regulatory Guide 1.143. The 2-1/2 inch pipe size is required to minimize pressure drop while maintaining maximum flow rates. This eliminates the need for operating at high pressures. Hard piping and welded pipe fittings have been selected to minimize crevices and the possibility of leaks. The standpipe between the resin transfer container and the surge tank will be 1-inch diameter carbon steel.

5.3.10 Valves

Valves are shown in the various figures. Valves in the 2-1/2 inch recirculation lines will be gate, diaphragm, or ball valves to minimize pressure drop.

Specific designs will be evaluated to minimize retention of contaminants. Most valves will be manually operated and constructed of stainless steel. Valves installed to control pressure and water level in the surge tank will be controlled automatically. The majority of the valves required to operate the system are located on the 280'-6" elevation as shown in Figure 12. These valves are in close proximity to the control station which includes the majority of instrumentation required to monitor and control the resin removal process equipment.

5.3.11 Instrumentation and Controls

Sufficient instrumentation will be provided to safely operate the system unde controlled conditions. For ease and safety of operation, the water level control in the surge tank is automatic. Maintaining a constant pressure in the resin transfer container (pump inlet pressure) will permit the operator to control system flow and pressure by adjusting the valve directly downstream of the recirculation pump. Radiation detectors will be installed at various locations to monitor expected changes in contamination levels as the resin and debris are transferred from the demineralizers. Pressure drop across the containers will be monitored to indicate performance of the filters. Flow meters will be provided to indicate instantaneous flow to and from the system. The Remote Controlled Transporter Vehicle (RCTV), shown in Figure 21, can be utilized to visually monitor the demineralizer cubicles for valve leakage and can install radiation detectors in the cubicles for monitoring the decrease in gamma radiation as the cesium is eluted to SDS and as the resin and debris are transferred to the resin transfer container. Temperature can be monitored as chemicals are added to ensure that no unexpected exothermic reactions are taking place. Provisions are also included to sample the effluent entering and leaving the containers to provide information on the contents of the containers and on the condition of the liquid prior to releasing it to the SDS through the charcoal filter.

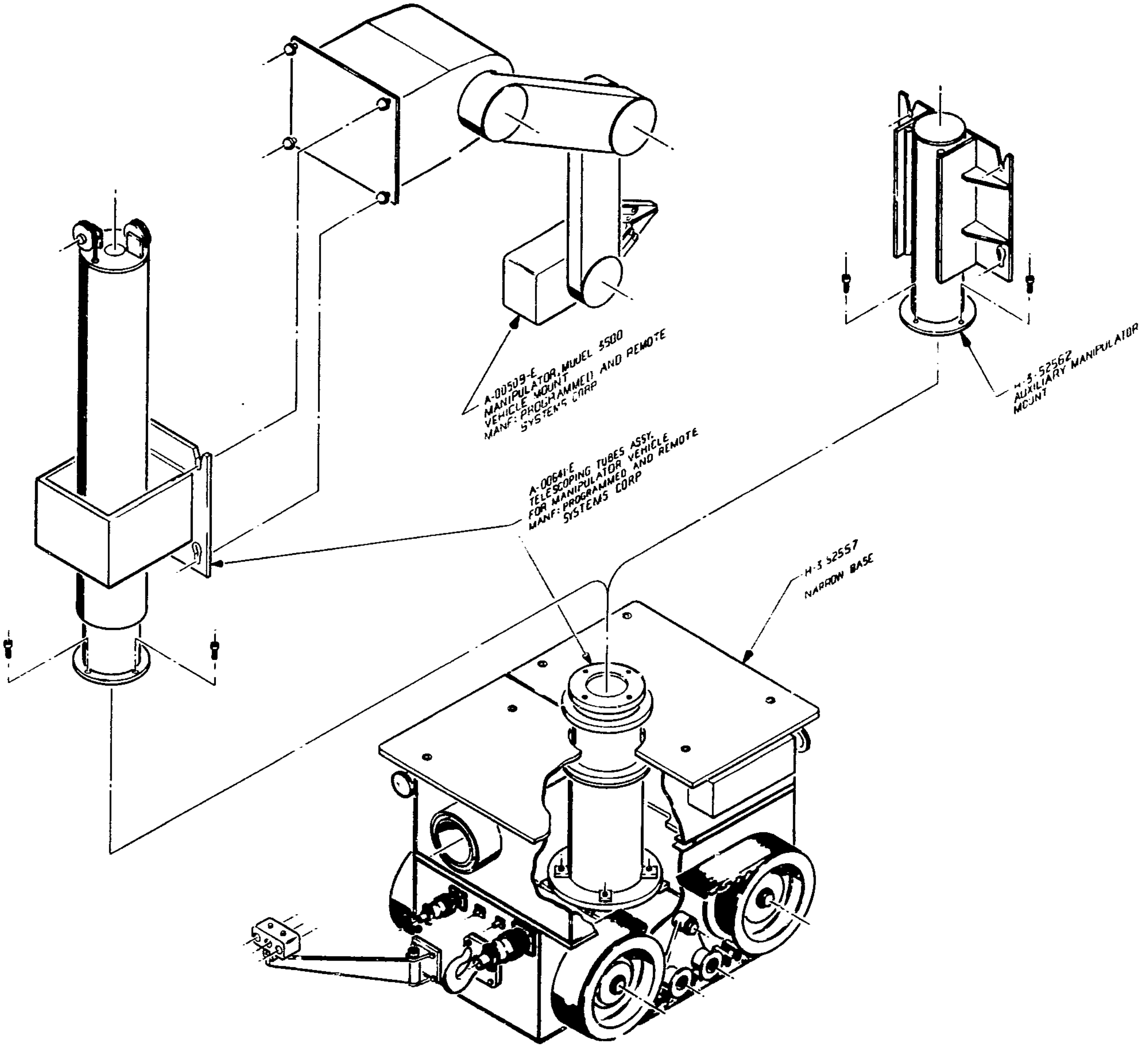

FIGURE 21. Remote Controlled Transport Vehicle.

5.3.12 Shielding

A major objective in the selection of tie-in points, routes for temporary piping, and the location of the major process equipment items discussed herein was to minimize radiation exposure to personnel during installation and operation of the resin removal process equipment. With the exception of a relatively short segment of temporary piping in the Hayes gas analyzer room, and the temporary piping near the resin removal process equipment, the majority of the existing and temporary piping that will be used to transfer resin will be in nonaccessible areas. These areas include the demineralizer cubicles, filter cubicles and valve alley on the 305' elevation and the valve room on the 280'-6" elevation. The remaining areas will require the installation of temporary shielding and possibly temporary exclusion of personnel from certain locations during resin transfer operations.

5.4 OPERATING PROCEDURES

Detailed operating procedures will be prepared as a part of the final design. The general process steps are discussed in Section 5.1.2 and include the operations outlined below.

5.4.1 Pneumatic Test of Demineralizer Piping System

Prior to filling and pressurizing the system with processed or demineralized water the piping systems that will be used during the resin removal process will be tested to assure integrity of the pressure boundary. Procedures will be prepared to pneumatically test the system and to determine leak rates, if any. Steps will be included to attempt to locate any significant leaks so that an assessment can be completed regarding the feasibility of repair.

5.4.2 System Fill and Recirculation to Remove Complex Compounds

This procedure covers initial fill and venting of the system and establishes recirculation at a low upward flow rate in the first demineralizer to be processed. Any complex compounds that are released from the irradiated resin will be circulated through the charcoal filter during operation under this procedure. This procedure will include the necessary steps and check points to assure that the instrumentation and controls are operating satisfactorily as an integrated system.

5.4.3 Upflow Recirculation to Remove Cesium

This procedure covers operation of the chemical injection system to displace cesium from the cation resin. This operation is performed while recirculating at a low upward velocity in the demineralizer. Cesium (and other solubles) in the effluent from the demineralizer are recirculated through the system. Samples will be taken to assure compatibility with the SDS and EPICOR II systems prior to release to these systems. Upon release, makeup water is supplied to the surge tanks. This feed and bleed procedure is continued until the radiation levels due to cesium stabilize.

5.4.4 Upflow Recirculation to Transfer Resin

This procedure covers recirculation in the upward direction through the demineralizer at maximum flow velocity (approximately 1-1/4 feet/minute) to induce carryover and transfer of the resin to the resin transfer container. The procedure will include instructions for adjusting and monitoring flow rates in the hydrocyclone overflow and underflow lines to optimize the rate of resin and debris removal from the demineralizer. Minor differences between the operation of the automatic surge tank level control system at high and low flow rate will be explained. The procedures will include instructions for monitoring the dose rates from the demineralizer and the resin transfer container during the transfer process.

5.4.5 Downflow Recirculation to Transfer Resin and Debris

This procedure covers recirculation through the system in the opposite direction to transfer the higher density resin beads and larger debris particles that cannot be removed by the relatively slow upflow velocity (1-1/4 feet/min) through the demineralizer. The procedure will address the special precautions required to prevent plugging the resin sluice line and will cover those contingency operations that will be required in the event the system piping becomes clogged with resin and debris.

5.4.6 Resin and Debris Transfer to Shipping Container

This procedure covers the operations required to generate a slurry in the resin transfer container and transfer this slurry to the shipping containers. Operation of the shipping container sampling equipment will be described. The procedure will include those steps required to backflush, isolate, vent, disconnect and remove and reinstall a new shipping container by using remotely actuated tooling.

5.4.7 Dewatering and Degassing in Preparation for Interim Onsite Storage and Offsite Shipment

This procedure covers those operations required to assure prevention of hazardous accumulations of hydrogen in the shipping container and charcoal filters after the container and filter have been removed from the system.

5.4.8 System Flushing

This procedure provides instructions for flushing the existing and temporary systems with water following the transfer of all resin and debris to the shipping containers. A procedure for unplugging and backflushing the normal demineralizer inlet lines and top laterals will be included. The procedure will not include the use of decontamination solutions although they may ultimately be necessary to cleanup the system. Fiberscope viewing of the tank interior will be performed through the resin fill line to verify the extent of cleanup. A radiation survey of the system will be performed prior to and after flushing.

6.0 PACKAGING AND SHIPPING DEMINERALIZER CONTENTS

Removal of the resin and debris from the demineralizers cannot be separated from the packaging, handling, storage and shipment. Two types of resin containers (liners) are currently in use at TMI-2 to perform these functions for SDS and EPICOR II. These were the only types of containers considered for use in the resin and debris removal system.

6.1 SHIPPING CONTAINER DESCRIPTION

The EPICOR II liner (Figure 22) is 4' dia x 4' high, of carbon steel, and is normally filled with resin for filtering low level radioactive water. The liners have a 32 cu ft capacity and weigh 3000 lb. They have been shipped with as much as 2000 Ci of activity inside the CNS 8-120 (Figure 23) or the HN200 casks. However, the CNS 8-120 cask which weighs 58,000 lb overloads the truck and thus requires overload highway permits. The HN200 is only available one week per month presenting a scheduling problem. These containers are presently being shipped to the Idaho National Engineering Laboratory (INEL) for storage, research, and disposal. The total loading of the demineralizers of approximately 10,500 Ci of ^{137}Cs would require that six containers be used if the 2000 Ci limit is retained.

The SDS liners (Figure 24) are 2' dia x 4'-5" high, of stainless steel, and normally filled with zeolite for filtering high level radioactive water. They contain 8 cu ft of zeolite and weigh about 1200 lbs. They are limited to 60,000 Ci of ^{137}Cs activity in the CNS1-13C cask (Figure 25). Therefore, The limiting factor in loading these liners is volume. The approximately 44 ft^3 of resin and debris from the demineralizers will require the use of six SDS liners. These containers are presently being shipped to Rockwell Hanford Operations (RHO) for storage in an approved overpack container designed by RHO. A comparison of the physical characteristics of these two liners is shown in Table X.

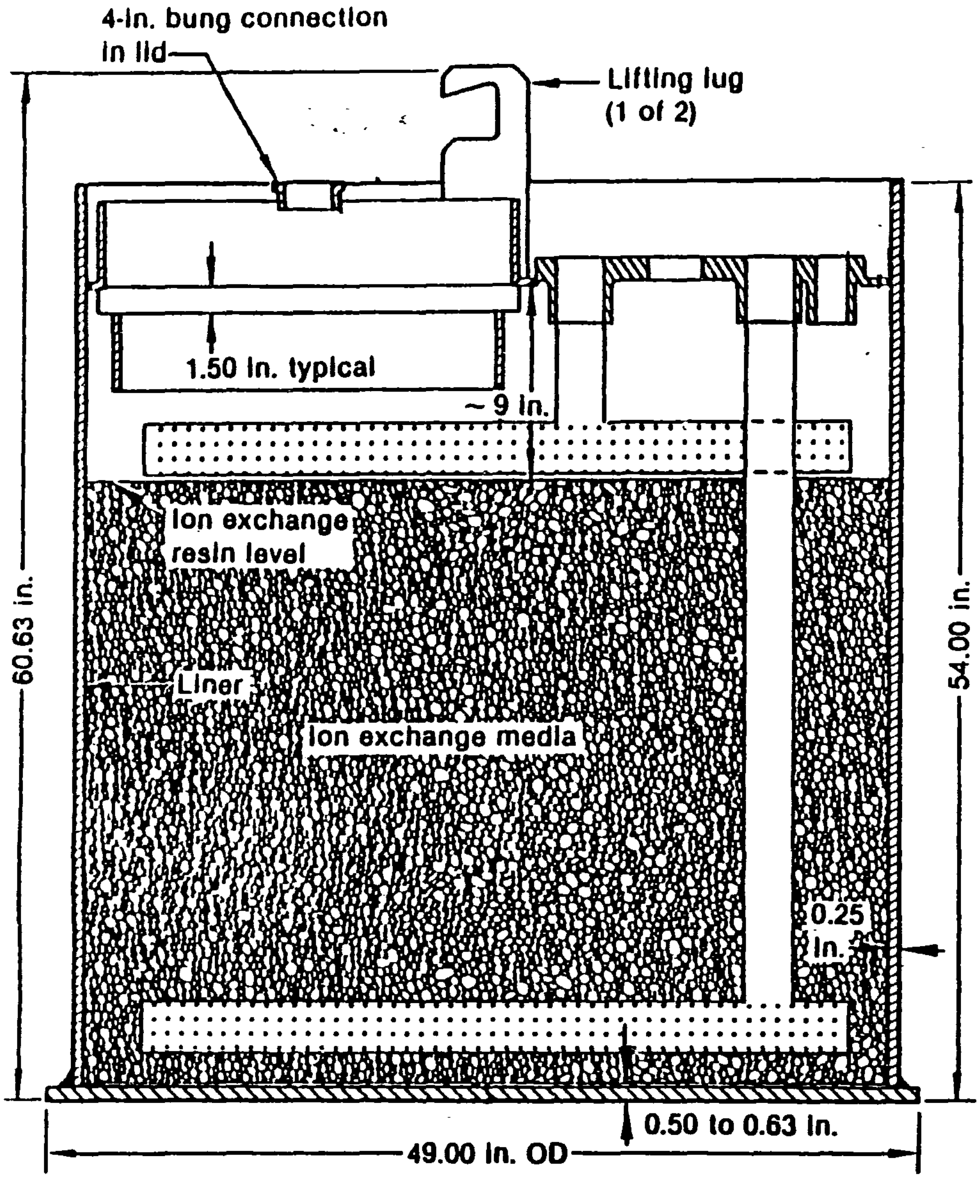

FIGURE 22. EPICOR II Liner.

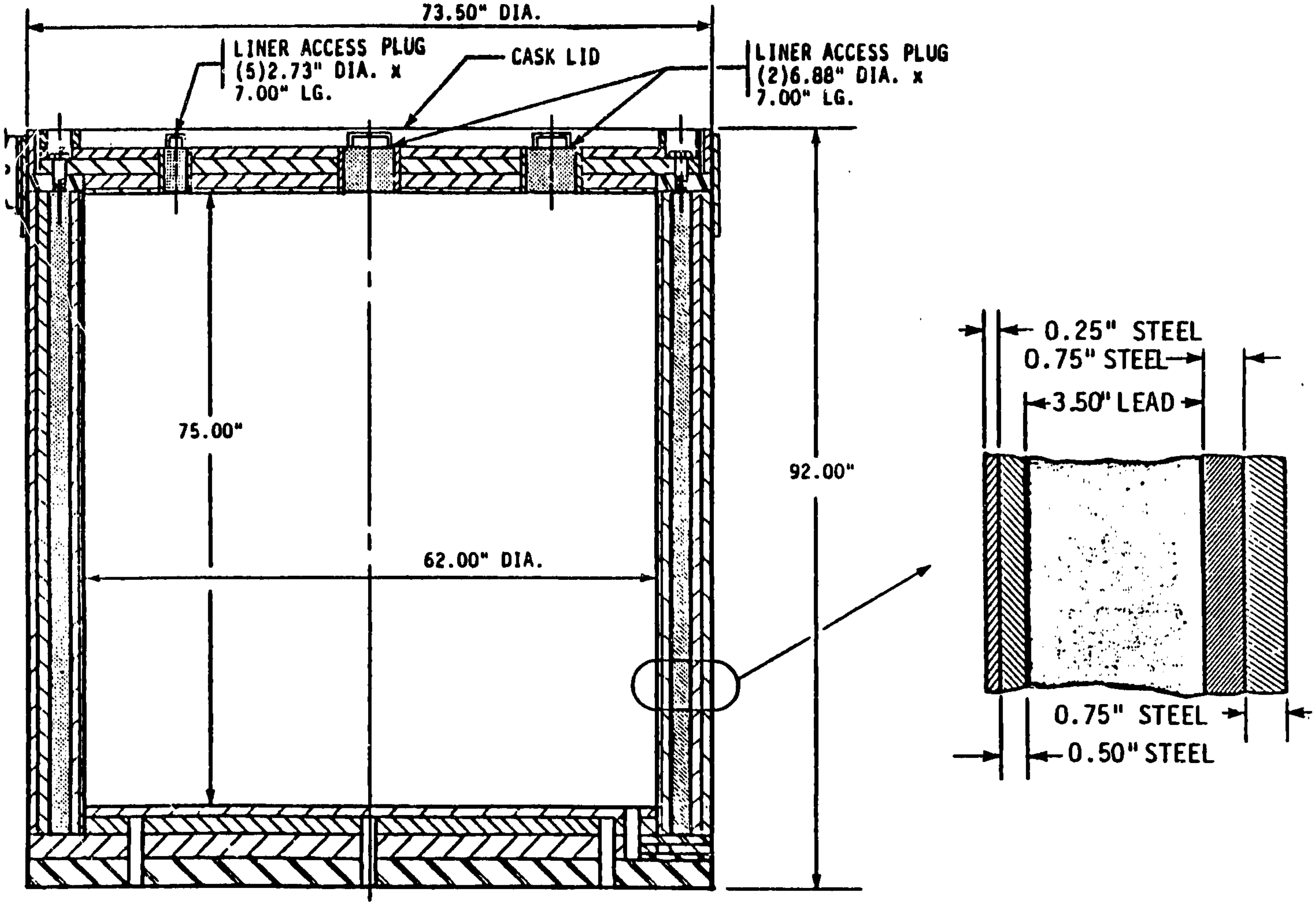

FIGURE 23. CNS 8-120 Cask.

SUBMERGED DEMINERALIZER SYSTEM RESIN LINER

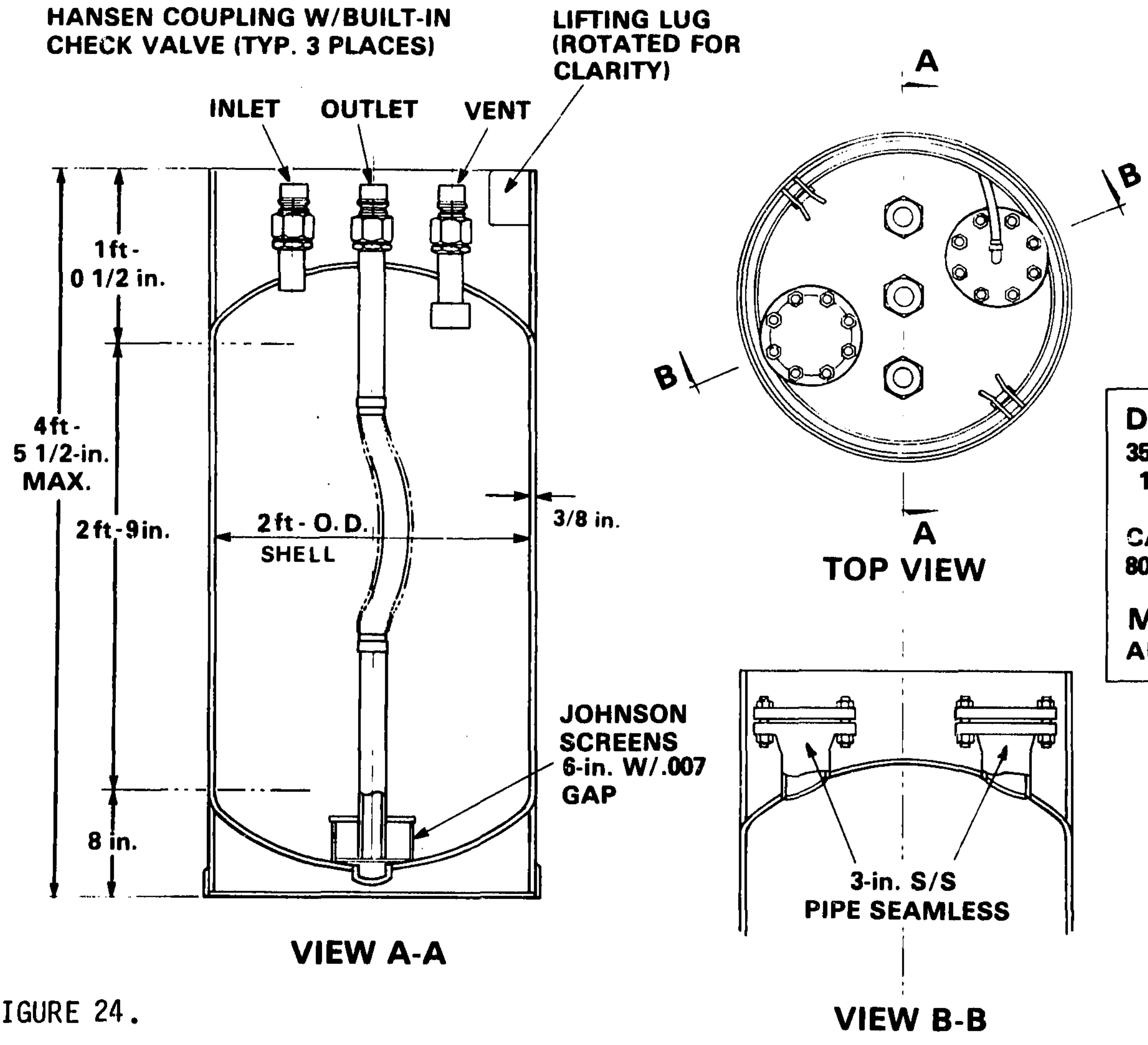

DESIGN PRESSURE
350 psig @ 400°F
15 psig @ 850°F

CAPACITY
80 U.S. GAL.

MATERIAL
AUST. STAINLESS STEEL

HEDL 8302-132.1

FIGURE 24.

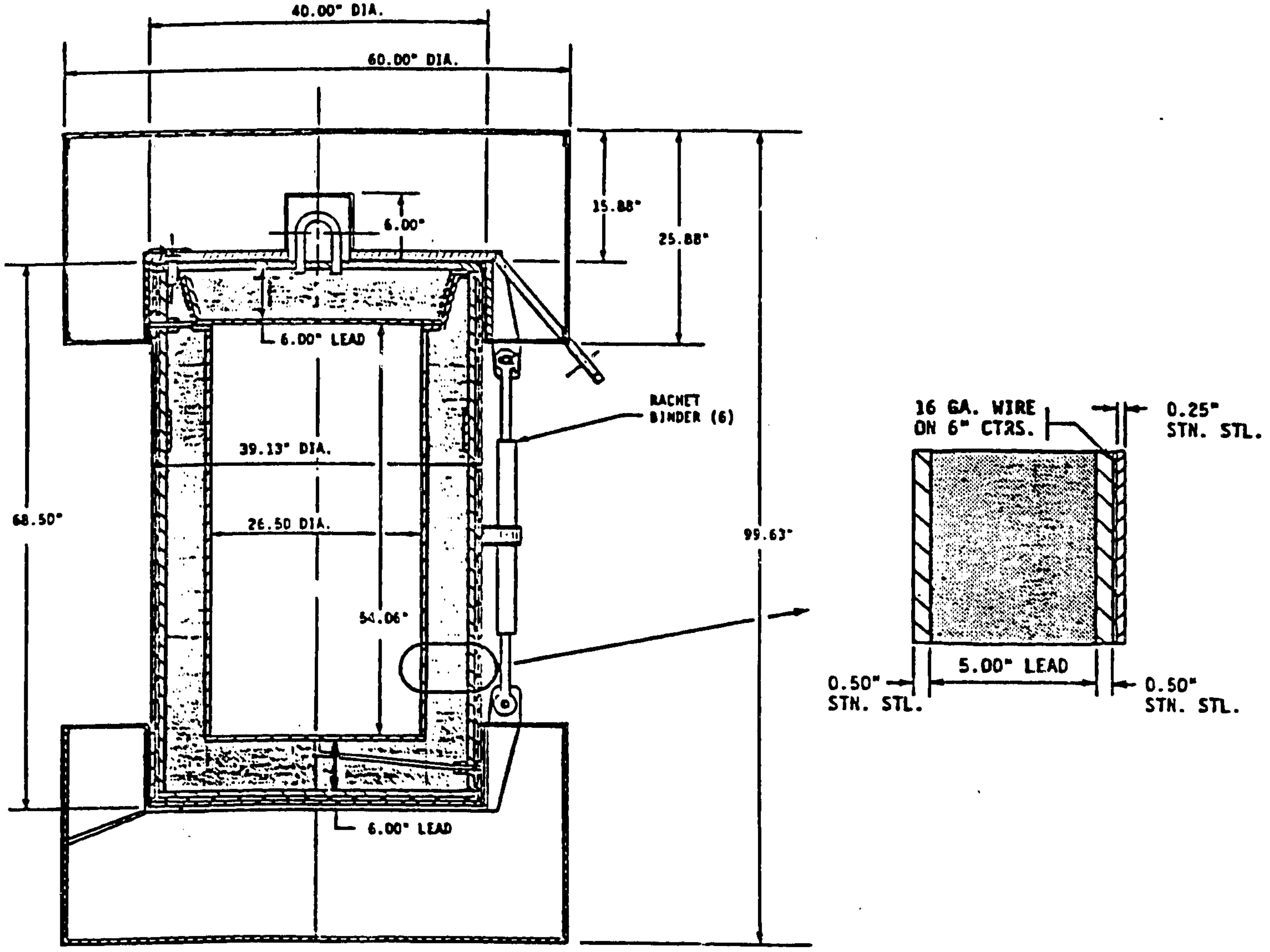

FIGURE 25. CNS1 13C Cask.

Table X

Liner Comparison

	SDS Liners	EPICOR Liners
Capacity	8 ft^3	32 ft^3
Material	stainless steel	carbon steel
Operating Pressure	350 psig	3 psig
Ci Capacity (^{137}Cs)	6.0×10^4	2.0×10^3
How Stored at TMI	in fuel pool	in concrete module

6.2 SHIPPING CASK DESCRIPTION

The shipping casks will serve several functions as part of the removal system. These functions are:

A. Personnel shielding of the resin capture container and charcoal filter during operation of the removal system.

B. Personnel shielding and lifting fixture for the resin capture containers and charcoal filters during transfer to the spent fuel pool for interim storage.

C. Personnel shielding of the resin capture containers and charcoal filters during shipment to the designated DOE laboratory.

These various functions dictate that at least two casks, and preferably three or four, be available for the duration of the demineralizer clean-up operations. Table XI describes the availability and shielding capabilities of all known casks for SDS and EPICOR liners.

Table XI

Shipping Cask Comparison

	SDS Liners		EPICOR Liners		
Cask Ident.	CNS1-13C	GE1600	CNS8-120	HN200	SN1
Number Avail.	1	6	2	1	1
Owned by	DOE	GE & Chem Nuclear	Chem Nuclear	Hittman	GPU
Shielding	4.5" Pb	6.2" Pb	4.5"Pb	4.3"Pb	4"Pb
Max rem/hr	*4500	*6000	*550	*500	
Weight, lb	24,000	24,000	58,000	44,000	60,000
TRU License	NO	In Concrete	NO	NO	NO

*based on ^{60}Co

The transuranic activity in the demineralizers dictates that their contents be packaged, stored and shipped as TRU waste. The following actions will be taken to obtain an amendment to the cask license for TRU waste or fissile content of any cask used:

A. An engineering analysis of the inner liner will be required, to prove that it can withstand the same conditions as the cask may be subject to. This has been done by DOE for the SDS liners and the CNS1-13C cask.

B. The amendment will cover dewatered resins, dewatered charcoal filters and other TRU or fissile material that may be shipped.

C. The amendment will be obtained for the CNS1-13C and GE 1600 cask.

D. An amendment can be obtained in 3 to 6 months.

If it is determined that the resin, or parts thereof, are not wanted for R&D programs, they can be transferred, diluted (making them non-TRU) and disposed of commercially. Hittman Nuclear and Chem Nuclear do this type of work routinely.

6.3 LINER/CASK SELECTION

During selection of the appropriate container and cask WHC considered the following criteria:

A. Handling and Loading - The monorail beam on the 305 ft operating level has a capacity of 25,000 pounds. The weight of a SDS liner with a CNS1-13C or GE1600 cask is within this crane's capacity.

B. Storage - The SDS and EPICOR liners are both currently stored onsite at TMI.

C. Demineralizer Contents Activity - The amount and type of activity which the casks will be required to shield is not known with complete certainty. For this reason, it is prudent to obtain the most shielding attainable.

D. Available quantity - As previously mentioned, at least two casks will be required. There are a sufficient quantity of GE1600 casks currently available.

Based upon these criteria, it is readily apparent that the preferred liner/cask combination is the SDS liner shielded by either the CNS1-13C or GE1600 cask.

6.4 WASTE DISPOSAL SUMMARY

The waste resulting from the clean-up of the demineralizers will consist of both abnormal and commercially disposable waste. The abnormal waste will consist of the following:

A. Six SDS type liners containing demineralizer contents. It is expected that at least two liners, but possibly all six will contain TRU waste.

Due to the nature of the removal process and the location of the uranium in the tank, the fuel is likely to be removed during the fast downflow step with the final portion of the resin. Therefore, the fuel could possibly be concentrated in the bottom of the transfer container and transferred into a single shipping container (for each demineralizer). However, there is no assurance that the fuel will not be mixed with the resin. Therefore, measurements will be made at TMI with the Compton recoil gamma-ray spectrometer to determine the amounts of fuel in the six shipping containers and the charcoal filter(s) before shipping. Sufficient gamma-ray activity will be present to allow counting in an approximately point source geometry as described by Reference 3.

B. One or two SDS type liners containing charcoal. These liners could possibly contain fuel fines and resin fines. The level of contamination may preclude commercial disposal.

The commercially disposable waste will consist of the following:

A. One EPICOR size (4 ft x 4 ft) carbon steel container.

B. Two 150 gal carbon steel tanks.

C. Approximately 405 ft of 2-1/2 inch stainless steel piping.

D. Approximately 205 ft of 1 inch stainless steel piping.

E. Four to six removal process pumps (including spares).

F. Miscellaneous control system components including valves.

The abnormal waste will be disposed of in accordance with DOE/NRC/GPU agreements. The commercially disposable waste will become the responsibility of GPU.

7.0 SAFETY CONSIDERATIONS

The operations required to remove the resin and debris from the makeup and purification demineralizer have been assessed on a preliminary basis to assure safety of plant equipment and personnel. An in depth assessment of the TRU content is reported in references 2 and 3 and is discussed in Section 3.0 of this document. The remaining items that require evaluation from a safety standpoint include exposure of personnel to radiation, hydrogen generation related concerns, exothermic reactions due to chemical addition and the specific design features of the resin removal equipment.

7.1 RADIATION AND SHIELDING

A preliminary radiation and shielding analysis has been completed (Appendix C) to provide an estimate of the radiation levels that will exist during the resin removal operations. Included in the analysis is an estimate of the shielding required to maintain general area radiation levels around the piping, resin transfer container and shipping containers to workable levels. Assumptions and highlights from this analysis are provided below.

7.1.1 Radiation Levels from 2-1/2 Inch Pipe

Assumptions:

A. 3500 curies of ^{137}Cs in the demineralizer prior to start of operations (average specific activity of 4.5 m Ci/cm^3)

B. Pipe length of 20 ft. (Radiation Source)

C. Volume of total system (piping, resin transfer container, and demineralizer) approximately 1000 gallons

D. The specific activity of contaminants in the piping is reduced by a factor of 5 due to adding approximately 800 gallons of water to the recirculating system.

Radiation Levels:

A. At a distance of 5 feet from the surface of unshielded pipe: 1700 m rem/hr.

B. At a distance of 5 feet from pipe shielded with 2 inches of lead: 9 m rem/hr.

7.1.2 Radiation Levels from 300 Gallon Resin Transfer Container

Assumptions:

A. Average specific activity of 4.5 m Ci/cm^3 (assumes elution of ^{137}Cs is not effective).

B. Container is one-half full of resin (150 gal) and is in a dewatered condition.

Radiation Levels:

A. At a distance of 5 feet from side of tank (no shielding): 23,000 m rem/hr.

B. At a distance of 5 feet from side of tank with 3 in. of lead shielding: 11.5 m rem/hr.

7.1.3 Radiation Levels from 80 Gallon Shipping Container

Assumptions:

A. 3500 curies of ^{137}Cs in the demineralizer prior to start of operations (average specific activity of 4.5 m Ci/cm^3)

B. Shipping container filled with resin having specific activity of 4.5 m Ci/cm^3

Radiation Levels:

A. At a distance of 5 feet from the side of the container (no shielding): 9900 m rem/hr.

B. At a distance of 5 feet from side of container with 5 in. of lead and 1.25 in. of steel shielding (equivalent to CNS1-13C shipping cask): 0.02 m rem/hr

7.1.4 Radiation and Shielding Assessment

The examples above indicate that personnel radiation exposure will not be excessive if reasonable amounts of shielding materials are used. Piping runs that are routed through areas that are accessible to personnel will be covered with lead bricks (assuming pipe runs are on floor) similar to the shielding methods employed for other temporary systems at TMI-2, e.g., SDS. Shielding will be designed for the overhead pipe runs that tie into the resin fill lines in the Hayes gas analyzer room to permit personnel access to this area during resin transfer operations.

7.2 HYDROGEN GENERATION

Although some hydrogen will continue to be generated during the resin removal process, this will not result in an unsafe condition since the process provides for venting of all gasses through the surge tank to the Waste Gas System. Note that an inert cover gas is maintained on the surge tank at all times. Prior to initiating the resin removal process a nitrogen purge will have been established on both demineralizers as a part of the prior activities associated with obtaining gas and resin samples.

Hydrogen and oxygen generation in the resin shipping containers (modified SDS liners) will be addressed in the preliminary design to assure that flammable limits will not be exceeded during shipment and storage of these vessels. Dewatering, drying, degassing and catalytic recombination will be evaluated and tested to assure that hydrogen and oxygen concentrations due to radiolysis of the irradiated organic resin will be maintained at less than 4 percent and 5 percent, respectively. A thorough evaluation of the hydrogen and oxygen generation aspects will be completed in the process of obtaining the required amendments to the license for the shipping container (see Section 6.3). This evaluation will use the experience gained to date on SDS and EPICOR II shipments of high dose rate zeolite beds and organic resins.

7.3 EXOTHERMIC REACTIONS DUE TO CHEMICAL ADDITION

The only chemicals planned for addition to the system are dilute solutions of sodium borate. No exothermic reactions are anticipated and this will be verified at ORNL by adding these solutions to samples of resin that will be removed from the demineralizers prior to the start of resin removal operations.

7.4 RESIN REMOVAL PROCESS EQUIPMENT

Process piping will be designed in accordance with ANSI B31.1 and the resin transfer container will be designed and constructed in accordance with Section VIII of the ASME Boiler and Pressure Vessel Code. Maximum system pressure downstream of the recirculation pump and hydrocyclone will not exceed approximately 65 psig. The shipping container and charcoal filter container are existing container designs and are capable of withstanding pressures up to 350 psig. Instrumentation will be provided for complete monitoring of all pertinent system parameters. All electrical equipment will be designed and installed in accordance with applicable electrical codes.

8.0 DEMINERALIZER RESIN RESEARCH AND DEVELOPMENT PROGRAM

As a part of the March, 1982 Memorandum of Understanding between the U. S. Nuclear Regulatory Commission and the U. S. Department of Energy, it was agreed that "DOE will also take possession of and retain purification system resins either for a R&D program of generic value or for storage or disposal on a reimbursable basis." The loadings of the resins as shown in Table VI exceed the levels acceptable for commercial disposal. The light water reactor industry generates highly radioactive resin wastes and has an interest in the development of commercially feasible disposal methods which stabilize the wastes and reduce their stored volume. The following sections will describe programs for chemical digestion and vitrification of the resins which can be accomplished at Hanford should DOE decide to pursue an R&D program.

As part of the previously described fuel assessment program the demineralizers were instrumented with solid state track recorders. This technology can also be utilized to assess the size distribution of fuel particles. A research and development program is also described which would demonstrate this methodology.

8.1 CHEMICAL DIGESTION OF ION EXCHANGE RESINS

8.1.1 Purpose

The purpose of this research effort would be to demonstrate the economics and technical feasibility of volume reduction and stabilization of reactor ion exchange resins using chemical digestion technology. The process converts ion exchange resin to CO_2 and H_2O and a low volume, nonreactive residue. The program includes: 1) bench scale demonstration of digestion of contaminated TMI ion exchange resin in existing hot cells at Hanford, 2) laboratory tests of radionuclide distribution, and 3) an economic and safety assessment to establish the economics of commercial application of the process.

8.1.2 Need

Spent ion exchange resins generated by commercial nuclear power plants represent a significant volume of radioactive waste produced. While various methods of packaging the resins for disposal are being evaluated, little work is underway to treat resins whose contamination levels exceed those provided for in 10CFR61.55-56. Past experience with incineration of ion exchange resins has been only partially successful. While some work has successfully been done on use of chemical digestion systems to volume reduce the ion exchange resins, the work was for TRU contaminated resins and did not fully evaluate treatment of highly radioactive reactor resins. Pilot scale demonstration of this technology for stabilization and volume reduction is necessary to enable technology transfer directly to industry.

8.1.3 Scope

The work is based on previous work performed by WHC on acid digestion of combustible nuclear wastes, including ion exchange resins. Recent WHC studies have shown that ion exchange resin is readily destroyed by chemical digestion in sulfuric acid using hydrogen peroxide as an oxidant. The resin is converted to CO_2 and H_2O, and a small volume of nonreactive residue. This program will demonstrate the key elements necessary to apply this technology in the commercial nuclear power industry to treatment of spent reactor resins. The key elements include: 1) bench scale demonstration of chemical processing of radioactive ion exchange resin in existing hot cell facilities at Hanford; 2) analytical tests to determine radionuclide distribution in the proposed chemical system; and 3) economic and safety assessment of chemical processing of reactor resins.

While chemical digestion has been demonstrated for transuranic waste, certain key hardware and program elements remain to be demonstrated for beta-gamma contaminated resins. These include continuous resin feeding, process simplification from substitution of H_2O_2 for HNO_3, and remote operability/maintainability of equipment. Tests are also required to evaluate treatment of volatile off-gas components such as iodine.

Equipment will be assembled for bench scale testing in an existing hot cell during the first quarter. Bench scale tests to determine the distribution and control requirements for radionuclides in the off gas and solid residue will be conducted. Primary emphasis will be evaluating state of the art emission control techniques and their effectiveness with off gas from the chemical digestion systems. The by-products of this process are prepared for in-situ glassification and subsequently buried. Data from these activities will be analyzed and a formal report will be written.

Data from these tests will be used to complete a preliminary conceptual design and cost estimate for a waste resin treatment unit. The relative economics and safety of a resin treatment facility will be evaluated in comparison with alternative options including packaging, shipment, and burial. A formal report will be written on the results. Follow on radioactive demonstration scale tests of ion exchange resin digestion will be defined.

8.2 VITRIFICATION OF DEMINERALIZER RESINS

8.2.1 Introduction

Vitrification to a borosilicate glass product is the DOE reference process for immobilizing high-level liquid wastes. PNL has completed full-scale nonradioactive and radioactive vitrification of zeolites and bench-scale nonradioactive vitrification of organic resins. This work was done in support of the TMI-2 cleanup. SDS zeolites and EPICOR II organic resins were generated during decontamination of waste water after the accident. The suitability of the vitrification process and product for ultimate disposal of these special nuclear wastes has been successfully demonstrated. This technology would be appropriate for TMI-2's highly-contaminated makeup and purification demineralizer resins. There are high TRU levels in this material so it cannot be disposed of by shallow land burial. Prior to receiving the actual resin, a nonradioactive demonstration of the process and equipment would be completed. PNL would also complete a transportation risk analysis.

8.2.2 Process Considerations

8.2.2.1 Vitrification Process Definition

A process will be designed and demonstrated to immobilize the resin as a glass product by incinerating the resin with glass formers at 1050-1150^{o}C in a joule-heated ceramic melter. The process will be demonstrated from receipt of the shipping container through production of the vitrified resin. Based on an ash content of 10% by weight (10 lb ash, 100 lb resin) and a waste loading of 15% (15 lb ash, 100 lb glass), there will be two 12-in. dia canisters filled with 6 ft of glass product from processing all of the TMI resin. This figure is very conservative and could be considerably less based on the results of glass development tests once the actual composition of the resin is determined from sample analysis.

The resin will be fed to the melter through a "drop tube" submerged below the surface of the molten glass. This will ensure good contact during incineration and, therefore, good retention of the ash in the glass. The glass also serves as a "scrubber" for removing volatile species before they escape to the off-gas system.

8.2.2.2 324 Building Description and Limitations

The demonstrations will be performed by PNL in the 324 Building, which is located in the 300 Area about 5 miles north of Richland, Washington. This building is equipped with facilities for both nonradioactive and radioactive work and has been utilized for high-level waste vitrification studies for the past 15 years. A floor plan of this facility is shown in Figure 26.

All of the nonradioactive activities will be performed in the PNL Engineering Development Laboratory (EDL). This modular-sectioned laboratory provides space for engineering development of chemical processes, instrumentation and equipment ranging in size from lab to full scale. Various vitrification and effluent treatment equipment that has been developed by PNL as part of the DOE

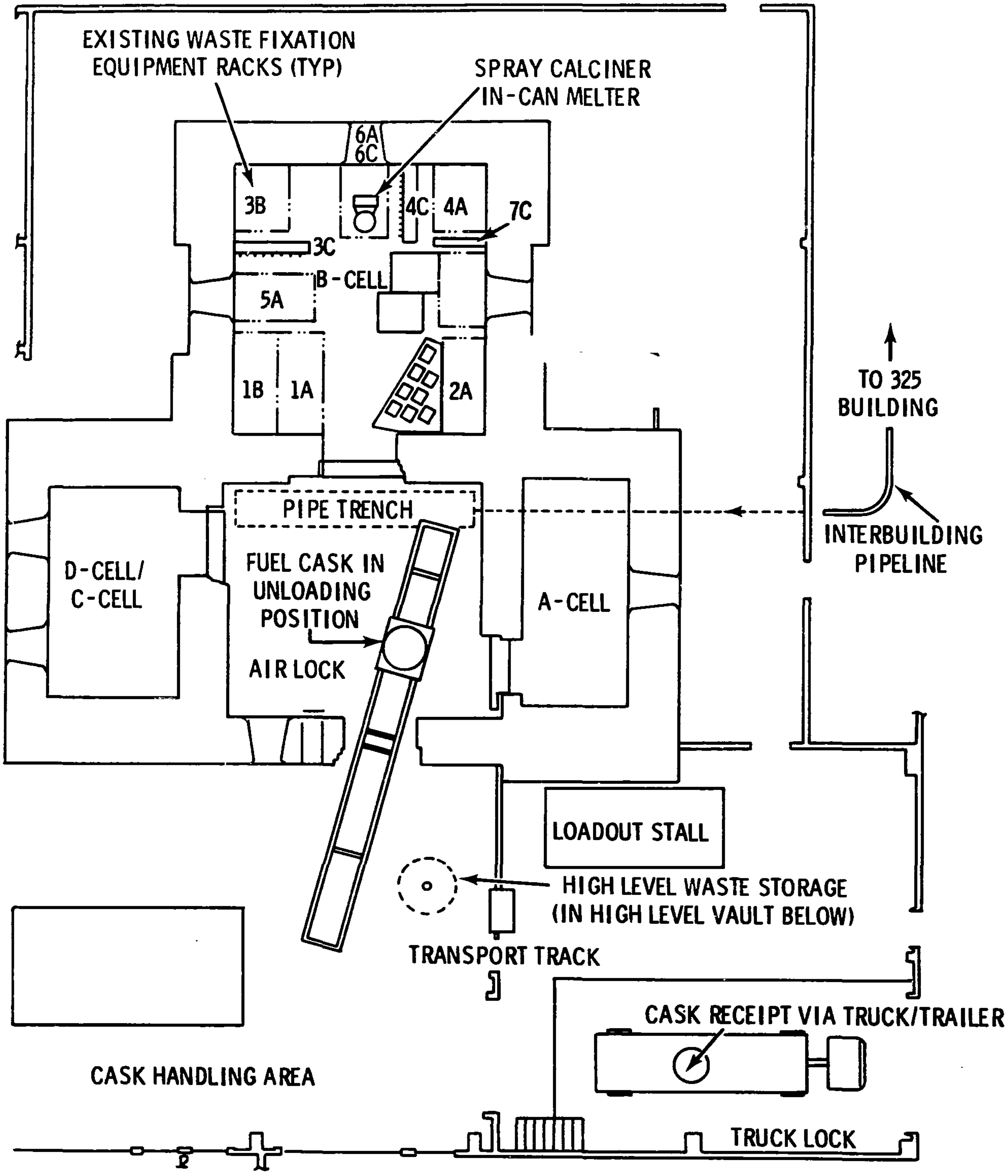

FIGURE 26. Plan View - 324 Building Radiochemical Engineering Cells.

National High-Level Waste Immobilization Program is presently installed in the laboratory. To the extent practical, this equipment will be utilized in this program.

The radioactive demonstration will be performed in the Radiochemical Engineering Cell Complex (Figure 26). Currently, a 30-40 L/h ceramic melter is being installed in B-Cell with feed and effluent treatment systems. This program will also use this equipment to the extent possible.

8.2.3 Process Development

8.2.3.1 Glass Development

A glass formulation will be defined for incorporating this particular resin ash into a borosilicate glass product. The objective of these tests is to maximize the waste (ash) loading and radionuclide retention while maintaining product quality comparable to commercial and defense high-level waste borosilicate glasses. Similar work with organic materials has already been completed at PNL and will be the basis for this task.

8.2.3.2 Melter Feed System

A system will be designed and developed for removing the resin from the shipping container, blending it with glass-forming chemicals and processing it to the melter. It is uncertain whether the resin can be processed as a solid or must be slurried and processed as a solution.

8.2.3.3 Nonradioactive Demonstration

A nonradioactive demonstration will be conducted in PNL's pilot-scale ceramic melter. It will be necessary to modify this melter to add a drop tube. The objectives of this demonstration are to demonstrate the melter feed system for organic resins and verify the process at production scale prior to completing it in the radiochemical cell. During these operations, optimum feed rates will be determined, effluent compositions analyzed and product quality verified. A report will be issued summarizing the results of this demonstration.

8.2.4 Transportation and Risk Analysis

To assure safe transportation and handling of the actual TMI resin, an assessment of risk to waste handling personnel and the public is required. PNL would perform a study to evaluate personnel risk as a result of changes in material characteristics and package conditions in transport, as well as the risk from radioactive releases resulting from transportation accidents. This evaluation will use available information on the transport and handling environment, shipping package integrity, and material characteristics or properties. On the basis of this information, procedures for handling the containers will be evaluated, and areas that are significant contributors to risk will be identified.

8.2.5 Radioactive Demonstration

The radioactive demonstration will be completed in B-Cell in the existing equipment. It may be necessary to add feed system components. It will be necessary to modify the melter to add the drop tube. No modifications to the effluent system are anticipated. During operations, effluent samples will be taken and product quality verified.

The B-Cell melter will have already completed an in-depth safety analysis and Operational Readiness Review prior to startup. It is assumed that most of that safety documentation will be applicable to this process. Only addendums to cover handling and processing of organic materials will be required.

8.3 PARTICLE SIZING USING SOLID STATE TRACK RECORDER AUTORADIOGRAPHY

During the accident at TMI-2 on March 28, 1979, fuel was dispersed to various locations throughout the primary reactor cooling system, including makeup and purification demineralizers A and B. As a part of the demineralizer recovery program, the ion exchange resin material from the demineralizers will be available for inspection. Information on particle size distributions of the fuel in these resins will be useful in order to gain knowledge on the nature of the mechanism of transport of the fuel to demineralizers A and B.

Described herein is a method for sizing of these fuel particles using solid state track recorder (SSTR) autoradiography. Also, related measurements to determine total uranium, total plutonium, and total ^{235}U are described.

8.3.1 Methods

The use of SSTRs in autoradiographic applications has been described previously (see, for example, References 4-7). SSTRs record the passage of ionizing particles such as alpha particles or fission fragments as latent tracks which can be developed by chemical etching to a size visible with a microscope. An example of an alpha particle autoradiograph is shown in Figure 27, which is taken from Reference 4. In this case, an air sampler filter was placed in firm contact with a cellulose nitrate SSTR. The star pattern of tracks was formed by alpha particles which originated from a particle of plutonium which was entrapped in the filter. The total number of tracks present is proportional to the decay rate of the plutonium, the time of exposure to the SSTR, and the total number of plutonium atoms present. Since the detection efficiency of the SSTR may be determined, the amount of plutonium present may be calculated and related to particle size. Figure 28 shows a fission fragment radiograph of the same particle after exposure to neutrons in close contact with a mica SSTR. Here, the number of tracks is directly proportional to the number of fissionable atoms present, the cross section for neutron induced fission, and the total fluence of neutrons. Again, the number of atoms present can be determined from the number of tracks. In Reference 4 the ratio of

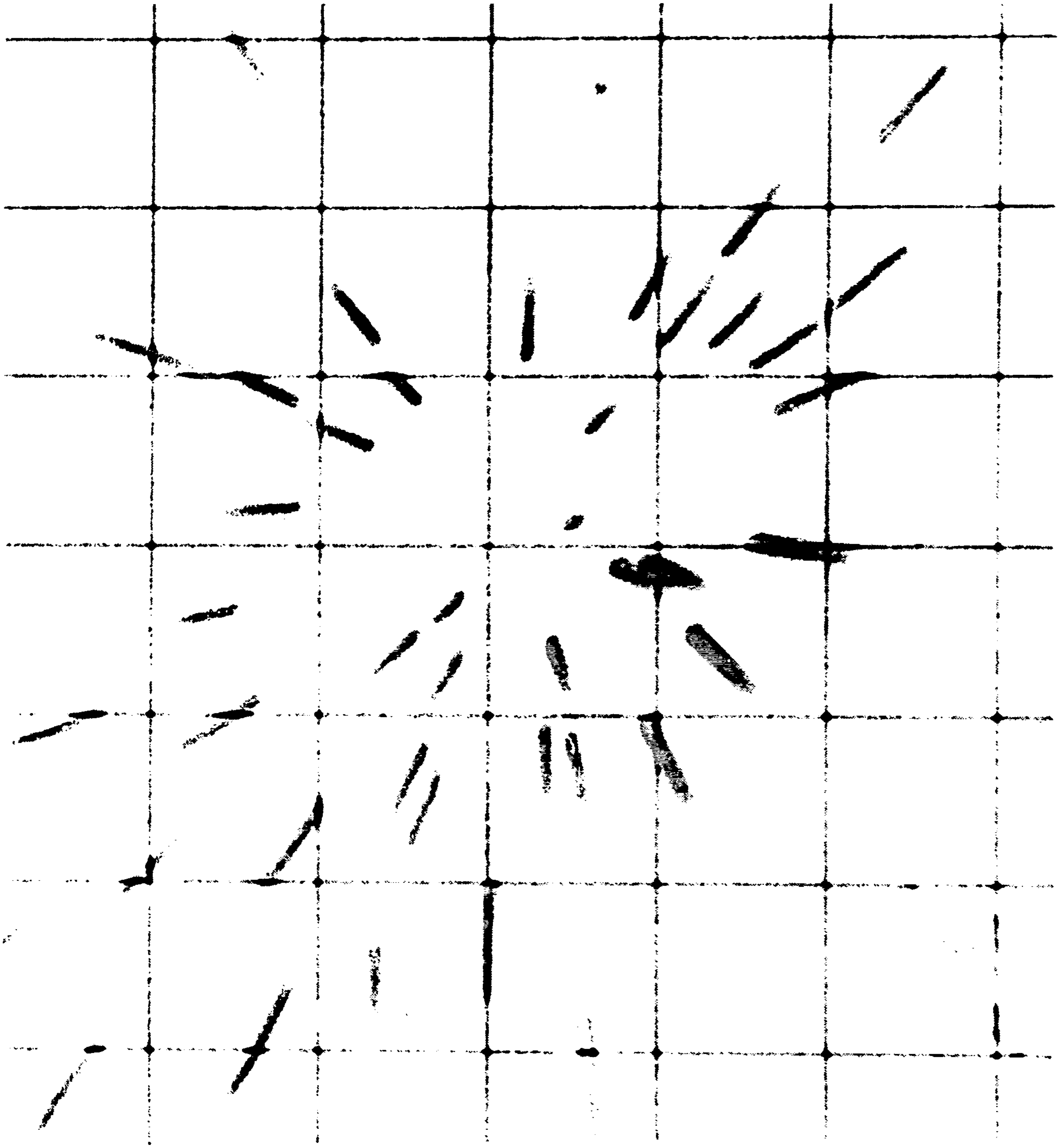

Figure 27 Alpha Autoradiograph of a Particle Containing Plutonium. Magnification of the Cellulose Nitrate SSTR is 400X, and the Grid Size is 12.9 Micrometers.

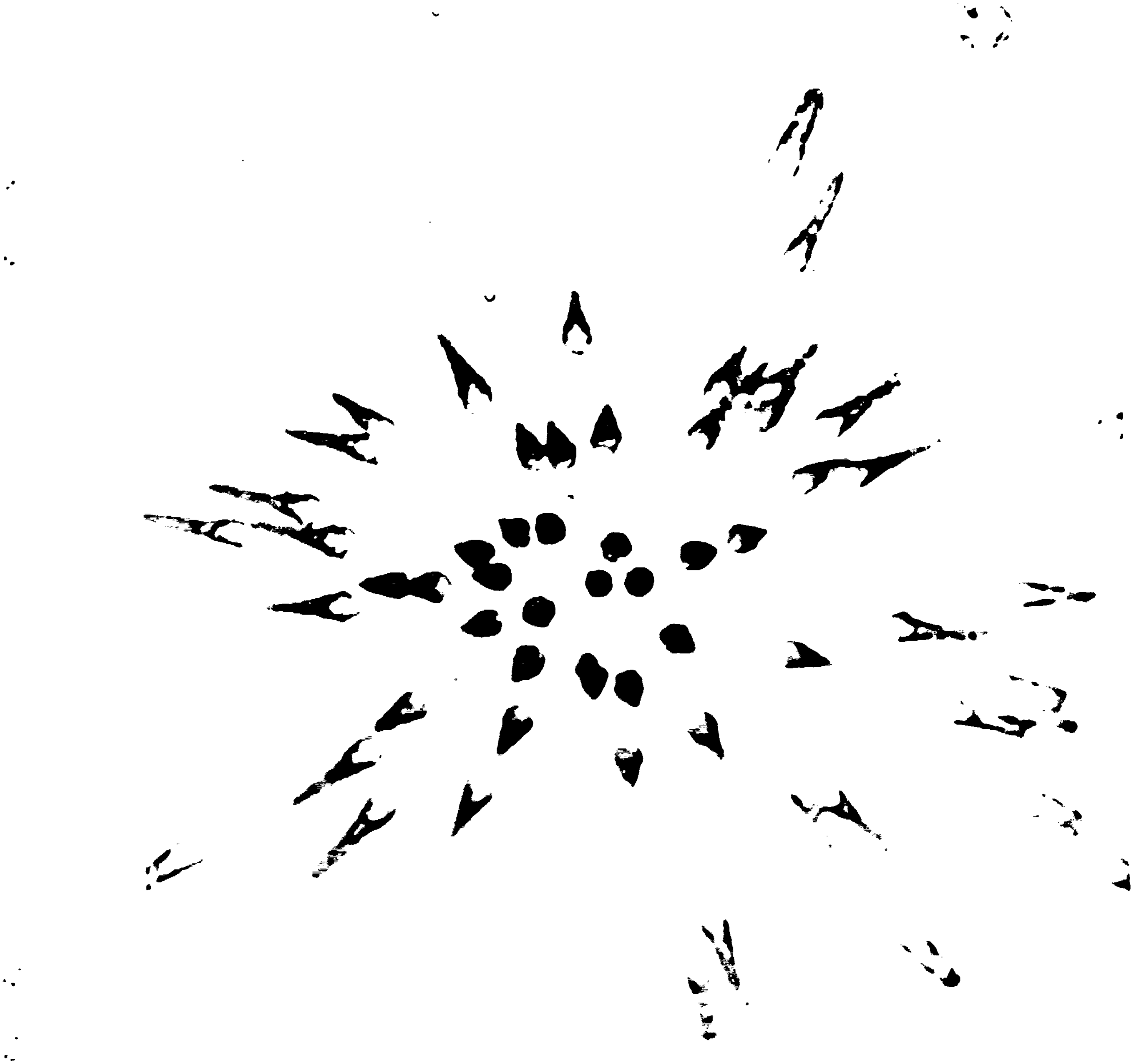

Figure 28. Radiograph of Neutron-Induced Fission Fragments from a Particle Containing Plutonium. Magnification of the Mica SSTR is 400X, and the Grid Size is 12.9 Micrometers.

fission tracks to alpha particle tracks was shown to be proportional to the ratio of fission cross section to decay rate. This latter ratio can be used to identify which isotope or mixture of isotopes is present in the particle.

Recently the method has been extended to solid metallic samples. Sectioned weld samples which contained plutonium were alpha autoradiographed using CR-39 SSTRs to determine the amounts of plutonium present. Figure 29 shows the results of four weld autoradiographs. Not only can the total amount of plutonium present be determined from the total number of tracks, but the physical form and distribution of the plutonium can be seen to be different. In welds one and two, a narrow region of particulate plutonium is present whereas non-particulate plutonium appears to be distributed throughout the weld in cases three and four. These four weld autoradiographs are shown at higher magnification in Figure 30, where individual alpha particle tracks in the CR-39 SSTR are more apparent. In Figure 31, high magnification photomicrographs of individual track clusters resulting from plutonium particles are shown for the weld one case. Here, individual particle sizes can be determined from the number of tracks in the cluster.

8.3.2 Applications to TMI-2 Demineralizer Resin R&D

TMI-2 demineralizer A has been shown in References 2 and 3 to contain a total of 1.1 to 1.6 kg of fuel. This fuel is most likely present in the form of undissolved oxide particles and has been shown to be concentrated in the tank at the 309' elevation. The amount of fuel present in demineralizer B is less than the amount in demineralizer A. Although data could be obtained directly on particle sizes of the fuel in the resin by filtration methods, adherence of fuel particles to larger resin particles could cause misleading results. Alpha particle autoradiographs can be used to obtain information on particle sizes directly, resulting in data that is more directly related to the physical form of the fuel as it passed through the primary cooling system from the core to the demineralizers. In order to obtain quantitative data on the amount of fuel present, the alpha specific activity must be determined. The National Reactor Dosimetry Center (NRDC) which is operated by the Irradiation Environment Group

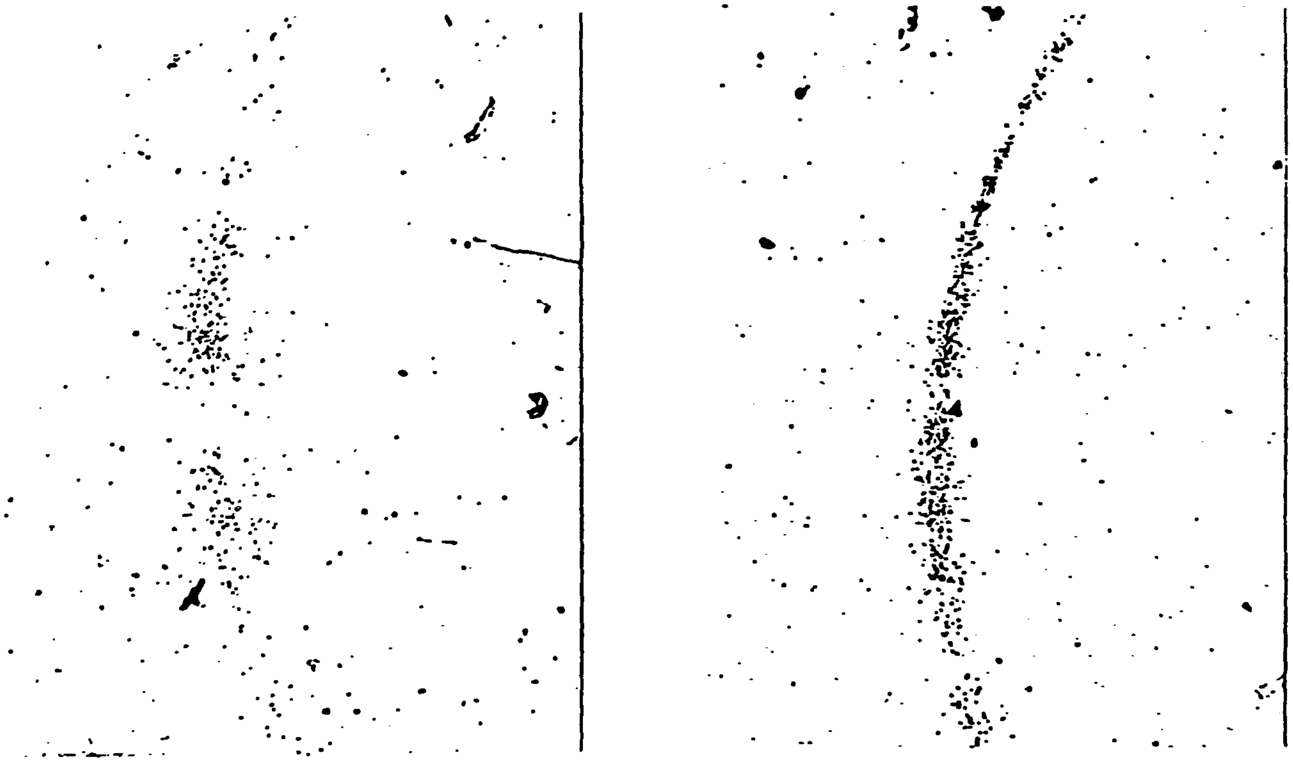

Weld #1

Weld #2

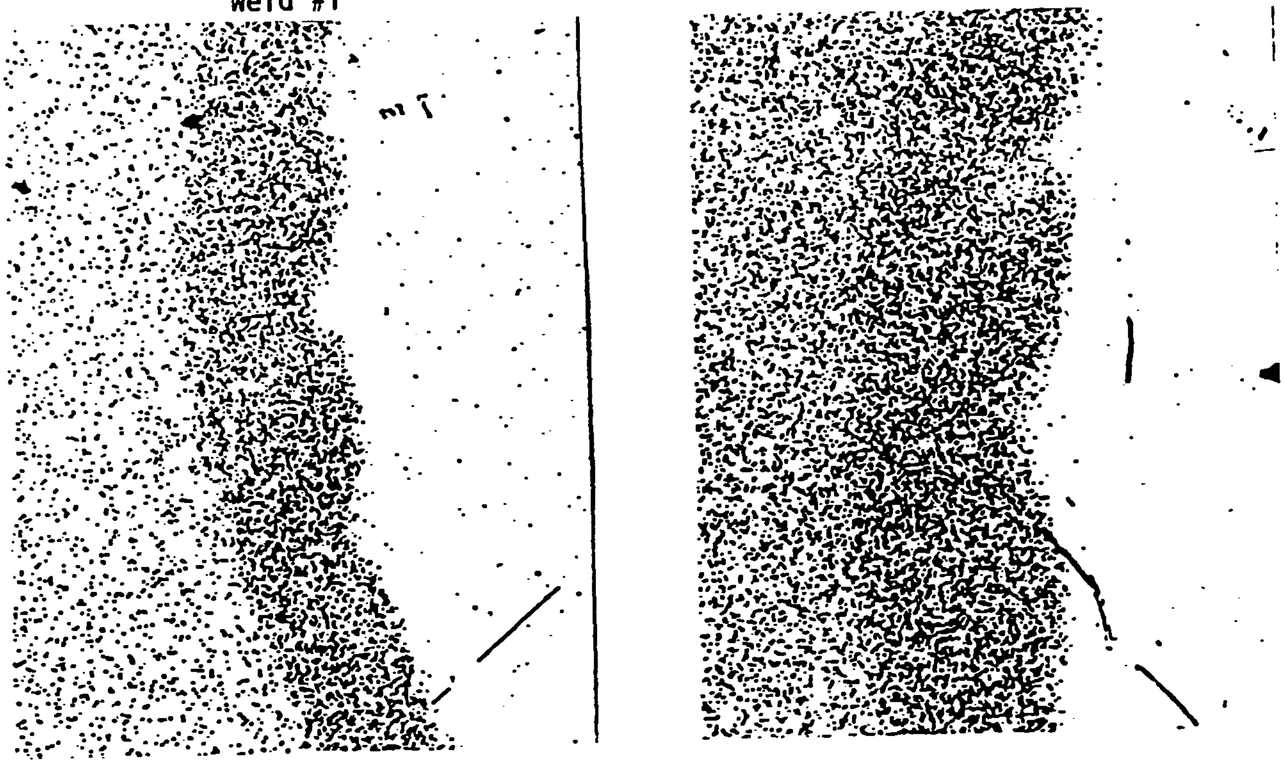

Weld #3

Weld #4

Figure 29. Autoradiographic Comparison of Four Different Welds. Magnification is 52X.

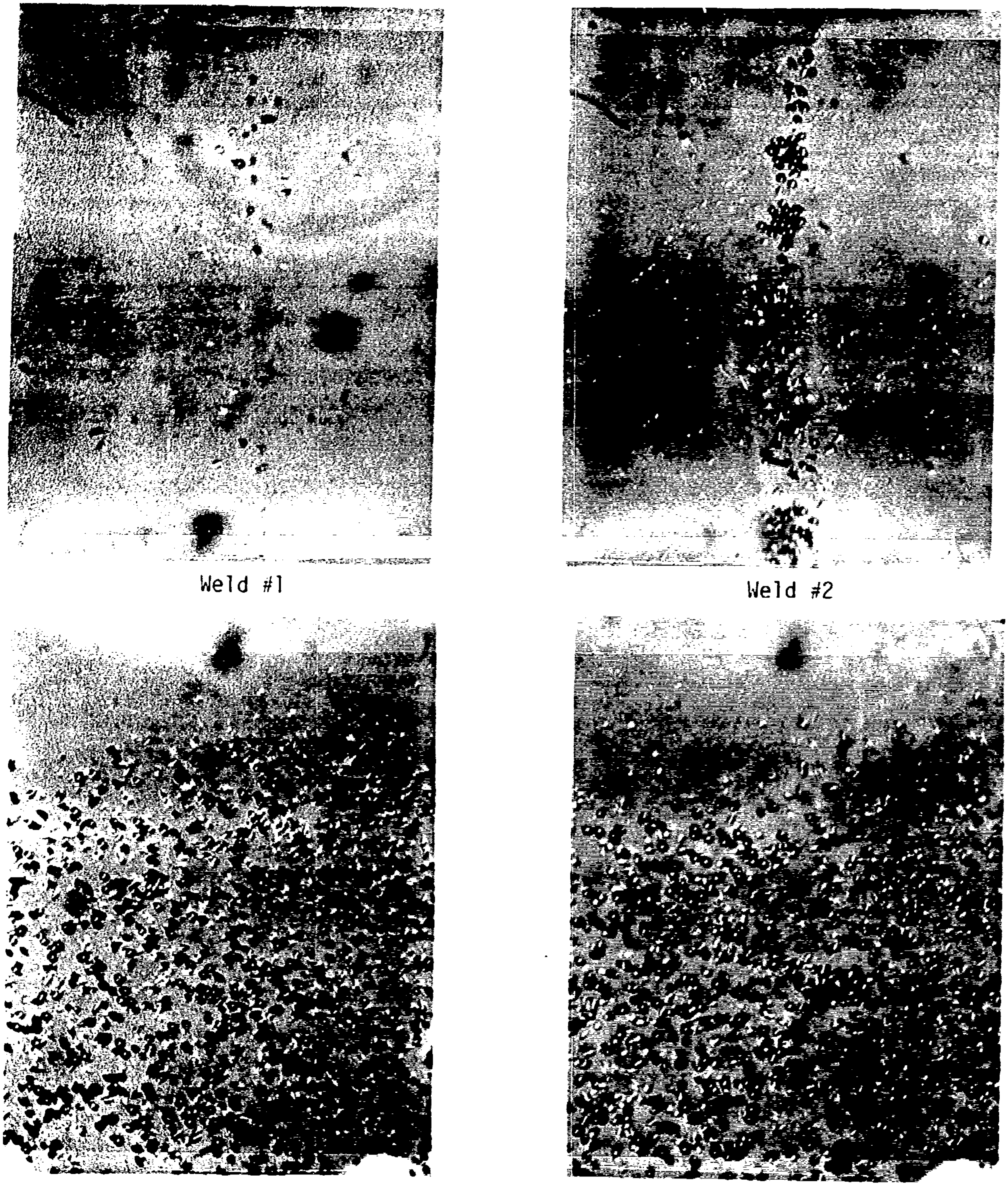

Weld #1

Weld #2

Weld #3

Weld #4

Figure 30. Autoradiographic Comparison of Four Different Welds. Magnification is 200X.

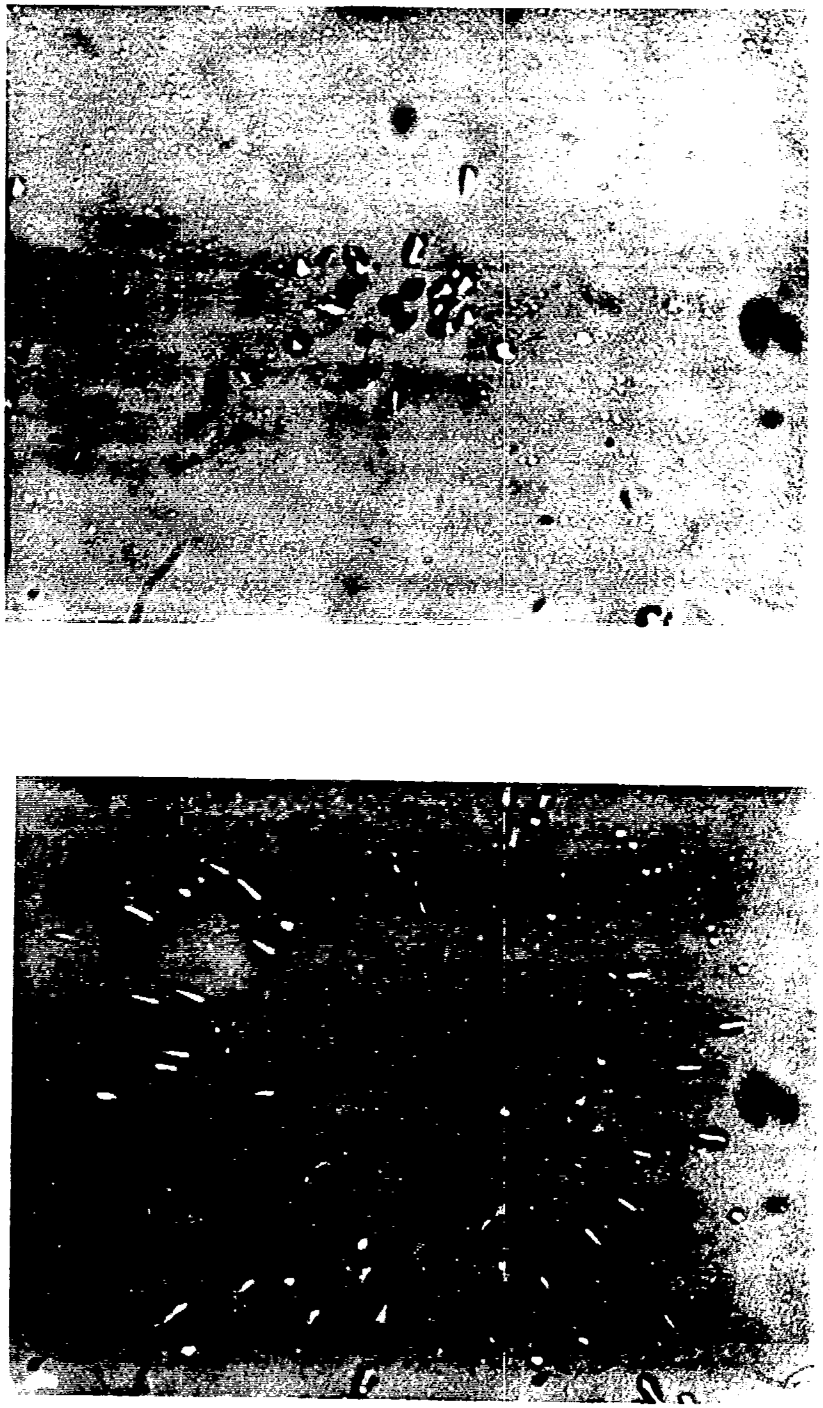

Figure 31. High Magnification Photomicrographs of an Alpha Autoradiograph of Weld #1. Typical Track Clusters Resulting from Particulate Alpha Sources Can be Seen. The Magnification is 400X.

(IEG) at WHC and the associated FTR Dosimetry Measurement Laboratories have alpha spectrometry equipment available for this purpose. Low and high geometry alpha counting chambers coupled with high resolution alpha spectrometers can be used to determine the alpha activities present in the fuel.

References 8 and 9 indicate a specific activity for TMI-2 fuel of about 7.7 x 10^9 α/sec/kg, but due to the nonuniform power density of the core, the alpha specific activity will vary with core location and should be calibrated directly using representative samples of fuel from the demineralizers. Table XII contains the individual contributions to the alpha decay rate from the various alpha emitting isotopes present (^{241}Am which is formed by decay of ^{241}Pu has been omitted from this table, but will contribute to the total alpha decay rate). Direct alpha spectrometry of TMI-2 fuel such as that contained in the demineralizers would yield an alpha spectrum consisting mainly of peaks from the plutonium isotopes with the main contribution being from ^{239}Pu. Approximately 1% of the total alpha activity is due to isotopes of uranium. Although the alpha particle energies for the uranium isotopes are generally lower than those of the plutonium isotopes, the less intense uranium peaks will be separable from the low energy continuum of the higher energy and more abundant plutonium alpha particles. The major contributors to the uranium alpha activity are ^{238}U and ^{234}U. Both of these isotopes should be good indicators of total uranium present since they are less affected by burnup than ^{235}U.

Of more interest from a criticality safety and materials accountability point of view is the ^{235}U content of the fuel which will depend on burn-up and will vary with local power density. The ^{235}U content can be determined directly by thermal neutron induced fission fragment radiography.

In summary, SSTR autoradiographic methods can be applied to measurements on TMI-2 demineralizer resins as follows:

TABLE XII

TMI-2 FUEL SPECIFIC ALPHA ACTIVITY

(Data Adapted from Reference 9)

Isotope	Atom%	(sec^{-1})	Specific Activity (dps/g)*	Fractional Activity
^{233}U	0.00472	1.380×10^{-13}	1.669×10^{4}	2.176×10^{-3}
^{234}U	0.02353	8.980×10^{-14}	5.415×10^{4}	7.063×10^{-3}
^{235}U	2.32090	3.121×10^{-17}	1.856×10^{3}	2.421×10^{-4}
^{236}U	0.07778	9.381×10^{-16}	1.870×10^{3}	2.439×10^{-4}
^{238}U	97.57308	4.916×10^{-18}	1.229×10^{4}	1.603×10^{-3}
^{233}Pu	0.06151	2.503×10^{-10}	9.425×10^{5}	1.229×10^{-1}
^{239}Pu	90.76092	9.110×10^{-13}	5.062×10^{6}	6.602×10^{-1}
^{240}Pu	7.64249	3.110×10^{-13}	1.572×10^{6}	2.050×10^{-1}
^{241}Pu	1.47076	$(1.530 \times 10^{-9})(2.45 \times 10^{-5})$	3.375×10^{3}	4.402×10^{-4}
^{242}Pu	0.06433	5.837×10^{-14}	2.299×10^{2}	2.999×10^{-5}

*Assuming (atom % U)/(atom % Pu) = 418.6

1. Alpha particle autoradiography to yield particle size distribution data using the plutonium alpha activity of the fuel.

2. Thermal neutron induced fission radiography to yield particle size distribution data based on the ^{235}U content of the fuel.

These measurements can be coupled with alpha spectrometric data on the same samples to determine uranium content. Thus, information is obtained on the total ^{235}U content, the total plutonium content, and the total uranium content as well as information on particle size distributions.

In addition, ratios of track counts obtained in (1) and (2) above can be used to detect any possible variations in the $^{239}Pu/^{235}U$ ratio on a particle-by-particle basis since the same particle can be located in both radiographs. In the TMI-2 case, the relative startup core power density variation is estimated to be about 0.8-1.2, both axially and radially (Reference 10). With SSTR radiography, 10% measurements are possible on a particle-by-particle basis. Since the TMI-2 core was only operated for 100 full power days, ^{235}U burn-up is not significant and the $^{239}Pu/^{235}U$ ratios should be a direct measurement of ^{239}Pu burn-in which will be related to the relative core power density distribution. Since TMI-2 was in the first cycle of operation, theoretical calculations of ^{239}Pu burn-in should be relatively reliable, leading to the possibility of correlating the measured $^{239}Pu/^{235}U$ ratio with the core location of individual particles. Consequently, any correlation of the $^{239}Pu/^{235}U$ ratio with particle size should shed some light on the mechanisms of core degradation and transport through the cooling system at the time of the accident.

8.3.3 Experimental Plan

Following removal of the resin from TMI-2 demineralizers A and B, approximately 44 ft^3 of resin will be placed in six separate containers. Due to the nature of the removal process and the location of the uranium in the tank, the fuel is likely to be removed during the downflow flush with the final portion of resin. Therefore, the fuel could possibly be concentrated in two of the six containers.

Initially, measurements will be made at TMI with the Compton recoil gamma-ray spectrometer to determine the amounts of fuel in the six resin containers and the charcoal filter before shipping. Sufficient gamma-ray activity will be present to allow counting in an approximately point source geometry as in Reference 3.

Following these measurements and shipment of the resin to WHC, representative samples of the resin will be obtained from the containers. It is assumed that a representative sample can be obtained from each of the six containers with forty samplings. These representative samples will be homogenized and aliquoted to produce thin layer samples of the resin and fuel. These samples will be dried and fixed to a backing for subsequent radiographic and alpha spectrometric measurements.

Initially, alpha spectrometry will be performed to determine the total uranium and plutonium content of the samples. The total uranium content will then be compared with the results of the Compton recoil gamma ray spectrometry to check for consistency.

The same samples will be subjected to alpha autoradiography by placing them in firm contact with CR-39 SSTRs. Several autoradiographs with different exposure times will be made to obtain more optimal statistics for the entire size range of the particle size distribution. These CR-39 radiographs will be etched in 6.2N NaOH at 25°C to develop the tracks and mounted for microscopic scanning. Initially, the SSTR autoradiographs will be scanned on the Hanford Automated Optical Track Scanner to determine the coordinates of the clusters on individual SSTRs. These clusters will subsequently be located and manually scanned to determine the track count for each individual cluster. Calibration radiographs of standard ^{240}Pu and ^{239}Pu actinide deposits will be used to calibrate the optical efficiency of the CR-39 SSTRs to allow quantitative calculations of the amount of plutonium present in each particle. The total number of clusters counted will be determined by the accuracy requirements for definition of the particle size frequency distribution.

The same resin samples will be remounted in firm contact with mica SSTR and subjected to a thermal neutron irradiation using a suitable neutron source. Following the irradiation, the mica SSTR radiographs will be etched with 49% HF at 20°C for 30 minutes to reveal the fission fragment tracks. The scanning procedure for the mica SSTRs will be similar to that outlined for the CR-39 SSTRs. A ^{235}U standard deposit in firm contact with a mica SSTR will be included in the irradiation to allow a quantitative calculation of the ^{235}U present in the resin samples. Fudicial markers on both the CR-39 and mica SSTRs will allow identification of track clusters resulting from an individual particle to be correlated in separate radiographs.

Particle size information will be tabulated for both the ^{239}Pu and ^{235}U radiographs and $^{239}Pu/^{235}U$ ratios will be determined on a particle-by-particle basis and attempts will be made to identify correlations between $^{239}Pu/^{235}U$ ratios and particle sizes.

A report will be issued on the results containing information on total uranium, total plutonium, total ^{235}U, particle size distributions, and $^{239}Pu/^{235}U$ ratios as a function of particle size. In addition to the information needed for the demineralizers recovery program, these can be used to deduce information on poossible mechanisms of core breakup and transport to the demineralizers and elsewhere.

9.0 REFERENCES

1. K. K. S. Pellay and G. L. Palau, "Radiolytic Effects on Ion Exchangers During the Storage of Radioactive Wastes," International Conference on Radioactive Waste Management, Winnipeg, Manitoba, September 1982, LA-UR-82-2281.

2. F. H. Ruddy, J. H. Roberts, R. Gold, C. C. Preston and J. A. Ulseth, "Solid State Track Recorder Neutron Dosimetry Measurements for Fuel Debris Assessment of TMI-2 Demineralizer-A", HEDL-SA-2834, December 1982.

3. J. P. McNeece, B. J. Kaiser, R. Gold, and W. W. Jenkins, "Fuel Content of the Three Mile Island Unit 2 Makeup Demineralizer," HEDL-TC-2301, December 1982.

4. B. Center and F. H. Ruddy, "Detection and Characterization of Aerosols Containing Transuranic Elements with the Nuclear Track Technique," Analytical Chemistry 48, 2135 (1976).

5. B. Center, "Detection and Characterization of Airborne Environmental Transuranic Particulate Matter Using the Nuclear Track Technique," Thesis, Washington State University (1975).

6. J. H. Roberts, V. P. Kafalenos, and T. J. Yule, "Characterization of Aerosols Containing Fissionable Elements Using Solid-State Track Recorders," in Solid State Nuclear Track Detectors: Proceedings of the 9th International Conference, F. Granzer, Et al. (ed.), Pergamon, Oxford (1978), p. 669.

7. R. L. Fleischer, P. B. Price, and R. M. Walker, Nuclear Tracks in Solids: Principles and Applications, University of California Press, Berkeley, CA (1975).

8. Letter, J. J. McCown to H. M. Burton, "TMI-2 Containment Building Sump Sludge," September 10, 1982.

9. Letter, J. J. McCown to H. M. Burton, "Analysis of TMI-2 Reactor Coolant Bleed Tank 'A' Sludge Sample," December 9, 1982.

10. C. Whitmarsh (Babcock & Wilcox), private communication of unpublished calculations, February 3, 1983.

APPENDIX A

TMI-2 DEMINERALIZER RESIN SCOPING TESTS

Pacific Northwest Laboratory

L. A. Bray

E. C. Martin

Battelle
Pacific Northwest Laboratories

Project Number

Internal Distribution

D. E. Knowlton
H. H. Van Tuyl
LAB/LB-File

Date October 20, 1982
To M. K. Mahaffey, 337 Bldg./1N, HEDL
From L. A. Bray
Subject TMI-2 Demineralizer Resin Removal - Activity 2

Scoping experiments were performed on identical resins to determine probable forms after exposure to estimated dose levels and temperature. The results of this work performed in FY-82 are attached.

Major conclusions are:

- At dose levels of 2×10^9R both dry and wet IRN-150 Li-form resin will remain in a particulate form.
- Sluicing tests indicate that exposed resins will sluice more readily than as received resin.
- The gas analyses taken during ^{60}Co irradiation show that large amounts of H_2 (20-90 mole%) are formed without an equivalent amount of oxygen. The products of irradiation are probably H_2 and H_2O_2. No oxygen is released in an organic medium probably because the H_2O_2 depletes itself in an oxidative process.
- Resin irradiated to 1.7×10^9R in H_2O show a weight and volume loss of ~ 50%.
- Resin heated to 260°C lost 63w% but retained its original structure. At 538°C the resin structure was completely destroyed using a N_2 atmosphere, was a solid mass, and was changed into coke.

LAB:df

Attachments

DESCRIPTION OF ACTIVITY 2

Objectives

Sluicing Without Treatment - Evaluate existing resin condition based on Hanford experience. Perform low-cost scoping tests of the resin and make an assessment as to sluicability to guide further concept studies. Identify probable forms and desired processing prior to packaging for shipment.

Time Period

August-September, 1982

Description

Sluicing Without Treatment

- literature study of resin and condition
- resin testing
- recommendations for sluicing

Procedure

Obtain sample of IRN-150 (H-form) from Rohm and Haas. Determine resin condition and pretreatment. Build pressure cans to be used in the ^{60}Co facility and schedule tests. Obtain analytical data.

- gas samples
- gas volume (determine pressure buildup)
- determine physical changes in resin.

Prepare letter report and assess need for follow-on program.

Conditions for Tests

	A	B*
Temperature, °C	65	102-107
Irradiation Rate	8×10^6 R/h	8×10^6 R/h
Gas Samples Taken	2	2
Gas Volume Check	Daily	Daily
Resin Volume, cm^3	410	124
H_2O Volume, cm^3	145	~ 0

---

* Resin pretreated by heating (183°C) in N_2 for approximately 22 hours.

ATTACHMENTS

Page

Figures

Tables

Letter

FIGURE 1 ^{60}Co Test Equipment

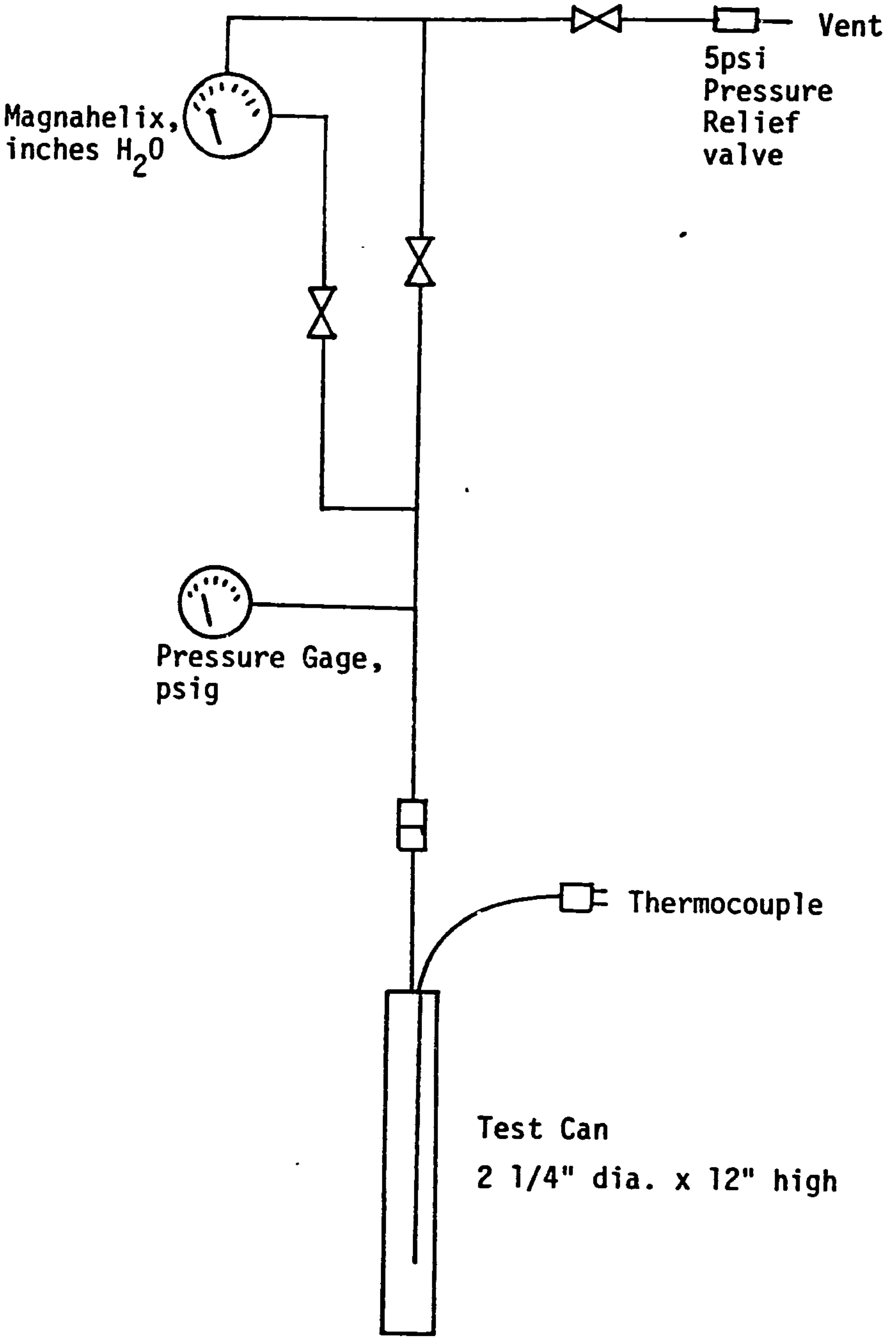

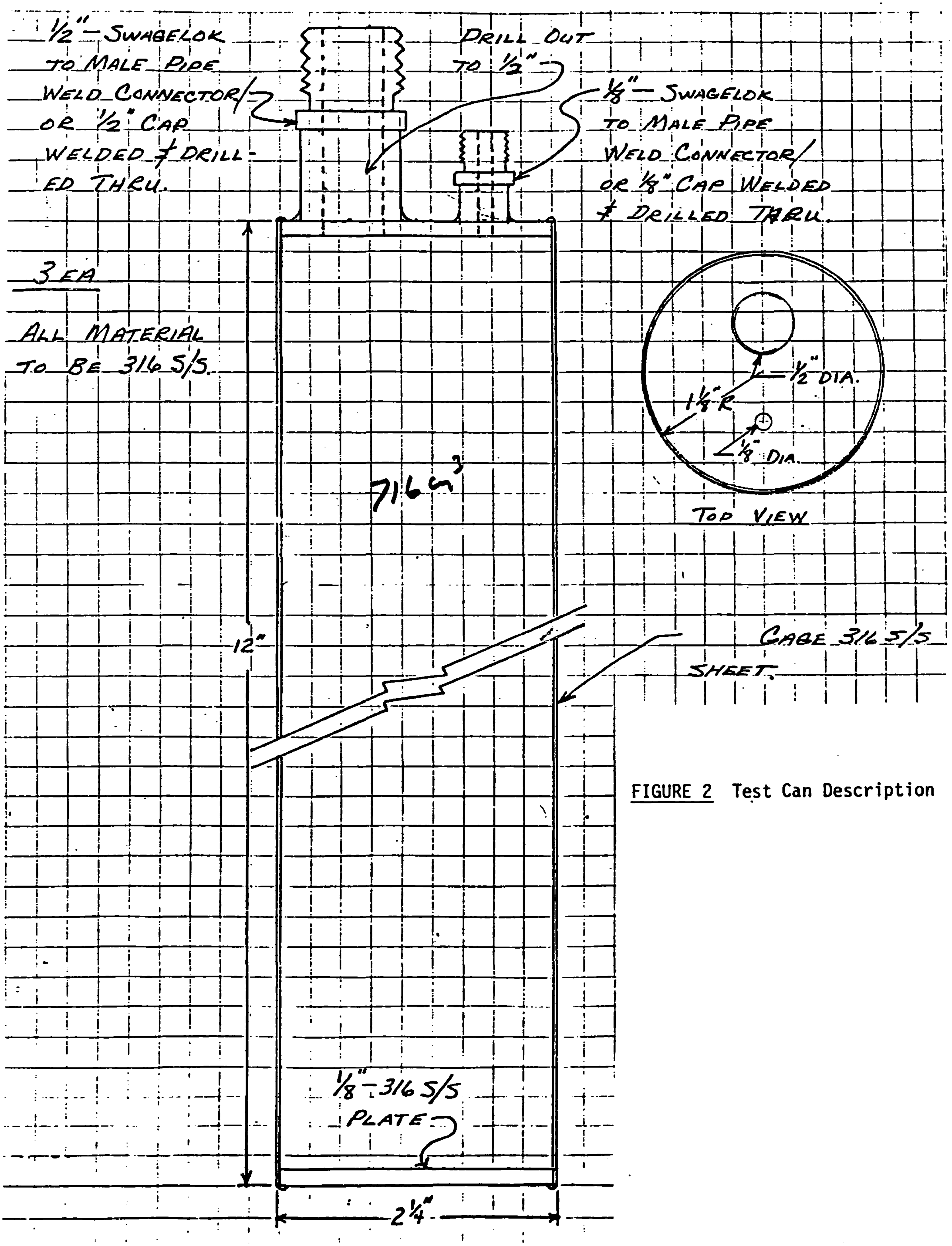

FIGURE 2 Test Can Description

TABLE 1. Test Conditions and Results for Test A (wet)

Objective

To submit IRN-150 resin in H_2O to a dose of 2 x 10^9R

Results

IRN-150 (LiOH form)
Dose: 1.74 x 10^9R @ 8.01 x 10^6R/hr
Temperature of Test Can: 142-151°F
Average Gas Presure Increase During Test: 21 inches of H_2O/hr @STP
Average Volume of Gas Generated: 41 cm^3/hr

Weight Change During Test

	Original	Final	Percent Change
Resin	281.1g	134.7g	-52w%
H_2O	145.2g	282.7g	+94.4w%

Volume Change During Test

	Original	Final	Percent Change
Resin	410 cm^3	177.5 cm^3	-56.7v%
H_2O (pH8.9)	145 cm^3	274 cm^3	+89v%

TABLE 2. Test Conditions and Results for Test B (dry)

Objective

To heat the resin at 360°F (steam temperature at 150 psig) and to submit this resin to a dose of 2×10^9R.

Results

IRN-150 (LiOH form)
Dose: 1.72×10^9R @ 8.01×10^6R/hr
Temperature of Test Can: 215-225°F
Average Gas Pressure Increase During Test: 0.1 inches of H_2O/hr @STP
Average Volume of Gas Generated: 2.3 - 3 cm^3/hr

	Weight Change During Test			
	Original	After Heating(c)	Final	Percent Change(a)
Resin	281g	104.7g (95.3)(b)	94.7g	-62.7w% (-0.6w%)

	Volume Change During Test			
	Original	After Heating(c)	Final	Percent Change(a)
Resin	~ 400 cm^3	~ 124 cm^3	~ 124 cm^3	-69v%

(a) No change in volume and weight was detected during irradiation.
(b) An analytical sample (9.4g) was removed prior to ^{60}Co treatment.
(c) Resin pretreated by heating at 360°F (183°C) in N_2 for approximately 22 hours.

TABLE 3. Gas Analysis of Samples Taken During ^{60}Co Tests[a]

	Test A (mole %)		Test B (mole %)	
	25 hrs	217 hrs	24 hrs	217 hrs
CO_2	--	3.8	28	10
O_2	<0.95	0.4	3.6	--
N_2	--	3.4	17.1	--
CO	--	0.1	0.5	--
He	<0.01	<0.01	<0.01	<0.01
H_2	84	91	20	58
CH_4	--	1	17.9	30
Trimethylamine	15	--	9.3	0.7
C_xH_y	--	0.15	1.4	0.4
C_2H_x	--	0.4	--	0.9
Methylamine	--	0.15	--	--
Benzene	--	0.05	--	--

(a) The test equipment was backfilled with argon prior to ^{60}Co irradiation to eliminate air.

Observation

The lack of oxygen in the analysis has been of considerable interest. A review of this subject by E. C. Martin (BNW) follows.

Gamma Irradiation of Aqueous Solutions - E. C. Martin

Gamma irradiation of pure water or dilute aqueous solutions should not be construed to be another form of electrolysis. The "molecular" products or irradiation are not H_2 and O_2 but rather $H_2$and H_2O_2. The "radical" products are the hydrated electron, hydrogen atom, hydroxyl and perhydroxyl radicals.(1)

---

(1) J. W. T. Spinks, An Introduction to Radiation Chemistry, 2nd Edition, Wiley-Interscience, NY, London, Sydney, Toronto, (1976), p. 257.

The hydrated electron and hydrogen atom act as "reducing radicals" since they frequently bring about reduction of dissolved substances. Hydroxyl and perhydroxyl (HO_2) radicals and hydrogen peroxide are described as the "oxidizing products" since they tend to bring about oxidation.

In the presence of organic materials hydrogen peroxide is capable of forming peracids (RCO_3H), which in turn can generate diols from α-β unsaturated ketones hydrocarbons. Epoxides are produced from α-β unsaturated by hydrogen peroxide in a base media. Cleavage of α-keto acids and α-diketones likewise is possible with basic hydrogen peroxide. A base catalyzed reaction between a nitrite and hydrogen peroxide to form the corresponding amide has been reported. Thus, in an organic medium most hydrogen peroxide that has been generated will have depleted itself in an oxidative process.

TABLE 4. IRN-150 Heat Tests

Objective

To heat IRN-150 Li-form resin to determine changes in physical properties with temperature.

Procedure

The as-received resin was pretreated with LiOH, washed with H_2O and filtered to remove excess water. Samples (100g) of resin were weighed out. Each portion of resin was placed in a glass tube and heated (225-1000°F) in a tube furnace in a 500 cm^3/min. stream of N_2.

Conclusion

IRN-150 heated from 100°C to 260°C lost 31-63w% but retained the structure of the original resin. At 400°C the resin lost 75w% and was black. At 538°C the resin was completely destroyed.

Results

Temperature		Heat	Initial	Final	Loss of Wt.	
°F	°C	Cycle, hr	Wt, g	wt, g	g	w%
225	100	25	101.8	70	31.8	31.2
358	181	~ 16.5	156.7	58.8	97.7	62.5
500	260	~ 22	99.3	37.0	62.3	62.7
750	400	~ 22	99.7	24.7	75.0	75.2
1000	538	~ 20	97.7	18.4	79.3	81.2

TABLE 5. Picture of Treated Resins*

Pictures Obtained

1) IRA-150 Mixed Bed (As Received, Li-Form)
2) IRA-150 Cation Resin
3) IRA-150 Anion Resin
4) Resin Heated to 225°F in N_2 for ~ 24 Hours
5) Resin Heated to 360°F in N_2 for ~ 24 Hours
6) Resin Heated to 500°F in N_2 for ~ 24 Hours
7) Resin Heated to 750°F in N_2 for ~ 24 Hours
8) Resin Heated to 1000°F in N_2 for ~ 24 Hours
9) Test A, 1.7×10^9 R (Wet)
10) Test B, 1.7×10^9 R (Dry)

---

*Pictures were delivered under separate cover and are not included in this information.

TABLE 6. Resin Removal by Sluicing

Objective

To determine differences in sluicing ability of new resin and resin treated to a dose of 2 x 10^9R.

Procedure

The expansion of ion exchange resin as a function of the rate of water upflow was used to compare new IRN-150 resin with resins from Tests A and B.

Each resin was placed in a glass ion exchange column 127 cm tall by 3.85 cm in diameter, filled with water. The settled height of the resin and the demarkation line between cation and anion resin was determined. Water was then introduced at the bottom of the column and its flow volume determined by catching the overflow in a 500 ml graduate as a function of time. As the water flow increased, the resin bed expanded and was measured.

Conclusion

IRN-150 Li-form resin irradiated to a dose of 1.7 x 10^9R, both dry and in H_2O, will sluice more readily than new untreated resin. Tests using 710 cm^3 (Table 6A) and 170 cm^3 (Table 6B) of new IRN-150 were compared with Test A (wet) irradiated resin (Table 6C), and Test B (dry) irradiated resin (Table 6D). A loss of organic meterials from the resin structures into the aqueous phase during irradiation (Test A) and during water uptake after irradiation and prior to testing (Test B), decreased their specific gravity and therefore, were more easily sluiced than new resin. Results are shown in Figure 3.

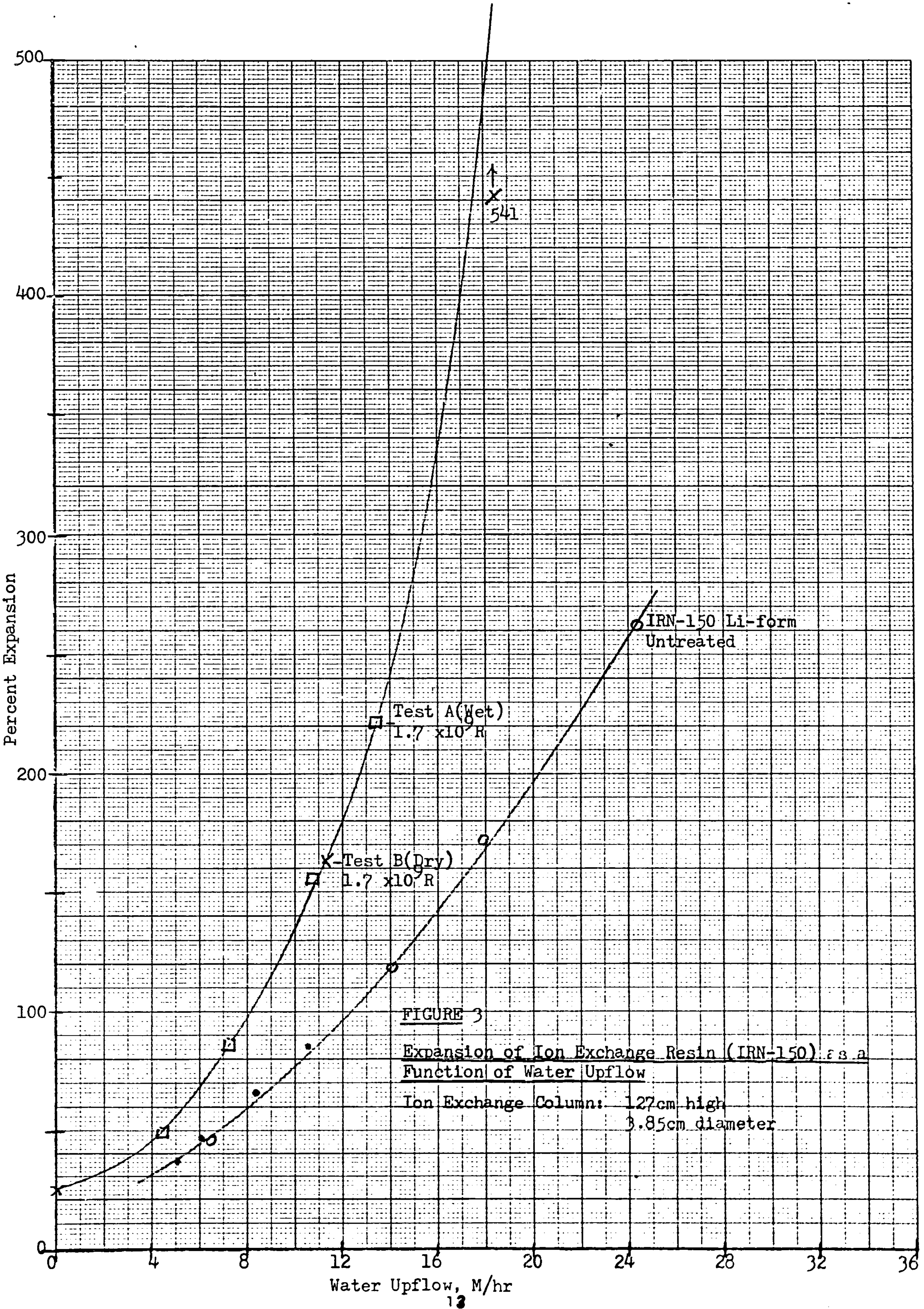

FIGURE 3

Expansion of Ion Exchange Resin (IRN-150) as a Function of Water Upflow

Ion Exchange Column: 127cm high
3.85cm diameter

TABLE 6A.

Objective: To Determine Expansion of IRN-150 Li-Form Resin as a Function of Water Flow - As Received

Conditions: 710 cm^3 IRN-150 - 230 cm^3 IRN-77 (Li Form)
- 480 cm^3 IRN-78 (OH Form)

Ion Exchange column - 127 cm High
3.85 cm diameter

Results

		Bed Depth					
Water Upflow		IRN-77		IRN-78		TOTAL	
cm^3/min.	M/hr	cm	% Expansion	cm	% Expansion	cm	% Expansion
0	0	19.5	0	42.0	0	61.5	0
100	5.2	21.5	10.3	63.0	50	84.5	37.4
115	6.0	23.0	17.9	67.0	59.5	90.0	46.3
158	8.2	25.0	28.2	76.5	82.1	101.5	65.0
203	10.5	26.5	35.9	86.5	105.9	113.0	83.7

Observations: The bed separated into two bands with the IRN-77 on the bottom.

TABLE 6B

Objective: To Determine Expansion of IRN-150 Li-Form Resin as a Function of Water Flow - As Received

Conditions: 125.8g (wet) IRN-150, ~ 170 cm^3

Ion Exchange column - 127 cm high
3.85 cm diameter

Results

		Bed Depth					
Water Upflow		IRN-77		IRN-78		TOTAL	
cm^3/min	M/hr	cm	% Expansion	cm	% Expansion	cm	% Expansion
0	0	5.0	0	9.7	0	14.7	0
123	6.4	6.0	20.0	15.5	60	21.5	46
270	14.0	7.5	50.0	24.5	153	32.0	118
345	17.9	9.0	80.0	31.0	220	40.0	172
469	24.3	10.0	100.0	43.0	343	53.0	261
1304	67.6	Settled resin, 7 cm high (~ 81 cm^3). Remaining resin went over top of column.					

TABLE 6C.

Objective: To Determine Expansion of Resin After Dose of 1.7 x 10^9R - Test A (Wet)

Conditions: 134.7g (wet), ~ 177 cm^3

Ion Exchange Column - 127 cm high
3.85 diameter

Results

Water Upflow		Bed Depth Total	
cm^3/min.	M/hr	cm	% Expansion
0	0	14.5	0
86	4.4	21.5	48
139	7.2	27.0	86
205	10.7	37.0	155
259	13.4	48.0	221
303	15.7	No Line	
909	47.1	Settled resin, 4 cm high (~ 46 cm^3). Remaining resin went out over top of column.	
1304	67.6	Only 10.5 cm^3 resin remaining in column.	

No distinct band between resins. Cation and anion beads appear to be attracted to each other.

TABLE 6D.

Objective: To Determine Expansion of Resin After Dose of 1.7 x 10^9R - Test B (Dry)

Conditions: 128.3g (wet), soaked dry resin in H_2O for 24 hours

Ion Exchange Column - 127 cm high
3.85 cm diameter

Results

		Bed Depth					
Water Upflow		Bottom Band		Top band		Total	
cm^3/min.	M/hr	cm	% Expansion	cm	% Expansion	cm	% Expansion
0	0	10.1	0	4.5	0	15.6(14.8)*	0
6	0.3	10.7	6	8.8	96	19.5	25
150	7.8	12.7	26	15.6	247	28.3	81
214	11.1	14.2	41	26.8	496	41.0	163
357	18.5	17.5	73	~ 82.5	1733	~ 100.0	541
1304	67.6	Settled resin, 8.5 cm high (~ 98 cm^3).					

* Mixed bed was less in volume than after separation.

TABLE 7.

DESCRIPTION OF ION EXCHANGE RESIN

TMI-2 DEMINERALIZER, IRN-217 (99.99% Li-7-OH)

Amberlite IRN-150 Mixed Bed Resin(a) 1/1 Chemical Equivalent

	IRN-77 Cation Exchange	IRN-78 Anion Exchange
Volume, %	40	60
Moisture, %	55	60
Volume Capacity, Meq/ml	1.75(b)	1.2(b)
Screen Analysis, on 16 mesh	5 max	5 max
thru 50 mesh	0.5	0.5
Active Sites	$- SO_3^- {}^+Li$	$N-(CH_3)_3^+ OH^-$

(a) Purchased as a mixed bed resin containing strongly acidic sulfonic cation exchange resin in the H^+ form (IRN-77), and a stongly basic anion exchange resin in the OH form.

(b) 0.7 Meq/ml of IRN-150.

INDEPENDENCE MALL WEST PHILADELPHIA, PA. 19105, U.S.A. TELEPHONE (215) 592-3000
CABLE ADDRESS: ROHMHAAS TELEX 845-247 TWX 710-670-5335

REPLY TO.
3475 INVESTMENT BLVD.
SUITE NO. 9
HAYWARD, CALIF. 94545
(415) 785-7000

ROHM AND HAAS COMPANY

August 2, 1982

Mr. Jack Ryan
Battelle N. W.
P. O. Box 999
Richland, Washington 99352

Dear Jack:

As we discussed by telephone, Amberlite IRN-217 is the lithiated version (99.99% Li-7-OH) of Amberlite IRN-150. Amberlite IRN-150 is a one to one chemically equivalent (or 60 percent by volume anion exchange resin, 40 percent cation exchange resin) mixture of Amberlite IRN-77 and IRN-78. Typical properties for these components are listed below:

	Amberlite IRN-77	Amberlite IRN-78
Moisture Content, %	55 max	60 max
Volume Capacity, Meq/ml	1.75 min	1.2 min
% regenerated, as supplied		
H form	98 min	--
OH form	--	90 min
Screen Analysis		
on 16 mesh	5 max	5 max
thru 50 mesh	0.5 max	0.5 max

I hope that this information will be useful to you. If I can be of any further assistance please contact me.

Very truly yours,

E. C. Feeney

E. C. Feeney

ECF/sn

TMI-2 Demineralizer Resin Removal - Activity 2

L. A. Bray and E. C. Martin
Pacific Northwest Laboratory
Richland, Washington 99352

Experiments were continued on IRN-150 Li-form resin after exposure to estimated dose levels and temperature. The results of this work performed in FY 83 are reported herein.

Major conclusions are that:

- 40-70% of the cation sites and >90% of the anion exchange sites are lost due to irradiation damage for wet IRN-150 Li-form resin at $\sim 2 \times 10^9$ R.

- No cation sites and >90% of the anion exchange sites are destroyed due to preheating the resin to 360°F and irradiation of the dry resin at $\sim 2 \times 10^9$ R.

- The anion exchange sites are destroyed (76% at 225°F and 99% at 500°F) when the IRN-150 is heated in an inert gas. No cation capacity was shown to be lost below 500°F.

- The sodium borate solution eluted Cs from partially and fully loaded new and wet irradiated resin. Only 67% of the Cs was eluted from fully-loaded heat-treated dry-irradiated resin. No elution was obtained for dry-irradiated partially loaded resin after 10 CV of sodium borate solution had been used to treat the resin. Discrepancies between results for fully-loaded Cs columns (Table 4) and partially loaded columns (Table 6) have been noted. Resolution would have required additional work.

E. C. Martin has completed an analysis of a water sample saturated after irradiation (2×10^9 R, Test A) to determine its elemental analysis, infrared, and ultraviolet spectrum.

Objective

Determine the exchange capacity (cation) for new and ^{60}Co treated resin (IRN-150, Li-form).

Results

In previous work, lithium treated IRN-150 was irradiated using a ^{60}Co source to 1.74×10^9 R. Two tests were completed:

Test A	Resin, cm^3	g (wet)	Solution, g
Initial	410	281	145.2
Final	177.5	134.7	274
Test B			
Initial	410	281	None
Final	--	104.7 (dry)	None

Additional samples of Li treated resin were heated in inert gas at 225°F, 500°F 750°F, and 1000°F.

In order to determine the cation capacity of the new and treated resins, weighed samples of wet resin were treated with acid, and the resulting solutions analyzed for lithium. The results (Table 1) show that the new Li-treated resin has a cation capacity of 0.61 meq/cm^3. After being irradiated (Test A), the capacity was 0.2-0.4 meq/cm^3. The remaining lithium was found in the aqueous solution. When the Li-treated resin was dried before irradiation (Test B), no cation capacity was lost as indicated by a Li cation capacity of 0.65 meq/cm^3.

TABLE 1. Lithium Analysis of New and Treated IRN-150 Resin

	Resin		Lithium	Capacity
	cm^3	g (wet)	Found, g	meq/cm^3
New resin	410	281.1	1.74	0.61
Resin Test A	177.5	134.7	0.21 (0.48)[a]	0.17 (0.4)[a]
Solution Test A	(4.6g/L x 0.274L)		1.26 (72.4%)	
Resin Test B	11.1	8.375	0.050	0.65

(a) By difference between new resin and Li found in solution.

Objective

Determine the exchange capacity (cation and anion) for new, heat treated and ^{60}Co treated resins by loading the exchangers with NaOH or HCl. The loaded exchangers were then eluted with HNO_3, and the resulting solutions analyzed for Cl^- and Na^+.

Results

Samples of new resin or resin from Tests A and B, as well as resins heated to 225°F and 500°F, were treated with either NaOH or HCl and washed with H_2O. The resulting loaded resins were eluted with HNO_3, and the resulting solutions analyzed for Na^+ or Cl^-. The results (Table 2) show that the cation capacity was not destroyed for either dry or wet irradiation (Test A or B) or resins heated to 500°F. Test A resin does show that the capacity is two-thirds of that for new resin, 0.4 vs. 0.6 meq/cm^3, and confirms the lithium results shown in Table 1. The results also show that the anion capacity of the IRN-150 is destroyed by the dry and wet irradiation (1.7×10^9 R) and by increasing the temperature from 225°F (0.15 meq/cm^3) to 500°F (0.006 meq/cm^3).

TABLE 2. Capacity of IRN-150 Resin as a Function of Treatment

Procedure: Samples of new or resin from Test A, B, and heated samples 225°F and 500°F were treated with either NaOH or HCl and washed with H_2O. The resulting resins were eluted with HNO_3 and analyzed for Na^+ or Cl^- ion.

Results:

	cm^3	g (wet	Na Found, mg	Capacity, meq Na/cm^3	Cl Found, mg	Capacity, meq Cl/cm^3
Initial Resin	7.29	5	98.5	0.59	164.5	0.64
Test A	6.59	5	61.5	0.41	5.85	0.025
Test B	11.1	8.375	164.0	0.64	6.15	0.016
225°F	11.0	8.110	174.5	0.68	57.0	0.15
500°F	10.9	8.155	171.3	0.68	2.5	0.006

Objective

Determine if a sluicing solution containing boric acid and sodium borate (3,500 ppm B, 1,000 ppm Na) at a pH of 7.8 will remove Cs from a loaded column.

Results

Five gram (wet) samples of new and irradiated resins were placed in small ion exchange columns. Each resin was treated by the addition of 80 ml of 0.475 M Cs (5.05 g) containing ^{137}Cs tracer. The columns were then H_2O washed, and the amount of Cs retained on the exchanger determined by difference between the effluent and the feed. The results are shown in Table 3. The resin capacity using cesium is similar to those results shown in Table 1 for lithium.

TABLE 3. Cs Loading of New and Treated IRN-150 Resin

	Resin		Cs Loaded, g/g Resin	Capacity, meq/cm^3
	cm^3	g (wet)		
New Resin	6.625	5	0.079	0.45
Resin Test A	7.55	5	0.031	0.16
Resin Test B	7.55	5	0.170	0.85

The above columns were then washed with three 50 ml volumes (~7 column volumes) of solution containing 0.087 M $Na_2B_4O_7$ and 0.235 M H_3BO_4 at a pH of 7.82. The results are shown in Table 4. The results show that with large volumes (21 CV) of borated water that the cesium is removed from new resin and resin irradiated (2 x 10^9 R - wet). The Test B resin (2 x 10^9 R - heated to 360°F) appears to be more diffcult to elute.

TABLE 4. Removal of Cs from New and Irradiated IRN-150 Resin Resin Using H_2O Containing Sodium Borate

50 ml Volumes (~7 CV) of Sodium Borate, pH 7.8	% Cesium Removed from Loaded Ion Exchange Resin		
	New Resin	Test A	Test B
1	68.4	79.1	31.0
2	25.6	22.3	23.3
3	12.4	6.9	12.2
% removed after ~21 CV	106.4	108.3	66.5

Objective

Determine if a solution containing boric acid and sodium borate will remove Cs from a partially loaded ion exchange resin.

Results

After completion of the above work, a second case was considered. Will the elution of a partially cesium loaded ion exchange resin be as efficient as one loaded to capacity?

Ten gram (wet) samples of new and irradiated resins were placed in ion exchange columns. Each resin was treated by loading 30 ml of 0.058 M Cs (0.23

g Cs) containing ^{137}Cs tracer on the column. The columns were then washed with 70 ml of H_2O. Essentially 100% of the Cs was loaded in each case as shown in Table 5.

TABLE 5. Cesium Loading on New and Irradiated IRN-150 Resin

	Resin		% of Feed	
	cm^3	g (wet)	Loaded	Cs Loaded, g/g Resin
New Resin	13.25	10	96.5	0.022
Resin Test A	15.10	10	~100	0.023
Resin Test B	15.10	10	~100	0.023

The above three columns were then washed with ten 15 ml volumes of sodium borate solution, and the fraction of the loaded cesium was determined in the effluent. The results (Table 6 and Figure 1) show that 90% of the cesium loaded was eluted from new and Test A resin in 55 CV and 13 CV, respectively. Test B resin (2 x 10^9 R - heated to 360°F) did not elute.

TABLE 6. Elution of Cs from Partially Loaded New and Treated IRN-150 Resin Using H_2O Containing Sodium Borate

	Percent of Feed in Effluent		
15 ml Volumes (1 CV) of Sodium Borate, pH 7.8	New Resin	Test A	Test B
1	1.4	0.9	0.01
2	2.7	5.9	0.01
3	2.8	11.6	--
4	3.0	13.7	0.01
5	3.2	12.3	0.01
6	3.8	11.1	0.01
7	3.9	9.2	0
8	4.0	7.0	0
9	4.1	6.0	0
10	4.2	5.3	0
% removed after 10 CV	33	83	0.1

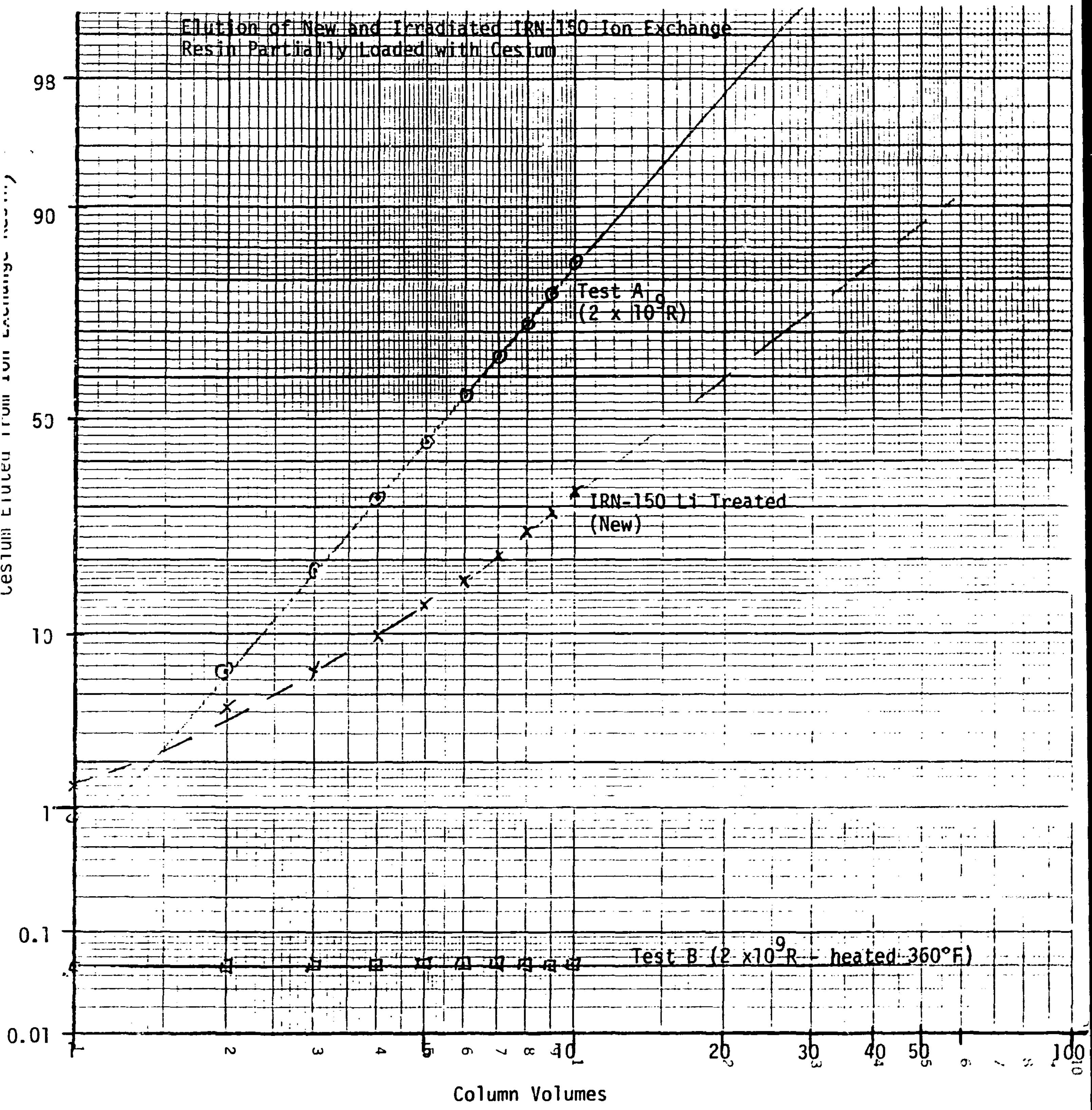

FIGURE 1. Elution of New and Irradiated IRN-150 Ion Exchange Resin Partially Loaded with Cesium

FURTHER ANALYSES ON TMI RESIDUE DEGRADATION PRODUCTS

A sample of water and TMI resin (in its lithium form) was irradiated to 1.7×10^9 R in a ^{60}Co source. The aqueous solution was separated by filtration from the solid resin material. 10 mL of the aqueous solution obtained in this manner was evaporated in air to yield 0.6 g of a yellow-orange residue. After drying in a desiccator, this residue was examined to determine its elemental analysis, infrared, and ultraviolet spectrum.

Elemental Analysis

A 7.391 mg sample was examined. The elemental analysis was determined to be:

C	10.52%
H	3.59
N	6.87
S	20.06
P	<0.01
	41.04%

Ash from the sample amounted to 4.342 mg or 58.75%. This ash is the residue that remained after the organic material was destroyed at high temperature in a stream of oxygen. Probably the ash consists of metallic compounds, in this case most likely only lithium sulfate. If this is the case, then the percentage of lithium would be about 7.42% of the sample.

An effort to determine a molecular formula for the residue, based on this analysis, was not successful as indicated by Table 7:

TABLE 7. Determination of Molecular Formula for Residue

Elements	Weight Percentage	Percentage ÷ Atomic Wt	Normalized Ratio
C	10.52	0.88	1.80
H	3.59	3.56	7.27
N	6.87	0.49	1.00
S	20.06	0.63	1.29
Li (from ash)	7.42	1.07	2.18
O (difference)	51.54	3.22	6.57

The empirical formula is

$$C_{1.8}H_{7.27}NS_{1.29}Li_{2.18}O_{6.57}$$

A molecular weight is needed to attempt a true formula. Unfortunately, after the yellow-orange residue was dried, it no longer could be completely dissolved in any common solvent. (Molecular weights are frequently determined by either freezing point or boiling point changes caused by a substance being dissolved in a suitable solvent.) The residue was found to be insoluble in:

Water
Chloroform
Toluene
Benzene
Methyl ethyl ketone
Dioxane
Dimethyl formamide
Acetonitrile
Ethanol
Tetrahydrofuran
Methyl cellusolve
Dichloroethylene

Conclusions: Results of the empirical formula indicate that probably many compounds resulted from the irradiation process. As a consequence, it is not possible to assign a formula based on the elemental analysis.

Spectral Evidence

The aqueous solution was examined in a Hewlett-Packard 8450A Uv/Vis Spectrophotometer to determine the extent of aromaticity or conjugated unsaturation present in the residue. There did not appear to be any aromatic rings or any appreciable unsaturation since the ultraviolet spectrum was featureless except for end absorption (i.e., at 200 nm and lower).

Infrared Spectroscopic Examination

A KBr pellet was prepared from ~1.5 mg of the desiccator-dried yellow-orange solid residue and 260 mg of KBr. The materials were ground to an intimate mixture, pressed at ~18,000 psi under vacuum, and examined using a Nicolet MX-1 Fourier Transform Infrared Spectrophotometer.

Attached is a spectrum of the residue. The first peak at 3451 cm^{-1} appears to be a water peak. It may be the residue which had been dried in the desiccator still retained some water. Additional drying must be performed, and the spectrum redetermined to decide whether this water peak is an integral part of the molecule or only an artifact caused by insufficient drying. This broad peak obscures smaller peaks that now appear only as small shoulders. The first shoulder at ~3250 cm^{-1} may be due to a bonded OH of a carboxylic acid.

The peak at 2973 is characteristic of aliphatic organic compounds. The presence of aromatic or alkene compounds would have produced absorption at 3100-3000 cm^{-1}. There is no indiction of any significant amounts of these compounds.

The strong peak at 1658 cm^{-1} can be assigned as a carbonyl absorption due to an amide group

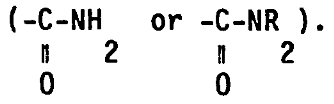

$(-\underset{\underset{O}{\|}}{C}-NH_2 \text{ or } -\underset{\underset{O}{\|}}{C}-NR_2)$.

The strong absorptions between 1200 and 1050 cm^{-1} may be identified as the sulfur-oxygen stretching frequencies of a sulfur-containing molecule such as a sulfate, sulfonate or sulfone. The presence of sulfur, found in the elemental analysis, gives support to this assignment.

A search was made of the infrared spectra library, but it did not uncover any spectrum that included all of these peaks. This unsuccessful search tends to give support to the idea that the yellow-orange residue is a mixture of compounds.

APPENDIX B

IN SITU TREATMENT OPTIONS FOR THREE MILE ISLAND DEMINERALIZER RESIN

Westinghouse Hanford Company

M. D. Crippen

W. O. Greenhalgh

IN-SITU TREATMENT OPTIONS FOR THREE MILE ISLAND DEMINERALIZER RESIN

CONTENTS

FIGURES

TABLES

IN-SITU TREATMENT OPTIONS FOR THREE MILE ISLAND DEMINERALIZER RESIN

I. SUMMARY

Four areas of in-situ treatment were considered: dissolution; in-situ solidification; chemical oxidation/dissolution; and other miscellaneous processes. Further examinations were made of those processes that appeared likely to succeed under the criteria of safety and efficiency and a number of laboratory scouting tests were made. These options are listed and results discussed. At this time, certain chemical oxidation/dissolution systems appear to be the most promising options although other options are feasible.

II. INTRODUCTION

This report summarizes preliminary results to date in exploring in-situ treatment of two tanks of demineralizer ion exchange resin at TMI.

The objective of this program is to convert the resin material and associated radioactive isotopes presently in the resin and tanks to a safe controllable waste form suitable for transport to and ultimate disposal at a designated repository. Criteria for evaluating options included safety, efficiency, and a reasonable overall expected cost. The need to make a product from in-situ treatment which would be compatible with ultimate disposal was considered in the study, but time did not permit detailed cost estimates or engineering the subsequent disposal steps.

III. OPTIONS

A. DISSOLUTION

This term refers to the physical solvation of a solid by a solvent. If the solvent were to be evapoarted, the solid would be recovered unchanged; i.e., chemical bonds are not permanently altered. A number of laboratory chemicals such as alcohols, ketones, chlorinated hydrocarbons, etc., are able to solvate a wide range of organic compounds. However, highly polymerized structures, like ion exchange resins, tend to be insolubable in most solvents.

Table 1 lists the solvents that were tried. None of the solvents had the desired effect, which is not surprising, considering the stable nature of the resins. Some of the more promising solvents were studied in more depth, but none were satisfactory. In the initial tests, 1 gram of resin was placed in 10 ml of test solvent and the solvent with resin was agitated for at least an hour with ultrasonic waves in a warm (50°C) water bath. Immediately after the test, the solvent was removed, the resin dried, and the final resin weight was compared with the initial weight to determine the weight dissolved. The more promising solvents were then refluxed with the resin at the boiling temperature of the test solvent. However, little or no improvement was apparent.

B. CHEMICAL OXIDATION/DISSOLUTION

This term refers to the permanent alterations in chemical bonds which promote a physical change in the resin. At this point one should digress and discuss the state of the resin itself. The original material was a mixture of monomers of styrene and vinyl structures with inroganic radicals such as sulfonates ($-SO_3$). These monomers were linked together in long chains to obtain a high molecular weight compound (liquid at normal conditions) with a number of active sites for interacting with ions in the aqueous phase. These long chains were then cross-linked and treated to yield a large surface area, hard solid labled "ion exchange resin."

Under certain conditions of use the chemical activity of the resins may change. Radiation dosage and heat both tend to promote more cross-linkage (only a small fraction of the cross-links were made in the original manufacture) which often leads to some loss of the ion exchange function. Melting or fusing of the resin ruins the material for ion exchange purposes because of the loss of surface area. If heating continues to the state of charring a large number of chemical bonds are broken, some material escapes as vapors, and the remaining solid material is chemically inactive except under the most severe conditions.

TABLE 1: CHEMICAL DISSOLUTION OF ION EXCHANGE RESIN

Solvent	% Dissolved	Solvent	% Dissolved
Acetone	3	West Safe Solvent	ND
Xylene	7	Cyclo Hexane	4
Tetrahydrofuran	6	Formaldehyde	2
Methanol	8	Benzyl Ether	ND
Ethanol	10	Methyl Sulfoxide	ND (swelling)
Glycerin	ND*	Nitromethane	ND
Pyridine	ND	Acetonitrile	ND
Chlorobenzene	9	Hydrazine Monohydrate	3
Chloroform	2	KOH sat. Methanol	2
Chlorethylene	3	KOH sat. Ethanol	6
Toluene	9	n-Butyl Alcohol	ND
Methylene Chloride	16	Dioxane	0.8
Methyl Isobutyl Ketone	8	Dimethyl Formamide	ND
Ether	9	Carbon Tetrachloride	ND
37% Formaldehyde	9	KOH sat. Butanol	ND
Isopropyl Alcohol	6	30% Hydrogen Peroxide (no iron)	7
Dioctal Pthalate	12		
Vinyl Acetate	ND (swelling)		
n-Dodecane	ND		
Penetrating Oil 22-D	2		
Benzene	8		
Nitrobenzene	ND (colored)		
Acetic Anhydride	ND (colored)		
Ethyl Acetate	ND		
Benzaldehyde	ND		
Dimethyl Aniline	ND		
Fluorad (FC-24)	Dehydrated		

*ND is used as an abbreviation for "none detected".

The most promising resin oxidation/dissolution system appears to be the iron-catalyzed hydrogen peroxide system. The hydrogen peroxide reverses the polymeric process and breaks up the cross-linkages that link the resin monomers together.(1) Resin reaction parameters determine the amount of degradation that occurs. Resin may merely be degraded to fine pumpable solids like those shown in Figure 1, or the resin may be degraded to polymer chains small enough to completely dissolve in the reaction media as shown in Figure 2. Prior research(1) indicated that only 10% of the resin is oxidized to CO_2 and the rest stays in solution; for our purposes that is quite acceptable. Several lab tests were run with encouraging results. The resin was rapidly degraded at reasonable temperatures ($\leq$90°C) and concentrations ($\leq$15% H_2O_2). The rate appeared to be controllable by manipulating temperature and concentration. However, this system may have difficulties converting melted or charred resin because of the reaction mechanisms. This should be explored in further testing.

Other systems were explored which are known for their ability to chemically oxidize most organic materials. An example is dichromate in concentrated sulfuric acid which is used to clean laboratory glassware. The major difficulty with such systems is that they result in large quantities of waste solution to be neutralized and solidified. The resulting solids would be an order of magnitude larger in volume than the original resin.

Permanganate in either alkaline or acidic media may also be used and is similar to dichromate in its oxidizing power. It has similar problems in terms of waste solutions and also forms an insoluble product (MnO_2) which can add complexity to subsequent tank cleaning efforts.

Another oxidizing system is available which has advantages - Ce(IV) in HNO_3. Previous work at HEDL on metallic parts decontamination showed the ceric to be effective in oxidizing paints and coatings. It was further tried on resin with encouraging results. The ceric oxidizes the resin to CO_2 and water while reducing to cerous ion. The cerous is continuously regenerated to ceric in an electrolytic cell and reused. Since the initial solution can be recirculated between the resin tank and the cell and results in only gasous products, the eventual material to be solidified is modest.

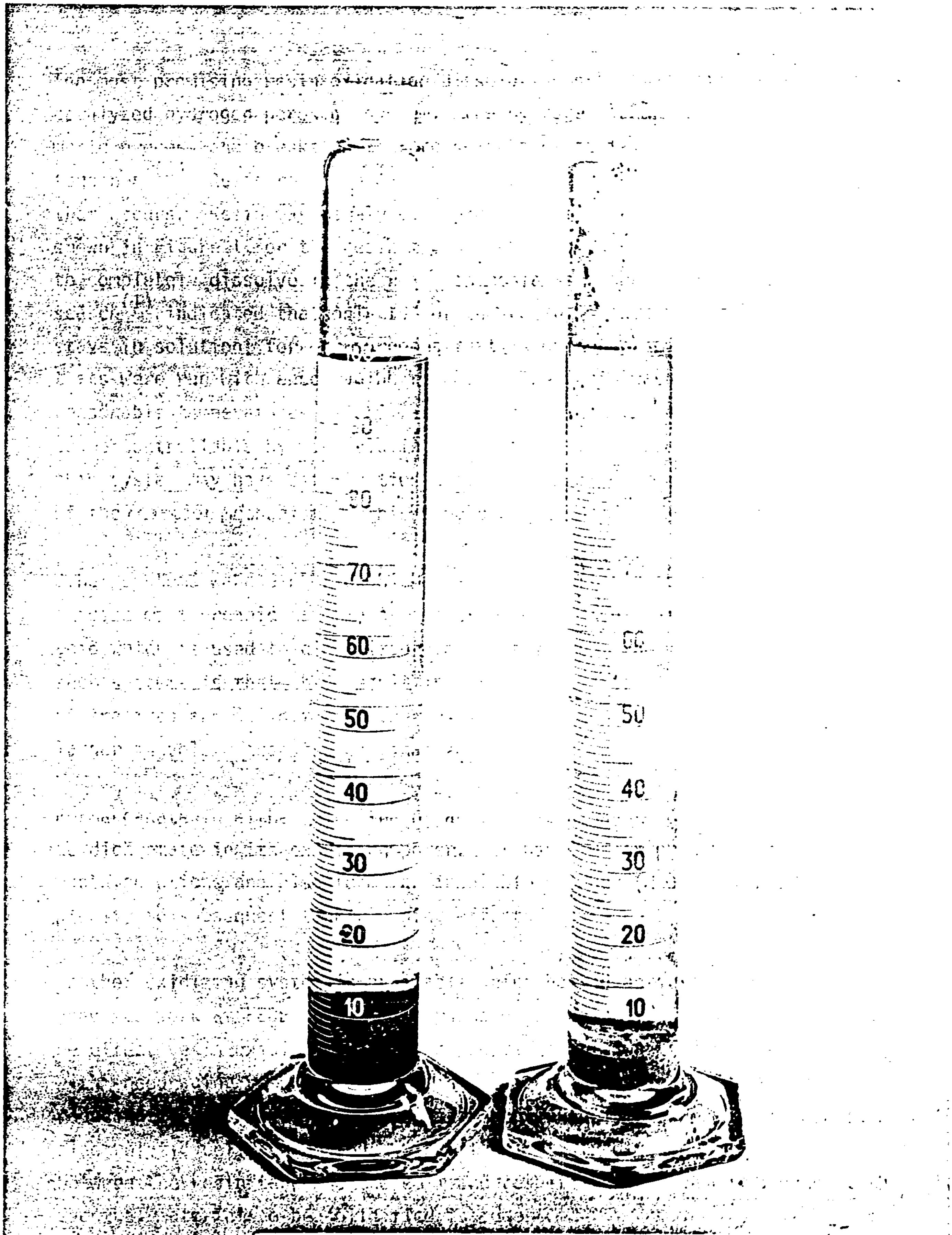

FIGURE 1 IRON CATALYZED DEGRADATION OF TMI ION EXCHANGE RESIN.

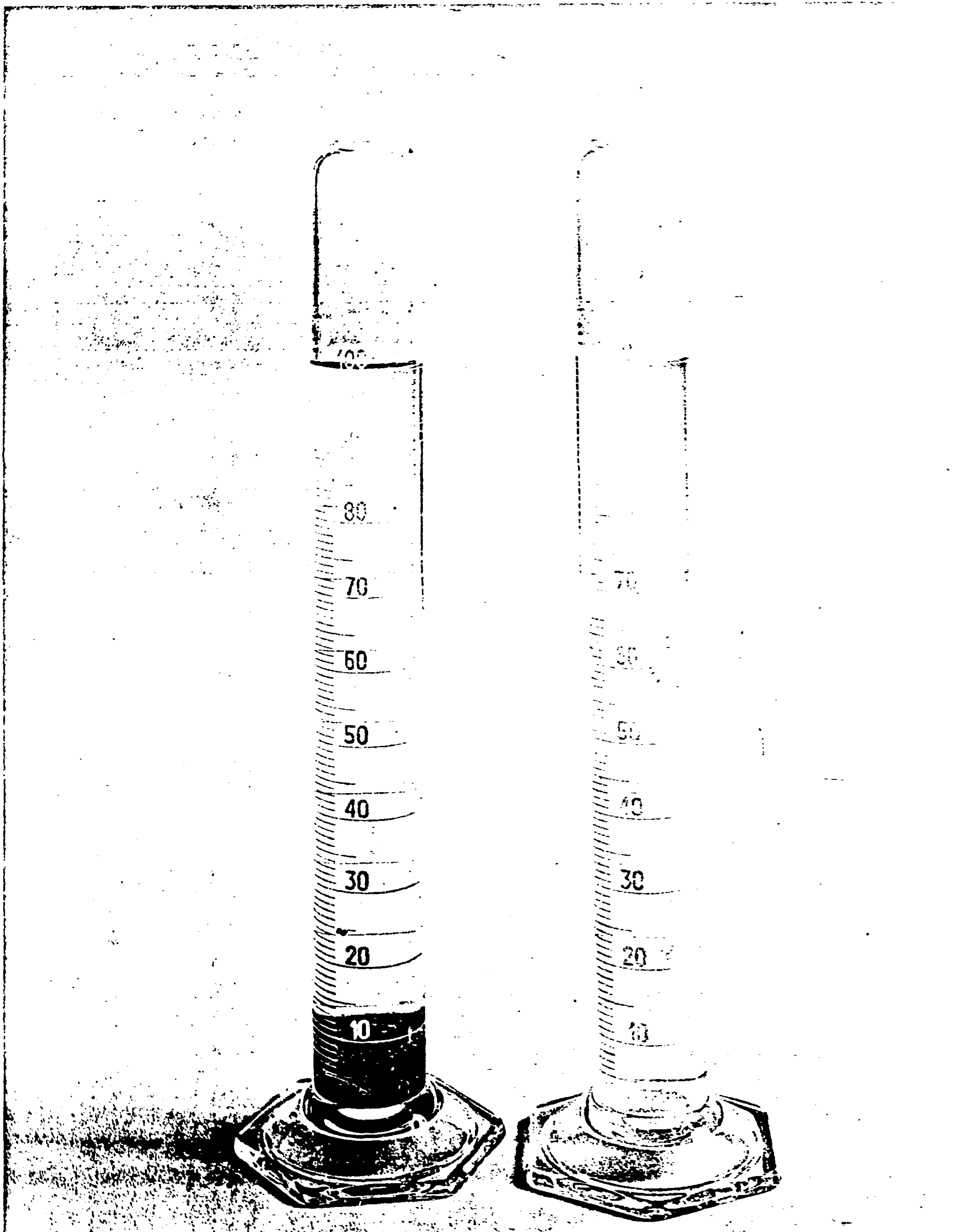

FIGURE 2 IRON CATALYZED DEGRADATION AND DISSOLUTION OF ION EXCHANGE RESIN.

Several lab tests were run with mixed results. The resin was degraded but the apparent reaction rate was slow and did not readily respond to changes in temperature and concentration. However, the ceric-nitric acid system has been shown to dissolve high temperature fired oxide fuel, both uranium and plutonium, and therefore provides an option whereby the resin can be degraded while dissolving the oxide fuel in the same process.

One other major system investigated was concentrated sodium hypochlorite solution (12-15% chlorine). Sodium hypochlorite apparently breaks up monomer chains as well as cross-linkages. It will also react with carbonized resin (elemental carbon). However, the overall reaction rate for the sodium hypochlorite system was substantially slower than for the corresponding hydrogen peroxide system.

C. OTHER

There are several known acid digestion systems which could be considered for dissolution or oxidation of resin. An acid digestion liquid that attacks organics and releases nitrogen for nitrogen analysis was tested with little or no positive dissolving results. The acid digestion liquid H_2SO_4-HNO_3 used 240-250°C to wet combust nuclear waste has been previously tested and proven to destroy ion exchange resin. But the use of this acid digestion option is unlikely because of the difficulty in maintaining the temperature of the demineralizer vessel at 240-250°C. However, it too will chemically dissolve and/or alter ceramic oxide fuel.

Further work with acid digestion systems wasn't considered because of the general problems associated with these systems. There is the problem of vessel corrosion. Although the tank would not be likely to leak during acid digestion processes, the vessel could not be coded for a return to its present use. There is also doubt about the suitability of present valves to withstand the high temperature acid because of elastomer seals and their design.

H_2O_2 could be substituted for the HNO_3 in an acid digestion system and the digestion conducted at a slightly lower temperature. However, one would have essentially all of the problems as noted above so this variation was not further investigated.

Another option considered was microwave burning. Previous work(2) indicated that the resin could be dried, melted, and pyrolized a layer at a time in a controlled manner. The soot and tars produced by pyrolysis are less concentrated than more typical combustion but are likely to cause filter plugging problems. The addition of air would also permit significant oxidation and a reduction of tars and soot. However, little development work has been done and significant time/money would be required to bring this process to the point where it could be used with reasonable confidence.

D. SOLIDIFICATION

There are two types of solidification media: organic and inorganic. Examples of the organic are urea formaldehyde, the Dow polymer system, and bitumen. These were not considered in detail because of radiation dose limitations. These materials will degrade at similar dosage levels to the original resins so the long-term effects would be similar to the pesent problems.

The main inorganic binder is Portland cement.* Much previous work has been done on cementation of resins.(3) The phase diagram, Figure 3, shows that there is enough space in the tank to make an acceptable mix. The triangle indicates the optimum composition for this tank. Compositions in this zone appears to have sufficient cement to prevent solidification product expansion due to resin swelling.(3) This of course would have to be verified with the Rohm and Haas IRN-150 resin and to make product expansion and compression-strength measurements to verify cement quality.

IV. DISCUSSION

A. GENERAL CONSIDERATIONS

An analysis was done to determine heat losses and cooling times. Assuming natural convection and radiant transfer as the loss mechanism, boiling conditions could be maintained in the tank with a modest heat input of 10 kW (see Fig. 4). This figure may shift somewhat depending on air flows thru the cell; losses

---

*Plaster of Paris could be used with similar results; its main advantage is its superior compatability with high sulfate loadings from, for example, sulfuric acid.

FIGURE 3.

WATER-CEMENT-RESIN PHASE DIAGRAM

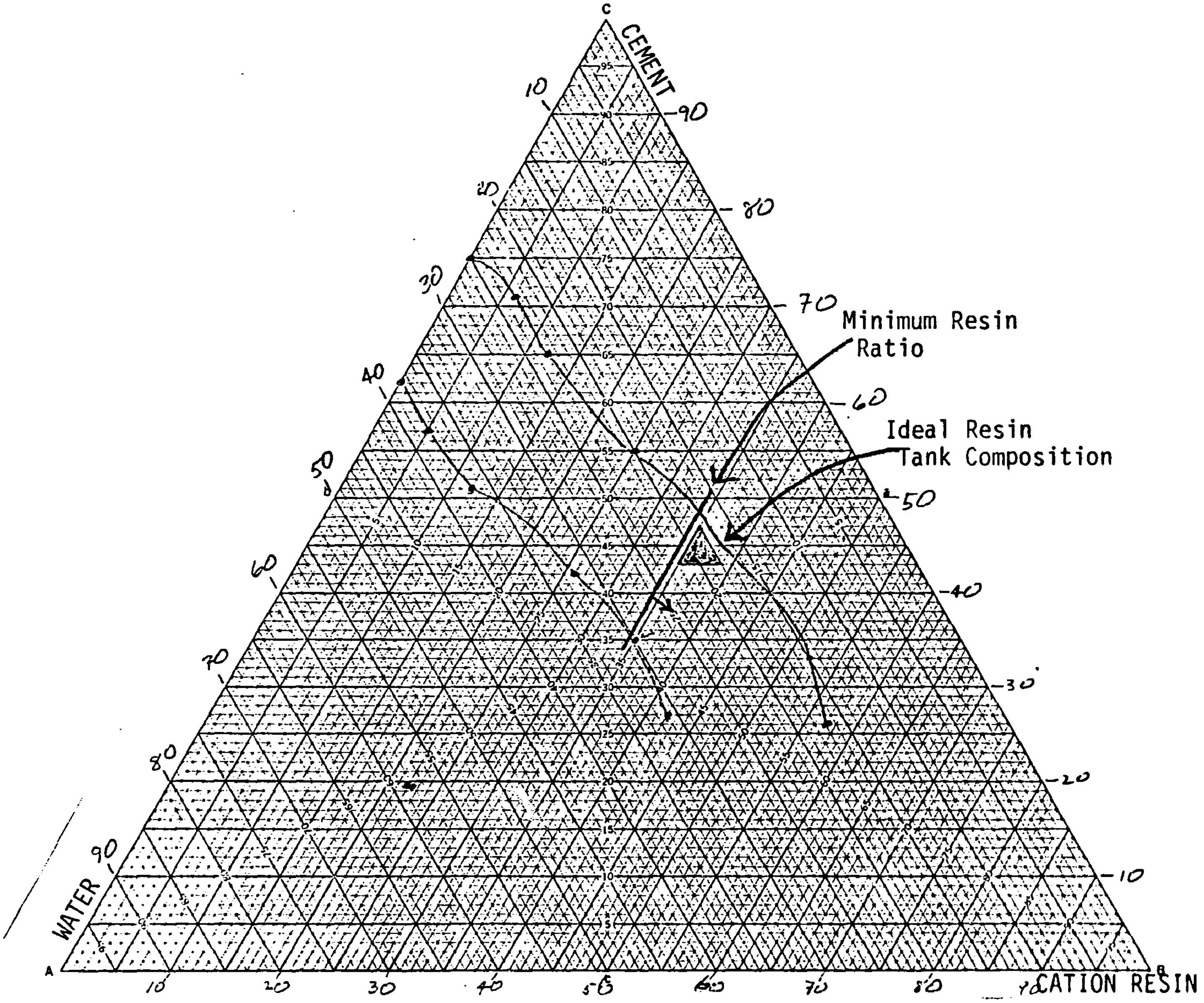

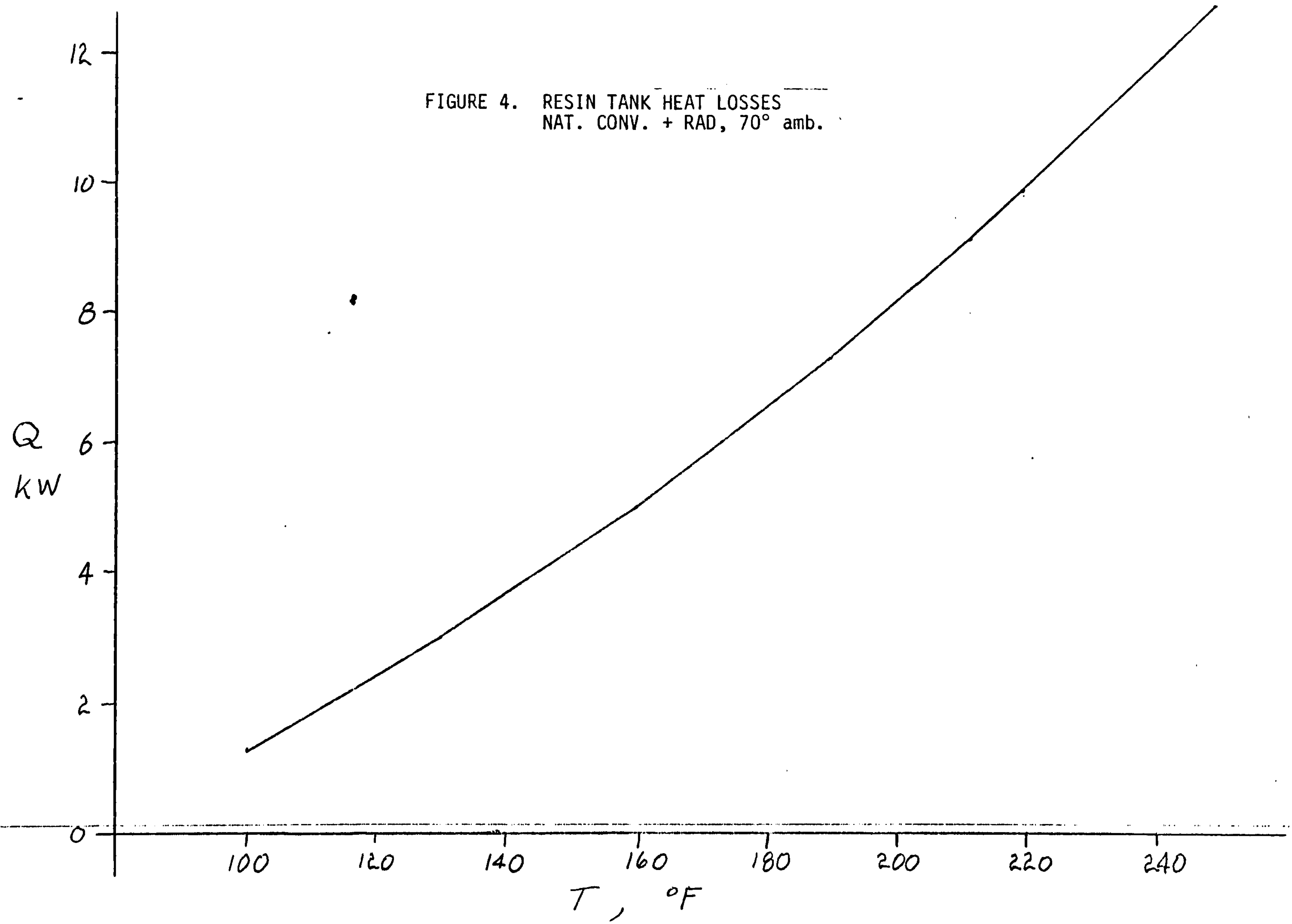

FIGURE 4. RESIN TANK HEAT LOSSES
NAT. CONV. + RAD, 70° amb.

from connecting piping were not included and could amount to a similar quantity if connections are made at some distance from the cell. Figure 5 shows the vessel temperature decay assuming even distribution inside. The thermal capacity is 2.0 kWh/°C and the maximum heating/cooling rate for a recirculating loop is about 180 kW or 1.54°C/min.

It can be seen that the cooling rate and heat capacity of the tank would not give enough temperature control in the event of a run-away reaction. The safest control would be to operate just under the boiling point (by temperature and pressure control) so that the nearly infinite heat sink of the boiling water could be used.

Figure 6 shows an off-gas clean-up system. This is based on RADTU experience (4 yrs of successful operation) so it may be confidently employed. The mist eliminator may not be necessary, but will trap particles of submicron size. Heated HEPA filters are used so that a stream containing corrosive gases can be passed without filter degradation.

This system will not trap volatile isotopes so if they are present extra equipment would have to be provided or the gas vented to another system with such capability.

Since the only vent from the vessel is a 3" line, the off-gas rate would be somewhat restricted. As a safety margin, the design rate should be limited to 1/10 of the flow that might cause equipment damage. From this it can be inferred that the reaction rate would be on the order of a few cubic feet per hour of wet resin which would mean a processing time on the order of several days. That does not seem excessive considering the time required for other events in the clean-up sequence.

Liquids may be pumped to and from the tanks thru two pipes (each 2 1/2" dia.) that end in upper and lower distribution headers; the holes in the headers are 3/16". There is a 3" line in the top head and a 2" in the bottom head designed for resin movement thru the tank and a 1" instrument line is also available.

FIGURE 5. TANK TEMP DECAY 70° amb.

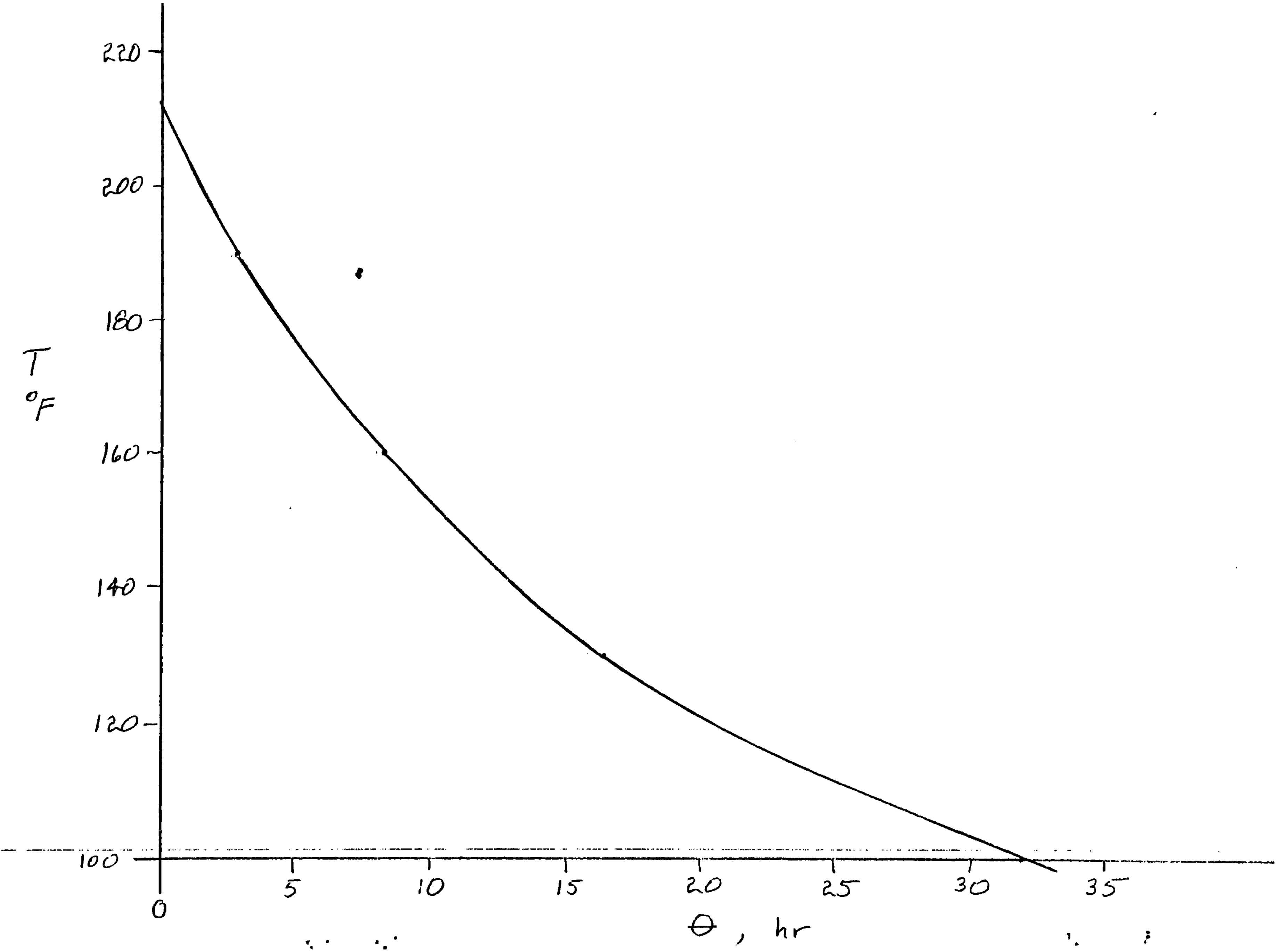

24 Sep 82

FIGURE 6. OFF-GAS

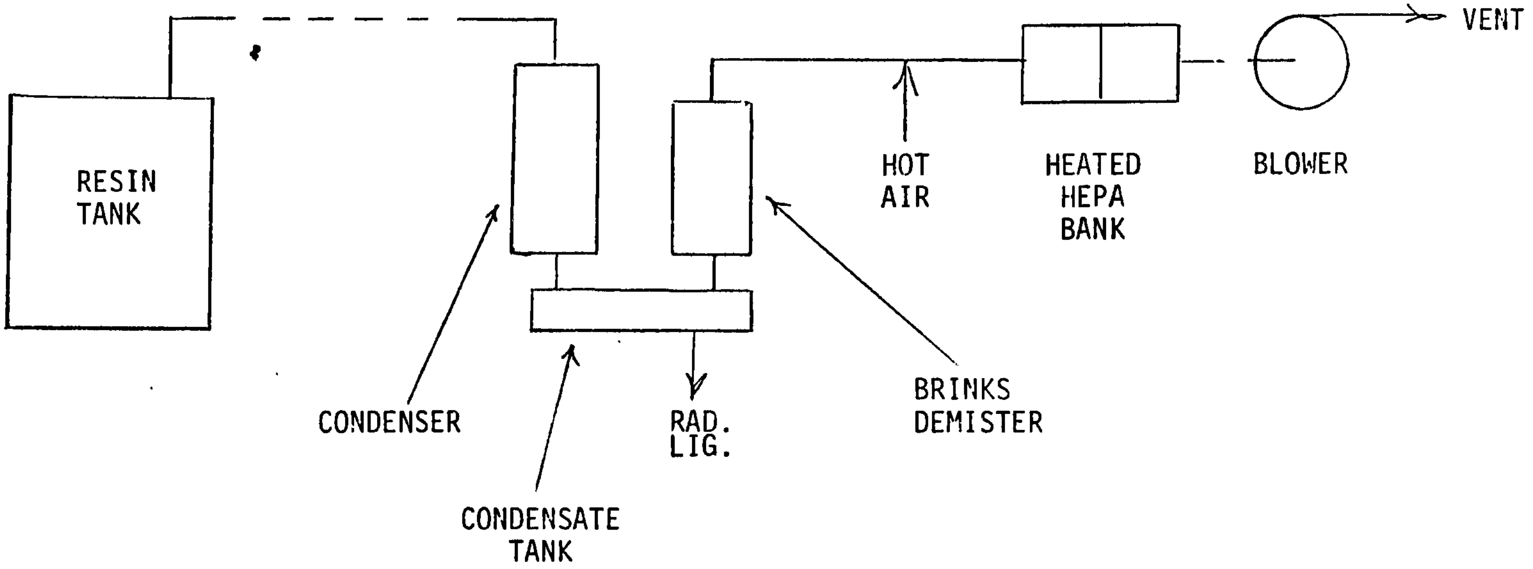

A large access port on the top (approximately 12") could provide entry for a mixer and cement or other solidifying agent. Impeller blades would have to be guided around the top distribution assembly (it has 12 arms) and the exact position of the shaft and motor may have to be adjusted because of the arms. There are no baffles or internal structures in the tank except for the top and bottom distributors.

During the period of most chemical reactions, the vessel will be self-stirring. All of the reactions under serious consideration give at least some gas evolution (plus water vapor) which results in effervescence and could be used effectively for vessel mixing.

B. REACTION HAZARDS

A consulting contract was made with a firm specializing in reaction safety of chemical systems. They determined that the reaction rate is very dependent on the concentration of catalytic iron for the hydrogen peroxide system, and that care must be taken to maintain adiabatic conditions in laboratory tests so that results will be meaningful for a large tank.

It was also determined that run-away reactions can be achieved with low concentrations (6%) of hydrogen peroxide and certain resins under special conditions. To avoid this possibility, they suggest using a small amount of high concentration oxidant in a small volume of resin. This encourages an uncontrolled reaction in the local area where the heat and vapors generated are within the capability of the off-gas system to handle. By conducting the concentrated peroxide to the tank in this way, a fairly even overall reaction rate is obtained and nearly all of the peroxide is consumed at any one time. Since even a small concentration of peroxide does not accumulate in the presence of the resin, no large-scale uncontrolled reaction can occur.

C. OPTIONS

Based on present knowledge, lab tests, and preliminary calculations, we feel that the following alternatives are viable for an in-situ treatment of this resin:

1. Solidification - A mechanical stirring with the addition of Portland cement and water to achieve a solidified mass in the existing tank. The end product would be a sealed container of solid material suitable for burial.

2. Dissolution - An addition of iron catalyzed hydrogen peroxide to chemically desolve the resin. Addition of off-gas clean-up equipment is required. No liquid recirculation is needed as temperature and reaction rate would be controlled by vacuum and altering the water-hydrogen peroxide ratio being added to the tank. The end result would be a tank of liquid that could be solidified by cement or other available means; evaporation of this liquid is NOT recommended because of the high molecular weight organics present. Use of a concentrated sodium hypochlorite system is a slower alternative treatment option to hydrogen peroxide.

3. Chemical Oxidation - Dichromate would be added to a sulfuric acid solution as the oxidizer. An off-gas system would be required to treat the evolved gases and a liquid recirculation and heating system would be necessary. As oxidant is replenished, a purge stream would arise that must be neutralized. The end result would be a large quantity of solution to be solidified with cement or plaster of paris; intermediate evaporation could be done.

There are other options that might give better results than the above but would require considerable development. Table 2 & 3 illustrates the conflicting requirements for this problem.

V. RECOMMENDATIONS

We recommend in-situ reaction by means of iron catalyzed hydrogen peroxide following the general scheme of Figure 7. After the reaction has terminated, a visual examination will be required to determine if umpumpable solids remain. If not, the liquid may be pumped to the soldification system.

If there are solids that cannot be removed from the tank, then solidification in the tank can be used. This is a decision that must be made on the spot taking into account the then current situation.

TABLE 2

SUITABILITY OF TREATMENT SYSTEMS vs RESIN STATE (Summary)

System	Fresh Resin	Spent Resin	Irradiated or Melted	Char
Solvents	No	No	No	No
Chem Oxidation	Yes	Yes	Yes	Yes
Chem Oxidation Disolution	Yes	Yes	?	No
Solidification	Yes	Yes	Yes	Yes
Digestion	currently installed equipment is incompatible			

TABLE 3

SPECIFIC TREATMENTS
vs RESIN STATE

Option	Dissolution of Resin Only	Dissolution of Resin & Fuel	Dissolution of Carbonized Resin
Catalyzed Hydrogen Peroxide	good	N/A	N/A
Hypochlorite	good	N/A	acceptable
Ceric-Nitric Acid	acceptable	acceptable	questionable
Chromic Acid Sulfuric Acid	good	good	questionable
Acid Digestion	good	good	good

FIGURE 7. IN-SITU REACTION SCHEME FOR A HYDROGEN PEROXIDE PROCESS

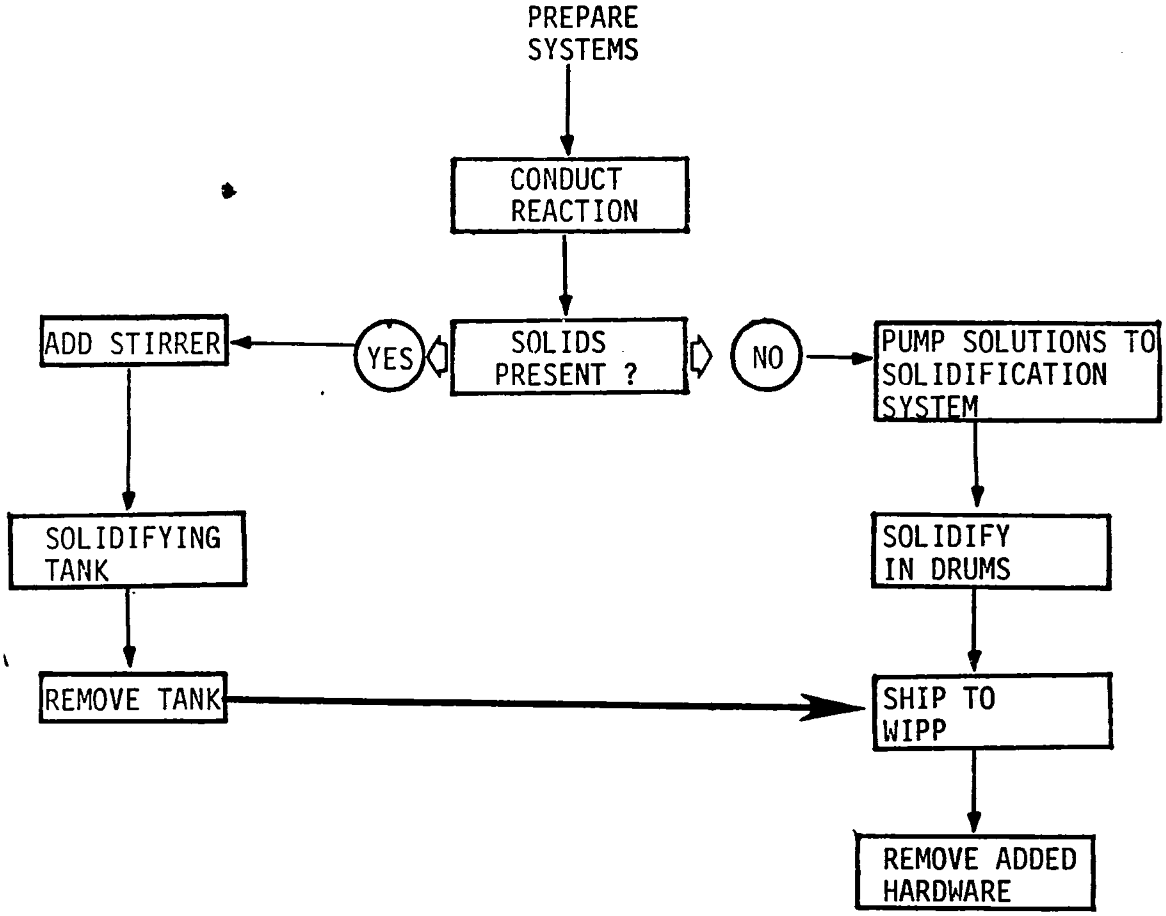

While extensive development of the recommended process is not required, some testing will be necessary to better define operating parameters and to evaluate the behavior of the actual resin product which may be charred, or extensively cross-linked due to radiolysis. This change in state may have effected the dispersability, solubility, and other properties of the resin. The tests which should be run include:

- Cementation of the actual resin product in the tank.
- Dissolution of the actual resin product in the tank.
- Reactions rates of this specific resin as a function of reactant concentration and temperature. Heat evolution rate needs to be measured.
- Pretreatment and solidification or peroxide reaction product liquids.

VI. REFERENCES

1. N. F. Bibler and E. G. Orebaugh, Iron-Catalyzed Dissolution of Polystyrene-sulfonate Cation Exchange Resin in Hydrogen Peroxide, DP-MS-74-56, E. I. duPont de Nemours & Co.

2. Feasibility of Applications of Microwave Technology for Nuclear Power Plant Radioactive Waste, EPRI-NP-2334, Chem-Nuclear Systems, Inc., Bellevue, WA, April 1982.

3. R. E. Lerch, Division of Waste Management, Production, and Reprocessing Programs Progress Report for January-December 1976, HEDL-TME 77-40, pp. 33-41, April 1977.

APPENDIX C

TMI-2 RESIN REMOVAL RADIATION AND SHIELDING ANALYSIS

Westinghouse Hanford Company

A. D. Wilcox

Westinghouse Hanford Company

From: Radiation and Shield Analysis
Phone: 6-2414 W/D-1
Date: March 8, 1983
Subject: SHIELDING ANALYSIS OF TMI-2 DEMINERALIZER RESIN REMOVAL SYSTEM

To: W. W. Jenkins W/B-84

cc:	RA Bennett	W/D-3	LM Martinson	W/A-51
	WL Bunch	W/D-1	EJ Renkey	W/B-17
	MK Mahaffey	W/B-63	DL Swannack	W/B-84
			ADW:File/LB	

References: (1) Memo, DL Swannack to WL Bunch, "TMI-2 Demineralizer Resin Removal," January 14, 1983.

(2) Memo, MK Mahaffey to EJ Renkey, "Specific Activity of Resin Based on Cs-137," December 17, 1982.

Radiation analyses of the principal components of the TMI-2 demineralizer resin removal system have been completed as requested by Reference 1. Dose rate traverses and shielding curves are provided to assist in the system design.

Analysis

The gamma radiation dose rates for the TMI-2 resin removal system were calculated with the QAD point kernel radiation analysis program. The system components were modeled separately for this analysis. The resin sluice filter tank was modeled as a cylinder with a 2 foot diameter and a height of 3 feet. The lines were modeled as 2, 2.5 and 3 inch diameter pipes with a length of 20 feet.

The gamma ray source terms are based on 3500 curies of ^{137}Cs in the resin in the bottom 2.5 feet of the A demineralizer(2) with an average specific activity of 4.5 mCi/cm^3. The gamma ray source terms are given in Table 1.

Results and Discussion

The unshielded gamma ray dose rates for the filter tank are given in Figure 1 along axial and radial traverses from the tank. The unshielded dose rates from the lines are given in Figure 2 with the shielded dose rates for the tank in Figure 3 and for the lines in Figure 4.

These dose rates are for system components filled with undiluted resin from the A demineralizer. In use, the unshielded dose rate at the desired distance from a component would be found from Figure 1 or 2. This value would be reduced by the dilution in the resin removal system. Then the necessary attenuation would be calculated and the corresponding amount of shielding determined from Figure 3 or 4.

As an example, at 10 feet from the 2.5 inch line, the unshielded dose rate is $\sim$3200 mrem/hr from Figure 2. If the dilution were 4 to 1, this would become 3200/5 = 640 mrem/hr. If the desired dose rate were 2 mrem/hr, the attenuation would be 640/2 = 320. In Figure 4 the unshielded contact dose rate for the 2.5 inch line is $\sim 3.2\times10^5$ mrem/hr. Attenuated by a factor of 320, this becomes $3.2\times10^5/320 = 10^3$ mrem/hr. In Figure 4 it can be seen that it takes 2.2 inches of lead or 4 inches of steel to reduce the dose rate on the 2.5 inch line to 10^3 mrem/hr. This is also the amount of shielding that will be needed to reduce the dose rate to 2 mrem/hr at 10 feet from the 2.5 inch line for the resin diluted 4 to 1.

The dimensions of some system components, such as pumps and valves, are not specified at this time. These components will be less significant as radiation sources than the filter tank, and Figures 1 and 3 could be used to provide very conservative estimates of dose rates and shielding for such components.

In view of the uncertainties associated with the radioactivity in the demineralizers and in the distribution within the resin removal system, it is recommended that the shielding be conservative.

A. D. Wilcox

Concurrence:

W. L. Bunch, Manager
Radiation and Shield Analysis

llr

Attachments: Table 1
Figures 1-4

TABLE 1

TMI-2 DEMINERALIZER RESIN GAMMA PHOTON SOURCE TERMS

Group #	Mean Energy (MeV)	Gamma Source Terms (photons/sec-cm^3)
1	0.15	2.5+6
2	0.25	0.0
3	0.35	0.0
4	0.475	1.5+6
5	0.65	1.52+8
6	0.825	3.67+7
7	1.0	3.99+5
8	1.225	3.26+5
9	1.475	1.21+6

FIGURE 1 UNSHIELDED TMI-2 DOSE RATES

From Resin Sluice Filter Tank

Containing TMI-2 Demin. Resin

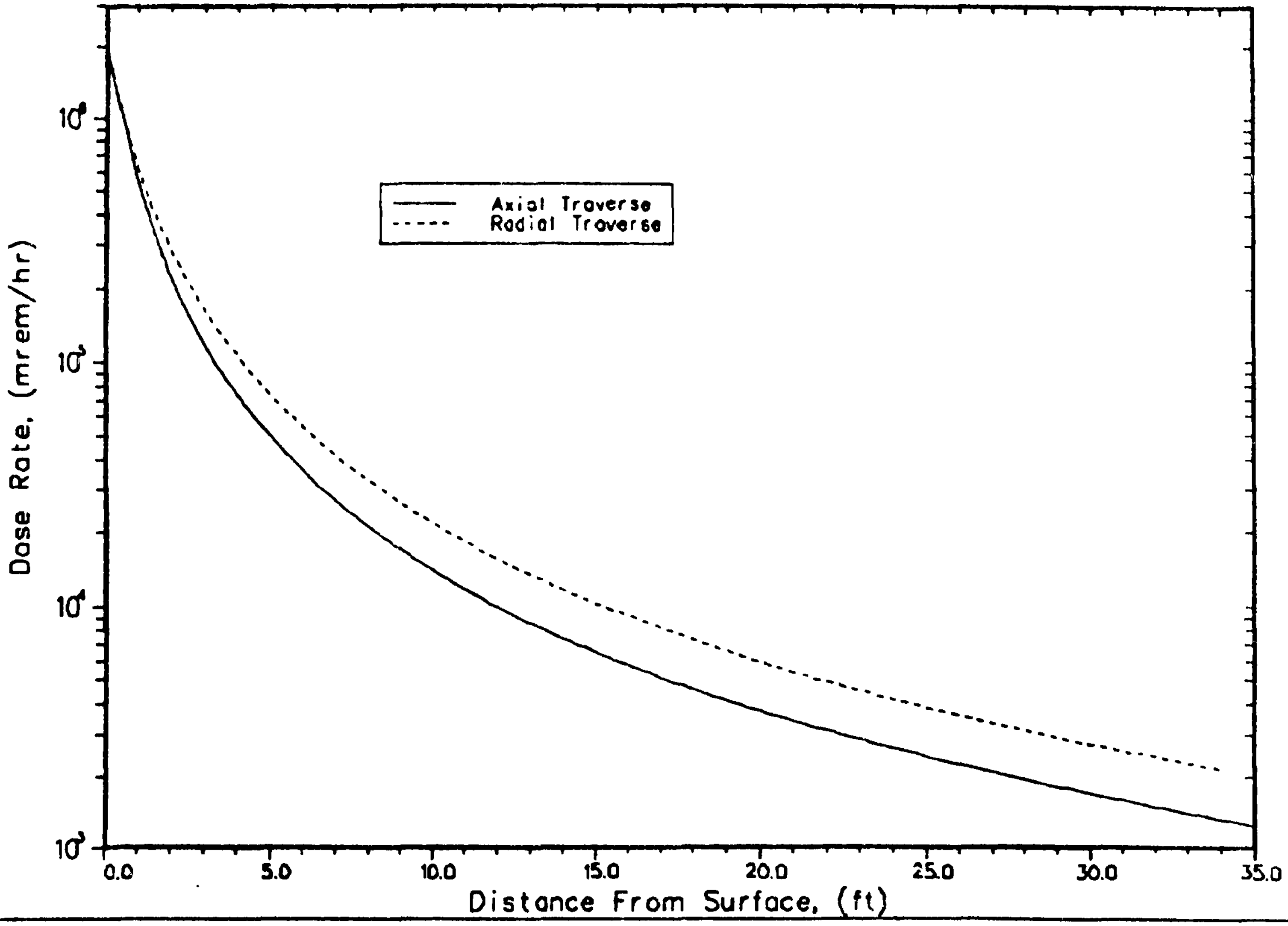

FIGURE 2 UNSHIELDED TMI-2 DOSE RATES

From Resin Sluice Lines

Filled With TMI-2 Resin

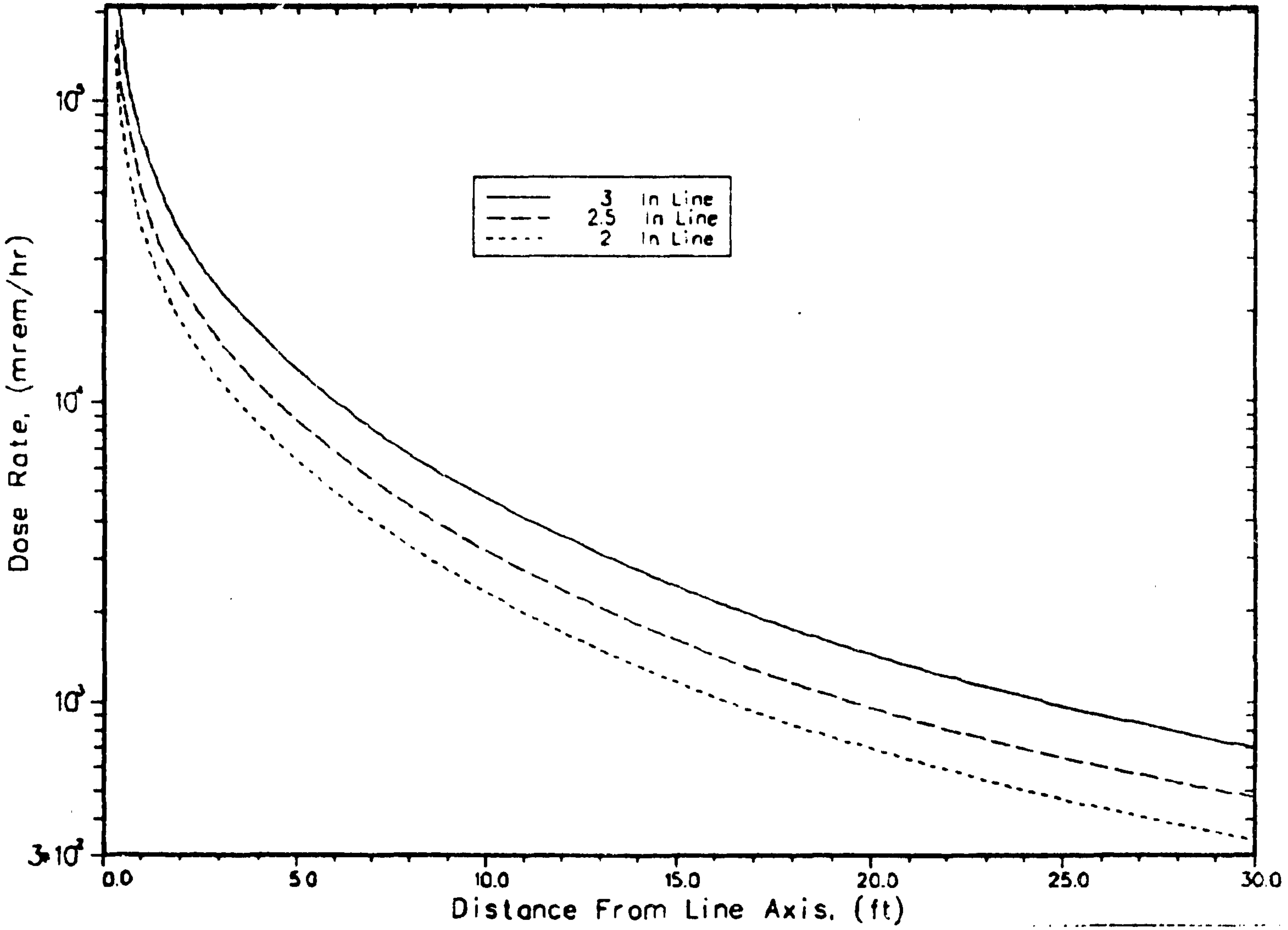

FIGURE 3 SHIELDED TMI-2 DOSE RATES
From Resin Sluice Filter Tank
Containing TMI-2 Demin. Resin
Dose Rates On Shield Surface

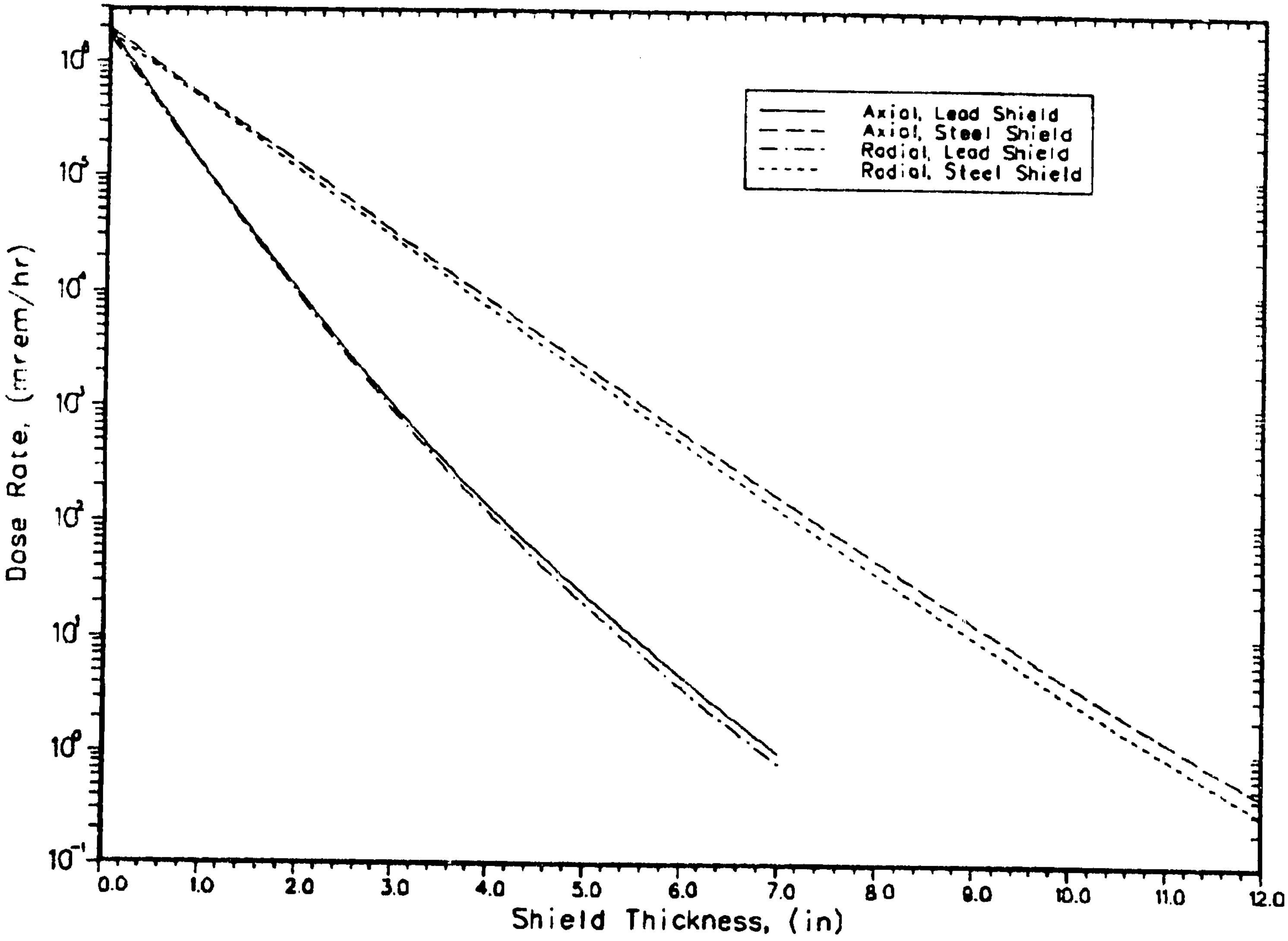

FIGURE 4 SLUICE LINE DOSE RATES

Dose Rates On Shield Surface
Line Size And Shielding Noted
Lines Filled With TMI-2 Resin

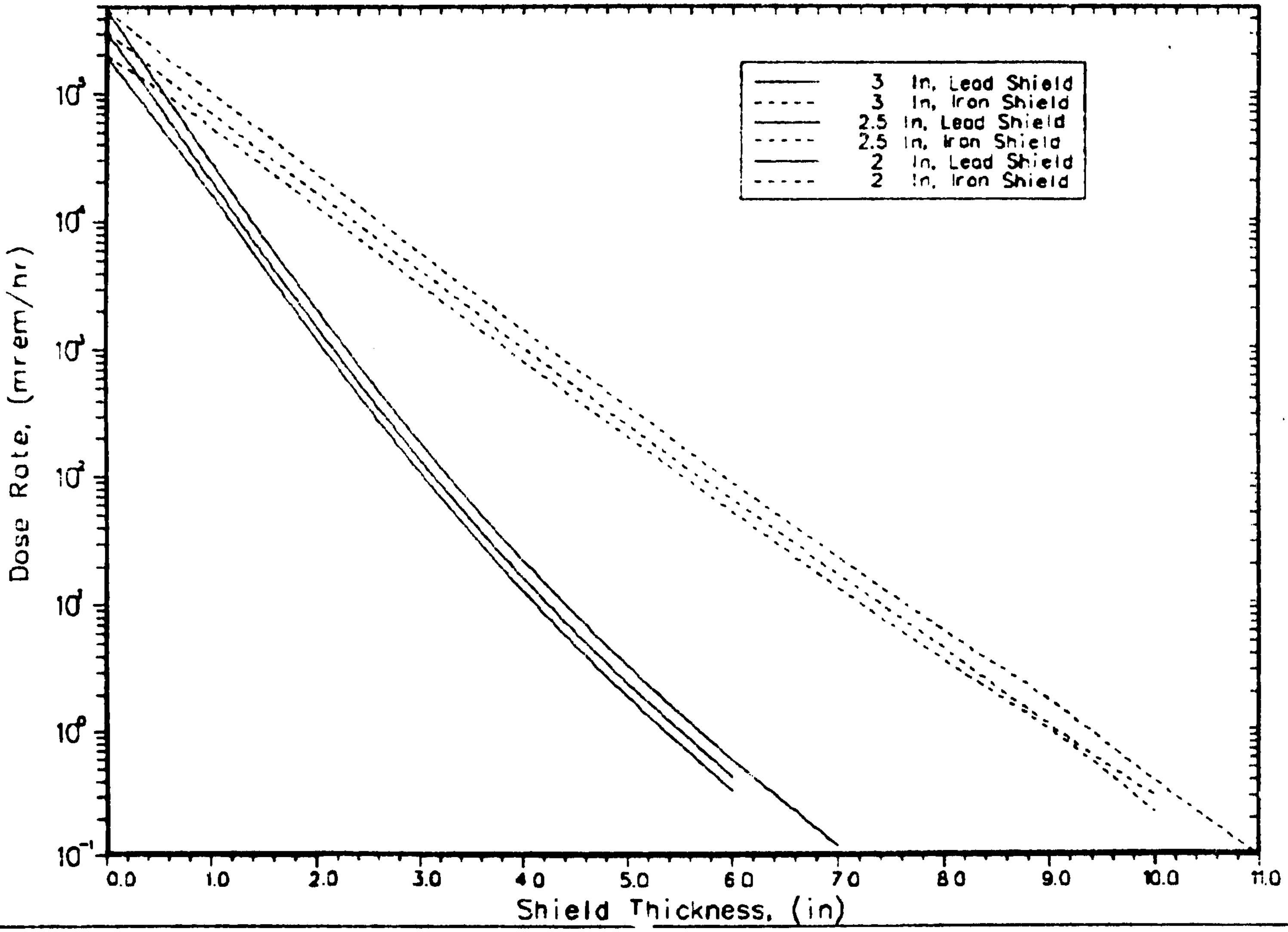

IN-SITU TREATMENT OPTIONS FOR THREE MILE ISLAND DEMINERALIZER RESIN--REPORT NO. 2

Compiled by:
W. O. Greenhalgh
M. D. Crippen

February 1983

IN-SITU TREATMENT OPTIONS FOR THREE MILE ISLAND DEMINERALIZER RESIN

CONTENTS

there is a big question as to what conditions the demineralizer resin was exposed to during the accident. Particularly in question are what changes could have occurred to the resin in the event it was exposed to a temperature excursion above the normal rated 160°F operating temperature and pressures from atmospheric to 150 psi (relief valve pressure setting). A series of small samples were autoclaved at various temperatures in water vapor and nitrogen atmospheres maintained at 150 psi. The four hour autoclaved samples are shown in Figure 1. The temperature at which the autoclaved samples were treated varied going from left to right (1) control-room temp., (2) 200°F, (3) 300°F, (4) 400°F, (5) 500°F, (6) 600°F, (7) 650°F. The respective densities measured were 0.81, 0.71, 0.71, 0.69, 0.70, 0.59, and 0.57.* There was approx. a vial full of resin used in each sample at the start of the run, so the volume shown is indicative of the volume changes that occurred to the resin. It should be noted that the last two samples contain black or carbonized beads. The four hour treatment time was selected because it was the maximum time they could be autoclaved and still be finished in an eight hour shift. The actual TMI resin conditions that we were trying to duplicate could have been much different in regards to the time variable.

In another autoclave experiment, a pint of resin was autoclaved for 130 hours at the 650°F maximum autoclave temperature to better determine what a lenghty temperature-pressure excursion might do to the resin. Figure 2 shows the resin in its Vycor glass reaction container. The container initially was filled to about 90% full. The end product appears to be about 120% of the original container volume. The measured density for the residual resin material is about 0.17 g/cc. The top outer exposed surface is hard to the touch, but the bulk material is very friable and crumbles rather easily. Structurally, there appeared to be little or no bead form, rather the material looked much like a solid foam product with variable sized voids.

---

*Note: These first autoclaved samples were first loaded with LiOH, whereas in later experiments the Rohm and Haas IRN-150 resin was used straight from the package.

Fig. 1: RESIN AUTOCLAVED 4 HR AT 150 PSI NIT.--TEMP: Control, 200, 300, 400, 500, 600, 650°F.

Fig. 2: RESIN AUTOCLAVED 130 HR AT 150 PSI NITROGEN AND 650°F.

B. Heat Treated Resin

Resin material was prepared for dissolution studies by heating a pint of it at 500°F, 600°F, and 750°F in air. Figure 3 shows the mixed bed resin prior to treatment. Figures 4, 5, and 6 show the resin after 6 hours of heat treatment at 500, 600, and 750°F respectively. It should be noted the particle size of the heat treated resin is indeed smaller than the non-treated resin. Also, the resin treated at 600 and 750°F both appear to be completely carbonized. Though apparently carbonized they are not as degrated as the 130 hour autoclaved sample. In contrast the 4 hour autoclaved sample at 650°F shown in Figure 7 is not wholly carbonized, but is more comparable with the 500°F, 6 hour sample shown in Figure 4. The degree of oxidation-dissolution of these residual resin materials should give a good indication of whether the agents will be effective against carbonized resin.

Further heat treatment work was undertaken to gain a better understanding of the amount of degradation that can occur with the resins at carbonizing temperatures. Moist resin was dried overnight, then heated to near constant weight at 500°F (260°C), then 24 hrs at 600°F, and 24 hrs at 750°F. The results are listed in Table I. It should be noted that the resulting weight and volume of the residual resin is a third or less than that of the original moist material. Thus resin heated to the above moderate temperatures would be expected to exhibit substantial degradation marked by significant volume and weight decreases.

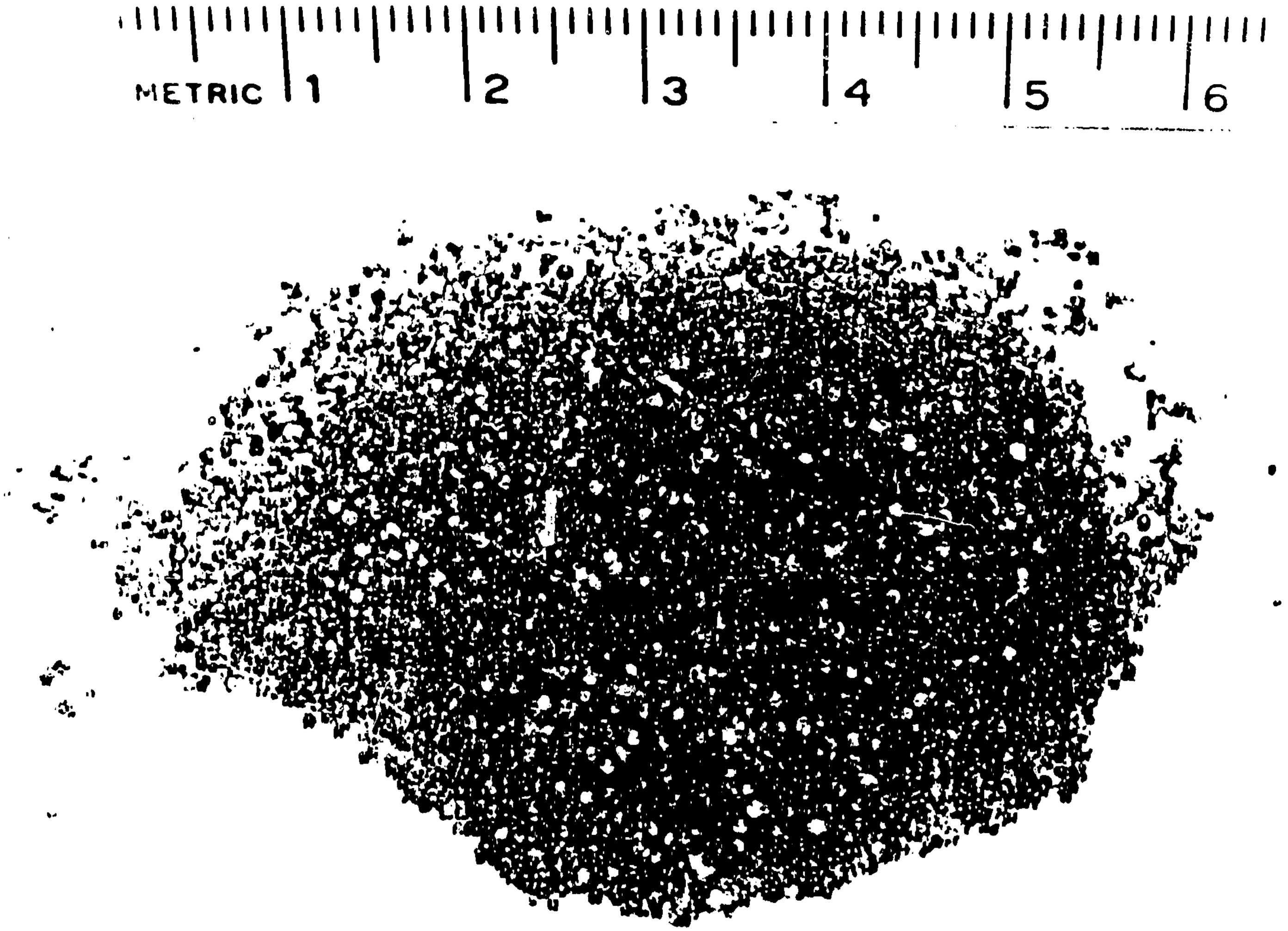

Fig. 3: MIXED BED RESIN--NO TREATMENT.

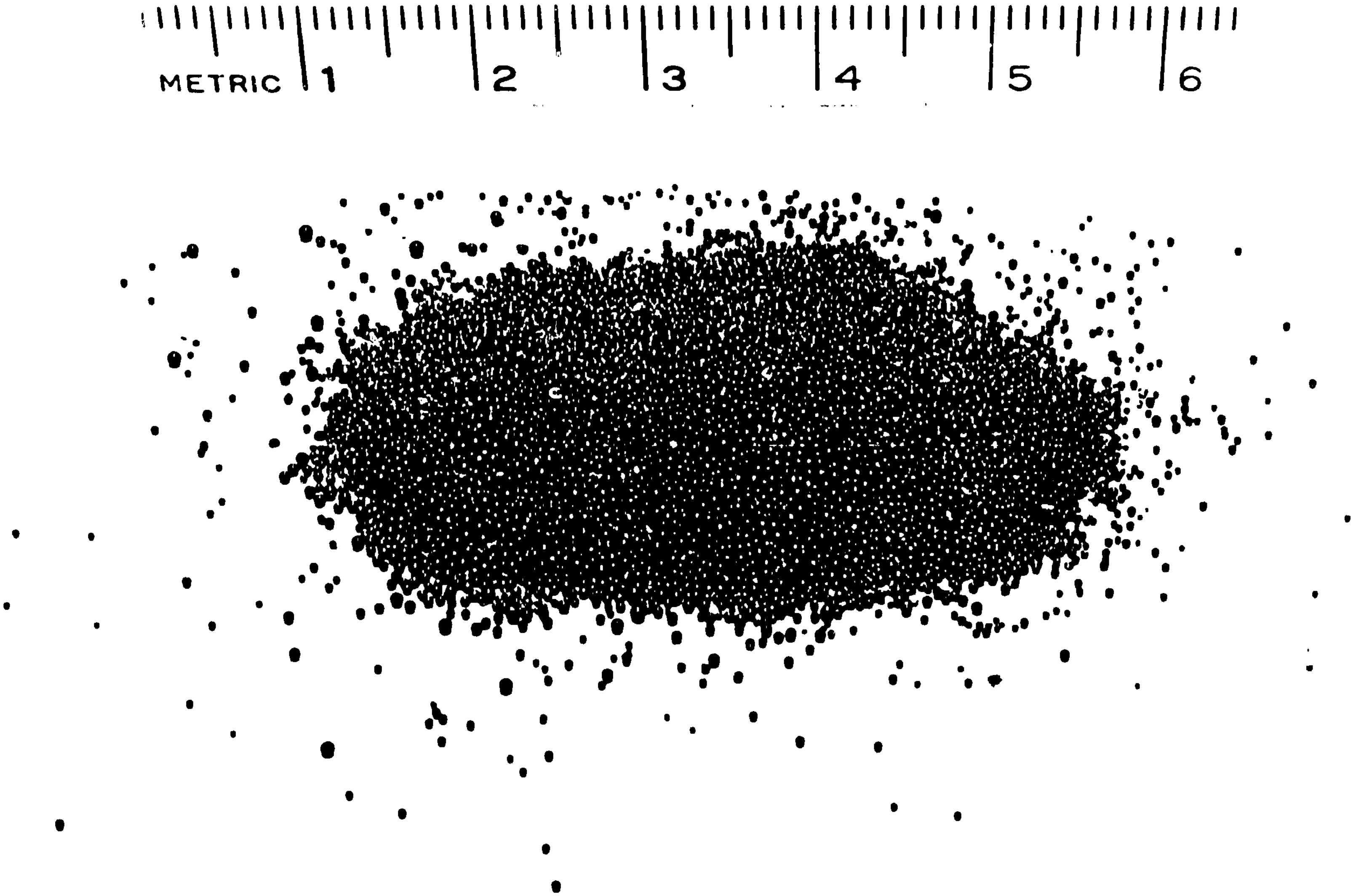

Fig. 4: MIXED BED RESIN HEATED IN AIR TO 500°F FOR 6 HR.

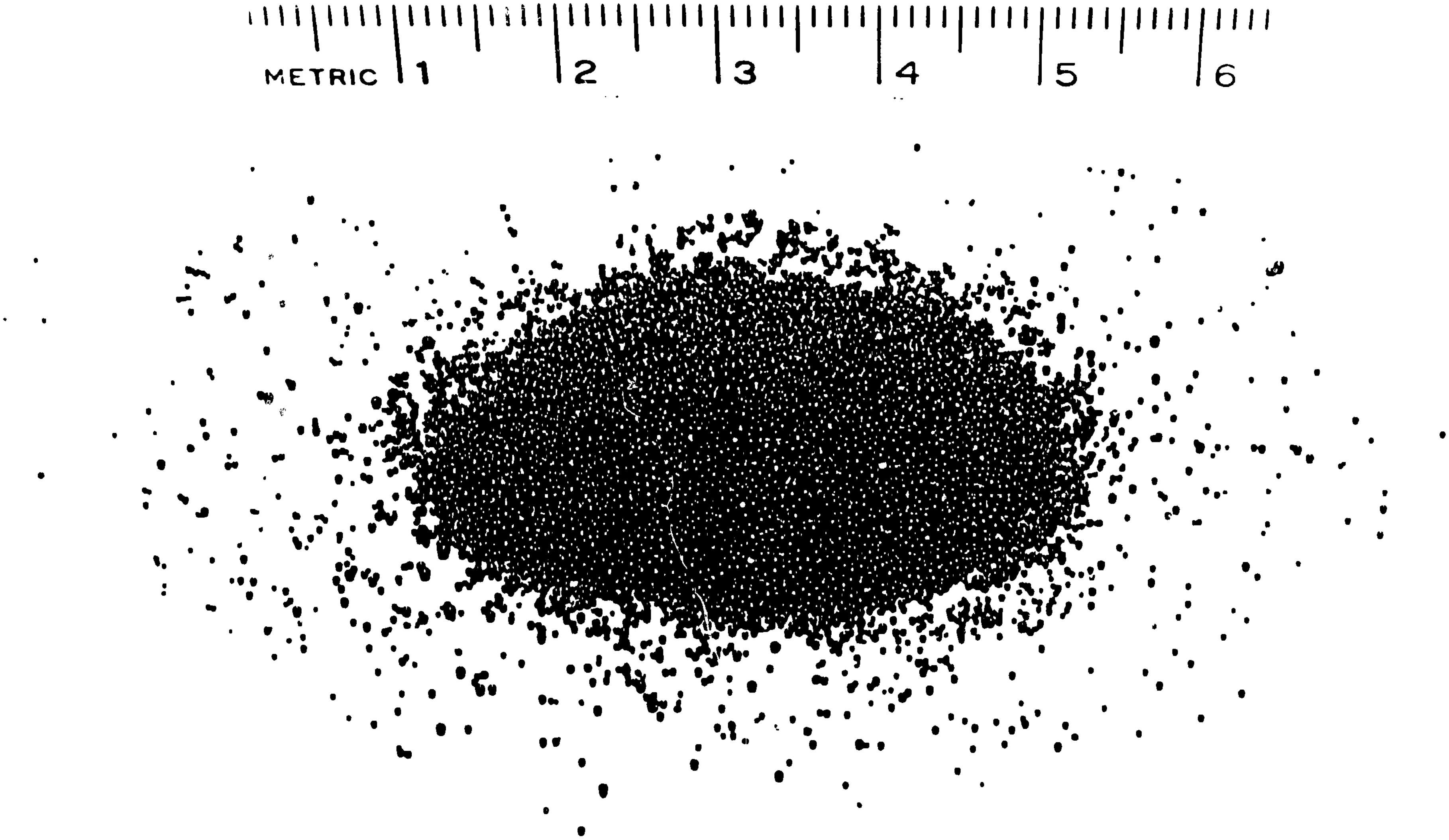

Fig. 5: MIXED BED RESIN HEATED IN AIR TO $600^{\circ}F$ FOR 6 HR.

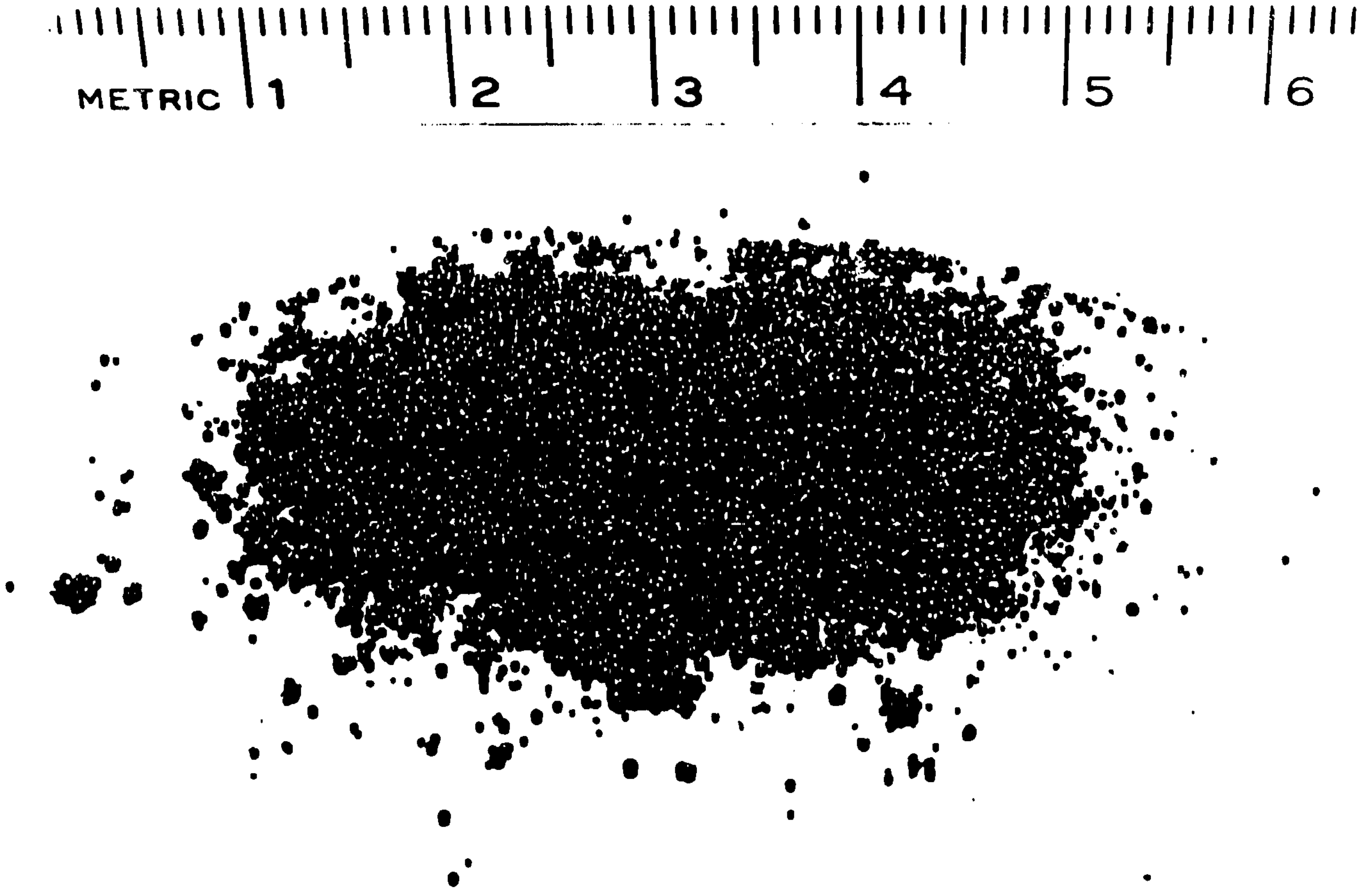

Fig. 6: MIXED BED RESIN HEATED IN AIR TO 750°F FOR 6 HR.

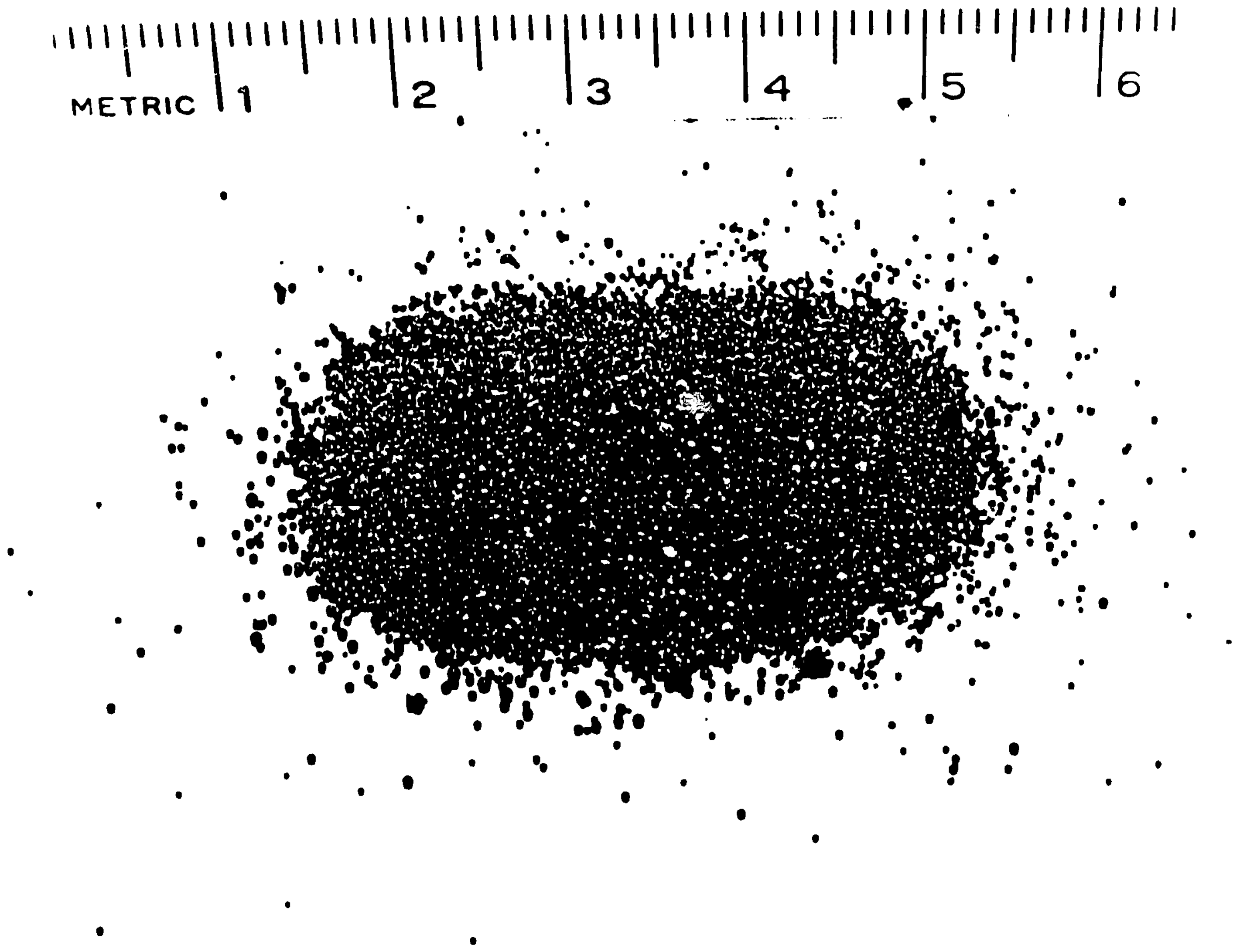

Fig. 7: MIXED BED RESIN AUTOCLAVED IN 150 PSI NITROGEN FOR 4 HR.

Table I: HEAT TREATMENT OF TMI RESIN IN AIR

Resin Treatment	Time Interval (hr)	Accum. Time (hr)	Resin Weight (g)	Weight Percent (%)	Resin Volume (cc)	Resin Density (g/cc)	Resin Color
Control	---	---	66.8824	100	100	0.67	orange
Drying	20 hr in Vac.	---	38.701	58	60	0.65	brown
Bake at 500°F	2	2	27.424	41	44	0.62	dk brn.
"	2	4	27.254	41	39	0.69	brn,blk.
"	2	6	26.771	40	38	0.70	near blk
"	6	12	25.561	38	36	0.71	black
"	18	30	24.740	37	35	0.72	"
"	22	52	24.275	36	34	0.72	"
"	64	116	23.226	35	33	0.71	"
Bake at 600°F	24	---	20.090	30	33	0.61	"
Bake at 750°F	25	---	16.832	25	32	0.52	"

C. Oxidation /Dissolution of Carbonized Resin

Material from the 500, 600, and 750°F heat treated resin discussed in Section B, and the 130 hr autoclaved resin was tested for low temperature oxidation/dissolution with catalyzed hydrogen peroxide and sodium hypochlorite. The results of the experimental runs are listed in Table II below:

Table II: LOW TEMPERATURE DIGESTION OF CARBONIZED RESIN

Run No.	Resin Description	Reactant Vol.(ml)	Cat. or Additives	Reaction Time (hr)	Ratio Digested	Percent Digested	UO Dis (g/1
			15% HYDROGEN PEROXIDE				
1.	Control	1000	5g Cat.	1 1/4	21.12/27.11	78	---
2.	Control	1000	1g Cat.	1 1/2	dissolved	100	---
3.	500°F	1000	1g Cat.	2	15.59/25.04	62	---
4.	600°F	1300	1g Cat.	7	8.80/17.11	51	---
5.	750°F	1000	1g Cat.	4	1.35/10.92	12	---
6.	130 hr, 650° Auto.	1500	1g Cat.	8	0.33/9.52	3	
7.	" "	1500	No Cat., 3 M HNO_3	6	0/6.14	0	---
8.	Control with UO_2 Fuel Pellets	1100	1g Cat.	4	All Degraded	100% fines	0.06
			12-15% SODIUM HYPOCLORITE				
1.	Control	2000	---	8	17.07/24.80	69	---
2.	Control	1500	20g $Mg(CLO_4)_2$	4	26.57/27.04	98	---
3.	500°F	1000	---	8	11.53/21.67	53	---
4.	600°F	1500	---	8	10.73/19.98	54	---
5.	750°F	1000	---	4	4.45/7.95	56	---
6.	750°F	2500	---	24	14.074/19.69	71	---
7.	130 hr, 650° Auto.	1500	19g $Mg(CLO_4)_2$	6	0.69/5.41	13	---
8.	Control with UO_2 Fuel Pellets	1000	---	6	12.25/18.55	66	<0.01

IV. CONCLUSIONS

A. Hydrogen peroxide processing cannot be relied upon to digest the TMI resin if it is completely carbonized.

B. Sodium hypochlorite processing will perform better than hydrogen peroxide on digesting carbonized resin even though the hydrogen peroxide is much better digesting agent on the non-carbonized resin.

C. Hydrogen peroxide appears to have some small dissolving affect on UO_2 type fuel pellets, particularly if the pellets are broken or powdered. No fuel affect was detected with the sodium hypochlorite agent.

D. No work was performed with the higher temperature oxidizers/dissolvers. However, enough work has been done in the past on sulfuric-nitric acid digestion work to know that the carbonized resin could be completely oxidized and dissolved by that system.

E. Moderate temperature treatment of the resin in itself significantly degrades the resin, typically to about 1/3 the original volume and weight of the resin. The resin beads themselves,if not destroyed, shrink in size allowing easier passage of treatment or immobilization liquid.

V. RECOMMENDATIONS

1. An attempt should be made to determine the relative status of the Demineralizer resin beds, namely, if the the bead resins are (a) reasonably intact and non-degraded;(b) partially degraded or (c) extensively degraded and carbonized.
2. If the resin is considered reasonably intact and non-degraded and dissolution of the resin is sought, then use of the low temperature iron catalyzed hydrogen peroxide is recommended as a first option*and sodium hypochlorite as a second option.
3. If the resin is considered partially degraded, then low temperature chemical dissolution is not nearly as practical; however, alternating dissolution cycles of catalyzed hydrogen peroxide followed by sodium hypochlorite should be sufficient to convert the resin to a solution or a fine slurry.
4. If the resin is considered fully degraded and carbonized, then a high temperature dissolution such as sulfuric-nitric acid at about 250°C (480°F) is recommended. If this seems too difficult then the low temperature sodium hypochlorite dissolution is recommended with provision for lengthy digestion times and lots of liquid reactant.

---

*Note: Suggested dissolution approach: Add 0.001 $\underline{M}$ iron catalyst and 0.001 $\underline{M}$ acid such as sodium bisulfate with sufficient water to just cover the resin. Then slowly add 30% H_2O_2 while monitoring the gas evolution. Do not add more than one resin volume of reactant until the reaction has consumed most of the added peroxide. A line for liquid condensate or overflow on the off-gas system will be required.

APPENDIX

HAZARDS RESEARCH
CORPORATION
Fire and Explosion Hazards Evaluation

200 EAST MAIN STREET • ROCKAWAY, NEW JERSEY 07866 • 201-627-4560

LITERATURE REVIEW
OF
SOLUBILIZATION OF ION EXCHANGE RESINS
BY HYDROGEN PEROXIDE
AND
BY NITRIC ACID

HRC Report 5272

Appendix A

January 1983

Submitted by:

Robert C. Putnam

Robert C. Putnam, Ph.D.
Senior Scientist

Approved by:

Chester Grelecki

Chester Grelecki, Ph.D.
Chief Scientist

CONTENTS

I. Hydrogen Peroxide Solubilization of Ion-Exchange Resin

A. Cation-Exchange Resins

1. Iron Catalyzed Dissolution of Polystrenesulfonate Cation - Exchange Resin in Hydrogen Peroxide

Ind. Eng. Chem. Prod. Res. Dev. Vol. 15, No. 2, 1976

Behler, N.E. and Orebaugh, E.G.

This article discusses the dissolution of cross-linked polystyrene sulfonate cation-exchange resin (Dowex 50W) in dilute Fe-H_2O_2. The ammonium or sodium form of the resin completely dissolves in 1 hr. at 80^oC using 6% H_2O_2 and 0.001 M Fe^{2+} or Fe^{3+}, in 0.1 M HNO_3 (0.63%).

Factors that impede dissolution are those which decrease sorption of Fe ions, namely: resin form, acidity, radiation dose and Fe complexing agents. To be effective, intermediates from Fe-catalyzed decomposition of H_2O_2 must be formed on the surface or within the resin bead.

Increasing cross-linkage increases dissolution time. It appears that intermediates attack cross-linkages and allow soluble polysulfonates to form. The dissolution is exothermic to the extent of 0.8 kcal/g of dry resin.

The following further observations were made:

a. Fe^{2+} and Fe^{3+} have the same catalytic effect.

b. No dissolution occurred with 0.1 M HNO_3 in the absence of Fe^{2+} and Fe^{3+}.

c. At ≤ 0.003 M Fe^{2+} the resin expanded to 1.5 times the original slurry volume and then dissolved to a clear solution occupying the original volume.

d. At $\geq$0.005 Fe^{2+} the reaction was very effervescent and nearly uncontrollable.

e. Substitution of 0.1 M H_2SO_4 for 0.1 M HNO_3 did not affect the dissolution times indicating NO_3^- is not necessary for dissolution.

f. Dissolution time increased with increasing acidity.

The general test mixture was:

Dowex 50W - X8
200-400 mesh, NH_4^+ form
30 vol. % slurry at 75-80°C
6% H_2O_2
0.1 M HNO_3
0.001 M Fe $(NO_3)_3$

2. Exchange Adsorption of Ions by Organic Zeolites, JACS 64 2818 (1947) Boyd, G.E., Schubert, J., and Adamore, A.W.

Amberlite IR-1 (cationic) with HNO_3 above 2N concentration showed energetic reactions and if H_2O_2 was present complete dissolution of the resin occurred.

A study of those exchange reactions using radioisotopes was made, and it was found that the exchange adsorption of cations from strong electrolytes was governed by the magnitudes of their charges and by the radii of their hydrated ions. An exception is hydrogen ion that apparently can be taken up as H_3O^+ or simply as H^+ depending on the strength of the acid of the base exchanger. With synthetic exchangers having methylene or sulfonic acids on the nucleus responsible for adsorption, hydrogen ion is one of the most weakly adsorbed, in contrast with clays, proteins and many other substances that have weak organic acids (-COOH) or weak inorganic acids (H_2SiO_3, H_3AlO_3), where hydrogen ion is the most strongly adsorbed. It seems probable in the latter that it is adsorbed as H^+. For the synthetic resins the adsorption affinity was:

$$La^{3+} > Y^{3+} >> Ba^{2+} >> Cs^+ > Rb^+ > K^+ > Na^+ > H^+ > Li^+$$

3. Stability of Sulfonated Cross-Linked Ion-Exchange Resin in Hydrogen Peroxide

J. Phys. Chem 61, 832 (1957), William Wood

Cation-exchange resins in the sodium form do not lose their exchange capacity at 150°C under pressure, but they undergo crosslink degradation when heated in the presence of hydrogen peroxide.

Crosslink degradation also occurs in the hydrogen form in the presence of H_2O_2 (10-50%) and is considerably increased by traces of Fe or Cu. Nickel and zinc show no effect. It appears that the degradation is brought about by those cations which bring about the decomposition of H_2O_2.

If the Fe concentration is high enough, the whole resin goes into solution. There was no loss of active groups in the decrosslinked resin on a weight basis. Temperature, peroxide concentration and the quantity of Fe all affect the degree of degradation.

4. Ion Exchange Resin Catalyst Stability in in-situ Epoxidation

J Am Oil Chem. Soc. 35 (7) p. 331 (1958)

Wm. Wood and J. Termini, The Permutit Co.

Effect of Fe Contamination of H_2O_2 on Resin Stability

The following mixture:

10 ml dry resin (Permutit QH) (hydrogen form)
35 mg Fe
35 ml H_2O_2 (10%)

was heated 3 hours at 60°C and the resin completely dissolved.

The Permutit QH originally contained less than 0.005% Fe. The 35 mg. Fe was equivalent to 0.9% Fe on the dry resin weight.

Increasing the resin crosslinking from 10 to 15% is not very effective in counteracting the solubilizing effect of iron contamination.

The DTA (tetrasodium salt) used for complexing the Fe decreased the amount of resin dissolved, but at high Fe levels, its effectiveness was not significant.

Comparison of titration curves of the undegraded and of the solubilized resin indicated some desulfonation and formation of weaker acid groups.

5. Stability of Ion Exchange Membranes in Hydrogen Peroxide

CA. 83, 60022 g (1975)

Zh. Prikl. Khim. (Leningrade) 1974, 47 (9), 2007-10 (Russ)
Bykov, S.J., Gorokhova, A.N.; Gorelova, E.N., Popov, A.A.;
Gracheva, R.F. (U.S.S.R.).

Examination of resistance of various cation exchange membranes to H_2O_2 showed the most stable were heterogeneous membranes based on KU-2, a sulfonated exchange resin on Teflon and polyamide support. Exchange capacity was insignificantly decreased after 300 hr. in H_2O_2 solutions, except for a 40% H_2O_2 solution in which a significant degradation occurred. A decrease of pH with increasing concentration of H_2O_2 solution was observed for KU-2.

B. Anion-Exchange Resins

1. Degradation of Anion-Exchangers in Aggressive Media
Report I. Effect of Hydrogen Peroxide in the Presence
of Copper Sulfate on Strongly Basic Anion-Exchangers
of Type I
CA 84:22582C (1976)
Rev. Poum. Chim. 1975, 20 (6) 839-54 (Fr.)
I. Petrariu, Pamfilia Petrariu, FL. Popescu and
Cornelia Luca
(Inst. Chem. Macromol. "Petru Poni", Iasi, Rom.)

Type I

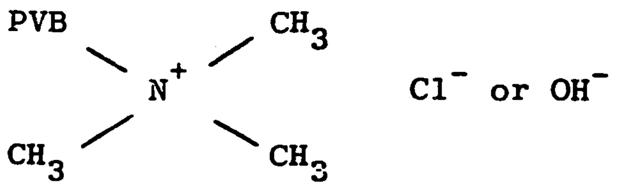

Poly (vinyl benzyl trimethyl ammonium) chloride

In the reaction of the strongly basic anion-exchange resin with H_2O_2 there are three principal processes:

1. Absorption of H_2O_2 by the resin
2. Catalytic decomposition of H_2O_2
3. Decomposition of the resin by H_2O_2

The present work has shown that degradations and decomposition of the resin structure is increased by an increase in temperature of treatment, by an increase in the concentration of H_2O_2 and by the addition of $CuSO_4$. The addition of $CuSO_4$ plays the most important part, catalyzing the decomposition of the H_2O_2 and thus accelerating the degradation process.

During degradation the total basic capacity and the strong basic capacity both decrease, but the weak basic capacity increases.

In the presence of H_2O_2 and $CuSO_4$ deamination of the resin greatly increased with time of treatment. Some dealkylation also occurred, but only slightly increased with time. In the absence of $CuSO_4$ both deamination and dealkylation were negligible. The foregoing data is based on the changes in the strong base capacity of the resin caused by 30% H_2O_2.

In H_2O_2 alone the Cl^- form of the resin is most stable. In H_2O_2 plus $CuSO_4$, the OH^- form of the resin is most stable. If one desires to solubilize the resin, it is evident that H_2O_2 plus $CuSO_4$ should be used with the resin in the Cl^- form. At 80°C using 30% H_2O_2 the resin is completely solubilized regardless of whether it is in the OH^- or Cl^- form. The composition used for study was:

10 ml. 30% H_2O_2
1 g. Resin
0.0188 g. $CuSO_4 \cdot 5\ H_2O$

DTG curves were shown and some energies of activation were estimated for various degradation steps.

Report II Action of H_2O_2 in the presence of $CuSO_4$ on Anion-Exchangers Containing Quaternary Ammonium Groups of Type II.

CA <u>84</u> 141061 s (1976)

Rev. Roum. Chim, <u>1975</u>, 20 (8) 1167-82 (Fr.)

TYPE II

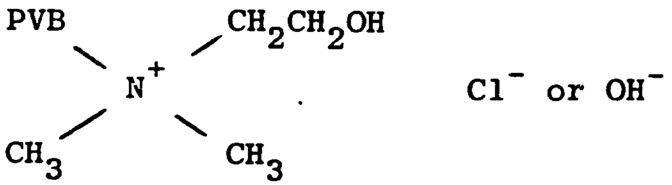

Poly (vinyl benzyl dimethyl-2-hydroxyethyl ammonium) chloride

The results for degradation of the Type II structure showed a general correlation with the results reported for the degradation of the Type I structure.

2. Ion Exchange Resin Solubilization.

Shell Chemical Corp.

Summary of Research Data

Concentrated Hydrogen Peroxide.

A diagram of a system using benzene as representative of ion-exchange resins shows that to avoid the explosive region for H_2O_2/H_2O the maximum starting concentration should not exceed 49%.

Strongly basic resins such as Dowex -1 in the hydroxide form should not be used as the basicity of this form causes excessive decomposition of much lower strength peroxide solutions.

C. Fenton's Reagent and Metal Complexes.

1. Metal Catalyzed Oxidation of Organic Compounds, Sheldon & Koch, Acad. Press. 1981

Fenton's Reagent consists of ferrous salts and H_2O_2, and is an example of the enhancement of the oxidizing power of H_2O_2 by the presence of a metal catalyst.

Many acidic oxides such as MoO_3 and WO_3 catalyze reactions of H_2O_2 by formation of inorganic peracids. This is also true of permonosulfuric acid (Caro's Acid) and the reaction of H_2O_2 with chromates is also well known. In general it has been found that the combination of ROOH and metal catalyst is generally far superior to that of H_2O_2 and metal catalyst for epoxidation. This is attributed to the presence of water in H_2O_2 systems.

For practical use in dissolving ion-exchange resin, a water system is necessary. Experimental work on the comparative effectiveness of H_2O_2 in the absence and presence of H_2SO_4 or using pre-made Caro's Acid should shed light on this matter. The addition of iron salts such as ferric and ferrous chloride and the presence of CrO_3 or chromates may well give results of interest.

For further information on Caro's Acid (peroxymonosulfuric acid) in hydrogen peroxide with sample organic compounds acting as fuel for oxidation see the Shell Chemical Corporation Report mentioned under IB2.

2. Fenton's Reagent-Historical.

Ferrous and ferric ion complexes with carbohydrates are oxidized by H_2O_2. Fenton's reaction here (1) seems similar to the oxidation of glucose and fructose by copper acetate. The amount of peroxide reacting was very dependent upon pH and was nearly constant at pH 4.12-5.28. Küchlin (2) also found that the Fe^{++} catalyst was sterochemically specific in the oxidation of glucose giving different rates with α and β glucose. In the oxidation of fructose he (3) found the oxidation reaches a maximum at pH 3.2-5.4. The effect of temperature on the rate was small in strong acid, but increased with rise of pH. The initial reaction velocity was proportional to the concentration of catalyst, but independent of the presence of Fe^{3+}. The rate was not quite proportional to the sugar concentration and was practically proportional to the H_2O_2 concentration.

Oxidation of glycolic acid by Fenton's Reagent showed that no complexes were formed. The decomposition of H_2O_2

by ferrous salts was stated to be a chain reaction where each Fe^{2+} caused several moles of H_2O_2 to react and that the Fe^{3+} formed was inactive.

The decomposition of H_2O_2 (5) in the presence of ferrous salts (Fenton's Reagent) formed OH and HO_2 radicals and converted various α-amino acids to α-keto acids. Free radicals were also generated by x-ray irradiation of dilute aqueous solutions in the presence of oxygen, and formed α-keto acid and aldehydes.

3. Oxidation by Free Radicals from Fenton's Reagent and by Irradiation.

a. The action of Fenton's Reagent on aqueous solutions of phenol were studied (6). It was found Fe^{3+} produced complexes with phenols and that the Fe^{2+}/Fe^{3+} system entered into redox processes with the products. The Fe^{3+} was again reduced to Fe^{2+} contributing to the stationary Fe^{2+} concentration of the system. With the phenol system it was found particularly difficult to obtain reproducible results. Phenol often reacted violently under conditions where nitrobenzene reacted moderately. However, secondary reactions could be inhibited by relatively small amounts of fluoride ion or pyrophosphate. The action of acid fluoride or phosphate was to complex Fe^{3+} and this influenced the mechanism of the action of Fenton's Reagent itself. Thus it appeared that the rate of Fe^{3+} was more important than previously assumed. It was felt that the OH radical formed was of primary importance in the hydroxylation reaction of phenol. The HO_2 radical was also capable of dehydrogenating an aromatic compound:

$$RH + HO_2 \rightarrow R + H_2O_2$$

This reaction is about 25 kcal less exothermic than the corresponding reaction of the OH radical because of differences in the bond energies of H-OH and $H-O_2H$.

b. X-ray radiation of phenol solutions and their conversion to dihydroxy and other derivatives was studied at length and found to correspond in many ways to the results obtained by using Fenton's Reagent. A total dose of 1×10^6 E.U.(300 min. at a dose rate of 3000 E.U./min) was used as well as lower dosages. At the wavelength of the x-rays used, 1 E.U. equals about 1 roentgen (R). Oxygen present in water saturated with air was found to suffice for only a dose of 6×10^4 E.U. For greater dosages, the experiments were carried out in the absence of oxygen. Solutions saturated with oxygen at 1 atm were only sufficient for a dose of ca 2.5×10^5 E.U.

c. Experiments with a mixed γ-ray-neutron source were carried out. The neutron source was a 1 g. Ra-Be source giving ca 1×10^{10} γ-ray quanta and ca 1×10^6 neutrons per second so that only a small fraction of the energy absorbed was due to the neutrons. Earlier work was confirmed that with a constant γ-ray intensity the yield was about twice as great when the mixed radiation was used. Considering the low neutron intensity this was remarkable. If carried out in the presence of oxygen, the difference between the yields from γ and γ-n sources disappears. Hence the cause of the difference in vacuum is the formation of oxygen by neutrons.

d. Similar work to the treatment of phenol was carried out with chlorobenzene in aqueous solution using Fenton's Reagent and separately using x-radiation. The data indicated action by HO and HO_2 radicals as before and correlated with other data. Dechlorination was pH independent and increased with oxygen present.

e. Bibliography

(1) A. Th. Küchlin and J. Boeseken, Proc. Acad. Sci. Amsterdam 32, 1218-34 (1929)

(2) A. Th. Küchlin, Rec. Trav. Chim, 51, 887-913 (1933)

(3) A. Th. Küchlin, Biochem Z. 261, 411-24 (1933)

(4) Stefan Goldschmidt and Stefan Pauncz, Ann. 502, 1-19 (1933)

(5) G.R.A. Johnson, G. Scholes, and J. Weiss, Science 114, 412-12 (1951)

(6) G. Stein and J. Weiss, J. Chem. Soc, 1951 3265-74

(7) G.R.A. Johnson, G. Stein and J. Weiss, J. Chem. Soc 1951 3275-8

II. Nitric Acid Solubilization of Ion Exchange Resin

A. Ion-Exchange Resins

1. Process for Making Water-Soluble Sulfonated Vinyl Aromatic Resins.

USP 2,669,557 (1953)

Robert M. Wheaton assignor to the Dow Chemical Co.

HNO_3 (30-90%), preferably at 35-70%, is used at 1-10 parts by weight of solution per part of copolymer at 90-120°C with agitation to effect solution with NOx being vented from the reaction zone. The solution is then evaporated in vacuo and the residue crushed and used as a thickening agent for synthetic latices or as a dispersing agent.

B. Hazards Using Nitric Acid

1. Explosion Hazards Using Nitric Acid in Ion-Exchange Equipment

Chem. Eng. Nov. 17, 1980 Calvin Calmos,

Water Purification Associates

This article discusses the hazards in using nitric acid in contact with weak and strong base anion-exchangers, and with strong acid cation-exchangers. The incidents noted deal with HNO_3 concentrations of 12% and upward. The obvious dangers of using a strong oxidizing agent with organic materials is apparent and indicates the use of HNO_3 with ion-exchange resins is to be avoided. If used, it should not be allowed to remain present with the resin in stagnant condition, nor should treatment occur over long periods or at greatly elevated temperatures. Nitric acid should not be used where ammonium ions are present because of the possible formation of ammonium nitrate or of ammonium salts of nitrated species.

III. Effect of Radiation on the Acid Solubilization of Ion-Exchange Resins

HRC Report 4137C, February 18, 1980, R. Putnam & C. Grelecki.

The purpose of this program was to run safety qualification tests on a waste disposal procedure. A digestion flask containing sulfuric acid was brought to 250-260°C. Nitric acid (70%) was fed into the sulfuric acid at a given rate. A prepared sample of ion exchange resin was then injected and the decomposition gases measured and analyzed. Samples of cationic and anionic resins were tested untreated, acid treated, and radiation treated. The radiation treated samples were each given an integrated exposure of 200 Mr (megarads).

Dowex 50 x 8 (cationic) at the highest feed levels of the resin, gave a higher yield when irradiated than when untreated. Dowex 1 x 4 (anionic) gave reduced gas yields both when acid treated and when irradiated.

Permutit SK (anionic) showed some increase in gas yields when irradiated.

The maximum rate of gas evolution was high only for the following.

Dowex 50 x 8 (cationic)	untreated
"	acid
"	irradiated
Dowex 1 x 4 (anionic)	untreated

The exposure of the TMI-2 Demineralizers as of March, 1982 is reported to have been about 2000 Mr.

A tank read 120 R/hr. 2 feet from tank wall.

B tank read 20 R/hr 7 feet from tank wall.

The readings were made about March, 1982.

IV. Stability of Hydrogen Peroxide

A. General Stability of Hydrogen Peroxide

ACS Monograph #128 (1955) by Schumb, Satterfield, and Wentworth

1. Surface to Volume Ratio

Experiments in Pyrex glass vessels at 50°C has shown that the decomposition rate of pure hydrogen peroxide solution is roughly proportional to the surface to volume ratio over a considerable range; i.e. the heterogeneous decomposition on the walls of laboratory-size vessels is usually far faster than the homogeneous decomposition. (1, 6)

Decomposition is greatly affected by the condition of the surface, the presence of inhibitors, the alkalinity of the glass, and passivation by HNO_3 or H_2O_2

2. Effect of Temperature

Decompositon rates of very pure unstabilized H_2O_2 solutions at temperatures of 50 to 70°C have shown the rate to increase by a factor of 2.2 for a 10°C rise. The temperature coefficient a is defined by:

$(T_2-T_1) \log a = 10 \log (k_2/k_1)$ where k_1 and k_2 are the reaction rate constants at temperatures T_1 and T_2. Data well support this. Measurements indicated a ratio of 40/1 for the increase from 50°C to 96°C. The equation gives a 38/1 ratio.

When ferric salts are added the coefficient is less than 2.2 indeed as low as 1.6. With a stannate stabilizer it was never below 2.2 and sometimes rose to 2.4. The temperature coefficient is an approximation to the Arrhenius expression and would not be expected to apply over a wide temperature range.

At room temperature 90% H_2O_2 will suffer less than a 1% decrease in content in several months. At 100°C it will lose 2% in 24 hours.

3. Effect of pH on Pure Hydrogen Peroxide

Measurement of decomposition vs. pH of H_2O_2 adjusted by addition of NaOH or H_2SO_4 shows a minimum around 4.2 for different concentrations from 10.9-65.6% H_2O_2 at 50°C. For the pH measurement the solution was diluted 1:10 to obtain all positive pH values for comparison since measurement at greater than 90% H_2O_2 by the glass electrode gave negative readings. For lower concentrations of H_2O_2 the effect of pH becomes increasingly important. Some authors think the variations are due to impurities introduced by the agents used to adjust the pH (12, 13). Vary careful experiments (1) with very pure anhydrous H_2O_2 showed a decrease in stability always occurred with a decrease in pH regardless of stabilizer content or acid used.

For ordinary H_2O_2 at low concentration (10.9%), the decomposition rate rapidly increased proceeding from pH 3.5 to 2.5.

4. Effect of pH on Impure Hydrogen Peroxide

Trace metals in 90% H_2O_2 show a peak in the decomposition vs. pH curve at about 3.5 pH, not found with pure H_2O_2. The peak may occur at a very small interval (about one pH unit). With Fe^{3+} (0.3 ppm at 30°C) it occurs at 3.7 pH. This has been interpreted (3, 14) as due to hydrolyses of the ferric salt to a colloidal hydrous oxide of large catalytically active surface in contact with the H_2O_2 solution. It is known that the growth of micelles from aqueous ferric salts reaches a maximum at about pH 3.6. The rapid fall in decomposition rate with further increase of pH (say to 4.0) is believed to be due to coagulation of the colloid and consequent reduction of surface area.

Increasing the iron concentration increases the decomposition rate for 90% H_2O_2 at 50°C, and the rate of increase varies with the pH. At pH 1.6 raising the Fe^{+++} concentration from 0.3 to 1.0 raises the decomposition rate from 0.030 to 0.050% per hour. At pH 3.2 the rate rises from 0.067 to 0.165% per hour.

When considering the use of catalyzed H_2O_2 to dissolve ion exchange resins, the existence of a peak of decomposition for Fe^{3+} at about pH 3.5, signifies that there is an area where decomposition and consequent dissolution may become very rapid. This can be of advantage for the dissolution, but should be controlled by using a low concentration of H_2O_2 and a controlled feed. Knowing the overall energy that can be released for the reaction would enable one to estimate the temperature levels that may be reached.

5. Effect of Radiation on Stability

It is well known that ultraviolet light causes decomposition of H_2O_2 (16) and that reducing the radiation reaching the material increases the stability. Other reference to radiation in work performed by Hazards Research Corp. has been discussed under III - Effect of Radiation on the Acid Solubilization of Ion-Exchange Resins.

6. Representative Stability Studies

Rates of decomposition have been reported as follows for 90% unstabilized peroxide (12):

30°C	1%/yr.
66°C	1%/wk.
100°C	2%/day
140°C	rapid

Pressure had no effect on the rate.

It has been found that mixed catalysts may show a greater effect on the decomposition rate than the sum of the two separately. For 90% H_2O_2 the following rates were found:

0.16 ppm	Fe^{3+}	0.010%/hr.
0.16 ppm	Cu^{2+}	0.015%/hr.
Combined		0.085%/hr.

One observer (22) noted that the presence of chloride in with the metal cation increased the decomposition rate 40-fold, showing the catalytic effect of an anion rather than a second cation.

Agitation of H_2O_2 solution (23) may cause bubbling due to release of oxygen supersaturation but no increase in the decomposition rate occurs due to agitation.

1. E.M. Roth and E.S. Shanley, Inc. Eng. Chem, 45, 2343 (1953)
3. W.C. Schumb, Ind. Eng. Chem. 41, 992 (1949)
6. W.C. Schumb, unpublished work of the M.I.T. Hydrogen Peroxide Project.
12. E.S. Shanley and F.P. Greenspan, Ind. Eng. Chem. 39, 1536 (1947)
13. V.W. Slater, Chemistry & Industry, 1945, 42
14. W.C. Schumb and J.R. Doyle, Abstracts of Papers, XIIth Int. Cong. of Pure and Appl. Chem., p. 508, Sept. 1951.
16. J. Buchi and V. Kurer, Pharm. Acta. Helvetica, 15, 59 (1940)

22. N. Uri, J. Phys. and Colloidal Chem. 53, 1070 (1949)

23. F.A. Gilbert and N. Michaelis, P.B. Report 98779 (1948)

B. Purification of Hydrogen Peroxide

USP 2, 676, 923 (1954) James H. Young to E.I. du Pont de Nemours and Company

This related to the purification of H_2O_2 by cation-exchange resins (Dowex 50) using a pH of 0-3.6 (preferably 0.7-2.5), to remove heavy metals. It is ineffective if more than 1% of the ion-exchange capacity is used for binding the heavy metals.

Crude H_2O_2 was completely decomposed by heating 10-15 hours at 100°C. After passage through the resin colums the losses of active oxygen were only 0.5 - 3.0 % in 15 hours at 100°C.

Purification of 25-75% H_2O_2 is most practical. If the amount of bound impurities is very-high, contact with the resin may be dangerous. H_2O_2 (35%) will react with resin heavily contaminated with iron. If the resin is regenerated first to at least 99% of its capacity, little decomposition of peroxide or reaction with the resin occurs.

To determine when the resin needs regeneration, treat it with twice its weight of 10% sulfuric acid for 10 minutes. Drain it off and determine the iron content by the potassium thiocyanate calorimetric method. When the Fe content exceeds

30 ppm, it needs regeneration. Preferably, it should be regenerated when the Fe content exceeds 15 ppm. When ready for use the Fe content should preferably be 0-1 ppm.

Ordinary temperatures up to 40°C may be used for treatment of the H_2O_2. The concentration of H_2O_2 should be at least 25% but preferably not above 50% or it may explode.

C. Decomposition of Hydrogen Peroxide

1. MCA Data Sheet

Mfg. Chemists Assn.

Chemical Safety Data Sheet SD-53 (1969)

Many contaminants at amounts less than 0.1 ppm can greatly increase the decomposition rate of hydrogen peroxide solution. Cu, Cr and Fe are especially harmful. Alkaline hydrogen peroxide solutions are even far more susceptible to decomposition by metal contaminants, the rate being greatly increased over the comparable acid solutions.

The rate of decomposition is affected by temperature and increases 2.2 fold for each 10°C in the range from 20 to 100°C.

Note that a heat rise of 1-2°C/hr. at 30-35°C means that eruption is certain unless checked by external cooling, dilution or stabilization.

2. Hydrogen Peroxide Determination in the Presence of Chromate.

Anal. Chem. 26 355 (1954) Joseph Rynasiewicz.

Knolls Atomic Power Lab., General Electric Co., Schenectady, New York

Ion-exchange resins were used to remove chromate from hydrogen peroxide solutions to enable the solutions to be analyzed. Mixed resins and anionic resins were found to adsorb H_2O_2 at high pH, which could be released for analysis by acidification. The rate of decomposition of peroxide in slightly alkaline sodium chromate solutions was dependent on pH, temperature, and chromate concentration.

The amino group in the anion-exchange resin appears to be responsible for the uptake of hydrogen peroxide.

D. Concentrated Hydrogen Peroxide

Summary of Research Data on Safety Limitations (1959)

Shell Chemical Corporation

1. The liquid phase system containing only H_2O_2 and H_2O appears safe from explosion at room temperature up to about 96% H_2O_2

2. The vapor phase of H_2O_2/H_2O system is explosive when it contains 26 mol% (40 wt.%) at one atmosphere.

3. Explosive regions in systems of hydrogen peroxide and organic compounds indicate that explosions are generally not possible if the final solutions contain less than 30% (by wt.) H_2O_2.

4. Ion-exchange resins or plastic such as PVC can explode with concentrated H_2O_2.

5. Immiscible systems can explode at interfaces.

6. The use of H_2SO_4 with H_2O_2 leads to the formation of peroxymonosulfuric acid (H_2SO_5). This material may cause detonations with organics. Quaternary systems (anionic resins) are conveniently acidified with H_2SO_4 rather than with HNO_3 which may lead to nitration and explosive decomposition. However, in the presence of H_2O_2, the concentration of H_2SO_4/H_2O must be kept low to avoid forming H_2SO_5. Explosion studies with sample organics with $H_2O_2/H_2SO_4/H_2O$ have been performed and indicate the existence of an induction period during which H_2SO_5 is being formed, before autodetonation occurs.

E. Rate of Hydrogen Peroxide Decomposition in Nitric Acid Solutions.

C.A. 77 144276g (1972)

Ind. Eng. Chem., Process Des. Develop.

1972, 11 (4), 547-9 (Eng.)

Miner, Frank J.; Hagan, Paul G., Dow Chemical Co.

Rate constants were determined for the decomposition of H_2O_2 in HNO_3 solutions as a function of HNO_3, H_2O_2, and an impurity mixture (Fe, Cr, Rb, Na, Cu)

HNO_3 (1.7-4.1 M) (10.2-22.8%)

H_2O_2 (2.3-4.9 M) (7.7-15.2%)

The runs were carried out at the boiling point.

The effect of HNO_3 concentration on the rate constant was small at 1.7-2.9 M, but increased at 2.9 - 4.1 M. The effect of the impurity concentration was linear increasing over the whole range. the H_2O_2 concentration had no effect.

F. Structure and Catalytic Properties of Chromium Complexes on Cation - Exchange Resin Surfaces

React. Kinet. Catal. Lett. 1977 6 (4), 443-8 (Eng.)
Mikhailova, D; Andrew, A. (Inst. Org. Chem., Sofia, Bulg.)
CA 87 74025 e (1977)

The type of bonding of Cr^{3+} on the surface of cation exchange resin was studied. Complexes of Cr^{3+} with ethylene diamine were obtained by direct synthesis on the surface. Coordination to N bases increases the catalytic activity of Cr^{3+} ions in H_2O_2 decomposition.

G. Study of the Catalytic Activity of Ion-Exchange Complexes in a Hydrogen Peroxide Decomposition Reaction

Kopylova, V.D., Frumkins, E.L; Mochalova, L.A.; Saldadze, K.M. (Mosk, Kooper. Inst., Moscow, USSR) Katal, Soderzh. Nanesennye Komplesky, 1980, 25-8 (Russ) Edit. by Ermakov, Yu. I. Akad. Nauk SSSR, Sib. Otd. Inst. Geol. Geofix.: Novosibirsk, USSR.

The catalytic activity of cation exchange KB-4 which contained Cu^{3+} and carboxylic groups was studied in liquid phase decomposition of H_2O_2. It increased with increasing concentration of low mol wt. ligand (NH_3) in the first coordination sphere of Cu^{3+} until the NH_3/Cu^{3+} ratio was 3 and then remained unchanged. The highest catalytic activity was shown by KB-4 containing about 0.5 mg-ion Cu^{3+}/g. KB-4.

V. Summary

The following is an abbreviated summary of the data presented.

S-IA1. Iron Catalyzed Dissolution

a. The Na or NH_4 form of cation-exchange resin (Dowex 50W) dissolves in 1 hour at 80°C in the following mixture:

6% H_2O_2
0.001 M Fe^{2+} or Fe^{3+}
0.1 M HNO_3 (0.63%)

b. Dissolution in (a) is impeded by factors that decrease sorption of Fe ions, such as:

resin form
acidity
radiation dose
Fe complexing agents
increased cross-linkage

c. Dissolution is exothermic (0.8 kcal/g resin)

d. Fe^{2+} and Fe^{3+} have the same catalytic effect.

e. 0.1 M HNO_3 does not effect dissolution in the absence of Fe^{2+} and Fe^{3+}

f. At $\leq$0.003 M Fe^{2+} the resin expanded to 1.5 times the original slurry volume and then dissolved.

g. At $\geq$0.005 Fe^{2+} the reaction was nearly uncontrollable

h. Nitrate ion is not necessary for dissolution.

i. Dissolution time increased with increasing acidity.

S-IA2. Exchange Adsorption of Ions by Organic Zeolites

a. Amberlite IR-1 (cationic) reacts energetically with HNO_3 and dissolves if H_2O_2 is present.

b. Exchange of cations from strong electrolytes is controlled by the size of the charge and the radii of the hydrated ions.

c. Hydrogen ion may be taken up as H_3O^+ or as H^+ depending on the strength of the acid of the base exchanger.

d. Adsorption affinity for synthetic resins shows the following order:

$$K^+ > Na^+ > H^+ > Li^+$$

S-IA3. Stability of Sulfonated Cross-Linked Resin in Hydrogen Peroxide.

a. The Na form of cation-exchange resin does not lose its exchange capacity at 150°C under pressure, but shows cross-link degradation in the presence of H_2O_2.

b. The hydrogen form degrades in the presence of H_2O_2 (10-50%) and more with traces of Fe or Cu. Ni and Zn show no effect.

c. The degradation is brought about by the cations that decompose H_2O_2.

d. Sufficient Fe brings complete dissolution.

e. There is no loss of active groups in decrosslinked resin on a weight basis.

f. The degree of degradation depends on temperature, peroxide concentration, and Fe level.

S-IA4. Ion Exchange Resin Catalyst Stability in in-situ Epoxidation

a. Permutit QH (cationic) in the hydrogen form, dissolved in 10% H_2O_2 in the presence of 0.9% Fe on the dry resin basis, in 3 hours at 60°C.

b. Increasing cross-linking from 10 to 15% is not very effective in counteracting the solubilizing effect of Fe.

c. EDTA decreases the amount of resin dissolved, but is not very effective at high Fe levels.

S-IA5. Stability of Ion-Exchange Membrane in Hydrogen Peroxide.

a. Heterogeneous membranes of a cationic-exchange resin, KU-2, on Teflon and polyamide were most resistant to H_2O_2. Exchange capacity was little decreased in 300 hr. in H_2O_2 except when the concentration was 40% H_2O_2.

b. Increasing the H_2O_2 concentration decreased the pH.

S-IB1. Degradation of Anion-Exchangers in Agressive Media.

a. Reaction of strongly basic anion-exchangers show three principal processes in reaction with H_2O_2

(1) Absorption of H_2O_2 by the resin

(2) Catalytic decomposition of H_2O_2

(3) Decomposition of the resin

b. Degradation of the resin is increased by elevation of temperature, increase in H_2O_2 concentration, and by addition of $CuSO_4$.

c. During degradation, the total basic and the strong basic capacity both decrease, but the weak basic capacity of the resin increases.

d. With H_2O_2 and $CuSO_4$ deamination greatly increased with treatment time. Some dealkylation occurred but only slightly increased with time.

e. The Cl^- form of the resin is most stable in H_2O_2.

f. In H_2O_2 plus $CuSO_4$, the OH^- form is most stable.

g. To solubilize using H_2O_2 plus $CuSO_4$, the Cl^- form should be used.

h. At 80°C using 30% H_2O_2 the resin is completely solubilized whether in OH^- or Cl^- form. The composition used for study was:

10 ml. 30% H_2O_2
1 g. Resin
0.0188 g. $CuSO_4 \cdot 5\ H_2O$

i. DTG Curves were shown and activation energies for some steps were estimated.

S-IB2. Ion Exchange Resin Solubilization

a. Model experiments using benzene as a substitute fuel for ion-exchange resins indicates 49% H_2O_2/H_2O as the maximum concentration to avoid the explosive region. Dowex-1, a strongly basic resin in the hydroxide form, should not be used due to excessive decomposition in much lower strength peroxide.

S-IC. Fenton's Reagent and Metal Complexes

1. Fenton's Reagent (H_2O_2 + Fe^{2+}) is an example of the enhancement of the oxidizing power of H_2O_2 by a metal catalyst.

2. Many acidic oxides such as MoO_3 and WO_3 do the same as Fe^{2+} by formation of inorganic peracids.

3. The formation of peroxymonosulfuric acid (Caro's Acid, H_2SO_5) from H_2SO_4 and H_2O_2 is another example.

4. The reaction of H_2C_2 with chromates and dichromates leads to the formation of peroxo complexes of Cr (IV, V and VI) having various oxidizing powers and some being explosive.

5. Amine complexes from CrO_3, H_2O_2 and ethylene diamine or NH_3 are known, the latter noted under IV G.

6. For epoxidation ROOH plus metal catalyst is superior to H_2O_2 plus metal catalyst due to the presence of water in the latter. For ion-exchange solution, however, water is necessary.

7. Historical work with Fenton's Reagent showed:
   a. Oxidation of glucose was stereospecific.
   b. Oxidation of fructose reached a maximum at pH 3.2-5.4.
   c. In the oxidation of glycolic acid no complexes were formed and the oxidation was a chain reaction forming OH and HO_2 radicals.

d. Alpha - Amino acids were converted to α-keto acids by free radicals generated by x-ray irradiation of dilute aqueous solution in the presence of oxygen.

8. Fenton's Reagent oxidized phenol to dihydroxy benzenes and further oxidation products, and the reaction was often violent.

9. Fluoride ion and pyrosphate ion were found to be good inhibitors for the reaction by complexing Fe^{3+}.

10. The radical OH was thought to be of primary importance in oxidation of phenol by Fenton's Reagent.

11. The x-ray radiation of phenol solutions gave products similar to those produced by Fenton's Reagent using dosages up to 1×10^6 E.U. (about 1 megaroentgen, MR).

12. Mixed γ-ray/neutron radiation gave a yield of product about twice that with the γ-ray alone even though the neutron intensity was low.

S-II. Nitric Acid Solubilization of Ion-Exchange Resin

A. Ion-Exchange Resins.

1. HNO_3 (35-70%) at 1-10 parts per part of resin at 90-120°C dissolves cation-exchange resins.

B. Hazards Using Nitric Acid

1. Avoid the use of HNO_3 of 12% or more concentration with ion-exchange resins because of the oxidation power and formation of nitrated species. Never use where NH_4^+ is present.

S-III. Effect of Radiation on the Acid Solubilization of Ion - Exchange Resins (Note: R = Roentgens, r = rads, Mr = Megarads)

1. The degree of decomposition of irradiated (200 Mr) cation-exchangers was greater than untreated. For anionic one sample showed reduced and another a slight increase over the untreated.

2. The maximum rate of decomposition was high for cationic, untreated, acid treated and irradiated; for anionic it was high for untreated.

S-IV. Stability of Hydrogen Peroxide

A. General Stability of Hydrogen Peroxide

1. The decomposition rate of H_2O_2 is roughly proportional to the surface to volume ratio.

2. The decomposition rate of H_2O_2 with temperature increases by a factor of 2.2 for a 10°C rise. The addition of Fe^{2+} may drop the factor to as low as 1.6.

3. H_2O_2 (90%) at ambient temperature decreases less than 1% in content over several months. At 100°C it decreases 2% in 24 hours.

4. Minimum decomposition of H_2O_2 is at pH 4.2 for 10.9-65.6% H_2O_2 at 50°C.

5. For lower concentrations of H_2O_2, pH becomes increasingly important relative to stabilization.

6. For ordinary H_2O_2 (10.9%) the decomposition rate rapidly increases in going from pH 3.5 to 2.5.

7. Fe^{3+} at 0.3 ppm at 30°C in 90% H_2O_2 shows a narrow (1 pH unit) high peak of decomposition at 3.7 pH, thought to be due to formation of a colloidal hydrous oxide of large catalytically active surface.

8. For resin solubilization the existence of this peak may be an advantage or a danger depending on the quantity and rate of energy release.

9. Increase of Fe concentration increases the rate of decomposition for 90% H_2O_2 at 50°C, and the rate varies with the pH.

10. In the temperature range of 30-100°C the rate of decomposition of unstabilized 90% peroxide ranges from 1%/yr. to 2%/day with no effect of pressure shown on the rate.

11. Mixed catalysts may show a greater effect on the decomposition rate than the sum of the two separately on 90% H_2O_2.

12. The presence of chloride anion with the metal cation increased the decomposition rate 40-fold showing the catalytic effect of an anion rather than a second cation.

13. Agitation did not increase the decomposition rate.

S-IV.B. Purification of Hydrogen Peroxide.

1. H_2O_2 may be purified by cation-exchange resins at pH 0.7-2.5 to remove heavy metals. It is ineffective if more

than 1% of the exchange capacity is used for binding the heavy metals.

2. Crude H_2O_2 is completely decomposed in 10-15 hours at 100°C.

3. Purification of 25-75% H_2O_2 is most practical, however, above 50% it may explode.

4. If the amount of impurities is very high, contact of 35% H_2O_2 with the resin may be dangerous.

5. If the resin is regenerated to 99% capacity little decomposition of H_2O_2 occurs.

6. Fe content of the resin should preferably be 0-1 ppm before use.

S-IV.C. Decomposition of Hydrogen Peroxide

1. MCA Data Sheet

a. Cu, Cr, and Fe greatly increase the decomposition rate of H_2O_2.

b. Alkaline H_2O_2 is even more susceptible to decomposition by metals than acid solutions.

c. A heat rise of 1-2°C/hr. at 30-35°C means that eruption is certain unless checked by cooling, dilution, or stabilization.

2. Hydrogen Peroxide Determination in the Presence of Chromate.

a. Ion-exchange resins may be used to remove chromate from H_2O_2 to enable the latter to be analyzed.

b. Mixed resins and anionic resins absorb H_2O_2 at high pH, which can be released by (acidification)

c. The rate of decomposition of H_2O_2 in slightly alkaline sodium chromate solutions is dependent on pH, temperature, and chromate concentration.

d. The NH_2 group in the anion-exchange resin appears to be responsible for the uptake of H_2O_2.

S-IV.D. Concentrated Hydrogen Peroxide Summary

1. The vapor phase system of H_2O_2/H_2O is explosive at 26 mol% (40 wt.%) at one atmosphere.
2. Systems of H_2O_2 and organics are generally not explosive if the final solutions contain less than 30 wt.% H_2O_2.
3. Concentrated H_2O_2 may explode with ion-exchange resins or plastics such as PVC.
4. Immiscible systems may explode at interfaces.
5. Peroxymonosulfuric acid (Caro's Acid) (from H_2SO_4 and H_2O_2) may explode with organics.
6. Anionic resins are preferably acidified with H_2SO_4 rather than HNO_3 to avoid nitration. The concentration of H_2SO_4 should be kept low to avoid formation of Caro's Acid with H_2O_2.
7. Explosion studies with organics and Caro's Acid (H_2SO_5) show the existence of an induction period while H_2SO_5 is being formed.

S-IV.E. Rate of Hydrogen Peroxide Deomposition in Nitric Acid Solutions.

1. Rate constants for the decomposition of H_2O_2 in HNO_3 solution as a function of HNO_3, H_2O_2 and an impurity mixture (Fe, Cr, Pb, Ni, Cu) were determined at the boiling point.

2. The effect of HNO_3 was small at 1.7-2.0 M, but increased at 2.9-4.1 M.

3. The effect of impurity was linear over the whole range.

4. The H_2O_2 concentration had no effect.

S-IV.F. Catalytic Properties of Chromium Complexes on Cation-Exchange Resin Surfaces.

1. Complexes of Cr^{3+} with ethylene diamine were synthesized directly on the surface.

2. Coordination to N bases increases the catalytic activity of Cr^{3+} ions in H_2O_2 decomposition.

S-IV.G. Catalytic Activity of Ion-Exchange Complexes in Hydrogen Peroxide Decomposition.

1. The highest catalytic activity of cation-exchanger KB-4 containing Cu^{3+} and carboxylic groups for decompositions of H_2O_2, was achieved at a 3/1 ratio of NH_3/Cu^{3+} and was shown by KB-4 containing 0.5 mg-ion Cu^{3+}/g KB-4.

VI. Recommendations

Based on a general study of the implications of the foregoing summary, the following recommendations for experimental work are offered to provide some present data to assist in drawing conclusions as to a possible preferred procedure for disposal of the TMI ion-exchange resin.

1. Laboratory Studies

Carry out laboratory studies on the solubilizing of Amberlite IRN 217 mixed bed resin with cation/anion ratio of 3:2.

- a. Agents
  - (1) 5%, 10%, 20% H_2O_2
  - (2) $Fe\ (NH_4)(SO_4)_2 \cdot 12\ H_2O$ (ferric)
    $FeCl_3 \cdot 6\ H_2O$
    $Fe\ (NH_4)_2\ (SO_4)_2 \cdot H_2O$ (ferrous)
    $FeCl_2 \cdot 4\ H_2O$
    $Fe(SO_4)_2 \cdot 7\ H_2O$
    $Fe(SO_4)_3 \cdot n\ H_2O$
    Chromium compounds and complexes
- b. General Conditions
  - (1) Ambient and elevated temperatures
  - (2) Open and closed systems.
  - (3) Variation of pH
- c. Resin Conditions
  - (1) Non-irradiated
  - (2) γ-irradiated
  - (3) γ and neutron-irradiated
  - (4) Treated with:

KOH	NaOH	NH_4OH	H_2SO_4
KCl	NaCl	NH_4Cl	HCl

d. Inhibitors

(1) Fluoride and pyrophosphate ions

(2) Search for others

2. Larger Scale Studies

In carrying out the laboratory studies, as information is gathered, the projected program would be adjusted to avoid duplication, remove experiments indicated to be unfruitful, and enlarge areas of promise. Based on the results, larger scale studies, in the vicinity of 4 liters if so desired, would be instituted to gather information and provide data for scaleup.

DISTRIBUTION - HEDL-7335

DOE/RL - KR Absher
PFX Dunigan, JR. (3)
JJ Schreiber
FR Standerfer

EG&G/TIO - GJ Quinn (5)

PNL - LA Bray
DE Knowlton

RHO - RE Smith

WHC - MD Crippen W/C-31
EA Evans W/C-23
WM Gajewski W/B-82
R Gold W/C-39
RD Hensyel W/A-5
WW Jenkins W/B-84
MK Mahaffey W/B-80
IF Marshall W/C-123 (2)
LM Northey W/B-84
EJ Renkey W/B-17
FH Ruddy W/C-39
WN McElroy W/C-39
WJ McShane W/B-12
DL Swannack W/B-84
HH Yoshikawa W/C-44
Central Files W/C-123 (2)

ORNL - A Malinouskas

LASL - J. Halbig

GPU Nuclear
TMI-2 DIVISION

TECHNICAL PLAN

MAKEUP AND PURIFICATION DEMINERALIZERS RESIN REMOVAL

Prepared by:
TMI-2 Technical Planning Department
GPU Nuclear, Inc. - Bechtel National, Inc.

TPO/TMI-072

TPO/TMI-072
Revision 0
August 1983

TECHNICAL PLAN

MAKEUP AND PURIFICATION DEMINERALIZERS RESIN REMOVAL

Technical Planning Department

Approval
Director, Technical Planning

Concurrence
Manager, Recovery Programs

Concurrence
Director, Site Operations

Concurrence
Director, Radiation Control

INTRADEPARTMENTAL REVIEW AND APPROVAL

Responsible Engineer	C. A. Nagin
Manager, Waste Management Planning	Cynthia G Hitz
Manager, Decontamination Planning	
Manager, Reactor Disassembly and Defueling	(for GE Stillman)
Manager, Data Management and Analysis	Victor R. Fricke
Supervisor, Technical and Administrative Services	A. Baroggio for G. W. Brothers
Deputy Director, Technical Planning	Raphael S Daniel

ACKNOWLEDGEMENT

The content of this plan represents the work and cooperation of many individuals. Considerable input from persons in Engineering, Operations, Safety Review, Radcon, and several Department of Energy (DOE) contractors is gratefully acknowledged.

SUMMARY

This plan describes the activities and systems required to remove and dispose of the contents of the makeup and purification demineralizers. The plan utilizes the submerged demineralizer system (SDS), in-plant letdown, and spent resin systems with some additions and modifications.

The plan is presented in three major phases: Phase I -- the removal of soluble radioactivity prior to transferring any solids; Phase II -- the modification of the spent resin system and design and installation of a solidification system, if necessary; and Phase III -- the actual resin transfer and solidification. Phase I and Phase II can proceed in parallel.

The preparation of the resins for offsite shipment is scheduled for the end of 1984, consistent with GPU Nuclear's commitment to the Nuclear Regulatory Commission. Based on ORNL analyses, success in performing these operations on schedule is likely.

The final resin waste form is a major issue that must be resolved because the quantities of waste and number of shipments will vary greatly between disposal at commercial sites versus DOE destinations. This also applies to any SDS vessels generated as a result of liquid radwaste processing. This plan assumes that solidification of the makeup and purification demineralizer resins is required.

CONTENTS

SECTION PAGE

SECTION PAGE

SECTION PAGE

TABLES

FIGURES

SECTION 1.0
INTRODUCTION

1.1 OBJECTIVE

This plan addresses the removal, transport, and disposal of the contents of the demineralizers in the Three Mile Island Unit 2 (TMI-2) makeup and purification system. The purpose is to present the selected technical methods for removal and waste processing.

1.2 BACKGROUND

The demineralizers in the TMI-2 makeup and purification system accumulated significant quantities of fission products and fuel debris during and subsequent to the March 1979 accident. Except for the reactor systems, the demineralizers contain the greatest amount of contaminated material at TMI-2. Until recently, the physical condition of the demineralizers and their contents were unknown. The radiation and thermal exposure to the installed resins were sufficient to cause severe degradation. (The "B" demineralizer resin sample did not show significant damage, however, the "A" demineralizer requires further characterization.) There was also concern that the demineralizer vessels contained large quantities of fuel. (We now know there are less than 4 kilograms of fuel in both vessels; Reference 1.) Thus a significant effort was conducted to determine the state of the demineralizer contents and to develop this plan. This effort is now completed.

Operations to decontaminate the demineralizers will be complex because of the degraded condition of their contents and the high radiation levels in the demineralizer cubicles. The demineralizers and components within the cubicles are not available for personnel access. If these resins were to be transferred by normal procedures, other plant areas and systems normally used for resin disposal would see radiation levels in excess of design.

The demineralizer characterization project is reported in References 1 through 4. The characterization project started in May 1982 and was completed in June 1983. The results of that effort provide the bases for this plan. Summaries of the characterization project results are in Appendices A and B.

System options are reported in Reference 5. The selected system approach is presented in this plan.

1.3 SCOPE

This plan addresses removal and disposal of the contents of the demineralizers in the makeup and purification system.

Decontamination of the demineralizers after contents removal and decontamination of the upstream and downstream portions of the makeup and purification systems are not in the scope of this plan. These activities are covered in the Integrated Plan for AFHB Characterization/Stabilization/Decontamination, TPO/TMI-049 (Reference 6).

1.4 CRITERIA

The criteria for this project are:

- Maximize use of existing systems to the extent practicable
- Minimize the possibility of creating new hotspots while transferring demineralizer contents
- Maximize use of remote operations techniques for high radiation areas to the extent practicable
- Provide operational decoupling among major project phases to allow operational flexibility and plan modifications to suit actual results achieved.

1.5 APPROACH

The plan is presented in three phases:

Phase I: Rinsing and eluting the demineralizer contents without moving solids (Section 3.1)

Phase II: Modifying the spent resin system, and sluicing and solidifying normal resins for a system test (Section 3.2)

Phase III: Sluicing, solidifying, and disposing of the purification demineralizer contents (Section 3.3).

Phases I and II can proceed in parallel. Completion of both is a prerequisite for Phase III.

There are schedule and system interfaces of this project with the auxiliary and fuel handling building (AFHB) system decontamination effort. There are also interfaces with the processing for disposal of other in-plant resins and sludges.

Section 2.0 of this plan presents systems descriptions required for completing the phases of the project. Section 3.0 is a work sequence for the project. Section 4.0 describes the project's interface with other projects.

SECTION 2.0

SYSTEMS DESCRIPTIONS

The makeup and purification demineralizer removal activity has been separated into three phases as shown in Figure 2-1. This figure shows that Phase I and Phase II must be completed before Phase III is begun. These prerequisite phases can proceed in parallel if resources are available. The following section describes each phase in more detail.

2.1 SYSTEM DESCRIPTION FOR PHASE I

In Phase I, soluble radioactivity (primarily cesium 137) will be removed from the resins and processed by the SDS system. This will reduce the dose rate in the demineralizer cubicles and sluice path to the spent resin system, and will minimize the handling problems caused by radiation of the sluiced demineralizer contents.

The activity will be removed by rinsing and eluting the resins. The flow path for this phase is shown in Figure 2-2. The resins will be rinsed by batching borated water into the demineralizer vessels, fluffing the resin, and decanting the water. Essentially the same operation will take place during eluting, however, chemicals such as sodium hydroxide and sodium borate will be added to the flush water to further displace the radioactive isotopes.

For these operations, the flow rate will be maintained between one and five gallons-per-minute to minimize the carryover of suspended solids. The resulting velocity through the demineralizers will be between 0.1 and 0.6 inch-per-minute. These velocities are capable of suspending resin particles of 8 to 20 microns and fuel particles of 1 to 3 microns. To guard against particle carryover and operational upsets, a guard filter will be installed.

The total flow required through each demineralizer is estimated to be 3000 gallons. This estimate is based on three volume exchanges for rinsing and three for elution. The anticipated procedure is to batch feed about 250 gallons, soak, fluff, settle, and decant. As the cesium concentrations are

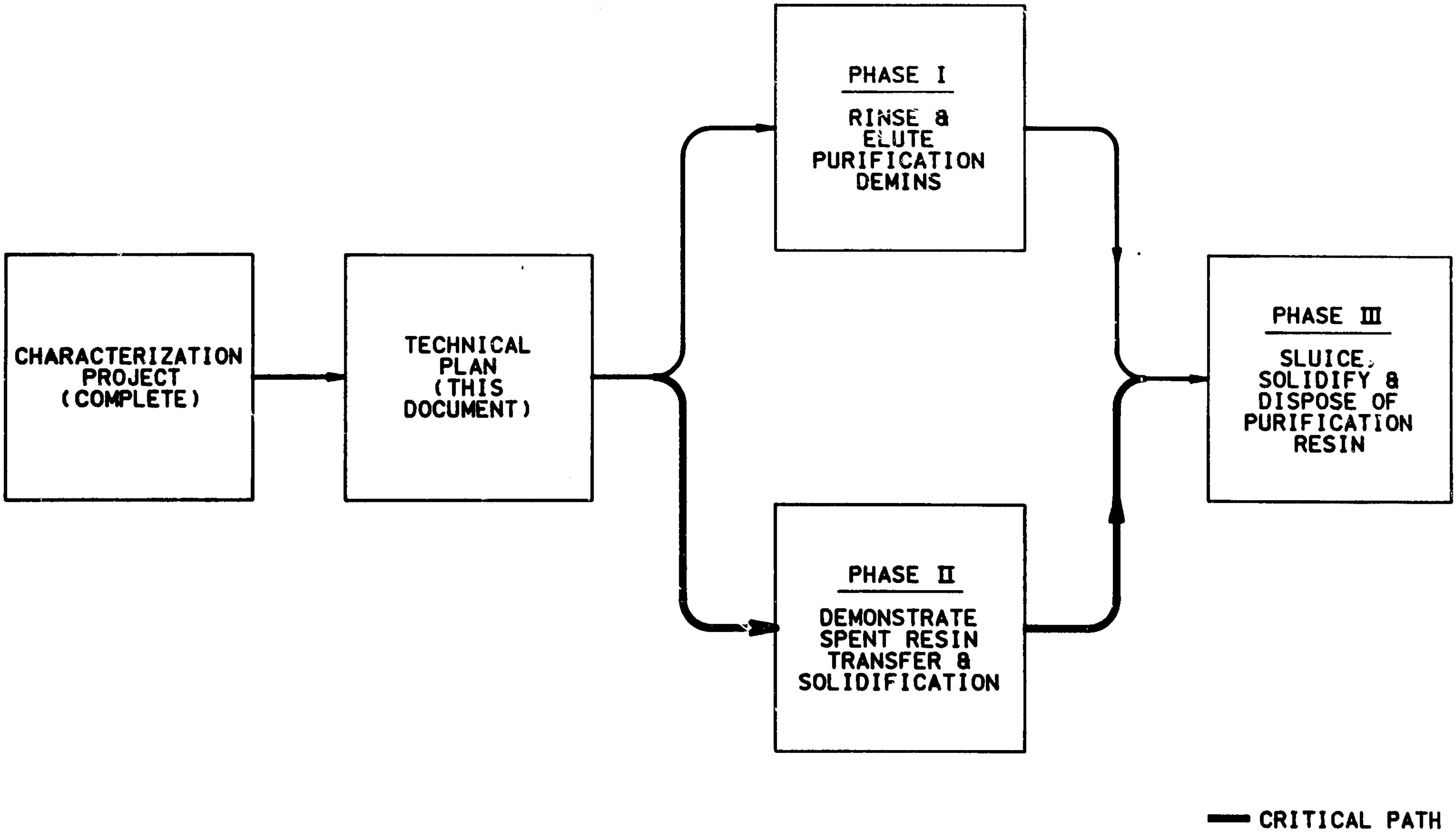

FIGURE 2-1

MAKE-UP AND PURIFICATION DEMINERALIZER RESIN REMOVAL PLAN OVERVIEW

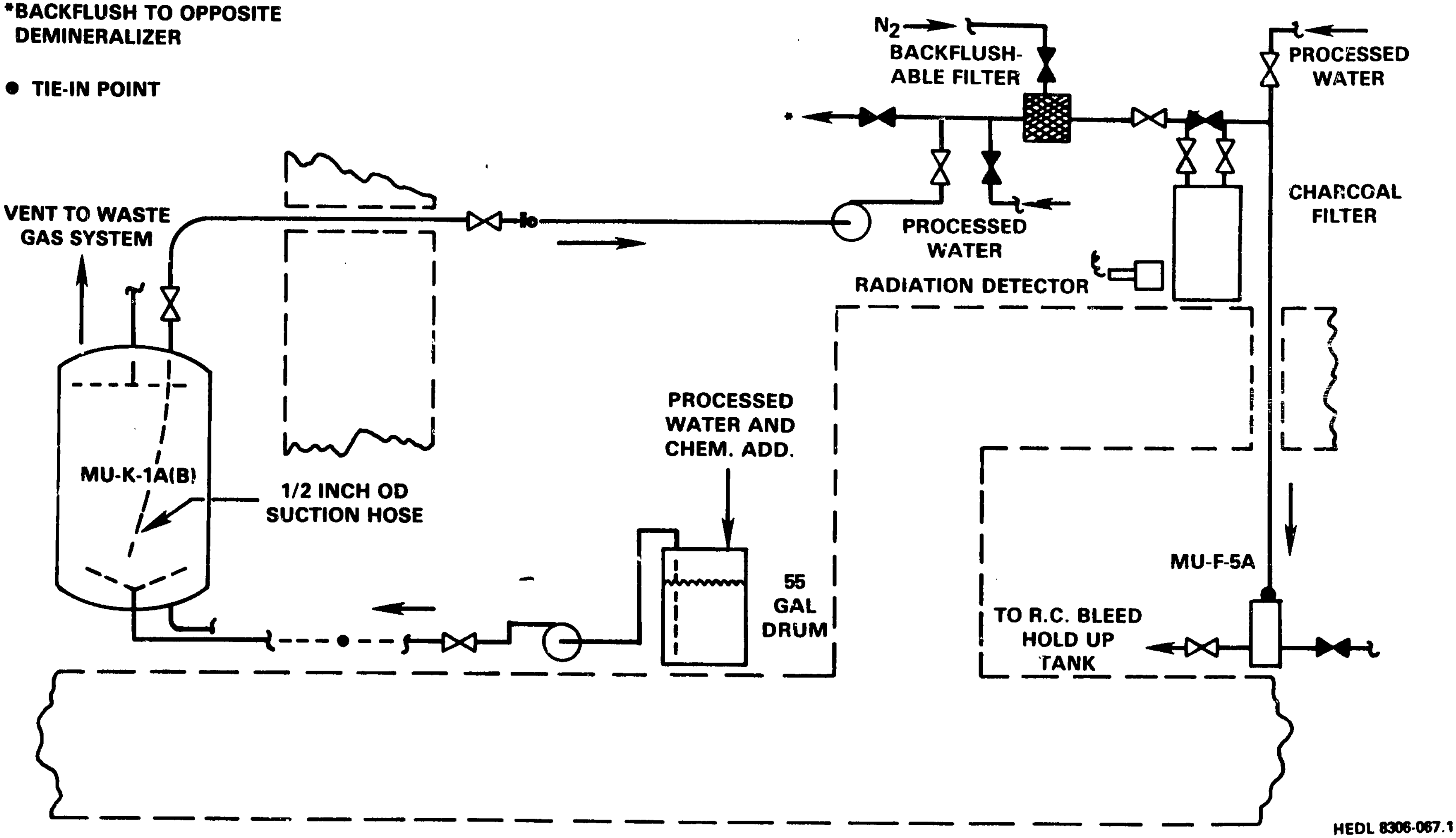

FIGURE 2-2
SCHEMATIC FOR RINSE AND ELUTION

expected to be very high, the discharge stream will be diluted with additional process water immediately downstream of the filter. These steps can be repeated more than three times if it appears that further removal of soluble radioactivity will be accomplished.

2.1.1 Equipment Description

For the most part, Phase I will use existing in-plant systems with the addition of a skid for water and chemical addition and for filtering and diluting the demineralizer effluent. A remote control tracked vehicle (LOUIE) will be used for radiation and video monitoring in the demineralizer cubicles.

The locations of these hardware additions are shown in Figure 2-3. They are individually discussed below.

2.1.1.1 Rinse Water Supply and Eluting Chemical Addition

A water feed is required to rinse and elute the demineralizer contents. This will be accomplished by connecting a process water supply, via hoses, to the existing connection for demineralized water addition. Alternatively, the water may be batched through the resin fill line. This modification is necessary because rinse water will be borated processed water and not plant demineralized water. A small batch tank will be required for chemical addition during elution steps. The water addition control station is conceptually shown in Figure 2-3 as being located in the Hayes gas analyzer room. This location allows both the dilution/elution feed and decant operations to be controlled from this room.

2.1.1.2 Effluent Filtration of Organics

Degradation of the resins within the demineralizer has resulted in organic compounds that will become suspended in the rinse and elution water. It is preferred that these compounds not pass into other portions of the letdown system or to the SDS. (It should be noted, however, that absolute filtration

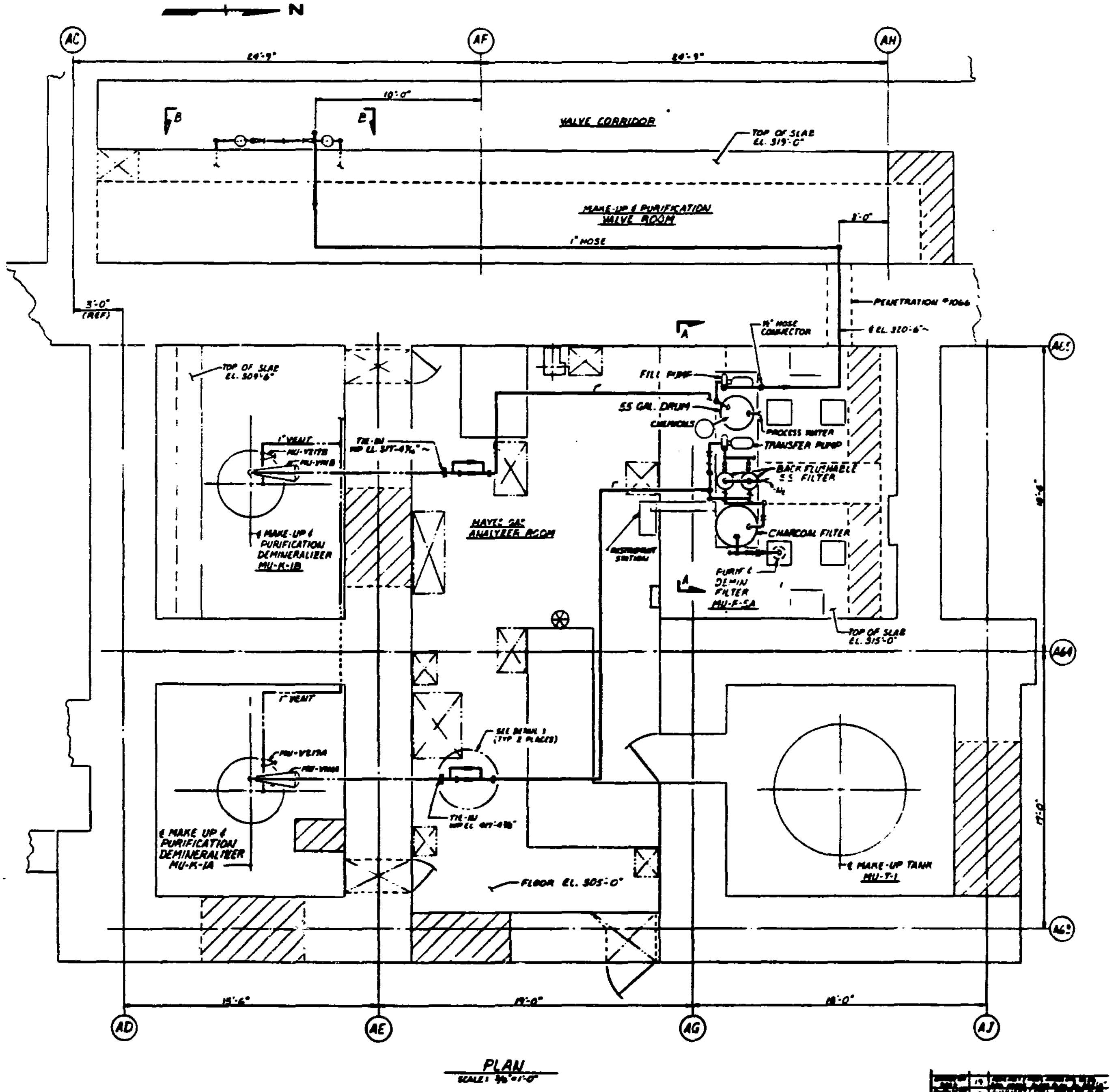

FIGURE 2-3
LOCATION SKETCH FOR RINSE AND ELUTION

of organics is not a requirement). To remove organics, a charcoal filter will be installed on the mezzanine of the Hayes gas analyzer room. The filter will be tied into the resin fill lines for the inlet and into the top of MUF-5A housing for the outlet. The filter will be housed in its own shielding and will be removed as a unit after the organics removal is complete.

2.1.1.3 Guard Filter For Particulates

A guard filter will be placed in the effluent line ahead of the organics filter. This guard filter has three purposes:

- To guard against the transfer of bulk solids out of the demineralizers that might be caused by flow transients during rinsing and elution

- To prevent resin and fuel fines transfer into the letdown piping and bleed tanks

- To prevent loading the organics filter with radioactive particulates, which would create a potential disposal problem.

Conceptually, the guard filter will be a sintered metal backwashable unit. The backwash flow path goes to the demineralizer opposite the one being pumped out. The backwash capability prevents this filter from becoming abnormal waste containing high TRU content and alleviates any plugging problems.

2.1.1.4 LOUIE

LOUIE is an existing remote control tracked vehicle that will be provided by the DOE for this project to obtain radiological information and data from within the demineralizer cubicles during the various operations. Similar information may also be required in the spent resin tank rooms during Phase III. In addition to radiation data, video inspection for suspected leaks and to verify valve operation will be useful tasks for LOUIE.

2.2 PHASE II SYSTEM DESCRIPTION

Phase II activities prepare the spent resin system for handling the sluiced demineralizer contents and provide for removing the material from the plant. This phase also demonstrates complete spent resin and solidification systems operation with material that is not as radioactive as the purification demineralizer contents.

A flow diagram for the sluicing and solidification process is shown in Figure 2-4.

2.2.1 Equipment Description

To a large extent these processes will use existing systems; however, some significant modifications and additions are planned. The modifications required to support demineralizer sluicing and solidification are individually discussed below. The locations of hardware additions are shown in Figure 2-5.

2.2.1.1 Spent Resin System Tie-ins to Solidification Skid

The existing spent resin pump discharge and the recirculation return line were installed to connect to TMI-1 systems. They wind their way beneath the El. 305' floor to the northwest corner of the auxiliary building at El. 305'. To minimize the runs of such pipe and to minimize uphill sluicing, the solidification process equipment will be located adjacent to the spent resin transfer pump cubicle, as shown in Figure 2-5. As a result, the existing pump discharge and return piping will be cut and a short recirculation loop will be installed, as shown in Figure 2-4. This addition will be permanent and should meet Regulatory Guide 1.143 design specifications. It will allow connection, by hoses, to the temporary solidification unit.

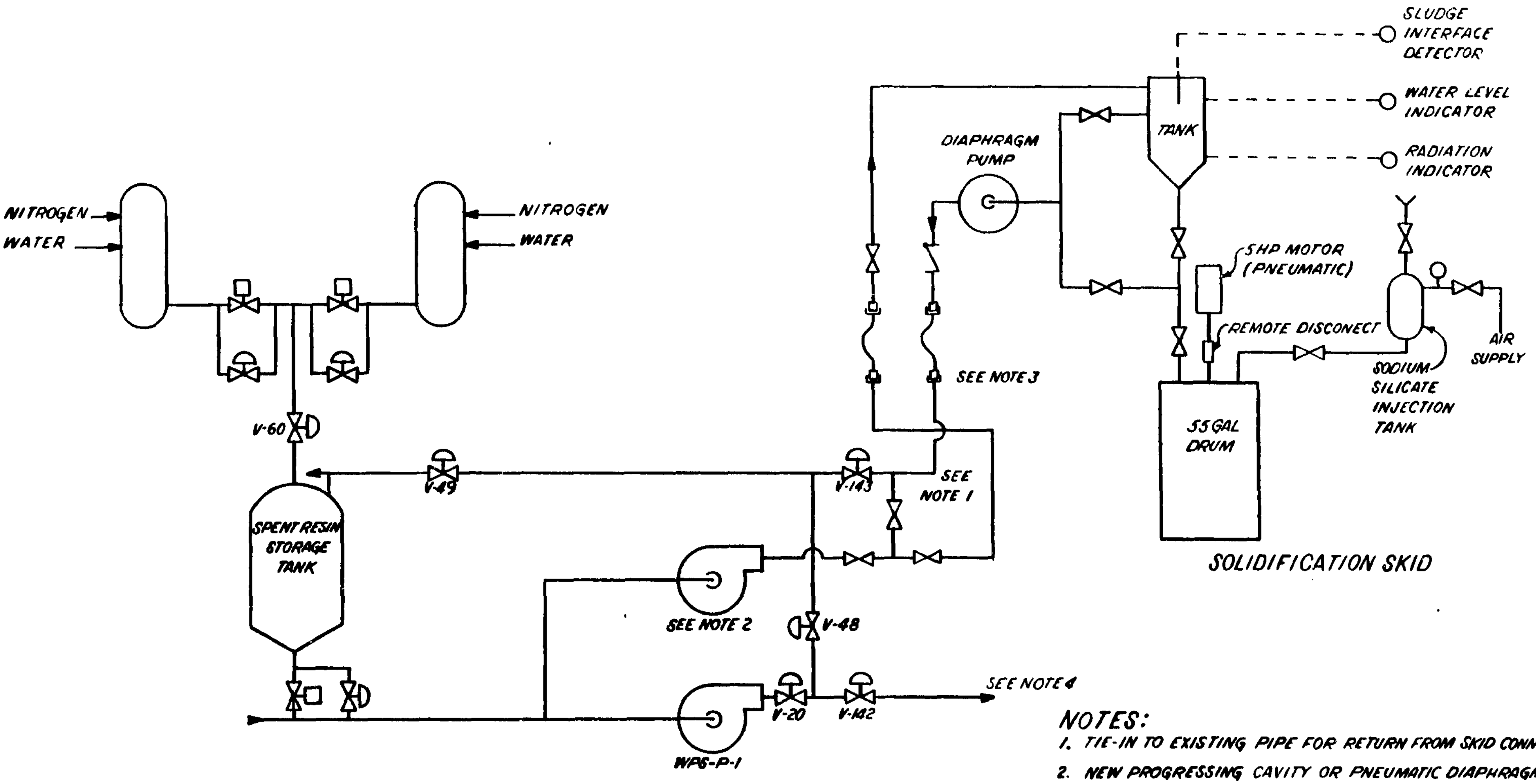

FIGURE 2-4
SLUICE AND SOLIDIFICATION SCHEMATIC

NOTES:

1. TIE-IN TO EXISTING PIPE FOR RETURN FROM SKID CONNECTIONS
2. NEW PROGRESSING CAVITY OR PNEUMATIC DIAPHRAGM PUMP AND CONNECTING PIPE.
3. NEW CONNECTIONS FOR SOLIDIFICATION SKID.
4. TIE-IN TO EXISTING PIPE FOR DEWATERING LINE TO A RECEVING TANK.

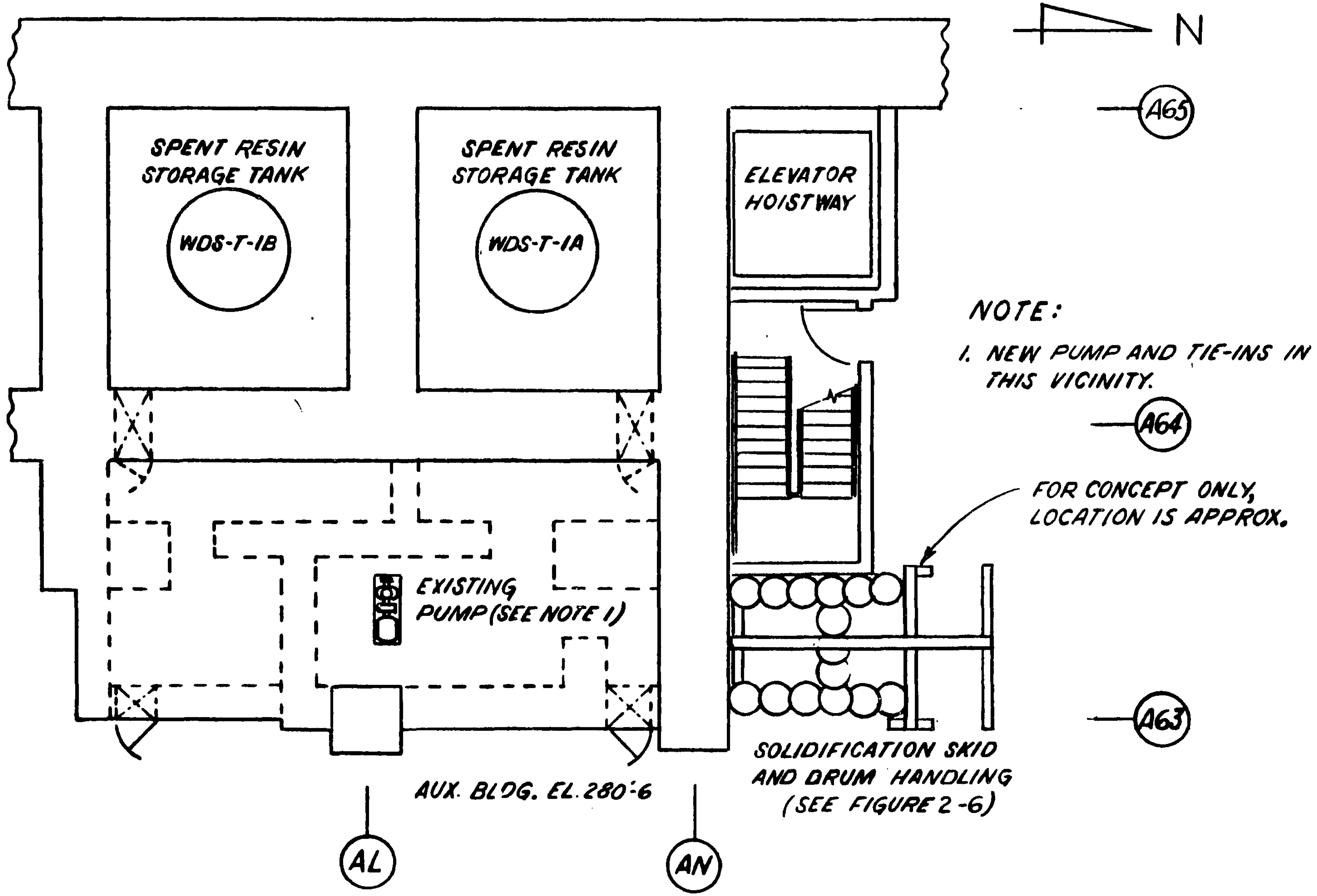

FIGURE 2-5
LOCATION SKETCH, SPENT-RESIN SYSTEM

2.2.1.2 Transfer Pump Addition

The installed resin transfer pump is a a centrifugal pump designed for low solids concentration water. A progressive cavity or pneumatic diaphragm pump more suitable for dense slurries should be installed in parallel with the existing pump.

The existing pump should not be removed because it will be useful for pumping water during dewatering and decanting operations when there is no need to move solids. If the installation of the additional pump creates undue difficulties with regard to piping and valve installation, then consideration can be given to replacing the existing pump.

2.2.1.3 Spent Resin Tank Dewatering Pipeline Connection

The current method for dewatering spent resin tanks is to drain them through a sparging line to the floor drain in the cubicle. To avoid recontaminating the auxiliary building sump, this method will be replaced. A dewatering line will be added that will allow water to be pumped to a tank such as the reactor coolant bleed tank B, from which it can be processed with SDS or EPICOR II.

2.2.1.4 Solidification Skid

A conceptual sketch of the solidification skid is shown in Figure 2-6. The solidification skid consists of a waste batch control tank, solidification equipment, and handling equipment including a transfer bell.

The focus of the skid will be a cone-bottomed batch control tank (20 to 30 gallons per batch) with appropriate radiation, solids, and water level instrumentation. The batch tank will be located immediately above the waste drum. This will allow operators to adjust the amount of waste to be solidified prior to dumping it into the solidification container, thereby insuring that disposal regulations are met. It will also prevent drum overfilling.

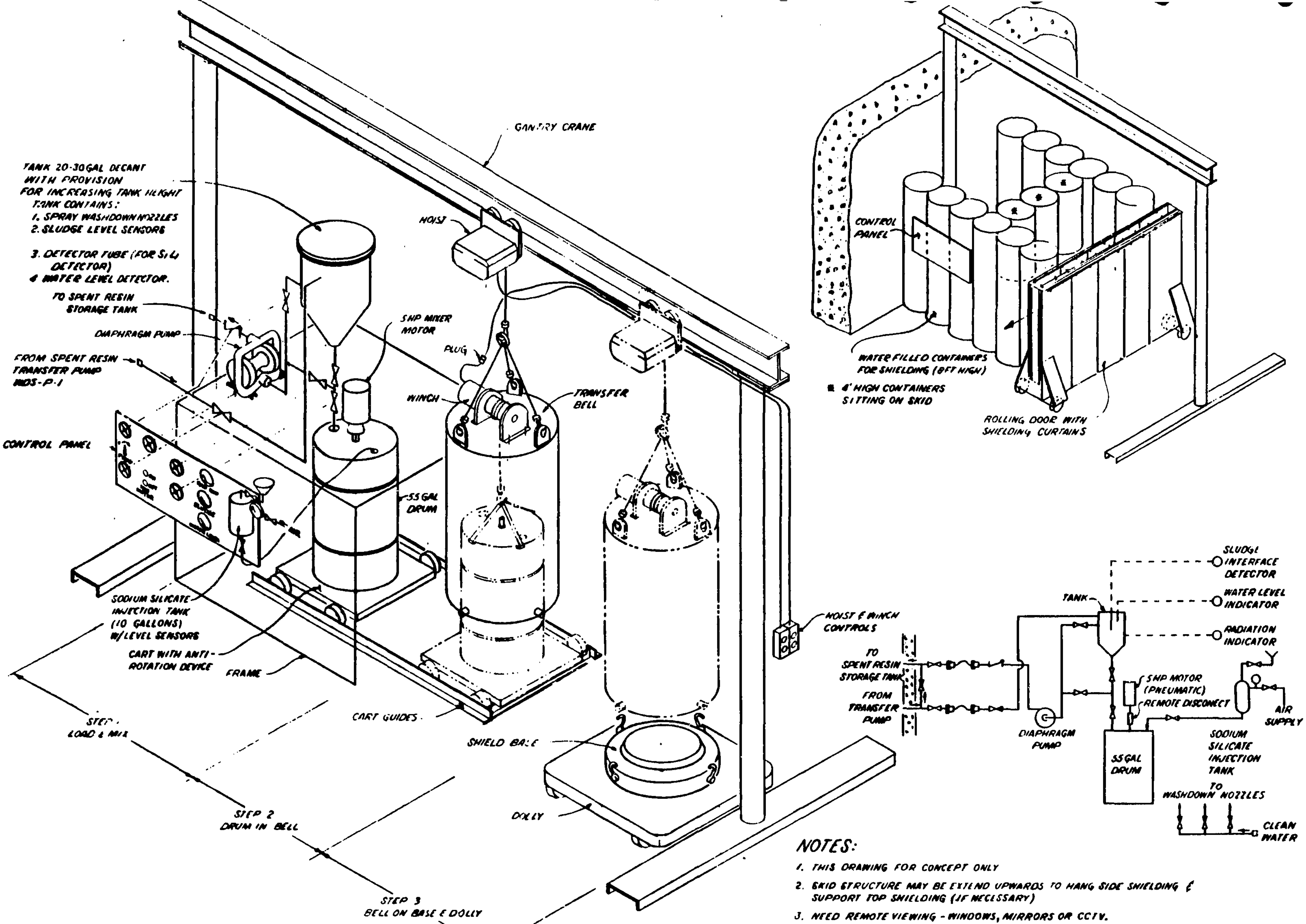

NOTES:

1. THIS DRAWING FOR CONCEPT ONLY
2. SKID STRUCTURE MAY BE EXTEND UPWARDS TO HANG SIDE SHIELDING & SUPPORT TOP SHIELDING (IF NECESSARY)
3. NEED REMOTE VIEWING - WINDOWS, MIRRORS OR CCTV.
4. VALVES ON SKID MAY BE PNEUMATIC.
5. SUITABLE AREA MONITORS & ALARMS REQUIRED.
6. SUITABLE VENTILATION & FILTERING REQUIRED.

FIGURE 2-6
SOLIDIFICATION SKID CONCEPT

The system will use 55-gallon drums with a sacrificial mixer. This size was chosen to simplify the handling of solidified waste from El. 280' to El. 305' for transfer to interim storage. The drums will be loaded with cement prior to receiving waste material.

A pump and several valves will also be required, as will drum positioning, anti-rotation, and indexing features. Shielding will, for the most part, be portable; however, it will be an integral part of the design. There will be several cleanout water flush points, valved and manifolded to a common connection point.

2.2.1.5 TRU Detection System

One possible process control parameter would be the radiation of the batch control tank on the solidification skid. The feasibility of the detecting TRU quantities in this manner is currently being investigated by DOE. If feasible, a detection system will be included with the skid.

2.2.1.6 Drum Handling

Once solidified, the drummed waste will be transferred to storage awaiting shipment. A shielded handling system including a transfer shield will be integrated with the skid design. The system is shown in Figure 2-6.

2.3 PHASE III

Phase III is the actual sluicing, solidification, and disposal of the purification demineralizer resins. Phase III uses the equipment installed in Phase II.

SECTION 3.0

WORK SEQUENCE DIAGRAM

The work sequence is shown on three seperate diagrams representing the Phase I, Phase II, and Phase III activities. These are Figures 3-1, 3-2, and 3-3, respectively.

3.1 PHASE I ACTIVITIES

Steps 1-33 are required to complete the work defined as Phase I. The lead for several of these activities will be assumed by off-island DOE contractors and is indicated on the figures by heavy outlining.

3.1.1 Letdown System Operability (Steps 1-5)

Steps 1-5 of the sequence verify letdown system operability to allow filling and emptying of demineralizers by backwards flow via the letdown line and demineralizer bypass to a radwaste tank, which will be a batch feed tank for the SDS. Flow should be avoided to portions of the letdown piping upstream of the bypass line as well as to the fill lines, sluice lines, and other connected systems.

Check the new filter installations for tightness and the ability to remove them. Operability test procedures should be written.

The assembly of test gear, Step 3, is potentially a time-consuming activity due to limited access to many areas.

3.1.2 Safety Evaluation and Procedures (Steps 6-8)

Procedures will be required for filling, rinsing, fluffing, and eluting the demineralizer contents, which will be conducted in accordance with the process flow sheet specifications. The review of these procedures will include a safety review.

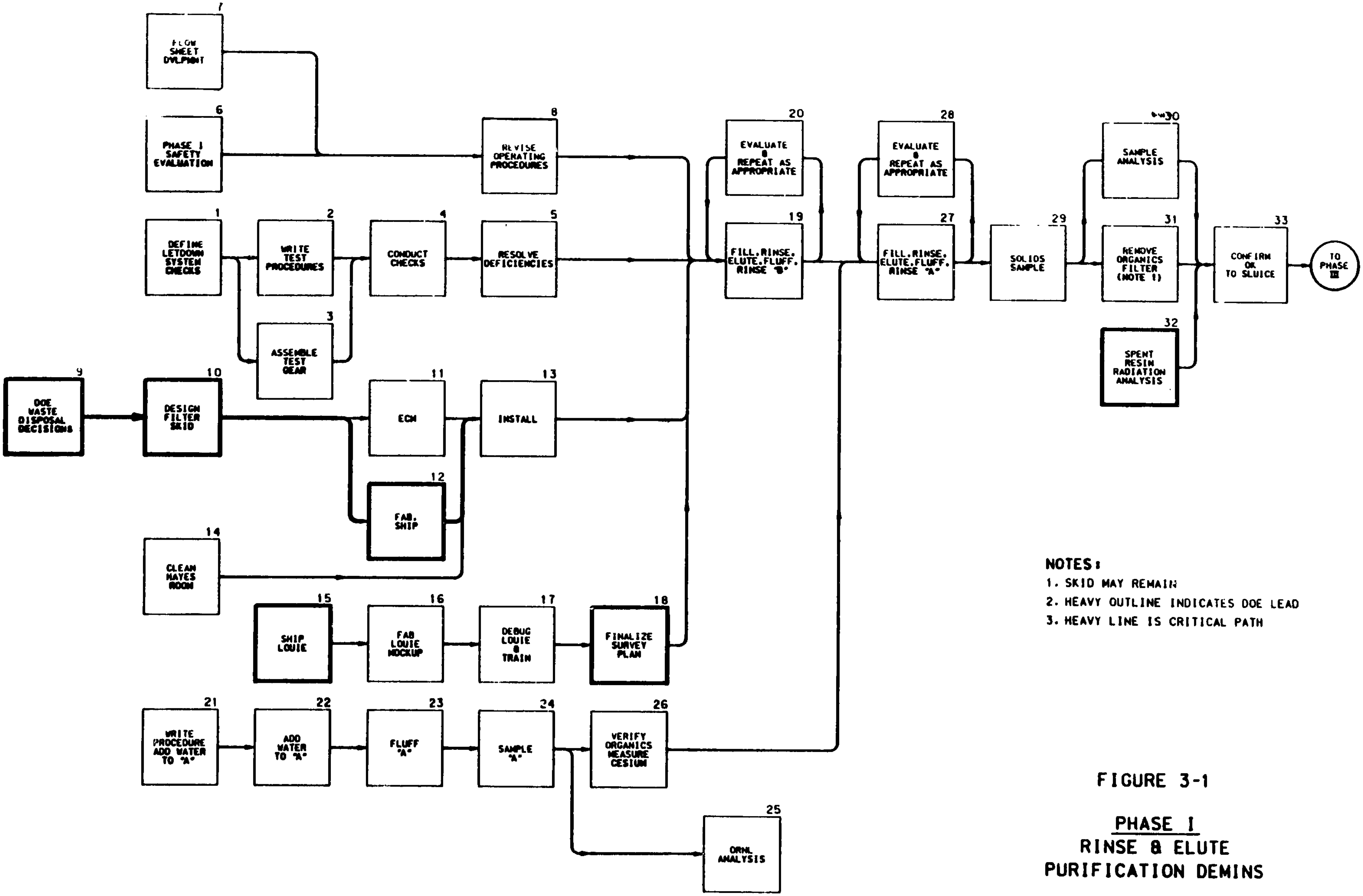

NOTES:

1. SKID MAY REMAIN
2. HEAVY OUTLINE INDICATES DOE LEAD
3. HEAVY LINE IS CRITICAL PATH

FIGURE 3-1

PHASE I
RINSE & ELUTE
PURIFICATION DEMINS

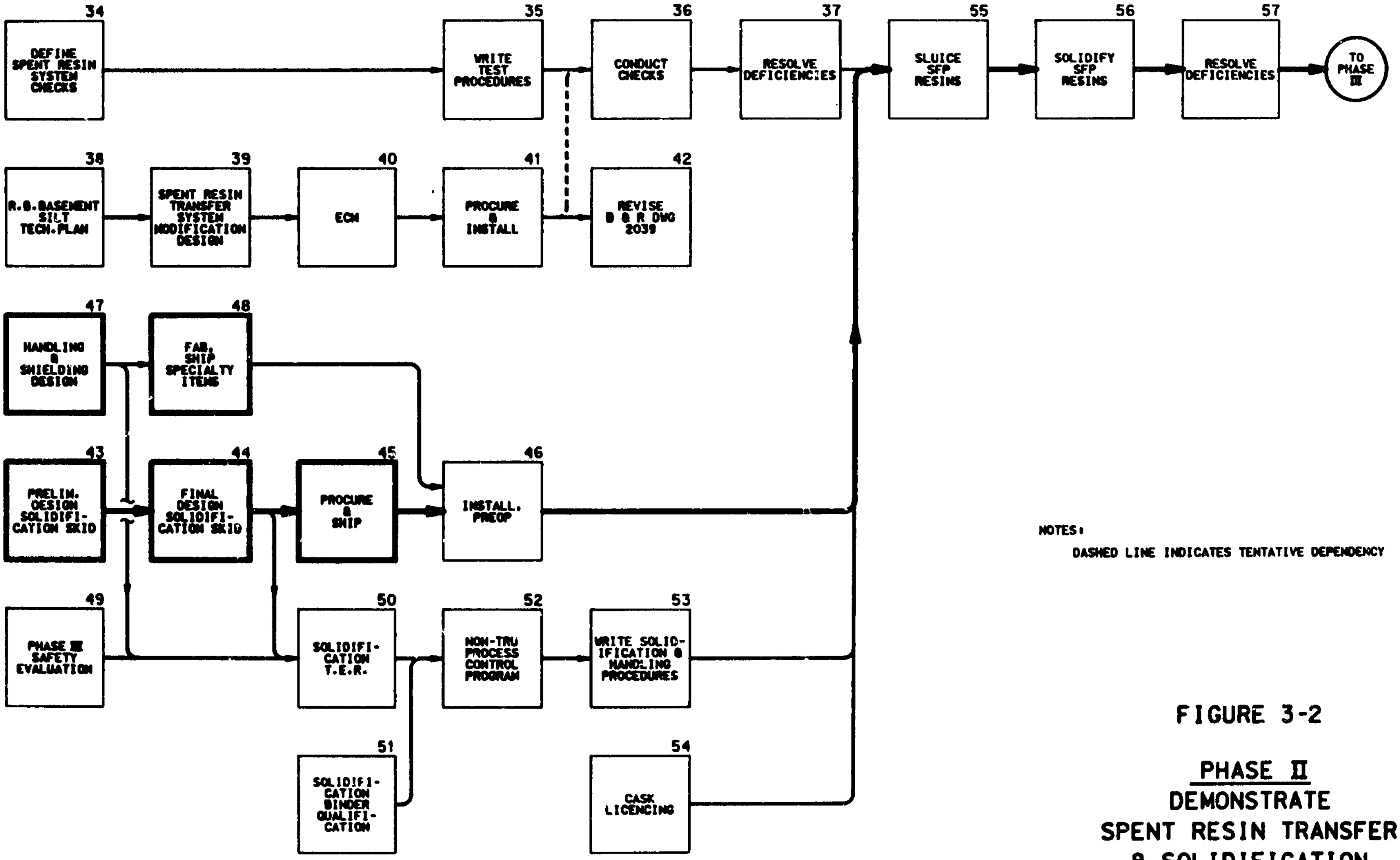

NOTES:

DASHED LINE INDICATES TENTATIVE DEPENDENCY

FIGURE 3-2

PHASE II
DEMONSTRATE
SPENT RESIN TRANSFER
& SOLIDIFICATION

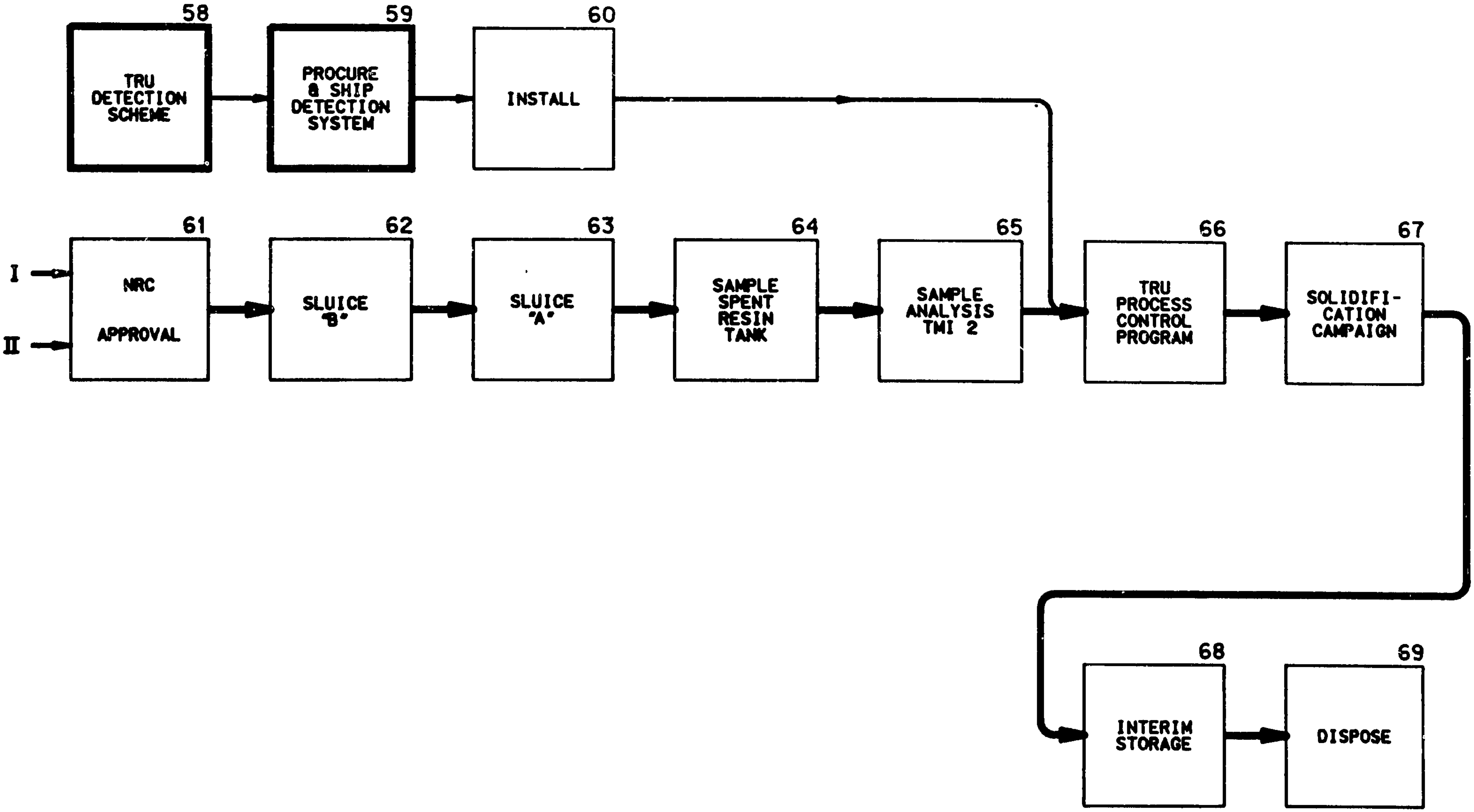

FIGURE 3-3

PHASE III
SLUICE, SOLIDIFY & DISPOSE
OF PURIFICATION RESIN

3.1.3 Waste Disposal Decisions (Step 9)

The quantities of solidified waste for various disposal scenarios are presented in Table 3-1. As can be seen, minimum volume disposal as TRU waste results in significant savings of operational effort and can result in significant savings in disposal cost if DOE, in accordance with the abnormal waste Memoranda of Understanding, can quote a reasonable disposal price.

A similar situation exists for SDS processing of the soluble activity. There are approximately 15,000 curies of Cs-137 in the two demineralizers. From a system performance standpoint, this activity can be deposited in one or two SDS vessels. However, commercial waste disposal limits (10 CFR 61) would limit this to about 1,000 curies per vessel, this results in about 15 vessels.

The waste disposal destination is therefore an issue that should be addressed soon in order to establish firm processing plans.

TABLE 3-1
PURIFICATION DEMINERALIZER RESIN
WASTE VOLUME BASED ON 4kg FUEL*

LIMITING FACTOR	DRUMS
1. Current U. S. Ecology License	200
2. 10 CFR 61 (Category C)	25
3. Max Solidifiable Conc. (Approximate)	15
4. Unsolidified	7

---

* Assumes cesium will be mostly removed during rinse and elution.

3.1.4 Filter Skid Sequence (Steps 10-13)

The design, fabrication, and delivery of the organic and particulate filters (see Sections 2.1.1.2 and 2.1.1.3) will be handled by DOE. Installation includes checkout of spent filter handling as well as installation in the system flow path.

3.1.5 Hayes Room Cleanup (Step 14)

The Hayes gas analyzer room requires several actions before proceeding. For example, the valves installed for the characterization project leak and must be fixed, the temporary cubicle entry doors must be removed, the radioactive gas sample rack will probably have to be relocated to make room for the filter skid installation, and the makeup filter cubicle must be decontaminated.

3.1.6 LOUIE (Steps 15-18)

The remote control transport vehicle is described in Section 2.1.1.4. As with the characterization project where SISI was used, a floor plan mockup should be constructed for exercising LOUIE and for operator training. The survey plan will specify the observations and data to be taken and should be used for training. No formal written procedures are required for LOUIE, as it is not a part of installed systems and there are no safety consequences in the event of its failure. In the event of failure, other remote devices such as FRED may be used.

3.1.7 "B" Operations (Steps 19-20)

The initial rinsing and eluting will be carried out on the "B" demineralizer. The "B" demineralizer will be filled, rinsed, eluted, fluffed, and re-rinsed before this process is begun on demineralizer "A". Although the "B" demineralizer contains more radioactivity than the "A" demineralizer, it contains less fuel, remains wet, and is better characterized by direct sample analysis results.

3.1.8 Fill and Resample "A" (Steps 21-26)

Because of sampling difficulties, the "A" demineralizer conditions are not as well know as those in demineralizer "B" even though the "A" demineralizer has been more extensively characterized by non-destructive techniques. A repeat of the previous sampling procedure is not planned before proceeding because there is no reason to believe that it will be any more successful. Therefore, it has been decided to partially fill "A" with water in an attempt to dissolve any crust and to wet the resin.

A sample of the "A" demineralizer will be drawn to verify the organics filter design and to obtain some idea of the amount of soluble cesium in the demineralizer.

3.1.9 "A" Operations (Steps 27-28)

Following the removal of soluble radioactivity from the "B" demineralizer, a similar procedure will be performed on the "A" demineralizer. These steps are a repeat of Section 3.1.7 but are for the "A" demineralizer. The degree of success with "B" and the results of the "A" water sample will provide information for processing "A".

3.1.10 Sample Demineralizer Contents (Steps 29-30)

After the elution of "A", the solids in both demineralizers will be sampled to determine the amount of radioactivity remaining. This will define the quantity of resin to be sluiced to the spent resin tanks.

3.1.11 Remove Organics Filter (Step 31)

After rinsing and eluting both demineralizers, there is no longer a need for the organics filter and thus it may be removed so it will not interfere with future resin sluicing operations.

The water addition and guard filter portions of the skid, however, may remain to support sluicing and later decontamination efforts.

3.1.12 OK To Sluice (Steps 32-33)

After the rinse and elution steps are conducted, the adequacy of existing shielding in the spent resin transfer system will be evaluated. To support this evaluation, an analysis will be conducted to predict the expected dose rate in various areas, particularly the spent resin tank cubicles, as a function of the radioactivity remaining in the demineralizers. The results of this analysis can be compared with the original shielding design basis.

The results of this comparison will determine whether the demineralizer contents should be sluiced and solidified in smaller batches than currently planned or whether additional shielding is required. After plan modification Phase I will be complete.

3.2 PHASE II ACTIVITIES

Steps 34-57 define the activities required to complete Phase II. Phase II prepares the spent resin system for handling the sluiced demineralizer contents and provides for removing the material from the plant. This phase also includes a demonstration run of the entire spent resin transfer system and solidification system by sluicing the spent fuel pool resins to the spent resin tanks with subsequent solidification. Like the particulate and organics filter skid in Phase I, the design and formation of the solidification and organics filter will be by a DOE contractor.

The detailed requirements for this phase are discussed in Section 2.2. A more detailed discussion of the logic sequence in Figure 3-2 follows.

3.2.1 Spent Resin System Operability (Steps 34-37)

This sequence is functionally the same as for the purification letdown system (Section 3.1.1). However, in this case there will be several modifications to the spent resin system, and therefore Figure 3-2 shows that these should be installed before the checks. In actual practice, it may be possible to conduct much of the testing before some of the modifications. These are operational decisions and beyond the scope of this plan.

3.2.2 RB Basement Silt Removal Technical Plan (Step 38)

A technical plan for removal of the reactor building basement silt is scheduled. This silt will likely require solidification prior to disposal. Therefore, this step identifies the need to investigate the potential for using the spent resin tanks and the make-up and purification solidification skid for the silt. Due to the different handling characteristics of the silt, some additional modifications are likely. These modifications must be identified and accommodated prior to contaminating the transfer and solidification system with the make-up and purification demineralizer resins.

3.2.3 Spent Resin Transfer System Modifications (Steps 39-42)

As described in Section 2.2, some hardware modifications to the spent resin system will be required. As these will be permanent changes, an engineering change memorandum (ECM) is required.

In addition to the ECM sketches, this plan calls for a revision of the P&ID for the spent resin system as a minimum. This is because this drawing will be necessary for operation of the system. It would also be prudent to revise the consolidated P&ID that was drawn for this project (Dwg. No. 2E-533-21-001), as it shows the purification demineralizers and spent resin system on one sheet and will be very useful for operators.

3.2.4 Solidification Skid (Steps 43-46)

The solidification skid described in Section 2.2.1.4 is required before any resins are sluiced. This sequence could possibly be the most limiting critical path for this project because considerable work is required.

3.2.5 Handling and Shielding (Steps 47-48)

The removal of the solidified drums from the solidification skid will require handling equipment and special shielding. This activity should be coordinated with the solidification skid design. This equipment may include transfer bells, hoists, and dollies. These are described in Section 2.2.1.6.

3.2.6 Solidification Operational Preparation (Steps 49-53)

The solidification skid is a new system. Although it is temporary, it is expected to stay in place for an extended period of time. Thus the development of operational procedures for solidification will be preceded by a technical evaluation report (TER) and associated safety review. Before the TER can be completed, the skid, shielding, and waste handling designs must be available.

A process control program (PCP) will be required for solidification batch control to ensure that solidification requirements are met and transportation and disposal limits are not exceeded. The demonstration operations in Phase II are not expected to create TRU contaminated waste because they will be conducted with pre-accident resins. Therefore, the PCP need not address TRU concentrations during Phase II operations.

Step 53 recognizes the Technical Position on waste form recently issued by NRC (Reference 7). This step is the test required to qualify the selected solidification binder.

3.2.7 Amend Cask License (Step 54)

A cask license may be required to ship the TRU contaminated waste. For example, if the CNS-113-C cask were to be used, it would have to be licensed for 200 grams of fuel.

3.2.8 System Demonstration (Steps 55-57)

These steps call for sluicing of the spent fuel pool cleanup system resins to demonstrate the operation of the modified spent resin system and the new solidification skid. These resins are mildly radioactive and should indicate any system deficiencies without risk of significant contamination or personnel exposure. When deficiencies are resolved, these systems should then be ready to process the purification system demineralizer contents.

3.3 PHASE III ACTIVITIES

Phase III involves the removal and disposal of the purification demineralizer solids. If significant radioactivity is removed in Phase I, then sluicing should be a routine operation. The system requirements for this phase are discussed in Section 2.3.

3.3.1 TRU Detection Scheme (Steps 58-60)

Because there is some fuel and thus TRU isotopes in the demineralizers, the concentration of this material in the final waste will have to be closely controlled to ensure burial limits will not be exceeded. Thus, a method of measurement is required for the final PCP. The feasibility of direct measurement of gamma activity to infer the TRU concentration is currently being investigated. For this project, since the soluble cesium will be removed before the solids are sluiced, insoluble cesium as well as cerium may be an acceptable measurement isotope. Should neither prove feasible, then direct control of solids quantity will be required (and difficult).

The TRU measurement hardware will be coordinated with the solidification skid design. It will not be necessary to have it in place for the Phase II demonstration, although this would be preferable.

3.3.2 Sluice Campaign (Steps 61-63)

It is anticipated that NRC concurrence will be required before sluicing the resins from the purification demineralizers. Phase I and II completion should provide sufficient assurance of safety to obtain this approval.

This plan calls for sluicing both demineralizers into one spent resin tank. This will "homogenize" the contents of both demineralizers, minimizing the sampling requirements consistent with ALARA principles. These samples will be used for solidification media proportioning to keep the final radioactive concentrations below disposal limits. As discussed previously, if the rinse and elution steps are not sufficiently effective in removing cesium, then these operations may be carried out individually for each demineralizer and possibly for smaller batches. This will complicate the PCP because several samples will probably be needed.

3.3.3 Solidification and Disposal Campaign (Steps 64-69)

The Phase II PCP will be revised for TRU control for the solidification campaign. The PCP revision will depend on the method for relating radiation to solids quantities, the results of a sample of the contents of the spent resin tank, and waste disposal destination decisions that will affect allowable concentrations (see Section 3.1.3). Sufficient samples will be taken to assure good waste characterization. These samples in combination with external radiation measurements will be used to define the quantity of waste in each drum.

The material will be solidified in 55-gallon drums that can be staged in the auxiliary building or individually transported to interim storage prior to shipping for disposal.

3.4 MILESTONE SCHEDULE

An overview milestone schedule for the previously described project activities is shown in Figure 3-5. This schedule shows that the commitment to the NRC to have material ready for shipment by the end of 1984 is achievable. Engineering is working on a detailed schedule.

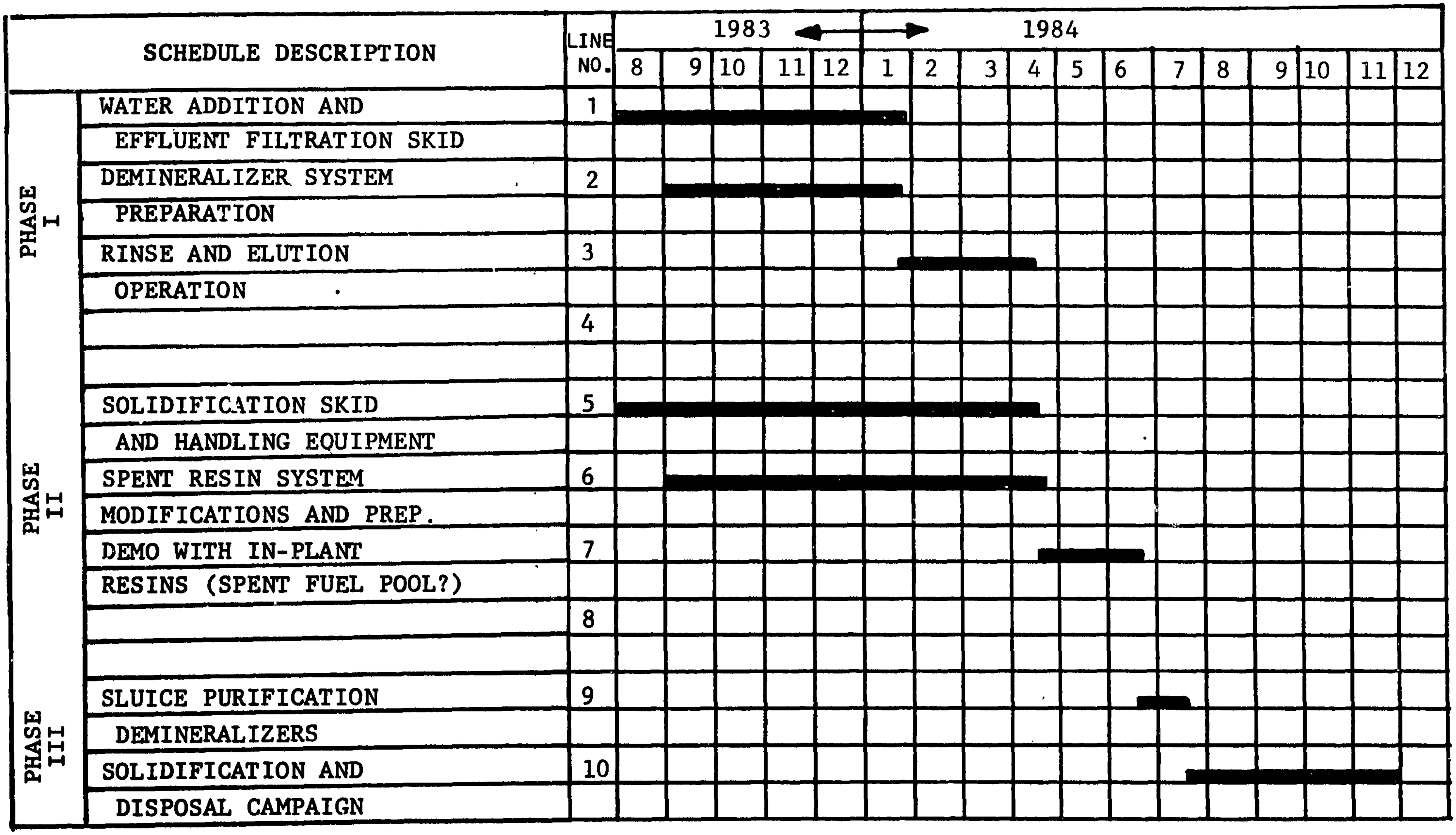

FIGURE 3-4

SCHEDULE OVERVIEW

SECTION 4.0

INTERFACE WITH OTHER PROJECTS

4.1 INTERFACE WITH SYSTEMS DECONTAMINATION

4.1.1 Schedule Interface

The goal of the project is to have the resin from the makeup system demineralizers ready to ship by the end of 1984. Plans for decontamination of all systems outside the scope of this plan are delineated by the Integrated Plan for AFHB Characterization/Stabilization/Decontamination, TPO/TMI-049, (Reference 6). The relationship between the implementation of these two plans will be shown on Recovery Programs Integrated Intermediate Schedules. Implementation of both activities is expected to begin in 1983. AFHB decontamination operations are expected to extend over a significant period of time. However, it is clear that the demineralizers must first be emptied before decontamination or removal of the debris and their associated piping is attempted. These decontamination activities may have to be rescheduled if the demineralizer project is not completed.

4.1.2 Isolation Boundaries

Establishing the boundaries for the demineralizer processing project is not prescribed here and is left as an operational decision.

4.2 INTEGRATION WITH OTHER DEMINERALIZER RESIN DISPOSAL

The activities sequence diagram shows sluicing of spent fuel cleanup demineralizers as a prerequisite to purification demineralizer sluicing. The purpose is to first "test" the system with less radioactive waste.

Other in-plant resins can be processed in the campaign with the spent fuel cleanup and the purification demineralizer resins for operational efficiency. Resins that have been identified as candidates are cleanup demineralizers and evaporator condensate.

4.3 INTEGRATION WITH REACTOR BUILDING BASEMENT SILT PROCESSING

A technical plan for processing the reactor building and AFHB silt is currently being written. It will recommend that the silt be pumped to the spent resin tanks for settling. The solidification skid also would be used for basement silt since the same problem of controlling TRU concentrations also applies in this effort. Use of the spent resin tanks for this purpose will require some modifications. These modifications should be accomplished, if possible, prior to sluicing of purification demineralizer resins. These modifications are not yet fully investigated, however, they are expected to be:

- A method to decant water from a spent resin tank
- Additional agitation features to break up consolidated silt at the tank bottom
- Additional instrumentation to determine silt quantities and concentration

REFERENCES

1. HEDL-7285. "Fuel Content of the TMI-2 Makeup Demineralizers"

2. Letter to G. Quinn, EG&G/TMI from A. P. Malinauskas, ORNL, dated June 13, 1983.

3. LASL-Q-4183-317. "NDA Measurements of the Demineralizers at TMI-2".

4. HEDL-7335. "Resin and Debris Removal System Conceptual Design."

5. HEDL-7377. "Planning Study, Resin and Debris Removal System, Makeup and Purification Demineralizers: TMI-2."

6. Technical Planning Department. Technical plan for the integrated plan for AFHB characterization/stabilization/decontamination. TPO/TMI-049. Revision 0. June 1983.

7. NRC Technical Position on Waste Form, May 1983.

APPENDIX

SUMMARY OF CONTENTS OF MAKEUP AND PURIFICATION DEMINERALIZERS

Resin Scoping Tests

A series of scoping tests were run at Pacific Northwest Laboratories (PNL) in an attempt to simulate the radiation and thermal degredation of the resins in the makeup and purification system. PNL irradiated a sample of IRN-150 mixed bed resin (similar to those used at TMI-2) to an accumulated dose of 1.7 x 10 rad with an external ^{60}Co source. The estimated cumulated doses experienced by the makeup and purification resins was between 1 and 5 x 10^9 rad. The results of these tests indicated a significant loss in resin volume and a corresponding increase in resin density. Samples of the resin were also heated to various temperatures and studied for degradation effects and products. Samples subjected to both radiation and heating showed significant weight loss (50-60%) and loss of functionality but remained sluicable up to 750°F. The estimated maximum temperature experienced by the resins in the makeup and purification system was 360°F. The gases released during the radiation and heating processes were sampled and analyzed. The major gas generated was hydrogen (80-90%).

In-Cell Surveys

A number of in-cell surveys were performed to determine the quantity of fission products and fuel in the demineralizers. Westinghouse Hanford Corporation (WHC) provided a small robot equipped with a TV camera and a dose rate monitor for the initial surveillances inside the cubicles. Gamma dose rate profiles augmented by TLD vertical dose profiles were also performed in the "A" demineralizer cubicle. Uncertainties involved in the interpretation of these data for assaying the quantity of fuel present in the demineralizers led to the performance of several additional in-cell surveys using more sophisticated non-destructive assay techniques.

Solid State Track Recorders (SSTR) were used to assess the neutron flux at the "A" demineralizer tank surface, thereby determining the quantity of fuel present. The SSTR data confirmed the tank was dry above the 309' elevation and estimated the quantity of fuel to be 1.7 ± 0.6 kg U.

The second technique for fuel measurement involved the scanning of the gamma spectrum from the "A" demineralizer tank using Si(Li) compton recoil spectrometry. Using equipment supplied by WHC, a scan of the "A" demineralizer tank through an existing penetration yielded the quantity of ^{144}Ce and ^{137}Cs present in the tank. From these data, an estimate of fuel of 1.3 ± 0.6 kg U was obtained.

The third technique applied to the fuel assay of the demineralizer resins was the use of a Be (γ,n) spectrometer system supplied by Los Alamos National Laboratory (LASL). The results of these scans showed the "A" demineralizer fuel content to be 2-7 kg and the "B" demineralizer to be $\sim$0.7 kg of U.

A summary of the data concerning the demineralizers known prior to sampling is given in Table I. It can be seen from the data in this table that the best estimate of conditions in the demineralizers are:

1. The resins have shrunk and settled
2. There is only a small volume of liquid in the tanks
3. More fuel and core debris are in the "A" demineralizer
4. Neither demineralizer has a significant quantity of fuel
5. The "B" demineralizer has more Cs activity
6. Piping and equipment in cubicles are in satisfactory condition

TABLE I

Estimated Demineralizer Loadings
Based NDA Characterizations

	Initial	A Vessel	B Vessel
1. Resin			
Volume, ft^3	50	22	22
Weight, lb	2,139	1,025	1,025
^{137}Cs, Ci	0	3,500	7,000
^{134}Cs, Ci	0	270	540
2. Liquid			
Volume, ft^3	44	3	3
Weight, lb	2,746	193	193
3. Debris			
U, lb		5	1
Core Debris, lb		95	19
^{137}Cs, Ci		177	35
^{134}Cs, Ci		16	3
^{106}Ru, Ci		21	4
^{144}Ce, Ci		28	5
^{125}Sb, Ci		116	23
TRU, Ci		0.5(a)	0.1(a)
4. Gas			
Volume, ft^3		54	54
Temp, °F		80	80
Pressure, psig		11	10.5

(a) α activity only

GAS SAMPLING

With the results of the resin scoping tests and non-destructive assay measurements in hand, sampling of the demineralizers began. The first task was to sample, depressurize and purge each demineralizer of its trapped gases.

This was accomplished by modifying the instrument lines leading to the Barton differential pressure gauge (MUDPAH-4517) located in the Hays Gas Analyzer Room. The installation of a temporary gas line to permit venting to the waste gas decay tanks was installed with the capability of adding diluent gas (nitrogen). After clearing of liquid in the instrument lines, samples of the gases were taken and analyzed on-site and at an off-site laboratory (WHEDL). The results of these analyses are summarized in Table II.

TABLE II

Analysis Results of Makeup and Purification Demineralizer Gas Samples Taken During Venting

	Results		
Analysis	Sample 1 A-demin	Sample 2 A-demin	B-demin*
Kr (ppm)	<6	<6	<6
Xe - 136 (ppm)	0.8	0.8	2
Xe - 134 (ppm)	0.6	0.7	1.5
Xe - 132 (ppm)	0.7	0.8	1.8
Xe - 131 (ppm)	8	7	19
Xe - 129 (ppm)	0.2	0.3	0.6
CO_2 (mole %)	0.47	0.44	2.75
Ar (mole %)	0.10	0.01	0.03
O_2 (mole %)	<0.01	0.02	<0.01
N_2 (mole %)	91.6	91.4	8.69
CO (mole %)	<0.2	<0.2	<0.2
He (mole %)	<0.01	<0.01	<0.01
H_2 (mole %)	7.59	7.15	81.3
CH_4 (mole %)	0.21	1.02	7.28
Kr - 85 (UCi/cc)	0.043	0.043	0.20

* No D_2, He - 3 or HT detected

Using gauges installed in the temporary gas venting system, the best estimate of the initial gas pressures on the demineralizers were 8 psig on the "B" demineralizer and 4 psig on the "A" demineralizer. The "A" demineralizer was diluted with nitrogen gas during the liquid clearing operations. It can be seen from these analyses that the principal gas was hydrogen with some nitrogen and very little oxygen. This suggests that oxygen scavenging is occurring thus preventing the build up of a potentially explosive atmosphere. The demineralizers were vented and purged with nitrogen to less than 2% residual hydrogen.

Resin Sampling

Following the safe venting and purging of the demineralizers, modifications necessary to sample the resins in the tanks were begun. Sampling was accomplished by cutting the resin fill line in the Hays Gas Analyzer Room and installing a new ball valve on the 3" lines for each demineralizer. Special sampling tools, designed and fabricated by NUS Corporation, were used to obtain samples of the material in both tanks with minimum contamination and exposure to personnel. Samples were obtained by probes inserted through the diaphragm valves in the resin fill lines and into the resin beds through the top of the tanks. The "A" demineralizer sample was very difficult to obtain due to the presence of a crust over the resin which was later confirmed by a visual fiberscope survey. The "B" demineralizer was found to contain a layer of water covering the resin. Two samples of the "B" demineralizer were obtained. The results of the analyses of these samples performed at ORNL are shown in Table III. The conclusions that can be drawn from these results are:

TABLE III
Analytical Results for TMI - Columns A & B

		April 1983		May 1983		
Units	El.	B-Solution	B-Solid	B-2 Liq.	B-2 Solid	A Solid
ppm	B	3000		3000	>200	>200
	C	1000 ppm		900 ppm	>10%	>10%
ppm	Na	7000		~10,000	>1000	>1000
ppm	Mg	<1		<1	2	5
ppm	Al	10		10	70	50
ppm	Si	<3		<3	<5	<5
ppm	P	0.1		0.1	<1	4
ppm	SO_4	9600		6000	15,000	10,000
ppm	Cl	5		20	30	20
ppm	K	3		0.8	4	4
ppm	Ca	20		10	30	50
ppm	V				1	<0.1
ppm	Cr	0.3		0.6	5	<1
ppm	Mn	0.2		0.1	5	10
ppm	La				3	~1
ppm	Ba				<1	40
ppm	Cs*	30		30	100	100
ppm	129-I*					100
ppm	Te*	<1		<1	30	10
ppm	Sn				~2	
ppm	In	0.2		0.3	30	300
ppm	Cd	<1		<1	60	1000
ppm	Ag	0.4		2	30	600
ppm	Rh				≤3	≤3
ppm	Mo					200
ppm	Nb	<.1		<.1	<1	1
ppm	Zr	1		1	6	500
ppm	Sr*	1		<1	1	4
ppm	Rb*	6		4	15	15
ppm	As	<.5		<.5	<1	2
ppm	Zn	<.2		0.2	<1	<1
ppm	Cu	1		0.3	<1	2
ppm	Ni	0.5		0.6	40	100
ppm	Co	<.1		<.1	<1	3
ppm	Fe	10		10	200	700
ppm	U	0.064	1620	0.109	283+	1250
ppb	Pu	0.72	3550	0.64	787+	3520
μCi/g	134Cs	0.181E3	0.778E3	0.101E3	1.13E3	15
μCi/g	137Cs	2.64E3	11.2E3	1.48E3	16.9E3	220
μCi/g	90Sr	0.014E3	0.49E3	9.46	0.88E3	200
μCi/g	60Co					1.98
μCi/g	125Sn					7.4
μCi/g	144Ce					9.9
	pH	5.7		5.3		

*Fission Product + normal.

+ = Values suspect - rechecks in progress.

TABLE III (Continued)

		April 1983		May 1983				
Units	El.	B-Solution	B-Solid	B-2 Liq.		B-2 Solid		A Solid
At %	234U	0.022	0.023	0.023**		.026		.022
At %	235U	2.23	2.46	2.5**		2.17		2.35
At %	236U	0.128	0.072	~.1**		0.10		0.072
At %	238U	97.62	97.45	97.5**		97.70		97.55
At %	238Pu	≤0.07	<.05	<.1		<.1		<.1
At %	239Pu	87.85	91.0	84.4		82.88		89.87
At %	240Pu	10.29	7.6	13.8	-	13.25		8.75
At %	241Pu	1.79	1.4	1.82		3.87	+	1.38
At %	242Pu	<.05	<.05	<.1		<.1		<.1

Original Sample

R at contact (110 Liq. & Solid) (7)

Insoluble Residue ~20 mg/ml ~500 mg/ml (dry)

**Small aliquot.

+ = values suspect - rechecks in progress.

---

1. The "A" demineralizer contains more fuel and core debris.
2. The "B" demineralizer liquid contains at least 500 Ci ^{137}Cs.
3. The "B" demineralizer resin is sluicable.
4. The "A" demineralizer sample may not be representative of resin.
5. The "A" demineralizer resin has a crusted appearance and severe channeling exists.
6. The "A" demineralizer is dry.